Springer Series on Polymer and Composite Materials

Susheel Kalia
Krzysztof Pielichowski *Editors*

Polymer/POSS Nanocomposites and Hybrid Materials

Preparation, Properties, Applications

Springer

Springer Series on Polymer and Composite Materials

Series editor

Susheel Kalia, Army Cadet College Wing, Indian Military Academy, Dehradun, India

More information about this series at http://www.springer.com/series/13173

Susheel Kalia · Krzysztof Pielichowski
Editors

Polymer/POSS Nanocomposites and Hybrid Materials

Preparation, Properties, Applications

Springer

Editors
Susheel Kalia
Army Cadet College Wing
Indian Military Academy
Dehradun, India

Krzysztof Pielichowski
Department of Chemistry
and Technology of Polymers
Cracow University of Technology
Kraków, Poland

ISSN 2364-1878 ISSN 2364-1886 (electronic)
Springer Series on Polymer and Composite Materials
ISBN 978-3-030-02326-3 ISBN 978-3-030-02327-0 (eBook)
https://doi.org/10.1007/978-3-030-02327-0

Library of Congress Control Number: 2018960349

This Springer imprint is published by the registered company Springer Nature Switzerland AG
The registered company address is: Gewerbestrasse 11, 6330 Cham, Switzerland

Preface

This book provides an overview about polymer nanocomposites and hybrid materials with polyhedral oligomeric silsesquioxanes (POSS). Among inorganic nanoparticles, functionalized POSS are unique nanobuilding blocks that can be used to create a wide variety of hybrid and composite materials, where precise control of nanostructures and properties is required. Polyhedral oligomeric silsesquioxanes have the general formula $(RSiO_{1.5})_n$, where n is an integer and R can be a large number of substituents including hydrogen, alkyl, aryl, alkenyl, phenyl, halogen and siloxy groups. Incorporation of POSS moieties into (organic) polymer matrix influences on the mechanical, thermal and flammability behaviour of composites and hybrid organic–inorganic materials in which the components are intimately mixed, where at least one of the component domains has a dimension ranging from a few tens to several nanometres, and there are chemical bonds (covalent or iono-covalent bonds) between the components. Importantly, POSS-containing materials can be biofunctionalized by linking, e.g., peptides and growth factors through appropriate surface modification in order to enhance the hemocompatibility of cardiovascular devices made of these materials. This reference work includes a description of synthesis routes of POSS and POSS-containing polymeric materials (e.g. based on polyolefins, epoxies, polyurethanes and polyamides), as well as presentation of POSS role as reinforcing agent and flame retardant. Finally, decomposition and ageing processes are outlined.

The main objective of this book is to explicate some important features of polymer nanocomposites and hybrid materials with polyhedral oligomeric silsesquioxanes. The first chapter of this book discusses main synthetic approaches used to prepare completely and partially condensed polyhedral oligomeric silsesquioxanes such as sol–gel technique, microwave irradiation procedures. A brief description of the characterization techniques used to analyse the properties of POSS is also reported here. Chapter "Design and Synthesis of Hybrid Materials with POSS" aims to provide the essential aspects related to design and fabrication of organic–inorganic hybrid structure based on polymeric materials and polyhedral oligomeric silsesquioxane. Chapter "Self-assembly of POSS-Containing Materials" presents an overview of selected contributions to the field of POSS-based nanohybrid materials. This chapter

discussed 3D nanonetworks, templating with POSS, POSS-containing hybrid materials for optoelectronics, supramolecular bioactive POSS nanoassemblies and self-assembly of POSS at the interface.

Chapters "Polyolefins with POSS" to "Dielectric Properties of Epoxy/POSS and PE/POSS Systems" include the polyolefins, polyurethanes, polyamides and epoxies-based nanocomposites with polyhedral oligomeric silsesquioxanes, respectively. Various mechanical, thermal, dielectric properties of POSS-containing polymer-based nanocomposites are also discussed in these chapters. Chapter "Porous Hybrid Materials with POSS" highlights the porous hybrid materials based on polyhedral oligomeric silsesquioxane. This chapter reviews the properties and importance of porosity of POSS and POSS hybrid materials. Chapter "Rubbers Reinforced by POSS" presents an extensive overview of rubbers reinforced with POSS. The role of POSS surface functional groups in controlling the properties of the synthesized rubber composites is discussed in this chapter. Chapter "POSS as Fire Retardant" summarizes the latest development on the POSS-based fire-retardant polymer composite materials mainly in terms of the class of polymers including epoxy resins, polycarbonates, polyesters, polyolefins, polystyrene, polyurethanes, vinyl esters, acrylics and cotton fabrics. In Chapter "POSS Hybrid Materials for Medical Applications", POSS hybrid materials for medical applications, including dental materials, drug delivery systems, tissue engineering applications and bioimaging, are described. Importantly, POSS structure and properties, especially its non-toxicity, make it possible to apply this kind of nanoparticles for suitable modification of materials for use in medicine and pharmacy. The role of organic–inorganic hybrid materials with POSS for coating applications has been described in Chapter "Organic–Inorganic Hybrid Materials with POSS for Coatings". The effect of POSS addition on the mechanical, surface, flame retardant and corrosion resistance properties is also discussed in this chapter. Chapter "Decomposition and Ageing of Hybrid Materials with POSS" discusses the decomposition and ageing of POSS-based hybrid materials. Thermal behaviour of most common POSS–polymer composites, namely epoxies, polypropylene, polystyrene, polylactide, polyimides and polyurethane, has been reported in this chapter.

All the 13 chapters in this book are contributed by renowned researchers from academia and research laboratories across the world. It should be a useful source for scientists, academicians, research scholars, material engineers and industries. This book will be supportive for undergraduate and postgraduate students in Institutes of Polymer Science & other Technical Institutes, and Technologists & Researchers from R&D laboratories working in this area.

The editors would like to express their gratitude to all the chapter contributors, who have contributed to this interdisciplinary book. Both the editors would like to thank their research teams for helping them in the editorial work. Finally, we gratefully acknowledge permissions to reproduce copyright materials from a number of sources.

Dehradun, India — Susheel Kalia
Kraków, Poland — Krzysztof Pielichowski

Contents

About the Editors

Dr. Susheel Kalia is an Associate Professor and Head in the Department of Chemistry at Army Cadet College Wing of Indian Military Academy, Dehradun, India. He was a Visiting Researcher in the Department of Civil, Chemical, Environmental and Materials Engineering at the University of Bologna, Italy, in 2013 and held a position as Assistant Professor in the Department of Chemistry at the Bahra University and Shoolini University, India, until 2015. He has around 80 research articles in international journals along with 11 books and 11 chapters in his academic career. His research interests include polymeric composites, bio- and nanocomposites, conducting polymers, nanofibres, nanoparticles, hybrid materials and hydrogels. He is an experienced book editor, and he has edited a number of successful books (with Springer and Wiley), such as "Cellulose Fibers: Bio- and Nano-Polymer Composites", "Polymers at Cryogenic Temperatures", "Polysaccharide Based Graft Copolymers", "Organic–Inorganic Hybrid Nanomaterials", "Polymeric Hydrogels as Smart Biomaterials", "Biopolymers: Environmental and Biomedical Applications", "Polymer Nanocomposites based on Organic and Inorganic Nanomaterials", "Biodegradable Green Composites". He is the main editor of the "Springer Series on Polymer and Composite Materials". In addition, he is a member of a number of professional organizations, including the Asian Polymer Association, Indian Cryogenics Council, the Society for Polymer Science, Indian Society of Analytical Scientists and the International Association of Advanced Materials.

Prof. Krzysztof Pielichowski is the Head of the Department of Chemistry and Technology of Polymers, Cracow University of Technology, and is an expert in polymer (nano)technology and chemistry, particularly in the areas of polymer nanocomposites with engineering polymers and hybrid organic–inorganic materials, including those containing polyhedral oligomeric silsesquioxanes (POSS) and nanocrystalline cellulose. Special attention is dedicated to the assessment of nanocomposites impact on the environment at all stages: preparation, characterization and recycling. He is currently performing a research programme in the area of preparation of engineering polymer nanocomposites with improved thermal and mechanical properties for construction applications. He is the co-author (or editor) of eight books and over 120 papers with impact factor.

He is the editor of the book series titled "Modern Polymeric Materials for Environmental Applications", and he has been a recipient of a number of international and national awards, such as Kosciuszko Foundation Award in 2000, Fulbright Fellowship Award in 2003 and the Rector of CUT Award in 2010 and 2016. He also has been a consultant or cooperating with a number of companies, such as ABB and Grupa Azoty. He is the President of the Polish Society of Calorimetry and Thermal Analysis and was a member of the Management Committee of the European Union COST Action MP0701 "Composites with Novel Functional and Structural Properties by Nanoscale Materials". He is a member of the Committee of Chemistry of the Polish Academy of Sciences and Commission of Technical Sciences of the Polish Academy of Arts and Sciences. He has served as a reviewer of a number of projects and research papers over the last decade and supervised eleven Ph.D. theses (completed) and four currently running.

Synthesis Routes of POSS

Enrico Boccaleri and Fabio Carniato

Abstract The study of the chemistry of materials containing Si–O bonds was in the past mainly applied to both inorganic silica and minerals or to organic silicones field in which the R_2SiO unit dominates. However, in the last decade, the field of silsesquioxane chemistry with general composition $RSiO_{3/2}$ has grown dramatically and many structures have been proposed in the literature. The idea of this chapter is to make an overview of the main synthetic approaches used to prepare completely and partially polyhedral oligomeric silsesquioxanes (POSS), highlighting the advantages and the weakness of each procedure. A brief description of the characterization techniques used to analyze the physicochemical properties of POSS was also carried out.

Keywords Polyhedral oligomeric silsesquioxanes · POSS synthesis
Close-cage POSS · Open-cage POSS · Cleavage · Corner capping
Hydrosilylation · Functionalization

1 Introduction

The polyhedral oligomeric silsesquioxanes (POSS) are a class of condensed three-dimensional oligomeric organosiliceous compounds with cage frameworks with different degrees of symmetry, sometimes addressed also as "spherosiloxanes" as topologically equivalent to a sphere.

E. Boccaleri (✉) · F. Carniato
Dipartimento di Scienze e Innovazione Tecnologica, Università del Piemonte Orientale, Viale Teresa Michel 11, 15121 Alessandria, Italy
e-mail: enrico.boccaleri@uniupo.it

F. Carniato
e-mail: fabio.carniato@uniupo.it

E. Boccaleri
Nova Res S.r.l., Via D. Bello 3, 28100 Novara, Italy

S. Kalia and K. Pielichowski (eds.), *Polymer/POSS Nanocomposites and Hybrid Materials*, Springer Series on Polymer and Composite Materials,
https://doi.org/10.1007/978-3-030-02327-0_1

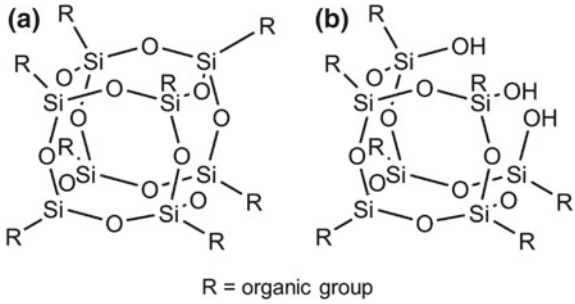

Fig. 1 Completely (**a**) and partially condensed POSS (**b**)

The term silsesquioxane dovetails the stoichiometry of the compound meaning that each silicon atom is bonded to one-and-a-half oxygen (sesqui-) and to a hydrocarbon (-ane) by a condensation reaction leading to ($RSiO_{1,5}$) bond units.

The initial discovery of silsesquioxanes dates back to 1946, when Scott [1] described completely condensed methyl-substituted silsesquioxanes. Although he was not able to assign the exact structure, he was able to determine that the general formula was $((CH_3)SiO_{3/2})_{2n}$, in which n was an integer. Nine years later, the molecular structure of a series of organosilsesquioxanes was determined via single-crystal X-ray diffraction by Barry et al. [2]. They first showed the cubic or hexagonal prismatic shape of the completely condensed molecules.

As in all the silicates, the silicon atoms show a tetrahedral arrangement and are located on the corners of the polyhedron and the oxygens are located on the edges (corner-sharing two tetrahedral silicon atoms).

Among the family of silsesquioxanes, the oligomeric structures can be divided into two important groups: the completely condensed POSS [3] and the partially condensed POSS [4–6] (Fig. 1). In the first case, POSS shows a totally closed-cage structure with the silicon atoms localized on the apices of the cage; in the second case, POSS is characterized by an opened-cage structure with dangling Si–OH groups. For this reason, the large variety of fully condensed and incompletely condensed POSS can refer to the general formula $(RSiO_{1,5})_a(H_2O)_{0.5b}$. In this expression, a and b are integer numbers ($a = 1, 2, 3 \ldots$ and $b = 0, 1, 2, 3 \ldots$) and are related to each other by the following equations:

$$a + b = 2n \quad (n = 1, 2, 3, \ldots)$$
$$b \leq a + 2$$

and R is a covalently bonded organic group.

The definition of these two terms expresses thus the composition of a specific POSS compound, but cannot give information about the structure, as, especially for larger molecules and silanol-containing structures, isomeric forms can be present. The definition of the above terms, a and b, is not the only way to identify the composition of a POSS. The most trivial nomenclature is to state the number of organic silsesquioxane units present in the system, as, i.e., octa-R-silsesquioxane. Another

Table 1 Brief summary of the silicone nomenclature

Number of Si–O bonds	Type of unit
1	M unit
2	D unit
3	T unit
4	Q unit

possibility to define POSS structure requires the use of the silicone nomenclature summarised in Table 1 and related to the number of Si-O bonds per Si unit.

Different synthetic procedures are proposed in the literature for the preparation of completely and partially condensed POSS, spanning from solgel syntheses to cleavage of completely condensed POSS and corner-capping reactions often used for the preparation of mono- and bifunctionalized POSS. Further strategies, such as the hydrosilylation of available POSS (typically applied to obtain T_8R_8, T_8R_7R', and $T_8R_{7-n}R'_n$ POSS) and microwave-assisted procedures have been also explored.

2 Synthetic Methodologies

2.1 Solgel Synthetic Procedures

looseness-1One of the strategies to prepare both completely and partially condensed POSS is the solgel procedure. This synthetic approach can be described as a multistep hydrolysis/condensation pathway. The first step is the hydrolysis of an organosilane precursor [7–10] in aqueous solution with the formation of low molecular weight species (step i) (Fig. 2). In the subsequent step, these precursors participate in condensation reaction with each other, leading to the formation of oligosiloxanes (step ii) (Fig. 2). The chemical nature of the final products (ranging from lower oligosiloxane dimers or tetramers, to polyhedral oligomeric silsesquioxanes like the tri- and tetrasilanol silsesquioxanes, to polymeric species) is governed by the thermodynamic [11–13] and kinetic parameters and by the solubility of the products.

Sprung and Guenther [9, 10] and later Brown and Vogts [8] studied in detail the hydrolytic condensation of different organosilanes $RSiX_3$ (R = methyl, ethyl, phenyl), and they observed that the formation mechanisms relative to condensation of the silanol monomer is based on the sequence of linear, cyclic, polycyclic, and polyhedral silsesquioxanes.

A chemical control of the final structures of the product is difficult to achieve following such synthetic approach because a large number of parameters influence each step of the reactions.

In detail, the physical and chemical factors are the following:

I. The nature of R and X groups
II. The solvent used in the synthesis

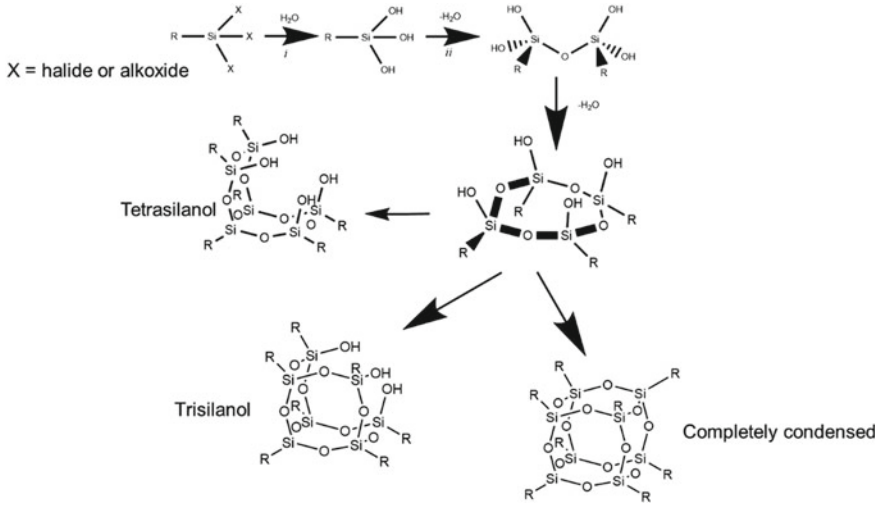

Fig. 2 Multistep hydrolysis/condensation reaction to obtain POSS

III. The amount of added water to the reaction and rate of addition
IV. The temperature
V. pH
VI. Reaction time.

(i) *The role of R group*

The role of R is much more important, as it can influence the reaction path for both steric and electronic effects. The steric factors strongly influence the buildup of the cage structure, as the hindrance of bulky groups can prevent the further condensation of the silanol units: In fact, while hindered precursors can lead to incompletely condensed silsesquioxanes (i.e., cyclohexyl- and cyclopentyl-substituted silanes), small substituents (e.g., methyl [9, 14] or hydrogen [15]) tend to give completely condensed species.

The electronic effects, for example, the inductive +I donation, can operate on hydrolytic step kinetic: For a series of alkylchlorosilanes, the increase of the hydrocarbon chain length slows down the rate of hydrolysis [16]. Furthermore, the presence of α unsaturated groups as $–CH_2=CH_2$ on the silicon proved to operate a stabilization of the five-coordinated Si intermediate for $d\pi - p\pi$ effect.

The role of X on the silane reactivity has to be coupled to the effect of this substituent on the solubility of the final POSS product: This is another factor of key importance, as a lower solubility of the product POSS means a higher synthesis rate [17].

(ii) *The role of X functionality*

The chemical nature of X group does not show an important effect on the silsesquioxanes synthesis, because it plays an effective role during the first step of the process. However, when X is a chloride group, the condensation reaction can be very fast, because of the formation of hydrochloric acid (HCl) which results in an autocatalytic species in the condensation step.

(iii) *The nature of the solvent*

Besides the effects on the solubility of the products of the reaction seen above, the role of the solvent has to be considered in the general scheme of the condensation reaction. Suitable polar solvents as an alcohol or an ether can in fact form stabilizing hydrogen bonds with silanol groups of alkoxy groups and can favor the formation of unsaturated species [17]. Moreover, the solvent can lower the energy of the intermediate species of the condensation reaction, thus favoring the formation of highly condensed structures [11, 12].

(iv) *The amount of added water and rate of addition*

These two parameters act on the concentration of the silanols in the reaction and on the kinetic of the condensation: While it is desirable to keep the concentration of the formed silanol low by a slow careful addition of water, as mentioned above, the kinetic effect cannot be easily handled and the precise effect is still unclear.

(v) *The temperature*

The temperature increase, acting both on the condensation kinetics and on the solubility of the product, causes the drift of the reaction toward highly condensed species. For these reasons, the syntheses leading to molecular species are usually at room temperature and often at subambient temperature.

(vi) *The pH*

As in solgel polymerization, the condensation of the silanol groups is catalyzed both by acidic and basic conditions. Molecular polyhedral products seem to be favored in low pH media, while polymeric species are commonly obtained with high pH values [18].

(vii) *The reaction time*

The synthesis of oligosilsesquioxanes, typically in the very first synthetic procedures set up, is often very low processes, showing precipitation times up to 36 weeks. In these cases, the collection of the reaction products after a short time leads to different products due to the rapid condensation of the intermediate species. In other syntheses, further crystal separations can be obtained by recrystallization of mother liquors and washing waters [19].

Completely condensed silsesquioxanes (POSS) exhibit the general formula $(RSiO_{1,5})_a(H_2O)_{0.5b}$ with $b = 0$ and $a \geq 4$, with different R substituents. In general, they are colorless crystalline substances, showing usually high volatility. This property, their density, and their melting point are also related to the nature and length of the R substituent (e.g., in octa(alkylsilsesquioxanes) the m.p. and density decrease with growing chain length while the volatility increases), while for a given substituent, the highest melting point and lower volatility are shown by the octameric system. This one, thanks to its stability, can be obtained as principal product, while smaller ($a = 4$, 6) and larger cage systems (mainly $a = 10$ and $a > 12$) are less common and often known only as by-products. For this reason, we will focus our survey on the octameric T_8 POSS system.

The cubic structure is an idealized representation of the real geometry, where the tetrahedral geometry of the Si causes the oxygen atoms to point out the cube edges.

After the early synthesis of the $R = CH_3$ species, prepared by Scott in 1946, [1] completely condensed silsesquioxane was obtained as main or by-products starting from monosilanes containing R groups, ethyl, [20] *n*-propyl, [21] *n*-butyl, [21] *n*-pentyl, [22] *n*-hexyl, [23] cyclohexyl, [2] phenyl, benzyl, and various substituted phenyl groups [22, 24, 25].

In many of these cases, further functionalization of the cage via the organic branches was made difficult by the presence of scarcely reactive alkyl groups.

A successful example was given by Feher et al. who prepared a series of highly functionalized POSS starting from p-$XCH_2C_6H_4SiCl_3$ monomers. These monomers were condensed in $[p\text{-}XCH_2C_6H_4SiO_{1.5}]_8$ compounds, and the reactive group on the organic moieties was post-reacted.

Partially condensed POSS is open-cage silsesquioxanes where a vertex is unoccupied by a Si atom and the dangling bonds are saturated with hydrogens. The presence of highly reactive silanols on a pseudo-cubic cage paved the way toward the corner-capping reactions with differently functionalized silane monomers or metal-containing groups.

The typical incompletely condensed silsesquioxane was prepared by Brown et al. [8] and then optimized by Feher et al. [26]. The synthetic method they proposed is based on a slow, kinetically controlled hydrolytic condensation of cyclohexyltrichlorosilane in aqueous acetone, let standing at room temperature. The crude product, which by NMR proved to be a mixture of three species, the heptameric open cube (45%), the completely condensed 6-term POSS (40%), and another pseudo-cubic octameric compound (15%), starts precipitating after about 2 months and continues the formation up to 36 months, to reach a yield of about 85% based on $CySiCl_3$. The formed precipitate can be periodically cropped without influencing the precipitation process, but as far as the reaction proceeds, an increase in the open-cube heptasilsesquioxane and a decrease of the condensed six-membered one were found.

Some years later, the same group [4] succeeded in improving the efficiency of the synthesis (obtaining the heptameric species in 7 days) and, by the use of monomeric precursors $RSiCl_3$ with different organic R groups, proved that the uncompletely condensed cage is a prerogative of aliphatic cyclic compounds but different behavior was observed: e.g., when R = cyclopentyl, the open-cube octameric species is

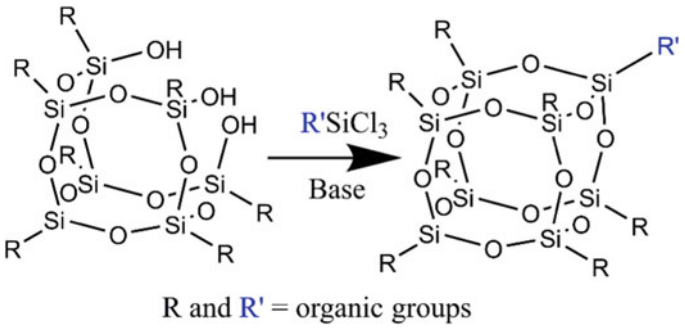

Fig. 3 Scheme of the corner-capping reaction

almost the unique product, while when R = cycloheptyl, another open-cage product a hexameric edge missing structure was obtained. In the case of cyclopentyl and cycloheptyl derivatives, refluxing the reaction mixture gave a significative increase to the reaction rate.

By using a high-speed experimentation results, Pescarmona et al. proposed a synthesis of the heptameric trisilanol silsesquioxane in acetonitrile instead of acetone which dramatically reduced the time of synthesis (18 h) and improved the yield (64%).

2.2 Corner Capping of Partially Condensed POSS

T_8R_8 and monofunctionalized T_8R_7R' POSS can be also synthesized starting from parent partially condensed silsesquioxanes through corner-capping reaction. In Fig. 3, a general reaction from the partially condensed silsesquioxane ($R_7Si_7O_9(OH)_3$) and the chloro- or alkoxysilane precursor, in the presence of a base, is reported. Feher et al. [26–28] gave a strong contribution to the optimization of the corner-capping reaction, aiming to develop novel systems for single-site heterogeneous catalysis. As a general comment, this reaction produces good yields and a large plethora of T_8R_7R' POSS was obtained. One of the main advantages of this synthetic approach is the possibility to introduce in the apex of silica cage-specific reactive groups (–NH_2, –SH, Cl, vinyl, etc.). For instance, $T_8R_7(CH_2)_3NH_2$ POSS with different R groups (i-Bu, c-C_5H_9, or Ph) were prepared.

The modification of the molar ratio of partially condensed POSS and silane precursor can influence the structure and properties of the final product. Indeed, there are manuscripts that report on the bridged compounds prepared with high yields by addition of chlorosilane to 2 equiv. of partially condensed POSS [29].

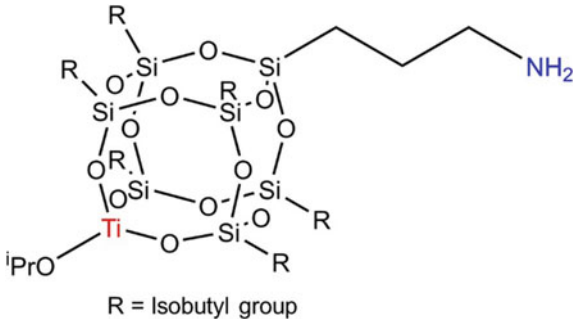

Fig. 4 Structure of bifunctional Ti–NH_2POSS

2.3 Cleavage of Completely Condensed POSS

An alternative way to obtain open-cage silsesquioxane with respect to the solgel procedure was reported by Feher et al. [5] that have set up a general method of cleavage of completely condensed silsesquioxanes. They showed that the addition of excess of HBF_4 OMe_2 and BF_3OEt_2 to a solution of $(cC_6H_{11})_8Si_8O_{12}$ in $CDCl_3$ or C_6D_6 gives a smooth reaction after standing for several hours or brief refluxing, causing the formation with a 85% yield of a fluoride-substituted silsesquioxane with a missing edge. The treatment with Me_3SnOH and aqueous HCl leads to a dihydroxylated open-cage system. The Si–F bond formation was proved not to be the driving force of the reaction, as the same reaction was tested successfully with triflic acid. The general validity of this approach was demonstrated as with the same method, and $R_6Si_6O_9$ cage compounds were cleaved [30].

The optimization of consecutive cleavage and corner-capping steps on a substituted starting material opens the way toward the insertion of two distinct functionalities (organic groups or metal ions) in the same cage, thus obtaining bifunctional POSS. The wide variety of silanes precursors and metal salts guarantee a fruitful production of class of novel materials. In the literature, a novel Ti-containing aminopropylhexaisobutyl-POSS (Ti–NH_2POSS) (Fig. 4), bearing in the structure an amino functionality and a titanium center, was efficiently obtained [31]. Ti–NH_2POSS has been prepared following two synthetic steps: (i) The commercially available completely condensed aminopropyl heptaisobutyl-POSS is corner-cleaved with aqueous tetraethylammonium hydroxide (TEAOH 35 wt%) in THF solution; (ii) in the second step, partially condensed POSS undergoes a corner-capping reaction with Ti(i-PrO)$_4$ in chloroform in order to obtain Ti–NH_2POSS [31]. Following a similar procedure, bifunctional POSS containing together amino/carboxylic and luminescent entities was also prepared in view of potential biomedical applications [32].

2.4 Hydrosilylation for the Preparations of T_8R_8, T_8R_7R', and $T_8R_{7-n}R'_n$ POSS

T_8R_8 Compounds

The hydrosilylation for the preparation of T_8R_8 POSS is typically supported by platinum catalyst and is based on the reaction from T_8H_8 or $T_8(OSiMe_2H)_8$ and alkene or alkyne substrates. Such reaction produces high yields, but it suffers from some drawbacks. The first one is the problem of forming different isomers of the product difficult to separate with conventional chromatography techniques. The second one is related to a parallel reaction with the oxygen sites of the substrate if present in the structure of the alkene and alkyne reactants. On the basis of the nature of organic moieties, it should be considered that most of these reactions show preferential substitution for β-position over α. However, following the discovery of a practical synthetic route to T_8H_8, hydrosilylation became one of the most common substitutions due to its simplicity and the often high yield of hydrosilylated products.

Numerous substituents can be introduced in the POSS structure, passing from aliphatic to aromatic and reactive functionalities.

In the literature, there are also some reactions that occur starting from T_8R_8 POSS bearing in the structure unsaturated organic groups with Si–H species [33].

Hydrosilylation can be also applied to bifunctional T_8R_7R' compounds containing two different substituents.

T_8R_7R' Compounds

The syntheses using hydrosilylation of a variety of T_8 POSS derivatives containing two different substituents are also performed. Exactly as in the case of T_8R_8 hydrosilylation reactions, the large number of the T_8R_7R' products of hydrosilylation is obtained from the reaction of T_8 POSS and bearing Si–H functionalities and unsaturated species. However, some exceptions are reported in the literature for $T_8R_7CH_2CH{=}CH_2$ (R = $-(CH_2)_2CF_3$ or –c–C_5H_9) [34, 35] and $T_8R_7CH{=}CH_2$ ($Si[OSiMe_2(CH_2)_2T_8Cy_7]_4$ and $O(SiMe_2OSiMe_2(CH_2)_2T_8Ph_7)_2$) [36, 37]. For these compounds, the reactions are more efficient if compared with parent reactions directly involving T_8-silyl species.

Only four cases in the literature reported the reaction of T_8H_8 POSS with unsubstituted alkyl derivatives in a specific molar ratio to obtain T_8H_7R' products (R′ = $-(CH_2)_3CO_2$-*n*-$C_{16}H_{33}$, *n*-$C_{19}H_{39}$, *n*-$C_{21}H_{43}$, *n*-$C_{23}H_{47}$) [38, 39]. The yields of the products appeared low in respect to other hydrosilylations, but the final products showed reactive groups not involved in the first reaction that can be exploited to introduce more type of functionalities on the same POSS cage.

$T_8R_{(7-n)}R'_n$ *Compounds*

Modifying the molar ratio of the two reactants, it is possible to generate POSS with general chemical composition $T_8R_{(7-n)}R'_n$. These reactions often tend to produce a mixture of numerous substitutional isomers, in many cases difficult to differentiate, since it requires the predominance of the $T_8(OSiMe_2H)_{7-n}R_n$ as reactant. This can be

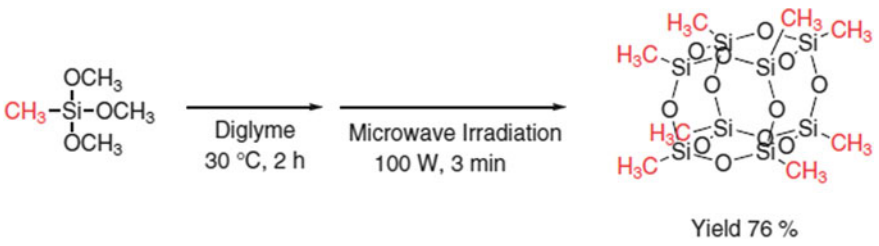

Fig. 5 Synthesis of octamethylsilsesquioxane under microwave irradiation. Reprinted from [41] © 2010 with permission of The Chemical Society of Japan

a strong limitation to possible applications of these compounds where a fine chemical control of the product is required.

2.5 Microwave Irradiation Procedures

Often, the procedure above described to prepare completely and partially condensed POSS requires long reaction times with yields in many cases not so high. These limitations pushed some research groups to develop synthetic strategies with high performances, in terms of cost, yields, and reaction times. In parallel, the green chemistry has been receiving progressively more attention in the last decades. The moderate use of organic solvents is increasingly required aiming to reduce environmental pollution.

In this scenario, microwave irradiation is a good alternative to the traditional synthetic methodologies and many papers have published about microwave-assisted chemical reactions [40]. In fact, microwave procedure ensures fast and direct heating of the solution, reducing the reaction to few minutes and increasing the pure product yields. Such procedure was also applied for the preparation of octamethylsilsesquioxane, starting from methyltrimethoxysilane in the presence of base catalyst. Under microwave irradiation (power 100 W) for few minutes, a yield of 76% of POSS was achieved (Fig. 5) [41].

Analogously, also octavinyl polyhedral oligomeric silsesquioxane was synthesized through the hydrolytic condensation of vinyltriethoxysilane using a domestic microwave oven, obtaining interesting results in reduced reaction times [42].

Microwave-assisted methods can be also applied to prepare partially condensed POSS. In the literature, cyclopentyltrisilanol $(c\text{-}C_5H_9)_7Si_7O_9(OH)_3$ was prepared by the hydrolytic condensation of the cyclopentyltrichlorosilane in acetone and water. The reaction under microwave irradiation resulted to be shorter in time if compared with the traditional synthetic approaches [43].

2.6 *High Yield and/or Facile Functionalization Methods for Novel Functional POSS—An Overview*

The spreading of application of POSS is related to the capability to make them prone to play relevant roles in chemistry, based on their manifold features of organicinorganic species, ligands, reinforcing agents, catalytic supports, etc.

On one side, the research on functionalization methods was driven by the need to overcome some possible drawbacks of conventional direct synthetic methods based on hydrolytic condensation of organotrichlorosilanes or organotrialkoxysilanes, as the presence of HCl and HBr can harness some organic functionalities, whereas the presence of some specific functional groups on R (i.e., hydroxyl groups) is poorly compatible with moisture-sensitive species as halosilanes. For instance, Marciniec and coworkers optimized the hydrolytic condensation reactions of silane precursors by using specific catalysts. For instance, dibutyltin dilaurate catalyst, largely used in the silicone synthesis, was used for the preparation of octakis (3-chloropropyl) octasilsesquioxane, obtaining the product in high yield and short times [44].

The literature is extremely rich in functionalized POSS synthesis, characterization, and application, and a complete overview is out of the scope of this chapter. However, several noteworthy methodologies that are actually tracing perspectives for novel functional roles for POSS will be briefly reported.

A generally claimed effective approach to the functionalization of organic groups of POSS is the use of the so-called click chemistry. According to the definition of Sharpless et al. [45], click reactions are widely applicable and simple to perform, can be conducted in easily removable or benign solvents, provide high yields, and produce only by-products that can be removed without using chromatographic techniques. A good overview of this approach on POSS is given in the work by Dong et al. [46].

Typical "click" reactions include Cu(I)-catalyzed [3 + 2] azide–alkyne cycloaddition (CuAAC), strain-promoted azide–alkyne cycloaddition (SPAAC), Diels–Alder cycloaddition, thiol-ene addition/thiol-X reaction (TEC), and oxime ligation.

As reported, to comply to "click" features, POSS must be made "clickable" basically in two ways, either during the cage synthesis by direct co-hydrolysis of functional silanes with "click" functionalities or with a post-condensation substitution to attach "clickable" group(s).

Specifically, "clickable" groups are alkynes, cyclooctynes, alkenes, azides, thiols, amines, etc.

A summary of "clickable" POSS building blocks that have been successfully synthesized and used in the literature is reported in Fig. 6.

As the literature reports, thanks to the possible orthogonality of these syntheses, combined application of recursive "click" reactions speeds up and favors the assessment of synthetic process with a limited number of reaction steps and convenient purification procedures.

A widespread functionalization is the thiol-ene click chemistry using photocatalytic processes [47].

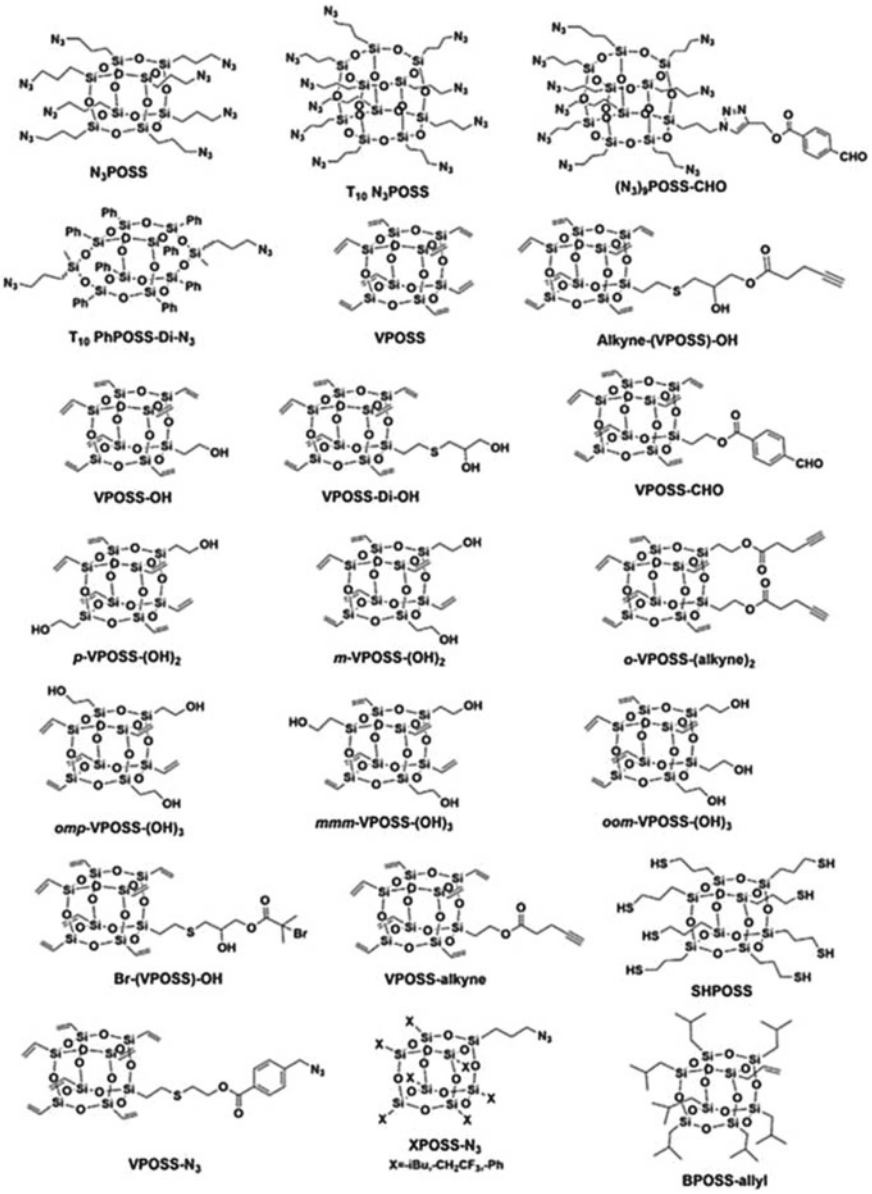

Fig. 6 Scheme of thiol-ene functionalization method on POSS. Reprinted from [46] © 2017 with permission of Elsevier

This pathway is often practiced due to the availability of vinyl-containing POSS. The starting point can basically be octavinyl T_8 or vinyl T_8R_7; as said in general for click processes, thiol-ene reaction shows several advantages: It is rapid, tolerant

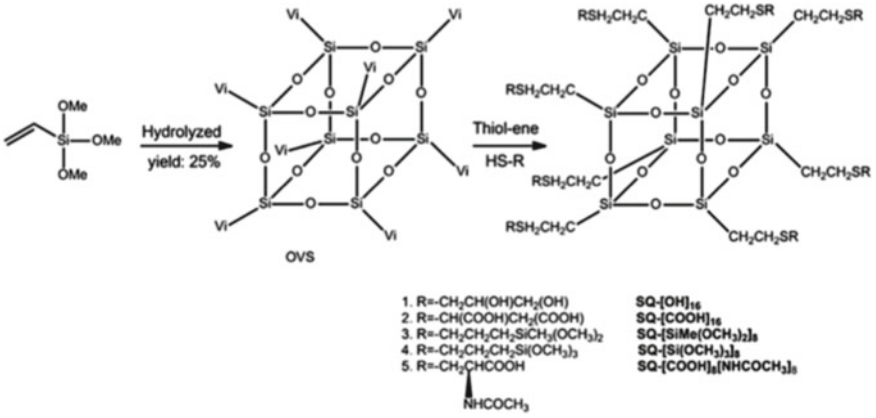

Fig. 7 Scheme of thiol-ene functionalization method on POSS. Reprinted from [47] © 2015 with permission of Elsevier

versus high water and oxygen; it requires mild conditions, low-cost catalysts and leads to high yield [48–50]. Its use on POSS is reported in the literature [51–55]. The general approach to multifunctional POSS is shown in the scheme (Fig. 7).

Basically, within 20 min, the dissolution of vinyl POSS and thiols in THF, in the presence of a photoinitiator and a 500 W UV lamp (365 nm), leads to a plethora of thioether-substituted POSS. In addition to thiol-ene chemistry, thiol–Michael reaction mediated by base or nucleophiles is another "click" approach enlarging the perspective of this kind of functionalizations [56]. In thiol–Michael reaction, a base-/nucleophile-mediated addition of a thiol group across activated double bonds is carried on. This approach is considered as a way to avoid radical recombination during the reaction, with minimum side products, and particularly powerful for samples with high molecular weight tails, bulky thiol ligands, or UV-absorbing functionalities.

Noteworthy methods for the functionalization of an open-cage POSS with the formation of Si–O–Si bonds without the formation of acidic by-products are reported using Sc(III) trifluoromethanesulfonate [57]. They can be applied to monosilanol POSS, disilanol POSS, trisilanol POSS, and tetrasilanol POSS (double-decker POSS), featuring high yields (76–98%) under mild conditions to append specific silanes based on the 2-methylallyl functionality. The reaction occurs at room temperature with the formation of isobutylene as the only by-product, which is neutral and harmless.

To address other organic reactions onto the cage substituent, a simple way to obtain octa-bromo-, octa-azido-, and octa-amino-functionalized POSS and further conversion to 3-propylurea-substituted POSS was reported by Schäfer et al. [58] carried on with simple chemical pathway and high yield. The protocol includes a series of reactions based on octaanionic cubic POSS (silylation of octaanionic cubic POSS, bromination, azidation, hydrosilylation, urea transformation) leading

an overall conversion of 83–88% where precursors are chosen to be air and moisture stable.

As an alternative to hydrosilylation, H_8T_8 has been used for the dehydrogenative reaction with alcohols to produce the octaalkoxylated POSS derivatives using different alcohols (2-hydroxyethyl methacrylate, 2-hydroxypropyl methacrylate, diphenylmethanol, triphenylmethanol, tricyclohexylmethanol) [59]. The reactivity was found to increase for tertiary, secondary, and primary alcohols, respectively, with secondary alcohols able to provide alkoxylated-cage silsesquioxanes preventing the condensation to polymers due to the lower hydrolyzability due to the steric hindrance of the groups constrained onto the POSS cage.

3 Characterization Procedures

The features of POSS, that make them similar both to siliceous materials and organic molecules, open a wide scenario in their characterization, making also useful typical techniques that are addressed to the study of molecular systems than materials.

3.1 NMR Characterization of POSS

For instance, the presence of Si atoms in the cage makes them suitable to the characterization with ^{29}Si NMR that, thanks to the solubility of POSS in several solvents, can be carried on in solution.

The use of ^{29}Si NMR can provide information of the nature of the cage structure. Completely condensed POSS is featured by chemically and magnetically identical Si atoms that are well highlighted by very simple NMR spectra.

Once reactions are carried on involving POSS, this technique allows to control the cage integrity, but it can also be profitably used for the control of cleavage reactions.

As reported in Fig. 8 and in Ref. [33], completely condensed POSS dissolved in deuterated solvents shows proton-decoupled ^{29}Si NMR spectra featured by a single signal due to the eight equivalent Si nuclei in the POSS cage, with chemical shifts (standard TMS) ranging between −65 and −80 ppm, being sensitive to the organic substituents.

With the same technique, the presence of isomers, resulting in a more complex pattern, can be inferred. ^{29}Si NMR is employed as well during the exploitation of reactions on POSS species. In particular, reactions lead to the cleavage of the cage (i.e., to achieve a T_7 $R_7Si_7O_9(OH)_3$ product) or corner-capping processes to produce T_8R_7R' and $T_8R_6R'R''$ compounds. In these cases, the differences of the Si species lead to multiple peaks due to the different chemical environment of Si atoms in the cage. Open-cage structures (when mainly deriving from cubic precursors) have typically three peaks with integration ratio 3:1:3, one due to the presence of three

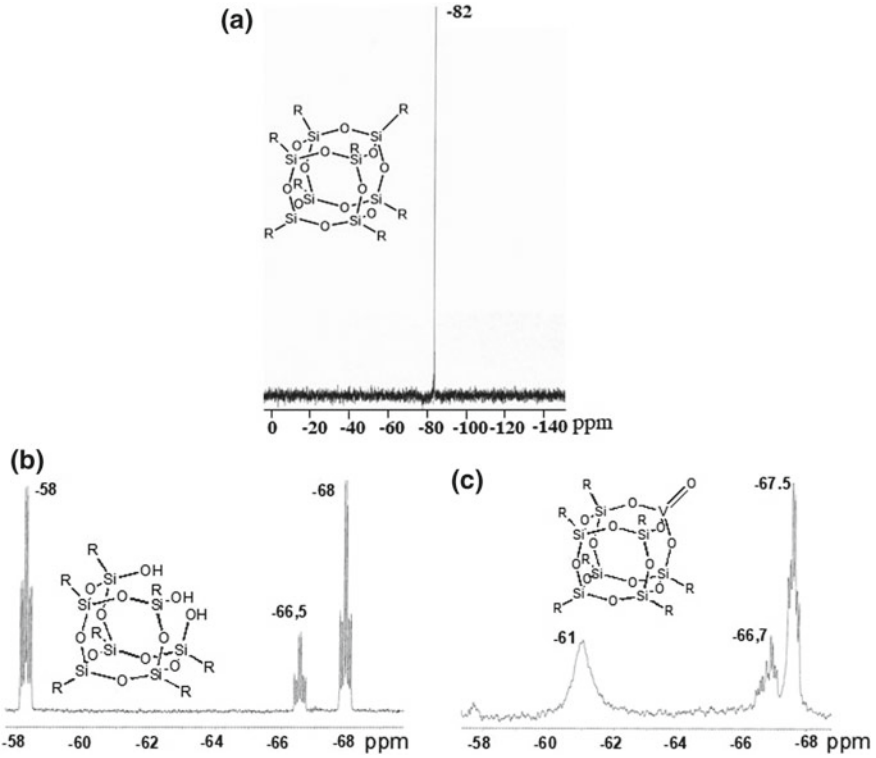

Fig. 8 NMR spectra of T_8R_8 (R=H) POSS (**a**), partially condensed isobutyl T_7R_7 POSS (R = isobutyl), and V-isobutyl T_7R_7POSS (**c**). Reprinted from [60] © 2007 with permission of Wiley

OH-bearing Si around −58 ppm, one related to the apical atom, and the third related to the three vicinal nuclei.

Monofunctionalized cubic-cage POSS has a similar behavior, but with an integration ratio of 1:3:4 for the functional group-bearing Si, the neighbors and the remaining nuclei, respectively.

The combination of the integration ratio and chemical shift was also employed to control and assess the statistical occurrence of open-cage functional POSS; the cleavage on aminopropyl isobutyl POSS highlighted by ^{29}Si NMR the occurrence of the co-presence of Si–OH units sided by the aminopropylic fragment.

Liquid NMR can also be used to determine the resonance of other nuclei as ^{1}H and ^{13}C to assess the identity of the pendant group especially when modifications (as corner capping or hydrosilylation) are carried on. Relevantly, the chemical shift of ^{13}C signals has highlighted a relevant feature of the cubic silica-like cage in terms of electronic interaction with the pendant groups. In fact, according to Li et al. [61], the cage effect on the organic fraction is electron withdrawing, with a role similar to a CF_3 group. For this reason, the reactivity of both the organic functionalities on

the cage (i.e., aromatic groups) and the silanol acidity in open-cage systems toward inorganic surfaces proved to be unusual.

The same technique has been widely used on solid-state samples (^{29}Si SS-NMR) using the molecular-like signals of Si nuclei of POSS to distinguish the nature of these compounds and to confirm the cage preservation when submitted to solid-state transformation (i.e., thermal annealing or melt extrusion of polymers).

3.2 Vibrational Spectroscopy

Other relevant techniques for the characterization of POSS materials and derived reaction products are vibrational spectroscopies; for this purpose, IR and Raman are almost equivalent in the information, though, due to the reduced effect of intra- and inter-molecular coupling effects, Raman spectra are often simpler and less affected by solid-state effects. Furthermore, Raman spectra can be easily carried on also on gel-like systems, with respect to IR classical sampling methods. The evidence of the hybrid nature of these materials is clear in the IR spectra, where the organic fragments present as substituents on the apical Si atoms can be identified using characteristic frequency tables employed in organic chemistry. IR spectroscopy highlights as well the inorganic cage features. Relevantly, the Si–O asymmetric stretching mode frequency of cage-like structures has a specific range (around 1100 cm^{-1}) that differs from polymeric ladder-like silsesquioxanes (1030–1055 cm^{-1}) [62, 63] and it is often checked as a proof of the retention of the cage structure when chemical treatments are carried on. As well, bending modes for Si–O–Si units are commonly found around 550–560 cm^{-1}.

IR and Raman spectra are useful also for the identification of the occurrence of the reactions of cleavage and corner capping. Trisilanol POSS species are clearly identified by two main signals, due to Si–O–H stretching and bending modes found commonly at 3250 and 890 cm^{-1}. The occurrence of these features with the preservation of the other fingerprint signals of the parent close-cage POSS (especially with a limited broadening of the Si–O asymmetric stretching mode) is a good confirmation of the occurrence of an effective cleavage of the cage. It is noteworthy that the silanol stretching modes are relevantly red-shifted when compared with common silica surfaces, and broadened by a significant interaction that are consistent with the expected high acidity/reactivity and a pronounced proton concentration due to the geometrical constraints.

IR and Raman spectra, hence, can also allow the evaluation of the occurrence of corner-capping reactions, restoring the features of a close-cage POSS.

These spectra have been also successfully employed in assessing the occurrence of corner capping with metal precursors. In this case, vibrational spectroscopies can highlight some further information. In fact, in the region around 900 cm^{-1} the occurrence of specific vibrational signals due to Si–O–Me stretching modes can be found (see, for instance, Fig. 9) [31].

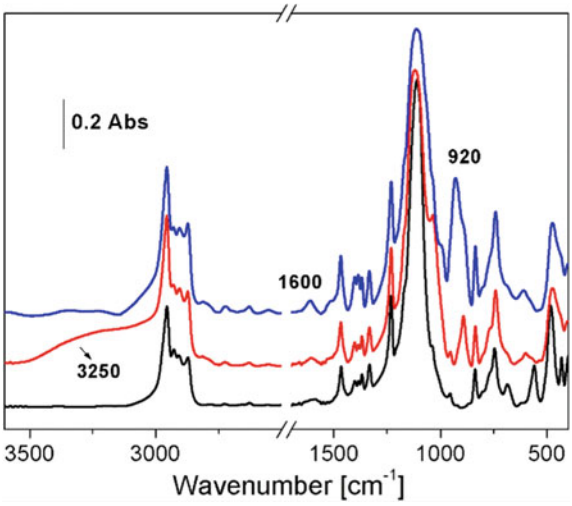

Fig. 9 IR spectra of completely condensed T_8R_7R' (R = isobutyl, R′ = aminopropyl) (black), partially condensed T_7R_6R' aminopropyl hexaiso-butyl-POSS (red), and the bifunctional Ti–NH_2POSS (blue)

3.3 X-Ray Diffraction

Considering the nature of POSS molecular systems, that is responsible for their homogeneity and structural identity as 3D nanomaterials, a part of the characterization of such species can pass through X-ray single crystal and powder diffraction.

Close-cage POSS structures reported in the literature for their structure by single-crystal X-ray diffraction are over 100. A survey on the reported structures provides as reliable cage dimensions ca. 3.11 Å as edge length, 4.40 Å as face diagonal, and 5.39 Å as the body diagonal.

Considering the application of POSS in material science, the use of powder X-ray diffraction is widespread. Depending on the nature of the R groups, POSS is more or less prone to crystallization. This is directly evident in their physical form, as they can range from powders to gel to liquid depending on the length of the alkyl group (see Fig. 10, for instance).

Basically, POSS single-crystal-derived crystallographic structures (deposited in the Cambridge Crystallographic Database) show that the role of pending organic groups is diriment in order to achieve an ordered sphere-like packing or a lower symmetry arrangement. Almost half of the structures are triclinic, while the remaining half are distributed evenly between monoclinic and rhombohedral (that means hexagonal packing of the POSS spheres) systems. This evidence suggests that the crystalline structure of POSS systems is a balance of the tendency of the cages to give tight packing, while the R group nature and conformational arrangement cooperatively hinder the optimal space filling.

This evidence is confirmed analyzing the behavior of isobutyl R_8T_8 POSS under variable temperature [64] (Fig. 11). As shown by DSC, at 48–55 °C the material undergoes a structural rearrangement that, under variable temperature in situ Raman-

Fig. 10 Picture of POSS materials, fully condensed octaisobutyl T_8R_8 (left), polyethylene glycol (PEG, chain length $C_n = 10$) T_8 POSS (center), fully condensed octaisooctyl T_8R_8 (right)

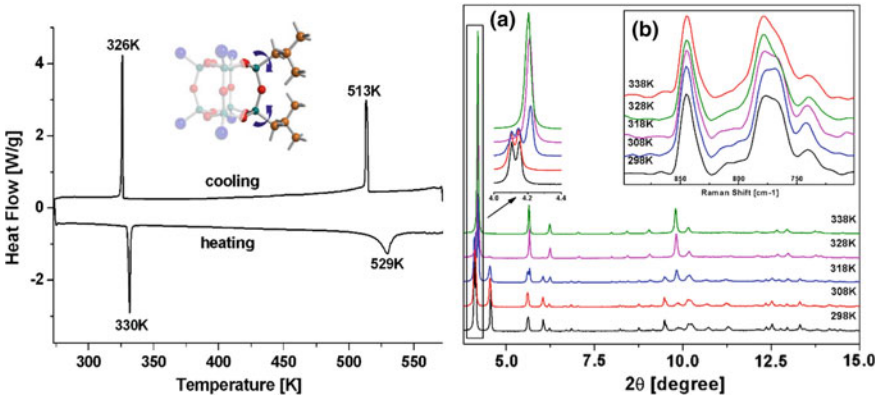

Fig. 11 Left: DSC profile under nitrogen flow of T_8R_8 isobutyl POSS; right: X-ray profiles (**a**) and Raman spectra (**b**) of T_8R_8 isobutyl POSS at variable temperature. Adapted from [64] © with permission of The Royal Society of Chemistry

XRPD experiments on synchrotron radiation, shows a cooperative conversion of the crystalline phase from monoclinic to rhombohedral. A further investigation using also SS-NMR and simulations on molecular mechanics, dynamics, and quantum chemical calculations highlights that the high-temperature crystalline phase occurrence is related to the presence of spheroid-like behavior of POSS cages with disordered isobutyl chains, due to conformational mobility operated dynamically by the increase of thermal motion.

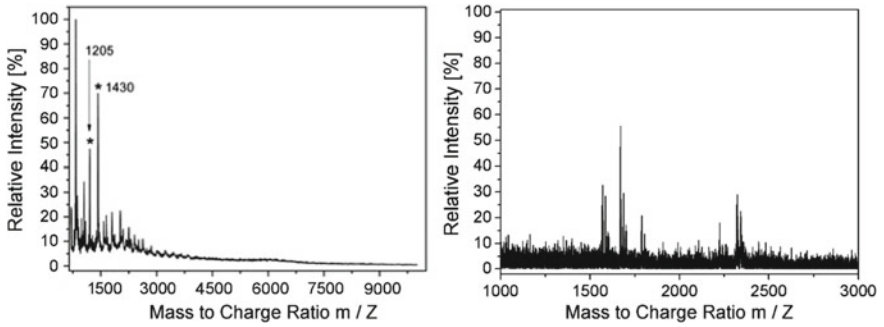

Fig. 12 Mass spectrum of Eu(III)-POSS (left) and a condensed oligomeric POSS (right) incorporated into a resin of sinapinic acid. Adapted from [65, 66] © 2014 and 2015 with permission of The Royal Society of Chemistry

3.4 MALDI-TOF Characterization

As a good guideline for the identification and characterization of POSS species, based on the molecular nature of these materials, the use of techniques allowing the determination of the molecular weight is relevantly employed. In particular, matrix-assisted laser desorption/ionization (MALDI) and electrospray injection (ESI) techniques have been applied on different POSS, with the goal of identifying the nature of the species, in order to evaluate the completion of a functionalization reaction or to assess or discard the presence of oligomers (i.e., dimeric species) or polymeric products given by the synthetic procedures.

For example, MALDI-TOF was employed to evaluate the nature of M-POSS with the main goal of assessing the coordination around the metal centre [65] (Fig. 12). In the specific case, the ionization of Eu(III)-POSS in a sinapinic acid matrix showed the presence of monomeric species containing Eu(III)-modified cage with an expanded coordination by solvent molecules (i.e., water, THF) and matrix fragment (as sinapinic acid).

Considering the ability of this technique to analyse high molecular weight species, it was employed to highlight the formation of oligomers obtained by thermal condensation of POSS monomers [66]. The presence of signals centred at 1600 and 2400 m/z resulted consistent with dimer and trimer structures, respectively (Fig. 12).

3.5 XPS Characterization

The use of X-ray photoelectron spectroscopy is sometimes reported in the characterization of POSS materials. More frequently, it has been employed in the determination of the surface distribution of POSS in polymer-based composites. Its application on POSS materials involves the basic features of this technique, allowing the identifica-

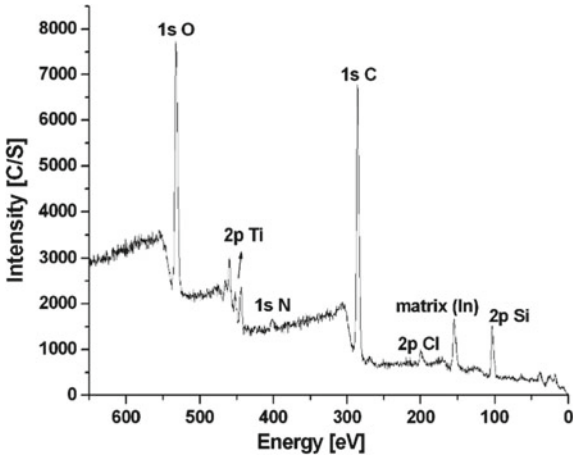

Fig. 13 XPS spectrum of bifunctional Ti–NH_2POSS. Reprinted from [31] © 2008 with the permission of The Royal Society of Chemistry

tion of almost all the elements in the periodic table. Hence, it has proved to be very useful for the determination of the composition of specific POSS products.

XPS emissions can provide quantitative information on light and heavy elements and can be profitably employed in the determination of multifunctional POSS. For instance, in Fig. 13, a bifunctional POSS based on the co-presence of an amino-functionalization on one corner and a Ti site was confirmed in its composition via this technique.

Furthermore, the fine structure of XPS signals allowed the study of the POSS interaction with surfaces (in particular H_8T_8 on gold) that showed a different chemical environment for 1 Si over 8, suggesting a vertex-based interaction of POSS with the surface [67].

3.6 SEC-GPC Characterization

POSS materials have a mass range that is composed of the cubic-cage (Si_8O_{12}) weight (41,672 u.m.a.) increasing depending on the type of the substituents. According to their solubility in organic solvents, their chemical compositional homogeneity and the possibility to form mixtures of isomers with different number of Si atoms, techniques as gel permeation chromatography (GPC), have been employed for the characterization and assessment of purity of POSS products.

3.7 TGA Characterization

The thermogravimetric behavior of POSS has been studied considering the peculiar features of these materials that resembles, for their composition, half-way between silicones $(R_2SiO)_n$ and silica SiO_2.

The thermal behavior of POSS is extremely different when heating is performed under inert or oxidative conditions, i.e., under nitrogen/argon or oxygen/air, respectively.

Under inert conditions, upon heating in temperature ramp up to 800 °C (10 °C/min), most of the close-cage POSS (R = methyl, isobutyl, isooctyl) are dominated by the occurrence of sublimation, in the temperature range between 160 and 350 °C and with a shift toward higher temperatures related to the increase of the chain length. Residues around 5–15 wt% reported, e.g., by Bolln et al. [68] are addressed as the formation of siloxane structures.

When degradation is carried on in air, higher residues, from 30 to 50%, are reported, with a higher weight loss for POSS with longer chains.

The thermal behavior of POSS has been detailed by coupling the information obtained by TGA and DSC with the use of GC–MS analyses, flash pyrolysis, and the analysis of the residues with FT-IR, FT-Raman, and XRPD [69, 70].

For isobutyl R_8T_8, the thermal heating under inert gas provides an almost negligible residue due to the main occurrence of evaporation upon melting, also confirmed by the investigation of the evaporation process using GC–MS and pyrolysis—GC–MS. The GC run of a solution of isobutyl R_8T_8 provides a single peak (confirming the purity of the sample), with a MS profile of the compound showing the gradual loss of 2-methylpropene caused by the ionization up to the formation of H_8T_8.

In comparison, pyrolysis–GC–MS at 600 and 800 °C highlights by-products after GC separation that suggests an increased release of organic species (i.e., ethane to condensed unsaturated molecules), favoring the conversion of the cage to silica.

The conversion to silica is evidenced by the thermal degradation under air, where a relevant residue is observed, whose amount depends on the heating rate. Low heating rates (such as 1 °C/min) produce a significantly high stable residue (46 wt% up to 800 °C), while high rates (viz. 100 °C/min) result in low residues as 20 wt%.

Isothermal experiments at 200, 300, and 500 °C show that lower temperatures promote a superficial transformation that retains further POSS species, while higher temperatures make the volatilization more relevant. The investigation of the residues using FT-IR, FT-Raman, and XRPD confirms the conversion of Si–R to Si–O bonds, operated by the peroxidation of the isobutyl fragment that can lead to residual Si–H fragments or to Si-centered radicals that can be the precursors of the siliceous residue.

A similar study was carried on systematically on H_8T_8 and R_8T_8 (R = methyl, isobutyl, and isooctyl). As expected, ramp heating in nitrogen up to 800 °C resulted mainly in evaporation, with the exception of H_8T_8, that gave an 18 wt% of residue for the occurrence of redistribution reactions leading to a silica fraction [71–75]. Upon heating in air, relevant amounts of residue (about 27 wt%) were found for isobutyl and isooctyl POSS, whereas lower amounts for H POSS (17 wt%) and negligible residue

for octamethyl POSS. This result is in agreement with the degradation mechanism due to oxygen presence, where primary carbons are poorly reactive. The behavior of octaphenyl POSS is significantly different; residues in nitrogen and air are 70 and 40%, respectively. This evidence, in the case of inert gas atmosphere, considering also the higher melting temperature of Ph-POSS, can be related to the entrapment of homogeneously distributed carbon derived from the phenyl degradation. In air, instead, the residual fraction corresponds to the quantitative conversion of POSS to silica as final product that can be quantitatively achieved also heating the carbon-containing residue produced by the degradation in inert conditions under air.

Again, on the thermal behavior of POSS, it is noteworthy to cite the study on open-cage systems. Mantz et al. [76] studied the degradation of $R_8Si_8O_{11}(OH)_2$ POSS (R = cyclohexyl) under inert gas. A two-step mechanism was found, with a preliminary homopolymerization of the macromers and a subsequent degradation of the organic fractions leading to a final inorganic silica residue.

On trisilanol systems, Zeng et al. [77] reported the formation of a viscous liquid under isothermal conditions (280 °C) in inert gas, with a full conversion to silica when heating or isothermal treatment is performed in air. Similarly, Marchesi et al. [66] reported the formation of a transparent gel-like product from the thermal heating at 170 °C of partially condensed isobutyl POSS under nitrogen for 2–6 h. The formation of oligomeric species consistent with dimeric and trimeric units was observed. The gel-like material proved to be stable upon heating up to 240 °C.

4 Conclusions

Since their discovery, on 1946, POSS has shown their potentiality to become a true field of research, as a series of issues are involved around their nature, preparation, characterization, and later application. In addition, several of their features have shown a growing interest in the main innovation trends in chemistry and material science.

For example, the assessment of the synthetic procedures has been part of the emerging interests on silicon chemistry and solgel processes, considered nowadays as one of the most promising processes for sustainable innovative materials.

The relevance of the hybrid features of POSS, filling actually the gap between organics and inorganics especially in the field of materials, was well perceived in the late 1980s at the University of California-Irvine by Dr. Joe Lichtenhan in challenging their mass production, promoting them in aerospace applications and with Dr. Joe Schwab in the 1990s delivering POSS technology out of the Air Force Research Laboratory founding a company on POSS, Hybrid Plastics, with manufacturing capacity reaching multiton scale [78].

With these achievings and their intrinsic nature of hybrid nanoscaled materials, POSS has gained a leading role in the twenty-first-century scientific challenge based on nanotechnology, affording a fully chemical bottom-up approachable to elegantly design and achieve multifunctional materials with chemical and structural homo-

geneity and features. The exploitation of their role has grown significantly thanks to the capability to scale up the synthetic procedures and to allow their use in applicative contexts, but much more with the development and widening of the crossing science regarding organic reactions on the R groups. With the mastering the all-round definition of the features of these extraordinary molecules, the wide scenario of functional POSS that can be produced by the use of organic functionalization protocols onto the inorganic cage has boosted once more the role of POSS as building blocks for designed materials built at nanoscale level.

References

1. Scott DW (1946) Thermal rearrangement of branched-chain methylpolysiloxanes. J Am Chem Soc 68:356
2. Barry J, Daudt WH, Domicone JJ, Gilkey JW (1955) Crystalline organosilsesquioxanes. J Am Chem Soc 77:4248
3. Feher FJ, Soulivong D, Lewis GT (1997) Facile framework cleavage reactions of a completely condensed silsesquioxane framework. J Am Chem Soc 119:11323
4. Feher FJ, Budzichowski TA, Blanski RL, Weller KJ, Ziller JW (1991) Facile syntheses of new incompletely condensed polyhedral oligosilsesquioxanes: [(c-$C_5H_9)_7Si_7O_9(OH)_3$], [(c-$C_7H_{13})_7Si_7O_9(OH)_3$], and [(c-$C_7H_{13})_6Si_6O_7(OH)_4$]. Organometallics 10:2526
5. Feher, FJ Soulivong D, Eklund AG (1998) Controlled cleavage of $R_8Si_8O_{12}$ frameworks: a revolutionary new method for manufacturing precursors to hybrid inorganic–organic materials. Chem Commun 13:399
6. Feher FJ, Terroba R, Ziller JW (1999) A new route to incompletely-condensed silsesquioxanes: base-mediated cleavage of polyhedral oligosilsesquioxanes. Chem Commun 22:2309
7. Voronkov MG, Lavrent'yev VI (1982) Top Curr Chem 102:199
8. Brown JF, Vogt LH (1965) The polycondensation of cyclohexylsilanetriol. J Am Chem Soc 87:4313
9. Sprung MM, Guenther FO (1955) The partial hydrolysis of methyltriethoxysilane. J Am Chem Soc 77:3990
10. Sprung MM, Guenther FO (1955) The partial hydrolysis of ethyltriethoxysilane. J Am Chem Soc 77:3996
11. Kudo T, Gordon MS (1998) Theoretical studies of the mechanism for the synthesis of silsesquioxanes. 1. Hydrolysis and initial condensation. J Am Chem Soc 120:11432
12. Kudo T, Gordon MS (2000) Theoretical studies of the mechanism for the synthesis of silsesquioxanes. 2. Cyclosiloxanes (D3 and D4). J Phys Chem A 104:4058
13. Jug K, Wichmann D (2000) MSINDO study of large silsesquioxanes. J Comp Chem 21:1549
14. Vogt LH, Brown JF (1963) Crystalline methylsilsesquioxanes. Inorg Chem 2:189
15. Frye CL, Collins WT (1970) Oligomeric silsesquioxanes, $(HSiO_{3/2})_n$. J Am Chem Soc 92:5586
16. Andrianov KA (1968) The methods of elementoorganic chemistry. Naura, Moscow, p 589
17. Pescarmona PP, van der Waal JC, Maxwell IE, Maschmeyer T (2001) A new, efficient route to titanium–silsesquioxane epoxidation catalysts developed by using high-speed experimentation techniques. Angew Chem Int Ed 40:740
18. Brinker C, Scherer G (2013) Sol-gel science—the physics and chemistry of sol-gel processing, 1st edn. Academic Press, Boston
19. Agasksar PA (1991) New synthetic route to the hydridospherosiloxanes Oh-$H_8Si_8O_{12}$ and D5h-$H_{10}Si_{10}O_{15}$. Inorg Chem 30:2707
20. Wiberg E, Simmler W (1956) Silanole. I. Stabilität und Kondensationsverhalten von Organosilandiolen. Z Anorg Allg Chem 283:401

21. Oisson K (1958) An Improved Method to Prepare Octa-(alkylsilse-squioxanes)(RSi)8O_{12}. Arkiv Kemi 13:367
22. Sprung MM, Guenther FO (1958) Copolymers of butadiene and unsaturated acids: crosslinking by metal oxides. J Polym Sci 28:17
23. Andrianov KA, Izmailor BA (1976) Hydrolytic polycondensation of higher alkyltrichlorosilanes in concentrated hydrochloric acid. Zh Obshch Khim 46:329
24. Brown F, Vogt LH, Prescott PI (1964) Preparation and characterization of the lower equilibrated phenylsilsesquioxanes. J Am Chem Soc 86:1120
25. Olsson K, Gronwall C (1961) On octa-(arylsilsesquioxanes),($ArSi)_8O_{12}$. 1. phenyl, 4-tolyl, and 1-naphthyl compounds. Arkiv Kemi 17:529
26. Feher FJ, Newman DA, Walzer JF (1989) Silsesquioxanes as models for silica surfaces. J Am Chem Soc 111:1741
27. Feher FJ (1986) Polyhedral oligometallasilsesquioxanes (POMSS) as models for silica-supported transition-metal catalysts. J Am Chem Soc 108:3850
28. Feher FJ (1989) Polyhedral aluminosilsesquioxanes: soluble organic analogs of aluminosilicates. J Am Chem Soc 111:7288
29. Gieβmann S, Fischer A, Edelmann FT (1982) Silyl-functionalized silsesquioxanes: new building blocks for larger Si–O-assemblies, including the first Si–Si-bonded silsesquioxanes. Z Anorg Allg Chem 2004:630
30. Feher FJ, Walzer JF (1991) Synthesis and characterization of vanadium-containing silsesquioxanes. Inorg Chem 30:1689; Field LD, Lindall CM, Maschmeyer T, Masters AF (1994) The synthesis and characterization of decaphenyltitanocene dichloride, [$Ti(\eta^5$-$C_5Ph_5)_2Cl_2$], and of [$Ti(\eta^5$-$C_5Ph_5)((c$-$C_6H_{11})_7Si_7O_{12})$], the first pentaphenylcyclopentadienyl polyhedral oligosilsesquioxane. Aust J Chem 47:1127
31. Carniato F, Boccaleri E, Marchese L (2008) A versatile route to bifunctionalized silsesquioxane (POSS): synthesis and characterisation of Ti-containing aminopropylisobutyl-POSS. Dalton Trans 1:36
32. Olivero F, Renò F, Carniato F, Rizzi M, Cannas M, Marchese L (2012) A novel luminescent bifunctional POSS as a molecular platform for biomedical applications. Dalton Trans 41:7467
33. Cordes BD, Lickiss PD, Rataboul F (2010) Recent developments in the chemistry of cubic polyhedral oligosilsesquioxanes. Chem Rev 110:2081
34. Meguro S, Yamahiro M, Watanabe K (2007) Chem Abstr 146:184612; Jpn Kokai Tokkyo Koho JP 2007015977, 2007
35. Fu BX, Lee A, Haddad TS (2004) Styrene−butadiene−styrene triblock copolymers modified with polyhedral oligomeric silsesquioxanes. Macromolecules 37:5211
36. Pan G, Mark JE, Schaefer DW (2003) Synthesis and characterization of fillers of controlled structure based on polyhedral oligomeric silsesquioxane cages and their use in reinforcing siloxane elastomers. J Polym Sci Part B: Polym Phys 41:3314
37. Haseba Y (2004) Chem Abstr 140:261477; Jpn Kokai Tokkyo Koho JP 2004083757, 2004
38. Goto R, Shimojima A, Kuge H, Kuroda K (2008) A hybrid mesoporous material with uniform distribution of carboxy groups assembled from a cubic siloxane-based precursor. Chem Commun 46:6152
39. Shimojima A, Goto R, Atsumi N, Kuroda K (2008) Self-assembly of alkyl-substituted cubic siloxane cages into ordered hybrid materials. Chem Eur J 14:8500
40. Galema SA (1997) Microwave chemistry. Chem Soc Rev 26:233
41. Iwamura T, Adachi K, Chujo Y (2010) Simple and rapid eco-friendly synthesis of cubic octamethylsilsesquioxane using microwave irradiation. Chem Lett 39:354
42. Penso I, Cechinatto EA, Machado G, Luvison C, Wanke CH, Bianchi O, Soares MRF (2015) Preparation and characterization of polyhedral oligomeric silsesquioxane (POSS) using domestic microwave oven. J Non-Cryst Solids 428:82
43. Janowski B, Pielichowski K (2008) Microwave-assisted synthesis of cyclopentyltrisilanol (c-$C_5H_9)_7Si_7O_9(OH)_3$. J Organomet Chem 693:905
44. Marciniec B, Dutkiewicz M, Maciejewski H, Kubicki M (2008) New, effective method of synthesis and structural characterization of octakis(3-chloropropyl)octasilsesquioxane. Organometallics 27:793–794

45. Kolb HC, Finn MG, Sharpless KB (2001) Click chemistry: diverse chemical function from a few good reactions. Angew Chem Int Ed 40(11):2004
46. Li Y, Dong X, Zou Y, Wang Z, Yue K, Huang M, Liu H, Feng X, Lin Z, Zhang W, Zhang W, Cheng SZD (2017) Polyhedral oligomeric silsesquioxane meets "click" chemistry: rational design and facile preparation of functional hybrid materials. Polymer 125:303
47. Xue L, Li L, Feng S, Liu H (2015) A facile route to multifunctional cage silsesquioxanes via the photochemical thiol–ene reaction. J Organomet Chem 783:49
48. Hoyle CE, Bowman CN (2010) Thiol-ene click chemistry. Angew Chem Int Ed 49:1540
49. Lowe AB (2010) Thiol-ene "click" reactions and recent applications in polymer and materials synthesis. Polym Chem 1:17
50. Dondoni A (2008) The emergence of thiol-ene coupling as a click process for materials and bioorganic chemistry. Angew Chem Int Ed 47:8995
51. Gao YJ, Eguchi A, Kakehi K, Lee YC (2004) Efficient preparation of glycoclusters from silsesquioxanes. Org Lett 6:3457
52. Rozga-Wijas K, Chojnowski J (2012) Synthesis of new polyfunctional cage oligosilsesquioxanes and cyclic siloxanes by thiol-ene addition. J Inorg Organomet Polym 22:588
53. Xu JW, Li X, Cho CM, Toh CL, Shen L, Mya KY, Lu XH, He CB (2009) Polyhedral oligomeric silsesquioxanes tethered with perfluoroalkylthioether corner groups: facile synthesis and enhancement of hydrophobicity of their polymer blends. J Mater Chem 19:4740
54. Li LG, Xue L, Feng SY, Liu HZ (2013) Functionalization of monovinyl substituted octasilsesquioxane via photochemical thiol-ene reaction. Inorg Chim Acta 407:269
55. Wu Y, Li LG, Feng SY, Liu HZ (2013) Hybrid nanocomposites based on novolac resin and octa(phenethyl) polyhedral oligomeric silsesquioxanes (POSS): miscibility, specific interactions and thermomechanical properties. Polym Bull 70:3261
56. Li Y, Su H, Feng X, Wang Z, Guo K, Wesdemiotis C, Fu Q, Cheng SZD, Zhang W (2014) Thiol-Michael "click" chemistry: another efficient tool for head functionalization of giant surfactants. Polym Chem 5:6151
57. Kaźmierczak J, Kuciński K, Hreczycho G (2017) Highly efficient catalytic route for the synthesis of functionalized silsesquioxanes. Inorg Chem 56(15):9337
58. Schäfer S, Kickelbick G (2017) Simple and high yield access to octafunctional azido, amine and urea group bearing cubic spherosilicates. Dalton Trans 46(1):221
59. Tsukada S, Sekiguchi Y, Takai S, Abe Y, Gunji T (2015) Preparation of POSS derivatives by the dehydrogenative condensation of T_8H with alcohols. J Ceram Soc Jpn 123(1441):739
60. Carniato F, Boccaleri E, Marchese L, Fina A, Tabuani D, Camino G (2007) Synthesis and characterisation of metal Isobutylsilsesquioxanes and their role as inorganic–organic nanoadditives for enhancing polymer thermal stability. Eur J Inorg Chem 4:585
61. Li Q, Zhou Y, Hang X, Deng S, Huang F, Du L, Li Z (2008) Synthesis and characterization of a novel arylacetylene oligomer containing POSS units in main chains. Eur Polym J 44:2538
62. Desmartin Chomel A, Dempsey P, Latournerie J, Hourlier-Bahloul D, Jayasooriya UA (2005) Gel to glass transformation of methyltriethoxysilane: a silicon oxycarbide glass precursor investigated using vibrational spectroscopy. Chem Mater 17:4468
63. Baney RH, Itoh M, Sakakibara A, Suzuki T (1995) Silsesquioxanes. Chem Rev 95:1409
64. Croce G, Carniato F, Milanesio M, Boccaleri E, Paul G, van Beek W, Marchese L (2009) Understanding the physico-chemical properties of polyhedral oligomeric silsesquioxanes: a variable temperature multidisciplinary study. Phys Chem Chem Phys 11:10087
65. Marchesi S, Carniato F, Boccaleri E (2014) Synthesis and characterisation of a novel Europium(III)-containing heptaisobutyl-POSS. New J Chem 38:2480
66. Marchesi S, Carniato F, Palin L, Boccaleri E (2015) POSS as building-blocks for the preparation of polysilsesquioxanes through an innovative synthetic approach. Dalton Trans 44:2042
67. Owens TM, Nicholson KT, Fosnacht DR, Orr BG, Banaszak Holl MM (2006) Formation of mixed monolayers of silsesquioxanes and alkylsilanes on gold. Langmuir 22:9619
68. Bolln C, Tsuchida A, Frey H, Mulhaupt R (1997) Thermal properties of the homologous series of 8-fold alkyl-substituted octasilsesquioxanes. Chem Mater 9:1475

69. Fina A, Tabuani D, Carniato F, Frache A, Boccaleri E, Camino G (2006) Polyhedral oligomeric silsesquioxanes (POSS) thermal degradation. Thermochim Acta 440:36
70. Fina A, Tabuani D, Frache A, Boccaleri E, Camino G (2005) In: Le Bras M, Wilkie C, Bourbigot S (eds) Fire retardancy of polymers: new applications of mineral fillers. Royal Society of Chemistry, Cambridge, UK, pp 202–220
71. Calzaferri G, Hoffmann R (1991) The symmetrical octasilasesquioxanes $X_8Si_8O_{12}$: electronic structure and reactivity. J Chem Soc Dalton Trans S:917
72. Loboda MJ, Toksey GA (1998) Understanding hydrogen silsesquioxane-based dielectric film processing. Solid State Technol 41:99
73. Liou HC, Pretzer J (1998) Effect of curing temperature on the mechanical properties of hydrogen silsesquioxane thin films. Thin Film Solids 335:186
74. Siew YW, Sarkar G, Hu X, Hui J, See A, Chua CT (2000) Thermal curing of hydrogen silsesquioxane. J Electrocem Soc 147:335
75. Yang CC, Chen WC (2002) The structures and properties of hydrogen silsesquioxane (HSQ) films produced by thermal curing. J Mater Chem 12(4):1138
76. Mantz RA, Jones PF, Chaffee KP, Lichtenhan JD, Gilman JW, Ismail IMK, Burmeister MJ (1996) Thermolysis of polyhedral oligomeric silsesquioxane (POSS) macromers and POSS−siloxane copolymers. Chem. Mater 8:1250
77. Zeng J, Bennett C, Jarrett WL, Iyer S, Kumar S, Mathias LJ, Schiraldi DA (2005) Structural changes in trisilanol POSS during nanocomposite melt processing. Compos Interfaces 11:673
78. Hybrid plastics website: https://hybridplastics.com

Design and Synthesis of Hybrid Materials with POSS

Ayesha Kausar

Abstract This chapter describes essential aspects related to design and fabrication of organic–inorganic hybrid structure based on polymeric materials and polyhedral oligomeric silsesquioxane (POSS). POSS is a class of organosilicic three-dimensional compounds with cage or non-cage framework. The POSS nanoparticle possesses size of few nm and has monodisperse and rigid structure. The POSS nanoparticle also has unique capability to reinforce numerous polymers (polyamide, epoxy, polyurethane, poly(vinyl chloride), poly(ethylene glycol), etc.). Various strategies have been adopted for the incorporation of POSS into polymer matrices via chemical cross-linking or physical blending. The design and structure of final hybrids have been found to influence by POSS surface functional groups and POSS content. Owing to POSS nanometer size and exceptional features, the hybrid materials own superior structural and functional properties such as mechanical strength, thermal stability, optical properties, low toxicity, and biocompatibility. The state of POSS-containing polymer hybrids with respect to current challenges and future prospects has also been described. The focus of this article is to present an account of fundamental understanding of structure, functional properties, synthesis, and design challenges of POSS-containing polymer hybrids.

Keywords POSS · Polymer · Hybrid · Synthesis · Cross-linking

1 Preface

Polyhedral oligomeric silsesquioxane (POSS) is nanostructure having general formula $(RSiO_{3/2})_n$ [1]. R in the formula may be a hydrogen atom or an organic functional group (alkyl, acrylate, hydroxyl, or epoxide). POSS is also referred to as silica nanoparticle constituting silica cage core and organic functional groups attached to

A. Kausar (✉)
School of Natural Sciences, National University of Sciences and Technology (NUST), H-12 Islamabad, Pakistan
e-mail: dr.ayeshakausar@yahoo.com

S. Kalia and K. Pielichowski (eds.), *Polymer/POSS Nanocomposites and Hybrid Materials*, Springer Series on Polymer and Composite Materials,
https://doi.org/10.1007/978-3-030-02327-0_2

cage corners. In other words, POSS is a hybrid inorganic/organic structure. POSS consists of both organic and inorganic elements, i.e., an inner core of inorganic silicon and outer core of oxygen and other organic constituents. POSS is also known as one of the smallest nano-sized inorganic particles. The nano-size, structure, and functionalization of POSS lead to essential physical properties such as thermal stability, mechanical properties, dielectric features, and optical properties [2, 3]. POSS nanoparticle imparts functional properties, structural stability, and processability to polymer/POSS hybrids. In addition, inclusion of POSS in polymers as nanofiller may cause superior thermal stability, and electrical, thermomechanical, permeability, and nonflammability properties [4–6]. POSS nanoparticle with outer layer of organic functional group has been found to compatible with polymers. The unique combination of organic (polymer) and inorganic phases (POSS) may bring about enhanced hybrid performance [7, 8]. The characteristics and performance of polymer/POSS depend on the successful incorporation of POSS particles in polymers. Using suitable technique, POSS has been reinforced in polymers through physical blending as well as chemical cross-linking. Usually POSS is physically mixed with POSS via melt mixing [9]. However, the chemical cross-linking can be induced through in situ method, solution technique with ligand or linker induced interaction between polymer and POSS. Aggregation of POSS nanoparticle may result through physical modes. Surface functionalization of nanoparticle and polymer can be achieved by chemical routes, which may consequence covalently linked polymer/POSS hybrids [10]. In this chapter, initially essential features and structure of POSS have been conversed. Main objective was to highpoint the preparation and design strategies used so far for polymer/POSS hybrid. Comprehensive research on these hybrids may lead to wide range of academic and commercial significance. Future prospects and related challenges have also been stated.

2 Polyhedral Oligomeric Silsesquioxane (POSS)

POSS is an important category of organosilicic three-dimensional compounds having caged or non-caged framework of silica core and organic functional group attached to the corners. Consequently, POSS consists of both inorganic and organic substituents. Inorganic silicon form inner core, while organic constituents form outer layer. Structure of POSS may range from molecular silica to multifunctional POSS molecules [11]. On POSS surface, when all the organic groups are non-reactive form molecular silica. POSS is known as monofunctional or MonoPOSS, when one organic group is reactive. If there are more than two functional groups on the surface, POSS is referred to as multifunctional or MultiPOSS. The variation in organic groups attached to the surface and type of cage structure may form different derivatives of silsesquioxane or POSS molecules. POSS can be often classified as caged or non-caged structures [12]. These categories have range of varied POSS structures (Fig. 1). However, cage-like POSS molecules have gained more research interest [13]. The T8 cubic inorganic core made up of silicon–oxygen ($R_8Si_8O_{12}$) and Q8 structure ($R_8Si_8O_{20}$) have gained

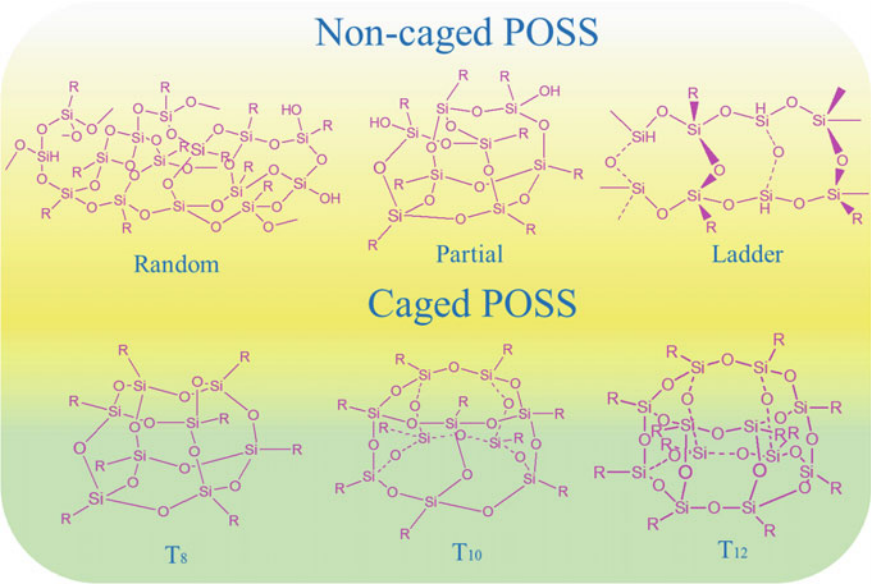

Fig. 1 POSS classified into caged and non-caged silesquioxane structure

noteworthy importance. The 'T' and 'Q' are used for silicon atoms bonded to three or four oxygen atoms, respectively [14]. The organic groups attached to the surface are also called vertex groups. POSS is a silsesquioxane molecule, which may yield oligomeric organosilsesquioxane through chemical reaction.

A simple example is the preparation of octakis[(3-glycidoxypropyl) dimethylsiloxy]-octasilsesquioxane [15]. It has been prepared by using tetramethylammonium hydroxide, dimethylchlorsilane methanol, tetraethoxysilane, and allyl glycidyl ether. Initially, octakis(dimethylsiloxy)octasilsesquioxane was synthesized and then octakis(dimethylsiloxy, 3-glycidoxypropyl)octasilsesquioxane was obtained using suitable functional molecules (Fig. 2). POSS is nonvolatile, odorless, and environmentally friendly compound. Apex group functionalization has been used to attain high-performance cage nanoparticle. In polymers, POSS reinforcement may cause improved thermal and mechanical properties [16]. Accordingly, POSS may also improve the flame retardance of the matrix polymers [17]. POSS dispersion in polymers may cause several beneficial effects to the polymers such as enhance mechanical strength, modulus, nonflammability, and rigidity [18]. The main obstruction to the design and synthesis of polymer/POSS materials is the aggregation of POSS nanoparticle. It is an important challenge encountered during the large-scale production of polymer/POSS hybrids. Development and use of suitable technique to prepare and disperse POSS nanoparticle in polymer matrix along with the development of optimum chemical bonding and interface interaction must be the research focus for high-performance polymer/POSS hybrids. POSS nanostructures have shown promise in catalyst supports, scaffolds for drug delivery, and imaging.

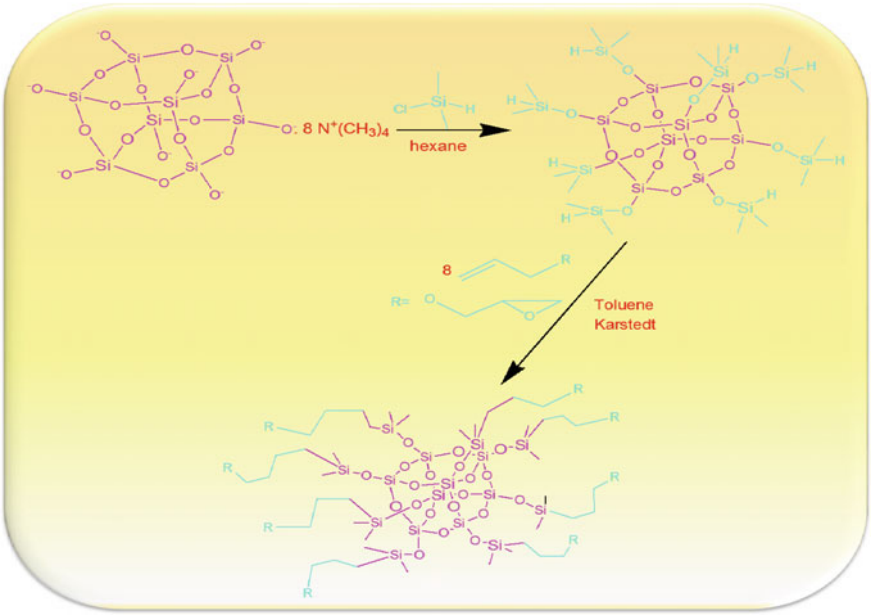

Fig. 2 Synthesis of octakis(dimethylsiloxy)octasilsesquioxane and octakis(dimethylsiloxy, 3-glycidoxypropyl) octasilsesquioxane

3 Polymer/POSS Hybrid Nanomaterial

Hybrid material is basically a composite consisting of two or more different constituents. Usually, the constituents in hybrid materials have physical interactions between them. However, according to some definitions, hybrid materials may consist of two or more components linked together by covalent bonds. When one of the constituents in hybrid material is at nanometer level, it is known as hybrid nanomaterial or nanohybrid. Hybrid material usually consists of inorganic and organic components. Mixing of nanolevel phases may lead to a homogeneous mixture with characteristics different than the original phases. In the case of polymer/POSS hybrids, factors such as POSS content, POSS functionalization, polymer/POSS interaction, and mode of cross-linking influence the final hybrid structure [19]. For the functionalization of POSS compounds, three approaches have been generally adopted including (i) corner-capping reactions of POSS compounds; (ii) addition/substitution reactions of edge groups; and (iii) condensation reaction of functional organosilanes [16]. Capping reaction may involve the introduction of monomer, e.g., methylacrylate to POSS molecule using trichlorosilane as a capping agent. Similarly, other functional groups such as styryl monomer may be introduced on POSS surface via corner-capping reactions using coupling agents. The condensation reaction of functional organosilanes and hydrolytic removal of silicon atom from POSS molecule may produce variety of

condensed POSS molecules. The functionalization of POSS compounds promotes their dispersion and compatibility with the polymer matrix. Amalgamation of POSS with polymer causes several enhanced characteristics in hybrid structure depending on nanofiller dispersion, content, and morphological contour. The functionalization of POSS molecules may allow controlled chemical reaction between the functional nanofiller and polymer matrix. The affinity between polymer chains and POSS has been estimated using theoretical calculations, spectral, and morphology analysis. POSS loading has led to improvement in range of functional properties of hybrids compared with the neat polymer. POSS and functional POSS nanofillers have not only been introduced in homopolymers, but also incorporated in block copolymer matrices. The behavior of POSS reinforcement in block copolymers is, however, different than that of homopolymer/POSS hybrids. POSS-containing block copolymer hybrids have been fabricated using living polymerization, bulk polymerization, free radical reaction, and other advanced polymerization approaches. In the case of block copolymers, reinforcement of nanofiller may cause self-assembly phenomenon in the hybrid materials. POSS nanofiller has been used for the self-assembly studies in bulk phases or blocks, where periodically well-organized nanostructures were produced. Development of ordered nanostructure relies on the block copolymer/POSS interaction parameters, volume fraction between the blocks, polydispersity, degree of polymerization of copolymers, etc. Hence, in the presence of POSS nanofiller, block copolymers can develop in situ interactions and may self-assemble to form nanostructures in bulk. Improved physical properties of polymer/POSS materials are desirable characteristics for several technical applications. Moreover, structure–property relationship in polymer/POSS systems has been investigated to define and modify the design and solicitation of these materials. Polymers such as poly(ethylene glycol), polystyrene, poly(vinyl chloride) (PVC), polyamide, epoxy, poly(methyl methacrylate) (PMMA) has been grafted with functional POSS compounds (Fig. 3). Polymer/POSS hybrid has been found with enhanced thermal stability and glass transition compared with neat polymers [20]. Surface functionalization and interfacial interactions have caused superior dielectric and mechanical properties relative to pristine polymers. Inert nature and biocompatibility of POSS have also led to significant biomedical applications [21].

4 Interaction in Polymer/POSS

Polyhedral oligomeric silsesquioxane forms an interesting class of organosilicon compounds with tri-dimensional cage structure. Studies on polymer/POSS materials have shown hybrid inorganic–organic nature, which conglomerates the properties of organic polymers and ceramics [22]. The silicon–oxygen framework possesses high degree of flexibility, and tunable solubility, and reactivity [23]. These properties can be functionalized using organic substituents on POSS. Wide range of functional groups may include alkyl, phenyl, vinyl, alcohol, carboxylic acid, sulfonic acid, epoxide, halide, imide, acrylate, methacrylate, thiols, silane, silanol, etc.

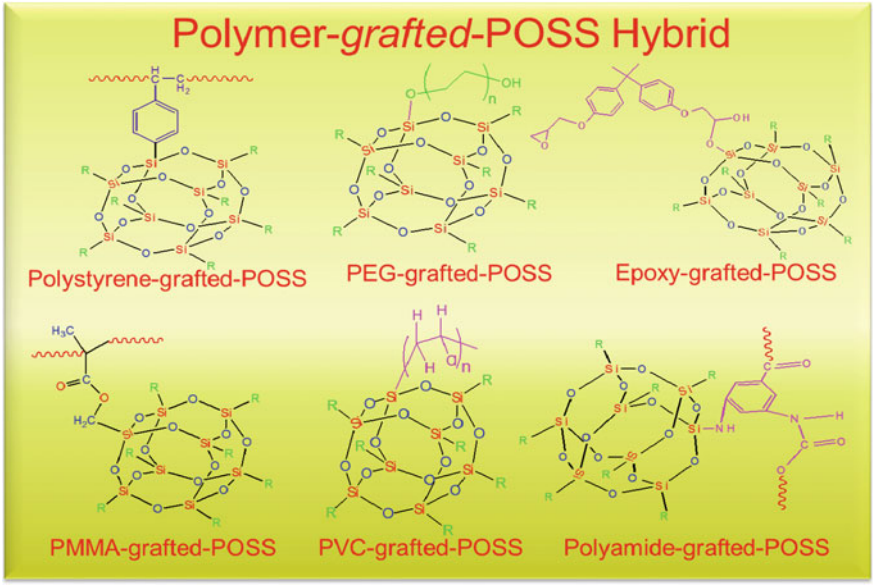

Fig. 3 POSS grafted with different polymers

[24–26]. The chemical nature of matrix can be tailored using desired vertex group. The compatibility of polymer/POSS hybrids strongly relies on the polarity match of polymer and POSS molecules [27]. In this regard, reactive vertex groups can be preferred to attain chemical bonding between polymer chain and POSS [28]. The improved processability, thermal stability, nonflammability, and oxidative resistance of materials are austerely correlated with the physical/chemical interaction between the matrix/POSS molecules [29]. The non-covalent interactions such as π–π and hydrogen bonding has been detected. For example, silanol-based POSS molecules may condense with hydroxyl-containing matrix form hydrogen bonding in hybrid [30]. POSS may also form unwavering covalent bonds with the polymer matrix. Furthermore, the structure of inorganic cage and organic vertex group of POSS also affect the reinforcement effects in polymer/POSS hybrids. Type of vertex group and interfacial interaction are also crucial to determine the filler dispersion and morphology of hybrid properties. These hybrids have been prepared using various processing techniques. During melt blending (one of the important method), POSS molecules act as plasticizer and affect the final material characteristics. Here, strong interaction between matrix/nanofiller may illustrate anti-plasticizing effect. The incorporation of POSS may lead to high viscosity values and improved rigidity. The glass transition temperature of hybrids has also been found to influence by POSS type, content, and physical/chemical interaction between matrix/nanofiller. Similarly, these factors also affect the mechanical, thermal, rheological, and other important physical properties of polymer/POSS hybrids.

Self-assembly phenomenon has received considerable interest in the field of block copolymers and hybrids. Self-assembly has been found to develop well-organized nanostructure or nano-pattern. Both the covalent and non-covalent interactions (hydrogen bonding, electrostatic interactions, van der Waals forces, etc.) have found to be involved in the self-assembly of copolymers and hybrids [31]. Wide range of self-assembled nano-organized architectures has been designed with varying morphologies and characteristics. Commonly observed self-assembled morphologies involve cylinders, spheres, rods, lamellae, gyroid, and range of other forms. The periodicities generated during hybrid synthesis depend on processing technique, polymer type, nanofiller, content, temperature, pH, solvent, etc. Initially, self-assembly was supposed to be originated from the phase and morphology differences between the different types of polymer blocks. Later, with the development of nanomaterials, self-assembly was found to be spontaneously initiated using nanoparticles. Self-assembly studies have revealed that the inorganic constituents such as POSS may act as initiator to instigated ordered structures in organic molecules. Consequently, the self-assembly behavior of polymer/POSS hybrids has been investigated in thin films, bulk, and solution form. The self-assembled morphology of POSS-containing polymeric hybrids was outstandingly different than that of conventional amphiphilic polymers. Such type of organic–inorganic architectures may have potential for promising applications such as micro and nanoelectronics, optics, medicine, etc.

5 Design and Fabrication Strategies for Polymer/POSS Hybrid

A variety of POSS nanostructures have been prepared containing reactive functionalities for grafting, surface bonding, and polymerization with other materials [32, 33]. POSS nanoparticle has been incorporated in polymers via simple blending, copolymerization, grafting, or other covalent linking approaches [34]. POSS reinforcement in polymers may lead to affective developments in physical properties. Generally, POSS has been found to enhance the mechanical properties, thermal and oxidation resistance, and nonflammability of polymers. POSS has been reacted with wide range of thermoplastic and a few thermoset systems. Addition of POSS in polymers has not caused dramatic changes in processing parameters; however, conditions need to be optimized for better dispersion of nanoparticle in matrix. For better dispersion, POSS is usually solubilized in monomer and incorporated in polymer or copolymer mixture. In this way, POSS may form better binding with the polymer, and less POSS aggregation and phase separation have been observed [35]. Variety of polymers (polyamide, poly(methyl methacrylate), polyurethane, poly(vinyl chloride), biodegradable polymers, etc.) have been reinforced with POSS. Physical methods, chemical interaction, and chemical copolymerization have been used for polymer/POSS interaction. For chemical interlinking, POSS has been functionalized with various reactive groups. A seg-

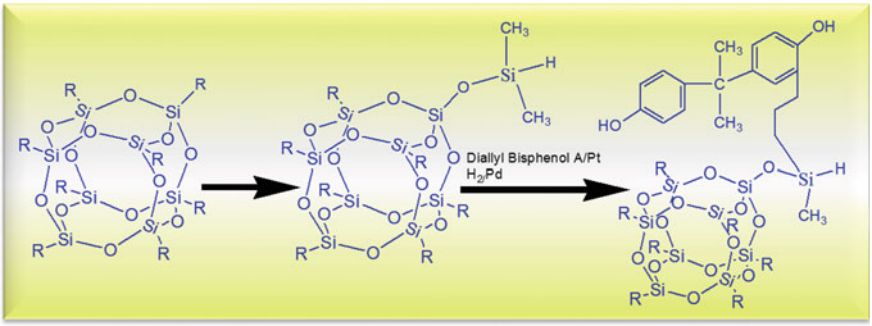

Fig. 4 Route to octacyclohexyl-POSS, with R = cyclohexyl, hydrido-POSS, and BPA-POSS

mented polyurethane has been developed using 4,4'-methylenebis(phenylisocyanate) (MDI) hard segment, polytetramethylene glycol (PTMG) soft segment, and 1,4-butanediol (BD) chain extender [36, 37]. The polyurethane has been reinforced with POSS [38, 39]. The polyurethane system containing POSS cage-like molecules pendent to polymer chain has been reported [40]. The copolymer forms random sequence of PTMG soft segments and MDI hard segment. The polymer was chain-extended by using 1-[3-(propylbisphenolA)propyldimethylsiloxy]-3,5,7,9,11,13,15 heptacyclohexylpenta-cyclo [9.5.1.13,9.15,15.17,13] octa-siloxane (BPA-POSS) (Fig. 4). In this way, POSS was chemically inserted in the hybrid design via molecular reinforcement in hard segment. Incorporation of POSS in epoxy polymer led to enhanced mechanical strength, permeability, high glass transition temperature (T_g), and nonflammability [41, 42]. A series of epoxy/POSS hybrids have been prepared containing 0–15 wt% nanofiller content [43]. Mechanical blending method was used for the purpose. POSS nanoparticle was amine functionalized to form POSS-NH_2 and 4,4′-diaminodiphenyl sulfone (DDS) used as curing agent (Fig. 5). The molten mixture was poured in a mold preheated at 120 °C. The amount of DDS was considered according to the number of epoxy groups. Epoxy/POSS hybrids have also been designed by reaction of octaepoxy-silsesquioxane (OECh) with an epoxy-amine system [44]. The OECh was used to replace diglycidyl ether of bisphenol A (DGEBA) with an aromatic diamine 4,4'-(1,3-phenylenediisopropylidene) bisaniline (BSA).

Environmental-friendly or biodegradable polymers such as polyethylene glycol (PEG) have also been processed with POSS for automotive, packaging, electronics, and textile industry [45, 46]. Aminopropylisobutylpolyhedral oligomeric silsesquioxane was melt compounded with poly(lactic acid) (PLA) and poly(ethylene glycol) (PEG) to form plasticized hybrids [47]. The modified POSS was found to reduce the melt viscosity of the hybrids, so act as lubricating agent. The nanofiller also influenced the thermal properties of hybrids. Correspondingly, poly(lactic acid) and poly(ethyleneglycol)-functionalized polyhedraloligomericsilses-Quioxane (PEG-POSS) hybrids were designed using melt blending [48]. The radiation-induced cross-linking behavior of neat PLA and PLA/PEG-POSS hybrids were explored. The

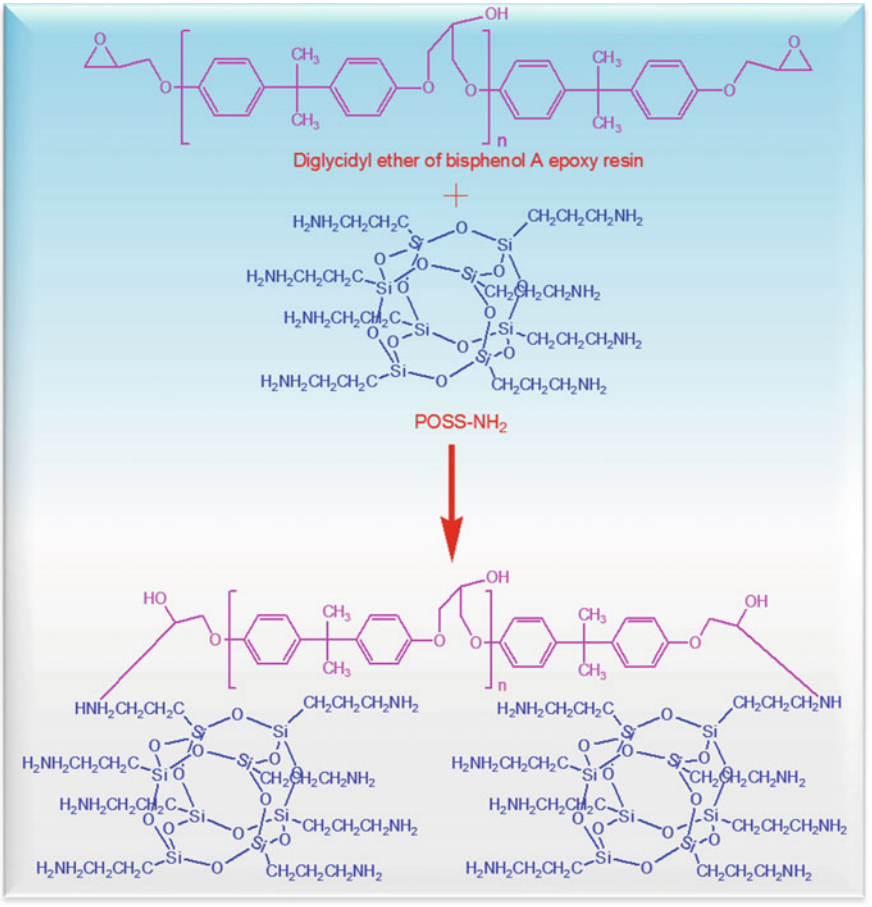

Fig. 5 Chemical reaction of octa(aminopropyl)silsesquioxane (POSS-NH_2) and diglycidyl ether of bisphenol A epoxy resin

cross-linking occurred by electron beam irradiation even at low absorbed dose. The cross-linking degree was increased extraordinarily with an increase in the absorbed dose to 20 kGy. POSS has also been grafted with different types of polyamide. Aliphatic polyamide/POSS hybrids have been reported [49]. Polyamide-6/POSS hybrid has been prepared through the polymerization of ε-caprolactam in the presence of ε-caprolactam-functionalized POSS [50].

POSS tethered aromatic polyamide hybrids have been prepared using Michael addition between maleimide-containing polyamide and amino-functionalized POSS (Fig. 6) [51]. Polyamide/POSS hybrid membrane has shown high water flux, salt rejection, and membrane properties compared with pure PA membranes [52–54]. The polyvinyl chloride (PVC) was reinforced with methacryl-POSS and dioctyl phthalate (DOP) in matrix through melt blending process [55]. The PVC and POSS hybrid was

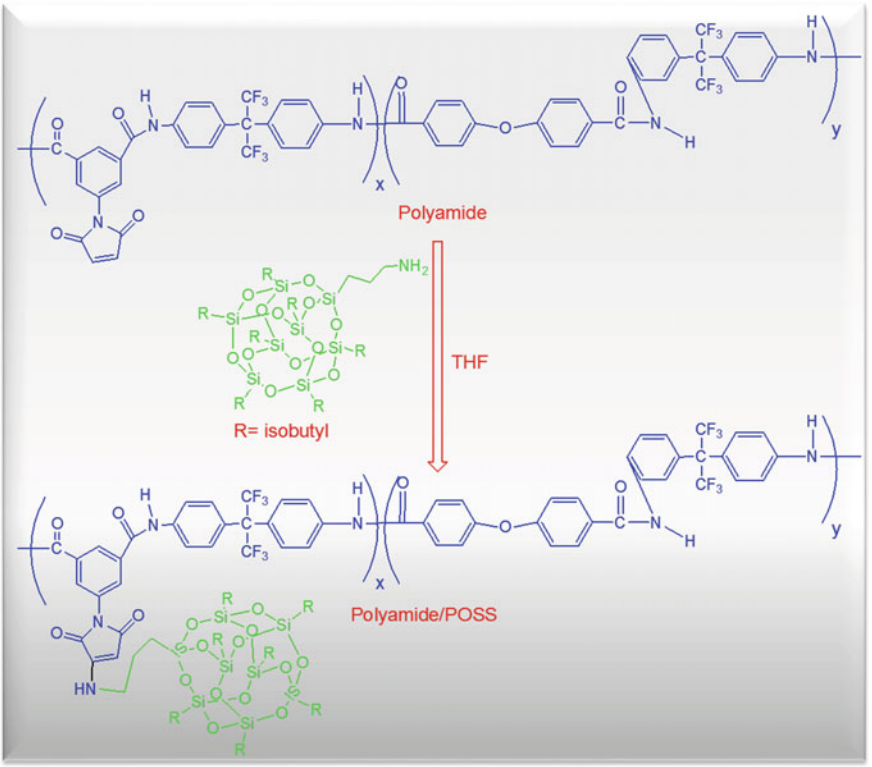

Fig. 6 Preparation of polyamide-tethered POSS hybrid

found transparent with fine dispersion up to 15 wt% loading. However, methacryl-POSS formed submicron-sized aggregates above 15 wt%. Addition of DOP also improved the miscibility of methacryl-POSS in PVC matrix [56]. Polystyrene (PS) and polypropylene (PP) were also used to design PS/POSS and PP/POSS hybrids [57, 58]. Dimeric and oligomeric Al- and Zn-containing isobutyl POSS were reinforced into PP matrix via melt blending [59]. The degradation pathways for POSS derivates were found to involve evaporation and oxidation. Metal-containing POSS resulted in improved thermal stability of hybrids. Poly(methyl methacrylate) (PMMA)/POSS hybrids have been prepared by bulk polymerization [60]. The thermal and flame stabilities of hybrids were evaluated using thermogravimetric analysis (TGA) and cone calorimetry. The number of attempts to design various combinations of polymers and POSS or functional POSS compounds involves melt blending, mechanical mixing, as well as chemical interaction routes. The nanoparticle dispersion, mechanical, thermal, flammability, rheological, cross-linking, and other physical characteristics have been measured and compared to approach an ultimate high-performance polymer/POSS motif.

Few important and conventional types of polymerization techniques need to be mentioned here for the fabrication of polymer/POSS hybrids such as atom transfer radical polymerization (ATRP), ring-opening metathesis polymerization (ROMP), reversible addition–fragmentation chain transfer polymerization (RAFT), and click chemistry. These techniques have shown their significance, particularly in the formation of self-assembled polymers and block copolymers hybrids with functional POSS molecules. As mentioned in the preceding section that the incorporation of nanoparticles may initiate periodicity in copolymers, therefore, the design of self-assembled polymer/POSS hybrids is essential to deliberate. ATRP has been used to develop an important class of self-organized star-shaped POSS-containing hybrids [61]. Polymerization of methylmethacrylate (MMA) monomer using octabromide POSS as initiator may yield the star-shaped hybrids. Monomer as well as initiator concentrations were kept low for ideal conversion of monomers to a ordered poly(methyl methacrylate) (PMMA)/POSS hybrid. Moreover, the star-shaped POSS-containing PMMA had narrow molecular weight distribution. ROMP has also been used as an effective technique to form self-assembled hybrids. Using ROMP, POSS-containing hybrid diblock copolymer of 2-endo-3-exo-5-norbornene-2,3-dicaboxylic acid trimethyl ester has been produced. The norbornene monomer has also been converted to a well-defined self-assembled polymer with POSS via ROMP [62]. In this technique, the norbornene ethyl POSS monomer was processed using Ru-based catalyst. RAFT polymerization has also yielded self-assembled star-shaped hybrids [63]. Here, azido-terminated PMMA was produced and attached to octa-alkyne-POSS core to form a well-organized structure. In this method, octa-alkyne-POSS acted as RAFT agent. It was important to control the molar ratio of MMA/RAFT agent to control the polymerization degree and morphology of final hybrid. Another successful approach to form self-assembled polymer/POSS hybrids is click chemistry. It is a rather simple way to conjugate polymer blocks and POSS together [64]. Copper-catalyzed Huis-gen 1,3-dipolar cycloaddition catalyst has been commonly used in this technique. Click chemistry has also been combined with the RAFT, ATRP, or ROMP polymerization techniques to form new self-assembled polymeric architectures using advanced method [65]. Click reaction between polymer chain and POSS molecules may form hemi-telechelic POSS-containing hybrids [66].

6 Structure–Property Relationship in Polymer/POSS Hybrid System

To acquire full knowledge of this field, it is essential to investigate and understand the structure–property relationship in the designed polymer/POSS hybrid systems. Effect of structural parameters on final properties of polymer/POSS hybrids with functional nanoparticles has been studied using different techniques [27]. Hoy's method, solubility parameters, and morphology analysis have been used to explore

the affinity between polymer and POSS sample. Investigations revealed that the POSS nanoparticles acted as plasticizer for the polymer chains. Thus, POSS functionality, dispersion, and content have been found responsible for better compatibility between the matrix and nanofiller. Slight differences in the morphology and solubility parameter of POSS and matrix may cause aggregation of nanofiller in matrix. Furthermore, type of processing technique may significantly influence the interaction between the matrix and POSS functional groups. Incorporation of inorganic appropriate amount of POSS framework and suitable polymerization technique may also form self-assembled network in hybrids. Incorporation of different POSS content, POSS functionality, polymer type, processing technique and parameters, may lead to pronounced effects on the properties of resulting hybrids. Very high POSS loadings may increase the system rigidity by enhancing the glass transition temperature, crystallinity, and damping factor of the nanocomposite system. Structure–property relationship of such polymer/POSS systems can be investigated using rheological measurements and solubility parameters. High nanofiller loading beyond optimum concentration may deteriorate the mechanical and tribological properties of the hybrids, while the thermal stability of the system may increase. On the other hand, fine dispersion of POSS molecules in matrix may decrease friction between organic macromolecules and POSS, reduce entanglement density of polymer chains, and so increase the free volume. Thus, glass transition temperature and crystallinity of the system may decrease. Consequently, POSS molecules act as plasticizers for organic matrices. However, the plasticization efficiency depends on the type of interaction between polymer and hybrids, and nature and length of pendent organic group attached with POSS [67]. POSS with closed-cage structure and short organic pendent groups are more prone to aggregation, while long pendent functionalities and open-cage structure may offer increased free volume in the hybrid. Besides, multifunctional POSS may also possess good miscibility with the organic matrix and disperse well. Influence of the structure of organic substituent of POSS on hybrid properties has been investigated using range of techniques such as scanning electron microscopy, transmission electron microscopy, atomic force microscopy, wide-angle X-ray diffraction, etc. [68].

7 Challenges and Future Scenarios

Polymer/POSS hybrid materials have gained noteworthy curiosity owing to nanoscopic structure and advance functional properties compared with conventional hybrid materials. POSS compounds own true hybrid inorganic–organic architecture having inner inorganic framework of silicone and oxygen. The inner inorganic core is covered by organic substituents and polar functional groups. The surface groups can be nonreactive or reactive depending upon the desired design of polymer/POSS. POSS is actually smallest possible particles of silica. Incorporation of POSS nanoparticle in thermoplastic/thermoset polymeric matrices by physical or chemical cross-linking has provided an excellent route to high-performance hybrids.

POSS reinforcement has impacted the mechanical, thermal, glass transition, as well as biomedical properties of final materials. POSS surface functionalization has also performed crucial role in governing hybrid characteristics. Modification of POSS has also considerably improved its dispersion in polymer matrix. Constant dispersal of POSS nanoparticle in matrices caused improvement in physical properties. Alternatively, non-functional POSS have not been found compatible with matrix, so cannot be dispersed uniformly. Moreover, meager dispersion may result in microphase separated systems, which may not offer appropriate reinforcement [69, 70]. Usually, POSS units chemically bound with polymer do not cause phase separation. Consequently, functional POSS possesses significant recompenses over other current filler technologies. The POSS content also plays imperative role in determining thermal, mechanical, and other structural properties of POSS-containing hybrids. The materials may exhibit superior physical properties depending on the amount of POSS present in the matrix. Optimum nanofiller loading level needs to be identified to attain better results. Though polymer/POSS hybrids possess outstanding physical properties, large-scale production of these materials for potential commercial applications is limited due to high cost [71]. Despite significant upgrading in design and functional characteristics of polymer/POSS hybrids, still there are number of challenges that need to be addressed. However, substantial advancement has been made in controlling POSS interaction and distribution with polymers, well-defined structure–property relationships need to be defined. Interaction in polymer/POSS and modified polymer/POSS hybrids require more research and knowledge for the contribution of both the components.

Research on polymer/POSS hybrids is getting huge attention. These hybrids are still under research and require more attention to explore on large industrial scale. Fabrication and preparation of polymer/POSS hybrids are versatile and economical technology, though there are certain problems in processing of these materials. Solution processing of these hybrids requires the use of less hazardous organic solvents. In this regard, several studies have employed melt mixing method; however, POSS aggregation and agglomeration are major problems in this case. In situ polymerization have been adopted using suitable surfactants and initiators to better compatiblize polymer with POSS. The properties of polymer/POSS also depend on the POSS content. Nevertheless, above optimum POSS concentration, self-interaction between POSS cages cause aggregation. The appropriate design and processing conditions are definitely needed to attain fine dispersion of POSS in matrix, even at higher concentration. The design of modified POSS with desired functionalities may develop strong optimum interaction with matrix to enhance the overall miscibility. In this way, new high-performance functional material can be developed for industrial applications such as aerospace and automotive materials, electronics, energy devices, coatings, desalination membranes, adsorbents, packaging materials, etc. The polymer/POSS hybrids have developed several superior features such as mechanical strength, thermal stability, optical properties, low toxicity, and biocompatibility. The research so far has mentioned few significant applications of polymer/POSS hybrids in textiles, fire-retarding materials, gas transport membranes, and biomedical. Though, improvement in rheological, mechanical, and thermal properties must be focused for

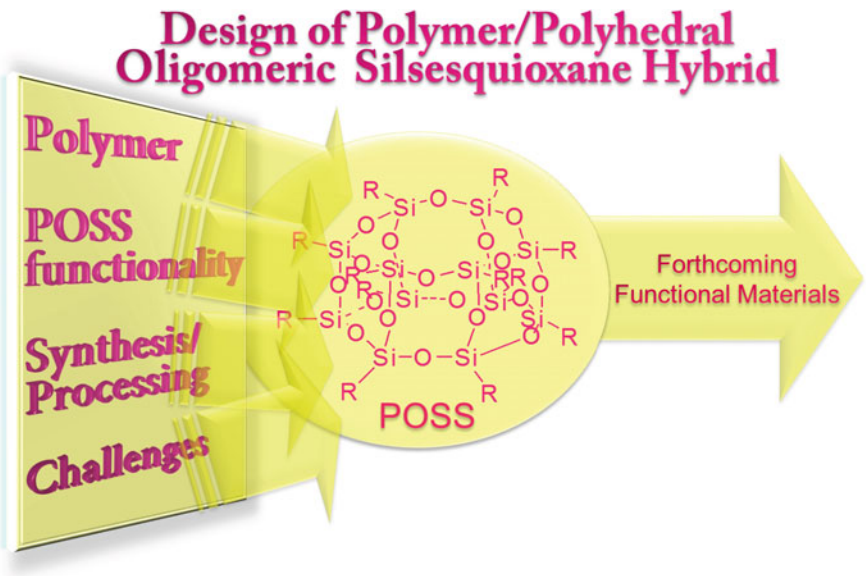

Fig. 7 Prospects of polymer/POSS hybrids

extensive future use in these and new areas. In the future, a suitable redirection is needed to study the processing of various polymers with modified POSS compounds for tailoring the desired high-performance characteristics (Fig. 7).

8 Summary

This chapter summarizes significant and versatile research on polymer/POSS hybrid materials. POSS nanoparticle has been amalgamated in thermoplastic as well as thermoset polymer matrices using solution method, in situ procedure, melt mixing, physical blending method, and other techniques. Final design of polymer/POSS hybrid depends on the mode of reinforcement using physical integration, chemical cross-linking, and covalent bonding. The miscibility and intermolecular interaction of organic–inorganic interpenetrating network of polymer/POSS have played essential role in determining the material characteristics. Surface functionalization of POSS has been employed to improve its compatibility with polymer matrices. Successful dispersion of POSS in polymer matrices depends on surface interaction such as polar interaction, van der Waals forces, hydrogen bonding, etc. in matrix nanofiller. These interactions may control POSS dispersion in polymeric matrices. Though, sometimes inter-particle interactions may result in the aggregation of particles. However, performance of hybrid materials has been enhanced by using different functional vertex groups, still there are several desired features need to be achieved.

Research on specific functionalization of POSS and its mode of integration in matrix is, consequently, indispensable to design high-performance hybrids. Nevertheless, standard models are definitely essential to attain unique designs of polymer/POSS hybrids, i.e., needed for research and industrial community. Established knowledge of structure–property relationship in these hybrids needs to be to develop. Functional properties and interaction of polymer/POSS necessitate profound studies related to optimum design and processing conditions. One can imagine future nanostructured polymer/POSS materials of great variety and designs being industrialized. Coupling of functional polymers with POSS chemistry may be utilized to build regular three-dimensional repeating structures and networks of polymer/POSS having nanophases. These hybrid materials have found relevance in miscellaneous areas such as aerospace, textile, devices, and biomedical appliances. Although, noteworthy developments have been reported for these hybrids, yet there are several design challenges needed to be addressed in these technical fields.

References

1. Kausar A (2017) State-of-the-art overview on polymer/POSS nanocomposite. Polym-Plast Technol Eng 1–20
2. Cordes DB, Lickiss PD, Rataboul F (2010) Recent developments in the chemistry of cubic polyhedral oligosilsesquioxanes. Chem Rev 110:2081–2173
3. Waddon AJ, Coughlin EB (2003) Crystal structure of polyhedral oligomeric silsequioxane (POSS) nano-materials: a study by X-ray diffraction and electron microscopy. Chem Mater 15:4555–4561
4. Devaraju S, Vengatesan MR, Selvi M, Kumar AA, Alagar M (2012) Synthesis and characterization of bisphenol-A ether diamine-based polyimide POSS nanocomposites for low K dielectric and flame-retardant applications. High Perform Polym DOI:0954008311433606
5. Dalwani M, Zheng J, Hempenius M, Raaijmakers MJ, Doherty CM, Hill AJ, Wessling M, Benes NE (2012) Ultra-thin hybrid polyhedral silsesquioxane–polyamide films with potentially unlimited 2D dimensions. J Mater Chem 22:14835–14838
6. Tian B, Gao J, Wang C, Huo L (2015) Synthesis of methylacryloypropyl-POSS/poly (fluorine-acrylate) core-shell nanocomposites and effect on thermal properties of materials. Polym-Plast Technol Eng 54:771–778
7. Li S, Simon GP, Matisons JG (2010) The effect of incorporation of POSS units on polymer blend compatibility. J Appl Polym Sci 115:1153–1159
8. Roy R, Komarneni S, Roy DM (1984) Multi-Phasic ceamic composites made by sol- gel technique. Mater Res Soc Symp Pro 32:347–359
9. McNally T, Murphy WR, Lew CY, Turner RJ, Brennan GP (2003) Polyamide-12 layered silicate nanocomposites by melt blending. Polymer 44:2761–2772
10. Lichtenhan JD, Otonari YA, Carr MJ (1995) Linear hybrid polymer building blocks: methacrylate-functionalized polyhedral oligomeric silsesquioxane monomers and polymers. Macromolecules 28:8435–8437
11. Kuo SW, Chang FC (2011) POSS related polymer nanocomposites. Prog Polym Sci 36:1649–1696
12. Cordes DB, Lickiss PD, Rataboul F (2010) Recent developments in the chemistry of cubic polyhedral oligosilsesquioxanes. Chem Rev 110:2081–2173
13. Zhou H, Ye Q, Xu J (2017) Polyhedral oligomeric silsesquioxane-based hybrid materials and their applications. Mater Chem Front https://doi.org/10.1039/c6qm00062b

14. Barry AJ (1946) Viscometric investigation of dimethylsiloxane polymers. J Appl Phys 17:1020–1024
15. Jeziorska R, Świerz-Motysia BARBARA, Szadkowska A, Marciniec B, Maciejewski H, Dutkiewicz MICHAŁ, Leszczyńska IRENA (2011) Effect of POSS on morphology, thermal and mechanical properties of polyamide 6. Polimery 56:809–816
16. Lim S-K, Hong E-P, Choi HJ, Chin IJ (2010) Polyhedral oligomeric silsesquioxane and polyethylene nanocomposites and their physical characteristics. J Indus Eng Chem 16:189–192
17. Mantz RA, Jones PF, Chaffee KP, Lichtenhan JD, Gilman JW, Ismail IMK, Burmeister MJ (1996) Thermolysis of polyhedral oligomeric silsesquioxane (poss) macromers and posssiloxane copolymers. Chem Mater 8:1250–1259
18. Zhou Z, Cui L, Zhang Y, Zhang Y, Yin N (2008) Preparation and properties of POSS grafted polypropylene by reactive blending. Eur Polym J 44:3057–3066
19. Wang X, Xuan S, Song L, Yang H, Lu H, Hu Y (2011) Synergistic effect of POSS on mechanical properties, flammability, and thermal degradation of intumescent flame retardant polylactide composites. J Macromol Sci B 51:255–268
20. Wang W, Guo Y-L, Otaigbe JU (2009) The synthesis, characterization and biocompatibility of poly(ester urethane)/polyhedral oligomeric silesquioxane nanocomposites. Polymer 50:5749–5757
21. Guo Y-L, Wang W, Otaigbe JU (2010) Biocompatibility of synthetic poly(ester urethane)/polyhedral oligomeric silsesquioxane matrices with embryonic stem cell proliferation and differentiation. J Tissue Eng Regener Med 4:553–564
22. Wu J, Haddad TS, Mather PT (2009) Vertex group effects in entangled polystyrenepolyhedral oligosilsesquioxane (POSS) copolymers. Macromolecules 42:1142–1152
23. Gnanasekaran D, Madhavpan K, Reddy RSR (2009) Developments of polyhedral oligomeric silsesquioxanes (POSS), POSS nanocomposites and their applications: a review. J Sci Ind Res 68:437–464
24. Dintcheva NTz, Morici E, Arrigo R, La Mantia FP, Malatesta V, Schwab JJ (2012) UV-stabilisation of polystyrene-based nanocomposites provided by polyhedral oligomeric silsesquioxanes (POSS). Polym Degrad Stab 97:2313–2322
25. Markovic E, Matisons J, Hussain M, Simon GP (2007) Poly(ethylene glycol) octafunctionalized polyhedral oligomeric silsesquioxane: WAXD and rheological studies. Macromolecules 40:4530–4534
26. Zhao H, Shu J, Chen Q, Zhang S (2012) Quantitative structural characterization of POSS and octavinyl-POSS nanocomposites by solid state NMR. Solid State Nucl Mag 43:56–61
27. Dintcheva NTZ, Morici E, Arrigo R, La Mantia FP, Malatesta V, Schwab JJ (2012) Structure-properties relationships of polyhedral oligomeric silsesquioxane (POSS) filled PS nanocomposites. Express Polym Lett 6:561–571
28. Lu CH, Wang JH, Chang FC, Kuo SW (2010) Star block copolymers through nitroxide-mediated radical polymerization from polyhedral oligomeric silsesquioxane (POSS) Core. Macromol Chem Phys 211:1339–1347
29. Iyer S, Schiraldi DA (2007) Role of specific interactions and solubility in the reinforcement of bisphenol A polymers with polyhedral oligomeric silsesquioxanes. Macromolecules 40:4942–4952
30. Liu H, Kondo S, Tanaka R, Oku H, Unno M (2008) A spectroscopic investigation of incompletely condensed polyhedral oligomeric silsesquioxanes (POSS-mono-ol, POSS-diol and POSS-triol): Hydrogen-bonded interaction and host–guest complex. J Organomet Chem 693:1301–1308
31. Zhang W, Müller AH (2013) Architecture, self-assembly and properties of well-defined hybrid polymers based on polyhedral oligomeric silsequioxane (POSS). Prog Polym Sci 38:1121–1162
32. Lichtenhan JD, Schwab JJ, Reinerth WA (2001) Nanostructured chemicals: a new era in chemical technology. Chem Innovat 31:3–5
33. Ellsworth MW, Gin DL (1999) Recent advances in the design and synthesis of polymer-inorganic nanocomposites. Polym News 24:331–340

34. Feher FJ, Weller KJ (1991) Synthesis and characterization of labile spherosilicates:[$(Me_3SnO)8Si_8O_{12}$] and [$(Me_4SbO)\ 8Si_8O_{12}$]. Inorg Chem 30:880–882
35. Haddad TS, Stapleton R, Jeon HG, Mather PT, Lichtenhan JD, Phillips S (1999) Nanostructured hybrid organic/inorganic materials. Silsesquioxane modified plastics. In Abstracts Of Papers Of The American Chemical Society. vol 217. pp U608-U608
36. Koberstein JT, Galambos AF, Leung LM (1992) Compression-molded polyurethane block copolymers. 1. Microdomain Morphol Thermomechanical Prop Macromol 25:6195–6204
37. Lattimer RP, Polce MJ, Wesdemiotis C (1998) MALDI-MS analysis of pyrolysis products from a segmented polyurethane. J Anal Appl Pyrol 48:1–15
38. Lewicki JP, Pielichowski K, De La Croix PT, Janowski B, Todd D, Liggat JJ (2010) Thermal degradation studies of polyurethane/POSS nanohybrid elastomers. Polym Degrad Stab 95:1099–1105
39. Devaux E, Rochery M, Bourbigot S (2002) Polyurethane/clay and polyurethane/POSS nanocomposites as flame retarded coating for polyester and cotton fabrics. Fire Mater 26:149–154
40. Fu BX, Hsiao BS, Pagola S, Stephens P, White H, Rafailovich M, Sokolov J, Mather PT, Jeon HG, Phillips S, Lichtenhan J (2001) Structural development during deformation of polyurethane containing polyhedral oligomeric silsesquioxanes (POSS) molecules. Polymer 42:599–611
41. Lee A, Lichtenhan JD (1998) Viscoelastic responses of polyhedral oligosilsesquioxane reinforced epoxy systems. Macromolecules 31:4970–4974
42. Mather PT, Jeon HG, Romo-Uribe A, Haddad TS, Lichtenhan JD (1999) Mechanical relaxation and microstructure of poly(norbornyl-poss) copolymers. Macromolecules 32:1194–2203
43. Zhang Z, Gu A, Liang G, Ren P, Xie J, Wang X (2007) Thermo-oxygen degradation mechanisms of POSS/epoxy nanocomposites. Polym Degrad Stab 92:1986–1993
44. Ramírez C, Rico M, Torres A, Barral L, López J, Montero B (2008) Epoxy/POSS organic–inorganic hybrids: ATR-FTIR and DSC studies. Eur Polym J 44:3035–3045
45. Iles A, Martin AN (2013) Expanding bioplastics production: sustainable business innovation in the chemical industry. J Cleaner Prod 45:38–49
46. Wu J, Ge Q, Mather PT (2010) PEG-POSS multiblock polyurethanes: synthesis, characterization, and hydrogel formation. Macromolecules 43:7637–7649
47. Turan D, Sirin H, Ozkoc G (2011) Effects of POSS particles on the mechanical, thermal, and morphological properties of PLA and plasticised PLA. J Appl Polym Sci 121:1067–1075
48. Jung CH, Hwang IT, Jung CH, Choi JH (2014) Preparation of flexible PLA/PEG-POSS nanocomposites by melt blending and radiation crosslinking. Radiat Phys Chem 102:23–28
49. Iyer S, Schiraldi D (2005) Synthesis and properties of copolymers of polyesters and polyamides with polyhedral oligomeric silsesquioxanes (POSS); comparison with blended materials. PMSE Prepr 92:326–327
50. Ricco L, Russo S, Monticelli O, Bordo A, Bellucci F (2005) ε-Caprolactam polymerization in presence of polyhedral oligomeric silsesquioxanes (POSS). Polymer 46:6810–6819
51. Liu YL, Lee HC (2006) Preparation and properties of polyhedral oligosilsequioxane tethered aromatic polyamide nanocomposites through Michael addition between maleimide-containing polyamides and an amino-functionalized polyhedral oligosilsequioxane. J Polym Sci Part A Polym Chem 44:4632–4643
52. Zhao F, Bao X, McLauchlin AR, Gu J, Wan C, Kandasubramanian B (2010) Effect of POSS on morphology and mechanical properties of polyamide 12/montmorillonite nanocomposites. Appl Clay Sci 47:249–256
53. Moon JH, Katha AR, Pandian S, Kolake SM, Han S (2014) Polyamide–POSS hybrid membranes for seawater desalination: effect of POSS inclusion on membrane properties. J Membr Sci 461:89–95
54. Pacheco F, Sougrat R, Reinhard M, Leckie JO, Pinnau I (2016) 3D visualization of the internal nanostructure of polyamide thin films in RO membranes. J Membr Sci 501:33–44
55. Soong SY, Cohen RE, Boyce MC, Mulliken AD (2006) Rate-dependent deformation behavior of POSS-filled and plasticized poly (vinyl chloride). Macromolecules 39:2900–2908

56. Soong SY, Cohen RE, Boyce MC (2007) Polyhedral oligomeric silsesquioxane as a novel plasticizer for poly (vinyl chloride). Polymer 48:1410–1418
57. Zheng L, Kasi RM, Farris RJ, Coughlin EB (2007) Synthesis and thermal properties of hybrid copolymers of syndiotactic poystyrene and polyhedral oligomeric silsesquioxane. J Polym Sci Part A Polym Chem 40:885
58. Rios-Dominguez H, Ruiz-Trevino FA, Contreras-Reyes R, Gonzalez-Montiel A (2006) Syntheses and evaluation of gas transport properties in polystyrene–POSS membranes. J Mater Sci 271:94–100
59. Fina A, Abbenhuis HCL, Tabuani D, Frache A, Camino G (2006) Polypropylene metal functionalised POSS nanocomposites: a study by thermogravimetric analysis. Polym Degrad Stab 91:1064–1070
60. Jash P, Wilkie CA (2005) Effects of surfactants on the thermal and fire properties of poly (methyl methacrylate)/clay nanocomposites. Polym Degrad Stab 88:401–406
61. Costa RO, Vasconcelos WL, Tamaki R, Laine RM (2001) Organic/inorganic nanocomposite star polymers via atom transfer radical polymerization of methyl methacrylate using octafunctional silsesquioxane cores. Macromolecules 34:5398–5407
62. Xu W, Chung C, Kwon Y (2007) Synthesis of novel block copolymerscontaining polyhedral oligomeric silsesquioxane (POSS) pendentgroups via ring-opening metathesis polymerization (ROMP). Polymer 48:6286–6293
63. Ye YS, Shen WC, Tseng CY, Rick J, Huang YJ, Chang FC, Hwang BJ (2011) Versatile grafting approaches to star-shaped POSS-containing hybrid polymers using RAFT polymerization and click chemistry. Chem Communicat 47:10656–10658
64. Moses JE, Moorhouse AD (2007) The growing applications of click chemistry. Chem Soc Rev 36:1249–1262
65. Agard NJ, Prescher JA, Bertozzi CR (2004) A strain-promoted 3 + 2azide-alkyne cycloaddition for covalent modification of blo-molecules in living systems. J Am Chem Soc 126:15046–15047
66. Zhang WA, Muller AHE (2010) Synthesis of tadpole-shaped PUSS-containing hybrid polymers via “click chemistry”. Polymer 51:2133–2139
67. Zhang Y, Lee S, Yoonessi M, Liang K, Pittman CU (2006) Phenolic resin–trisilanolphenyl polyhedral oligomeric silsesquioxane (POSS) hybrid nanocomposites: structure and properties. Polymer 47:2984–2996
68. Bizet S, Galy J, Gérard JF (2006) Structure-property relationships in organic − inorganic nanomaterials based on methacryl − POSS and dimethacrylate networks. Macromolecules 39:2574–2583
69. Chhabra P, Choudhary V (2010) Polymer nanocomposite membranes based on sulfonated poly(ether ether ketone) and trisilanol phenyl POSS for fuel cell applications. J Appl Polym Sci 118:3013–3023
70. Raftopoulos KN, Pielichowski K (2016) Segmental dynamics in hybrid polymer/POSS nanomaterials. Prog Polym Sci 52:136–187
71. DeArmitt C (2010) Polyherdral Oligomeric Silesquioxane Handbook. In: Phanom plastics. POSS and Hybrid Plastics are registered trademarks of Hybrid Plastics Inc., USA

Self-assembly of POSS-Containing Materials

Anna Kowalewska

Abstract Polyhedral oligomeric silsesquioxanes (POSS) are unique nanoscale compounds that play a very important role in nanotechnology and materials science. The three-dimensional hybrid molecular clusters can form a range of well-defined supramolecular structures, owing to their intrinsic ability for aggregation. The organization of POSS in the solid state provides a non-covalent "crystalline template" approach. Understanding the mechanisms behind the cooperative interactions in POSS-based materials allows for the tailored performance of the building blocks and is essential for the development of novel hierarchical hybrid materials. Numerous reports have been published on various aspects of POSS chemistry and technology. This chapter presents an overview of selected contributions to the field of POSS-based nanostructured materials and the phenomena operating at the nanolevel in the truly beautiful world of the self-assembling polyhedra.

Keywords Polyhedral silsesquioxanes · Self-assembly · Crystal packing Interface · Templating · Surfactants · MOF · Liquid crystals · Optoelectronics Advanced materials · Biomaterials

1 Introduction

Polyhedral oligomeric silsesquioxanes (POSS) are structurally well-defined, three-dimensional hybrid molecular clusters with a rigid inorganic nanocore surrounded by organic groups that can be modified to achieve the desired physicochemical properties. The term *silsesquioxane* describes their characteristic stoichiometry, where each silicon atom (*sil-*) is bonded to one-and-a-half oxygen (*-sesquiox-*) and to a hydrocarbon moiety (*-ane*). Octasilsesquioxane ($R_8Si_8O_{12}$, T_8) is POSS molecule, with quasi-spherical geometry of the siloxane core (Scheme 1). Species with spherosilox-

A. Kowalewska (✉)
Centre of Molecular and Macromolecular Studies, Polish Academy of Sciences, Sienkiewicza 112, 90-363 Łódź, Poland
e-mail: anko@cbmm.lodz.pl

S. Kalia and K. Pielichowski (eds.), *Polymer/POSS Nanocomposites and Hybrid Materials*, Springer Series on Polymer and Composite Materials,
https://doi.org/10.1007/978-3-030-02327-0_3

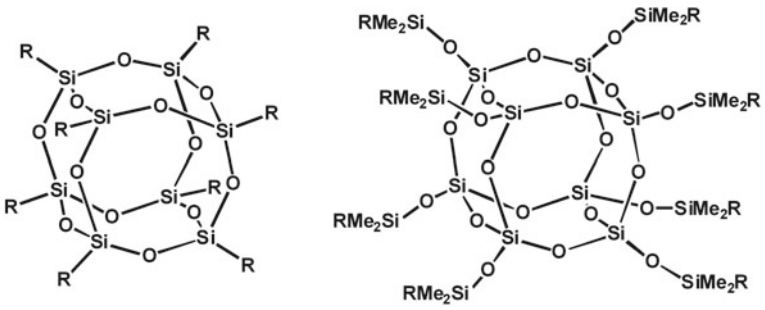

Scheme 1 Molecular structure of octahedral silsesquioxanes T_8R_8 and dimethylsiloxyspherosiloxanes Q_8MR_8

ane cage $(SiO_{4/2})_8$ surrounded by functionalized dimethylsiloxy groups ($OSiMe_2R$) (Q_8MR_8) also belong to the family of POSS compounds.

Over the last two decades, POSS have received an exceptional attention in macromolecular science and nanoengineering as building blocks for the synthesis of various organic–inorganic hybrids. Apart from their high symmetry and nanosize of the chemically robust framework, POSS are non-toxic and biocompatible. POSS show also excellent thermal characteristics [1], ultralow dielectric constant [2] and extraordinary oxygen plasma etching resistance [3, 4]. Well-defined structural features and tailor-made physicochemical properties make POSS ideal nanofillers for polymer composites [5, 6]. They can be blended into polymer matrices, grafted as side chains or acting as cross-linking sites. Their incorporation improves physicochemical properties of the material and its processing (glass transition temperature, thermal stability, mechanical performance) [7–13]. POSS can also influence the crystalline morphology of polymers facilitating or hindering the crystallization process [14, 15]. Polyhedral silsesquioxanes have been also used for the synthesis of more advanced materials such as light-driven artificial enzymes [16], biomaterials for tissue engineering [17], biocomposites [18], optical sensors [19] or scaffolds for controllable 3D π-conjugated luminophores [20].

Hierarchical structures are present in a range of POSS-based advanced materials, including amphiphilic macromolecules, nanoparticles and liquid crystals [21–24]. The structure of POSS and most POSS-derived shape amphiphiles is accurate without polydispersity. As a result, hierarchical nanoassemblies can be obtained with sharp interfaces between different domains and low defect density. It makes POSS ideal elemental building blocks for the preparation of diverse inorganic–organic hybrid materials by the bottom-up approach. Self-assembly is one of the methods most frequently used to obtain ordered structures. Non-covalent interactions such as intermolecular hydrogen bonding, π–π stacking and hydrophobic interactions are typically used as driving forces in the construction process. Understanding the phenomena directing the molecular packing of POSS is crucial for the effective design and control of hierarchical structures as well as physicochemical properties of POSS-based hybrid materials.

2 POSS Crystal Packing and Hierarchical Structures in the Solid State

The ability of POSS for self-assembling and formation of well-defined superstructures in solid state should be reviewed in the context of their morphology. Silsesquioxanes can be easily functionalized, and the respective synthetic methods for their preparation have been recently reviewed [25–31]. The nature of the organic periphery affects the molecular packing of POSS as well as their characteristic mesomorphic behaviour [32, 33]. The highest symmetry arrangement for octahedral silsesquioxanes with functional groups in each octant of Cartesian space would be the one with side substituents pointing away from the vertices of the core. In fact, the preferred way of organization and packing morphology of POSS molecules depend on several factors. The most important one is the type, size and structure of the organic substituents [34]. The way of side group distribution around the silsesquioxane core, closest distances and contacts between arms in the same molecular cage as well as other neighbouring cages can play a significant role in self-assembled systems. Monofunctional POSS (T_8R_8) bearing the same organic groups at each of silicon atoms and multifunctional (bifunctional or heterofunctional) POSS ($T_8R_{8-x}R'_x$) with more than one type of organic substituents can form completely different supramolecular assemblies.

2.1 Monofunctional POSS

A range of crystal-packing types and polymorphic forms have been described for silsesquioxanes bearing the same type of organic groups at each of silicon atoms. Majority of solid T_8R_8 crystallize in the triclinic space group *P*-1; nevertheless, monoclinic, tetragonal and rhombohedral structures have been also reported. X-ray diffraction studies revealed that T_8R_8 with relatively small alkyl or aryl substituents have molecular symmetry close to octahedral (O*h*), and their packing patterns are governed by the inorganic core [35–39]. Such species can be treated as spheres that are arranged hexagonally in the crystal structure in ABCA sequence [38, 40–42]. In such a pattern, molecules in one layer lie above the interstitial spaces in adjacent layers. The tiniest POSS molecules of T_8H_8 pack most closely in the trigonal *R*-3 ($^2C_{3i}$) crystal lattice [43, 44]. Organic substituents at silicon atoms prevent such close packing. Characteristic diffraction peaks in a single-crystal X-ray spectrum of an octahedral silsesquioxane appear at 2θ values corresponding to overall dimension of the molecules, body diagonal of the silsesquioxane cage [(1–11) plane, ~5.4 Å] and the distance between its opposite faces [(300) plane, ~3.1 Å] [25, 45]. The diffraction patterns of T_8R_8 with R = Me, Ph, vinyl or allyl suggest that the average value of the length of Si–O bonds in silsesquioxane cages is independent of the nature of the organic substituent [46]. Polymorphism phenomenon, which is the ability of

chemical compounds to exist in more than one crystalline structure, was observed for many POSS [39, 47–50].

T_8R_8 molecules bearing elongated side groups at the inorganic core exhibit a "rod-like" uniaxial symmetry [39, 47, 51–53]. In most cases symmetrical, radial arrangement of side substituents around the silsesquioxane cube is unfavourable for efficient packing in the crystal structure. Long side chains are much better accommodated if aligned orthogonally to the two opposite faces of the inorganic cube. Despite the rod-like structure and the arrangement in solid state similar to that of mesogenic groups along *b*-axis in liquid crystals, rod-like POSS do not belong to the class of smectic/nematic compounds. Side substituents control the type of packing of POSS in the crystal lattice. $T_8(n\text{-}C_nH_{2n+1})_8$ ($n = 7$, 8–14, 16, 18) are crystalline solids at room temperature owing to the intermolecular interactions and van der Waals attraction forces between *n*-alkyl chains [39, 47, 51–53]. The molecules are stacked in a lamellar or bilayer arrangement in triclinic (*P*-1) crystals. Similar structures are formed by *n*-alkanes C_nH_{2n+2} (n(even) = 6–26) [54]. The same type of solid-state packing (triclinic, *P*-1) was found for POSS with hetero-organic side groups, e.g. $T_8(CH_2CH_2CH_2SH)_8$ [55, 56], $T_8(CH_2CH_2CH_2Cl)_8$ [57, 58] and T_8(3-paramethoxyphenylpropyl)$_8$ [39]. Molecules of $T_8(CH_2CH_2CH_2SH)_8$ are additionally bound by weak S–H–S hydrogen bonds [56].

Side alkyl groups in rod-like $T_8(n\text{-alkyl})_8$ also crystallize in conformations similar to those characteristics for *n*-alkanes. Some POSS bearing *n*-alkyl groups are also polymorphic. The most efficiently packed crystal lattice is formed when alkyl chains are stacked parallel to each other in low-energy trans zigzag conformation. In some cases [e.g. $T_8(n\text{-alkyl})_8$, $n = 4$, 6], the alkyl arms can be distorted away from the molecular axis and interdigitated between the layers [47]. Molecular packing of $T_8(n\text{-}C_5H_{11})_8$ is quite unique. Side arms are spaced radially out of the core, giving rise to a "disc-like" arrangement of molecules in two-dimensional columnar structures [47]. A similar structure can be induced under appropriate crystallization conditions for otherwise rod-like $T_8(n\text{-}C_7H_{15})_8$ [47]. In the case of POSS with longer side chains [$T_8(n\text{-}C_8H_{17})$ and $T_8(n\text{-}C_{10}H_{21})$], an adjustment of molecules in the crystal network is required in order to obtain the most compact structure [47]. Side alkyl chains do not interdigitate but are tilted to the basal plane of POSS cages and aligned antiparallel to each other with respect to the layers that are separated by well-defined gaps.

Interestingly, despite all similarities, the hierarchical structures and packing morphologies of octasilsesquioxanes T_8R_8 and dimethylsiloxyspherosiloxanes Q_8MR_8 can differ significantly. It was found that the type of packing can be strongly altered if the size of the inorganic core increased. Moreover, flexible siloxane linkers (-$OSiMe_2$-) between alkyl groups and siloxane cages allow for greater mobility of side arms and larger distance between the free chain ends. It results in lower melting temperatures (T_m) of Q_8MR_8 compared to their T_8R_8 analogues. The effect seems to be more pronounced for species with small organic substituents. For example, ideally symmetric molecules of T_8Me_8 form rhombohedral crystals (space group *R*-3) [59] but those of only slightly larger $T_8(OMe)_8$ are triclinic (space group $P1\text{-}C_i$) [35, 60], while both T_8H_8 [43] and Q_8MH_8 [35, 37, 61] crystallize within trigonal-rhombohedral lattices (space group *R*-3). Interactions between substituents in Q_8MR_8

with long alkyl groups are more important than the increased mobility of side arms due to the presence of flexible dimethylsiloxane linker. Consequently, they govern the crystal packing of such molecules. For example, side alkyl arms of $T_8(n\text{-}C_{18}H_{37})_8$ and $Q_8M(n\text{-}C_{18}H_{37})_8$ point away in parallel way from the polyhedral core [51]. Both molecules are of rod-like shape, but crystals of Q_8MR_8 are more compact due to the interdigitation of long alkyl chains. Dimethylsiloxyspherosiloxanes octasubstituted with $R = -(CH_2)_2S(CH_2)_2(CF_2)_nCF_3$ ($n = 5, 7$) and their T_8R_8 analogues also belong to the same crystal group (triclinic $P1$) [37, 62].

The type of packing defines the course of melting of $T_8(n\text{-}C_nH_{2n+1})_8$. Melting temperatures are higher for species with longer side chains [36, 47, 53]. It can be ascribed to a larger extent of intermolecular interactions and more efficient packing. Yet, the increase in T_m exhibits an odd–even number effect due to the differences in packing geometry (parallelograms or trapezoids) and efficiency of intermolecular contacts, analogously to *n*-alkanes [54]. However, contrary to *n*-alkanes, $T_8(n\text{-}C_nH_{2n+1})_8$ ($n = 4$–11) did not show the odd–even effect in their experimentally (X-ray diffraction) estimated densities. The crystal density decreases on augmenting the length of side chains [47]. The effect was attributed to the separation of organic fraction by inorganic cubes and more efficient interdigitation of shorter side arms. For the same reason, the type of crystal packing determines thermal stability of $T_8(n\text{-}C_nH_{2n+1})_8$ [36, 47] and $Q_8M(n\text{-}C_nH_{2n+1})_8$ (linear, $n = 3$–8; and branched, $n = 5$–7) [37].

It was also found that melting temperatures of some rod-like POSS grafted with heterorganic side groups [56, 63] are higher than T_m of their *n*-alkyl analogues [53]. The effect was explained by strengthening the interactions between side chains due to the formation of hydrogen bonds.

2.2 *Heterofunctional POSS*

There are various synthetic pathways available for the preparation of heterofunctional POSS bearing more than one type of organic substituents at silicon atoms. Most reports published to date are focussed on octahedral silsesquioxanes of the T_8R_7R' type [29], sometimes named "monofunctional" due to the fact that only one of eight organic groups can be chemically modified.

Development of a synthetic procedure that would result in the desired heterofunctional silsesquioxanes is not an easy task. Co-hydrolysis of two different trifunctional organosilanes ($RSiX_3$, $X = Cl, OR'$) typically results in complicated, statistical mixtures of products [64]. T_8R_7R' are most often prepared in reactions of substitution or addition to one of eight reactive corner groups on the silsesquioxane core or by corner-capping of truncated trisilanol POSS [$T_7R_7(OH)_3$]. The latter procedure provides molecules of defined structure [65]. The majority of POSS obtained by the corner-capping strategy have seven chemically inert groups (e.g. Ph, *i*-Bu, *i*-Oct) and only one functional substituent that can be used for further modifications. However, the functionalization of the remnant organic moieties (if possible) leads to more elaborated systems. $T_8(CH{=}CH_2)_8$ is an ideal molecule for the preparation of

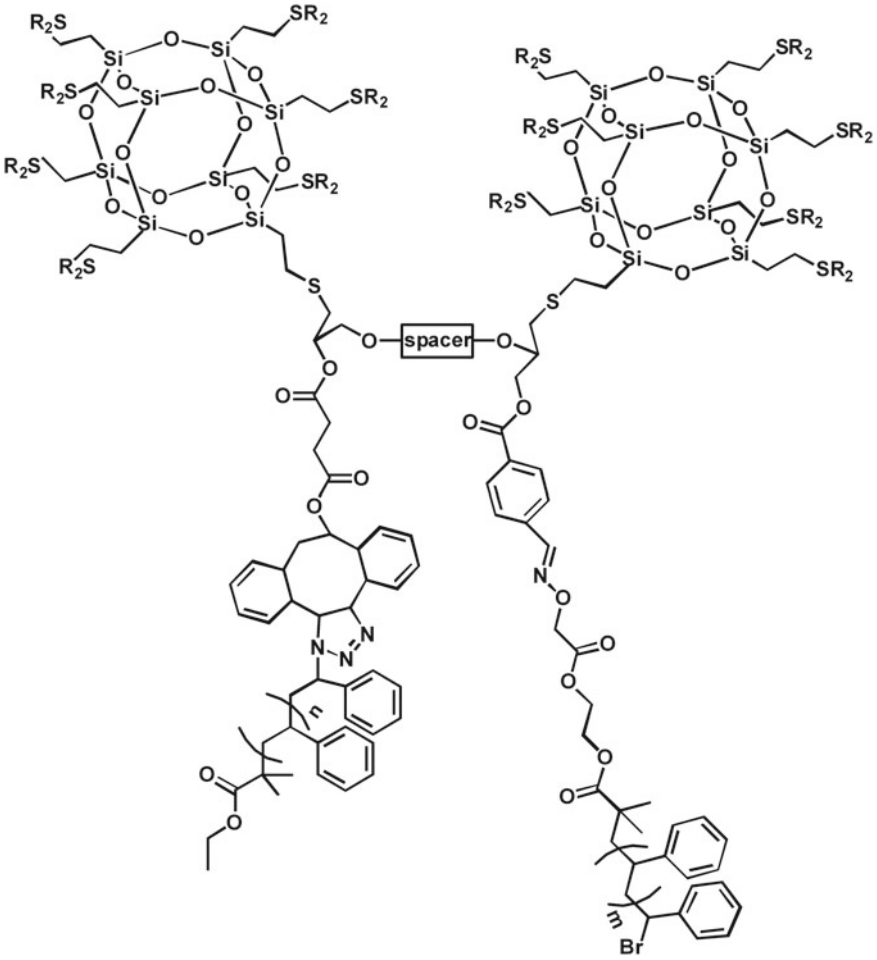

Scheme 2 Molecular structure of an asymmetric gemini surfactant (R = tert-butyl mercaptoacetate) [71]

such multifunctional products via "one corner" modification of the silsesquioxanes [66]. Procedures for anisotropic functionalization of $T_8(CH{=}CH_2)_8$ through reaction with triflic acid [30] or via thiol–ene chemistry [31] were developed. The resulting T_8R_7R' amphiphiles contain chemically distinct segments (e.g. hydrophilic and hydrophobic) connected via a covalent chemical bond. The products were used for the synthesis of various unsymmetrical macromolecules, such as shape amphiphiles based on polymer-tethered POSS [67–69], or asymmetric giant gemini surfactants (AGGS) of complex macromolecular structures (Scheme 2) [70–72]. The strategies for the preparation of such giant species can involve both "grafting-from" and "grafting-onto" procedures [22].

Other octafunctional POSS can be also selectively functionalized by monosubstitution at one of silicon atoms. For example, giant surfactants with acryloxyl-functionalized silsesquioxane heads were constructed from commercially available POSS and polystyrene. The head was subsequently functionalized with bulky ligands via thiol-Michael and thiol–ene addition of 2-mercaptoethanol, 1H,1H,2H,2H-perfluoro-1-decanethiol, 1-thio-β-D-glucose tetraacetate and 2-naphthalenethiol [73]. T_8H_7 monofunctionalized with a side group bearing azobenzene moiety was prepared by hydrosilylation of 4-butyl-4′-allyloxyazobenzene with T_8H_8 [74]. It was found that the bulky POSS ligands played an important role in the formation of cylindrical assemblies that were transformed into a mesostructured silica-like film. The *trans–cis* photoisomerization of azobenzene groups upon UV irradiation was also facilitated in the hybrid molecules.

Grafting of multiple functional groups onto POSS in two consecutive thiol–ene reactions resulted in a mixture of regioisomers (*para*-, *meta*-, *ortho*-) of bis-adducts that could be separated by flash column chromatography and isolated at synthetically useful quantities [31, 75, 76]. They were transformed into giant surfactants by the attachment of polystyrene chains [77]. Evidence was found for the influence of the tethering positions on the contributions of the system free energy (interfacial energy, head-to-head interactions and entropic energy of the tails). Upon increasing the temperature, the order–order transitions from lamellae to double gyroids were noted in the metaisomer, and from double gyroids to hexagonal cylinders in the orthoisomer (Fig. 1). It was observed that the order–disorder transition temperatures decreased in the order of *ortho*-, *meta*- and *para*-isomers.

POSS with cubic symmetry seem to be ideal candidates for the preparation of well-defined, bifunctional Janus-type "nanobricks". The term "Janus particle" (named after the two-faced Roman god of beginning and ending) was used for the first time by Pierre-Gilles de Gennes to define dissymmetric nanoscale objects with two distinct sides [78]. The structural directionality of each single particle results in unique physicochemical properties and is exceptionally promising for applications in nanoengineering, sensing, optical imaging and catalysis [79]. The synthesis of structurally well-defined and monodispersed Janus POSS is extremely challenging. Preparation of such molecules has been attempted from "half-cage" cyclic tetrasiloxanetetraol precursors [80–82]. However, the pioneering synthetic routes led to rather complex statistical mixtures of multifunctional cubes.

Recently, two reports have been published on the synthesis of true Janus POSS with a two-face substitution of silicon atoms in the inorganic core (Scheme 3). A structurally well-defined Janus nanocube of two chemically distinct opposed faces was obtained via symmetry controlled multiclick CuAAC functionalization of $T_8(CH_2CH_2CH_2N_3)_8$ with a conformationally constrained tetra-alkyne having an appropriate geometry and spatial orientation of the C≡C bonds [83]. Another nanometre-scale Janus silsesquioxane was synthesized through the cross-coupling of a "half-cube" cyclic sodium siloxanolate with another "half-cage" cyclic fluorosiloxane [84]. The structure of the isolated compound (triclinic, space group *P*-1) was confirmed by X-ray crystallography.

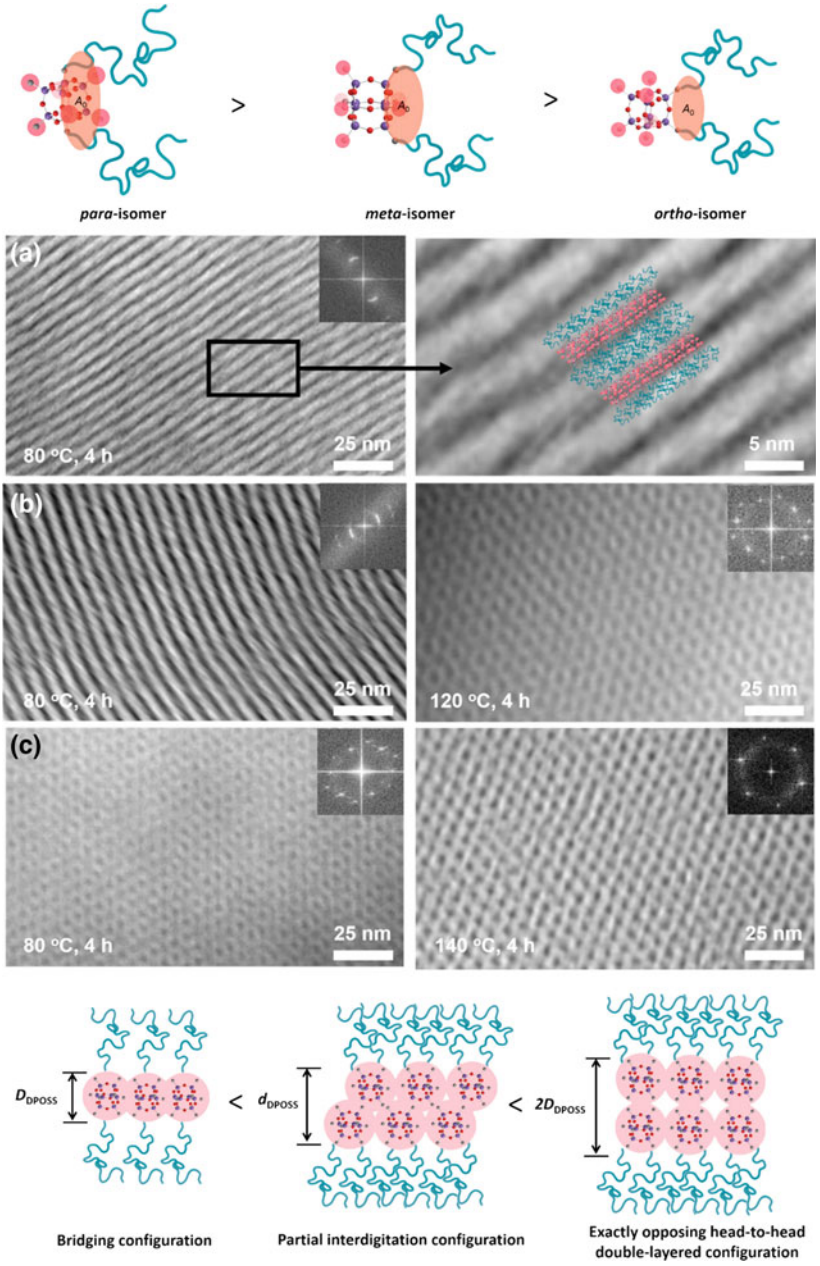

Fig. 1 Packing schemes of giant surfactant regioisomers with two PS chains and hydroxyl-functionalized POSS head, and variable temperature TEM images of microtomed samples and the corresponding diffraction patterns obtained from fast Fourier transformation of the images for **a** LAM phase of paraisomer at 353 K (the zoom-in view and the molecular packing model); **b** LAM phase of metaisomer at 353 K (left), and DG phase (right) of metaisomer at 393 K; **c** DG phase (left) of orthoisomer at 353 K and HEX phase (right) at 413 K. Adapted with permission from [77]. Copyright 2018 American Chemical Society

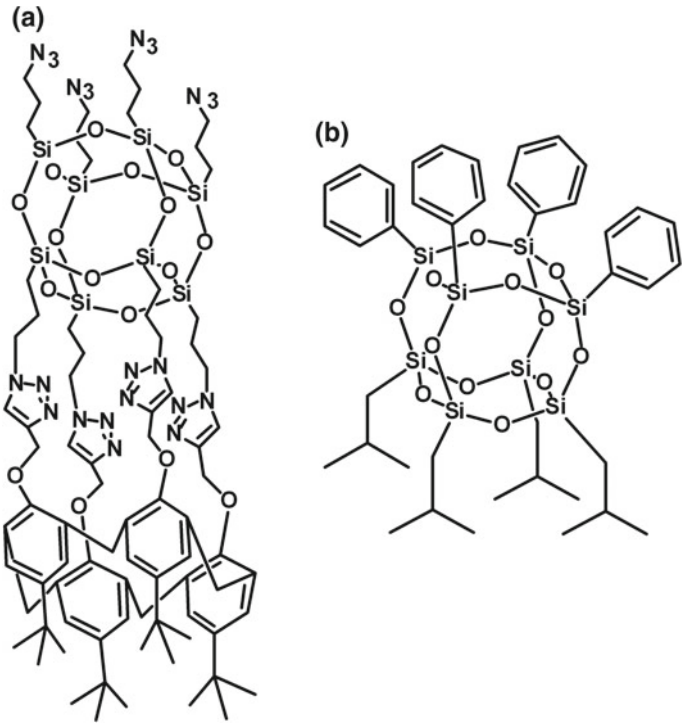

Scheme 3 Structure of octahedral "Janus" silsesquioxanes **a** 1,3,5,7-tetraazidopropyl-9,11,13,15-tetratriazolyl-calixarene-pentacyclo-[9.5.1.13,9.15,15.17,13]-octasiloxane [83] and **b** 1,3,5,7-tetraphenyl-9,11,13,15-tetraisobutyl-pentacyclo-[9.5.1.13,9.15,15.17,13]-octasiloxane [84]

3 Mesomorphic Behaviour of POSS Crystals

Thermally induced packing polymorphism due to the conversion from a metastable to a stable crystal structure can be observed for a range of polyhedral silsesquioxanes. It is an exceptionally important phenomenon that can be used for the design of self-assembled hierarchical systems based on crystal structures formed by POSS. The major solid–liquid phase transition of melting/crystallization can be accompanied for some octahedral silsesquioxanes by specific transformations in the solid state, involving changes of their crystal structure. For example, $T_8(n\text{-Pr})_8$ can exist in two forms: hexagonal (space group *R*3) above 272 K and triclinic (space group *P*1) below 272 K [42]. Three different crystal structures varying in unit cell dimensions, the space group and the conformation of cyclohexyl rings were observed for $T_8(\text{cyclohexyl})_8$ (*P*-1 triclinic, *R*3 rhombohedral and *P*4/n tetragonal) [39]. The packing morphology and thermal behaviour of some aryl-substituted POSS are also dictated by molecular interactions between the side groups [85]. For example, two

crystal structures [triclinic (*P*1 or *P*-1) and monoclinic (space group *P*2/m or *P*m)] were found for T_8Ph_8 [42].

The phenomena can be caused by increased molecular motions within the crystallites involving rotations in side groups or by a minor structural reordering of alkyl chain arms (without changes in the long-range order of the molecules). Compounds that exhibit such behaviour are known in organic chemistry as "plastic crystals" [86]. They interact weakly in the solid state and can be dynamically disordered with respect to the orientational degrees of freedom, e.g. by jump diffusion between a restricted number of possible orientations [87]. The term "rotor phase" or "rotatory phase" is also used if rotation of molecules is involved in the process. Classic plastic crystals are most frequently of globular shape, which provides little steric hindrance for reorientation and free tumbling about points of 3D crystal lattices.

Octahedral silsesquioxanes of spherical shape [e.g. $T_8(Me)_8$, $T_8(Et)_8$ and $T_8(i\text{-}Bu)_8$] are capable of free tumbling about their axes of symmetry which give rise to solid–solid state transitions that can be detected by a range of analytic methods (X-ray crystallography, calorimetry, Raman spectrometry and solid-state NMR spectroscopy). It was found that triclinic crystals of $T_8(i\text{-}Bu)_8$ undergo transformation into symmetric rhombohedral structures on heating via transitional formation of a monoclinic crystal cell [88, 89]. The phase transition involves fast and cooperative rotation of CH_3 units in *i*-Bu groups, as was shown by solid-state NMR experiments and Raman analysis [89]. The rotation helps POSS molecules to adopt a spheroid-like shape compatible with D3h symmetry and to fit into a rhombohedral lattice of *R*-3m space group.

$T_8(CH{=}CH_2)_8$ exists as a mixture of conformers with a small energy difference [90]. Vinyl groups at the silica core are fairly unhindered, and the methylene groups can rotate between three minimum-energy positions. It results in a change of crystal structure from triclinic (*P*-1) characteristic at $T < 233$ K [91] to hexagonal (space group *R*-3) at $T > 233$ K, leading also to the expansion of unit cell volume, which is characteristic to phase transitions of first order [90, 92–94]. Thermal solid–solid phase rearrangements were also noted for $T_8(n\text{-}Pr)_8$ [42], T_8Et_8 and $T_8(CDCH_2D)_8$ [95]. Four different crystal phases were observed at different temperatures for $T_8(CDCH_2D)_8$ [95]. The largest change in packing symmetry was noted at 257 K ($\Delta H = 47$ J/mol K) leading to the transition from asymmetric triclinic (space group *P*-1) to a highly symmetric rhombohedral unit cell (space group *R*-3). It involved also the expansion of the cell volume and a decrease in the number of molecules per unit. The motions of side groups in $T_8(CDCH_2D)_8$ became increasingly anisotropic if the temperature was lowered past the transition point, as indicated by solid-state ^{1}H NMR spectroscopy [95]. A similar phenomenon was observed for T_8Et_8 (at 253 K, $\Delta H = 28$ J/mol K) [95]. The transition from triclinic to a closely packed hexagonal (space group *R*-3) arrangement of molecules in the crystal structure was observed as well for $T_8(n\text{-}Pr)_8$ (272 K) [42], $T_8(i\text{-}Bu)_8$ (330 K) [89] and $T_8(CH_2CH_2CH_2Cl)_8$ (~400 K) [94]. Thermal characteristics of other T_8R_8 systems bearing heteroatoms in their side alkyl chains (e.g. $T_8(CH_2CH_2CH_2SH)_8$ [56] and octa(3-decanamidopropyl)-silsesquioxane [63]) suggest analogous behaviour. Surprisingly, plastic crystal phase transitions were not detected for T_8Me_8, $T_8(i\text{-}Pr)_8$ nor

$T_8(n\text{-Bu})_8$ [42]. However, neutron powder diffraction studies indicated a strongly temperature-dependent rotational dynamics of methyl groups in the crystal of T_8Me_8 [96]. The results exhibited different average lengths and vibrational energies of C–H bonds in methyl groups. Two methyl groups with shorter C–H bond lengths are situated the hexagonal *c*-axis and have C_3 site symmetry, while the other six methyls (not placed on symmetry axes or planes) are of C_1 site symmetry.

Rod-like polyhedral silsesquioxanes of elongated structure do not meet the criteria of classic "plastic crystals". Despite of this, POSS grafted with long *n*-alkyl groups (both $T_8(n\text{-alkyl})_8$ [47, 51, 53, 95] and $Q_8M_8(n\text{-alkyl})_8$ [37] derivatives) can exhibit specific solid–solid phase transitions in solid state due to increased mobility of their side chains. Thermally induced structural reordering can involve segmental motions including kinking and chain twisting out of the plane. Such mesomorphic transitions are usually of a small consequence. Most often only reversible change of unit cell size is observed, and the long-range crystal structure is not affected [53]. In the case of their $Q_8M_8(n\text{-}C_{18}H_{37})_8$ counterparts, no evidence of a thermally induced solid–solid phase transition was found despite a reversible lattice expansion before melting [51]. Such a solid-state behaviour can be ascribed to the presence of the flexible $OSiMe_2$ spacers between the inorganic core and the alkyl chains. Nevertheless, Q_8MMe_8, Q_8MH_8 and Q_8MVi_8 of spherical shape behave as plastic crystals and show endothermic rotor phase transitions at low temperatures [35].

Multitechnique (DSC, DRS, PALS, NMR and POM) variable temperature studies have been carried out to explain the differences in the "plastic crystal" behaviour between spherical and rod-like octahedral silsesquioxanes [94]. $T_8(CH{=}CH_2)_8$ and $T_8(CH_2CH_2CH_2Cl)_8$ were chosen as the respective models (Scheme 4). The pattern of multiple phase transitions in $T_8(CH_2CH_2CH_2Cl)_8$ can be also found for other POSS, such as $T_8(CH_2CH_2CH_2SH)_8$, but in the case of the octa(3-chloropropyl)silsesquioxanes they are well separated. It enabled much more precise analysis of their nature. It was found that both POSS undergo reversible thermally induced phase transitions in the solid state (Fig. 2) due to increased dynamics of the side groups. The mechanisms leading to the best position of molecules in most symmetrical crystal lattices vary for the species of different symmetry (Scheme 5). In the case of spherical $T_8(CH{=}CH_2)_8$, the thermal energy was used to increase dynamics of side groups. The single phase transition observed at 233 K is of first order. It leads to a change in the permittivity due to α-type structural relaxation (Fig. 3), as well as expansion of the crystal lattice and thermochromism of the material.

The respective low-temperature transition (at 250 K) for rod-like $T_8(CH_2CH_2CH_2Cl)_8$ involved a unique negative thermal expansion of crystals and their self-actuation. The effect is opposite to that observed for $T_8(CH{=}CH_2)_8$; nevertheless, both observed lattice expansion and contraction are of first order, as indicated by the respective changes of heat capacity. High-temperature transitions (350–400 K) of $T_8(CH_2CH_2CH_2Cl)_8$ are of a completely different nature. The increased mobility of side groups at elevated temperatures resulted in a gradual change of crystal structure and formation of a highly symmetric system. The observed transitions are of second order, as suggested by the gradual increase in ΔCp in the corresponding temperature range. The complex behaviour was reflected

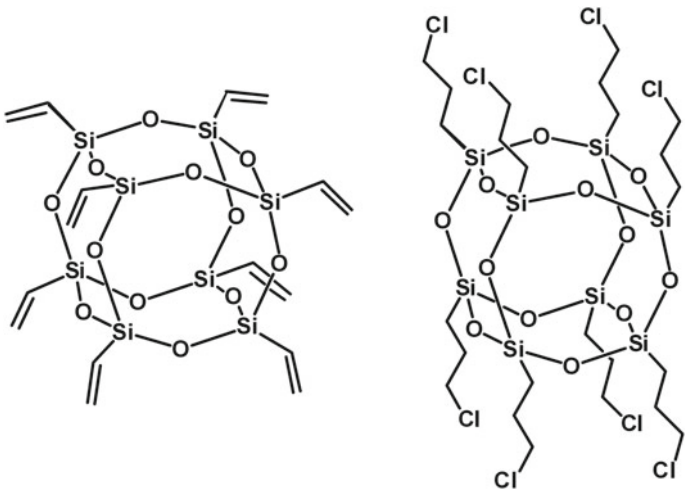

Scheme 4 Molecules of spherical $[T_8(CH{=}CH_2)_8]$ and rod-like $[T_8(CH_2CH_2CH_2Cl)_8]$ octasilsesquioxanes

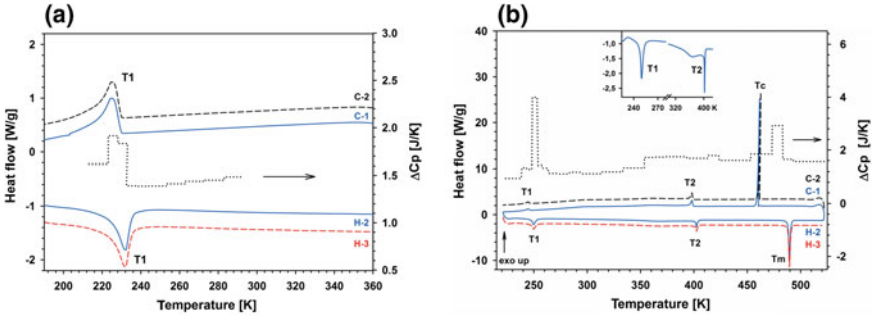

Fig. 2 DSC studies (heating and cooling runs) of phase transitions and changes of heat capacity (ΔC_p) recorded for **a** $T_8(CH{=}CH_2)_8$ and **b** $T_8(CH_2CH_2CH_2Cl)_8$ ([94]—reproduced by permission of the PCCP Owner Societies)

in unusual changes in the capacitance (Fig. 3) and fractional free volume of the material. The relaxation process due to the increased dynamics of 3-chloropropyl groups has a linear temperature dependency with low activation energy. The observed phenomena are important for molecular engineering of POSS-based well-defined hybrid materials capable of thermally induced structural transformations. Translation in solid state of rod-like molecules of POSS bearing reactive functions in their side alkyl chains can be of exceptional synthetic value, for example in POSS-based flexible networks of cooperative structural transformability via entropy-based subnet sliding.

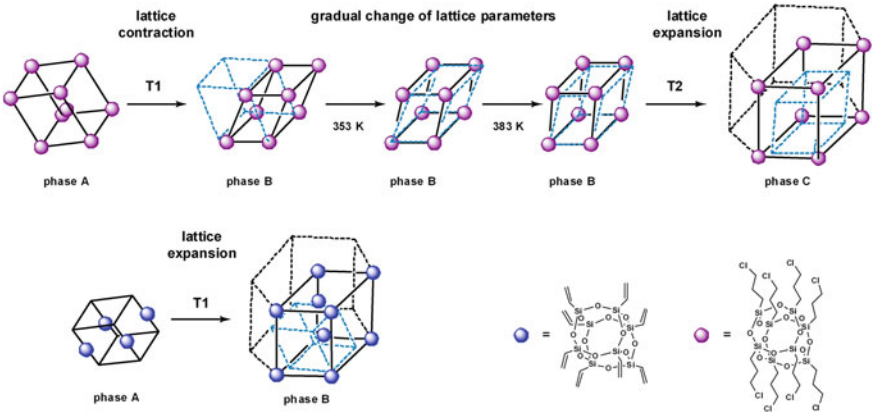

Scheme 5 Crystal lattice rearrangements on thermally induced solid-state phase transitions in $T_8(CH_2CH_2CH_2Cl)_8$ and $T_8(CH{=}CH_2)_8$ ([94]—reproduced by permission of the PCCP Owner Societies)

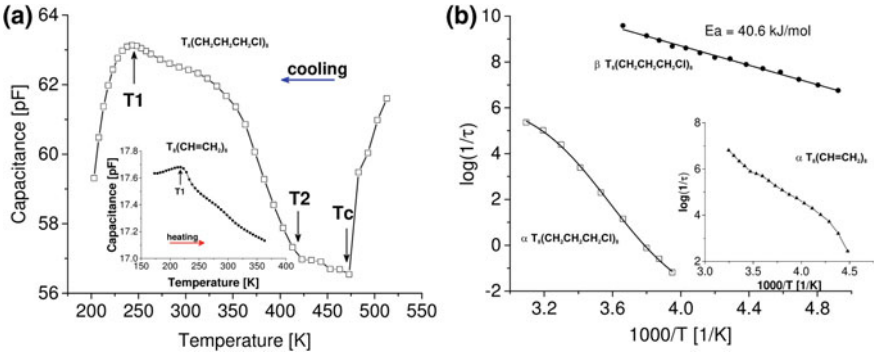

Fig. 3 Dielectric parameters as a function of temperature **a** capacitance plot and **b** temperature dependency of relaxation processes for $T_8(CH_2CH_2CH_2Cl)_8$ [insert $T_8(CH{=}CH_2)_8$] ([94]—reproduced by permission of the PCCP Owner Societies)

4 Advanced Hybrid Materials Based on POSS Self-assembling Phenomena

Single molecules of polyhedral silsesquioxanes can be regarded as organic–inorganic hybrid materials at the molecular level [24]. POSS molecules have been also successfully incorporated into a range of well-defined hybrid nanoarchitectures. The tendency to crystallize and formation of ordered nanostructures make POSS potential supramolecular "recognition elements" and crystalline templates in more complex systems. A wide range of nanotechnologies that were influenced by the phenomenon of the controlled self-assembly of silsesquioxane templates include preparation of nanoparticles of noble metals, quantum dots, complexes with DNA, metal–organic

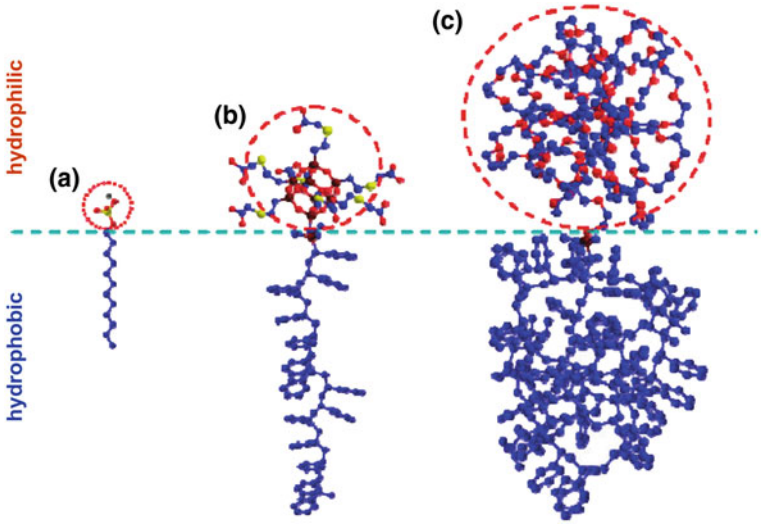

Scheme 6 Structural comparison of **a** typical small-molecule surfactant (sodium dodecyl sulphate); **b** giant hybrid surfactant with POSS head; and **c** typical amphiphilic diblock copolymer. Reprinted with permission from [100]. Copyright 2018 American Chemical Society

frameworks and materials for optoelectronics. They are discussed in the following part of the text.

4.1 Surfactants

Unsymmetrical multifunctional POSS (T_8R_7R') are of exceptional interest for a wide range of supramolecular systems, including amphiphilic moieties and surfactants [23, 97]. POSS of different geometrical and chemical symmetries with inorganic silsesquioxane heads monotethered with organic alkyl tails can form well-defined hierarchical structures. Adjustment of the length and branching of alkyl chains allows to tune intermolecular forces and molecular packing [98, 99]. Nanoscale arrangement of such building blocks in solid state is very important for materials engineering. Surfactants and block copolymers are capable of generating various thermodynamically stable micellar structures (spheres, cylinders and vesicles) in dilute solutions. Packing of such amphiphilic molecules depends on the equilibrium interfacial area of the ionic (hydrophilic) head at the critical micelle concentration (Scheme 6) [100]. Their self-assembly behaviours and the type of micellar structure are also determined by structural parameters (the size and chemical structures of immiscible parts and the overall size of molecule) and physical characteristics of experimental environments (solvent, concentration, pH value, temperature, additives) [22].

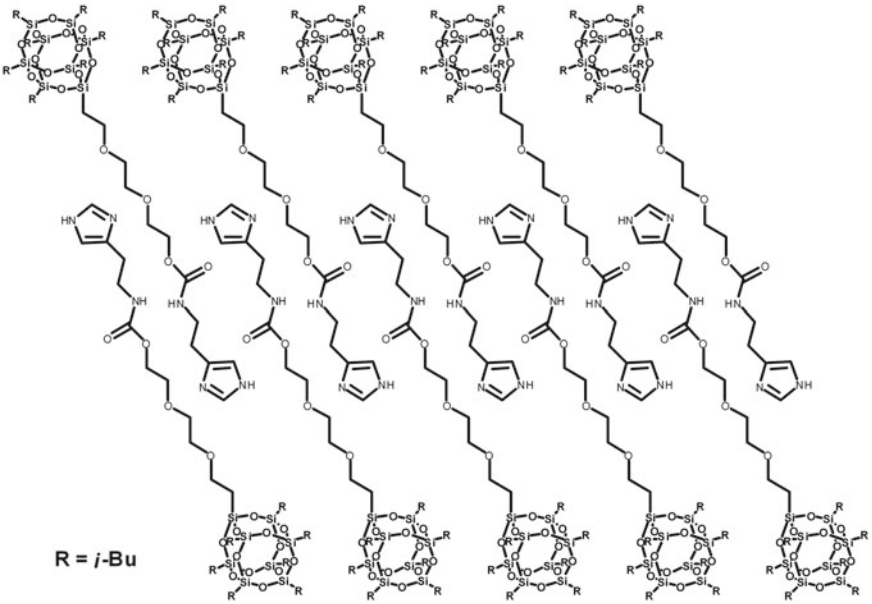

Scheme 7 "Head-to-head" interdigitated bilayer of amphiphilic POSS [102]

Molecular dynamics simulations revealed that attractive electrostatic POSS—POSS interactions in $T_8H_7(n\text{-}C_7H_{15})$ consisting of a silsesquioxane head and a single hydrophobic tail are responsible for association and clustering of inorganic cages [101]. Formation of a bilayer structure with sharp boundaries ("head-to-head", Scheme 7) is the preferred assembly mode for such molecules [98, 99, 101]. Even POSS with a relatively short organic tail at one corner of the cube can act as amphiphilic molecules of uniform molecular weight. To some extent, the order can be preserved even in the molten state since melting starts within the organic domain, prior to the decay of the inorganic lattice. The morphology at the nanometre scale and thermal properties can be changed with the length and number of branching in the side chains due to a minor structural reordering (rotation or translation) [98, 99]. Hydrophobicity of the organic tail is not a prerequisite for the organization of T_8R_7R' in solid state and at the interphase. The structure of such arrays can be controlled also by other factors. $T_8(i\text{-Bu})_7$ tethered with a hydrophilic organic tail terminated with imidazole group formed vesicles in water and well-defined interdigitated bilayer nanosheets in organic solvents due to the amphiphilic nature of the molecules in conjunction with hydrogen bonding from the carbamate groups [102].

Shape has been increasingly recognized as an important factor for the self-assembly of POSS derivatives. Diverse and complex structures can be created by an appropriate manipulation of the shape anisotropy of building blocks. Interesting effects were noted for amphiphilic POSS with long polymeric tails that enable a unique "bottom-up" strategy for the preparation of 2D nanostructures. The molecu-

lar geometry and enthalpy/entropy balance direct the organization of such species. Reduction of free energy guided by geometry (overall molecular shape) and properties (amphiphilic interactions) of those asymmetric molecules are the driving forces. It was observed that the hierarchical structures formed by giant surfactants, composed of various functionalized POSS heads tethered with polystyrene (PS) tails, are highly sensitive to the molecular topology. For example, grafting two PS tails to a POSS head shifted the boundaries between different ordered phases and altered the packing configurations of POSS, compared to the analogue with a single PS chain of equal molecular weight [104]. Two tri-armed organic–inorganic hybrids based on carboxylic acid-functionalized POSS with/without PS linkers self-assembled into hollow spherical nanostructures in water/organic mixed solvents [103].

Two completely different mechanisms and driving forces operate in the self-assembly process depending on the shape of macromolecules (Fig. 4). In the presence of PS linkers, the hybrid species resemble surfactants and form bilayer vesicles in a process driven by hydrophobic interactions. Single-layered, vesicle-like "blackberry"-type structures were obtained without polystyrene linkers. It was found that their formation was mediated by electrostatic interactions, with hybrids behaving like hydrophilic macroions. The alteration of the assembly size in response to the change of the solvent polarity was different for the two species. A remarkable sensitivity of highly ordered self-assembled structures to molecular topology was observed for giant surfactants composed of various functionalized POSS heads tethered with one or two polystyrene tails. It facilitated the engineering of various nanophase-separated structures with sub-10 nm features [104]. The boundaries between different ordered phases could be shifted to adjust the packing of POSS. It led to reduction of the self-assembled nanodomains. Their morphology depended also on the molecular details of functional groups on the silsesquioxane cages.

Asymmetric giant "bolaform-like" surfactants composed of PS chain end-capped with two different POSS [hydrophobic $T_8(i\text{-Bu})_7$ and hydrophilic derivatives of $T_8(CH{=}CH_2)_7$ with added thioglycerol] were able to form a range of structures in solid state, including hexagonally packed cylinders (Hex), double gyroids (DG), lamellae and body-centred cubic spheres (BCC) [105]. The morphology type depended on the compatibility between organic–inorganic segments, the length of PS linkers and the volume fraction of the hydrophilic domain. Hydrophilic POSS were phase-separated from the PS domains, whereas hydrophobic $T_8(i\text{-Bu})_7$ were associated within the polymer matrix. However, favourable interactions between $T_8(i\text{-Bu})_7$ governed their crystallization in the mixed phase if geometry of the confinement was appropriate. The crystalline packing within the self-assembled lamellae resulted in even higher phase separation. However, for other three phases with curved interfaces (DG, Hex and BCC), the polystyrene matrix and $T_8(i\text{-Bu})_7$ were completely miscible and amorphous. Further POSS-PS phase separation took place on flat interfaces. Various highly ordered mesophases were also produced by the self-assembly of other conjugates of hydrophilic POSS tethered with hydrophobic polystyrene tails [106]. The nanophase separation between the heads and tails leads to the formation of Frank–Kasper (F–K) and quasi-crystal phases of ordered spheroids. Increasing the

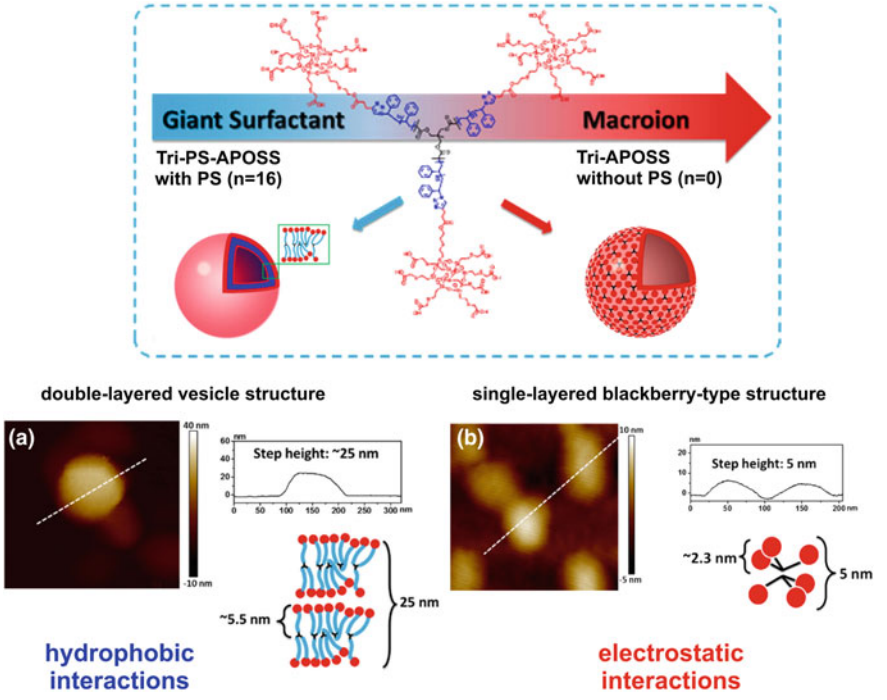

Fig. 4 Structures formed by tri-PS-POSS and tri-POSS hybrids without PS linkers—giant surfactant *vs* macroion; a) AFM images and height profiles of collapsed assemblies after solvent evaporation corresponding to models of the double-layer vesicle and blackberry structure. Adapted with permission from [103]. Copyright 2018 American Chemical Society

number of tails from one to four shifted compositional phase boundaries and stabilized F–K and quasi-crystal phases in regions typical to simple spheroidal micelles.

Polymeric chains of different chemical structure can be used as tails in the POSS-based surfactants. It allows for the formation of novel hybrid materials of specific properties and applicative potential. Giant linear and star-like surfactants with omniphobic perfluorinated POSS heads tethered onto the end point or junction point of diblock polystyrene-*b*-poly(ethylene oxide) (PS-*b*-PEO) copolymer (with fixed length of the PEO block) were capable of forming different ordered phases and phase transitions on changing the molecular weight of the PS block [107]. Varying shape anisotropy of block POSS-PEO copolymers (Scheme 8) was shown to have an effect on the melting (T_m) and recrystallization (T_r) temperatures of both the PEO and POSS layers as well as on the crystallinity of the PEO layer [108]. The crystallization of PEO drives the block copolymers to self-assemble into large nanothick sheets with one PEO crystalline layer sandwiched by two POSS layers. A decrease in T_m and T_r as well as disruption of the crystalline PEO layer and an increase in T_m of the POSS layer were observed with increasing number of POSS. Formation of unique hierarchical assemblies was observed for giant rod-like

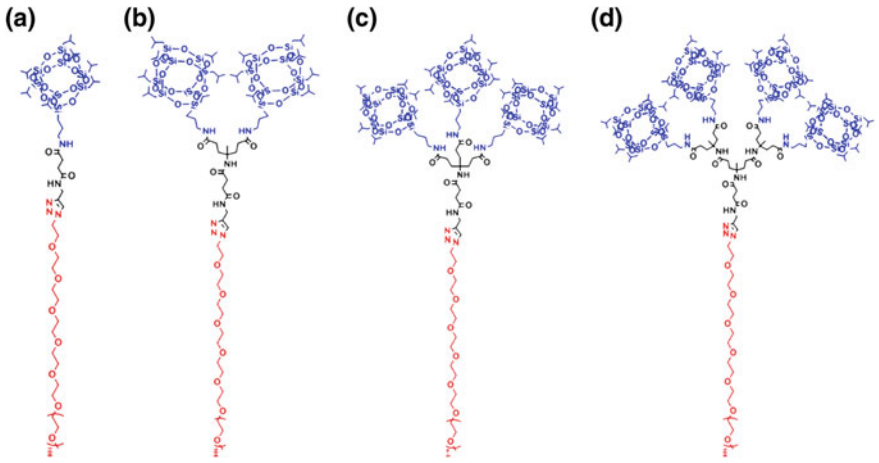

Scheme 8 Chemical structures of shape-anisotropic block copolymers consisting of POSS and PEO chains. Reprinted with permission from [108]. Copyright 2018 American Chemical Society

amphiphiles with perfluorinated $T_8[CH_2CH_2(CF_2)_7CF_3]_7$ heads and PEO or PS tails [109]. Due to the specific molecular geometry, the species did not interdigitate but were hexagonally packed within double-layered lamellae. The lamellae morphology in such systems depends on the structure of polymeric tails. The presence of electronegative fluorine atoms influenced melting properties of T_8R_7R' [$R = (CH_2)_2CF_3$; $R' = CH_3$; $(CH_2)_2C_6H_5$; $(CH_2)_2CF_3$; $(CH_2)_2(CF_2)_nCF_3$ ($n = 5,7,9$); $CH_2CH(CF_3)_2$; $(CH_2)_3OCF(CF_3)_2$] [110]. It can be explained by the strong interactions between fluorine and silicon atoms of neighbouring silsesquioxane cages, which results in a tighter packing. Spontaneous formation of concentric lamellae was observed for self-assembling giant surfactants consisting of $T_8(CH_2CH_2SCH_2CH_2(CF_2)_7CF_3)_7$ heads and flexible polymer tails [111]. Species having a single PS tail (POSS-PS), two different PS and PEO tails (PS-POSS-PEO) and a block copolymer tail (POSS-PS-*b*-PEO) were studied. Owing to the asymmetrical sizes of the head and tail blocks and the rectangular molecular interface between them, the giant surfactants can assume a truncated-wedge-like molecular shape. Their nucleation and growth during phase separation induced smooth morphological curvature during the self-assembly process, which resulted in the formation of curved and concentric lamellae.

Diblock amphiphilic copolymers with $T_8(i\text{-Bu})_7$ side groups grafted on only one block of [PHEMAPOSS-*b*-P(DMAEMA-*co*-CMA)] formed spherical micelles in water. The POSS core was thus surrounded by stimuli-responsive shells sensitive to changes of pH and redox potential [112]. The shells could be cross-linked by photodimerization of coumarin moieties (CMA). The subsequent etching of silsesquioxane structures with hydrofluoric acid left hollow polymeric capsules, suitable for the delivery of active agents in photodynamic therapy.

Evaporation-induced self-assembly of $T_8(OEt)_7(n\text{-alkyl})$ ($n = 16, 18, 20$) resulted in the formation of two-dimensional hexagonal columnar mesophases (p6mm). The

phenomenon was used for the preparation of organic–inorganic hybrids with well-ordered mesostructures and pore diameters governed by the size of *n*-alkyl groups. It was also shown that $T_8(OEt)_6(n\text{-alkyl})_2$ species with two alkyl chains randomly distributed about the silsesquioxane core could generate only lamellar structures [113]. This behaviour was attributed to the increase in space occupied by the head group and to the development of mesophases with higher curvature.

Telechelic macromolecules of two different POSS units symmetrically linked by hydrophilic organic spacers ("dumbbell-shaped") can also form unique structures on self-assembling in bulk. A specific phase separation was observed for amphiphilic $T_8(i\text{-Bu})_7\text{-}(CH_2)_3NHC(O)CH_2S(CH_2)_2\text{-}T_8(CH_2CH_2SCH_2COOH)_7$ [114]. The interlayer hydrogen bonding between carboxyl groups helped to the formation of a specific 3D crystal built of stacked 2D layers. Partial neutralization of –COOH groups with TBAOH broke the interlayer hydrogen bonds that were replaced by competitive electrostatic repulsive interactions. It resulted in the formation of 2D nanoplates. It was also shown that introduction of an excessive number of charges associated with one $T_8(CH_2CH_2SCH_2COOH)_7$ end group prevented completely the lateral growth of crystals. Dumbbell-shaped hybrids, terminated with two POSS molecules and containing poly(tert-butyl acrylate) linkers of three different molecular weights, formed different structures in aqueous solution at pH 8.5 depending on the length of the spacer [115]. The self-assembly of the shorter species resulted in ellipsoidal aggregates with a moderately uniform size, whereas the hybrids with the longest polyacrylate chain self-assembled into aggregates with a broad size distribution. $T_8(i\text{-Bu})_7\text{-}X\text{-}T_8(R'')_7$ (*X*—phthalic anhydride derivative, R''=$CH_2CH_2SCH_2COOH$, $CH_2CH_2SCH_2CH_2OH$ or $CH_2CH_2SCH_2CH_2C_6F_{13}$) formed bilayer head-to-head structures that were organized subsequently into a 3D orthorhombic lattice within a $Pna2_1$ symmetry group [116]. The formation of the ordered structure was associated with an endothermic transition of first order observed at 455 K. It was also demonstrated that the type of highly ordered supramolecular lattices (including a Frank–Kasper A15 phase) in amphiphilic systems built of $T_8(i\text{-Bu})_7$ and polar $T_8(R'')_7$ depended on the number of hydrophobic silsesquioxane ligands [117].

4.2 Hybrid POM–POSS Clusters and Related Structures

Supramolecular phase ordering of asymmetrical dumbbell-shaped nanoparticles of polyoxometalate–organic–POSS (POM–POSS) is quite unique. Such species of Janus-type characteristics (molecular Janus nanoparticles—MJPs) are derivatives of crystalline POSS [typically hydrophobic $T_8(i\text{-Bu})_7$] and polyoxometalates of a Wells–Dawson type $\{[P_2W_{15}V_3O_{62}](n\text{-}Bu_4N)_6\}$ [118, 119] or a Lindqvist type $\{Mo_6O_{18}N(n\text{-}Bu_4N)_2\}$ [114]. Synergistic self-assembly and nanoscale phase separation of POM- and POSS-containing zones is the thermodynamic driving force for the formation of hierarchical nanostructures [118]. POM–POSS self-assemble into 2D nanocrystals with double layers of crystalline POSS sandwiched between

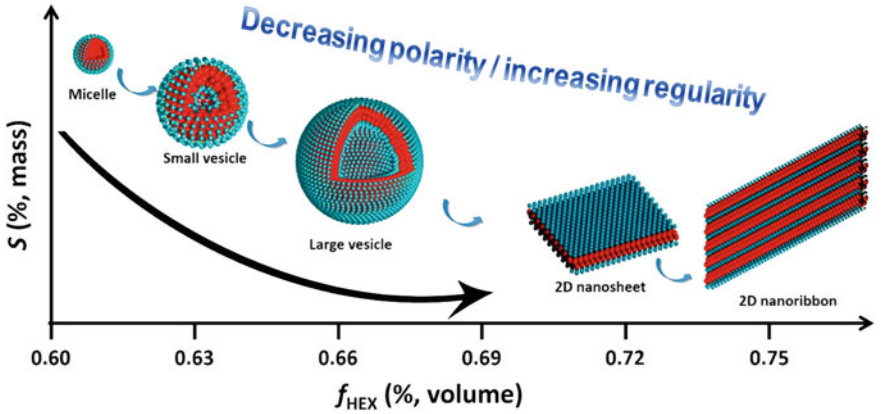

Fig. 5 Sheet-to-ribbon transitions due to the change in packing mode of POM–POSS clusters. Adapted with permission from [120]. Copyright 2018 American Chemical Society

two layers of inorganic species (Fig. 6). The dissimilar rigid clusters at molecule periphery form a brick-like packing in the solid state. The flexible linkers between POSS and POM provide a certain degree of freedom for an appropriate configuration adjustment. The thickness of double layers is controlled by separate crystallization of the nanoparticles. Other factors, such as solvent polarity, number of counterions and size of construction blocks, can change the crystallization mode of clusters of the same type and alter the nanoscale phase separation between incompatible parts [119].

The amphiphilic features of MJPs enable the *co*-clusters to self-assemble into diverse nanoaggregates in the liquid phase (micelles, vesicles, nanosheets and nanoribbons) by tuning the polarity of solvent used [120]. It was found that during the self-assembly process in solution, the increase in packing order causes the vesicle-to-sheet transition, whereas the change in packing mode results in the sheet-to-ribbon transitions (Fig. 5). In media of higher polarity, the *co*-cluster self-assembled into small bilayer vesicles in which a POM layer was sandwiched by the two POSS layers. The vesicle size increased with decreasing polarity of the solvent to break at $\varepsilon \approx 6.1$ and then finally convert into flat bilayer nanosheets at $\varepsilon \approx 5.6$. These changes are due the increasing packing order of the POM clusters that augments the bilayer rigidity. In solvents of low polarity ($\varepsilon \geq 5.3$), long nanoribbons were formed in which the POM–POSS co-clusters were arranged according to a fishbone-shape model with maximized electrostatic interactions between the POM blocks.

MJPs made of covalently linked α-Keggin-type polyoxometalate nanoclusters and $T_8(i\text{-Bu})_7(CH_2CH_2CH_2NH_2)$ self-assembled to form diverse nanostructures driven by secondary interactions among the building blocks and solvents via tuning molecular topology and solvent polarity [121]. Colloidal nanoparticles with nanophase-separated internal lamellar structures were formed initially in highly polar solvents (acetonitrile/water mixtures). Upon ageing, they turned gradually

into 1D nanobelt crystals. Stacked crystalline lamellae were dominant in less polar methanol/chloroform solutions. When $T_8(i\text{-Bu})_7$ heads were replaced with non-crystallizable T_8(cyclohexyl-SCH_2CH_2) groups, then colloidal spheres were also formed, but then failed to evolve further into crystalline nanobelts. Isolated two-dimensional nanosheets were obtained in less polar solvents. The nanosheets were composed of two inner crystalline layers of Keggin POM covered by two monolayers of disordered POSS (amorphous phase). Self-assembly of clusters with two $T_8(i\text{-Bu})_7$ heads was hardly sensitive to solvent polarity and was dominated by the crystallization of silsesquioxane cages that formed the crystalline inner bilayer, sandwiched by two outer layers of Keggin POM clusters (Fig. 6).

Analogous phenomena directed the type of supramolecular structures formed by derivatives of POSS and [60] fullerene (C60) [114]. Proper matching of the size of components at both ends of such dumbbell macromolecules is very important. Two-dimensional layer could be formed only if two $T_8(i\text{-Bu})_7$ residues were attached to one C60. Species having only one $T_8(\text{i-Bu})_7$ molecule tethered to C60 were too imbalanced in their size and did not crystallize [114]. Another asymmetric giant amphiphile composed of one [60] fullerene covalently linked with two $T_8(i\text{-Bu})_7$ moieties formed objects of the so-called one-and-half-layered structure [122]. The compositional asymmetry between C60 and $T_8(i\text{-Bu})_7$ led to a "sandwich-layered" molecular packing, where a single layer of C60 was sandwiched between double $T_8(i\text{-Bu})_7$ layers. Within these layers, the molecules further organized into crystalline arrays. This packing scheme repeated along the c-axis formed a 3D orthorhombic lattice (*P*nnm symmetry group).

4.3 3D Nanonetworks

Highly symmetric structures of octafunctional POSS can be exceptionally useful for the development of 3D hierarchical structures. Octahedral silsesquioxanes can be regarded not only as a platform for blending organic and inorganic modules at the molecular scale but also as building blocks or functional knots for the preparation of well-organized 3D networks. A range of advanced materials can be formed with POSS linked by covalent, supramolecular and coordinative bonds.

4.3.1 Well-Ordered Polymeric Networks

Organic–inorganic meso/macroporous covalent networks were obtained with POSS via a facile template-free strategy exploiting Schiff base chemistry [123]. The materials resulting from the combination of $T_8(CH_2CH_2CH_2NH_2)_8$ with terephthalic aldehyde were used as stabilizing supports for a palladium catalyst due to the presence of N-containing functionalities, large porosities and high BET surface areas. The resulting heterogeneous and recyclable catalyst of high activity and turnover frequency was employed in Suzuki–Miyaura reactions. Schiff base chem-

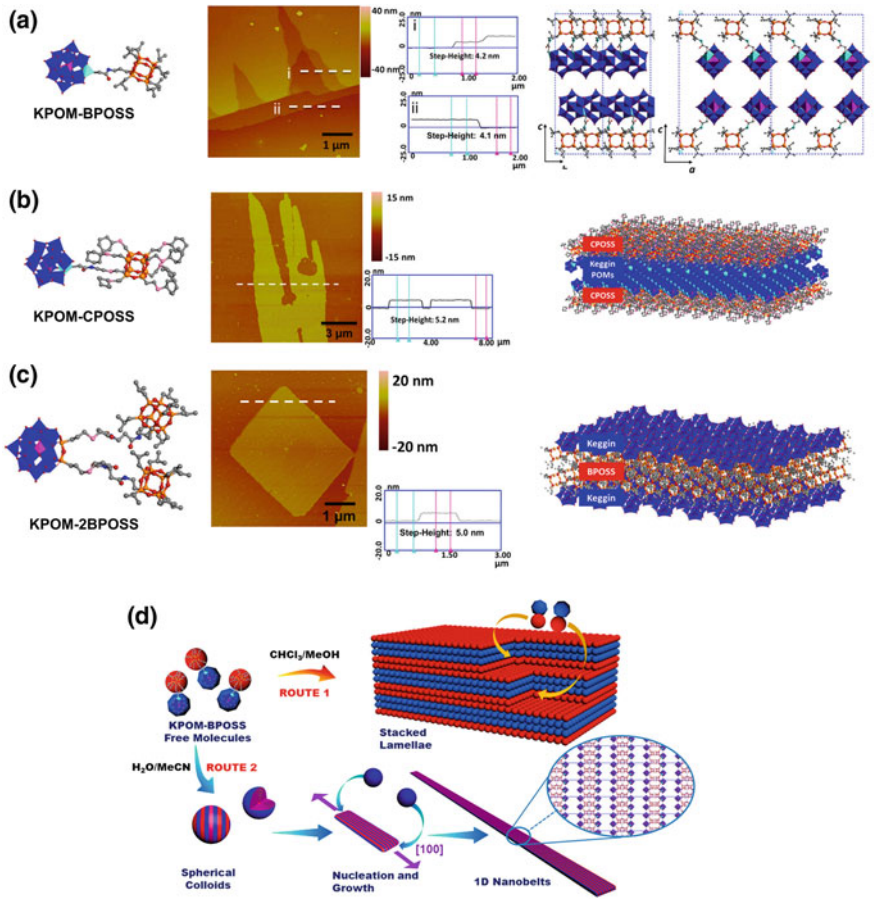

Fig. 6 **a**, **b** AFM height measurements of the flat-on single crystals (2D nanosheet morphology) of POM–POSS of different chemical structure and the respective perspective views of simulated crystal lattices; **d** the proposed mechanism of forming the stacked lamellae in chloroform/methanol and the 1D nanobelts in water/acetonitrile. (Adapted with permission from [121] Copyright 2018 American Chemical Society)

istry was also used for the preparation of a cross-linked silsesquioxane nanohybrid with $T_8(CH_2CH_2CH_2NH_3^+Cl^-)_8$ and glutaraldehyde as a dual cross-linking bridge [124]. Block-like irregular nanoparticles with specific surface area of 42.8 m^2/g were formed. The cross-linked nanohybrid was used as a solid-phase adsorbent for selective adsorption of acidic dyes (such as methyl orange) in aqueous solutions. Electrostatic interactions are the driving force for the adsorption (maximum adsorption capacity of 237.5 mg/g). The process was spontaneous and exothermic. The adsorbed molecules could be efficiently recovered using a methanolic solution of NaOH. The reusable adsorbent can be applied for wastewater treatment in dye industry.

A well-defined covalently linked microporous organic–inorganic nanohybrid framework was obtained with *p*-iodio-octaphenylsilsesquioxane by a Yamamoto-type of Ullmann cross-coupling [125]. This strategy provides an approach for constructing a wide variety of functionalized zeolite-like porous organic frameworks. Formation of well-ordered networks consisting of truncated octahedra [β-cages compared with Linde type A zeolite (LTA)] and truncated cuboctahedra (α-cages compared with LTA) with diameters of about 2 nm was confirmed by NMR spectroscopy and nitrogen adsorption. The inorganic silsesquioxane cubes were linearly linked by biphenyls, which led to the formation of micropores with the narrow pore size distribution and BET surface area of 283 m^2/g. The network was thermally stable up to 670 K in air and efficiently adsorbed benzene and water.

A cross-linked and thermostable fluorinated POSS-based network was prepared by thermal polymerization of trifluorovinyl ether groups (Scheme 9) [126]. The hybrid polymer network shows 5 wt% loss at ~610 K. It is transparent, of low water uptake, of low dielectric constant under both dry and wet conditions (<2.56) and of low dissipation factor ($<3.1 \times 10^{-3}$) in a wide range of frequencies from 40 Hz to 30 MHz. Such high-performance dielectric materials are suitable for microelectronics and fabrication of high-frequency printed circuit boards or integrated circuits.

POSS-based poly(ionic liquid)-like cationic networks of tuneable mesoporosities (surface area > 900 m^2/g) were formed with $T_8(CH_2Cl)_8$ and rigid N-heterocyclic cross-linkers (4,4′-bpy) [127]. When $T_8(CH_2CH_2CH_2Cl)_8$ with more flexible chloropropyl groups was used as the monomer, then the obtained material had a very low surface area (7 m^2/g). It indicates the importance of the rigidity of POSS for the generation of ordered structures. The resulting networks were applied as the supports for loading POM $PMo_{10}V_2O_{40}^{5-}$ (PMoV) as guest species through the anion-exchange process. The POSS–POM hybrid was used as efficient heterogeneous catalysts for H_2O_2-mediated oxidation of cyclohexane and aerobic oxidation of benzene. Hyperbranched polymeric networks of adjustable hydrophilic–hydrophobic properties were also prepared by controlled cross-linking of $T_8(CH{=}CH_2)_7(CH_2CH_2OH)$ followed by grafting PEG chains to residual vinyl groups [128]. The polymers exhibited a characteristic transition from micelle to vesicle in aqueous solutions.

Self-assembly of ordered nanoscale POSS superstructures was evidenced in semicrystalline covalently cross-linked nanocomposites of polyhedral silsesquioxane and poly-(ε-caprolactone) (POSS–PCL) [129]. Asymmetrical triblock copolymers with a single POSS moiety centred between two PCL chains were used for the formation of a shape memory network (Fig. 7). Both crystalline reflections of the PCL orthorhombic phase and POSS rhombohedral phase were shown if PCL was terminated with OH groups. It indicates independent crystallization due to microphase separation. Consequently, two long period spacings—one associated with POSS (long period of 66 Å) and the other associated with PCL lamellar nanophase (long period of 151 Å)—were shown in SAXS diffractograms. The nanostructure was dominated by crystallization of POSS. Coordination via hydrogen bonding between the inert corner isobutyl groups of POSS and the end groups of PCL diols facilitated crystallization of PCL chains. End-capping of PCL with acrylate groups was required for cross-linking but greatly reduced the crystalline order of POSS. End-capping prevented

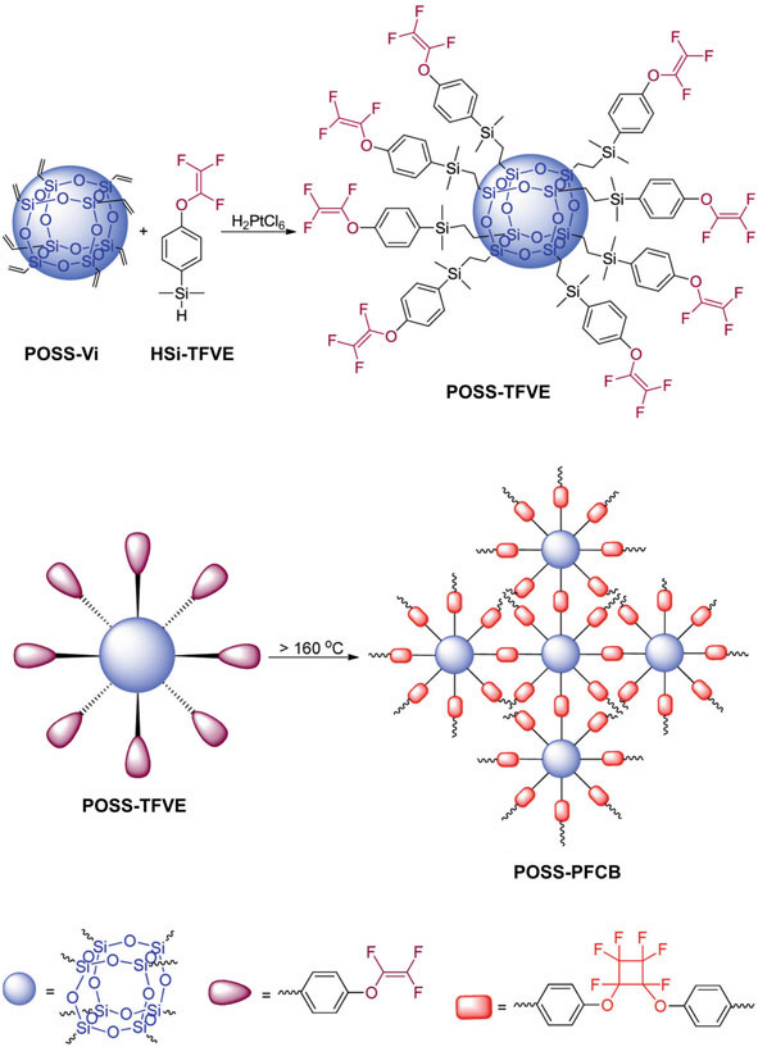

Scheme 9 Synthesis of a POSS-based network by thermal polymerization of trifluorovinyl ether groups. Adapted with permission from [126]. Copyright 2018 American Chemical Society

also the coordination between POSS and PCL, thus freeing the poly-(ε-caprolactone) chains for fold crystallization of the orthorhombic phase. Despite the architectural constraints, cross-linking with tetrathiol molecules supressed the crystallization of PCL, but did not hinder completely the formation of a superstructure in the material. POSS crystals embedded in amorphous PCL matrix were segregated as crystalline clusters organized as a highly ordered cubic phase.

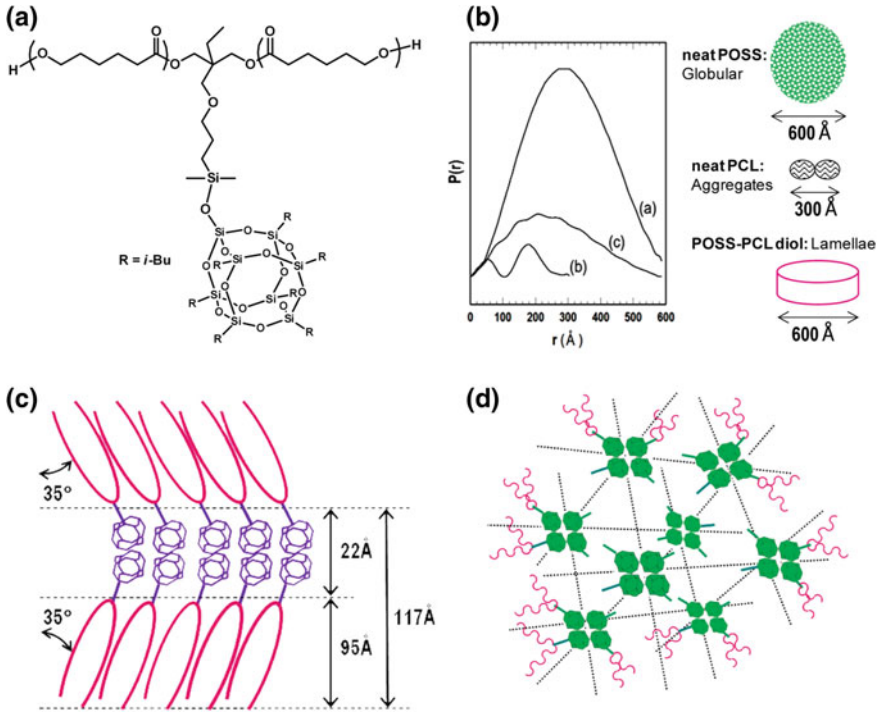

Fig. 7 Formation of hierarchical assemblies in POSS-poly-(ε-caprolactone) networks: **a** the structure of POSS-poly-(ε-caprolactone) hybrid; **b** pair distribution function plots P(r) derived from the SAXS data of (*a*) neat POSS, (*b*) neat PCL homopolymer and (*c*) monomeric POSS-CL diol nanocomposite; **c** the proposed long-range order of POSS-CL acrylate nanocomposites; **d** the model of cubic superstructure for the POSS–PCL network. Adapted with permission from [129]. Copyright 2018 American Chemical Society

Polycarboxyl octaphenylsilsesquioxanes $T_8(C_6H_5COOH)_8$ were used as nanofillers and macromolecular cross-linkers to cure diglycidyl ether of bisphenol A (DGEBA) with formation of ester bonds [130]. The network structures of the obtained inorganic–organic polymer nanocomposites and cross-linking densities were modulated by varying the amount of $T_8(C_6H_5COOH)_8$. The cured samples of POSS/DGEBA were transparent, and a homogeneous dispersion of POSS within the DGEBA matrix was evidenced. The silsesquioxane molecules opened up the organic segments between two cross-linking nodes, leading to an increase in the intersegmental distance. Consequently, the segmental mobility increased, resulting in decreased mechanical modulus and improved toughness of the networks.

4.3.2 Hydrogen-Bonded 3D Networks

Three-dimensional supramolecular assemblies and special type networks can be constructed by controlled assembly of well-defined POSS building blocks via hydrogen bonds. For example, octakis[*N*-(6-aminopyridin-2-yl)-undecanamide-10-dimethylsiloxy]-silsesquioxanes (POSS-C11-Py), self-assembled through hydrogen bonds, formed a physically cross-linked polymer-like structure with good mechanical properties [131]. POSS-C11-Py was transformed into a supramolecular ionomer (HCl-doped POSS-C11-Py) with both quadruple hydrogen-bonding and ionic side arms [132]. The obtained network could be fabricated into films with hierarchical microphase separation. HCl-doped POSS-C11-Py exhibited high proton conductivity and can be used for the preparation of proton-exchange membranes.

POSS bearing residues of carboxylic acids are interesting building blocks due to the propensity of –COOH groups to the formation of stable dimers. A mixture of octa[2-(p-carboxyphenyl)ethyl] and octa[2-(4-carboxy-1,1′-biphenyl)ethyl] silsesquioxanes assembled to form an ordered hybrid two-component network [133]. Networks of complementary hydrogen bonds were also obtained with $Q_8M_8(CH_2CH_2–C_6H_4OH)_8$ bearing side phenol groups by blending with reactive diblock copolymers, such as poly(styrene-*b*-2-vinylpyridine) (PS-*b*-P2VP), poly(styrene-*b*-4-vinylpyridine) (PS-*b*-P4VP) and poly(styrene-*b*-methyl methacrylate) (PS-*b*-PMMA) [134].

The strength of the formed hydrogen bonds was found to be the key feature affecting the morphologies of the hierarchical structures (lamellae, cylinders, body-centred cubic spheres, disordered). Formation of a lamellar phase of thermoreversible characteristics was reported for supramolecular networks with blocks of octakis(vinylbenzylthymine-siloxy)silsesquioxane (OBT-POSS) and octakis[(vinylbenzyltriazolyl)methyladenine-siloxy]silsesquioxane (OBA-POSS) linked by intermolecular complementary hydrogen bonds between adenine and thymine residues [135].

Tetrakis(nicotinoxymethyl)methane (TNMM) and octakis[dimethyl(4-hydroxyphenethyl)siloxy]-silsesquioxane (OP-POSS) were used as tetrahedral and cubic building blocks for the preparation of thermally reversible, 3D hydrogen-bonded transparent network [136]. FTIR spectroscopy provided clear evidence for the formation of intermolecular hydrogen bonds between the OP-POSS and TNMM units. The blend of 40 wt% TNMM in OP-POSS exhibited a single glass transition temperature at 310 K, which is a compromise between Tg of OP-POSS (~293 K) and the melting temperature of TNMM (~340 K), and indicated the low degree of local intermolecular thermal motions.

Self-assembled supramolecular structures were generated in mixtures of multidiamidopyridine-functionalized POSS (MD-POSS) and both mono- and bis-uracil (U)-functionalized poly(ethylene glycols) (U–PEG and U–PEG–U) due to the formation of strong complementary multiple hydrogen bonds between the diaminopyridine groups and uracil moieties [137]. The polymer-like supramolecular materials exhibited improved thermal properties upon increasing the content of MD-POSS. The interactions of uracils with MD-POSS hindered completely crys-

tallization of PEG-U. TEM imaging indicated that the interactions in the symmetric U–PEG–U systems were stronger and their structures were relatively more ordered.

Hydrogen-bonded silsesquioxane networks can be applied as advanced materials in biomedicine. For example, $T_8[CH_2CH_2CH_2N(CH_2CH(OH)CH_2OH)_2]_8$ (POSS-AH) was used for the preparation of pH-responsive aggregates with natural polysacharide hyaluronic acid that can be applied as cell immune barriers, drug and gene delivery systems and chemical sensors [138]. Smart self-healing hydrogels were developed using self-assembled colloidal micelles of POSS-AH and poly(acrylic acid) (PAA) [139]. The micelles could be cross-linked in situ by hydrogen-bonding and ionic interactions between POSS-AH and PAA chains, as well as by covalent bonds linking PAA and bis(*N*,*N*′-methylene-bis-acrylamide). The ratio of reversible physical bonds *vs* chemical cross-links determined the mechanical properties of the hydrogels.

Supramolecular association of molecules bearing silanol (Si-OH) groups is interesting not only because of the formation of hierarchical architectures due to hydrogen bonding. Such systems can be also cross-linked by covalent siloxane linkages generated by the condensation of silanol moieties. The procedure provides a soft-chemical approach to well-defined silica-like materials with molecularly designed structures. Supramolecular lamellar crystals were prepared by hydrogen bond-directed assembly of Q_8MOH_8 with silanol groups [140]. The anisotropic 2D assembly of cubic POSS is different from the 3D assembly of organosilanol-modified cage siloxanes. Drying and thermal treatment induced solid-state polycondensation towards the formation of ordered siloxane networks. Hybrid networks that were synthesized using cage silsesquioxanes bearing diphenylsilanol groups were less ordered due to the steric hindrance provided by bulky diphenylsilyl moieties [141]. A range of hydrogen-bonded 3D crystalline porous materials were also made of POSS with eight organosilanol groups $T_8(CH{=}CHC_6H_4SiR_2OH)_8$ (*R*=*i*-Pr, Ph) [142]. Selective inclusion of hydrocarbons into large cavities of the obtained hydrogen-bonding networks with adjustable porosity was shown, depending on the pore size. Hydrocarbons such as hexane and heptane were included in the open frameworks without interpenetration of one network into another. Perpendicular stacking of the benzene cluster as a guest hydrocarbon in the pores of $T_8(CH{=}CHC_6H_4Si(i\text{-}Pr)_2OH)_8$ and $T_8(CH{=}CHC_6H_4SiPh_2OH)_8$ was also found (Scheme 10).

4.3.3 Metal–Organic Frameworks and Metal Complexes Forming Hierarchical Structures

A range of non-covalent ligand–metal interactions between organic moieties and transition metal centres have been used for the preparation of metal–organic frameworks (MOF) [143–147]. The main advantage of such structures is their dynamic nature. They can be sensitive to various external stimuli (e.g. temperature, pH, light, solvents, concentration, ultrasound), which gives the material an ability to alter its response. Moreover, modification of the metal ion or the structure of ligands can be used to tune the electrochemical, magnetic or optical responses. The formation of

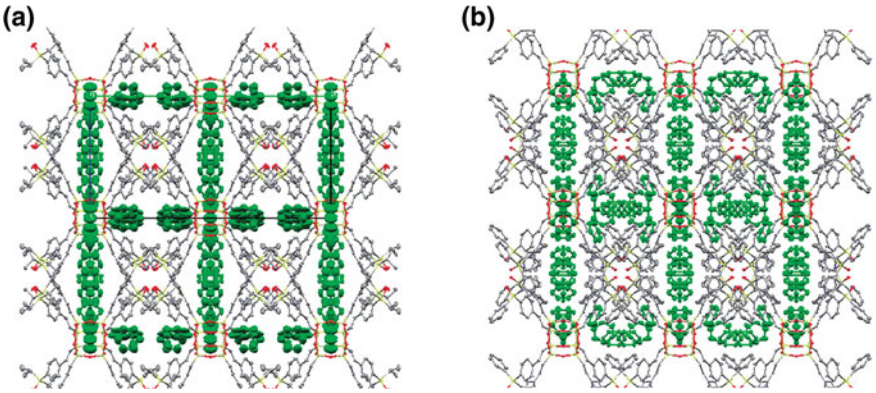

Scheme 10 Supramolecular 3D frameworks made of hydrogen-bonded POSS **a** $T_8(CH{=}CHC_6H_4Si(i\text{-}Pr)_2OH)_8$ and **b** $T_8(CH{=}CHC_6H_4SiPh_2OH)_8$ with included solvent molecules. Reprinted with permission from [142]. Copyright 2018 American Chemical Society

such long-range ordered/crystalline structures and extended networks requires the use of appropriate ligands with shape and functionality suitable for the coordinative ligation.

Octafunctional POSS can be successfully used as 3D ligands for the preparation of MOF. Rigidity of the inorganic cube used as a scaffold, as well as the presence of appropriate reactive groups at each silicon vertex, can increase effectively the symmetry of such hybrid networks and the concentration of doped metal cations. For example, metallo-supramolecular hybrid networks were obtained using $T_8[CH_2CH_2CH_2NHC(O)CH_2CH_2COOH]_8$ coordinated to copper ions [148] or terpyridine-functionalized POSS coordinated to Co(II) or Cu(II) [149]. The latter exhibited electrochromism during the cyclic voltammetry measurements, which makes them good candidates for electronic, optoelectronic and photovoltaic applications. The properties can be adjusted by the type of substituents at pyridine groups. The formed stable terpyridine metal complexes are completely reversible, and addition of a strong competitive ligand (HEDTA-Na_3) led to an efficient decomplexation. POSS decorated with eight terpyridine moieties were also used for the formation of 3D extended supramolecular structures by assembly with two different metal ions (Zn^{2+} and Fe^{2+}) (Fig. 8) [150]. TEM investigations further evidenced the tendency of 4metal@O-POSS to form a 3D organization with an irregular porous structure. The capability of the organic–inorganic hybrid network to trap solvent molecules was verified. Studies carried out with ^{1}H NMR as well as absorption and emission spectroscopy have shown that under selected conditions stable gels could be formed at room temperature. The gels were stable under ambient conditions.

The unique porous structure, large surface area and high pore volume make MOF especially attractive for catalysis, gas storage and separation or drug delivery [151]. They can be tailored for targeted chemical interactions but can also lose their crystallinity and pore ordering upon exposure to chemical compounds. Water can easily

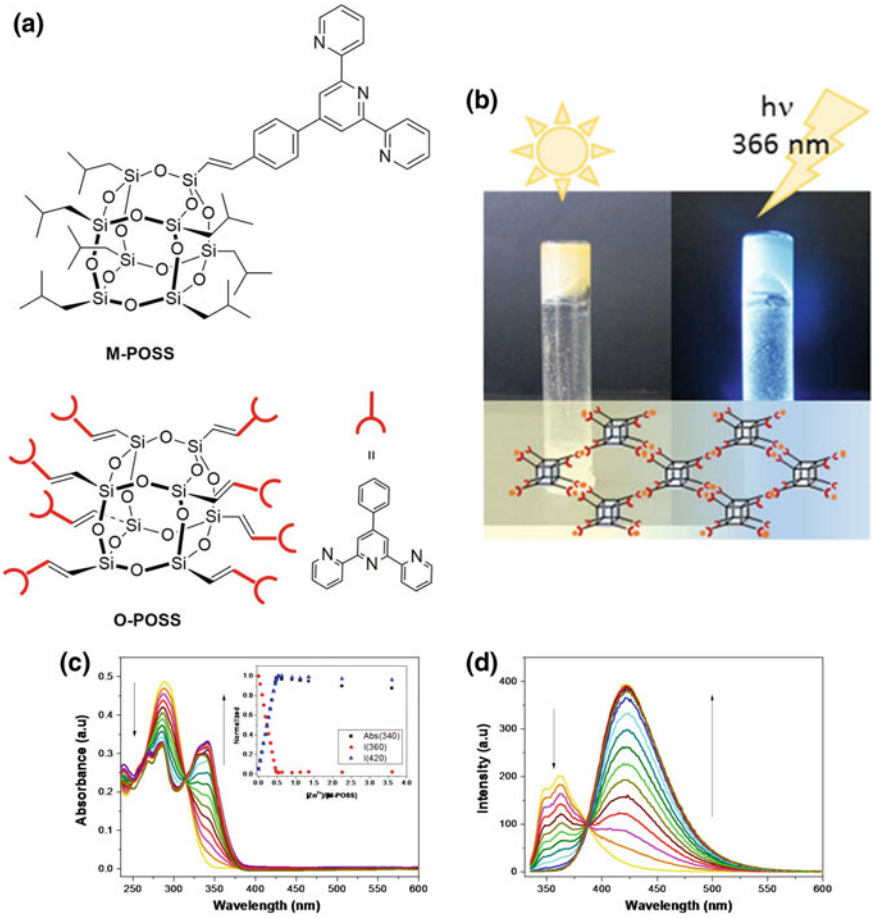

Fig. 8 **a** Structure of POSS bearing a single and eight terpyridine groups; **b** photograph of 4Zn@O-POSS gel without and with UV irradiation at 366 nm; **c** UV–Vis absorption spectra of M-POSS in CH_2Cl_2 (1×10^{-5} M) upon titration with $Zn(OTf)_2$ in EtOH (1.3×10^{-3} M) (the inset: normalized absorption changes at 340 nm (■) and the normalized emission intensity changes at 360 (●) and 420 nm (▲); **d** emission spectra of M-POSS in CH_2Cl_2 upon titration with $Zn(CF_3SO_3)_2$. Adapted with permission from [150] Copyright 2018 American Chemical Society

penetrate the pores and destroy the structure of some MOF by hydrolysis or replacement of ligands coordinated to metal centres. For example, porous MOF of copper trimesate [$Cu_3(BTC)_2$, HKUST-1] had large surface areas, high pore volume, relatively high chemical stability and good lability of coordinated solvents (including molecules of water) in the pores of the framework. The removal of coordinated water molecules from the $Cu_3(BTC)_2$ structure opens coordinatively unsaturated sites which is crucial for catalytic applications but detrimental for the stability of MOF. It is thus important to protect the structure of activated MOF against humidity,

retaining at the same time unhindered access of reagents to the inner parts of the network. Suitable POSS can be used for the purpose. For example, the stability of copper trimesate against moisture was enhanced by selective functionalization of the Cu sites on the outer surface of MOF with $T_8(i\text{-octyl})_7(CH_2CH_2CH_2NH_2)$ [152]. The protection of the surface of activated MOF against moisture was attributed to the hydrophobic nature of the long aliphatic chains. The same POSS were used for modification of other MOFs [low-symmetry rhombohedral MOF-74(Ni and Co) and high-symmetry cubic MIL-100(Fe)] [152]. The crystallinity of the MOF was intact during the modification, and the change of the mesoporous volume of MIL-100 was negligible due to the fact that the windows of MIL-100 are too small to let the POSS into the network. All the modified MOFs were hydrophobic, and $T_8(i\text{-octyl})_7(CH_2CH_2CH_2NH_2)$ successfully protected the outer metal sites on the surface.

In spite of not being formally MOF or MOF-related structures, some metal—POSS complexes can form unique hierarchical architectures. Their appropriate self-assembly can be used for the development of novel materials. For example, platinum(II) polypyridine complexes of d8 square-planar configuration exhibit interesting spectroscopic and luminescent properties due to Pt···Pt and π–π interactions. The characteristics can be changed by altering the molecular association and formation of metallogels or liquid crystals [153–155]. An alkynylplatinum(II) terpyridine complex functionalized with $T_8(CH{=}CH_2)_7$ groups exhibited solvent-induced self-association behaviour [156]. The obtained nanostructures were capable of "rings to rods" morphological transformations in media of different polarity due to the stabilization of Pt···Pt and π–π stacking as well as hydrophobic interactions between POSS moieties. Crystal-packing diagrams suggest a head-to-tail configuration for the dimeric structure. Other alkynylplatinum(II) terpyridine complexes functionalized with POSS exhibited multistage morphological transformations from spheres to nanoplates in response to solvent change through the interplay of hydrophilic, hydrophobic, Pt···Pt and π–π stacking interactions [157]. The intermolecular forces can be adjusted by appropriate structural modifications. If charged moieties were incorporated in the system, then drastic colour changes were observed in response to aggregation–disaggregation induced by changes in solvent polarity. The morphological transformations are associated with changes of spectroscopic characteristics and the complexes can be used as functional materials with sensing or imaging capabilities.

Functionalized POSS can be also complexed with lanthanide ions. Emission intensities of bare lanthanide ions Ln^{3+} are typically weak. Sensitization with organic ligands (the so-called antenna effect) can be a way to solve the problem. The use of POSS ensures uniform distribution of Ln^{3+} and prevents their aggregation at high concentrations. Hybrid luminescent complexes of Eu^{3+} and Tb^{3+} of highly saturated colour and good thermal stability were obtained with POSS dendrimers decorated with β-diketone moieties and incorporated in PMMA matrix [158]. Photo- and thermally stable complexes of Tb^{3+} and POSS bearing eight benzoic acid moieties also exhibited enhanced luminescent properties [159]. High luminescence combined with good stability and processability make those hybrid materials interesting candidates

for luminescent probes in bioassays, UV sensors, flat-panel displays, laser materials, optoelectronic devices as well as for crystal engineering.

4.4 Templating with POSS

Nanosized POSS, substituted on every corner of the inorganic cages with side groups acting as recognition units, are very interesting assembly motives. Formation of a "crystalline template" leading to controlled self-assembly of nanoparticles can be achieved by crystallization of POSS. It can be induced by intermolecular non-covalent interactions (hydrogen bonding, acid/base proton transfer and specific electrostatic forces) and allows for the formation of well-ordered hierarchical structures. Various self-assembling POSS has been applied as stabilizing templates for the preparation of metal nanoparticles, quantum dots and carbon dots. Owing to the presence of siloxane framework, POSS can be also used as sacrificial templates in porous materials.

4.4.1 Stabilizing Templates for Metal Nanoparticles

Nanoparticles (NPs) of noble metals (Au, Ag, Pd) exhibit unique physicochemical and electronic properties, different than those of bulk metal or metal atoms, due to the quantum size effect, high superficial surface areas and confinement of electronic states [160]. That is why, for example, nanocomposites containing Au NPs can act as ferromagnetics at room temperature despite the diamagnetic character of bulk gold [161]. Those peculiar properties make them very attractive for applications in advanced technologies, including optoelectronics, catalysis, sensing and biomedicine [162]. For example, palladium NPs of stable hierarchical structures are attractive for catalysis and hydrogen storage. Well-defined nanoparticles of silver can be applied as plasmonic devices, in photovoltaics, catalysis and for surface-enhanced Raman scattering (SERS) sensors. NPs of gold have high molar absorptivity in the visible region, but their aggregation results in colour changes due to mutually induced dipoles that depend on interparticle distance and aggregate size. The phenomenon can be applied in sensing systems. Bare metal nanoparticles can be prepared by employing various chemical methods (reduction of metal salts in solution) and physical techniques (laser ablation, resistive evaporation in vacuum, mechanic subdivision of metallic aggregates). However, undesired and uncontrolled aggregation and formation of droplets instead of well-dispersed films makes difficult preparation and use of such NPs in the condensed phase. It was found that the size and surface functionality of NPs of noble metals can be finely tuned using POSS as stabilizing templates.

Nanoparticles of gold can be stabilized via electrostatic interactions [163–166]. It was shown that pH-responsive Au NPs can be formed spontaneously on mixing $T_8(CH_2CH_2CH_2NH_3^+Cl^-)_8$ and tetrachloroauric acid under basic conditions [164]. Under the applied conditions, the amino groups reduce cations of Au(III) to Au(0) and

interact with the surface of Au NPs. The size of particle aggregates can be controlled by changing the molar ratio of $T_8(CH_2CH_2CH_2NH_3^+Cl^-)_8$ to Au NPs [165]. The affinity of Au NPs to organic solvents was modified via Michael addition of the aminopropyl groups on POSS to methyl acrylate. $T_8(CH_2CH_2CH_2NH_3^+Cl^-)_8$ was also used for the preparation of nanocomposites containing well-separated Au NPs. Amide bonds were formed in situ between the POSS moieties and COOH groups on the surface of gold primed with 11-mercaptoundecanoic acid [166, 167]. The phenomenon of electrostatic self-assembly allowed for the increase in interparticle spacing upon assembly with POSS. Modulation of the surface plasmon resonance band of Au NPs can be achieved in this way. A shift to higher wavelengths in solution and shift to lower wavelengths in the solid-state were observed as a result of different particle–particle dipolar interactions [167].

Sodium hydroxide was used to hydrolyse partially siloxane bonds of the adsorbed $T_8(CH_2CH_2CH_2NH_3^+Cl^-)_8$ to generate SiO^- species, which additionally stabilized Au NPs via electrostatic interparticle repulsion and hindered their aggregation [164]. The particles were pH-responsive, since addition of hydrochloric acid generated NH_3^+ ions that interacted with SiO^-, inducing reaggregation of NPs. It was also shown that $T_8(CH_2CH_2CH_2NH_3^+Cl^-)_8$ can help to the formation of well-dispersed homogenous NPs of silver, grown in a biphasic system on the interface between graphene oxide (GO) and $AgNO_3$ solution [168]. The obtained Ag NPs–POSS/GO nanocomposite can be used for electrochemical sensing of nitroaromatic compounds.

POSS bearing amine groups were also used as capping agents in the reductive growth of Pd nanocrystallites [169–171]. Studies on primary Pd NPs and their secondary aggregates suggest that the reductive growth of nanocrystallites can depend on the structure of POSS [169]. Uniform secondary Pd aggregates were obtained providing the POSS ligand was functionalized with amine groups in the hydrochloride form [$T_8(CH_2CH_2CH_2NH_3^+Cl^-)_8$]. The morphology of Pd core–shell NPs was determined by the ratio of self-interaction potentials of the ligands to their interaction with solvent. A correlation was found in Pd/POSS systems between sufficiently slow ligand diffusion kinetics of the reactive species and the growth rate of metal crystallites. Rapid diffusion of Pd prenucleating clusters was slowed by relatively slow-moving hydrochloride POSS ligands. It left time for reduction of NPs and their growth into nanocrystals. Pd nucleation does not seem to be preceded by formation of observable self-assembled POSS templates. DFT simulations suggested that the slow diffusion would result in regular spherical morphology of the aggregates, possibly due to the shift of the particle condensation equilibrium towards dissolution. More rapidly diffusing POSS ligands induced random structures and low solubility of nanoparticles after the syntheses.

$T_8(CH_2CH_2CH_2NH_3^+Cl^-)_8$ was used as well for stabilization and cross-linking of bimetallic microporous colloidal NPs made of Pd and Au [172]. The hybrid nanocomposites were generated by electrostatic interactions between Au NPs coated with 11-mercaptoundecanoic acid and aggregates of Pd capped with $T_8(CH_2CH_2CH_2NH_3^+Cl^-)_8$. The procedure resulted in precipitating of NPs of random shape. Stable colloids of spherical aggregates of Pd NPs coated with Au NPs can be obtained in a two-step process by reduction of palladium acetate in the presence of

$T_8(CH_2CH_2CH_2NH_3^+Cl^-)_8$ as a rigid template [171]. Bimetallic platinum–bismuth nanoparticles (Pt-BiNPs, 60% Bi) of blackberry-like morphology were prepared with $T_8(CH_2CH_2CH_2NH_3^+Cl^-)_8$ that played the role of both the morphology control agent and the carrier of electrocatalyst with corrosion resistance [173]. Their electrocatalytic activity (electro-oxidation of formic acid for fuel cell applications), effective CO tolerance and durability were enhanced with respect to commercial catalysts.

It was already mentioned that the surface of noble metals can be easily modified by chemisorption of thiols and sulphur-containing species. Several thiol-functionalized POSS were also used as protective ligands to stabilize NPs of Au, Pd or Ag in solution or as templates for their incorporation into thin films. POSS can also provide a synergistic effect for the surface coverage due to the presence of multianchor sites and hydrophobic interactions between POSS and the surface. For example, molecules of $T_8(i\text{-Bu})_7(CH_2CH_2CH_2SH)$ were applied as protective groups for the preparation of hybrid POSS-coated Au NPs of high stability in solid state [174]. Plate-like morphology of the POSS crystals led to the formation of a unique fern-like microstructure with hybrid POSS–Au NPs on its surface. Removal of the silsesquioxane templates resulted in sintering of nanosized Au islands. Au NPs covered with $T_8(i\text{-Bu})_7(CH_2CH_2CH_2SH)$ were also used for the preparation of polymer nanocomposites [161]. The particles were blended with poly(*n*-butyl methacrylate) randomly decorated with $T_8(i\text{-Bu})_7$ in the side chains. The increased compatibility between both components improved miscibility of Au NPs and the polymer matrix. The distribution of Au NPs was governed by interactions between POSS ligands grafted on the polymer chains and those adsorbed on the surface of gold.

Palladium NPs capped with POSS were prepared by ligand exchange of acetate groups on $Pd(OAc)_2$ with 1-dodecanthiol and $T_8(i\text{-Bu})_7(CH_2CH_2CH_2SH)$, followed by a thermal work-up [175]. High affinity of Pd to thiols led to the formation of cores composed of disordered aggregates. Nanosized storage vessels for Pd(0) atoms with transportation channels in the shell could be formed in this way. The nanoclusters were successfully employed as the catalytic system in a model Mizoroki–Heck coupling reaction.

Cubic silsesquioxanes not only can stabilize nanoclusters of noble metals, but also can provide reactive groups for chemical modification of the formed NPs shells. Diaminopyridine-functionalized octasilsesquioxanes (POSS-DAP) and thymine-functionalized gold nanoparticles (Thy–Au) formed well-defined and well-dispersed spherical aggregates on mixing due to the combined hydrogen-bond recognition and aggregation/crystallization of POSS moieties [176]. DAP units interact with Thy–Au nanoparticles through complementary three-point hydrogen bonds, and POSS nanoparticles were packed uniformly into larger nanocrystals. It was found that side-to-side rather than the face-to-face POSS–POSS packing was preferred. The same three-point hydrogen-bonding recognition motives were used for modification of gold surface covered with thymine-terminated self-assembled monolayers with DAP-functionalized POSS [177]. Hybrid inorganic–organic films were formed in this way showing that both chemical and physical nature of surfaces can be engineered by orthogonal deposition of POSS.

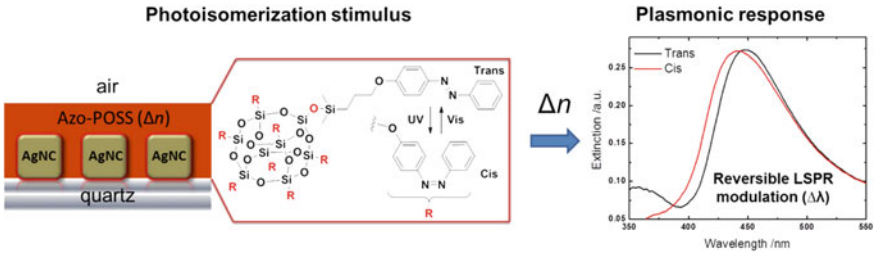

Fig. 9 Plasmonic response of Ag NPs coated with Azo–POSS matrix of adjustable refractive index. Reprinted with permission from [179]. Copyright 2018 American Chemical Society

The self-assembly process controlled by crystallization kinetics of POSS was employed for the preparation of hierarchical Ag NPs/POSS hybrids of branched morphology using $T_8(CH{=}CH_2)_8$ and $T_8(\text{cyclohexyl})_8$ [178]. Well-defined and stable Ag structures, which were left after the treatment on a hot plate at 523 K for 30 min in air, exhibited excellent SERS performance with high enhancement factors.

Hybrid POSS with azobenzene moieties in their side chains (Azo–POSS) were used as a stable photoactive coating for light-induced plasmonic modulations of embedded Ag nanostructures [179]. The refractive index of Azo–POSS conjugate could be altered owing to the *trans–cis* photoisomerization of azobenzene groups on irradiation with UV light (380 nm) (Fig. 9). The reversible changes resulted in 6 nm hypsochromic plasmonic shift in the plasmonic band of the embedded Ag NPs. Moreover, a polarization-dependent variation in reflectance was observed in the total internal refraction (TIR) regime.

POSS with polymeric chains grafted onto silsesquioxane cores were also used for the modification of the surface of noble metals. Hybrid polymer brushes with poly(ethylene glycol) (PEG) chains tethered to POSS via linkers containing thiolate moieties were chemisorbed on the surface of gold [180]. PEG-functionalized POSS were used to coat charged Au NPs of various shapes to aid their transfer into organic solvents [181]. Macromolecules built of thermoresponsive PNIPAM arms grafted to octahedral silsesquioxane core (POSS-*g*-PNIPAM) were explored as stabilizers for colloidal Au NPs [182]. Hybrid thermosensitive Au NPs were obtained. Their lower critical solution temperature (LCST) was decreased compared to POSS-*g*-PNIPAM.

A green solid-state synthetic method was implemented for the fabrication of POSS supported N-heterocyclic carbenes/imidazolium salts of palladium(II) complexes and well-dispersed Pd NPs of a very small size [183]. The prepared homogeneous and recyclable nanocatalyst was highly efficient in Suzuki–Miyaura cross-coupling reactions. The imidazolium moiety on POSS played a key role in the solubility of the catalyst.

Iron oxide nanoparticles can be used for many biological applications, including MRI contrast agents, magnetic separation or localization and thermal ablation. However, the effective use of magnetic nanoparticles depends on their size and composition, physical properties and surface chemistry capable of promot-

ing specific interactions with target biomolecules. Various octafunctional POSS were applied for preparation of well-dispersed metal oxide nanoparticles, biocompatible and transferable into aqueous solutions. For example, magnetic nanoparticles were prepared by exchange of the primary surface monolayer using anionic octa(tetramethylammonium)-POSS $\left(SiO_{4/2}\right)_8{}^{-}NMe_4{}^{+}$ (Fig. 10) [184]. They had excellent stability within biologically relevant pH ranges and salt concentrations and interacted with proteins via surface charge complementarity.

Interesting conjugated structures comprised of γ-Fe_2O_3 nanoparticles and PbSe nanocrystal quantum dots (NQDs) were prepared with the use of 2-aminoethanethiol and $\left(SiO_{4/2}\right)_8{}^{-}NMe_4{}^{+}$ hydrate [185]. Hydrogen bonds that were formed between water-soluble nanoparticles, PbSe NQDs functionalized with amine groups and γ-Fe_2O_3 NPs stabilized with POSS, allowed for hierarchical coupling and the formation of structurally conjugated fluorescing and magnetic nanoparticles. It was found that the hydrogen bonding occurred via the formation of a pseudo-ring, in which the $NH_3{}^{+}$ group was hydrogen bonded to the lone pairs of the siloxane oxygen in POSS and the O^{-} of the hydrate POSS was hydrogen bonded to one of the CH_2 groups in 2-aminoethanethiol (Scheme 11). The unique system can be used for biomedical applications such as biosensing, detection of cancer cells and drug delivery.

An amphiphilic star-shaped hybrid copolymer constructed of POSS core and poly(ε-caprolactone) arms terminated with β-cyclodextrin moieties assembled into hybrid micelles with hydrophobic POSS–PCL chain encapsulating Fe_3O_4 nanoparticles [186]. Good adsorption capacity of the hybrid micelles was shown in removal of bisphenol A from aqueous solutions due to the host–guest interactions with β-CD. The clusters were separated by an external magnetic field, which can be exploited for environmental protection. $T_8[CH_2CH_2CH_2NHCH_2CH_2CH_2Si(OEt)_3]_8$ was anchored on the surface of Fe_3O_4 nanomagnetics [187]. The resulting hybrid was employed as a magnetic nanocatalyst for high-yield synthesis of pyrans.

4.4.2 Stabilizing Templates for Quantum Dots

Colloidal quantum dots (QDs) are nanometric semiconductor particles of specific optical and electronic properties which can change as a function of both size and shape [188]. Because of their high photochemical stability, tuneable bandgap, high molar extinction coefficients, multiple exciton generation and strong light absorption, QDs are of wide interest and applicative potential for the preparation of transistors, LEDs, lasers, solar cells, quantum computing, bioimaging or inkjet printed semiconductors. The ability to control the structure of QDs is critical for the understanding of their collective properties and for the development of new materials and devices. Unfortunately, the undesired surface trap defects on QDs, induced by the dangling bonds of unsaturated atoms, are almost inevitable. They can cause low electron injection efficiency and high charge recombination in both the interior of QDs and at the interface with electrolyte. It limits severely the application of QDs in photovoltaics. Therefore, it is highly desirable to passivate surface defects on QDs. The trapping

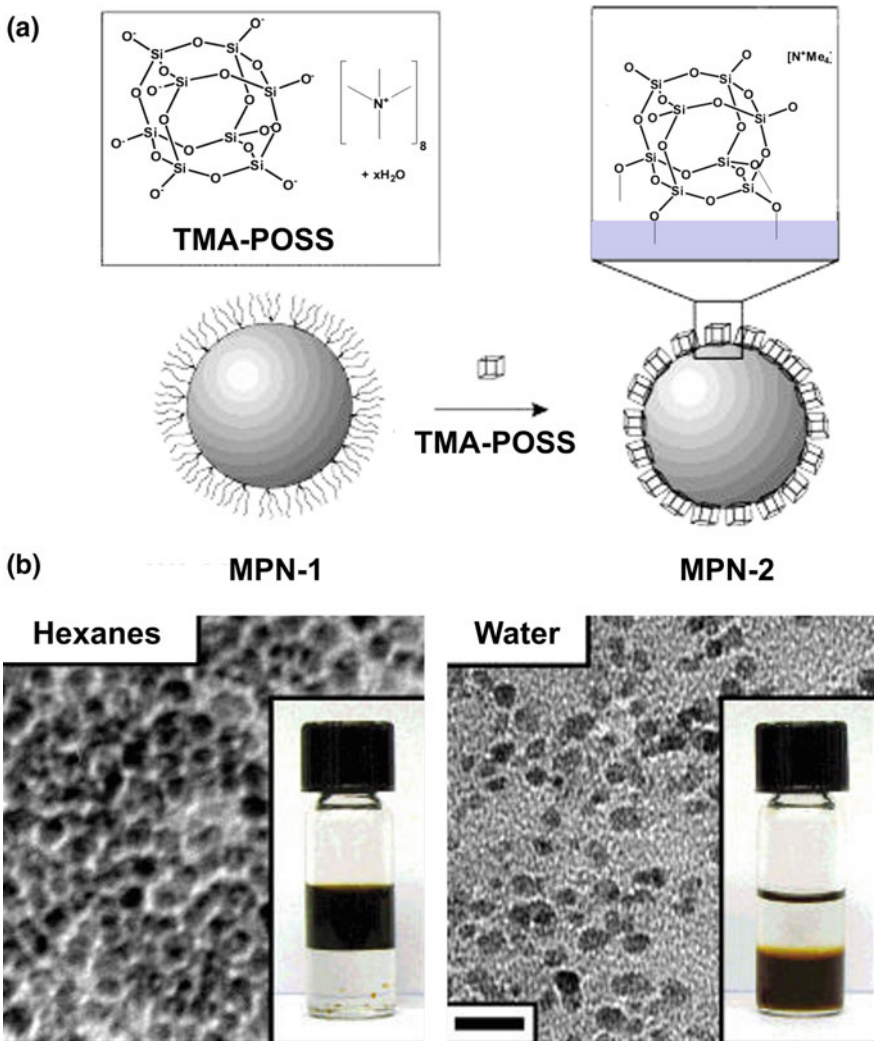

Fig. 10 Magnetic nanoparticles stabilized with $(SiO_{4/2})_8^-NMe_4^+$: **a** passive ligand exchange of the surface monolayer resulting in water-soluble nanoparticles; **b** TEM images of the primary magnetic nanoparticles (in hexanes) and the modified with POSS (in water). The insets show the transfer of particles from non-polar to polar solvent after the exchange (scale bar = 20 nm). Reprinted with permission from [184]. Copyright 2018 American Chemical Society

states can be efficiently suppressed by coating core QDs with small molecular ligands. POSS can also serve for the purpose as high-performance surface modification agents that can play an important role in the spatial stability. The bulky inorganic cage-like core of POSS makes them ideal steric stabilizers. It results in the forma-

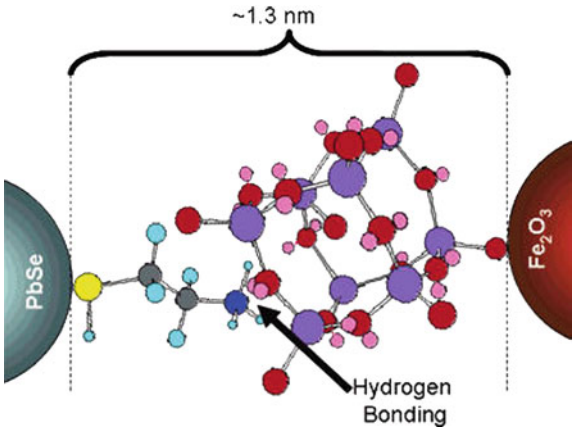

Scheme 11 Structure of a pseudo-ring made of hydrogen bonds between PbSe NQDs with grafted 2-aminoethanethiol and γ-Fe_2O_3 NPs stabilized with POSS. Reprinted with permission from [185]. Copyright 2018 American Chemical Society

tion of an inorganic shell around the core QDs (core/shell structure). POSS can also provide QDs with useful functionalities.

The presence of $T_8(i\text{-Bu})_7(CH_2CH_2CH_2SH)$ on the surface of CdSe QDs improved the photoelectric current, reduced the surface defects and increased the system stability [189]. The modified wurtzite phase QDs of variable sizes capped with POSS (Fig. 11) had desirable light-emission characteristics including photoluminescence quantum efficiencies and fluorescence lifetimes. They were used as efficient photosensitizers for TiO_2 nanotube (TNT) electron acceptor arrays. The silsesquioxane shell allows for the access of small electrolyte ions and electron transport from the surface of QDs. The $T_8(i\text{-Bu})_7(CH_2CH_2CH_2SH)$/CdSe QDs/TNT system exhibited better performance than the conventionally stabilized QDs. The prospective applications of such materials include memory devices, solar cells and semiconductor chalcogenide aerogels. It was also shown that simultaneous use of SH-POSS alongside two other ligands (mercaptosuccinic acid and D-cysteine) favourably reduced the cytotoxicity of CdTe QDs [190].

Well-defined aggregates of QDs with chemical cross-linkers offer desirable collective properties that cannot be found in the individual constituents. The effect depends on the size and nature of the components, the interparticle spacing and their hierarchical organization. Non-covalent assembly is a critical strategy to regulate both spacing and structure. Spherical nanohybrids made of $T_8(CH_2CH_2CH_2NH_3^+Cl^-)_8$ and Mn-doped ZnS QDs capped with 3-mercaptopropionic acid, spontaneously self-assembled in aqueous solutions and were used for quantitative detection of DNA [191]. It was shown that negatively charged phosphate groups in DNA double helix competed with negatively charged QDs in the formation of stable complexes with $T_8(CH_2CH_2CH_2NH_3^+Cl^-)_8$. Molecules of $T_8(CH_2CH_2CH_2NH_3^+Cl^-)_8$ were also used as capping agents to decrease surface defect density of CdTe QDs and to increase their power conversion efficiency (PCE) [192]. The current density and PCE of solar cells made of the POSS modified species was improved with respect to their analogues with bare CdTe QDs.

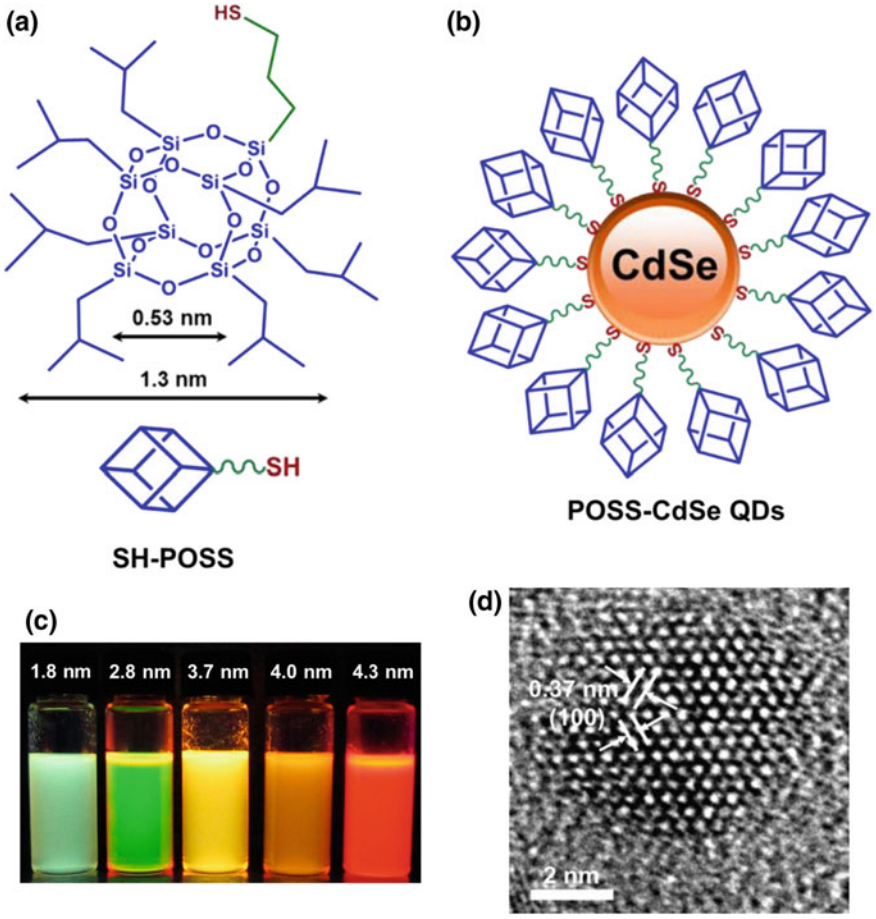

Fig. 11 **a** Chemical structure of $T_8(i\text{-Bu})_7(CH_2CH_2CH_2SH)$ and **b** schematic drawing of a CdSe QD capped with the POSS ligands; **c** the photoluminescence colour change of the POSS-CdSe QDs under a UV lamp during the growth; **d** HRTEM image of POSS-CdSe QDs. Adapted with permission from [189]. Copyright 2018 American Chemical Society

Carbon quantum dots (CDs) are nanosize carbon particles (<10 nm in size) of strong and tuneable fluorescence emission properties [193]. They can be used in biomedicine, optoelectronics, catalysis and sensing. The surface of CDs, characteristically covered with reactive COOH or OH groups, can be chemically modified and passivated with various organic, polymeric, inorganic or biological materials. By surface passivation, the fluorescence properties as well as physical properties of CDs (including dispersibility in various solvents) can be adjusted. CDs were functionalized with $T_8(i\text{-Bu})_7(CH_2CH_2CH_2NH_2)$ to make them superhydrophobic and enhance their photoluminescence and thermal stability [194]. The obtained nanohybrids can be applied as composite fillers, fluorescent liquid marbles and solid-state fluorescent

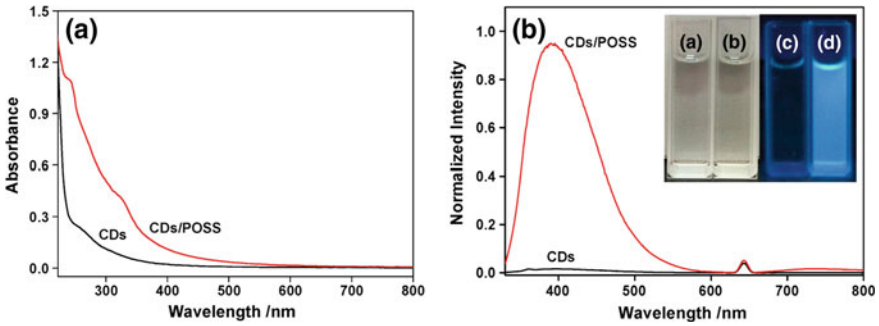

Fig. 12 **a** UV–Vis spectra and **b** fluorescence spectra for the bare CDs and POSS functionalized carbon dots (Cds/POSS) [the inset picture of bare CDs and CDs/POSS under visible (a/c) and UV (b/d) light]. Reprinted with permission from [195]. Copyright 2018 American Chemical Society

sensors. $T_8(CH_2CH_2CH_2NH_3^+Cl^-)_8$ was used as a passivation agent for CDs via formation of amide bonds with carboxylic groups on the surface of CDs [195]. The obtained CDs/POSS were dispersed in aqueous media. In addition to the characteristic features of carbon dots, they exhibited photoluminescence with quantum yield of 24% (Fig. 12), resistance to photobleaching and excellent photoluminescence stability in the presence of biological samples. Both the photoluminescent emission wavelength and the fluorescence intensity depend closely on the size of CDs. The hybrid CDs/POSS can be used for multicolour imaging in biological systems, as it was demonstrated with HeLa cells and MCF-7 cells. Water-soluble molecules of $\left(SiO_{4/2}\right)_8^-NMe_4^+$ were applied as a solid matrix for embedding water-soluble N,S-*co*-doped carbon dots [196]. Highly efficient solid-state luminophores with strong deep blue emission and a very high photoluminescence quantum yield (60%) were obtained.

4.4.3 Sacrifice Templates for Microporous Carbon Supercapacitors

Nanostructured carbon materials, such as graphene, graphene oxide, carbon nanotubes and fullerenes, have been considered promising candidates for a wide range of applications including organic electronics, supercapacitors, semiconductor devices and energy-storage materials [197]. Carbonization of organic precursors in the presence of various templates allows for the replication of the latter in the structure of the final product [198]. The characteristics of templated mesoporous carbons depend both on the employed carbon precursors and the template. The pore size and its distribution are of major importance in determining the performance of porous carbons used as electrode materials of supercapacitors. The maximum electrochemical double-layer (EDL) capacitance is delivered by microporous carbons of monodisperse pore size that matches the size of the desolvated/bare electrolyte ions. The presence of hierarchically interconnected pores or combination of interconnected

micro-/mesopores is an important parameter that can improve the electrochemical efficiency of carbon materials.

The physical and chemical functionalization of the carbon nanomaterials with POSS towards the development of novel hybrid nanostructures was very effective. POSS building blocks can be applied simultaneously as a carbon source and as sacrifice templates for generation of microporous carbons of hierarchical structure. Chemically cross-linked SixOy cage clusters embedded in N-doped carbon were prepared by thermal treatment of $T_8(CH_2CH_2CH_2NH_3^+Cl^-)_8$ in an inert environment [199]. Nanoscale Si-rich clusters distributed in a lighter matrix of N-doped carbon were formed at 1173 K due to chemical cross-linking and carbonization of the side chains of POSS. The material exhibited stable and high cycling, as well as rate capacity when used as a lithium-ion battery anode. The results can be ascribed to the "island–sea" morphology for the "clusters-in-carbon" hybrid structure that enhances interfacial interactions and facilitates charge conduction. Moreover, the small size of clusters with less compact Si–O active sites allow for smooth and complete lithium insertion/extraction. Such electrochemical properties are promising for energy-storage devices.

Molecules of T_8Ph_8 were used for the preparation of well-defined microporous carbon nanospheres [200–202]. The synthetic process included cross-linking of organic components and induced phase separation. It was followed by carbonization and subsequent removal of monodispersed silica domains [200]. The obtained porous material had large specific surface area, as well as excellent adsorption and supercapacitance properties. Ultrasmall Si particles were embedded in carbon matrix with this simple Si-carbon integration strategy. The downsizing of silicon particles in conductive carbon matrix of porous structure enhanced lithium-ion storage performance of Si-based anode [201]. Friedel–Crafts cross-linking of T_8Ph_8 shells resulted in the formation of continuous polymeric nanospheres with inorganic nanosilica wrapped in. The cross-linked nanospheres were converted into porous carbon matrix after high-temperature carbonization treatment and magnesiothermic reduction. Silsesquioxane cages (1.0 nm) were reduced and transformed into ultrasmall Si particles (4–10 nm).

A covalent bond-induced surface-confined cross-linking of T_8Ph_8 was used to construct 1D coaxial microporous carbon composites of the core made of carbon nanotubes (CNT) enveloped by microporous carbon shells ("CNT@micro-C on Fig. 13) [202]. The POSS building blocks were attached to the surface of acylated CNT. A cross-linked layer was formed with the thickness tailored from 6 to 20 nm. It was transformed into a microporous coating after carbonization of T_8Ph_8 and etching of the inorganic cages (BET surface area of about 570–1300 m^2/g). The obtained CNT@micro-C combined the structural advantages of CNT and microporous carbon (large surface area, high electrical conductivity, fast ion transfer speed and short ion transfer distance). CNT serves as electron motion pathway, and the 3D stacked microporous tube accelerates ion transfer rate and shortens ion transfer distance. As a consequence CNT@micro-C revealed superior supercapacitive performance (capacitance retention up to 86%) and can be used as an electrode material.

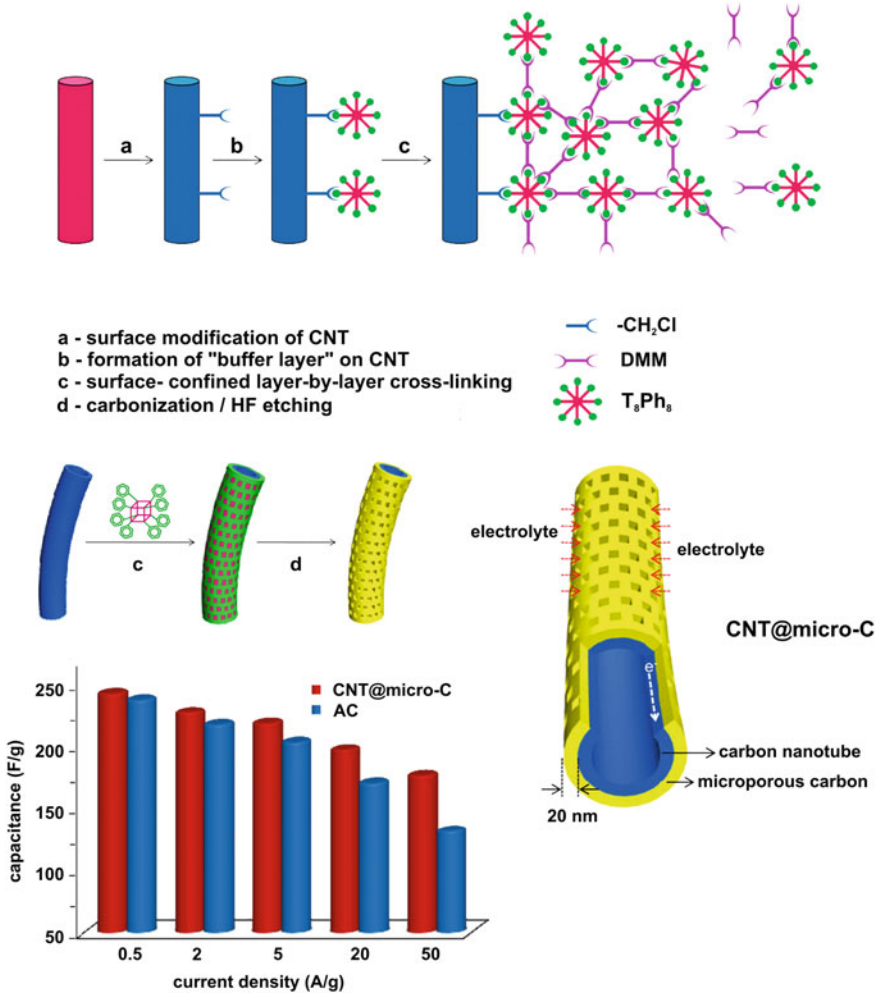

Fig. 13 Preparation and capacitive performance of 1D coaxial microporous carbon composite in the process of surface-confined cross-linking of T_8Ph_8 on the surface of CNT. Adapted with permission from [202]. Copyright 2018 American Chemical Society

Hierarchically porous carbon structures of high specific surface area (>2000 m^2/g), large pore volume and very good power performance were also formed by self-assembling of $T_8(C_6H_5NH_2)_8$ in the presence of block copolymers (Pluronic F127 and Pluronic F108) [203]. The block copolymer-assisted method combined the molecular-scale templating effect of POSS and good compatibility between aminophenyl groups and the block copolymers. Highly ordered mesopores (~4 nm) were formed due to soft templating by Pluronics. Two-dimensional hexagonal (p6 m) or body-centred cubic (Im3 m) mesopore arrangement could be obtained

by adjusting the composition of block copolymers. The presence of POSS template resulted in uniform micropores of ~1 nm diameter in the walls between mesopores. The mesopores facilitated fast transport of ions to fine micropores. Specific capacitance of the porous carbons after ~4 wt% nitrogen doping reached ~160 F/g in an ionic liquid electrolyte and ~ 210 F/g in 1 M H_2SO_4 aq.

4.5 POSS-Containing Hybrid Materials for Optoelectronics

POSS are suitable platforms for the preparation of high-performance materials of unique optoelectronic properties. Incorporation of POSS into organic matrices is of significant interest because of their distinct hybrid nanostructures, confined size effect and physical properties [204, 205]. The inorganic core does not show any significant optical properties and electronic conjugation. The small silica-like cage acts as a nanoparticle filler, and the organic substituents increase their compatibility with organic compounds. The rigid silsesquioxane core not only reinforces the mechanical properties of materials, but also acts as a isolating barrier because of its low thermal conductivity and small dielectric constant. The so-called nanoporous low-j materials of low electric constant are of high demand in microelectronics. They can be prepared by introducing air-filled voids into the bulk. The presence of closed nanopores, homogeneously distributed in the matrix, is required to preserve the electric and mechanical properties. It was found that dielectric constant of polyimide nanocomposites with grafted methacrylate (MA) side chains containing POSS can be tuned by varying the molar ratio of the grafted MA-POSS in the copolymer [206, 207]. POSS molecules formed crystalline nanoaggregates that could act as an isolating barrier. Materials of dielectric constants close to 2.2 were achieved if PI-*g*-PMA-POSS contained 23.5 mol% MA-POSS.

The enhancement of the optoelectronic performance is important for the development of organic light-emitting diodes (OLEDs), liquid crystal displays, AIE-based sensors and biodevices or electrochromic devices. Excessive π–π stacking in many organic luminescent materials causes a significant drop in their quantum yield in the solid state. The undesirable behaviour can be suppressed by generation of 3D structures with POSS scaffolds. The change of the crystal lattice leads to aggregation-induced emission (AIE) effects [208]. Analogously, POSS can disrupt conjugated polymer packing in electrochromic materials. It facilitates free ion movement and creates more accessible sites for the redox reactions.

4.5.1 Luminescent Materials

Derivatives of pyrene (Py) show characteristic large Stokes shift, strong absorbance, high quantum yield and good photochemical stability [209, 210]. The emission of monomeric pyrenes can be found in the ultraviolet part of the electromagnetic spectrum (380 nm), while the excimer emissions are in the range of 450–500 nm. Those

properties can be of advantage in light harvesting systems, especially if the energy is transferred from pyrene excimers to spectrally suitable acceptors. An efficient antenna system should have a very high molar extinction coefficient, excellent photostability and ability to transfer the energy. However, many hydrophobic organic luminophores (especially planar polycyclic aromatics) are efficient light emitters only when molecularly dissolved or dispersed in good solvents. In solid state, they require the presence of separators that would simultaneously prevent the excessive stacking and direct the luminophores in the solid state into their most perfect organization. Pyrene derivatives, due to their high quantum yield and strong affinity with various analytes, are widely used as fluorescent probes to study dynamics and conformational changes of polymers and biomacromolecules [211]. However, it is hard to prepare thin fluorescent Py films that would exhibit strong excimer emission in the solid state. In spite of pure excimer fluorescence of pyrene crystals, the spin-coated thin films of pyrene and its derivatives frequently exhibit weak or no excimer emissions due to the random packing of pyrene rings as a result of rapid evaporation of solvent during the coating process. Moreover, if the films are to be used as sensors, then Py rings should not be aggregated too tightly in order to allow for diffusion of analytes. The use of POSS substituted pyrenes can be a good solution to both problems. Simulation of electronic structures of T_8Ph_8 indicated that the highest occupied molecular orbitals (HOMOs) as well as the lowest unoccupied molecular orbitals (LUMOs) were localized on phenyl side groups [212]. It means that star-shaped organic luminescent dyes grafted on 3D POSS molecules can be less prone to self-quenching and have improved quantum efficiencies in photoluminescence and electroluminescence.

Indeed, the results obtained with several POSS-Py systems show the desired effect. For example, a supramolecular star-like, blue-light electroluminescent material with 4-uracilbutyl-1-methylpyrene units linked to the silsesquioxane core via a triple hydrogen-bonding array (U-Py/ODAP-POSS) exhibits strong and stable fluorescence emission and high quantum efficiency even at high temperatures (423 K) [213]. Good solution processing of U-Py/ODAP-POSS allowed for the preparation of an electroluminescence device of higher maximum brightness and higher luminance efficiency than those of the parent pyrene derivative. An organic–inorganic light-emitting material based on POSS grafted with dipyronecarbazol moieties (POSS–DPCz) is an effective chromophore with substantially improved fluorescence-colour purity and quantum yield compared to control DPCz without incorporated POSS [214]. The introduction of POSS within the chromophore matrix promoted the formation of 3D hierarchical nanostructures. POSS-DPCz exhibited excellent optoelectronic properties and high thermal stability, solution processability, good film-forming ability and efficient control of POSS dispersion. Photoluminescence and electrochemical analyses indicated, both in solution and in the thin films, that POSS cages effectively suppressed aggregation and enhanced the colour stability of DPCz. Spin-coated thin films of ester of 1-pyrenebutyric acid and $T_8(i\text{-Bu})_7$ bearing a single 1-(2,3-propanediol)propoxy chain (PBPOSS) exhibited strong excimer emissions at 475 nm when excited at 350 nm [215]. Spectroscopic studies indicated that the crystallization of silsesquioxane moieties in the films induced the formation

of pyrenyl excimers. A very fast fluorescence quenching was observed upon exposure to the vapours of nitroaromatic compounds. An eight triphenylamino-pyrenyl substituted POSS was designed as a highly sensitive and efficient sensing material of 3D symmetrical spatial conformation, high area-to-volume ratio, high molar extinction coefficient, multiple exciton transfer path and energy level suitable to detection of nitrate ester explosives [216].

Hybrid pyrene–silsesquioxane molecules with two pyrene rings anchored to a single inorganic core via flexible ether bonds (BPy-POSS of "butterfly-like" structure) were designed in order to enrich the fraction of intrinsic intramolecular pyrene dimers on the surface of ordered thin films made of $T_8(i\text{-Bu})_7$ [217]. Silsesquioxane moieties act as crystalline templates through POSS–POSS recognition and direct assembling of Py groups. The emission spectra of BPy-POSS in dichloromethane contained a large share of intramolecular and intermolecular excimers. The result was attributed to the easy rotation of two adjacent ether bonds and the π–π interactions of aromatic rings that facilitate the formation of pyrenyl dimers or aggregates. The fluorescence quenching was observed upon exposure to the vapours of nitrobenzene.

Interesting results were obtained with $T_8(CH{=}CH\text{-}Py)_8$ that exhibits enhanced fluorescence emission from pyrene–pyrene excimers. It was used for the preparation of solution processable emitting materials for OLEDS [218]. It was also shown that such hybrid systems can act as effective fluoride ion sensors in solutions with a π–π^* fluorescence enhancement or quenching, depending on the polarity of the solvent used [219]. The fluorine anion was pulled into the confined space of the silsesquioxane cage owing to electrostatic interactions with electron-deficient silicon atoms. The F^- ion occupies the central position within the cage, which resulted in a slight compression of the silsesquioxane framework [220, 221]. $T_8(CH{=}CH\text{-}Py)_8$ exhibited a significant fluorescence of pyrene–pyrene through space excimers in DMSO, while π–π^* fluorescence emission of monomeric pyrenes was dominant in THF. Fluoride encapsulation in high polarity solvents such as DMSO resulted in increase in the distance between Py groups and diminished the pyrene–pyrene fluorescence but enhanced π–π^* fluorescence emission. In THF, the POSS-F^- complex exhibited a significant excimer emission. The π–π^* effect was quenched and a colour change from light yellow to deep orange was observed as a result of the postulated formation of a charge-transfer (CT) complex among the pyrenyl rings.

Perylene diimide (PDI) is structurally related to pyrene (Fig. 14). Derivatives of PDI have attracted a significant attention as organic semiconductors due to their chemical and photochemical stabilities, as well as high extinction coefficients. The ordered supramolecular structures of perylene derivatives can be also applied as organic electronic devices, such as light-emitting diodes, photovoltaic devices, organic field effect transistors or electron transfer cascades. The self-assembling abilities of PDI and formation of one-dimensional nanostructures due to π–π interactions enable efficient long-range charge migration and increase the electrical conductivity. However, the extended π–π stacking can cause solution-processing problems as well as a significant drop of fluorescence quantum yield in concentrated solutions and in the solid state.

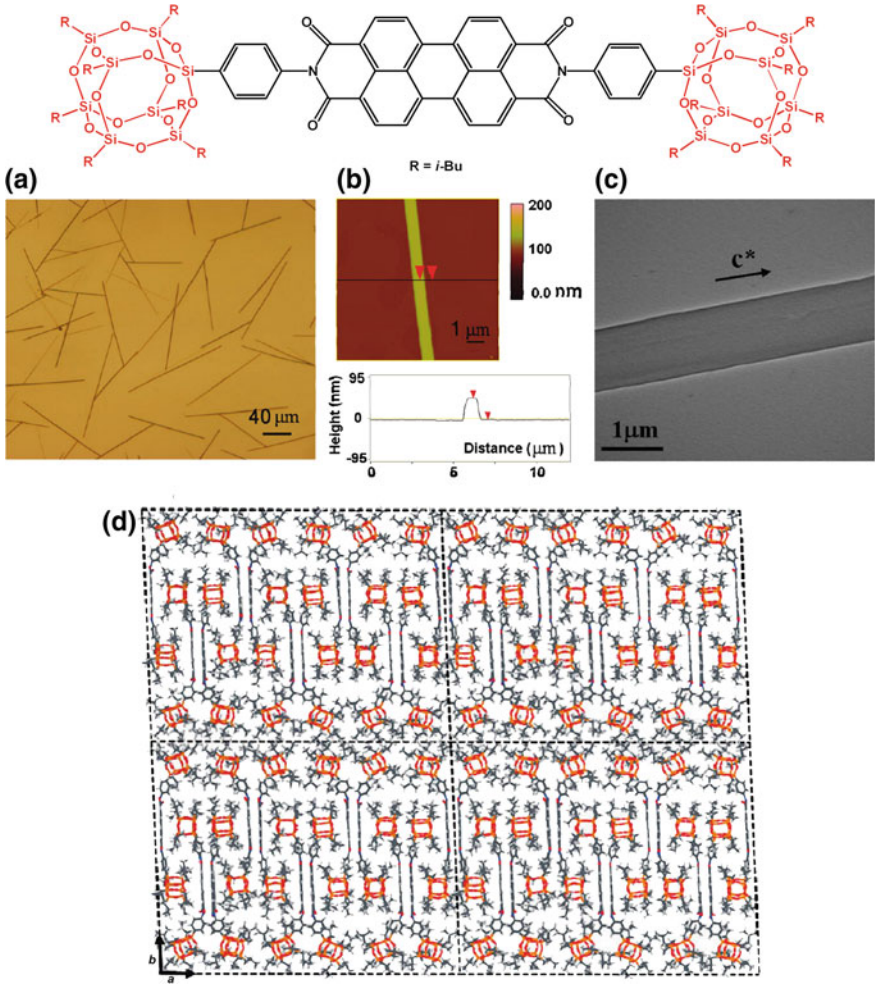

Fig. 14 **a** Optical microscopy image of single-crystalline nanobelts of POSS–PDI–POSS hybrid; **b** AFM image and a line-scan profile of the flat top of single-crystalline nanobelts and **c** TEM bright-field image of a single-crystal nanobelt; **d** molecular packing in the crystal lattice. Adapted with permission from [223]. Copyright 2018 American Chemical Society

Sterically hindered substituents, such as POSS, grafted at imide positions or bay regions of PDI can help to overcome these drawbacks and supress the undesirable effects. Microwave condensation of $T_8(i\text{-Bu})_7(CH_2CH_2CH_2NH_2)$ with a range of mono- and bis-anhydrides yielded the corresponding POSS imide derivatives including bis-phthalic POSS imide, bis-naphthalic POSS imide and bis-perylene POSS imide [222]. The latter displayed particularly strong fluorescence, with quantum yield approaching unity, while the photoluminescence of naphthyl bis/monoimide analogues was only very weak. The X-ray crystal structure of bis-perylene POSS

imide indicated good separation of perylene moieties. PDIs with bulky POSS substituents exhibited a unique supramolecular structure with a discrete dimer packing scheme, which can enhance fluorescence quantum yield in the solid state. Uniform and ultralong crystalline nanobelts with dimensions of 0.2 mm × 1 μm × 50 nm were self-assembled directly by slow evaporation of THF solutions containing symmetric POSS–PDI–POSS hybrids with rigid 1,4-phenylene linkers between the perylene moiety and side $T_8(i\text{-Bu})_7$ groups [223]. The steric hindrance of POSS makes it difficult to achieve a continuous stacking of PDIs. Instead, the molecules dimerized to maximize the π–π interactions and then packed as interdigitating building blocks. Crystal structure consists of six dimers as one supramolecular motif in one triclinic unit cell. It can account for anisotropic crystal growth and the nanobelts formation. Similar phenomena were noted for POSS–PDI–POSS with $T_8(i\text{-Bu})_7$ covalently attached to the PDI linker via flexible spacers [208]. The macromolecules formed ultralong crystalline microbelts with a length of several hundred micrometres. In the first step, the molecules formed dimeric structures (both in solution and in the solid state) that become building blocks of a monoclinic crystal lattice. Quantum yields of 100% (in solution) and 17.5% (in the solid state) were observed. The material was applied as a high-performance colorimetric and ratiometric fluorescent probe for rapid detection of fluoride anions.

However, the presence of bulky groups in PDI molecules does not inevitably promote the improvement of fluorescence quantum yields in the solid state. The self-aggregation behaviour of a series of symmetric PDI bisimide derivatives with bulky $T_8(i\text{-Bu})_7$ groups at imide nitrogens and bearing also side groups at the bay positions of the PDI spacer was studied [224]. The presence of POSS did not have large effects on the spectroscopic properties of PDIs in solution but changed the packing structure of the molecules and their emission in the solid state. It was found that fluorescence quantum yield in the solid state was determined by the type of packing structure. Most of the studied molecules were packed in a "face-to-face" mode, but with different longitudinal displacement. "J"-type interactions between the neighbouring molecules and improved quantum yields were observed if the longitudinal displacement was large. Small positional shifts resulted in "H"-type interactions and poor quantum yields.

Unsymmetrical hybrid PDI–POSS derivatives are well soluble in common organic solvents and show typical absorption and emission features of the perylene diimide fragment in solution, with a quantum efficiency close to unity [225]. The electronic absorption spectra of both, spin-coated films and powders, indicated a reduced fluorophore aggregation and significant quantum yield efficiencies (QY up to 70%) owing to the effect of POSS. Unsymmetrical POSS–PDI derivatives were also used for the preparation of more elaborated macromolecules and sensing systems. An amphiphilic fluorescent polymer of controlled molecular weight and low polydispersity, containing PDI and POSS, was synthesized by grafting perylene anhydride with $T_8(\text{iBu})_7(CH_2CH_2CH_2NH_2)$ and 2-bromoisobutyryl bromide to produce an ATRP macroinitiator for the radical polymerization of N-isopropylacrylamide [226]. Self-assembly of the resulting amphiphilic macromolecules was studied in aqueous solutions. It was found that the hybrid nanoparticles exhibited attractive high red

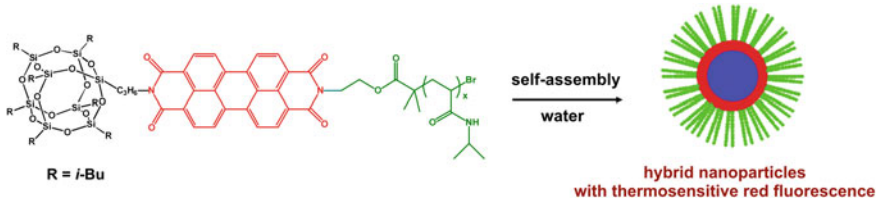

Scheme 12 Thermoresponsive micelles formed by self-assembled POSS–PDI–PNIPAM macromolecules. Reprinted with permission from [226]. Copyright 2018 American Chemical Society

fluorescence at 645 nm due to the incorporation of bulky POSS moieties. The fluorescence intensity of the self-assembled hybrids could be tuned due to the presence of thermoresponsive PNIPAM coronas (Scheme 12).

POSS were also applied as scaffolds for the preparation of other thermally stable solid-state emissive materials [20]. POSS decorated with rigid linear π-conjugated luminophores at each of eight vertices of silsesquioxane core formed intermolecular excimers in dilute solutions. However, the intrinsic luminescent properties of the monomer could be recovered if bulky alkyl chains were introduced to the luminophores. Similar optical properties were observed in the solid state, regardless the increase in steric hindrance. The preservation of electronic states and the lack of non-specific intermolecular interactions in the condensed state were attributed to the presence of rigid 3D inorganic scaffolds and the specific radial distribution of luminophores around the silica cubes. It was also demonstrated that the POSS-based hybrids exhibited bright blue emission beyond 473 K in the open air, which is interesting for advanced electroluminescent devices, displays and sensors. Hard-sphere-like aromatic polyamide dendrimers with POSS cores were synthesized up to the sixth generation using the divergent approach [227]. The intrinsic viscosities of the dendrimers reach the maxima at the fifth generation and have squashed sphere shapes on mica substrates even for the sixth generation. The shells of high-generation dendrimers are rigid owing to the restricted molecular motion of the crowded peripheral units. More intensive fluorescence emission was observed on increasing the generation number of dendrimers terminated with trifluoroacetamide groups, which points to the role of the constrained terminals in the enhancement of photoluminescence.

4.5.2 Liquid Crystals

Polyhedral silsesquioxane cores were also used for the preparation of disc-like or rod-like species of true liquid crystalline (LC) properties. The packing mode and the type of mesophase in such POSS-LC systems depends generally on side mesogens tethered to the inorganic core and their propensity towards formation of mesomorphic phases [228, 229]. However, despite the pseudo-spherical geometry of the core, molecules of POSS bearing long rigid mesogens typically are of cylindrical or rod-like shape and tend to form lamellar enantiotropic smectic A and smectic C phases

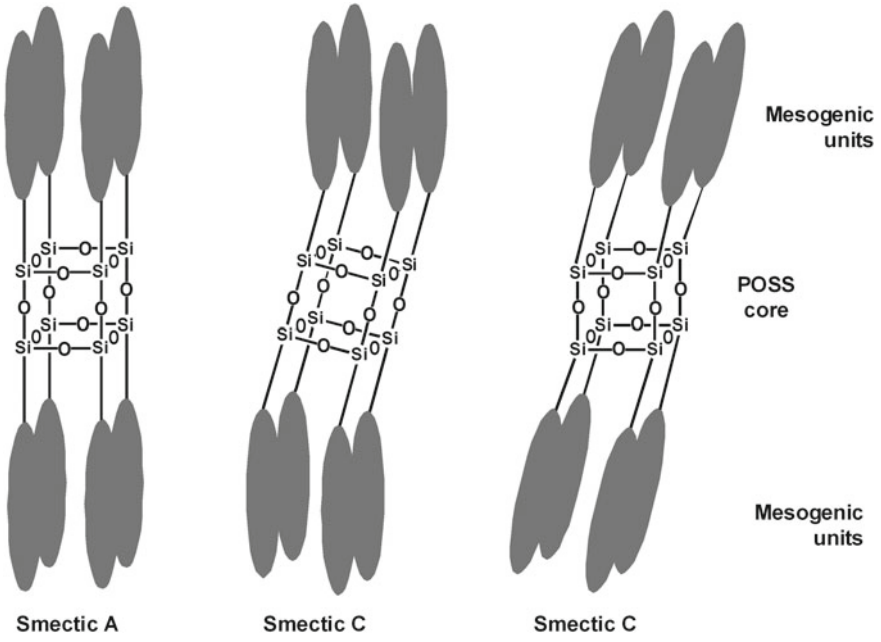

Scheme 13 Distribution of side groups with respect to the inorganic core in lamellar enantiotropic smectic A and smectic C phases formed by POSS grafted with long rigid mesogens [242]

on heating (Scheme 13) [230–233]. The clearing point of the smectic C to smectic A transition and Tg were lowered in the case of dendritic species, compared to the linear mesogens. The specific molecular topology can also play a very important role in the formation of supramolecular LC self-assemblies [234–241].

POSS octasubstituted with 4′-undecyloxybiphenyl-4-yl-4-octyloxy-2-(pent-4-en-1-yloxy)benzoate groups could form both nematic and hexagonal columnar mesophases [243]. Biaxial domains (cybotactic clusters) made of tilted layers, with spacing between layers determined by the length of the rigid part of the mesogenic unit, were observed in each of them in a wide temperature range. Such hybrid molecules can be used in organic optoelectronic devices or employed as sensitive fluorescent probes for detection of metal cations, acids, gases or explosives.

Unfortunately symmetrical silsesquioxanes can easily aggregate in organic LC media, which can result in undesired light scattering by macroscopic particles. Such systems must consist of completely separated phases to be effective. Formation of hierarchically ordered structures by hybrid heterofunctional T_8R_7R' makes them interesting candidates for the application in LC devices with vertical alignment (VA). POSS increase thermal stability of such systems. The required phase separation was obtained with $T_8(i\text{-Bu})_7$ monosubstituted with cyanobiphenyl group [244]. At high temperatures, they form an induced smectic phase and closely packed layered structures on mixing with 4-cyano-4′-heptyloxybiphenyl [245]. The molecules dispersed

in a nematic LC medium gradually diffuse to form a perfectly separated VA layer [244]. It was also found that LC hybrid materials of enhanced nonlinear optical characteristics [246]. and physicochemical properties [247] can be obtained if POSS are grafted with appropriate side groups that help their dispersion in LC media. Mixing POSS functionalized with azobenzene mesogens with a nematic LC matrix resulted in functional hybrid nanocomposites exhibiting reversible dynamic holographic properties [246]. They were capable of rapid, light-induced changes of refractive index due to conformational isomerization of azobenzene units.

Rigid polymers side-jacketed with mesogen groups and POSS can exhibit LC properties due to competitive self-assembling and separation of organic and inorganic phases [248, 249]. For example, rigid poly(terephthalates) with side-grafted POSS can act as rod-like supramolecular mesogens at high temperatures and form hexagonal columnar nanophase (2D Colh) [249]. At low temperatures, the hexagonal order is disrupted by crystallization of POSS. The separate self-assembling of organic and inorganic parts results in the formation of an inclusion complex [coexisting columnar nematic LC phase (Colh) and rhombohedral crystalline (KR) phase]. Interconverting LC phases [crystal (Cr) formed by POSS, coexisting Cr and hexagonal columnar (Colh) phase, and pure Colh phase] were also thermally induced in mesogen-jacketed poly(norbornenes) with side POSS groups [248]. Materials exhibiting chiral nematic phases can be useful in LC displays and electro-optical switches. POSS have been also used as cores for grafting various mesogens including simple molecules [250] and polymeric liquid crystals [251].

Interesting hierarchical structures were obtained with POSS functionalized with discotic side groups. Polyhedral silsesquioxanes bound to discotic triphenylene (TPE) molecules can form unique hierarchical structures owing to the separation of inorganic and organic phases and the tendency of both POSS and TPE to form well-organized mesophases. A unique hierarchical structure was formed by molecules of octafunctional $T_8(TPE)_8$ having peripheral alkyl chain arms of two lengths (C_5 and C_{12}) (Scheme 14). It was ascribed to the incompatibility between POSS and the hydrocarbon parts, favourable interactions among peripheral mesogens and decrease in entropy due to deformation of the silsesquioxane core [252]. The molecular topology was extremely important for the supramolecular self-assembly of the star-shaped supermolecules. It was found that the morphology and thermal characteristics of LC mesophases generated by such molecules depend on the length of spacers between POSS and TPE. Species with C_5 arms were amorphous, but those with C_{12} side chains could self-assemble into hierarchical mesophases. It was a result of the balance between microphase segregation and competition between interactions among peripheral mesogens and decreased entropy owing to the deformation of POSS core. A column-within-column superhexagonal columnar phase was formed by species with C_2 linkers between POSS and TPE. Molecules with C_6 spacers have an alternating POSS-TPE lamellar morphology with a rectangular columnar symmetry. An oblique columnar phase with inverted columnar morphology with four TPE columns arranged into a supercolumn within the POSS/alkyl chain matrix was found for the most separated hybrids with C_{10} linkers.

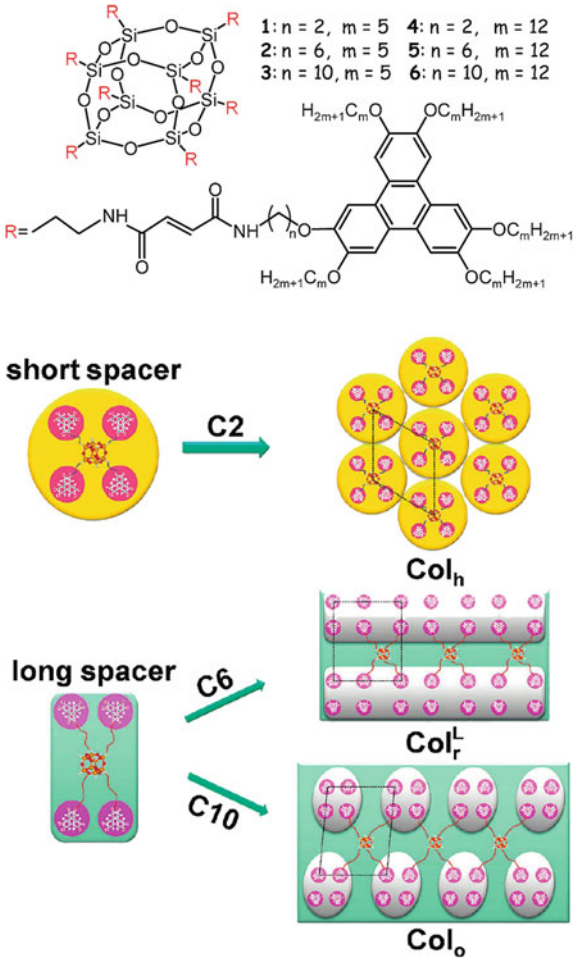

Scheme 14 Chemical structures of hybrid star molecules of $T_8(TPE)_8$ and schematic representation of their supramolecular self-assembly in the solid state (2D unit cells drawn in dotted lines). Adapted with permission from [252]. Copyright 2018 American Chemical Society

Nanophase separation between crystalline lamellae of heterofunctional POSS and liquid crystalline organic moieties was observed both for an asymmetric disc-cube dyad derivative of 2-hydroxy-3,6,7,-10,11-pentakis-(pentyloxy)-triphenylene and $T_8(i\text{-Bu})_7$ linked by a flexible C_{11} organic spacer (Scheme 15) and for 1:1 physical blend of POSS and TPE (Fig. 15) [253]. $T_8(i\text{-Bu})_7$ groups were stacked into an ABCA four-layer lamellar rhombohedral crystal (space group *R*-3*m*) characteristic to the parent POSS. True columnar mesophases were not obtained. The silsesquioxane assemblies were sandwiched between LC bilayers comprised of TPE molecules. In the physical blend, POSS and TPE formed the outer layers with triphenylenes interdigitating in the rhombohedral crystal structure. TPE molecules were oriented parallel to the lamellar normal. The arrangement is similar to homeotropic nematic discotic structures.

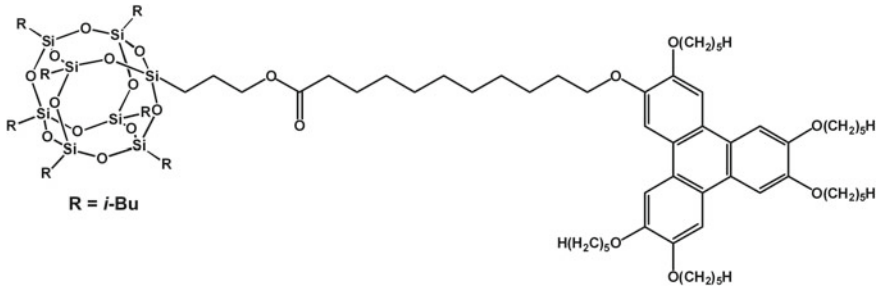

Scheme 15 Polyhedral silsesquioxane $T_8(i\text{-Bu})_7$ bound to the molecule of discotic triphenylene [253]

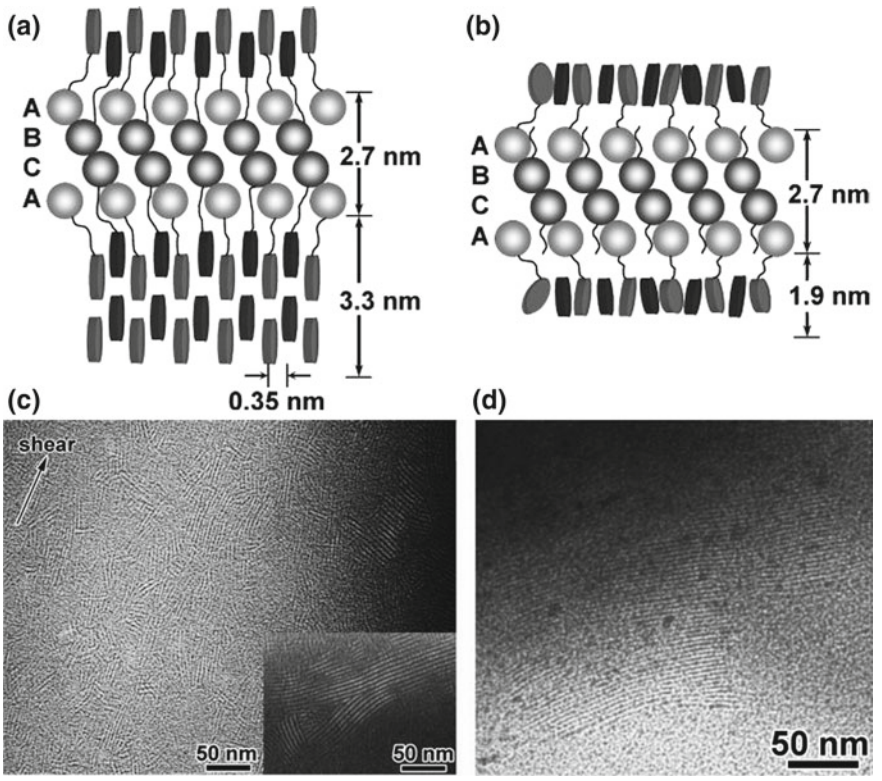

Fig. 15 Schematic representations of self-assembly at room temperature of **a** POSS-TPE (POSS ABCA stacked into a four-layer lamellar crystal and TPE discs formed staggered bilayer) and **b** 1:1 physical blend of POSS and TPE (interdigitating); **c** bright-field TEM micrographs of POSS-TPE; **d** TEM micrograph of 1:1 blend of POSS-TPE:POSS. Adapted with permission from [253]. Copyright 2018 American Chemical Society

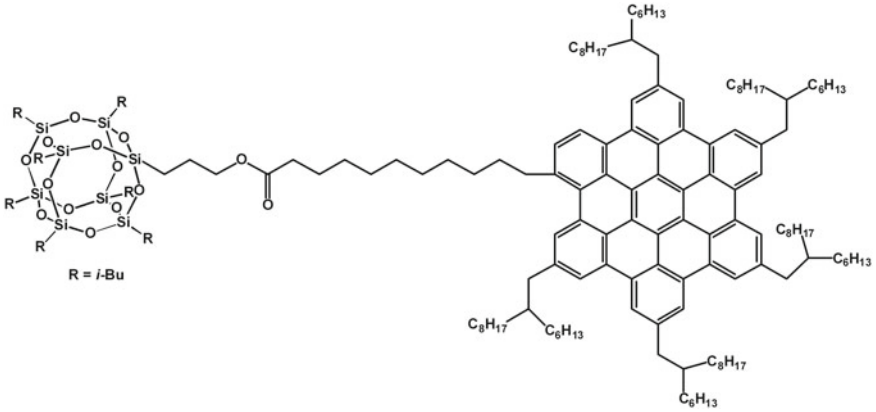

Scheme 16 $T_8(i\text{-Bu})_7$ grafted with hexa-peri-hexabenzocoronene [257]

Tetraphenylethylene can also act as a sensitive fluorescent probe to monitor the self-assembly of POSS molecules. Two nanohybrid dendrimers that were synthesized by grafting tetraphenylethene units onto $Q_8M(CH{=}CH_2)_8$ exhibited aggregation-induced emission (AIE) and high fluorescence quantum efficiencies in both dilute solutions and in the solid state [254]. They were also much more thermally stable than the parent tetraphenylethylene compounds. The emissions of nanoaggregates could be quenched by picric acid or Ru^{3+} ions, which suggests their possible use as highly sensitive chemosensors for explosives and metal ions. Incorporation of Schiff bases furnished the hybrid POSS nanoparticles with pH-responsiveness [255]. Rapid fluorescence quenching was observed under acidic conditions. It was also observed that $T_8(i\text{-Bu})_7$ monomodified with tetraphenylene groups exhibited monomer emission in organic solvents as well as AIE emission in THF/water [256]. Samples prepared separately from THF and THF/water had different hierarchical nanostructures. The flexible spacers between the organic moieties and POSS controlled the lamellar self-assembly and supressed the aggregation of luminophores.

POSS-based derivatives with the silica core grafted with hexa-peri-hexabenzocoronene (HBC) moieties (Scheme 16) are closely related to the POSS-TPE systems. It was found that POSS–HBC hybrids can form various complex self-assembled nanostructures, depending on the POSS content and topology of the molecule [257].

At ambient temperature, structures of low order were observed for molecules of a single $T_8(i\text{-Bu})_7$ linked to HBC, and of long-range hierarchical structures for larger species. The transition temperature increased with the POSS content. Species with two POSS molecules formed a supramolecular structure with a monoclinic unit cell coexisting with KR crystalline phase made of silsesquioxane moieties. HBC core surrounded with six POSS exhibited two order-to-order transitions (Colh coexisting with KR to Colh and Colh-to-BCC) but remained ordered within the experimental temperature range. It should be stressed that the complex BCC phase is quite

unique for a system built of rigid nanoparticles. The effect of the linker on the self-assembling properties of POSS–HBC dyads was investigated [258]. Hierarchically ordered monodisperse structures were obtained with high molecular precision that played an important role in self-assembling. Spacers that were too long or too short could not balance the competition between POSS and HBC moieties, which made them unable to form highly ordered structures at low temperatures. HBC–C_3–POSS dyad with the most suitable spacer consisting of three methylene units generated highly ordered orthorhombic structures. At high temperatures, 2D Colh structure was governed by the length of the flexible spacer between POSS and side HBC groups. All dyads (except the one with the longest spacer) produced hexagonal columnar 2D Colh structures at high temperatures.

4.5.3 POSS-Based Ionic Liquids

Ionic liquids (ILs) are non-volatile salts with unique physicochemical characteristics and melting temperature below 373 K. They have attracted considerable interest due to high ionic conductivity, high polarity, negligible vapour pressure, high thermal stability, non-flammability, high density, high heat capacity and wide electrochemical stability window. Due to the ability to dissolve a wide range of organic and ionic compounds, they can be also used as "green" solvents in conventional and catalytic reactions and separation–purification processes.

Several reports have suggested that POSS-based IL can be used as no-leaking, high-performance electrolytes [259–265]. The observed increased interest in application of POSS as ILs can be attributed to their unique 3D structure that can strengthen ion transportation abilities, high rigidity and thermostability, as well as the presence of functional substituents on the silica cores. The highly symmetric structure of POSS contributes to the suppression of the molecular mobility of ion salts and results in the formation of regular structures, leading to thermally stable, thermotropic IL crystals. It was shown that the temperature range in which hybrid POSS-ILs with various alkyl chain lengths exist in LC phase is enlarged because of the stabilizing effect of the inorganic core [260]. These well-ordered ionic moieties should be able to work as efficient cation carriers and scaffolds for ordering cations, as well as exhibit enhanced optical and magnetic properties. Thermally stable thermotropic IL crystals can be also used in electronic devices. The LC phase of the POSS-tethered ion salts was maintained until decomposition (no clearance point during heating).

The so-called room temperature ionic liquids were obtained with POSS [259, 261]. After tethering to the cubic core, the ion pairs are isolated and distributed in a star shape, which increase the exclusion volume, disrupt the aggregation of ion pairs and lead to decrease in T_m. The products are transparent and colourless, and those of high number of ionic pairs melt below 298 K. It can be attributed to the smaller enthalpy and entropy of fusion of POSS-IL [262]. It was also shown that tethering the ionic arms to the inorganic core led to the enhancement of hydrogen-bonding capability, as indicated by respective chemical shifts in ^{1}H NMR spectra.

The structural features of POSS can contribute more than its rigidity to the enhancement of thermal stabilities of POSS-based ILs. A large number of ion pairs tethered to POSS is essential to increase the temperature of their decomposition, but it is not the only factor that determines the thermostability. Comparative studies on polyanionic POSS with imidazolium cations tethered to the silsesquioxane core (POSS-Im) and the respective counterpart salts of single side chains revealed that the respective values of decomposition temperature (T_d) for POSS derivatives with 6 and 8 ionic pairs were higher than those of single-arm species and the parent POSS core. In contrast, POSS-Im2 and POSS-Im4 showed lower T_d (even than the single chain ion pairs).

Studies on the behaviour of ionic POSS in solution explained the macroion—counterion interactions [263]. Both positively and negatively charged POSS-IL with identical charges and similar sizes self-assembled into blackberry-type supramolecular structures in water/acetone mixtures. The phenomenon was found to be charge-regulated and driven by the counterion-mediated attraction. The size of blackberry structures increased upon increasing the acetone content. Negatively charged POSS self-assembled in polar solvents and formed less ordered supramolecular structures than the positively charged POSS. Those discrepancies were ascribed to different counterions and ionic domains of positively and negatively charged macroions, ionic strength in solution and the water-bridged hydrogen bonding between the monomers.

Ionic liquids of tuneable properties have found numerous applications in materials science (e.g. electrolytes for actuators, lithium batteries and fuel cells). Replacing liquid-state electrolytes with solid-state electrolytes can also improve the durability of dye-sensitized solar cells (DSSCs). Amorphous ionic conductors in the elastomeric state at the operating temperature of solar cells ensure good pore filling and improve the photovoltaic performance due to increased interfacial contact between the electrolyte and the TiO_2 film. Efficient amorphous ionic conductors for solid-state DSSCs were prepared by linking $T_8(CH_2CH_2CH_2Cl)_8$ to imidazolium iodides with propyl and allyl groups (T_g respectively at 278 and 279 K) [264]. Binary solid-state electrolytes were prepared by blending the ionic conductors and appropriate amount of iodine without any other additives. Good power conversion efficiency (6.29%) has been achieved with good long-term stability using an organic dye as the sensitizer. Stronger intermolecular π–π stacking interactions between the allyl groups and imidazolium rings are responsible for the higher conductivity and slower charge recombination than those observed for the propyl counterpart.

Cross-linking and solution extraction of ionic POSS was used for fabrication of inorganic–organic hybrid ionogels and scaffolds with well-defined mesopores (Scheme 17) [265]. High-performance ionogels with superior performance as lithium-ion batteries, excellent electrochemical stability and unique ion conduction behaviour were fabricated through cross-linking of functional groups on silsesquioxane cores and various cationic tertiary amines. The extraction of liquid components left hybrid scaffolds with well-defined, interconnected porous structure and covalently tethered ionic groups in local environment. The products were used as recyclable, heterogeneous catalysts for the CO_2-catalysed cycloaddition of epoxides.

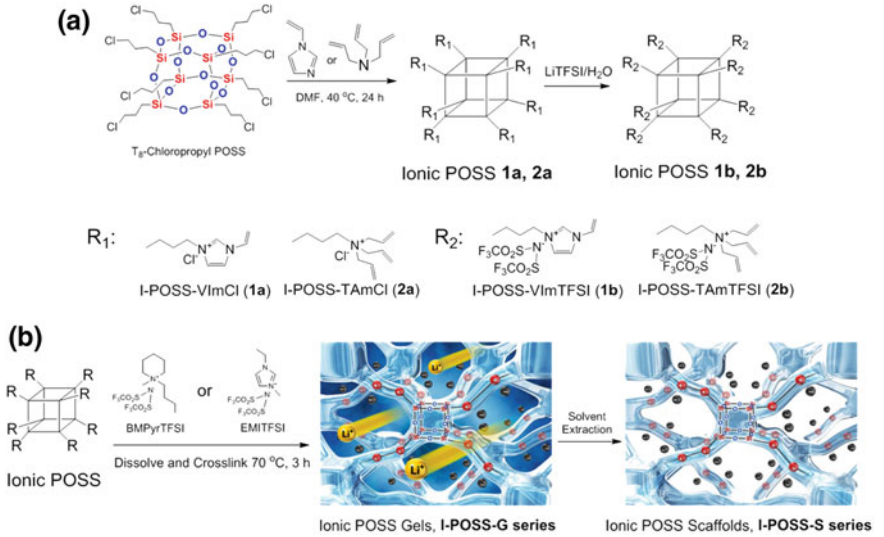

Scheme 17 Cross-linking of ionic POSS for the preparation of hybrid mesoporous ionogels. Adapted with permission from [265]. Copyright 2018 American Chemical Society

Three-dimensional hybrid species having POSS inorganic cores enveloped by coronas made of grafted organic macromolecules can assemble in solution into large-scale structures similar to multidendrimer aggregates with POSS-rich domains surrounded by POSS-poor domains [266]. The flexible chains of polymers attached to POSS tend to adjust their conformation in response to changes of the environment. When dissolved, such systems become more compact and deformed on increasing the concentration of the solution. POSS-poly(*N*-isopropylacrylamide) (PNIPAm)–poly(2-hydroxyethyl methacrylate) (PHEMA) copolymers were found to be dual-responsive to temperature and pH [267]. Similar pH-responsiveness was noted for imidazole-terminated POSS-poly(amidoamine) dendrimers of first and second generation [268]. The effect is structure dependent and the recorded pKa values decreased for larger species owing to electrostatic repulsions between neighbouring polar groups. Such hybrid systems can be used as functional smart materials for, e.g. encapsulation and controlled release of various cargo molecules. Ordered nanonetworks of ionic branched macromolecules, e.g. POSS-poly(amidoamine) (PAMAM) dendrimers of first and second generation terminated with imidazolium bromide residues [269], can be used as solid conductive materials. Formation of well-organized domains combined with segmental mobility of side chains facilitates charge transport in such hybrid polyelectrolytes. Existence of ionic domains for charge transport was confirmed with WAXS for thin films of PAMAM–POSS–PF_6 macromolecules of first and second generation [269].

Maximum ionic conductivity at 324 K was recorded for the POSS-core dendrimer of lower generation and smaller concentration of lithium ions. The observed VFT-

type behaviour indicated that segmental motions may contribute to long-range charge transport.

Hybrid amphiphilic POSS-IL of low T_g and good thermal stability were also prepared from $T_8(CH_2CH_2CH_2SH)_8$ and 1-allyl-3-methylimidazolium salts through the photochemical thiol–ene reaction. They self-assembled into perfect vesicles with "yolk–shell" structures, in which the anions formed the "shell" and POSS cages aggregated to form the "yolk" [270]. Water-soluble ionic dendrimers were prepared with $T_8(CH{=}CH_2)_8$ via subsequent thiol–ene addition and Menschutkin reaction [271]. The products can be modified via click chemistry and were also used for host–guest encapsulation of dyes, exhibiting an ultrahigh loading capability due to the regular structure and relatively big cavities.

4.6 Supramolecular Bioactive POSS Nanoassemblies

Molecular self-assembly plays an important role in biology and underlies the formation of a wide variety of natural biological structures with high level of precision and complexity. Nanotechnology aspires to create artificial materials, with hierarchical structures and tailored properties, exploiting principles that can be found in nature. Polyhedral silsesquioxanes have found application in biomedicine, drug delivery and diagnostics [272, 273]. Moreover, a broad range of bioinspired POSS-based hybrid systems was developed, including molecular recognition techniques based on peptides and DNA. POSS-based cargo peptide delivery system can be used for drug targeting and labelling in human cells [274]. Organic–inorganic hybrids, able to interact with poly(amino acids) via hydrogen bonds and exhibit smart pH-responsive and thermoresponsive properties, were made of water-soluble silsesquioxane nanoparticles with side tertiary amine moieties [275, 276]. It was also suggested that structures formed by POSS–polypeptide and POSS–DNA hybrids can be used in organic microelectronics (integrated circuit materials) [277, 278].

4.6.1 Polypeptides

Polypeptides are short chain macromolecules built of several amino acid monomers linked by amide bonds. They are closely related to proteins and can form hierarchically ordered structures (α-helices and β-sheets) stabilized by intra and intermolecular hydrogen bonds both in the solid state and in solutions [279]. The importance of peptides as self-assembling building blocks for the construction of nanobiomaterials is well known [280–282]. They offer a great diversity of biochemical properties (specificity, intrinsic bioactivity, biodegradability) and physical features (small size, conformation) and can be used as excellent structural units for the bottom-up fabrication of complex nanobiomaterials. Synthesis of poly(peptide-*b*-non-peptide) (rod/coil) block copolymers containing well-defined and rigid polypeptide segments has received a considerable attention due to their unique self-assembly behaviour and

well-designed 3D architectures that can mimic biological activity of more complex proteins.

POSS can be used for the preparation of block polypeptides of various molecular architectures (linear block, side grafted or of star shape). The hybrid silsesquioxane moieties attached to polypeptides can prevent uncontrolled aggregation of peptide nanoribbons and enhance α-helical conformation of the biomolecules in the solid state [273, 283, 284]. The hierarchical self-assembly via intramolecular hydrogen bonding between siloxane bonds and polypeptides or π–π interactions can play a significant role in the process. POSS–polypeptide copolymers exhibit a significant stability of α-helical conformation and superior thermal properties.

Various nanostructures featuring aggregated POSS and polypeptides in α-helical or β-sheet conformations can be obtained on adjusting the structure of macromolecules. Linear chains of poly(γ-propargyl-L-glutamate)-*g*-POSS copolymers (PPLG-*g*-POSS) were packed in the solid state as hexagonal cylinders featuring α-helical conformations and POSS aggregates [285]. Their block analogues with γ-benzyl-L-glutamate segments (PBLG-*b*-POSS) tend to form bilayer-like nanostructures (Fig. 16) [286, 287]. Incorporation of cube silsesquioxanes at the core of well-defined star PBLG-*b*-POSS copolymers also enhanced formation of α-helical structures [283]. The star-shaped macromolecules exhibited larger conformational stability than linear PBLG, which resulted in the change of liquid crystal ordering and alignment of PBLG chains in the solid state.

Hierarchical self-assembly of the organic–inorganic hybrid triblock copolymers polystyrene-*b*-poly(γ-propargyl-L-glutamate-*g*-POSS) [PS-*b*-(PPLG-g-POSS)] also resulted in the formation of cylindrical structures due to microphase separation in the diblock part of copolymers [277]. Grafting of POSS units onto side chains of PPLG enhanced the α-helical conformation in the solid state, induced hexagonal lattice packing and increased the thermal stability of α-helical secondary structures of polypeptide segments. Combination of PBLG segments with amyloidogenic short peptide (LVF) tethered to $T_8(i\text{-Bu})_7$ yielded a wide variety of hierarchical nanostructures [288]. Owing to π–π aromatic interactions between side chain phenyl groups in PBLG, the hybrid conjugate formed 2D hexagonal cylinders comprised of 18/5 α-helices. Removal of the side chain benzyl groups from the conjugate produced a pH-sensitive amphiphilic anionic homopolymers. The conjugate assembled into various spherical to square-shaped morphologies in aqueous media, depending on the ratio of hydrophobic/hydrophilic segments as well as the content of POSS.

4.6.2 DNA Complexes

Negatively charged double-stranded DNA is a unique biomacromolecule of helical conformation and long persistent length, capable of genetic information storage. It can be also used in catalysis, bioinformatics and for gene transfection. Efficient transfer to the cell and into the cell nuclei is the main challenge for transfection agents in gene therapy, in particular for plasmid DNA (pDNA) delivery. Understanding the structure–function relationship of cationic lipid-based gene transfection and mor-

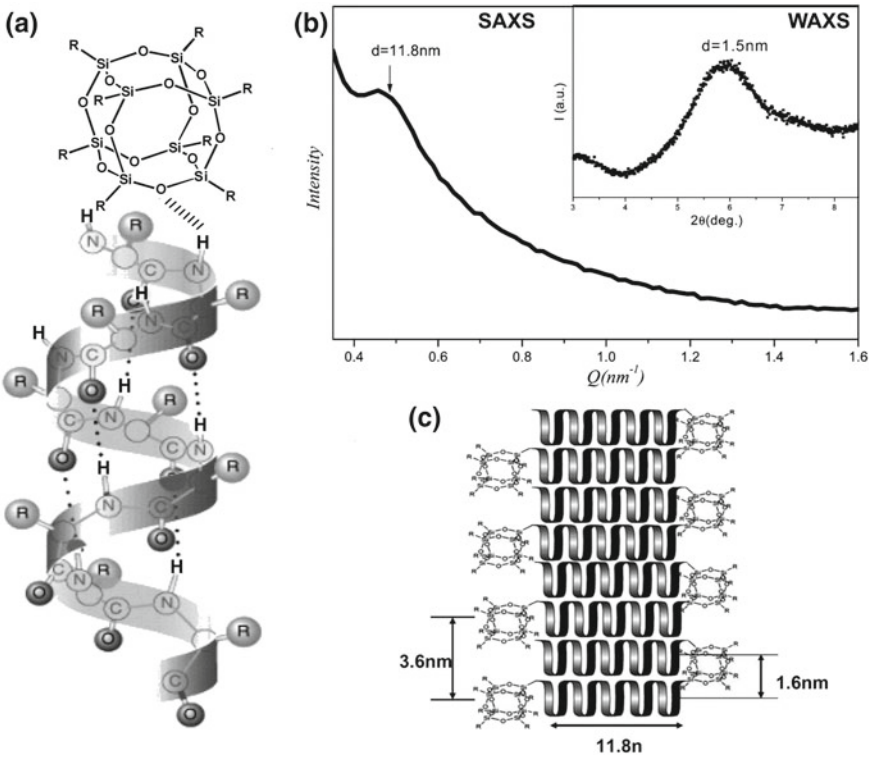

Fig. 16 **a** Intramolecular hydrogen-bonding interaction in POSS-b-PBLG copolymer, **b** schematic presentation of the nanoribbon formed in the network structure of the toluene gel of POSS-*b*-PBLG and its **c** SAXS and WAXS (inset) profiles. Adapted with permission from [287]. Copyright 2018 American Chemical Society

phology of the formed mesophase is crucial for the preparation of efficient carriers. The equilibrium morphology of lipoplexes is determined by the free energy balance among surface charge density, spontaneous curvature of the lipids and elastic properties of the lipid bilayers. Thermodynamically, the complexation is driven by the electrostatic interaction between negatively charged DNA and positively charged cationic lipids and the release of small-molecule counterions. Moreover, the transfection mechanism based on the polyplex interaction with the cellular membrane depends on the polymer architecture. Various cationic polymers show promising features as transfection vesicles that are able to enter cells by endocytosis and can be dissociated to release DNA for gene expression [289]. The polyplex dissociation is governed by the polymer chemistry and biodegradability. Several important reports have been published on superior gene transfection abilities of POSS–DNA polyplexes [290–292]. They can be also used as carriers of drugs into malfunctioning cells [293].

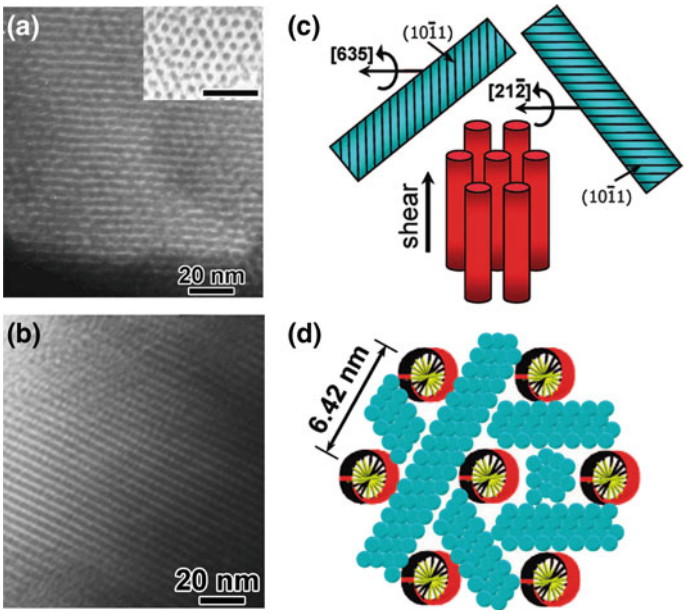

Fig. 17 Bright-field TEM micrographs of the DNA–imidazolium POSS complex having **a** the inverted hexagonal and **b** the lamellar phases; **c** representation of the DNA inverted hexagonal phase (red cylinders) and POSS crystal orientations (top bars) and **d** parallel and hexagonally aligned DNA cylinders and ABCA four-layer POSS lamellar crystals in the interstitials. Adopted with permission from [294]. Copyright 2018 American Chemical Society

POSS-based imidazolium salt was used as a cubic cationic lipid complexed with double-stranded DNA, and the mesophase self-assembly behaviour of the hybrid was studied [278]. Formation of an inverted hexagonal columnar (H_{II}^{C}) phase for the DNA–POSS-imidazolium salt complex above the melting point of POSS crystals was observed. The effect is a consequence of the induced negative spontaneous curvature of species made of bulky hydrophobic POSS tails and hydrophilic imidazolium head. Various self-assembled phase morphologies were obtained depending on the competition between the lamellar crystallization and the negative spontaneous curvature of cationic POSS-imidazolium lipids [294]. A lamellar phase was generated when the crystallization was relatively slow (e.g. isothermal crystallization at 403 K predominated by crystallization of POSS molecules), but if it was rapid (e.g. sample quenched to 273 K), then an inverted hexagonal phase was obtained with POSS lamellar crystals grown in the interstitials of DNA cylinders. In the latter case, the lipid negative curvature predominated the self-assembly process (Fig. 17). The double-stranded DNA retained the β-form helical conformation in the inverted hexagonal phase, whereas in the lamellar phase the helical conformation was largely destroyed, possibly due to the ionic complexation of POSS crystals at both sides of the DNA double strand.

POSS can be used for preparation of biosensors due to the formation of specific supramolecular assemblies. Cationic POSS were successfully applied as very sensitive probes for the detection of DNA by resonance light scattering [295]. It was shown that the electrostatic interactions of cationic POSS and DNA enhance the RLS signal.

Nucleoside triphosphates play crucial roles in a wide variety of biological events such as nucleic acid synthesis (building blocks for DNA and RNA), signal transduction, metabolism and enzymatic reactions. Precise POSS-based recognition system for triphosphates can be used for the construction of biosensors and biotechnological tools for monitoring biorelated reactions. Selective molecular recognition for nucleoside triphosphates, adenosine triphosphate (ATP), uridine triphosphate (UTP) and cytidine triphosphate (CTP), was observed inside the ligand-modified water-soluble hybrid gels composed of POSS [296]. It was found that the ligands inside the gels could form a stable complex only with the target nucleoside triphosphate that was able to participate in the complementary pattern of hydrogen bonds. A similar procedure with the affinity enhancement and the precise recognition of the hydrogen bond patterns was applied for the selective encapsulation of guanosine triphosphate (GTP) into POSS-based water-soluble polymers via the complex formation with the naphthyridine derivatives.

4.7 Self-assembly of POSS at the Interface

The investigation of silsesquioxane molecules contained at interfaces can be critical for the advancement in materials science and development of surface-based technologies. The results obtained in solution are not always useful for practical applications that often require immobilization of functional molecules at surfaces or interfaces (fabrication of sensors or functionalization of high-surface area materials). Solid and liquid surfaces are fundamentally different in many aspects including energy state, motional freedoms and adsorption of molecules. Consequently, they allow for the investigation of different properties of molecules. The lower dynamicity of the solid surface is advantageous for high-resolution observations. Motions of molecules on solid surfaces are often restricted. On the other hand, liquid surfaces (such as the air–water interface) are flexible and dynamic, with rapid diffusion of molecular components leading to mixing and rearrangements. The dynamic nature of liquid interfaces enables flexible control of nanostructures and molecular functions.

The surface behaviour of functionalized POSS is interesting from the point of view of the interfacial assembly process. It is also of importance regarding ultrathin film technologies and fast and sensitive signal transmission over short-time intervals. Very little is known about the morphologies that develop within 2D monolayers of POSS molecules. The comparative discussion of the properties of POSS positioned at solid or liquid surfaces included in the following sections.

4.7.1 Langmuir–Blodgett Films

General tendency of POSS for aggregation can be an obstacle for the preparation of well-organized thin films using typical methods such as spin coating. Deposition of POSS-based coatings as a result of specific interactions with the substrates [161, 170, 297] or by layer-by-layer deposition [298] is an exception. Langmuir–Blodgett (LB) technique can be at least a partial solution to the problem. The method exploits the phenomenon of particle self-assembly upon compression at the air–water interface and is a unique tool for inducing highly ordered layered structures with well-defined, molecular-level precision [299]. Molecules in such thin films are ordered in a quasi-smectic way. LB technique made a significant contribution to physical chemistry, nanotechnology and surface science. The general observations concerning Langmuir films can be applied to other coating technologies. Thin-film formation at the air–water interface by silicon containing polymeric materials is well known [300]. Polyhedral silsesquioxanes is another class of surface-active materials that can be used alone for the preparation of LB films or embedded as nanofillers in polysiloxane monolayers [300]. The rigid structure of POSS derivatives results in a more traditional Langmuir film behaviour.

Symmetrical T_8R_8 with short hydrophobic alkyl chains [e.g. $T_8(i\text{-Bu})_8$] do not form thin films at the air–water interface, despite their ability for crystallization due to interactions between side groups. Such POSS can be assembled into uniform Langmuir–Blodgett or Langmuir–Schaefer films only after cleaving one of siloxane bonds, which transform the molecules into amphiphilic species [301–304]. The open-cage $T_7(i\text{-Bu})_7OH_3$ is amphiphilic and formed Langmuir films, whereas its closed-cage analogue—$T_8(i\text{-Bu})_8$—formed only heterogeneous films at all surface concentrations. It was also shown that in contrast to trisilanolisobutyl-POSS, trisilanolcyclohexyl-POSS formed intricate structures in the collapse state, including rod-like domains at very high Π. These phenomena were attributed to dimerization of trisilanol POSS. It was also shown that molecules of amphiphilic open-cage $T_7(i\text{-Bu})_7OH_3$ form a 2D rugged monolayers on the surface of water, which undergo a counter-intuitive reversible crystallization [305]. The in-plane interparticle correlation peaks, characteristic of a 2D system, were replaced during the transition by intense localized spots. The finding was explained with a model that assumed crystalline periodic stacking of the $T_7(i\text{-Bu})_7OH_3$ dimers, relaxing upon decompression to retain the initial monolayer state.

Amphiphilic POSS can be also obtained by modification of the open-cage trisilanol POSS precursors. The effect of the kind of functional groups (polyether and fluoroalkyl) bound to two different open-cage POSS molecules not bearing silanol groups was studied regarding the formation of Langmuir monolayers [306]. Both derivatives were able to form insoluble Langmuir films at the air–water interface. They could be transferred onto quartz plates and changed wetting properties of the substrates. It was shown that structure and properties of the prepared monolayers (i.e. packing density, orientation of the molecules, stability, electric surface potential) depended on the chemical structure of the side groups grafted onto POSS core. The behaviour of T_8R_8 at the interface can change on increase in the length of side

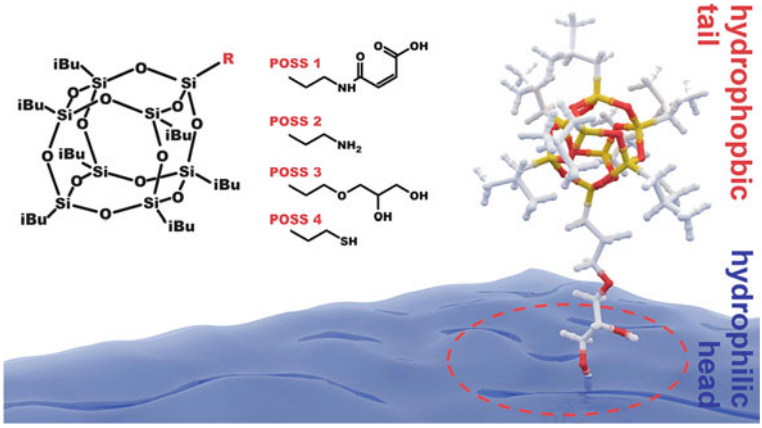

Scheme 18 Arrangement of $T_8(i\text{-Bu})_7R'$ at the air–water interface. Reprinted with permission from [308]. Copyright 2018 American Chemical Society

chains. All fluorocarbon POSS admixed with silica nanoparticles were able to form a hydrophobic LB film (condensed and rigid due to the incorporation of silica) [307]. It was observed that fluorinated POSS dispersed silica nanoparticles and prevented their aggregation. It was also found that the character of only one out of eight functional groups can have a great influence on the behaviour of POSS at the air–water interface. The Langmuir–Blodgett technique was applied for $T_8(i\text{-Bu})_7R'$ with hydrophilic heterorganic functional group R' (Scheme 18) [308]. Bifunctional amphiphilic POSS formed more easily well-organized films at the air–water interface.

However, it is not always the case and $T(i\text{-Bu})_7(CH_2CH_2CH_2SH)$ could form only 2D aggregates and multilayer films [308]. Analogously, amphiphilic POSS bearing two hetero-organic groups: $T(i\text{-Oct})_6(CH_2CH_2CH_2SH)_2$ and $T(i\text{-Oct})_4[CH_2CH_2(CF_2)_6CF_3]_2(CH_2CH_2CH_2SH)_2$ aggregated at the air–water interface [309]. Quite surprisingly, symmetric T_8R_8 with side groups containing heteroatoms easily formed Langmuir–Blodgett films. For example, a permeable but highly stable and reproducible Langmuir layer was obtained with $T_8(CH_2CH_2CH_2SH)_8$ [309]. The film could be transferred to a range of solid supports. Octakis[{2-(3,4-epoxycyclohexyl)ethyl}-dimethylsilyloxy]-octasilsesquioxanes of Q_8MR_8 type were assembled into a homogeneous monolayer that underwent a stepwise collapse with time [310]. It was found that the monolayer behaviour is totally different from that of typical amphiphiles. The $\Pi - A$ isotherm and equilibrium elasticity suggested formation of a liquid expanded monolayer. After the collapse, films of multilayer morphology were formed. Stepwise transitions from flake-like domains, then star-like structures, and finally aggregation into a ring network were observed. The formed unusual multilayer morphology is a consequence of side group reorganization, followed by a progressive decrease in the distance between the inorganic cores.

The importance of the balance between hydrophilic and hydrophobic parts for the stability of a Langmuir film was shown for two series of organic-functionalized

core–shell silsesquioxane derivatives (POSS-M)*p*-(*x*/*y*) with various compositions of hydrophobic and hydrophilic terminal groups. The studies were carried out in the bulk state and within mono- and multilayered Langmuir films at the air–water interface as well as on solid surfaces [311]. A mixture of silsesquioxanes (POSS-M) composed of polyhedra, incompletely condensed POSS species, ladder-type structures, linear structures, and all other possible combinations, was used. The two series of $(POSS\text{-}M)_{p\text{-}(x/y)}$ molecules were different in the hydrophobic–hydrophilic balance of their peripheral groups (*x* and *y* referring to the molar per cent of –OCONH–$C_{18}H_{37}$ tails and –OH for $(POSS\text{-}M)_{1-(x/y)}$ and the ratio of –OCONH–$C_{18}H_{37}$ tails and –OC-C_6H_4COOH terminal groups for $(POSS\text{-}M)_{2-(x/y)}$. The unit cell dimensions of the crystalline phase suggested the molecular packing with interdigitated peripheral tails of POSS cores. However, in the bulk state the presence of aromatic rings in $(POSS\text{-}M)_{2-(x/y)}$ series resulted in the crystal structure of lower symmetry than that of the $(POSS\text{-}M)_{1\text{-}(x/y)}$. The molecules that contained a sufficient amount of –OCONH-$C_{18}H_{37}$ tails exhibited double endothermic transition that was attributed to independent melting of alkyl chains, followed by the disassembly of the unit cells of (POSS-M) cores. The surface morphologies for the various hydrophobic–hydrophilic combinations at low surface pressure (0.5 mN/m) were found to be similar to those observed for the classical amphiphilic star polymers. However, at higher surface pressure (5 mN/m), a uniform monolayer was formed for POSS-M compounds with lower content of hydrophilic groups. The variation of terminal group composition led to diverse morphologies that ranged from one-dimensional and curved domains for low hydrophobic content to planar aggregates with increasing amount of hydrophobic alkyl chains. The surface morphologies resembled the two-phase solid–liquid state, typically observed for alkyl-containing hyperbranched systems. All hydrophilic–hydrophobic $(POSS\text{-}M)_{p-(x/y)}$ aggregated into uniform monolayer films at high surface pressure. The formation of multilayered structures was observed for $(POSS\text{-}M)_{p-(50/50)}$ with equal content of hydrophilic and hydrophobic groups (Fig. 18). The absence of hydrophobic segments in a fully hydroxylated $(POSS\text{-}M)_{1-(0/100)}$ compromised the ability to form a stable monolayer.

POSS have been also used as components of more elaborated systems aggregated at the air–water interface. Binary mixtures of cholesterol and octakis[{2-(3,4-epoxycyclohexyl) etyl}dimethylsilyloxy]octasilsesquioxane (OE-POSS) were compressed into Langmuir films [312]. The presence of two collapse points on the obtained isotherms was their most characteristic feature. The first point occured at similar surface pressures for all compositions, and it was attributed to the collapse of less-stable OE-POSS. The second one corresponded to the collapse of the cholesterol part. True mixed and homogenous films were not obtained, but phase separation and formation of microdomains of each component in the matrix of the other one was observed due to the differences in the molecular structure. Squeezing out less-stable OE-POSS molecules *co*-spread with cholesterol from the monolayer was noted after exceeding the collapse surface pressure of pure silsesquioxane. The system can be regarded as a simplified biomembrane model. The lack of the interactions between OE-POSS and biomembrane components represented by cholesterol suggests that

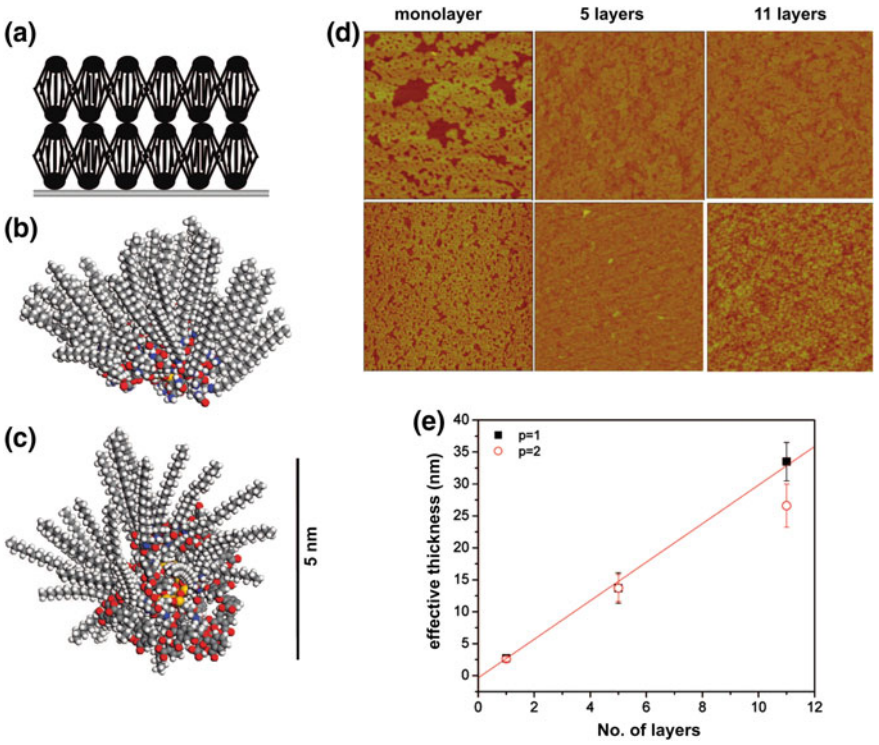

Fig. 18 **a** Multilayered LB film composed of amphiphilic silsesquioxane cores with alternating hydrophilic and hydrophobic peripheral groups; **b** $(POSS\text{-}M)_{1\text{-}(50/50)}$ and **c** $(POSS\text{-}M)_{2\text{-}(50/50)}$ with the alkyl chains stretched vertically, away from the hydrophilic surface; **d** AFM images of LB multilayers deposited at surface pressure of 10 mN/m; **e** plot of effective thickness *vs* number of layers for LB films of $(POSS\text{-}M)_{1\text{-}(50/50)}$ and $(POSS\text{-}M)_{2\text{-}(50/50)}$. Adapted with permission from [311]. Copyright 2018 American Chemical Society

such membranes would fluidize in the presence of functionalized POSS, which can be important for biomedical applications.

Aggregation behaviour of three star-shaped fluoropolymers containing POSS cores and grafted with side chains [POSS-(PMMA-*b*-PTFEMA)$_8$, POSS-(PTFEMA-*b*-PMMA)$_8$ and POSS-(PTFEMA-*b*-PMPEGMA)$_8$] was investigated at the air–water interface [313]. It was found that the surface pressure–mean molecular area isotherms exhibited four different regions. A pseudo-plateau corresponding to a "pancake-to-brush" transition was observed. The process of the relaxation of the monolayer was found to be related to the fast adsorption–desorption exchange of molecules and polymer segments on the surface and slow reconformation of the adsorbed macromolecules inside the adsorption layer. A variety of morphologies were observed for the LB films prepared at the air–water interface at different surface pressures, depending on the structure of the star-shaped copolymers.

4.7.2 Exfoliation of Silicate Clays

The well-defined structural features and tailor-made physicochemical properties, that can be tuned to enhance interfacial interactions, make POSS ideal nanofillers for polymer composites. Self-assembling phenomena strongly influence the behaviour of both small silsesquioxane molecules blended into polymers as well as tethered to polymer chains that can form crystalline domains in the organic matrix [5, 6, 314–316]. The aggregation or crystallization of POSS moieties used as nanofillers in polymeric systems as well as the interphase interactions can play a prominent role determining viscosity, melt elasticity and flammability of polymer nanocomposites.

However, POSS can be used not only as specialty nanofillers in polymer matrices, but they can also modify other materials used as additives in polymer composites. The self-assembling ability of POSS was used for intercalation of natural mineral clays, such as montmorillonite (MMT) [317]. Due to the special layered structure, adhesion, ion-exchange capacity and organic adsorption behaviour, MMT is frequently used in polymer composites to improve their chemical, physical, mechanical and thermal properties. Such polymer/clay nanocomposites have a wide range of applications as structural, coating and packaging materials. MMT is expandable and allows for intercalation the interlayer space with surfactant molecules up to the saturation limit. The surfactant concentration, dimensions as well as packing density determine the morphology of modified clays. POSS of T_8R_7R' type, because of their large molecular dimension, high thermal stability, biocompatibility, recyclability and poor flammability, were found to be good substitutes for alkyl ammonium tallow salts and 'onium ions in clay modification [318–321]. The rigid and cubic-shaped POSS can be absorbed into the clay galleries, but they cannot be arranged as flexibly as chain surfactants in the interlayer space. Once a double layer of POSS is assembled, then the *d*-spacing in expanded MMT is defined. The incorporation into the clay interlayer spacing results in the formation of "silicate clay" with a sandwich structure (Scheme 19). The interlayer spacing in composites with POSS intercalated into clay galleries is increased, and their thermo-oxidative stability is enhanced.

The chemistry and texture of POSS intercalated clays have been investigated for POSS bearing different functional groups that could interact with MMT. Amine-functionalized POSS can be intercalated into the layered clay via the onium exchange reaction. High concentration of POSS is not a prerequisite for the increase in the interlayer spacing. It was found that interlayer space of MMT modified with T_8(*i*-Oct)($CH_2CH_2CH_2NH_2$) was strongly dependent on the arrangement of POSS surfactant but less dependent on the POSS concentration [322, 323]. However, it is not always the case. Other reports on MMT-T_8(*i*-Oct)($CH_2CH_2CH_2NH_2$) complexes with a large interlayer distance and specific surface area were synthesized via ion-exchange reaction followed by freeze-drying treatment [324]. It was observed that the morphology of the POSS–MMT can depend on the POSS concentration, but also on pH of the suspension and the drying procedure. The tensile properties of the composites of POSS–MMT and poly(butylene terephthalate) were extensively improved as compared to the pristine PBT, due to the homogeneous dispersion of POSS–MMT in the polymer matrix (formation of a clay network).

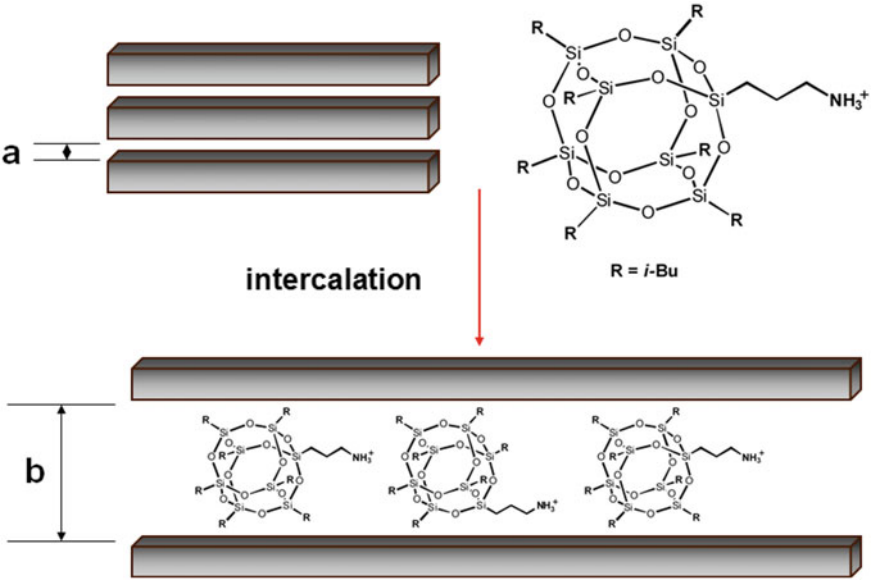

Scheme 19 Intercalation of mineral clays with POSS surfactants [5]

Clays modified with imidazolium-based surfactants are more thermally stable than those intercalated with their ammonium-based analogues. POSS-imidazolium derivatives were used as an organic modifier for MMT [325]. It was found that the self-assembled crystalline POSS domains are present in the clay interlayers but the solvent can change the efficiency of the ion-exchange reaction. The *d*-spacing of the exchanged clay is large (3.6 nm), accommodating a bilayer structure of the POSS-imidazolium molecules, even at low surfactant loading levels. It was observed that the structure and rigidity of the linker between the POSS and the cationic part interacting with MMT can be of significant importance. The packing structures of two types of POSS-imidazolium surfactants with different molecular rigidity intercalated in the intergalleries of MMT results in a bilayer packing structure with long axes of molecules largely tilted with respect to the basal plane [326]. The more flexible POSS-imidazolium cation formed a 2D ordered structure in the clay intergalleries, while the structure of layers formed by the rigid one were disordered (Scheme 20). Furthermore, the clay modified with the rigid surfactant exhibited increased interlayer *d*-spacings on reducing the surfactant loading. Formation of a more extended conformation of the POSS surfactant was postulated. The clay modified with the rigid POSS, despite the low organic content and disordered packing structure, has better thermal and thermo-oxidative stability than the more flexible one.

A range of interesting nanocomposites can be obtained using POSS–MMT hybrids. For example, nanocomposites of polylactide (PLA) reinforced with MMT modified with T_8(*i*-Bu)($CH_2CH_2CH_2NH_2$) were manufactured through melt-compounding [327]. It was found that the melt crystallization rates of the nanocom-

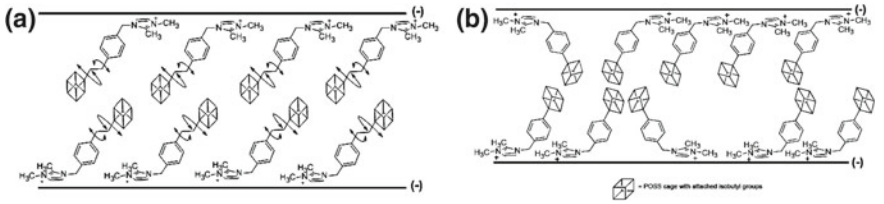

Scheme 20 Organization of rigid and flexible POSS in the interlayer galleries of MMT [326]

posite were enhanced remarkably in comparison with the neat PLA. The overall melt crystallization of PLA/POSS–MMT nanocomposites was found to be dominated by the heterogeneous nucleation and 3D spherulite growth. The isothermal crystallization analysis based on the Avrami model indicated higher spherulite nucleation density of PLA/POSS–MMT nanocomposites but identical spherulite growth rates (regardless of POSS–MMT content). It was also found that the crystalline morphological features of PLA were not influenced by the presence of POSS–MMT.

Poly(ethylene terephthalate) (PET)/montmorillonite nanocomposites were prepared on addition of a very small amount of $T_7Ph_7(OH)_3$ as a functional molecular spacer enhancing the degree of clay dispersion [328]. The trisilanol POSS was able to draw molecules of monomeric bis(2-hydroxyethyl) terephthalate into clay intergalleries, which allowed for their in situ polymerization between platelets of MMT. Moreover, $T_7Ph_7(OH)_3$ reacted with PET, further facilitating clay delamination and reinforcing the mechanical properties of the polymer due to the higher degree of flow-induced clay orientation.

MMT pretreated with a propargyl-containing primary intercalator was exfoliated into layers or sheets of nanoparticles through Huisgen [2 + 3] cycloaddition of singly or multiply azido-functionalized POSS to the propargyl derivative [329].

5 Conclusions and Perspectives

Polyhedral silsesquioxanes are nanoscale hybrid building blocks that can be used in template-free processes leading to the formation of nano- and micro-objects via "bottom-up" strategies. Formation of hierarchical superstructures by those unique self-assembling molecules plays an increasingly important role in materials science. Specific molecular packing and aggregation in the solid state are efficient tools enabling the control of morphology of POSS-derived hybrid materials, modulation of their physicochemical characteristics and performance.

Hierarchical structures formed by POSS can be used in applications related to energy, adsorption, separation and catalysis. Nanotechnologies exploiting self-organization of polyhedral silsesquioxanes and their crystallization patterns afford for the preparation of metal nanoparticles and quantum dots that can be used for high-resolution printing of defect-free microcircuits. Supramolecular materials based on

POSS can be also applied as surfactants, cargo vessels and templates. Understanding the cooperation and complementarity in POSS-based materials is essential for the design of such advanced systems. Precise control of the self-assembling process is the key factor for tailored organization of POSS.

References

1. Wang L, Du W, Wu Y, Xu R, Yu D (2012) Synthesis and characterizations of a latent polyhedral oligomeric silsesquioxane-containing catalyst and its application in polybenzoxazine resin. J Appl Polym Sci 126:150–155
2. Lee YJ, Huang JM, Kuo SW, Chang FC (2005) Low-dielectric, nanoporous polyimide films prepared from PEO–POSS nanoparticles. Polymer 46:10056–10065
3. Eon D, Raballand V, Cartry G, Cardinaud C, Vourdas N, Argitis P, Gogolides E (2006) Plasma oxidation of polyhedral oligomeric silsesquioxane polymers. J Vac Sci Technol B 24:2678–2688
4. Hirai T, Leolukman M, Liu CC, Han E, Kim YJ, Ishida Y, Hayakawa T, Kakimoto MA, Nealey PF, Gopalan P (2009) One-step direct-patterning template utilizing self-assembly of POSS-containing block copolymers. Adv Mater 21:4334–4338
5. Kuo S-W, Chang F-C (2011) POSS related polymer nanocomposites. Progr Polym Sci 36:1649–1696
6. Zhang W, Müller AHE (2013) Architecture, self-assembly and properties of well-defined hybrid polymers based on polyhedral oligomeric silsequioxane (POSS). Progr Polym Sci 38:1121–1162
7. Lim S-K, Lee JY, Choi HJ, Chin I-J (2015) On interaction characteristics of polyhedral oligomeric silsesquioxane containing polymer nanohybrids. Polym Bull 72:2331–2352
8. Mammeri F, Bonhomme C, Ribot F, Babonneau F, Dirè S (2009) New monofunctional POSS and its utilization as dewetting additive in methacrylate based free-standing films. Chem Mater 21:4163–4171
9. Żubrowska A, Piórkowska E, Kowalewska A, Cichorek M (2015) Novel blends of polylactide with ethylene glycol derivatives of POSS. Colloid Polym Sci 293:23–33
10. Kowalewska A, Fortuniak W, Chojnowski J, Pawlak A, Gadzinowska K, Zaród M (2012) Polymer nano-materials through self-assembly of polymeric POSS systems. Silicon 4:95–107
11. Grala M, Bartczak Z (2015) Morphology and mechanical properties of high density polyethylene-POSS hybrid nanocomposites obtained by reactive blending. Polym Eng Sci 55:2058–2072
12. Frone AN, Perrin FX, Radovici C, Panaitescu DM (2013) Influence of branched or unbranched alkyl substitutes of POSS on morphology, thermal and mechanical properties of polyethylene. Composites Part B 50:98–106
13. Sarkar B, Ayandele E, Venugopal V, Alexandridis P (2013) Polyhedral oligosilsesquioxane (POSS) nanoparticle localization in ordered structures formed by solvated block copolymers. Macromol Chem Phys 214:2716–2724
14. Martins JN, Bianchi O, Wanke CH, Dal Castel C, Oliveira RVB (2015) Effects of POSS addition on non-isothermal crystallization and morphology of PVDF. J Polym Res 22:224
15. Zhang D, Shi Y, Liu Y, Huang G (2014) Influences of polyhedral oligomeric silsesquioxanes (POSSs) containing different functional groups on crystallization and melting behaviors of POSS/polydimethylsiloxane rubber composites. RSC Adv 4:41364–41370
16. Jeon J-H, Tanaka K, Chujo Y (2014) Light-driven artificial enzymes for selective oxidation of guanosine triphosphate using water-soluble POSS network polymers. Org Biomol Chem 12:6500–6506

17. Teng CP, Mya KY, Win KY, Yeo CC, Low M, He C, Han M-Y (2014) Star-shaped polyhedral oligomeric silsesquioxane-polycaprolactone-polyurethane as biomaterials for tissue engineering application. NPG Asia Mater 6:e142
18. Wysokowski M, Materna K, Walter J, Petrenko I, Stelling AL, Bazhenov VV, Klapiszewski Ł, Szatkowski T, Lewandowska O, Stawski D, Molodtsov SL, Maciejewski H, Ehrlich H, Jesionowski T (2015) Solvothermal synthesis of hydrophobic chitin–polyhedral oligomeric silsesquioxane (POSS) nanocomposites. Int J Biol Macromol 78:224–229
19. Kakuta T, Tanaka K, Chujo Y (2015) Synthesis of emissive water-soluble network polymers based on polyhedral oligomeric silsesquioxane and their application as optical sensors for discriminating the particle size. J Mater Chem C 3:12539–12545
20. Gon M, Sato K, Tanaka K, Chujo Y (2016) Controllable intramolecular interaction of 3D arranged π-conjugated luminophores based on a POSS scaffold, leading to highly thermally-stable and emissive materials. RSC Adv 6:78652–78660
21. Asad U, Shakir U, Gul SK, Syed MS, Zakir H, Saz M, Muhammad S, Hazrat H (2016) Water soluble polyhedral oligomeric silsesquioxane based amphiphilic hybrid polymers: synthesis, self-assembly, and applications. Eur Polym J 75:67–92
22. Yu X, Li Y, Dong X-H, Yue K, Lin Z, Feng X, Huang M, Zhang W-B, Cheng SZD (2014) Giant surfactants based on molecular nanoparticles: precise synthesis and solution self-assembly. J Polym Sci Part B Polym Phys 52:1309–1325
23. Ullah A, Ullah S, Khan GS, Shah SM, Hussain Z, Muhammada S, Siddiq M, Hussain H (2016) Water soluble polyhedral oligomeric silsesquioxane based amphiphilic hybrid polymers: synthesis, self-assembly, and applications. Eur Polym J 75:67–92
24. Tanaka K, Chujo Y (2012) Advanced functional materials based on polyhedral oligomeric silsesquioxane (POSS). J Mater Chem 22:1733–1746
25. Lickiss PD, Rataboul F (2088) Fully condensed polyhedral oligosilsesquioxanes (POSS): from synthesis to application. In: West R (ed) Advances in organometallic chemistry, vol 57. Elsevier Inc., The Netherlands, pp 1–116
26. Cordes DB, Lickiss PD, Rataboul F (2010) Recent developments in the chemistry of cubic polyhedral oligosilsesquioxanes. Chem Rev 110:2081–2173
27. Cordes DB, Lickiss PD (2011) Preparation and characterization of polyhedral oligosilsesquioxanes. In: Hartmann-Thompson C (ed) Advances in silicon science, vol 3. Springer Science B. V., Berlin, pp 47–113
28. Laine RM (2005) Nanobuilding blocks based on the $[OSiO_{1.5}]_x$ ($x = 6, 8, 10$) octasilsesquioxanes. J Mater Chem 15:3725–3744
29. Marcolli C, Calzaferri G (1999) Monosubstituted octasilasesquioxanes. Appl Organomet Chem 13:213–226
30. Feher FJ, Wyndham KD, Baldwin RK, Soulivong D, Lichtenhan JD, Ziller JW (1999) Methods for effecting monofunctionalization of $(CH_2{=}CH)_8Si_8O_{12}$. Chem Commun 1289–1290
31. Li Y, Guo K, Su H, Li X, Feng X, Wang Z, Zhang W, Zhu S, Wesdemiotis C, Cheng SZD, Zhang W-B (2014) Tuning, "thiol-ene" reactions toward controlled symmetry breaking in polyhedral oligomeric silsesquioxanes. Chem Sci 5:1046–1053
32. Ye Q, Zhou H, Xu J (2016) Cubic polyhedral oligomeric silsesquioxane based functional materials: synthesis, assembly, and applications. Chem Asian J 11:1322–1337
33. Kowalewska A (2017) Self-assembling polyhedral silsesquioxanes—structure and properties. Curr Org Chem 21:1234–1264
34. Barry AJ, Daudt WH, Domicone JJ, Gilkey JW (1955) Crystalline organosilsesquioxanes. J Am Chem Soc 77:4248–4252
35. Auner N, Ziemer B, Herrschaft B, Ziche W, John P, Weis J (1999) Structural studies of novel siloxysilsesquioxanes. Eur J Inorg Chem 7:1087–1094
36. Bolln C, Tsuchida A, Frey H, Mülhaupt R (1997) Thermal properties of the homologous series of 8-fold alkyl-substituted octasilsesquioxanes. Chem Mater 9:1475–1479
37. Perrin FX, Nguyen TBV, Margaillan A (2011) Linear and branched alkyl substituted octakis(dimethylsiloxy)-octasilsesquioxanes: WAXS and thermal properties. Eur. Polym. J. 47:1370–1382

38. Waddon AJ, Coughlin EB (2003) Crystal structure of polyhedral oligomeric silsequioxane (POSS) nano-materials: a study by X-ray diffraction and electron microscopy. Chem Mater 15:4555–4561
39. Bassindale AR, Chen H, Liu Z, MacKinnon IA, Parker DJ, Taylor PG, Yang Y, Light ME, Horton PN, Hursthouse MB (2004) A higher yielding route to octasilsesquioxane cages using tetrabutylammonium fluoride, Part 2: further synthetic advances, mechanistic investigations and X-ray crystal structure studies into the factors that determine cage geometry in the solid state. J Organomet Chem 689:3287–3300
40. Larsson K (1960) Crystal structure of $(HSiO_{1.5})_8$. Arkiv foer Kemi 16:215–219
41. Larsson K (1960) Crystal structure of octa(methylsilsesquioxane), $(CH_3SiO_{1.5})_8$. Arkiv foer Kemi 16:203–208
42. Larsson, K (1960)Crystal structure of substituted octa(silsesquioxanes), $(RSiO_{1.5})_8$ and $(ArSiO_{1.5})_8$. Arkiv foer Kemi 16:209–214
43. Handke B, Jastrzębski W, Kwaśny M (2012) Klita, Structural studies of octahydridooctasilsesquioxane—$H_8Si_8O_{12}$. J Mol Struct 1028:68–72
44. Törnroos KW (1994) Octahydridosilasesquioxane determined by neutron diffraction. Acta Cryst C50:1646–1648
45. Cordes DB, Lickiss PD (2011) Preparation and characterization of polyhedral oligosilsesquioxanes. In: Hartmann-Thompson C (ed) Applications of polyhedral oligomeric silsesquioxanes, vol 3. Advances in silicon science. Springer Science B.V., The Netherlands, pp 47–113
46. Podberezskaya NV, Baidina IA, Alekseev VI, Borisov SV, Martynova TN (1982) X-ray structural study of silasesquioxanes. The crystal structure of octa(allylsilasesquioxane). J Struct Chem 22:737–740
47. El Aziz Y, Bassindale AR, Taylor PG, Stephenson RA, Hursthouse MB, Harrington RW, Clegg W (2013) X-ray crystal structures, packing behavior, and thermal stability studies of a homologous series of *n*-alkyl-substituted polyhedral oligomeric silsesquioxanes. Macromolecules 46:988–1001
48. Chinnam PR, Gau MR, Schwab J, Zdilla MJ, Wunder SL (2014) The polyoctahedral silsesquioxane (POSS) 1,3,5,7,9,11,13,15-octaphenylpentacyclo[9,5,1,13,9,15,15,17,13]-octasiloxane (octaphenyl-POSS). Acta Cryst C70:971–974
49. Morimoto S, Imoto H, Naka K (2017) POSS solid solutions exhibiting orientationally disordered phase transitions. Chem Commun 53:9273–9276
50. Zakharov AV, Masters SL, Wann DA, Shlykov SA, Girichev GV, Arrowsmith S, Cordes DB, Lickiss PD, White AJP (2010) The gas-phase structure of octaphenyloctasilsesquioxane $Si_8O_{12}Ph_8$ and the crystal structures of Si_8O_{12}(p-tolyl)$_8$ and Si_8O_{12}(p-$ClCH_2C_6H_4$)$_8$. Dalton Trans 39:6960–6966
51. Heeley EL, Hughes DJ, El Aziz Y, Williamson I, Taylor PG, Bassindale AR (2013) Properties and self-assembled packing morphology of long alkyl-chained substituted polyhedral oligomeric silsesquioxanes (POSS) cages. Phys Chem Chem Phys 15:5518–5529
52. Bassindale AR, Gentle TE (1993) Siloxane and hydrocarbon octopus molecules with silsesquioxane cores. J Mater Chem 12:1319–1325
53. Heeley EL, Hughes DJ, El Aziz Y, Taylor PG, Bassindale AR (2013) Linear long alkyl chain substituted POSS cages: the effect of alkyl chain length on the self-assembled packing morphology. Macromolecules 46:4944–4954
54. Boese R, Weiss H-C, Bläser D (1999) The melting point alternation in the short-chain n-alkanes: single-crystal X-ray analyses of propane at 30 K and of *n*-butane to *n*-nonane at 90 K. Angew Chem Int Ed 38:988–992
55. Dumitriu AMC, Cazacu M, Bargan A, Balan M, Vornicu N, Varganici C-D, Shova S (2015) Full functionalized silica nanostructure with well-defined size and functionality: Octakis(3-mercaptopropyl)octasilsesquioxane. J Organomet Chem 799–800:195–200
56. Kowalewska A, Nowacka M, Maniukiewicz W (2016) Octa(3-mercaptopropyl)octasilsesquioxane—a reactive nanocube of unique self-assembled packing morphology. J Organomet Chem 810:15–24

57. Marciniec B, Dutkiewicz M, Maciejewski H, Kubicki M (2008) New, effective method of synthesis and structural characterization of octakis(3-chloropropyl)octasilsesquioxane. Organometallics 27:793–794
58. Dumitriu A-M-C, Balan M, Bargan A, Shova S, Varganici C-D, Cazacu M (2016) Synthesis of functionalized silica nanostructure: unexpected conversion of cyanopropyl group in chloropropyl one during HCl-catalysed hydrolysis of the corresponding triethoxysilane. J Molec Struct 1110:150–155
59. Handke B, Jastrzębski W, Mozgawa W, Kowalewska A (2008) Structural studies of crystalline octamethylsilsesquioxane $(CH_3)_8Si_8O_{12}$. J Molec Str 887:159–164
60. Day VW, Klemperer WG, Mainz VV, Millari DM (1985) Molecular building blocks for the synthesis of ceramic materials: $[Si_8O_{12}](OCH_3)_8$. J Am Chem Soc 107:8262–8264
61. Provatas A, Luft M, Mu JC, White AH, Matisons JG, Skelton BW (1998) Silsesquioxanes: part I: a key intermediate in the building of molecular composite materials. J Organomet Chem 565:159–164
62. Xu J, Li X, Cho CM, Toh CL, Shen L, Mya KY, Lu X, He C (2009) Polyhedral oligomeric silsesquioxanes tethered with perfluoroalkylthioether corner groups: facile synthesis and enhancement of hydrophobicity of their polymer blends. J Mater Chem 19:4740–4745
63. Janeta M, John Ł, Ejfler J, Szafert S (2015) Novel organic-inorganic hybrids based on T_8 and T_{10} silsesquioxanes: synthesis, cage-rearrangement and properties. RSC Adv 5:72340–72351
64. Li G, Wang L, Ni H, Pittman CU (2001) Polyhedral oligomeric silsesquioxane (POSS) polymers and copolymers: a review. J Inorg Organomet Polym 11:123–154
65. Liu H, Puchberger M, Schubert U (2011) A facile route to difunctionalized monosubstituted octasilsesquioxanes. Chem Eur J 17:5019–5023
66. Li Y, Dong X-H, Zou Y, Wang Z, Yue K, Huang M, Liu H, Feng X, Lin Z, Zhang W, Zhang W-B, Cheng SZD (2017) Polyhedral oligomeric silsesquioxane meets "click" chemistry: rational design and facile preparation of functional hybrid materials. Polymer 125:303–329
67. Yue K, Liu C, Guo K, Yu X, Huang M, Li H, Wesdemiotis C, Chang SZD, Zhang W-B (2012) Sequential, "click" approach to polyhedral oligomeric silsesquioxane-based shape amphiphiles. Macromolecules 45:8126–8134
68. Li Y, Dong X-H, Guo K, Wang Z, Chen Z, Wesdemiotis C, Quirk RP, Zhang W-B, Chang SZD (2012) Synthesis of shape amphiphiles based on POSS tethered with two symmetric/asymmetric polymer tails via sequential "grafting-from" and thiol–ene "click" chemistry. ACS Macro Lett 1:834–839
69. Li Y, Wang Z, Zheng J, Su H, Lin F, Guo K, Feng X, Wesdemiotis C, Becker ML, Cheng SZD, Zhang W-B (2013) Cascading one-pot synthesis of single-tailed and asymmetric multitailed giant surfactants. ACS Macro Lett 2:1026–1032
70. Wang Z, Li Y, Dong X-H, Yu X, Guo K, Su H, Wesdemiotis C, Cheng SZD, Zhang W-B (2013) Giant gemini surfactants based on polystyrene–hydrophilic polyhedral oligomeric silsesquioxane shape amphiphiles: sequential "click" chemistry and solution self-assembly. Chem Sci 4:1345–1352
71. Su H, Li Y, Yue K, Wang Z, Lu P, Feng X, Dong X-H, Zhang S, Cheng SZD, Zhang W-B (2014) Macromolecular structure evolution toward giant molecules of complex structure: tandem synthesis of asymmetric giant gemini surfactants. Polym Chem 5:3697–3706
72. Li Y, Su H, Feng X, Yue K, Wang Z, Lin Z, Zhu X, Fu Q, Zhang Z, Cheng SZD, Zhang W-B (2015) Precision synthesis of macrocyclic giant surfactants tethered with two different polyhedral oligomeric silsesquioxanes at distinct ring locations via four consecutive "click" reactions. Polym Chem 6:827–837
73. Li Y, Su H, Feng X, Wang Z, Guo K, Wesdemiotis C, Fu Q, Cheng SZD, Zhang W-B (2014) Thiol-Michael "click" chemistry: another efficient tool for head functionalization of giant surfactants. Polym Chem 5:6151–6162
74. Guo S, Sasaki J, Tsujiuchi S, Hara S, Wada H, Kuroda K, Shimojima A (2017) Role of cubic siloxane cages in mesostructure formation and photoisomerization of azobenzene siloxane hybrid. Chem Lett 46:1237–1239

75. Shao Y, Yin H, Wang X-M, Han S-Y, Yan X, Xu J, He J, Ni P, Zhang W-B (2016) Mixed [2:6] hetero-arm star polymers based on Janus POSS with precisely defined arm distribution. Polym Chem 7:2381–2388
76. Han S-Y, Wang X-M, Shao Y, Guo Q-Y, Li Y, Zhang W-B (2016) Janus POSS Based on Mixed [2:6] Octakis-Adduct Regioisomers. Chem Eur J 22:6397–6403
77. Wang X-M, Shao Y, Xu J, Jin X, Shen R-H, Shen D-W, Wang J, Li W, Ni P, Zhang W-B (2017) Precision synthesis and distinct assembly of double-chain giant surfactant regioisomers. Macromolecules 50:3943–3953
78. De Gennes PG (1992) Soft matter (Nobel lecture). Angew Chem 104:856–859
79. Walther A, Müller AHE (2013) Janus particles: synthesis, self-assembly, physical properties, and applications. Chem Rev 113:5194–5261
80. Andrianov KA, Tikhonov VS, Makhneva GP, Chernov GS (1973) Synthesis of polycyclic tetramethyl-tetraphenylcyclooctasilsesquioxane. Bull Acad Sci USSR Div Chem Sci 22:928–928
81. Asuncion MZ, Ronchi M, Abu-Seir H, Laine RM (2010) Synthesis, functionalization and properties of incompletely condensed "half cube" silsesquioxanes as a potential route to nanoscale Janus particles. C R Chim 13:270–281
82. Tateyama S, Kakihana Y, Kawakami Y (2010) Cage octaphenylsilsesquioxane from cyclic tetrasiloxanetetraol and its sodium salt. J Organomet Chem 695:898–902
83. Blázquez-Moraleja A, Pérez-Ojeda ME, Suárez JR, Jimeno ML, Chiara JL (2016) Efficient multi-click approach to well-defined two-faced octasilsesquioxanes: the first perfect Janus nanocube. Chem Commun 52:5792–5795
84. Oguri N, Egawa Y, Takeda N, Unno M (2016) Janus-cube octasilsesquioxane: facile synthesis and structure elucidation. Angew Chem Int Ed 55:9336–9339
85. Yandek GR, Moore BM, Ramirez SM, Mabry JM (2012) Effects of peripheral architecture on the properties of aryl polyhedral oligomeric silsesquioxanes. J Phys Chem C 116:16755–16765
86. Brand R, Lunkenheimer P, Loidl A (2002) Relaxation dynamics in plastic crystals. J Chem Phys 116:10386–10401
87. Folmer JCW, Withers RL, Welberry TR, Martin JD (2008) Coupled orientational and displacive degrees of freedom in the high-temperature plastic phase of the carbon tetrabromide α–CBr 4. Phys. Rev. B 77:144205–144214
88. Kopesky ET, McKinely GH, Cohen RE (2004) Thermomechanical properties of poly(methyl methacrylate)s containing tethered and untethered polyhedral oligomeric silsesquioxanes. Macromolecules 37:8992–9004
89. Croce G, Carniato F, Milanesio M, Boccaleri E, Paul G, van Beek W, Marchese L (2009) Understanding the physico-chemical properties of polyhedral oligomeric silsesquioxanes: a variable temperature multidisciplinary study. Phys Chem Chem Phys 11:10087–10094
90. Bonhomme C, Tolédano P, Maquet J, Livage J, Bonhomme-Coury L (1997) Studies of octameric vinylsilasesquioxane by carbon-13 and silicon-29 cross polarization magic angle spinning and inversion recovery cross polarization nuclear magnetic resonance spectroscopy. J Chem Soc Dalton Trans 1617–1626
91. Taylor PG, Gelbrich T, Hursthouse MB University of Southampton, Crystal structure report archive 2000. http://ecrystals.chem.soton.ac.uk/838/
92. Baidina IA, Podberezskaya NV, Alekseev VI, Martynova TN, Borisov SV, Kanev AN (1980) The crystal structure of vinylsilasesquioxane $[C_2H_3SiO_{3/2}]_8$. J Struct Chem 20:550–554
93. Wu J, Wu ZL, Yang H, Zheng Q (2014) Crosslinking of low density polyethylene with octavinyl polyhedral oligomeric silsesquioxane as the crosslinker. RSC Adv 4:44030–44038
94. Kowalewska A, Nowacka M, Włodarska M, Zgardzińska B, Zaleski R, Oszajca M, Krajenta J, Kaźmierski S (2017) Solid-state dynamics and single-crystal to single-crystal structural transformations in octakis(3-chloropropyl)octasilsesquioxane and octavinyloctasilsesquioxane. Phys Chem Chem Phys 19:27516–27529
95. Poliskie GM, Haddad TS, Blanski RL, Gleason KK (2005) Characterization of the phase transitions of ethyl substituted polyhedral oligomeric silsesquioxane. Thermochim Acta 438:116–125

96. Jalarvo N, Gourdon O, Ehlers G, Tyagi M, Kumar SK, Dobbs KD, Smalley RJ, Guise WE, Ramirez-Cuesta A, Wildgruber C, Crawford MK (2014) Structure and dynamics of octamethyl-POSS nanoparticles. J Phys Chem C 118:5579–5592
97. Tanaka K, Chujo Y (2013) Unique properties of amphiphilic POSS and their applications. Polymer J 45:247–254
98. Wang L, Ishida Y, Maeda R, Tokita M, Hayakawa T (2014) Alkylated cage silsesquioxanes: a comprehensive study of thermal properties and self-assembled structure. RSC Adv 4:34981–34986
99. Wang L, Ishida Y, Maeda R, Tokita M, Horiuchi S, Hayakawa T (2014) Alkylated cage silsesquioxane forming a long-range straight ordered hierarchical lamellar nanostructure. Langmuir 30:9797–9803
100. Yu X, Zhong S, Li X, Tu Y, Yang S, Van Horn R, Ni CY, Pochan DJ, Quirk RP, Wesdemiotis C, Zhang W-B, Cheng SZD (2010) A giant surfactant of polystyrene-(carboxylic acid-functionalized polyhedral oligomeric silsesquioxane) amphiphile with highly stretched polystyrene tails in micellar assemblies. J Am Chem Soc 132:16741–16744
101. Zhou J, Kieffer J (2008) Molecular dynamics simulations of monofunctionalized polyhedral oligomeric silsesquioxane $C_6H_{13}(H_7Si_8O_{12})$. J Phys Chem C 112:3473–3481
102. Takeda M, Kuroiwa K, Mitsuishi M, Matsui J (2015) Self-assembly of amphiphilic POSS anchoring a short organic tail with uniform structure. Chem Lett 44:1560–1562
103. Zhang W, Chu Y, Mu G, Eghtesadi SA, Liu Y, Zhou Z, Lu X, Kashfipour MA, Lillard RS, Yue K, Liu T, Cheng SZD (2017) Rationally controlling the self-assembly behavior of triarmed POSS–organic hybrid macromolecules: from giant surfactants to macroions. Macromolecules 50:5042–5050
104. Yue K, Liu C, Huang M, Huang J, Zhou Z, Wu K, Liu H, Lin Z, Shi A-C, Zhang W-B, Cheng SZD (2017) Self-assembled structures of giant surfactants exhibit a remarkable sensitivity on chemical compositions and topologies for tailoring sub-10 nm nanostructures. Macromolecules 50:303–314
105. Wu K, Huang M, Yue K, Liu C, Lin Z, Liu H, Zhang W, Hsu C-H, Shi A-C, Zhang W-B, Stephen ZD, Cheng SZD (2014) Asymmetric giant "bolaform-like" surfactants: precise synthesis, phase diagram, and crystallization-induced phase separation. Macromolecules 47:4622–4633
106. Yue K, Huang M, Marson RL, He J, Huang J, Zhou Z, Wang J, Liu C, Yan X, Wu K, Guo Z, Liu H, Zhang W, Ni P, Wesdemiotis C, Zhang W-B, Glotzer SC, Cheng SZD (2016) Geometry induced sequence of nanoscale Frank-Kasper and quasicrystal mesophases in giant surfactants. PNAS 113:14195–14200
107. Hsu C-H, Dong X-H, Lin Z, Ni B, Lu P, Jiang Z, Tian D, Shi A-C, Thomas EL, Cheng SZD (2016) Tunable affinity and molecular architecture lead to diverse self-assembled supramolecular structures in thin films. ACS Nano 10:919–929
108. Yu C-B, Ren L-J, Wang W (2017) Synthesis and self-assembly of a series of nPOSS-b-PEO block copolymers with varying shape anisotropy. Macromolecules 50:3273–3284
109. Dong X-H, Ni B, Huang M, Hsu C-H, Chen Z, Lin Z, Zhang W-B, Shi A-C, Cheng SZD (2015) Chain overcrowding induced phase separation and hierarchical structure formation in fluorinated polyhedral oligomeric silsesquioxane (FPOSS)-based giant surfactants. Macromolecules 48:7172–7179
110. Kettwich SC, Pierson SN, Peloquin AJ, Mabry JM, Iacono ST (2012) Anomalous macromolecular assembly of partially fluorinated polyhedral oligomeric silsesquioxanes. New J Chem 36:941–946
111. Dong X-H, Ni B, Huang M, Hsu C-H, Bai R, Zhang W-B, Shi A-C, Cheng SZD (2016) Molecular-curvature-induced spontaneous formation of curved and concentric lamellae through nucleation. Angew Chem Int Ed 55:2459–2463
112. Zhang Z, Xue Y, Zhang P, Müller AHE, Zhang W (2016) Hollow polymeric capsules from POSS-based block copolymer for photodynamic therapy. Macromolecules 49:8440–8448
113. Shimojima A, Goto R, Atsumi N, Kuroda K (2008) Self-assembly of alkyl-substituted cubic siloxane cages into ordered hybrid materials. Chem Eur J 14:8500–8506

114. Liu H, Hsu C-H, Lin Z, Shan W, Wang J, Jiang J, Huang M, Lotz B, Yu X, Zhang W-B, Yue K, Cheng SZD (2014) Two-dimensional nanocrystals of molecular Janus particles. J Am Chem Soc 136:10691–10699
115. Zhang W, Yuan J, Weiss S, Ye X, Li C, Müller AHE (2011) Telechelic hybrid poly(acrylic acid)s containing polyhedral oligomeric silsesquioxane (POSS) and their self-assembly in water. Macromolecules 44:6891–6898
116. Li Y, Zhang W-B, Hsieh I-F, Zhang G, Cao Y, Li X, Wesdemiotis C, Lotz B, Xiong H, Cheng SZD (2011) Breaking symmetry toward nonspherical Janus particles based on polyhedral oligomeric silsesquioxanes: molecular design, "click" synthesis, and hierarchical structure. J Am Chem Soc 133:10712–10715
117. Huang M, Hsu C-H, Wang J, Mei S, Dong X, Li Y, Li M, Liu H, Zhang W, Aida T, Zhang W-B, Yue K, Cheng SZD (2015) Selective assemblies of giant tetrahedra via precisely controlled positional interactions. Science 348:424–428
118. Hu M-B, Hou Z-Y, Hao W-Q, Xiao Y, Yu W, Ma C, Ren L-J, Zheng P, Wang W (2013) POM–organic–POSS cocluster: creating a dumbbell-shaped hybrid molecule for programming hierarchical supramolecular nanostructures. Langmuir 29:5714–5722
119. Ma C, Wu H, Huang Z-H, Guo R-H, Hu M-B, Kĩbel C, Yan L-T, Wang W (2015) A filled-honeycomb-structured crystal formed by self-assembly of a Janus polyoxometalate–silsesquioxane (POM–POSS) co-cluster. Angew Chem Int Ed 54:15699–15704
120. Wu H, Zhang Y-Q, Hu M-B, Ren L-J, Lin Y, Wang W (2017) Creating quasi two-dimensional cluster-assembled materials through self-assembly of a Janus polyoxometalate-silsesquioxane co-cluster. Langmuir 33:5283–5290
121. Liu H, Luo J, Shan W, Guo D, Wang J, Hsu C-H, Huang M, Zhang W, Lotz B, Zhang W-B, Liu T, Yue K, Cheng SZD (2016) Manipulation of self-assembled nanostructure dimensions in molecular janus particles. ACS Nano 10:6585–6596
122. Lin M-C, Hsu C-H, Sun H-J, Wang C-L, Zhang W-B, Li Y, Chen H-L, Cheng SZD (2014) Crystal structure and molecular packing of an asymmetric giant amphiphile constructed by one C60 and two POSSs. Polymer 55:4514–4520
123. Zhang C, Leng Y, Jiang P, Lu D (2016) POSS-based meso-/macroporous covalent networks: supporting and stabilizing Pd for Suzuki-Miyaura reaction at room temperature. RSC Adv 6:57183–57189
124. Liu J, Yu H, Liang Q, Liu Y, Shen J, Bai Q (2017) Preparation of polyhedral oligomeric silsesquioxane based cross-linked inorganic-organic nanohybrid as adsorbent for selective removal of acidic dyes from aqueous solution. J Colloid Interface Sci 497:402–412
125. Peng Y, Ben T, Xu J, Xue M, Jing X, Deng F, Qiu S, Zhu G (2011) A covalently-linked microporous organic-inorganic hybrid framework containing polyhedral oligomeric silsesquioxane moieties. Dalton Trans 40:2720–2724
126. Wang J, Sun J, Zhou J, Jin K, Fang Q (2017) Fluorinated and thermo-cross-linked polyhedral oligomeric silsesquioxanes: new organic–inorganic hybrid materials for high-performance dielectric application. ACS Appl Mater Interfaces 9:12782–12790
127. Chen G, Zhou Y, Wang X, Li J, Xue S, Liu Y, Wang Q, Wang J (2015) Construction of porous cationic frameworks by crosslinking polyhedral oligomeric silsesquioxane units with N-heterocyclic linkers. Scientific Reports 5:11236
128. Li D, Niu Y, Yang Y, Wang X, Yang F, Shen H, Wu D (2015) Synthesis and self-assembly behavior of POSS-embedded hyperbranched polymers. Chem Commun 51:8296–8299
129. Alvarado-Tenorio B, Romo-Uribe A, Mather PT (2011) Microstructure and phase behavior of POSS/PCL shape memory nanocomposites. Macromolecules 44:5682–5692
130. Wang Z, Wang Z, Yu H, Zhao L, Qu J (2012) Controlled network structure and its correlations with physical properties of polycarboxyl octaphenylsilsesquioxanes-based inorganic–organic polymer nanocomposites. RSC Adv 2:2759–2767
131. Cheng C-C, Yen Y-C, Chang F-C (2011) Self-supporting polymer from a POSS derivative. Macromol Rapid Commun 32:927–932
132. Cheng C-C, Yen Y-C, Ko F-H, Chu C-W, Fan S-K, Chang F-C (2012) A new supramolecular film formed from a silsesquioxane derivative for application in proton exchange membranes. J Mater Chem 22:731–734

133. Voisin D, Flot D, Van der Lee A, Dautel OJ, Moreau JJE (2017) Hydrogen bond-directed assembly of silsesquioxanes cubes: synthesis of carboxylic acid POSS derivatives and the solid state structure of octa[2-(p-carboxyphenyl)ethyl] silsesquioxane. CrystEngComm 19:492–502
134. Lu Y-S, Yu C-Y, Lin Y-C, Kuo S-W (2016) Hydrogen bonding strength of diblock copolymers affects the self-assembled structures with octa-functionalized phenol POSS nanoparticles. Soft Matter 12:2288–2300
135. Wu Y-C, Shiao-Wei Kuo S-W (2012) Self-assembly supramolecular structure through complementary multiple hydrogen bonding of heteronucleobase-multifunctionalized polyhedral oligomeric silsesquioxane (POSS) complexes. J Mater Chem 22:2982–2991
136. Shih R-S, Lu C-H, Kuo S-W, Chang F-C (2010) Hydrogen bond-mediated self-assembly of polyhedral oligomeric silsesquioxane-based supramolecules. J Phys Chem C 114:12855–12862
137. Wang J-H, Altukhov O, Cheng C-C, Chang F-C, Kuo S-W (2013) Supramolecular structures of uracil-functionalized PEG with multi-diamidopyridine POSS through complementary hydrogen bonding interactions. Soft Matter 9:5196–5206
138. Lu L, Zhang C, Li L, Zhou C (2013) Reversible pH-responsive aggregates based on the self-assembly of functionalized POSS and hyaluronic acid. Carbohydrate Polym 94:444–448
139. Yang L, Lu L, Zhang C-W, Zhou C-R (2016) Highly stretchable and self-healing hydrogels based on poly(acrylic acid) and functional POSS. Chin J Polym Sci 34:185–194
140. Sato N, Kuroda Y, Abe T, Wada H, Shimojima A, Kuroda K (2015) Regular assembly of cage siloxanes by hydrogen bonding of dimethylsilanol groups. Chem Commun 51:11034–11037
141. Kawahara K, Tachibana H, Hagiwara Y, Kuroda K (2012) A spherosilicate oligomer with eight stable silanol groups as a building block of hybrid materials. New J Chem 36:1210–1217
142. Kawakami Y, Sakuma Y, Wakuda T, Nakai T, Shirasaka M, Kabe Y (2010) Hydrogen-bonding 3D networks by polyhedral organosilanols: selective inclusion of hydrocarbons in open frameworks. Organometallics 29:3281–3288
143. Farha OK, Hupp JT (2010) Rational design, synthesis, purification, and activation of metal–organic framework materials. Acc Chem Res 43:1166–1175
144. Stock N, Biswas S (2012) Synthesis of metal-organic frameworks (MOFs): routes to various MOF topologies, morphologies, and composites. Chem Rev 112:933–969
145. Meek ST, Greathouse JA, Allendorf MD (2011) Metal-organic frameworks: a rapidly growing class of versatile nanoporous materials. Adv Mater 23:249–267
146. Liu J, Chen L, Cui H, Zhang J, Zhang L, Su C-Y (2014) Applications of metal-organic frameworks in heterogeneous supramolecular catalysis. Chem Soc Rev 43:6011–6061
147. Cui YJ, Li B, He HJ, Zhou W, Chen BL, Qian GD (2016) Metal-organic frameworks as platforms for functional materials. Acc Chem Res 49:483–493
148. Banerjee S, Kataoka S, Takahashi T, Kamimura Y, Suzuki K, Sato K, Endo A (2016) Controlled formation of ordered coordination polymeric networks using silsesquioxane building blocks. Dalton Trans 45:17082–17086
149. Köytepe S, Demirel MH, Gültek A, Seçkin T (2014) Metallo-supramolecular materials based on terpyridine-functionalized polyhedral silsesquioxane. Polym Int 63:778–787
150. Carbonell E, Bivona LA, Fusaro L, Aprile C (2017) Silsesquioxane–terpyridine nano building blocks for the design of three-dimensional polymeric networks. Inorg Chem 56:6393–6403
151. Dang S, Zhu QL, Xu Q (2017) Nanomaterials derived from metal–organic frameworks. Nat Rev Mater 3, Article no. 17075
152. Sanil ES, Cho K-H, Hong D-Y, Lee JS, Lee S-K, Ryu SG, Lee HW, Chang J-S, Hwang YK (2015) A polyhedral oligomeric silsesquioxane functionalized copper trimesate. Chem Commun 51:8418–8420
153. Chan MHY, Ng M, Leung SYL, Lam WH, Yam VWW (2017) Synthesis of luminescent platinum(II) 2,6-bis-(N-dodecylbenzimidazol-2 '-yl)pyridine foldamers and their supramolecular assembly and metallogel formation. J Am Chem Soc 139:8639–8645
154. Zhang SL, Luo KJ, Geng H, Ni HL, Wang HF, Li Q (2017) New phosphorescent platinum(II) complexes with tetradentate CNNC ligands: liquid crystallinity and polarized emission. Dalton Trans 46:899–906

155. Chico R, de Domingo E, Dominguez C, Donnio B, Heinrich B, Termine R, Golemme A, Coco S, Espinet P (2017) High one-dimensional charge mobility in semiconducting columnar mesophases of isocyano-triphenylene metal complexes. Chem Mater 29:7587–7595
156. Au-Yeung H-L, Leung SY-L, Tam AYY, Yam VW-W (2014) Transformable nanostructures of platinum-containing organosilane hybrids: non-covalent self-assembly of polyhedral oligomeric silsesquioxanes assisted by Pt···Pt and π–π stacking interactions of alkynylplatinum(II) terpyridine moieties. J Am Chem Soc 136:17910–17913
157. Au-Yeung H-L, Tam AYY, Leung SY-L, Yam VW-W (2017) Supramolecular assembly of platinum-containing polyhedral oligomeric silsesquioxanes: an interplay of intermolecular interactions and a correlation between structural modifications and morphological transformations. Chem Sci 8:2267–2276
158. Li L, Feng S, Liu H (2014) Hybrid lanthanide complexes based on a novel β-diketone functionalized polyhedral oligomeric silsesquioxane (POSS) and their nanocomposites with PMMA via in situ polymerization. RSC Adv 4:39132–39139
159. Xu Q, Li Z, Chen M, Li H (2016) Synthesis and luminescence of octacarboxy cubic polyhedral oligosilsesquioxanes coordinated with terbium. CrystEngComm 18:177–182
160. Naka K, Chujo Y (2009) Nanohybridized synthesis of metal nanoparticles and their organization. In: Muramatsu A, Miyashita T (eds) Nanohybridization of organic-inorganic materials, vol XVI. Springer, Berlin, p 191
161. Kuo S-W, Wu Y-C, Lu C-H., Chang F-C (2009) Surface modification of gold nanoparticles with polyhedral oligomeric silsesquioxane and incorporation within polymer matrices. J Polym Sci Part B Poly Phys 47:811–819
162. Daniel M-C, Astruc D (2004) Gold nanoparticles: assembly, supramolecular chemistry, quantum-size-related properties, and applications toward biology, catalysis, and nanotechnology. Chem Rev 104:293–346
163. Naka K, Itoh H, Chujo Y (2004) Preparation of gold nanoparticles protected by a cubic silsesquioxane and their monolayer formation on a glass substrate. Bull Chem Soc Jpn 77:1767–1771
164. Imoto H, Ishida K, Sasaki A, Irie Y, Ito H, Naka K, Chujo Y (2015) Spontaneous formation of gold nanoparticles with octa(3-aminopropyl) polyhedral oligomeric silsesquioxane. Bull Chem Soc Jpn 88:653–656
165. Imoto H, Shigeyoshi S, Naka K (2015) Surface modification and aggregation control of gold nanoparticles via multifunctional stabilizer based on polyhedral oligomeric silsesquioxane. Bull Chem Sci Jpn 88:693–697
166. Wang X, Naka K, Itoh H, Chujo Y (2004) Self-organized nanocomposites of functionalized gold nanoparticles with octa(3-aminopropyl)octasilsesquioxane. Chem Lett 33:216–217
167. Carroll JB, Frankamp BL, Srivastava S, Rotello VM (2004) Electrostatic self-assembly of structured gold nanoparticle/polyhedral oligomeric silsesquioxane (POSS) nanocomposites. J Mater Chem 14:690–694
168. Bai W, Sheng Q, Ma X, Zheng J (2015) Synthesis of silver nanoparticles based on hydrophobic interface regulation and its application of electrochemical catalysis. ACS Sustain Chem Eng 3:1600–1609
169. Létant SE, Maiti A, Jones TV, Herberg JL, Maxwell RS, Saab AP (2009) Polyhedral oligomeric silsesquioxane (POSS)-stabilized Pd nanoparticles: factors governing crystallite morphology and secondary aggregate structure. J Phys Chem C 113:19424–19431
170. Naka K, Itoh H, Chujo Y (2002) Self-organization of spherical aggregates of palladium nanoparticles with a cubic silsesquioxane. Nano Lett 2:1183–1186
171. Naka K, Sato M, Chujo Y (2008) Stabilized spherical aggregate of palladium nanoparticles prepared by reduction of palladium acetate in octa(3-aminopropyl)octasilsesquioxane as a rigid template. Langmuir 24:2719–2726
172. Wang X, Naka K, Zhu M, Itoh H, Chujo Y (2005) Microporous nanocomposites of Pd and Au nanoparticles via hierarchical self-assembly. Langmuir 21:12395–12398
173. Chen T, Ge C, Zhang Y, Zhao Q, Hao F, Bao N (2015) Bimetallic platinum-bismuth nanoparticles prepared with silsesquioxane for enhanced electrooxidation of formic acid. Int J Hydrogen Energy 40:4548–4557

174. Lu C-H, Kuo S-W, Huang C-F, Chang F-C (2009) Self-assembled fernlike microstructures of polyhedral oligomeric silsesquioxane/gold nanoparticle hybrids. J Phys Chem C 113:3517–3524
175. Lu C-H, Chang F-C (2011) Polyhedral oligomeric silsesquioxane-encapsulating amorphous palladium nanoclusters as catalysts for Heck reactions. ACS Catal 1:481–488
176. Carroll JB, Frankamp BL, Rotello VM (2002) Self-assembly of gold nanoparticles through tandem hydrogen bonding and polyoligosilsequioxane (POSS)–POSS recognition processes. Chem Commun 1892–1893
177. Jeoung E, Carroll JB, Rotello VM (2002) Surface modification via 'lock and key' specific self-assembly of polyhedral oligomeric silsequioxane (POSS) derivatives to modified gold surfaces. Chem Commun, 1510–1511
178. Cai J, Chao L, Watanabe, A (2015) Facile preparation of hierarchical structures using crystallization-kinetics driven self-assembly. ACS Appl Mater Interfaces 18697–18706
179. Ledin PA, Russell M, Geldmeier JA, Tkachenko IM, Mahmoud MA, Shevchenko V, El-Sayed MA, Tsukruk VV (2015) Light-responsive plasmonic arrays consisting of silver nanocubes and a photoisomerizable matrix. ACS Appl Mater Interfaces 7:4902–4912
180. Ye X, Gong J, Wang Z, Zhang Z, Han S, Jiang X (2013) Hybrid POSS-containing brush on gold surfaces for protein resistance. Macromol Biosci 13:921–926
181. Wang F, Phonthammachai N, Mya KY, Tjiu WW, He C (2011) PEG-POSS Assisted facile preparation of amphiphilic gold nanoparticles and interface formation of Janus nanoparticles. Chem Commun 47:767–769
182. Zhang X, Hu Y, Liu R, Sun J, Fang S (2015) Thermosensitive gold nanoparticles based on star-shaped poly(N-isopropylacrylamide) with a cubic silsesquioxane core. Macromol Res 23:227–230
183. Mohapatra S, Chaiprasert T, Sodkhomkhum R, Kunthom R, Hanprasit S, Sangtrirutnugul P, Ervithayasuporn V (2016) Solid–state synthesis of polyhedral oligomeric silsesquioxane-supported N-heterocyclic carbenes/imidazolium salts on palladium nanoparticles: highly active and recyclable catalyst. ChemistrySelect 1:5353–5357
184. Frankamp BL, Fischer NO, Hong R, Srivastava S, Rotello VM (2006) Surface modification using cubic silsesquioxane ligands. Facile synthesis of water-soluble metal oxide nanoparticles. Chem Mater 18:956–959
185. Etgar L, Lifshitz E, Tannenbaum R (2007) Hierarchical conjugate structure of γ-Fe_2O_3 nanoparticles and PbSe quantum dots for biological applications. J Phys Chem C 111:6238–6244
186. Yuan W, Shen J, Lia L, Liu X, Zou H (2014) Preparation of POSS-poly(ε-caprolactone)-β-cyclodextrin/Fe_3O_4 hybrid magnetic micelles for removal of bisphenol A from water. Carbohyd Polym 113:353–361
187. Safaei-Ghomi J, Nazemzadeh SH, Shahbazi-Alavi H (2016) Novel magnetic nanoparticles-supported inorganic-organic hybrids based on POSS as an efficient nanomagnetic catalyst for the synthesis of pyran derivatives. Catalysis Comm 86:14–18
188. Evans CM, Cass LC, Knowles KE, Tice DB, Chang RPH, Weiss EA (2012) Review of the synthesis and properties of colloidal quantum dots: the evolving role of coordinating surface ligands. J Coordination Chem 65:2391–2414
189. Wang Y, Vaneski A, Yang H, Gupta S, Hetsch F, Kershaw SV, Teoh WY, Li H, Rogach AL (2013) Polyhedral oligomeric silsesquioxane as a ligand for CdSe quantum dots. J Phys Chem C 117:1857–1862
190. Rizvi SB, Yildirimer L, Ghaderi S, Ramesh B, Seifalian AM, Keshtgar M (2012) A novel POSS-coated quantum dot for biological application. Int J Nanomed 7:3915–3927
191. He Y, Wang H-F, Yan X-P (2009) Self-assembly of Mn-doped ZnS quantum dots/octa(3-aminopropyl)octasilsequioxane octahydrochloride nanohybrids for optosensing DNA. Chem Eur J 15:5436–5440
192. Zhao X, Ma R, Yang M, Yang H, Jin P, Li Z, Fan Y, Du A, Cao X (2017) Fabrication of POSS-coated CdTe quantum dots sensitized solar cells with enhanced photovoltaic properties. J Alloys Comp 726:593–600

193. Park Y, Yoo J, Lim B, Kwon W, Rhee S-W (2016) Improving the functionality of carbon nanodots: doping and surface functionalization. J Mater Chem A 4:11582–11603
194. Wang D, Liu J, Chen J-F, Dai L (2015) Surface functionalization of carbon dots with polyhedral oligomeric silsesquioxane (POSS) for multifunctional applications. Adv Mater Interfaces 3:1500439
195. Wang W-J, Hai X, Mao Q-X, Chen M-L, Wang J-H (2015) Polyhedral oligomeric silsesquioxane functionalized carbon dots for cell imaging. ACS Appl Mater Interfaces 7:16609–16616
196. Wang Y, Kalytchuk S, Wang L, Zhovtiuk O, Cepe K, Zboril R, Rogach AL (2015) Carbon dot hybrids with oligomeric silsesquioxane: solid-state luminophores with high photoluminescence quantum yield and applicability in white light emitting devices. Chem Commun 51:2950–2953
197. Potsi G, Rossos A, Kouloumpis A, Antoniou MK, Spyrou K, Karakassides MA, Gournis D, Rudolf P (2016) Carbon nanostructures containing polyhedral oligomeric silsesquioxanes (POSS). Curr Org Chem 20:662–673
198. Inagaki M, Toyoda M, Soneda Y, Tsujimura S, Morishita T (2016) Templated mesoporous carbons: synthesis and applications. Carbon 107:448–473
199. Kong J, Wei Y, Lu X, He C (2017) Cross-linking Si_xO_y cages with carbon by thermally annealing polyhedral oligomeric silsesquioxane: structures, morphology, and electrochemical properties as lithium-ion battery anodes. ChemElectroChem 4:49–55
200. Li Z, Wu D, Liang Y, Fu R, Matyjaszewski K (2014) Synthesis of well-defined microporous carbons by molecular-scale templating with polyhedral oligomeric silsesquioxane moieties. J Am Chem Soc 136:4805–4808
201. Li Z, Li Z, Zhong W, Li C, Li L, Zhang H (2017) Facile synthesis of ultra-small Si particles embedded in carbon framework using Si-carbon integration strategy with superior lithium ion storage performance. Chem Eng J 319:1–8
202. Li Z, Li Z, Li L, Li C, Zhong W, Zhang H (2017) Construction of hierarchically one-dimensional core–shell CNT@microporous carbon by covalent bond-induced surface-confined cross-linking for high-performance supercapacitor. ACS Appl Mater Interfaces 9:15557–15565
203. Liu D, Cheng G, Zhao H, Zeng C, Qu D, Xiao L, Tang H, Deng Z, Li Y, Su B-L (2016) Self-assembly of polyhedral oligosilsesquioxane (POSS) into hierarchically ordered mesoporous carbons with uniform microporosity and nitrogen-doping for high performance supercapacitors. Nano Energy 22:255–268
204. Ren Z, Yan S (2016) Polysiloxanes for optoelectronic applications. Progr Mater Sci 83:383–416
205. Li Z, Kong J, Wang F, He C (2017) Polyhedral oligomeric silsesquioxanes (POSSs): an important building block for organic optoelectronic materials. J Mater Chem C 5:5283–5298
206. Leu C-M, Chang Y-T, Wei K-H (2003) Polyimide-side-chain tethered polyhedral oligomeric silsesquioxane nanocomposites for low-dielectric film applications. Chem Mater 15:3721–3727
207. Chen Y, Kang E-T (2014) New approach to nanocomposites of polyimides containing polyhedral oligomeric silsesquioxane for dielectric applications. Mater Lett 58:3716–3719
208. Ben H-J, Ren X-K, Song B, Li X, Feng Y, Jiang W, Chen E-C, Wang Z, Jiang S (2017) Synthesis, crystal structure, enhanced photoluminescence properties and fluoride detection ability of S-heterocyclic annulated perylene diimide-polyhedral oligosilsesquioxane dye. J Mater Chem C 5:2566–2576
209. Vinnik FM (1993) Photophysics of preassociated pyrenes in aqueous polymer solutions and in other organized media. Chem Rev 93:587–614
210. Figueira-Duarte TM, Müllen K (2011) Chem Rev 111:7260–7314
211. Bains G, Patel AB, Narayanaswami V (2011) Molecules 16:7909–7935
212. Lin TT, He C, Xiao Y (2003) Theoretical studies of monosubstituted and higher phenyl-substituted octahydrosilsesquioxanes. J Phys Chem B 107:13788–13792
213. Chu Y-L, Cheng C-C, Chen Y-P, Yen Y-C, Chang F-C (2012) A new supramolecular POSS electroluminescent material. J Mater Chem 22:9285–9292

214. Cheng C-C, Chu Y-L, Chu C-W, Lee D-J (2016) Highly efficient organic–inorganic electroluminescence materials for solution processed blue organic light-emitting diodes. J Mater Chem C 4:6461–6465
215. Bai H, Li C, Shi G (2008) Pyrenyl excimers induced by the crystallization of POSS moieties: spectroscopic studies and sensing applications. ChemPhysChem 9:1908–1913
216. Gao Y, Xu W, Zhu D, Chen L, Fu Y, He Q, Cao H, Cheng J (2015) Highly efficient nitrate ester explosive vapor probe based on multiple triphenylaminopyrenyl substituted POSS. J Mater Chem A 3:4820–4826
217. Lu C-H, Tsai C-H, Chang F-C, Jeong K-U, Kuo S-W (2011) Self-assembly behavior and photoluminescence property of bispyrenyl-POSS nanoparticle hybrid. J Colloid Interf Sci 358:93–101
218. Yang XH, Giovenzana T, Feild B, Jabbour GE (2012) Sellinger, A Solution processeable organic–inorganic hybrids based on pyrene functionalized mixed cubic silsesquioxanes as emitters in OLEDs. J Mater Chem 22:12689–12694
219. Chanmungkalakul S, Ervithayasuporn V, Hanprasit S, Masik M, Prigyai N, Kiatkamjornwong S (2017) Silsesquioxane cages as fluoride sensors. Chem Commun 53:12108–12111
220. Bassindale AR, Pourny M, Taylor PG, Hursthouse MB, Light ME (2003) Fluoride-Ion encapsulation within a silsesquioxane cage. Angew Chem Int Ed 42:3488–3490
221. Pappalardo RR, Marcos ES, Lopez-Ruiz MF (1993) Solvent effects on molecular geometries and isomerization processes: a study of push-pull ethylenes in solution. J Am Chem Soc 115:3722–3730
222. Clarke D, Mathew S, Matisons J, Simon G, Skelton BW (2011) Synthesis and characterization of a range of POSS imides. Dyes Pigm 92:659–667
223. Ren X, Sun B, Tsai C-C, Tu Y, Leng S, Li K, Kang Z, Van Horn RM, Li X, Zhu M, Wesdemiotis C, Zhang W-B, Cheng SZD (2010) Synthesis, self-assembly, and crystal structure of a shape-persistent polyhedral-oligosilsesquioxane-nanoparticle-tethered perylene diimide. J Phys Chem B 114:4802–4810
224. Zhang Y, Zhang L, Liu H, Sun D, Li X (2015) Synthesis and aggregation properties of a series of dumbbell polyhedral oligosilsesquioxane-perylene diimide triads. CrystEngComm 17:1453–1463
225. Lucenti E, Botta C, Cariati E, Righetto S, Scarpellini M, Tordin E, Ugo R (2013) New organic-inorganic hybrid materials based on perylene diimide-polyhedral oligomeric silsesquioxane dyes with reduced quenching of the emission in the solid state. Dyes Pigm 96:748–755
226. Du F, Tian J, Wang H, Liu B, Jin B, Bai R (2012) Synthesis and luminescence of POSS-containing perylene bisimide-bridged amphiphilic polymers. Macromolecules 45:3086–3093
227. Matsumoto K, Nishi K, Ando K, Jikei M (2015) Synthesis and properties of aromatic polyamide dendrimers with polyhedral oligomeric silsesquioxane cores. Polym Chem 6:4758–4765
228. Mehl GH, Saez IM (1999) Polyhedral liquid crystal silsesquioxanes. Appl Organometal Chem 13:261–272
229. Saez IM, Goodby JW (2001) Chiral nematic octasilsesquioxanes. J Mater Chem 11:2845–2851
230. Haxton KJ, Morris RE (2009) Polyhedral oligomeric silsesquioxane dendrimers in silicon-containing dendritic polymers. In: Dvornic PR, Owen MJ (eds) Advances in silicon science. Springer Science + Business Media B.V., Berlin, pp 121–139
231. Saez IM, Goodby JW (2008) Supermolecular liquid crystals. In: Kato T (ed) Structure and bonding (Series Editor: Mingos DMP) liquid crystalline functional assemblies and their supramolecular structures, vol 128. Springer, Berlin, pp 1–62
232. Zhang C, Bunning TJ, Laine RM (2001) Synthesis and characterization of liquid crystalline silsesquioxanes. Chem Mater 13:3653–3662
233. Shibaev V, Boiko N (2009) Liquid crystalline silicon-containing dendrimers with terminal mesogenic groups. In: Dvornic PR, Owen MJ (eds) Advances in silicon science. Springer Science + Business Media B.V., Berlin, pp 237–283

234. Mehl GH, Goodby JW (1996) Liquid-crystalline, substituted octakis-(dimethylsiloxy)octasilsesquioxanes: oligomeric supermolecular materials with defined topology. Angew Chem Int Ed Eng 35:2641–2643
235. Saez IM, Goodby JW, Richardson RM (2001) A liquid-crystalline silsesquioxane dendrimer exhibiting chiral nematic and columnar mesophases. Chem Eur J 7:2758–2764
236. Keith C, Dantlgraber G, Reddy RA, Baumeister U, Prehm M, Hahn H, Lang H, Tschierske C (2007) The influence of shape and size of silyl units on the properties of bent-core liquid crystals—from dimers via oligomers and dendrimers to polymers. J Mater Chem 17:3796–3805
237. Pan Q, Chen X, Fan X, Shen Z, Zhou Q (2008) Organic–inorganic hybrid bent-core liquid crystals with cubic silsesquioxane cores. J Mater Chem 18:3481–3488
238. Białecka-Florjańczyk E, Sołtysiak JT (2010) Liquid crystalline silicon-containing oligomers. J Organomet Chem 695:1911–1917
239. Chiang I-H, Chuang W-T, Lu C-L, Lee M-T, Lin H-C (2015) Shape and confinement effects of various terminal siloxane groups on supramolecular interactions of hydrogen-bonded bent-core liquid crystals. Chem Mater 27:4525–4537
240. Pan Q, Gao L, Chen X, Fan X, Zhou Q (2007) Star mesogen-jacketed liquid crystalline polymers with silsesquioxane core: synthesis and characterization. Macromolecules 40:4887–4894
241. Wang X, Cho CM, Say WY, Tan AYX, He C, Chan HSO, Xu J (2011) Organic–inorganic hybrid liquid crystals derived from octameric silsesquioxanes. Effect of the peripheral groups in mesogens on the formation of liquid crystals. J Mater Chem 21:5248–5257
242. Saez IM, Goodby JW (1999) Supermolecular liquid crystal dendrimers based on the octasilsesquioxane core. Liq Cryst 26:1101–1105
243. Karahaliou PK, Kouwer PHJ, Meyer T, Mehl GH, Photinos DJ (2008) Long- and short-range order in the mesophases of laterally substituted calamitic mesogens and their radial octapodes. J Phys Chem B 112:6550–6556
244. Kim D-Y, Kim S, Lee S-A, Choi Y-E, Yoon W-J, Kuo S-W, Hsu C-H, Huang M, Lee SH, Jeong K-U (2014) Asymmetric organic–inorganic hybrid giant molecule: cyanobiphenyl monosubstituted polyhedral oligomeric silsesquioxane nanoparticles for vertical alignment of liquid crystals. J Phys Chem C 118:6300–6306
245. Kim N, Kim D-Y, Park M, Choi Y-J, Kim S, Lee SH, Jeong K-U (2015) Asymmetric organic–inorganic hybrid giant molecule: hierarchical smectic phase induced from POSS nanoparticles by addition of nematic liquid crystals. J Phys Chem C 119:766–774
246. Miniewicz A, Girones J, Karpinski P, Mossety-Leszczak B, Galina H, Dutkiewicz M (2014) Photochromic and nonlinear optical properties of azo-functionalized POSS nanoparticles dispersed in nematic liquid crystals. J Mater Chem C 2:432–440
247. Liu H-S, Jeng S-C (2013) Liquid crystal alignment by polyhedral oligomeric silsesquioxane (POSS)–polyimide nanocomposites. Opt Mater 35:1418–1421
248. Hou P-P, Gu K-H, Zhu Y-F, Zhang Z-Y, Wang Q, Pan H-B, Yang S, Shen Z, Fan X-H (2015) Synthesis and sub-10 nm supramolecular selfassembly of a nanohybrid with a polynorbornene main chain and side-chain POSS moieties. RSC Adv 5:70163–70171
249. Zhu Y-F, Liu W, Zhang M-Y, Zhou Y, Zhang Y-D, Hou P-P, Pan Y, Shen Z, Fan X-H, Zhou Q-F (2015) POSS-containing jacketed polymer: hybrid inclusion complex with hierarchically ordered structures at sub-10 nm and Angstrom length scales. Macromolecules 48:2358–2366
250. Mehl GH, Thornton AJ, Goodby JW (1999) Oligomers and dendrimers based on siloxane and silsesquioxane cores: does the structure of the central core affect the liquid-crystalline properties? Mol Cryst Liquid Cryst Sci Technol Sect A. Mol Cryst Liquid Cryst 332:455–461
251. Wang G, Xiong Y, Tang H (2015) Synthesis and characterisation of star-shaped liquid crystalline polymer with a POSS core. Liquid Cryst 42:1280–1289
252. Miao J, Zhu L (2010) Topology controlled supramolecular self-assembly of octa triphenylene-substituted polyhedral oligomeric silsesquioxane hybrid supermolecules. J Phys Chem B 114:1879–1887
253. Cui L, Collet JP, Xu G, Zhu L (2006) Supramolecular self-assembly in a disk-cube dyad molecule based on triphenylene and polyhedral oligomeric silsesquioxane (POSS). Chem Mater 18:3503–3512

254. Xiang K, He L, Li Y, Xu C, Li S (2015) Dendritic AIE-active luminogens with a POSS core: synthesis, characterization, and application as chemosensors. RSC Adv 5:97224–97230
255. Zuo Y, Wang X, Yang Y, Huang D, Yang F, Shen H, Wu D (2016) Facile preparation of pH-responsive AIE-active POSS dendrimers for the detection of trivalent metal cations and acid gases. Polym Chem 7:6432–6436
256. Zhou H, Li J, Chua MH, Yan H, Ye Q, Song J, Lin TT, Tang BZ, Xu J (2016) Tetraphenylethene (TPE) modified polyhedral oligomeric silsesquioxanes (POSS): unadulterated monomer emission, aggregation-induced emission and nanostructural self-assembly modulated by the flexible spacer between POSS and TPE. Chem Commun 52:12478–12481
257. Zhang M-Y, Zhou S, Pan H-B, Ping J, Zhang W, Fan X-H, Shen Z (2017) Structural complexity induced by topology change in hybrids consisting of hexa-perihexabenzocoronene and polyhedral oligomeric silsesquioxane. Chem Commun 53:8679–8682
258. Zhang M-Y, Gu K-H, Zhou Y, Zhou S, Fan X-H, Shen Z (2016) The synthesis and self-assembly of disc-cube dyads with spacers of different lengths. Chem Commun 52:3923–3926
259. Tan J, Ma D, Sun X, Feng S, Zhang C (2013) Synthesis and characterization of an octaimidazolium based polyhedral oligomeric silsesquioxanes ionic liquid by an ion-exchange reaction. Dalton Trans 42:4337–4339
260. Tanaka K, Ishiguro F, Jeon J-H, Hiraoka T, Chujo Y (2015) POSS ionic liquid crystals. NPG Asia Mater 7:e174
261. Tanaka K, Ishiguro F, Chujo Y (2010) POSS ionic liquid. J Am Chem Soc 132:17649–17651
262. Gon M, Tanaka K, Chujo Y (2017) Creative synthesis of organic-inorganic molecular hybrid materials. Bull Chem Soc Jpn 90:463–474
263. Zhou J, Yin P, Hu L, Haso F, Liu T (2014) Self-assembly of subnanometer-scaled polyhedral oligomeric silsesquioxane (POSS) macroions in ddilute solution. Eur J Inorg Chem 4593–4599
264. Zhang W, Wang Z-S (2014) Synthesis of POSS-based ionic conductors with low glass transition temperatures for efficient solid-state dye-sensitized solar cells. ACS Appl Mater Interfaces 6:10714–10721
265. Lee JH, Lee AS, Lee J-C, Hong SM, Hwang SS, Koo CM (2017) Multifunctional mesoporous ionic gels and scaffolds derived from polyhedral oligomeric silsesquioxanes. ACS Appl Mater Interfaces 9:3616–3623
266. Yuan G, Wang X, Wu D, Hammouda B (2016) Structural analysis of dendrimers based on polyhedral oligomeric silsesquioxane and their assemblies in solution by small-angle neutron scattering: fits to a modified two correlation lengths model. Polymer 100:119–125
267. Bai Y, Yang L, Toh CL, He C, Lu X (2013) Temperature and pH dual-responsive behavior of dendritic poly(*N*-isopropylacrylamide) with a polyoligomeric silsesquioxane core and poly(2-hydroxyethyl methacrylate) shell. Macromol Chem Phys 214:396–404
268. Naka K, Masuoka S, Shinke R, Yamada M (2012) Synthesis of first- and second-generation imidazole terminated POSS-core dendrimers and their pH responsive and coordination properties. Polym J 44:353–359
269. Naka K, Shinke R, Yamada M, Belkada FD, Aijo Y, Irie Y, Shankar SR, Smaran KS, Matsumi N, Tomita S, Sakurai S (2014) Synthesis of imidazolium salt-terminated poly(amidoamine)-typed POSS-core dendrimers and their solution and bulk properties. Polym J 46:42–51
270. Li L, Liu H (2016) Rapid preparation of silsesquioxane-based ionic liquids. Chem Eur J 22:4713–4716
271. Han J, Zheng Y, Zheng S, Li S, Hu T, Tang A, Gao C (2014) Water soluble octa-functionalized POSS: all-click chemistry synthesis and efficient host–guest encapsulation. Chem Commun 50:8712–8714
272. Ghanbari H, Cousins BG, Seifalian AM (2011) A nanocage for nanomedicine: polyhedral oligomeric silsesquioxane (POSS). Macromol Rapid Commun 32:1032–1046
273. Fabritz S, Hörner S, Avrutina O, Kolmar H (2013) Bioconjugation on cube-octameric silsesquioxanes. Org Biomol Chem 11:2224–2236
274. Hörner S, Fabritz S, Herce HD, Avrutina O, Dietz C, Stark RW, Cardosoc M, Kolmar H (2013) Cube-octameric silsesquioxane-mediated cargo peptide delivery into living cancer cells. Org Biomol Chem 11:2258–2265

275. Mori H, Saito S (2011) Smart organic–inorganic hybrids based on the complexation of amino acid-based polymers and water-soluble silsesquioxane nanoparticles. React Funct Polym 71:1023–1032
276. Mori H, Saito S, Shoji K (2011) Complexation of amino-acid-based block copolymers with dual thermoresponsive properties and water-soluble silsesquioxane nanoparticles. Macromol Chem Phys 212:2558–2572
277. Lin Y-C, Kuo S-W (2012) Hierarchical self-assembly structures of POSS-containing polypeptide block copolymers synthesized using a combination of ATRP, ROP and click chemistry. Polym Chem 3:882–891
278. Cui L, Zhu L (2006) Lamellar to inverted hexagonal mesophase transition in DNA complexes with calamitic, discotic, and cubic shaped cationic lipids. Langmuir 22:5982–5985
279. Mendes AC, Baran ET, Reis RL, Azevedo HS (2013) Self-assembly in nature: using the principles of nature to create complex nanobiomaterials. WIREs Nanomed Nanobiotechnol 5:582–612
280. Kricheldorf HR (2006) Polypeptides and 100 years of chemistry of a-amino acid *N*-carboxyanhydrides. Angew Chem Int Ed 45:5752–5784
281. Byrne M, Murphy R, Kapetanakis A, Ramsey J, Cryan S-A, Heise A (2015) Star-shaped polypeptides: synthesis and opportunities for delivery of therapeutics. Macromol Rapid Commun 36:1862–1876
282. Qi Y, Chilkoti A (2014) Growing polymers from peptides and proteins: a biomedical perspective. Polym Chem 5:266–276
283. Kuo S-W, Tsai H-T (2010) Control of peptide secondary structure on star shape polypeptides tethered to polyhedral oligomeric silsesquioxane nanoparticle through click chemistry. Polymer 51:5695–5704
284. Fabritz S, Hörner S, Könning D, Empting M, Reinwarth M, Dietz C, Glotzbach B, Frauendorf H, Kolmar H, Avrutina O (2012) From pico to nano: biofunctionalization of cube-octameric silsesquioxanes by peptides and miniproteins. Org Biomol Chem 10:6287–6293
285. Lin Y-C, Kuo S-W (2012) Hierarchical self-assembly and secondary structures of linear polypeptides graft onto POSS in the side chain through click chemistry. Polym Chem 3:162–171
286. Lin Y-C, Kuo S-W (2011) Self-assembly and secondary structures of linear polypeptides tethered to polyhedral oligomeric silsesquioxane nanoparticles through click chemistry. J Polym Sci Part A Polym Chem 49:2127–2137
287. Kuo S-W, Lee H-F, Huang W-J, Jeong K-U, Chang F-C (2009) Solid state and solution self-assembly of helical polypeptides tethered to polyhedral oligomeric silsesquioxanes. Macromolecules 42:1619–1626
288. Haldar U, Pan A, Mukherjee I, De P (2016) POSS semitelechelic Aβ17–19 peptide initiated helical polypeptides and their structural diversity in aqueous medium. Polym Chem 7:6231–6240
289. Rinkenauer AC, Schubert S, Traeger A, Schubert US (2015) The influence of polymer architecture on in vitro pDNA transfection. J Mater Chem B 3:7477–7493
290. Yang YY, Wang X, Hu Y, Hu H, Wu D-C, Xu F-J (2014) Bioreducible POSS-cored star-shaped polycation for efficient gene delivery. ACS Appl Mater Interfaces 6:1044–1052
291. Jiang S, Poh YZ, Loh XJ (2014) POSS-based hybrid cationic copolymers with low aggregation potential for efficient gene delivery. Org Biomol Chem 12:6500–6506
292. Jiang S, Poh YZ, Loh XJ (2015) POSS-based hybrid cationic copolymers with low aggregation potential for efficient gene delivery. RSC Adv 5:71322–71328
293. Loh XJ, Zhang Z-X, Mya KY, Wu Y-I, Hea CB, Li J (2010) Efficient gene delivery with paclitaxel-loaded DNA-hybrid polyplexes based on cationic polyhedral oligomeric silsesquioxanes. J Mater Chem 20:10634–10642
294. Cui L, Chen D, Zhu L (2008) Conformation transformation determined by different self-assembled phases in a DNA complex with cationic polyhedral oligomeric silsesquioxane lipid. ACS Nano 2:921–927

295. Zou Q-C, Yan Q-J, Song G-W, Zhang S-L, Wu L-M (2007) Detection of DNA using cationic polyhedral oligomeric silsesquioxane nanoparticles as the probe by resonance light scattering technique. Biosens Bioelectron 22:1461–1465
296. Jeon J-H, Kakuta T, Tanaka K, Chujo Y (2015) Facile design of organic–inorganic hybrid gels for molecular recognition of nucleoside triphosphates. Bioorganic Med Chem Lett 25:2050–2055
297. Liu Y-L, Liu C-S, Cho C-I, Hwu M-J (2007) Polyhedral oligomeric silsequioxane monolayer as a nanoporous interlayer for preparation of low-k dielectric films. Nanotechnology 18:225701
298. Wu G, Su Z (2006) Polyhedral oligomeric silsesquioxane nanocomposite thin films via layer-by-layer electrostatic self-assembly. Chem Mater 18:3726–3732
299. Ariga K, Yamauchi Y, Mori T, Hill JP (2013) 25th anniversary article: what can be done with the Langmuir-Blodgett method? Recent developments and its critical role in materials science. Adv Mater 25:6477–6512
300. Esker AR, Yu H (2012) Langmuir monolayers of siloxanes and silsesquioxanes. In: Owen MJ, Dvornic PR (eds) Silicone surface science, advances in silicon science. Springer Science + Business Media, Dordrecht
301. Deng J, Polidan JT, Hottle JR, Farmer-Creely CE, Viers BD, Esker AE (2002) Polyhedral oligomeric silsesquioxanes: a new class of amphiphiles at the air/water interface. J Am Chem Soc 124:15194–15195
302. Deng J, Hottle JR, Polidan JT, Kim H-J, Farmer-Creely CE, Viers BD, Esker AE (2004) Polyhedral oligomeric silsesquioxane amphiphiles: isotherm and Brewster angle microscopy studies of trisilanolisobutyl-POSS at the air/water interface. Langmuir 20:109–115
303. Deng J, Viers BD, Esker AR, Anseth JW, Fuller GG (2005) Phase behavior and viscoelastic properties of trisilanolcyclohexyl-POSS at the air/water interface. Langmuir 21:2375–2385
304. Wamke A, Dopierała K, Prochaska K, Maciejewski H, Biadasz A, Dudkowiak A (2015) Characterization of Langmuir monolayer, Langmuir-Blodgett and Langmuir-Schaefer films formed by POSS compounds. Colloids Surf A 464:110–120
305. Banerjee R, Sanya MK, Bera MK, Gibaud A, Lin B, Meron M (2015) Reversible monolayer-to-crystalline phase transition in amphiphilic silsesquioxane at the air–water interface. Sci Rep 5, No. 8497
306. Dutkiewicz M, Karasiewicz J, Rojewska M, Skrzypiec M, Dopierała K, Prochaska K, Maciejewski H (2016) Synthesis of an open-cage structure POSS containing various functional groups and their effect on the formation and properties of Langmuir monolayers. Chem Eur J 22:13275–13286
307. Dopierała K, Bojakowska K, Karasiewicz J, Maciejewski H, Prochaska K (2016) Interfacial behaviour of cubic silsesquioxane and silica nanoparticles in Langmuir and Langmuir-Blodgett films. RSC Adv 6:94934–94941
308. Paczesny J, Binkiewicz I, Janczuk M, Wybrańska K, Richter Ł, Hołyst R (2015) Langmuir and Langmuir–Blodgett films of unsymmetrical and fully condensed polyhedral oligomeric silsesquioxanes (POSS). J Phys Chem C 119:27007–27017
309. Kraus-Ophir S, Jerman I, Orel B, Mandler D (2011) Symmetrical thiol functionalized polyhedral oligomeric silsesquioxanes as building blocks for LB films. Soft Matter 7:8862–8869
310. Dopierala K, Wamke A, Dutkiewicz M, Maciejewski H, Prochaska K (2014) Interfacial properties of fully condensed functional silsesquioxane: a Langmuir monolayer study. J Phys Chem C 118:24548–24555
311. Gunawidjaja R, Huang F, Gumenna M, Klimenko N, Nunnery GA, Shevchenko V, Tannenbaum R, Tsukruk VV (2009) Bulk and surface assembly of branched amphiphilic polyhedral oligomer silsesquioxane compounds. Langmuir 25:1196–1209
312. Dopierała K, Maciejewski H, Prochaska K (2016) Interaction of polyhedral oligomeric silsesquioxane containing epoxycyclohexyl groups with cholesterol at the air/water interface. Colloids Surf B 140:135–141
313. Li Z, Ma X, Guan X, Qiang X, Zang D, Chen F (2017) Aggregation behavior of star-shaped fluoropolymers containing polyhedral oligomeric silsesquioxane (POSS) at the air–water interface. Colloid Polym Sci 295:157–170

314. Zhang W, Huang M, Su H, Zhang S, Yue K, Dong X-H, Li X, Liu H, Zhang S, Wesdemiotis C, Bernard Lotz B, Zhang W-B, Li Y, Cheng SZD (2016) Toward controlled hierarchical heterogeneities in giant molecules with precisely arranged nano building blocks. ACS Cent Sci 2:48–54
315. Raftopoulos KN, Pielichowski K (2016) Segmental dynamics in hybrid polymer/POSS nanomaterials. Progr Polym Sci 52:136–187
316. Zhou H, Ye Q, Xu J (2017) Polyhedral oligomeric silsesquioxane-based hybrid materials and their applications. Mater Chem Front 1:212–230
317. Chiu C-W, Huang T-K, Wang Y-C, Alamani BG, Lin J-J (2014) Intercalation strategies in clay/polymer hybrids. Progr Polym Sci 39:443–485
318. Kai J, Teo H, Toh CL, Lu X (2011) Catalytic and reinforcing effects of polyhedral oligomeric silsesquioxane (POSS)-imidazolium modified clay in an anhydride-cured epoxy. Polymer 52:1975–1982
319. Hojiyev R, Ulcay Y, Hojamberdiev M, Çelik MS, Carty WM (2017) Hydrophobicity and polymer compatibility of POSS-modified Wyoming Na-montmorillonite for developing polymer-clay nanocomposites. J Colloid Interf Sci 497:393–401
320. Zhao Y, Jiang X, Zhang X, Hou L (2017) Toughened elastomer/polyhedral oligomeric Ssilsesquioxane (POSS)-intercalated rectorite nanocomposites: preparation, microstructure, and mechanical properties. Polym Compos 38:E443–E450
321. Yei D-Y, Kuo S-W, Su Y-C, Chang F-C (2004) Enhanced thermal properties of PS nanocomposites formed from inorganic POSS-treated montmorillonite. Polymer 45:2633–2640
322. Zhao F, Wan C, Bao X, Kandasubramanian B (2009) Modification of montmorillonite with aminopropylisooctyl polyhedral oligomeric silsequioxane. J Colloid Interface Sci 333:164–170
323. Zhao F, Bao X, McLauchlin AR, Gu J, Wan C, Kandasubramanian B (2010) Effect of POSS on morphology and mechanical properties of polyamide 12/montmorillonite nanocomposites. Appl Clay Sci 47:249–256
324. Wan C, Zhao F, Bao X, Kandasubramanian B, Duggan M (2008) Surface characteristics of polyhedral oligomeric silsesquioxane modified clay and its application in polymerization of macrocyclic polyester oligomers. J Phys Chem B 112:11915–11922
325. Fox DM, Maupin PH, Harris RH Jr, Gilman JW, Eldred DV, Katsoulis D, Trulove PC, De Long HC (2007) Use of a polyhedral oligomeric silsesquioxane (POSS)-imidazolium cation as an organic modifier for montmorillonite. Langmuir 23:7707–7714
326. Toh CL, Xi L, Lau SK, Pramoda KP, Chua YC, Lu X (2010) Packing behaviors of structurally different polyhedral oligomeric silsesquioxane-imidazolium surfactants in clay. J Phys Chem B 114:207–214
327. Lee JH, Jeong YG (2011) Preparation and crystallization behavior of polylactide nanocomposites reinforced with POSS-modified montmorillonite. Fibers Polym 12:180–189
328. Toh CL, Yang L, Pramoda KP, Lauc SK, Lu X (2013) Poly(ethylene terephthalate)/clay nanocomposites with trisilanolphenyl polyhedral oligomeric silsesquioxane as dispersant: simultaneously enhanced reinforcing and stabilizing effects. Polym Int 62:1492–1499
329. Cui H-W, Kuo S-W (2012) Using a polyhedral oligomeric silsesquioxane surfactant and click chemistry to exfoliate montmorillonite. RSC Adv 2:12148–12152

Polyolefins with POSS

M. Pracella

Abstract The influence of POSS structure and mixing processes on the structural and morphological characteristics, and the thermal, mechanical and rheological behaviour of polyolefin/POSS nanocomposites have been reviewed in the present chapter. POSS molecules ($[RSiO_{1,5}]_p$) with various organic substituents (R), both of non-reactive and reactive type, have been examined. In particular, the properties of systems with polyethylene, polypropylene or ethylene–propylene copolymer matrix (HDPE/POSS, LDPE/POSS, PP/POSS, EP/POSS), and vinyl polymers (PS/POSS), containing linear and branched alkyl-substituted POSS have been analysed at various compositions and preparation conditions. The studies indicated that the length of alkyl groups on POSS molecules plays a fundamental role in determining the POSS dispersion degree in the polymer matrix during the melt mixing process, as well as the crystallization, thermal and mechanical behaviour of these composites. Then, the properties of binary and ternary systems containing polyolefin grafted with reactive groups (such as PP-*g*-MA) and POSS functionalized with amino groups (am-POSS)—able to induce grafting reactions of POSSs on the polymer chains in melt mixing—have been reported. It was demonstrated that the grafting promotes the compatibilization of the nanocomposites, increasing POSS dispersion up to molecular level and improving mechanical and thermal resistance. Moreover, the isothermal and non-isothermal crystallization processes and the crystalline morphology of polyolefin/POSS systems have been analysed with the aim of investigating the nucleation activity of POSS nanoparticles on the crystal growth and the overall crystallization kinetics of the polyolefin matrix.

Keywords Polymer composites · Polyolefins · Polysilsesquioxanes · Morphology Thermal behaviour · Mechanical properties · Reactive mixing

M. Pracella (✉)
National Research Council, Institute for Physical and Chemical Processes, c/o Department of Civil Engineering, University of Pisa, Largo L. Lazzarino 2, Pisa 56124, Italy
e-mail: mariano.pracella@diccism.unipi.it

S. Kalia and K. Pielichowski (eds.), *Polymer/POSS Nanocomposites and Hybrid Materials*, Springer Series on Polymer and Composite Materials,
https://doi.org/10.1007/978-3-030-02327-0_4

Nomenclature

EP	Ethylene–propylene copolymer
HDPE	High-density polyethylene
LDPE	Low-density polyethylene
PEO-*b*-PE-POSS	Polyethylene oxide-polyethylene-POSS triblock copolymer
PET	Polyethylene terephthalate
PIBMA	Poly(isobutyl methacrylate)
PMMA	Poly(methylmethacrylate)
PMMA-*b*-PMAPOSS	Polymethylmethacrylate-polymethacrylate POSS block copolymer
PP	Isotactic polypropylene
PP-*g*-MA	Maleic anhydride-grafted PP
PP-*g*-POSS	POSS-grafted PP
PS	Polystyrene
PA	Polyamide
PC	Polycarbonate
PS-*b*-PMAPOSS	Polystyrene-polymethacrylate POSS block copolymer
am2b-POSS	Aminoethyl-aminopropyl-heptaisobutyl-POSS
amb-POSS	Aminopropyl-heptaisobutyl-POSS
amo-POSS	Aminopropyl-heptaisooctyl-POSS
heptacyclopentyl-POSS	4,4′-Bis(heptacyclopentyl-T8-silsesquioxyl)phenyl ether
me-POSS	Methyl-POSS
oap-POSS	Octaaminophenyl-POSS
OIB-POSS	Octaisobutyl-POSS
OIO-POSS	Octaisoctyl-POSS
OM-POSS	Octamethyl-POSS
ph-POSS	Phenyl-POSS
POSS18	*n*-Octadecyldimethylsiloxy-POSS
POSS7b	4-Methyl-hexyldimethylsiloxy-POSS
POSS8	*n*-Octyldimethylsiloxy-POSS
POSS-NH_2	Amino-POSS
vi-POSS	Vinyl-POSS

1 Introduction

Polymeric nanocomposites containing polyhedral oligomeric silsesquioxanes (POSS) as dispersed inorganic nanofillers offer the opportunity to design advanced materials with high thermal and mechanical performances. These materials are attracting large growing attention from automotive, aerospace, electronics and biotechnology companies [1]. POSS molecules differ from other types of nanofillers

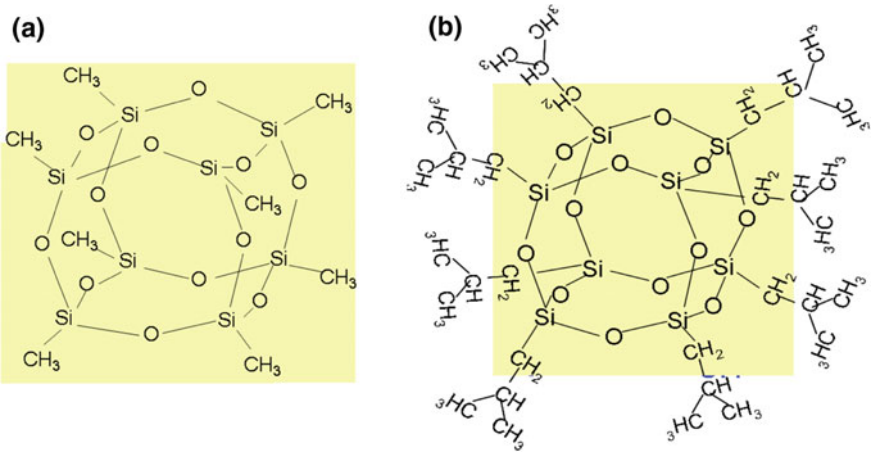

Fig. 1 Chemical structure of alkyl-substituted POSS: **a** octamethyl-POSS (OM-POSS), **b** octaisobutyl-POSS (OIB-POSS)

(e.g. organoclay, carbon nanotube, nanofibres) in several aspects: they can be dispersed in the polymer matrix at the level of individual molecules, therefore at a size much lower than the average dimension of conventional fillers.

POSS molecules—with general formula $[RSiO_{1,5}]_n$ where R is hydrogen or an organic group (alkyl, aryl or any of their derivatives) and $n = 6$–12—are characterized by a size in the range 1–3 nm and a high chemical versatility to form nanostructures with tailored dimensionality [2] (Fig. 1). The functionality, solubility and reactivity of these molecules can be easily changed through modifying the R side groups with various organic substituents, both of reactive and non-reactive type. Due to their great chemical flexibility, POSS molecules can be incorporated into polymers by copolymerization, grafting, or even blending using traditional processing methods.

The preparation and properties of various thermoplastics—as polyolefins [3, 4], polyethylene terephthalate [5], polystyrene, polymethylmethacrylate [6], polyamide [7, 8], polycarbonate [9, 10]—containing POSS molecules with different structure have been explored. Moreover, thermosets, such as epoxy [11, 12], elastomers [13] and liquid crystalline polymers, have been reinforced with POSS. In most cases, it has been found that adding POSS to the polymer matrix allows to improve thermal and mechanical properties.

Over the past decades, several papers have been focused on the structure–property relationships of polyolefin composites containing dispersed POSS molecules as nanofillers. It has been pointed out that the crystal morphology, the thermal stability, tensile properties and melt rheology of polyethylene and polypropylene composites containing alkyl-substituted POSS can be largely affected by the chemical structure, concentration and dispersion degree of POSS particles. The type and length of alkyl groups on POSS molecules play a fundamental role in determining the dispersion degree and the interactions with the polyolefin matrix during the mixing process

in solution or from the melt. In general, the weak interactions between POSS and organic polymer matrices, opposed to the strong self-interaction between the POSS units, frequently cause the formation of aggregates. Microscopic analyses showed that POSS with short alkyl substituents (e.g. R=CH_3) gave mainly rise to micron-sized crystalline aggregates, whereas those with longer alkyl substituents were quite homogeneously dispersed in the polyolefin matrix likely owing to a more favourable interaction of the long alkyl groups with the polymer chains, as compared to the intermolecular interactions between POSS units.

The effect of incorporation of POSS molecules with linear and branched alkyl substituents having different chain length has been extensively investigated for nanocomposites with high-density polyethylene (HDPE), low-density polyethylene (LDPE), polypropylene (PP), ethylene–propylene copolymers (EP) and polystyrene (PS) matrix (see Sect. 4.2). Depending on their molecular structure, POSS particles can significantly influence the crystallization processes of the polyolefin matrix by inducing a nucleating effect on the growth of polyolefin crystals, or even modifying the polymer crystal structure and the crystallinity, due to miscibility phenomena of the components in the amorphous phase.

The compatibility and thus the properties of polyolefin/POSS nanocomposites are expected to be markedly enhanced by promoting chemical interactions between the components during melt mixing, such as grafting reactions of POSS onto the polymer chains, which can lead to a fine dispersion of the filler into the polyolefin matrix. This can be achieved through melt mixing of polymer and POSS components bearing functional reactive groups. In the present chapter, the attention has been focused on nanocomposites obtained by reactive blending of maleic anhydride-grafted PP (PP-*g*-MA) with various POSS modified with amino groups (POSS-NH_2), giving rise to POSS grafting—by amide bonds—on the polyolefin chains in the melt (see Sect. 4.3). Finally, the effect of nanoparticle chemical structure, phase dispersion and surface interactions on some advanced applications of these systems has been discussed (see Sect. 4.4).

2 Polyolefin/POSS Nanocomposites

The properties of polymer/POSS nanocomposites are mainly dependent on the chemical structures of POSS and polymer components. Since the dispersion of POSS in the polymer matrix largely affects the chemical/physical characteristics of these materials, the method of preparation of such nanocomposites plays a key role. POSS units can be incorporated into polymer matrices by employing two distinct methods: *physical blending* and *chemical reaction* [1].

In *physical blending*, POSS nanoparticles are dispersed in the polymer by melt mixing or solvent casting. This method—the most common—presents several advantages, as a lower cost and the exploitation of processing technologies commonly employed for polymer compounding, such as batch mixing or melt extrusion. However, a major problem in physical blending is the control of POSS dispersion dur-

ing the mixing process, which closely influences the final properties of the resulting nanocomposites. In the *chemical reaction* method, POSS nanoparticles are bonded covalently to the polymer chains through grafting or polymerization reaction: monofunctional POSS, containing a reactive site (i.e. a double bond), can be introduced in the polymerization reaction to form, for example, polyethylene-POSS [14], polystyrene-POSS [15] or poly(methylmethacrylate)-POSS nanocomposites [2]. However, most of studied polyolefin/POSS systems were obtained by melt mixing or solution blending.

The property characterization of these systems includes optical (OM) and electron microscopy techniques (TEM, SEM, FESEM, EDS), atomic force microscopy (AFM), X-ray diffraction (SAXS, WAXS), Fourier transform infrared spectroscopy (FTIR), differential scanning calorimetry (DSC), thermogravimetric analysis (TG), tensile and rheological tests, dynamic mechanical thermal analysis (DMTA), as well as dielectric measurements.

2.1 Polyethylene/POSS

2.1.1 Crystal Structure and Morphology

Several studies have been carried out on the structure–property relationships of polyethylene/POSS nanocomposites. The crystallization behaviour and the properties of high-density polyethylene (HDPE) reinforced with octamethyl-POSS (OM-POSS) by means of physical blending were analysed by Joshi et al. [16]. It was found that under shear conditions during melt mixing OM-POSS was homogeneously dispersed on a molecular level in HDPE up to a content of 1 wt%. At concentrations higher than 1 wt%, POSS crystallized as nanocrystals, or it gave rise to crystalline agglomerates (10 wt% loading). OM-POSS did not affect the crystallinity and crystal structure of HDPE up to 5 wt% content, while it influenced the crystallization kinetics of HDPE reducing crystallinity and crystal perfection of HDPE at 10 wt% content.

The influence of POSS on the microstructure, thermal and thermomechanical properties of linear low-density polyethylene (LLDPE) was analysed at various nanofiller concentrations by Hato et al. [17]. A decrease of the crystallinity of the polyolefin matrix together with an increase of the thermal stability was reported for LLDPE/POSS nanocomposites. It was concluded that the addition of POSS particles resulted in a significant improvement in both the storage and loss moduli of the neat LLDPE, together with a substantial improvement in thermal stability.

The effect of incorporation of POSS molecules with long alkyl chain substituents—(*n*-octyldimethylsiloxy)octasilsesquioxane (POSS8), (*n*-octadecyldimethylsiloxy) octasilsesquioxane (POSS18) and (4-methylhexyldimethylsiloxy)octasilsesquioxane (POSS7b)—on the properties of HDPE and LDPE was investigated by Niemczyk et al. [18]. SEM analysis of HDPE/POSS showed that the morphology of nanocomposites with *n*-octyl-substituted POSS8

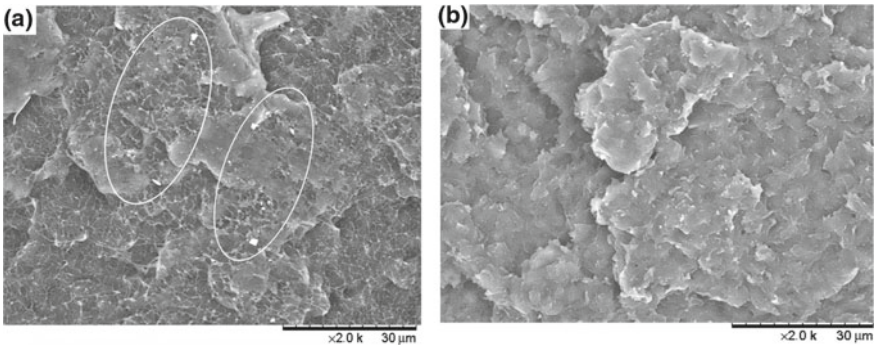

Fig. 2 SEM micrographs of nanocomposites of HDPE with **a** 5 wt% (*n*-octyldimethylsiloxy) silsesquioxane (POSS8) and **b** 5 wt% (*n*-octadecyldimethylsiloxy)silsesquioxane (POSS18). Reprinted from [18], Copyright 2016, with permission from Springer

(Fig. 2a) was less homogenous than that of nanocomposites with longer *n*-alkyl groups (POSS18) where no aggregates were observed (Fig. 2b).

Perrin et al. [19] studied nanocomposites of LDPE containing octakis(dimethylsiloxy)octasilsesquioxanes having both linear (P3-P8) and branched (P5b-P7b) alkyl substituents, the alkyl chain length varying between C3 and C8 for linear substituents, and between C5 and C7 for branched ones.

Small angle X-ray diffraction patterns of linear and branched POSS and related LDPE/POSS nanocomposites (PE3-PE8, PE-5b-PE-7b) are shown in Fig. 3. For all POSS and LDPE/POSS samples, the diffraction maxima are mostly shifted to lower 2θ angles with increasing the length of *n*-alkyl substituents, which indicates a significant influence of alkyl groups on the POSS dispersion. Changes in the position and intensity of maxima were also observed between nanocomposites containing branched and linear substituents (Fig. 3b–d), the maxima being shifted towards lower angles for branched POSSs with respect to linear POSSs, suggesting a higher compatibility of the branched ones with the polyolefin. A marked difference in the diffraction patterns of pure POSSs with respect to their nanocomposites was observed in the case of P6b and P7b branched samples. These POSSs are crystalline at room temperature (Fig. 3c) but no crystalline peaks were detected in SAXS spectra of the nanocomposites (PE-6b, PE-7b) containing these POSSs (Fig. 2d), indicating that only amorphous POSS aggregates are present in the LDPE matrix.

2.1.2 Thermal Properties

For polyethylenes containing POSS molecules with different alkyl chain substituents, it was found that the type and content of POSS significantly influenced the crystallization and melting behaviour, as well as the thermal stability of the nanocomposites.

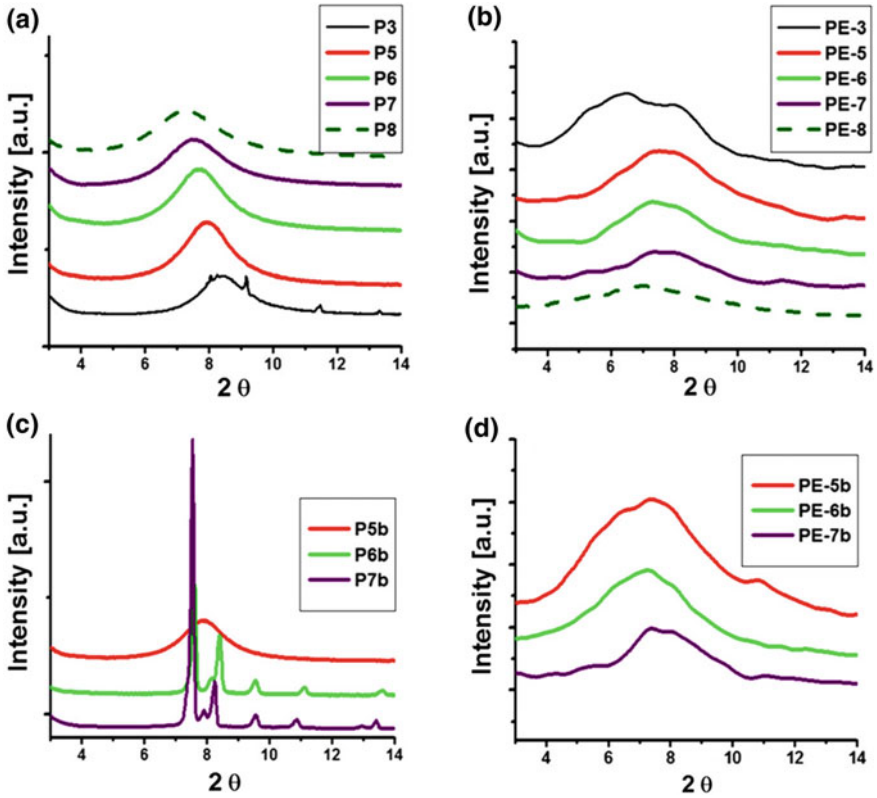

Fig. 3 Small angle X-ray diffraction patterns of **a** linear (P3-P8) and **c** branched (P5b-P7b) POSSs, and related LDPE/POSS nanocomposites with **b** linear (PE-3-PE-8) and **d** branched POSSs (PE-5b-PE-7b) (3 wt%). Reprinted from [19], Copyright 2013, with permission from Elsevier

Thermal and X-ray scattering techniques were used to probe the compatibility of the POSS molecules and subsequently the effect on the crystalline morphology during quiescent crystallization of PE [20, 21]. The miscibility and dispersion of the POSS molecules were found to increase with increasing the alkyl chain length of POSS substituents. POSS molecules with shorter alkyl chain showed aggregation forming POSS crystals in the PE matrix, but become progressively more dispersed as the alkyl chain length increased, suggesting better compatibility and interaction of the substituent groups with the PE chains. The POSS molecules in all cases were seen to act as nucleating agents regardless of their dispersion in the PE matrix, increasing the crystallinity, crystallization kinetics and influencing the lamellar morphology when compared with pure PE. The longer the alkyl chain substituent on the POSS molecules, the greater the POSS dispersion in the PE matrix at the same loading. The time-resolved SAXS data during the quiescent crystallization process showed that the long-range ordering and crystalline structure developed in the blends before

that in the pure PE. PE/POSS blends developed a more defined crystalline lamellar structure compared to neat PE.

Significant changes in the crystallization and melting behaviour were observed by Niemczyk et al. [18] for HDPE and LDPE nanocomposites containing POSS with short alkyl chain substituents (POSS8), as compared with the nanocomposites containing POSSs with longer chain substituents (POSS18): the former ones showed a higher nucleating effect on the crystallization of the polyolefin than the latter ones. However, the nucleating effectiveness of POSSs in the HDPE matrix was lower than that found in the LDPE matrix. In most cases, the incorporation of POSS particles into polyolefins caused an increase of the crystallinity degree of the nanocomposites.

The incorporation of POSSs enhances significantly the thermal stability of the polyolefin matrix. In fact, it has been inferred that the thermo-oxidative degradation of POSS leads to the formation of a silica-like residue which tends to accumulate on the material surface, forming a ceramic layer that acts as a protective barrier, reducing the flow of heat and gas into the nanocomposite. Fina et al. [22] reported that POSS molecules with methyl substituents were less thermally stable than POSS structures containing isobutyl or isooctyl groups. POSS molecules with short alkyl chain substituents undergo almost complete sublimation, while those with longer alkyl chain substituents evaporate above the POSS melting temperature.

The thermal stability of polyolefin/POSS nanocomposites is markedly influenced by the structure of the POSSs as well as by the nanofiller dispersion in the polymer matrix. Generally, for LDPE/POSS nanocomposites, the addition of POSS enhanced the thermal stability of these materials. TGA analysis under nitrogen also showed that the nanocomposites containing POSS with longer *n*-alkyl substituents (POSS18) exhibited the highest thermal stability [18]. Addition of POSS with branched alkyl substituents (POSS7b) into HDPE matrix decreased thermal stability of nanocomposites in comparison with those containing linear alkyl-substituted POSS and with the neat polymer. This is in agreement with the observation that longer alkyl chain substituents enhance the compatibility of POSSs with polymer chains, and thus the nanoparticle dispersion. The thermal stability in air of nanocomposites was improved with respect to neat polyolefins, especially at higher contents of POSS.

2.1.3 Mechanical Properties

The study of PE/POSS nanocomposites containing linear and branched POSS with various chain lengths indicated that the tensile properties are strictly depending on the chain structure of the POSS substituents. All the analysed systems displayed higher elongation and energy at break and lower Young's modulus as compared to neat PE; further, the nanocomposites showed higher tensile strength at break than neat PE. The simultaneous increase of both ductility and strength suggested that alkyl POSSs did not act as a typical plasticizer or a typical reinforcement.

Analysing the tensile properties of nanocomposites as a function of the length of POSS substituents, Perrin et al. [19] found that elongation at break, tensile strength and energy at break increase and the yield strength decreases with decreasing the

length of the linear alkyl groups, namely when the compatibility between POSS and PE decreases. It was concluded that POSSs with long flexible *n*-alkyl substituents do not induce reinforcing effects in the nanocomposites, whereas POSSs with branched alkyl substituents lead to an improvement of mechanical properties.

Similar results were reported by Frone et al. [23], who analysed nanocomposites of low-density polyethylene (LDPE) with two types of octakis(dimethylsiloxy)octasilsesquioxanes with linear (POSSl) and branched (POSSb) C5 substituents at various concentrations (0.5–8 wt%), prepared by melt mixing. For all LDPE/POSS nanocomposites, the mechanical tests revealed a significant improvement of tensile strength and elongation properties as compared to neat LDPE, the enhancement of mechanical properties being more pronounced for nanocomposites with branched POSSb (Fig. 4). An increase of POSS content causes a decrease of modulus especially for composites containing branched POSS (Fig. 4a). Smaller values of modulus were also observed by peak force Quantitative Nanoscale Mechanical (QNM) analysis for all nanocomposites. The addition of both linear and branched POSS induced an improvement of tensile strength at break, yield strength and elongation at break as compared to the neat LDPE. A marked increase of tensile strength was observed at 0.5 and 1 wt% POSSb concentration (Fig. 4b). Above these concentrations, the minor increase of tensile strength is probably due to the aggregation tendency of POSS molecules, as confirmed by AFM and XRD results. Both types of POSS displayed a similar increase of elongation at break for nanofiller concentrations higher than 3% (Fig. 4d).

2.1.4 Rheological Behaviour

For HDPE/OM-POSS composites, the complex viscosity data at different angular frequencies indicated that the interactive forces between POSS particles and HDPE matrix are weak van der Waals forces.

It has been shown that OM-POSSs are miscible in HDPE at concentrations $\leq$2 wt%, whereas are immiscible at concentrations $\geq$5 wt% and at temperature $\geq$180 °C [16]. At low concentrations (<1.0 wt%), POSS particles act as lubricants and lead to a significant decrease of viscosity as compared to neat HDPE, reaching a minimum at 0.25 wt% content (Fig. 5). With increasing POSS concentration, the polymer chain mobility decreases and viscosity increases: above 5 wt% POSS in HDPE, it forms a three-dimensional network of POSS nanocrystals which induces a gelation behaviour at low shear rate ($\omega = 0.1$ rad/s), as observed for composites of ethylene–propylene copolymer with POSS [24]. The miscibility at low concentrations—likely due to weak van der Waals interactions—leads to a fine dispersion of POSS particles into the HDPE matrix, and this could probably reduce chain entanglements increasing the free volume in the melt, which results in lower viscosity.

The effect of POSS addition on the temperature dependence of viscosity was evaluated by using an Arrhenius-type equation:

$$\eta = A\mathrm{e}^{E}\mathrm{a}/RT \tag{1}$$

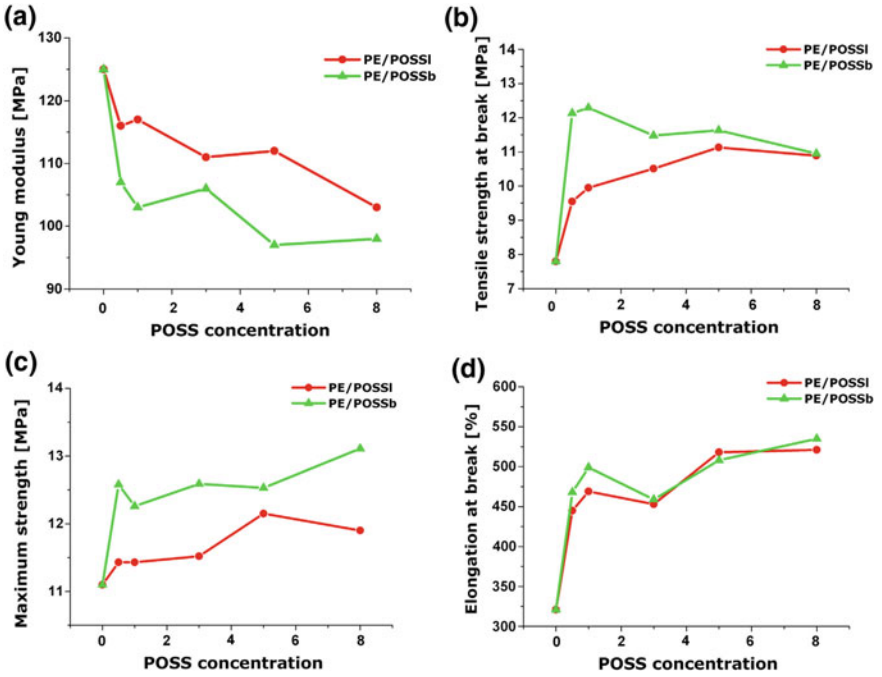

Fig. 4 Young's modulus (**a**), tensile strength (**b**), maximum strength (**c**) and elongation at break (**d**) of neat PE and PE/POSS nanocomposites containing linear alkyl POSS (POSSl) and branched alkyl POSS (POSSb). Reprinted from [23], Copyright 2013, with permission from Elsevier

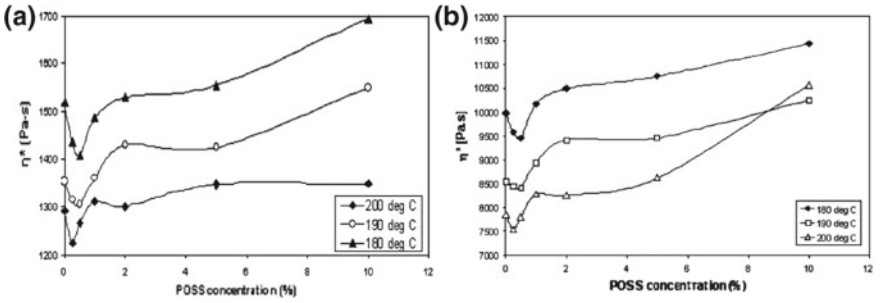

Fig. 5 Influence of POSS concentration on the complex viscosities η^* of HDPE/OM-POSS nanocomposites at **a** $\omega = 10$ rad/s and **b** $\omega = 1$ rad/s in the temperature range 180–200 °C. Reprinted from [16], Copyright 2006, with permission from American Chemical Society

where η is the zero-shear viscosity, R the gas constant, and E_a the flow activation energy.

Values of E_a were calculated for nanocomposites and HDPE from plots of $\log\eta$ (using the η^* data at $\omega = 0.1$ rad/s) versus $1/T$. The activation energy for POSS nanocomposites (21–24 kJ/mol) was found to be lower than that of neat HDPE

(26 kJ/mol), confirming that POSS at low concentrations helps to reduce the resistance to flow of the polyolefin. At higher concentrations, POSS particles give rise to aggregates, which physically hinder the flow increasing the viscosity (Fig. 5). Furthermore, DMTA analysis revealed a wide shift of α-transition peak of HDPE towards high temperatures for all HDPE/POSS as compared to neat polymer. This shift was accounted for by the presence of POSS in the intercrystalline regions, causing a restriction of the movement of HDPE chains [16].

2.2 Polypropylene/POSS

2.2.1 Crystal Structure and Morphology

Nanocomposites of isotactic polypropylene (PP) containing fully alkyl-substituted POSS (T8 cages) with different chain structure have been extensively investigated in the last decades. PP nanocomposites containing octamethyl-POSS (OM-POSS), octaisobutyl-POSS (OIB-POSS) and octaisoctyl-POSS (OIO-POSS) at different weight ratios, from 1 to 10 wt%, have been prepared by melt mixing in a Brabender Plasti-Corder or in miniextruder at temperatures $\geq$180 °C [25, 26]. OM-POSS and OIB-POSS are crystalline solids, whereas OIO-POSS is liquid at room temperature. The various nanocomposites have been analysed by optical and electron microscopy, WAXS, DSC, TGA, DMTA and tensile tests.

The POSS dispersion into PP matrix is strictly influenced by the chain length of alkyl groups. For composites with OM-POSS, the compatibility between POSS and PP was rather low, resulting in the formation of micro-aggregates both at low and high filler content (Fig. 6). Using OIB-POSS, a fine particle dispersion on a submicron scale was found within the polymer matrix at low filler content (3 wt%). Increasing OIB-POSS concentration resulted in changes of morphology: SEM and polarized optical microscopy (POM) analyses of sample with 10 wt% OIB-POSS (PP/OIB10) revealed the presence of PP spherulites that had grown around POSS crystal aggregates (Fig. 7).

PP/OIO-POSS samples displayed at any composition a very fine filler dispersion with no microscopic evidence of phase separation. All samples exhibited the characteristic spherulitic morphology of isotactic polypropylene with α-monoclinic crystal structure as confirmed by WAXS analysis. Traces of β- and γ-crystal phases were found only in PP/OIB-POSS sample at high POSS content.

Observation by polarized optical microscopy (POM) showed that for composites with OM-POSS the growth of PP spherulites occurred preferentially on the particle surfaces [26]. The spherulite growth rate G of neat PP and PP/POSS composites, measured by POM during isothermal crystallization at $T_{ic} = 130$ °C, is plotted in Fig. 8 as function of POSS content. For all samples, the spherulite radius increased linearly with time before the spherulites contact each other. In the nanocomposites, the growth rate G increased for OM-POSS content higher than 3 wt%, while in the presence of OIB-POSS and OIO-POSS resulted almost unaffected by the filler

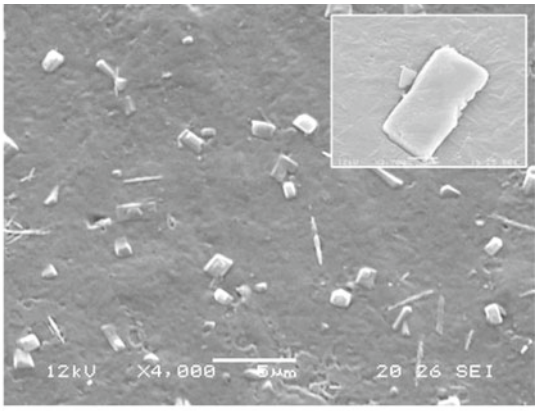

(a)

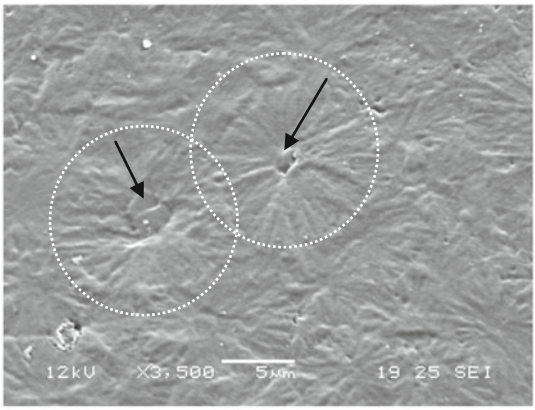

(b)

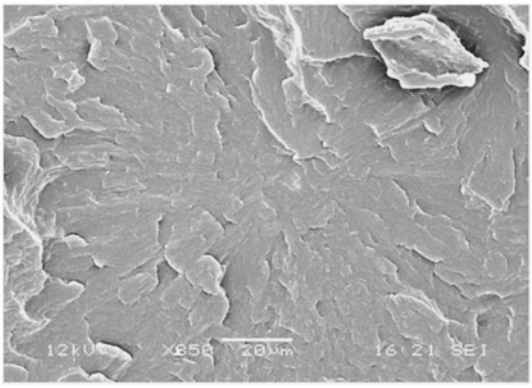

(c)

Fig. 6 SEM micrographs of fracture surfaces of **a** PP/OM-POSS (10 wt%) showing the presence of OM-POSS crystals; **b** PP spherulites grown on OIM-POSS (10 wt%) crystals (indicated by arrows); and **c** PP/OIB-POSS (3 wt%)

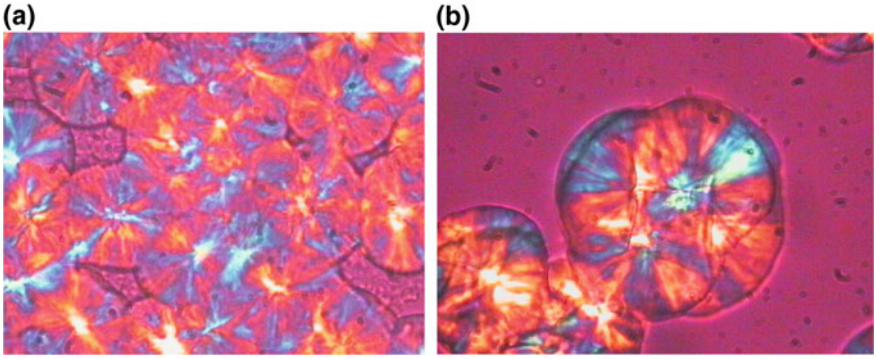

Fig. 7 POM micrographs of PP spherulites growing in composites: **a** PP/OM-POSS (10 wt%) and **b** PP/OIB-POSS (10 wt%) (spherulites nucleated on POSS crystals) during isothermal crystallization from the melt at $T_{ic} = 130$ °C (crossed Nicols). Reprinted from [26], Copyright 2006, with permission from John Wiley and Sons

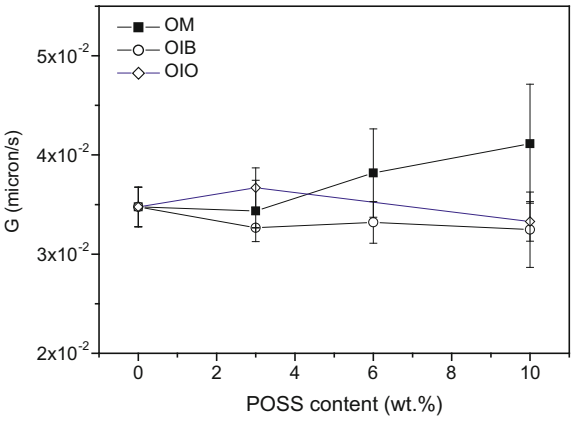

Fig. 8 Spherulite growth rate G as function of POSS content for neat PP and its nanocomposites with OM-POSS, OIB-POSS and OIO-POSS isothermally crystallized at $T_{ic} = 130$ °C. Reprinted from [26], Copyright 2006, with permission from John Wiley and Sons

content, as compared to neat PP. This suggests that the nucleation and the growth process of the spherulites from the melt are influenced by the type of alkyl substituent on the POSS cage and, in particular, by the interactions at the surface of POSS aggregates, which in turn depend on the filler concentration as evidenced by the microscopic analysis of PP/OM and PP/OIB samples.

For PP/OM-POSS nanocomposites with low nanofiller content ($\leq$3 wt%), isothermally crystallized in the temperature range 115–123 °C, Chen et al. observed a large increase of the spherulite growth rate G, compared to plain PP [27]. At temperatures above 123 °C, only minor changes of G were found with varying the POSS content. This behaviour was accounted for by assuming that POSS molecules first form nanocrystals that can act as a nucleating sites for PP, and then these nanocrystals aggregate together to form thread or network nanocrystal structures that can greatly

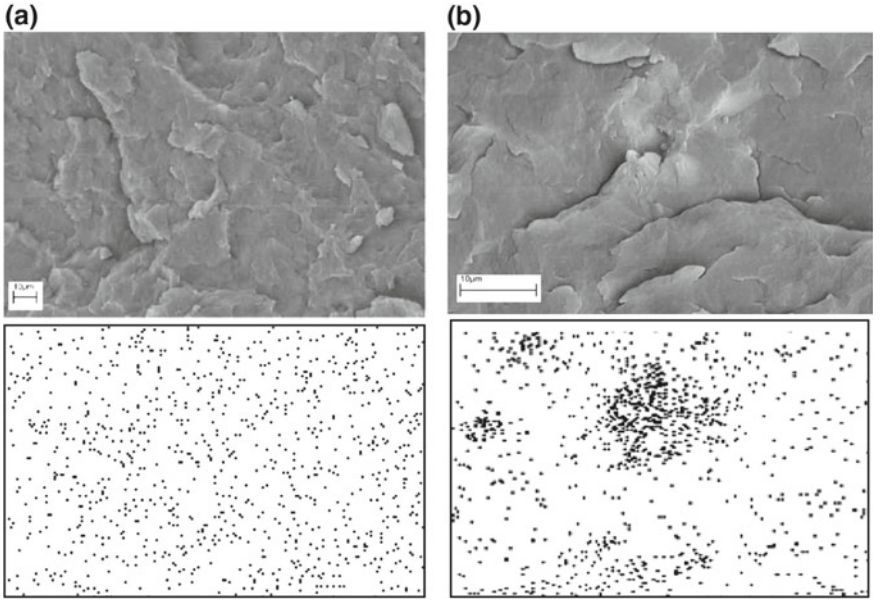

Fig. 9 SEM micrographs with EDS silicon mapping for PP filled with **a** 5% vinyl-POSS and **b** 5% phenyl-POSS. The distribution of black dots represents silicon presence. Reprinted from [28], Copyright 2010, with permission from Elsevier

disturb the transport of polymer molecules in the melt and the crystal growth, due to a rise in the energetic barrier of formation of critical nuclei.

PP blends with vinyl- and phenyl-substituted POSS have been also investigated, obtaining a submicronic POSS dispersion up to 5% POSS content [28]. As shown in Fig. 9, Energy Dispersive X-ray Spectroscopy (EDS) for silicon in PP blends with vinyl-POSS indicated a homogeneous particle distribution in the polymer matrix, whereas the morphology of PP loaded with phenyl-POSS was not homogeneous showing zones with different Si concentration.

2.2.2 Overall Crystallization Kinetics

Isothermal Crystallization Kinetics

The isothermal crystallization behaviour of PP and PP/POSS nanocomposites from the melt was examined by DSC in the temperature range $T_{ic} = 125–138$ °C [26]. The results indicated that the overall crystallization rate of PP increased in samples containing OM-POSS, while decreased in the case of samples with OIB-POSS and OIO-POSS, compared to the neat PP. The analysis of the isothermal kinetics was carried out using the Avrami model [29], according to Eq. (2):

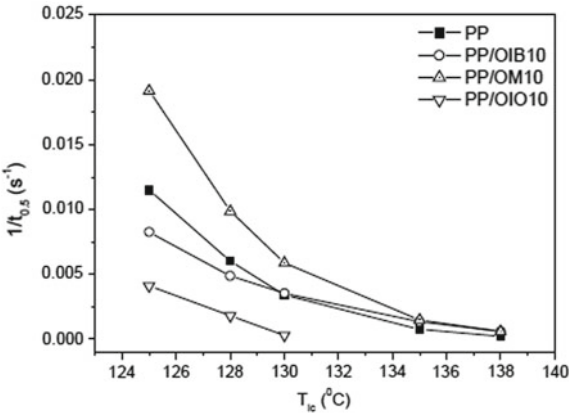

Fig. 10 Overall crystallization rate ($1/t_{0.5}$) of isothermally crystallized PP and PP/OM-POSS, PP/OIB-POSS, PP/OIO-POSS nanocomposites (10 wt% POSS), as a function of crystallization temperature (T_{ic}) in the range 125–138 °C. Reprinted from [26], Copyright 2006, with permission from John Wiley and Sons

$$X(t) = 1 - \exp\{K_n t^n\} \tag{2}$$

where $X(t)$ is the fraction of crystallinity developed at time t ($X(t) = X_c(t)/X_c(t=\infty)$) at a fixed T_{ic}, n is the Avrami exponent—depending on the nucleation mechanism and growth geometry of crystals—and K_n the rate constant, whose values can be determined from the slope and the intercept of linear plots of $\log\{-\ln[1 - X(t)]\}$ versus $\log t$, respectively. The Avrami exponent of the composites showed average values near to 3, in agreement with a three-dimensional (spherulitic) crystal growth initiated by heterogeneous nucleation.

In Fig. 10, the overall crystallization rate of PP and PP/POSS composites with 10 wt% POSS—expressed as the reciprocal of the crystallization half-time, $t_{0.5}$, determined from plots of $X(t)$ versus t—is plotted as function of T_{ic}. Composites with OM-POSS displayed a higher rate than plain PP at same T_{ic} and the rate increased with increasing the filler amount. Otherwise, composites with OIO-POSS and OIB-POSS (3–6 wt%) showed a marked decrease of crystallization rate; for $T_{ic} \geq 130$ °C, the sample with 10 wt% OIB-POSS showed a similar behaviour to PP. The temperature dependence of crystallization rate was thus related to the activation energy for the formation of critical nuclei, which was evaluated from the slope of linear plots of $\ln(1/t_{0.5})$—or $\ln K_n$—versus $1/(T_{ic}\Delta T)$, according to the kinetic theory of polymer crystallization [30]. The data obtained indicated that the activation energy for the crystal nucleation in PP/OM and PP/OIB samples (at low OIB content) was lower than that found for neat PP and PP/OIO composites.

Furthermore, knowing that for a crystallization process controlled by heterogeneous nucleation and spherulitic growth the kinetic constant ($K_{n=3} \propto N_h \cdot G^3$) is related to the number of heterogeneous nuclei per unit volume, N_h, and the growth rate, G, values of N_h were determined for the various samples at different T_{ic} [31]. It was found that PP/OM displayed the largest values of nucleation density compared to neat PP and other nanocomposites (Table 1).

Table 1 Nucleation density (nuclei/cm^3) of PP, PP/OM-POSS and PP/OIB-POSS samples with 3, 6, 10 wt% POSS content, isothermally crystallized at 125 and 130 °C. Reprinted from [26], Copyright 2006, with permission from John Wiley and Sons

T_{ic} (°C)	PP	PP/OM3	PP/OM6	PP/OM10	PP/OIB3	PP/OIB6	PP/OIB10
125	$8.8\ 10^9$	$1.9\ 10^{10}$	$2.0\ 10^{10}$	$2.3\ 10^{10}$	$3.3\ 10^8$	$1.0\ 10^8$	$4.0\ 10^9$
130	$1.5\ 10^9$	$8.3\ 10^9$	$2.9\ 10^{10}$	$2.0\ 10^{10}$	$6.0\ 10^7$	$2.5\ 10^7$	$3.9\ 10^9$

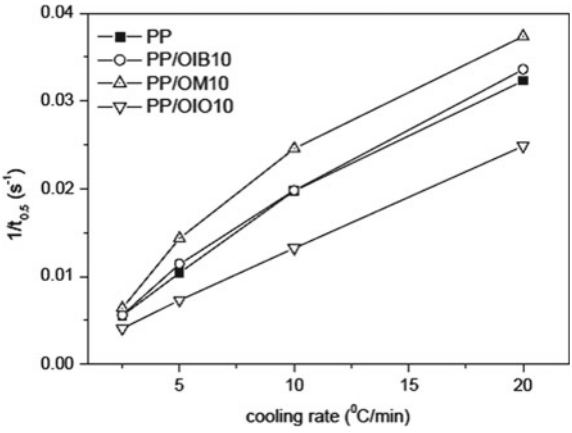

Fig. 11 Non-isothermal crystallization rate ($1/t_{0.5}$) as a function of the cooling rate for PP, PP/OM-POSS, PP/OIB-POSS and PP/OIO-POSS samples (10 wt% POSS). Reprinted from [26], Copyright 2006, with permission from John Wiley and Sons

Non-Isothermal Crystallization Kinetics

The onset and the crystallization peak temperature (T_{nc}) on the DSC thermograms of PP/POSS recorded at various cooling rates (2.5–20 °C/min) resulted to change with type and content of POSS. The addition of OM-POSS shifted the crystallization temperature to higher values, whereas addition of OIB and OIO-POSS moved T_{nc} to lower values as compared to plain PP at same cooling conditions. In all the examined range, the crystallization rate of PP is higher for PP/OM and lower for PP/OIO, as already observed for the isothermal crystallization. However, as shown in Fig. 11, these effects are depending on the cooling rate: at lower cooling rate (2.5 °C/min), all samples display a quite similar behaviour with little effect of the nanofiller.

The kinetics were analysed by using both the Avrami and the Ozawa theory [32]. According to the Ozawa model, the relative crystallinity $X(T)$ at a temperature T can be calculated as:

$$X(T) = 1 - \exp\{-K(T)/\alpha^m\} \tag{3}$$

where α is the cooling rate, m is the Ozawa exponent which depends on the dimension of crystal growth, and $K(T)$ is the cooling function related to the overall crystallization rate. According to Eq. (3), plots of log[–ln(1–$X(T)$)] versus t logα should give straight lines from which the values of m and $K(T)$ can be determined. The resulting plots for PP/POSS samples did not show linear trends indicating that m is not

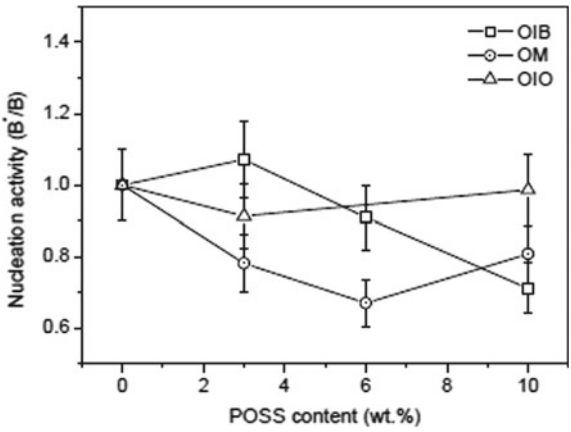

Fig. 12 Nucleation activity ($\Phi = B^*/B$) of octamethyl-POSS (OM), octaisobutyl-POSS (OIB) and octaisooctyl-POSS (OIO) in PP/POSS nanocomposites in non-isothermal crystallization conditions, as a function of POSS content. Reprinted from [26], Copyright 2006, with permission from John Wiley and Sons

constant with temperature and the cooling function could not be evaluated. However, other kinetic equations based on a combined approach of the two models have been satisfactorily applied to polyolefin nanocomposites with OM-POSS to relate the crystallinity change with cooling rate and temperature [4].

The nucleation activity Φ of the various samples was evaluated on the basis of non-isothermal crystallization kinetics according to the model proposed by Dobreva et al. [33]. Values of Φ were experimentally calculated at various cooling rates (α) from the slopes (B, B^*) of the linear relations:

$$\ln \alpha = \text{constant} - B/\Delta T_p^2 \tag{4}$$

$$\ln \alpha = \text{constant} - B^*/\Delta T_p^2 \tag{5}$$

where $\Delta T_p = T^\circ{}_m - T_c$ is the supercooling, B and B^* the values measured for neat PP and PP/POSS composites, respectively, and $\Phi = B^*/B$. For particles with no nucleation activity, $\Phi = 1$, while for very active substrates, Φ approaches zero.

The effect of the various POSS on the nucleation activity is shown in Fig. 12 as function of filler content [26]. It can be seen that OM-POSS displays a higher activity ($\Phi = 0.7$–0.8) at all examined compositions, whereas OIO-POSS is ineffective for nucleation ($\Phi = 1$) and OIB-POSS results to be effective only at a content of 10 wt% ($\Phi = 0.7$). It is interesting to notice that very similar results have been reported for composites of HDPE with OM-POSS which showed nucleation activity ($\Phi = 0.8$) for a POSS amount of 10 wt% [4].

2.2.3 Thermal Degradation Behaviour

The results of TGA analysis performed, both under nitrogen and in air, indicated that different POSS structures had different impacts on the thermal stability of PP/POSS nanocomposites. Thermal degradation of neat POSS compounds with long alkyl sub-

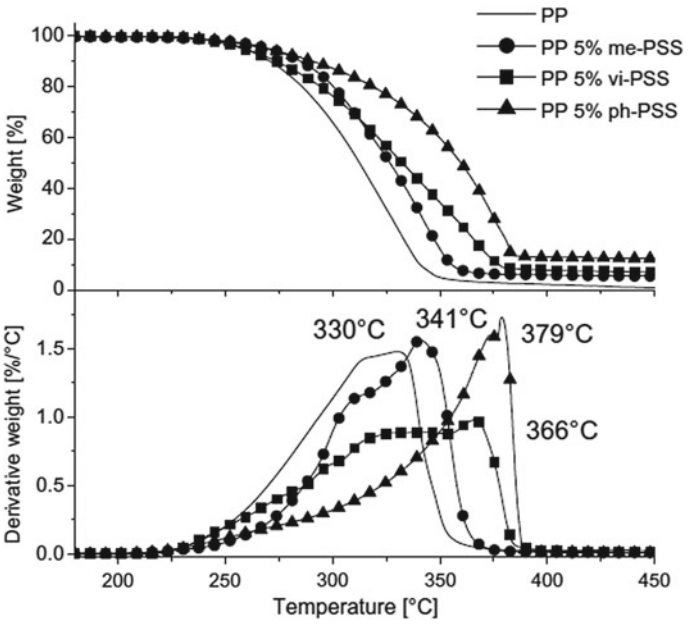

Fig. 13 TGA weight loss and derivative weight curves for neat PP and PP nanocomposites with 5% methyl-POSS (me-PSS), vinyl-POSS (vi-PSS) and phenyl-POSS (ph-PSS) in air. Reprinted from [28], Copyright 2010, with permission from Elsevier

stituents in air resulted differently than degradation under nitrogen. For PP nanocomposites containing *n*-octadecyl substituents (POSS18), higher maximum mass loss rate temperatures (T_{max}) were observed for samples with 1 and 5% filler content, compared with analogous PP nanocomposites containing *n*-octyl substituents (POSS8) [18].

For PP composites with methyl-POSS, vinyl-POSS and phenyl-POSS, it has been inferred that POSSs do not influence PP degradation under nitrogen, whereas they clearly affect the polymer stability under air [28]. In particular, composites with 1.5% POSS (inorganic Si–O fraction) showed only small improvements in thermoxidative stability with respect to neat PP; increasing the POSS content to 5%, the stability of composites appeared significantly improved, as shown by the shift of weight loss curves towards higher temperatures in Fig. 13.

Moreover, combustion tests showed improved performances in terms of lower combustion rate, due to the formation of a ceramic superficial layer acting as a protection towards degradation of the underlying material by limiting heat transfer and mass transfer. Nevertheless, it was noted that the ceramic superficial layer obtained from PP/POSS degradation generally appears thin and discontinuous, which is a limiting factor for its efficiency. The best performances were obtained with vinyl-POSS nanocomposites, which showed a reduction of the maximum Heat Release Rate and an increase of Limiting Oxygen Index value.

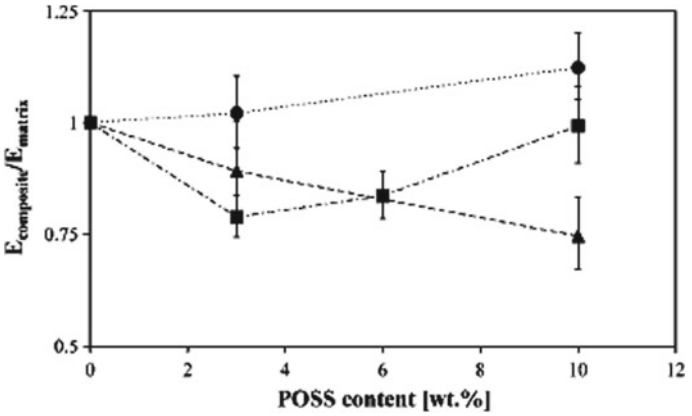

Fig. 14 Young's modulus of (●) PP/OM-POSS, (■) PP/OIB-POSS and (▲) PP/IO-POSS nanocomposites normalized to the modulus of neat PP, as a function of POSS content. Reprinted from [34], Copyright 2007, with permission from John Wiley and Sons

2.2.4 Mechanical Properties

Blends of polypropylene (PP) with (3–10 wt%) octamethyl-POSS (OM-POSS), octaisobutyl-POSS (OIB-POSS) or isooctyl-POSS (IO-POSS) were investigated to elucidate the effect of the alkyl group length on the mechanical behaviour of the blends [34]. Uniaxial tensile tests showed that the addition of OM-POSS induces an increase in Young's modulus and a reduction of the yield strength at all compositions, as compared to neat PP (Fig. 14).

Otherwise, the incorporation of OIB-POSS and IO-POSS caused a decrease of both Young's modulus and yield strength by increasing the POSS content. It was suggested that POSS behaves as particles having a siliceous hard core surrounded by a hydrocarbon soft-shell, which limits the stress transfer from the matrix to the core depending on the length of the alkyl groups.

Therefore, the different effects induced by POSS particles on the mechanical stiffness in composites with OM-POSS and IO-POSS (10 wt%) could be explained by assuming that, in the system with longer alkyl substituent, the presence of a thick soft-shell may hinder the stress transfer from the polymer matrix to the inorganic hard core of the particle, whereas in the system with OM-POSS the thin soft-shell makes possible a reinforcement action. In fact, for the same POSS content, the amount of inorganic material dispersed in the composite with IO-POSS is much lower than that dispersed in the composite with OM-POSS. Composites of PP with vinyl-POSS also displayed attractive mechanical performances, with higher elastic modulus, yield stress and elongation at break as compared to other composites and plain PP [28].

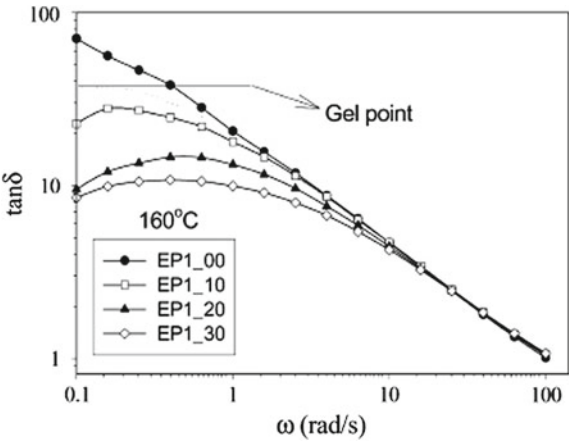

Fig. 15 Tan δ values versus frequency ω for neat EP (EP1_00) and EP/POSS nanocomposites with 10 wt% (EP1_10), 20 wt% (EP1_20) and 30 wt% (EP1_30) octamethyl-POSS at 160 °C. The extrapolated dotted line represents the gel point. Reprinted from [24], Copyright 2003, with permission from Elsevier

2.3 Ethylene–Propylene Copolymer/POSS

The structure, mechanical and rheological behaviours in the molten state of nanocomposites of ethylene–propylene copolymers (EP) with different ethylene content, containing octamethyl-POSS (OM-POSS) and octaisobutyl-POSS (OIB-POSS), were investigated by means of WAXD, dynamic mechanical analysis and oscillatory shear-, stress- and strain-controlled rheology [24].

The effect of POSS aggregation on the melt rheology and the mechanism of physical gelation of EP matrix in the presence of POSS nanoparticles were investigated. Oscillatory shear results showed that the EP/POSS nanocomposites exhibited a solid-like rheological behaviour compared with the liquid-like rheological behaviour of neat EPR. The rheological behaviour of neat EP copolymer was typical of polymer melts having a negative slope of tan δ over the entire frequency range examined (Fig. 15).

The introduction of POSS molecules drastically changed the rheology of EP: for EP/OM-POSS (10–30 wt%) nanocomposites, the tan δ slope became positive in the low-frequency region ($0.1 \leq \omega \leq 0.5$ rad/s) indicating a rheological transition from melt-like to solid-like ('Gel point' in Fig. 15). This behaviour was also observed in the nanocomposites at higher temperatures (180–200 °C) at all POSS contents. DMA results indicated that the values of glass transition temperature, T_g, and Young's modulus of the nanocomposites are higher than those of the neat copolymer, suggesting the existence of physical bonds between the POSS nanocrystals and polymer chains.

WAXD results showed the formation of nanocrystals aggregates, confirming that the unusual rheological behaviour of EP/POSS nanocomposites could be accounted for by the occurrence of interactions between same POSS molecules. Thus, it was concluded that two types of interactions contributed to the physical gelation in EP/POSS melts: the strong particle-to-particle interactions between the POSS crys-

tals and the weak particle-to-matrix interactions between the POSS crystals and the EP matrix.

2.4 Composites of Vinyl Polymers with POSS

The miscibility, the morphology and thermal behaviour of octaisobutyl-POSS (OIB-POSS) in polystyrene (PS), poly(isobutyl methacrylate) (PIBMA) and poly(methylmethacrylate) (PMMA) matrices, obtained by solution blending, were investigated over a wide composition range (25–75 wt% POSS) [6]. SEM and WAXS analyses showed a clear phase separation of the components in all blends and at all compositions examined. POSS crystallized within the polymer matrix and with increasing its concentration formed micron-sized aggregates with cubic structure. Similar crystal morphology has been observed in composites of PP with OIB-POSS [26]. The crystal size of POSS in PIBMA (and PMMA) matrices was smaller than that observed in PS matrix. Crystal–crystal transitions and melting points of POSS crystals did not change in the presence of polymer. PS/POSS blends did not show any significant change of glass transition temperature T_g, whereas for the other systems T_g was found to increase markedly with POSS content, likely due to different types of interaction between the POSS substituents and the polymer chains (both PIBMA and OIB-POSS contain isobutyl groups).

The thermal degradation of PS nanocomposites with heptacyclopentyl-bridged POSS at different POSS content (1–5 wt%)—synthesized by in situ polymerization of styrene in the presence of POSS—was studied and compared with that of nanocomposites containing heptaisobutyl-bridged POSS, in order to investigate the influence of the POSS cage substituents on the thermal stability of the nanocomposites [15].

POSS/PS nanocomposites exhibited a large improvement of thermal stability (both in terms of temperature at 5% mass loss and activation energy of degradation), with respect to PS and homologous isobutyl-bridged POSS/PS. The glass transition temperatures of the nanocomposites with heptacyclopentyl-bridged POSS were lower than those found for the composites containing isobutyl POSS due to the lower degree of crosslinking.

The photo-ageing behaviour of PS/POSS nanocomposites has been investigated by Dintcheva et al. [35]. POSS having different inorganic structure and organic substituents has been used in the preparation of nanocomposites with PS matrix, and the formulated films were subjected to accelerated weathering. Compared to pristine PS, it was found that PS/POSS samples developed a lower level of carbonyl and hydroxyl groups as a function of the exposure time, supporting a largely improved resistance of these nanocomposites to photo-degradation. It was concluded that the organic groups significantly influence the local morphology of the nanocomposite by controlling the POSS dispersion into the matrix, and its response to photo-oxidation.

3 Reactive Mixing of Polyolefins and POSS

3.1 Reactive Mixing Processes and Phase Interactions

It has been pointed out that the morphology, the thermal stability and tensile properties of polyolefins containing POSSs are strictly influenced by the chemical structure and dispersion degree of POSS nanoparticles. In general, due to the poor interactions between POSS and polymer matrices, the presence of coupling agents or even the chemical modification of the components becomes necessary to improve the compatibility of these materials [36]. Reactive blending is regarded as an efficient method for modifying and enhancing the properties of polymer/POSS nanocomposites. Compared with the physical blending, composites prepared by reactive blending may display improved mechanical and thermal properties due to the occurrence of stable chemical bonds between the components that can promote a homogeneous dispersion of the filler in the polymer matrix. Compatibilization may also be achieved by addition of a reactive functionalized polymer or copolymer, as third component, to a polyolefin composite containing modified POSSs.

Various methods of reactive mixing of polyolefins and POSS have been reported in the literature. Copolymers formed between ethylene and POSS (PE-*co*-POSS) were prepared and characterized by Zheng et al. [14, 37] using wide-angle X-ray scattering. In these copolymers, the POSS units, attached as pendant groups to the PE backbones, were found to crystallize as nanocrystals forming a lattice separate from that characteristic of polyethylene crystals. The POSS nanocrystals are covalently connected to the PE crystallites through an intermediate disordered interfacial region. It was concluded that in such copolymers POSS crystallizes as anisotropically shaped crystallites. The presence of POSS disturbs the crystallization of the polyolefin which results in smaller and disordered polyethylene crystallites.

Zhou et al. [38] grafted octavinyl-POSS to isotactic PP by reaction of double bonds of vinyl-POSS with polymer chains in the presence of dicumyl peroxide (DCP). The grafting reaction was verified by FTIR spectroscopy, Soxhlet extraction and Si elemental analysis, and then the properties of reactive blended (RB) samples were compared with those of samples obtained by physical blending (PB) of PP and POSS (without DCP). WAXD analysis showed that in physical blending POSS can act as β-nucleating agent for PP, indicating that POSS molecules exist as crystal in PP matrix (for POSS content $\geq$2 wt%), unlike the reactive blending composites where the crystalline β-form disappeared owing to the complete dispersion of grafted POSS in the PP matrix. This was further confirmed by DSC analysis and SEM microscopy.

As shown in Fig. 16, the crystallization peak temperature changed little for PB composites ($T_c = 120$ °C) at all compositions, while increased significantly in the case of RB samples ($T_c = 130$ °C) showing that the grafted POSS has a clear nucleating effect on PP chains. Further, the modulus of reactively mixed composites was found to increase in the presence of POSS, whereas it decreased in composites prepared by physical blending.

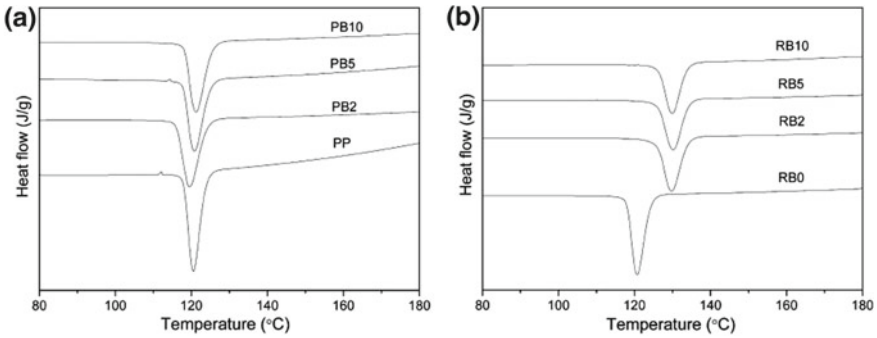

Fig. 16 DSC crystallization exotherms of PP and PP/vinyl-POSS composites (2–10 wt% POSS) prepared by **a** physical blending (PB) and **b** reactive blending (RB) (cooling rate: 10 deg/min). Reprinted from [38], Copyright 2008, with permission from Elsevier

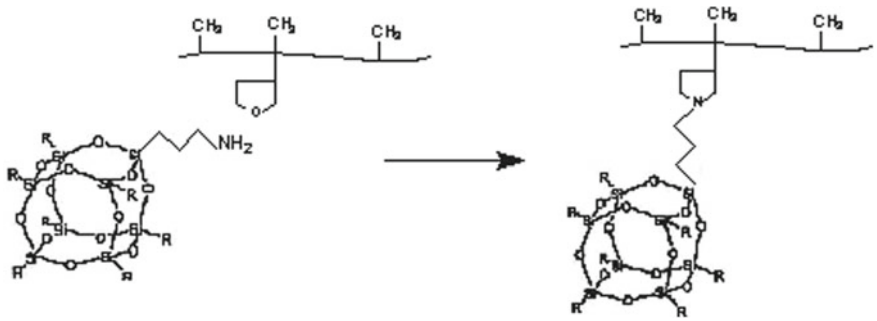

Fig. 17 Scheme of melt grafting reaction of aminopropyl-eptaisobutyl-POSS (amb-POSS) onto maleic anhydride-grafted PP (PP-*g*-MA) [39]

The polymer/filler interfacial interactions can be improved by melt mixing of polyolefin and POSS molecules containing both functional reactive groups that can interact with each other (Fig. 17). Hybrid nanocomposites obtained by blending maleic anhydride-grafted PP (PP-*g*-MA) and various alkyl POSS functionalized with end amino groups (Fig. 18): aminopropyl-heptaisobutyl-POSS (amb-POSS), aminoethyl-aminopropyl-heptaisobutyl-POSS (am2b-POSS) and aminopropyl-heptaisooctyl-POSS (amo-POSS) have been studied by Pracella et al. [39] and Grala et al. [40]. The properties of these systems have been then compared with those of (non-reactive) composites of PP homopolymer with same functionalized POSS and PP/POSS physical blends. Additionally, ternary composites of PP and amino-functionalized POSS additivated with PP-*g*-MA as compatibilizer were also investigated.

Grafting of POSS was evaluated by FTIR analysis and solvent extraction of unbound POSS. Figure 19 shows normalized FTIR spectra in the range of C=O absorptions from 1400 to 1900 cm^{-1}, obtained for neat PP and composites. In the reactive blend of PP-*g*-MA with am2b-POSS (curve 4), the carbonyl band (at

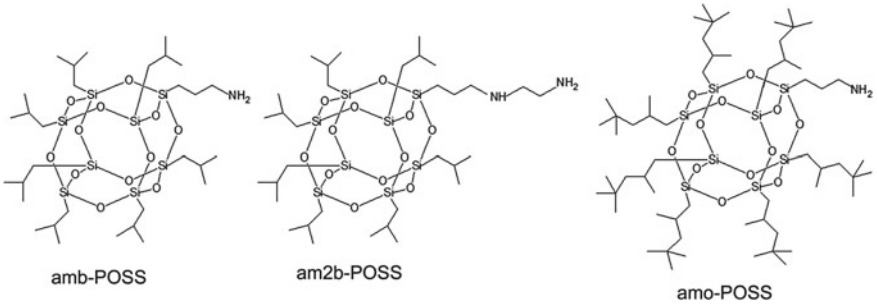

Fig. 18 Chemical structure of amine-functionalized POSS: aminopropyl-heptaisobutyl-POSS (amb-POSS), aminoethyl-aminopropyl-heptaisobutyl-POSS (am2b-POSS) and aminopropyl-heptaisooctyl-POSS (amo-POSS). Reprinted from [40], Copyright 2013, with permission from John Wiley and Sons

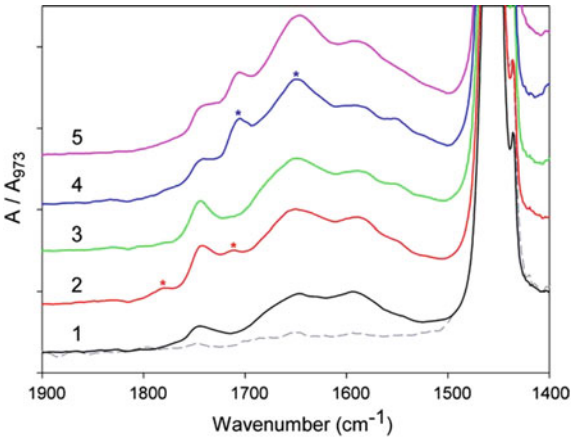

Fig. 19 Normalized FTIR spectra in the frequency range of C=O absorptions: (1) iPP, virgin pellet (broken line) and Brabender processed (solid line), (2) PP-*g*-MA, (3) iPP/am2b-POSS (5 wt%), (4) PP-*g*-MA/am2b-POSS (5 wt%) and (5) PP-*g*-MA/am2b-POSS (5 wt%) after Soxhlet extraction of ungrafted POSS. The curves were shifted vertically for clarity of presentation. Reprinted from [40], Copyright 2013, with permission from John Wiley and Sons

1710 cm^{-1}) almost disappeared and was replaced by a stronger peak at 1703 cm^{-1} (marked with *), characteristic of the imide group [41]. The formation of imide groups supported the reaction of anhydride groups with amine groups of am2b-POSS, i.e. grafting of POSS molecules on PP backbone. This imide peak remained practically unchanged after extraction of unbound am2b-POSS with THF.

Reactive systems based on maleic anhydride-grafted polypropylene (PP-*g*-MA) and Ti-containing amino polyhedral oligomeric silsesquioxanes (Ti-POSS-NH_2) have been also prepared by one-step reactive blending and compared with non-reactive PP/POSS systems [42]. The occurrence of reaction between the anhydride

groups of PP-*g*-MA and the amino groups of POSS molecules was confirmed by FTIR, whereas SEM analysis showed a nanometric dispersion of POSS into the polymer only in the presence of POSS-NH_2.

3.2 Morphology and Structure of PP-g-POSS Composites

The morphology of the various systems was examined by SEM on samples crystallized from the melt both in dynamic and isothermal conditions. All samples exhibited the characteristic spherulitic morphology of isotactic polypropylene (Fig. 20). For non-reactive binary systems of PP-*g*-MA and/or PP with OIB-POSS (5 wt%), SEM analysis of freeze-fractured surfaces showed a phase separation of OIB-POSS with formation of micron-sized aggregates in the interspherulitic zones and the presence of regular platelet-like POSS crystals at PP spherulite borders (Fig. 20a–c).

It was shown by energy dispersive spectrum (EDS) that these crystals consisted mainly of silicon with an intense peak at 1.7 keV (Fig. 20b), indicating that POSS preferentially aggregates and crystallizes into an ordered lattice within the polymer matrix. Similar phase-separated crystal textures were detected for am-POSS in the non-reactive PP/amb-POSS binary system (Fig. 20d). Otherwise, binary (PP-*g*-MA/amb-POSS) and ternary (PP/PP-*g*-MA/amb-POSS) composites with reactive components did not reveal any presence of POSS crystals or aggregates, indicating a very fine dispersion of the nanofiller into the polymer matrix, as confirmed by the results of EDS microanalysis showing a weak Si peak at 1.7 keV (Fig. 20e). This clearly supported the occurrence of POSS grafting onto PP-*g*-MA chains.

According to the above findings, WAXS spectra of non-reactive systems (PP-*g*-MA/OIB-POSS, PP/amb-POSS) displayed intense reflection characteristic of POSS crystals in 2θ range 6–12°, while no significant diffraction peaks relevant to POSS crystals were detected in the case of PP-*g*-MA/amb-POSS and PP/PP-*g*-MA/amb-POSS reactive samples (Fig. 21). Moreover, the appearance of POSS crystal reflections was accompanied by the presence of the peak of γ-form PP crystals ($2\theta = 20.07°$). It must be noticed that the growth of γ-form PP crystals has been also observed in reactive blends of modified PP (PP-*g*-AA, PP-*g*-GMA) with polyamides or polyesters [43].

3.3 Crystallization Behaviour and Thermal Degradation

The thermal behaviour of the composites resulted to be influenced by the chemical structure of the components and phase morphology. DSC thermograms showed that on cooling from the melt the crystallization temperature of PP-*g*-MA (113.6 °C) increased upon addition of OIB-POSS (118.5 °C) but decreased in the presence of amb-POSS (111.0 °C). This behaviour can be related to the dispersion degree of POSS within the polymer matrix, giving rise to crystal nucleation effects of PP chains

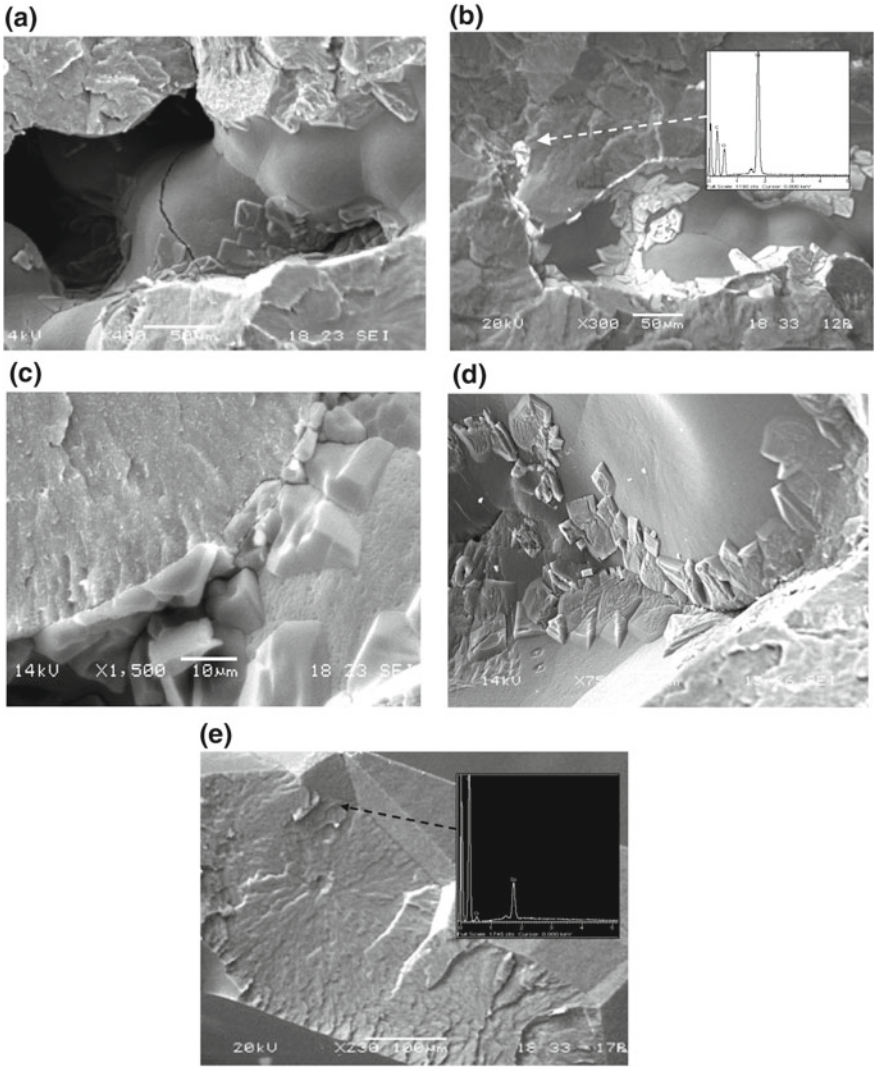

Fig. 20 SEM micrographs of fracture surfaces of binary composites (containing 5 wt% POSS): (a, b) PP-*g*-MA/OIB-POSS and (c) PP/OIB-POSS showing OIB-POSS crystals grown at the borders of impinged PP spherulites; (d) crystals of amb-POSS grown at the interface of PP spherulites in non-reactive PP/amb-POSS; (e) PP-*g*-MA/amb-POSS, isothermally crystallized at $T_c = 130$ °C, with EDS spectra of selected areas (indicated by the arrows)

at low dispersion (i.e. in the presence of crystals) of POSS in the non-reactive system (PP-*g*-MA/OIB-POSS), or to *retarded* crystallization of PP when the nanofiller is highly dispersed, as consequence of the chemical interactions in the reactive system (PP-*g*-MA/amb-POSS).

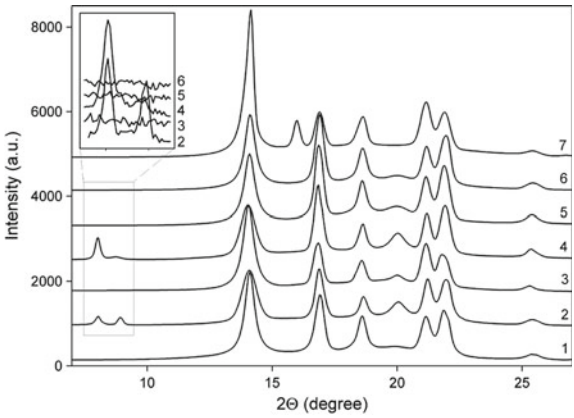

Fig. 21 WAXS spectra of melt crystallized composites and plain polymers: (1) PP-*g*-MA; (2) PP-*g*-MA/OIB-POSS; (3) PP-*g*-MA/amb-POSS; (4) PP/amb-POSS; (5) PP/PP-*g*-MA/amb-POSS (50/47.5/2.5); (6) PP/PP-*g*-MA/amb-POSS (75/23.5/1.25); (7) neat PP [39]

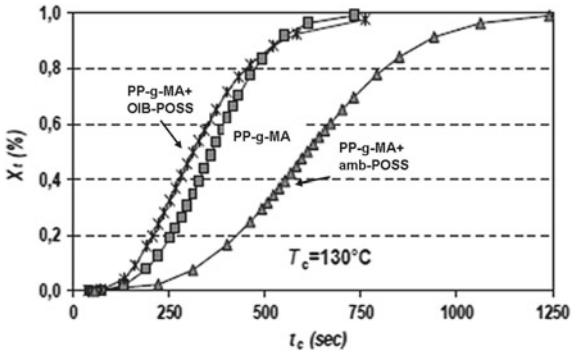

Fig. 22 Relative crystallinity fraction, X_t, as a function of crystallization time, t, at $T_c = 130$ °C for PP-*g*-MA/amb-POSS, PP-*g*-MA/OIB-POSS and plain PP-*g*-MA [39]

The isothermal crystallization kinetics of both functionalized and non-functionalized samples were examined in the temperature range 122–135 °C according to the Avrami model. The overall crystallization rate of PP-*g*-MA matrix was found to decrease markedly in reactive composites with amb-POSS, as compared to non-reactive composites with OIB-POSS and plain PP-*g*-MA (Fig. 22). On the other side, a higher crystallization rate was observed for PP-*g*-MA in composites with OIB-POSS, likely due to the nucleating effect of the nanofiller.

For samples containing the amino-functionalized POSS, the values of the Avrami exponent ($n = 3.5$–4) were higher than those recorded for neat PP-*g*-MA and PP-*g*-MA/OIB-POSS ($n = 3$), supporting that primary nucleation and growth of polymer crystals are strictly affected by the chemical interactions between the components, and thus by POSS dispersion. The sharp decrease of overall crystallization rate recorded for the PP-*g*-MA/amb-POSS sample is to be related to the strong polymer–nanoparticle interactions in the melt and thus to constraints on the movement of polypropylene chains caused by POSS grafting.

The analysis of melting behaviour of isothermally crystallized samples showed the occurrence of multiple melting peaks that could be ascribed to crystals of different

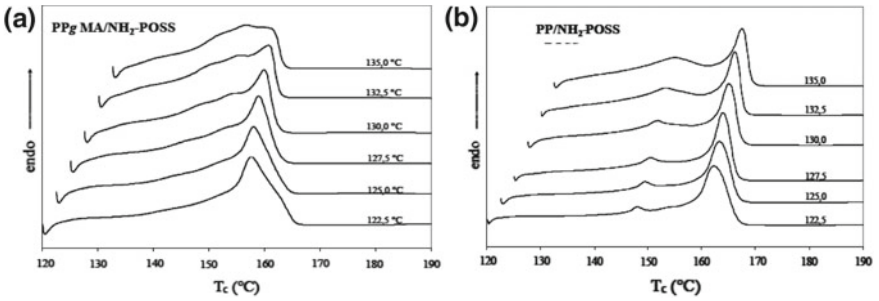

Fig. 23 DSC melting thermograms of composites of **a** PP-*g*-MA and **b** PP with 5 wt% amb-POSS (NH_2-POSS), isothermally crystallized at various T_c [39]

stability and structure (polymorphic α- and γ-forms), as well as to reorganization phenomena during heating (Fig. 23). The presence of γ-form crystals was detected only for plain PP samples.

Equilibrium melting temperatures, T°_m, of polypropylene crystals were calculated for the various samples by extrapolation (to the line $T_m = T_c$) of linear plots of the observed melting temperatures T_m versus T_c, according to Hoffmann–Week equation [44]:

$$T_m = T_m^{\circ}(\psi - 1)/\psi + T_c/\psi \tag{5}$$

where ψ is a parameter related to the fold length of primary nuclei. A significant change of T°_m from 177.0 °C for neat PP-*g*-MA to 172.5 °C for PP-*g*-MA/amb-POSS—compared to $T^{\circ}_m = 185$ °C for plain PP—was noticed for the reactive samples suggesting that the POSS nanoparticles were dispersed within the interlamellar amorphous region of PP spherulites. Accordingly, the results of SAXS analysis showed that the lamellar thickness of polymer crystals was influenced by the sample composition and crystallization conditions, and the estimated values of crystal thickness were lowered in the case of reactive system [40].

The thermal degradation behaviour of PP-*g*-MA/amb-POSS, PP/amb-POSS and ternary PP/PP-*g*-MA/amb-POSS composites was examined in the temperature range 100–600 °C both in nitrogen and air (Fig. 24). In nitrogen, all samples displayed the same trend almost independently of POSS functionalization. In air, a different behaviour was observed for PP-*g*-MA/amb-POSS which presented a large increase of the temperature of maximum weight loss rate (402 °C) as compared to PP-*g*-MA/OIB-POSS (310 °C) and plain PP-*g*-MA (338 °C), indicating that the finer dispersion of the grafted nanofiller in the compatibilized composite greatly improved the thermal stability of the polyolefin. This effect could be explained in terms of accumulation of POSS on the sample surface during the thermoxidative degradation, with formation of a ceramic layer acting as a protective barrier [22].

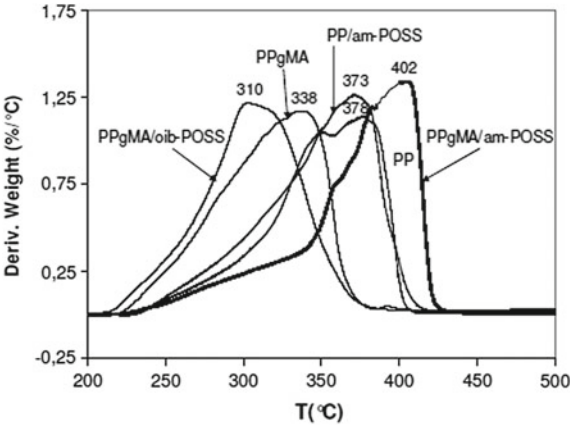

Fig. 24 Derivative weight loss from TGA analysis of PP/POSS and PP-*g*-MA/POSS composites and plain polymers in air [39]

3.4 Mechanical and Rheological Properties

Grafting with POSS causes also a reduction of PP crystallinity degree both in PP-*g*-POSS reactive hybrids and ternary systems (PP/PP-*g*-MA/amb-POSS), as well as deep changes in the properties of PP amorphous phase: the entanglement density increases, while flexibility and mobility of amorphous chains decrease. These structural changes affect the tensile properties of PP modified with POSS as elastic modulus and yield stress, both controlled by the crystalline phase, and the ultimate properties, which depend much more on the amorphous component. The morphology and mechanical properties of hybrids obtained by reactive melt-blending of PP and PP-*g*-MA with various amine-functionalized POSS (amb-POSS, amo-POSS and am2b-POSS) were extensively examined by Grala et al. [40].

SEM analysis revealed clear differences in the morphology of PP/POSS and PP-*g*-POSS composites (Fig. 25): in PP/POSS physical blends micron- and submicron-sized POSS crystals were observed, while no such crystals or aggregates were detected in samples obtained by reactive blending of PP-*g*-MA with POSS. SEM micrographs of iPP/amb-POSS blend evidence segregation of POSS from iPP and its rejection from the interior of growing PP spherulites to their growth front, and finally POSS crystals are collected within interspherulitic boundary regions (Fig. 25a). On the contrary, no traces of POSS crystals or aggregates were observed in PP-*g*-POSS hybrids for any POSS type and at any crystallization conditions (Fig. 25b–d), which may suggest the homogeneous distribution of POSS molecules.

The results of mechanical analysis of the ternary systems with different PP/PP-*g*-MA/aminoPOSS composition ratio are shown in Fig. 26. No marked variations were observed in the values of Young's modulus and yield stress (Fig. 26a, b) for samples with different content of PP-*g*-POSS copolymers (1.25–5.0 wt% POSS) compared to plain copolymers. Otherwise, larger variations were found in ultimate properties (Fig. 26c, d), especially in strain at break. Nevertheless, one can observe a clear dependence of the nominal ultimate strain on the type of POSS (Fig. 26d). The

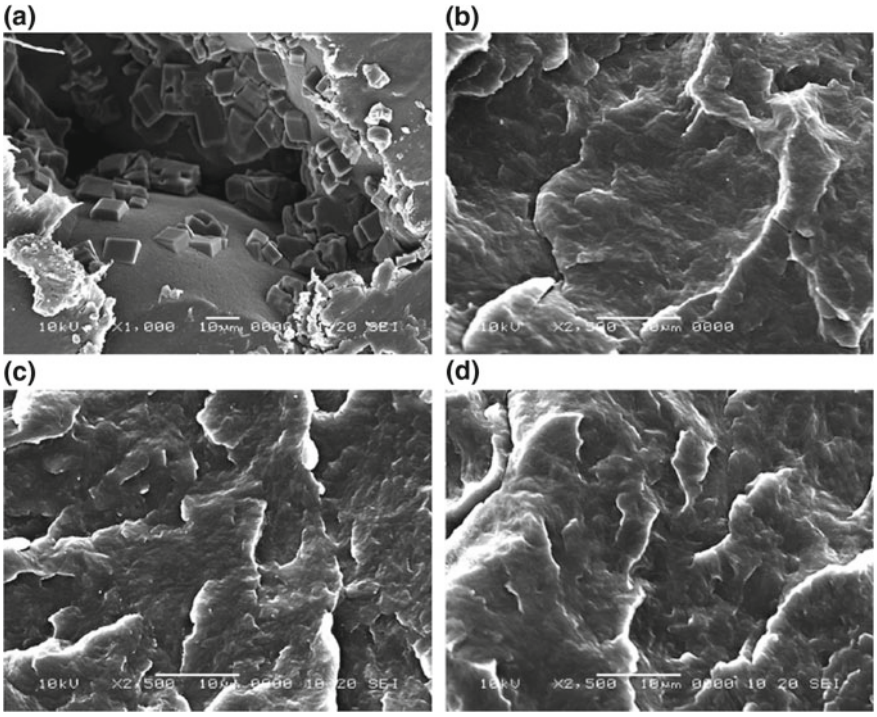

Fig. 25 SEM micrographs of freeze-fractured surfaces of: **a** PP/amb-POSS physical blend showing the presence of POSS crystals at the surface of PP spherulites (isothermally crystallized at 132 °C), **b** PP-*g*-amb-POSS, **c** PP-*g*-amo-POSS and **d** PP-*g*-am2bPOSS hybrids obtained by reactive blending. All samples contain 5 wt% of the respective POSS. Reprinted from [40], Copyright 2013, with permission from John Wiley and Sons

decrease of the strain at break is relatively small for systems containing amb-POSS, moderate in those with amo-POSS, and very large in samples containing am2b-POSS. The ability of large strain deformation is generally a property of the amorphous component and is controlled primarily by the molecular network of entangled chains in the amorphous phase [45]. Modification of PP by grafting with very bulky POSS molecules should induce large changes in the properties of the amorphous phase since all chain segments containing grafted POSS molecules reduce their ability to crystallize and to be incorporated into PP crystalline lamellae. Therefore, these segments must be redistributed into the *interlamellar* amorphous phase upon solidification. This could lead not only to a reduced crystallinity (with thinner crystals) as experimentally observed, but also to a more entangled molecular network within the amorphous phase. All above would result in a stiffer amorphous phase with reduced ability to large strain deformation, as compared to plain PP. A deeper modification of the properties of amorphous phase in samples containing PP-*g*-am2bPOSS was observed than in those with PP-*g*-amo-POSS and PP-*g*-amb-POSS (with same POSS

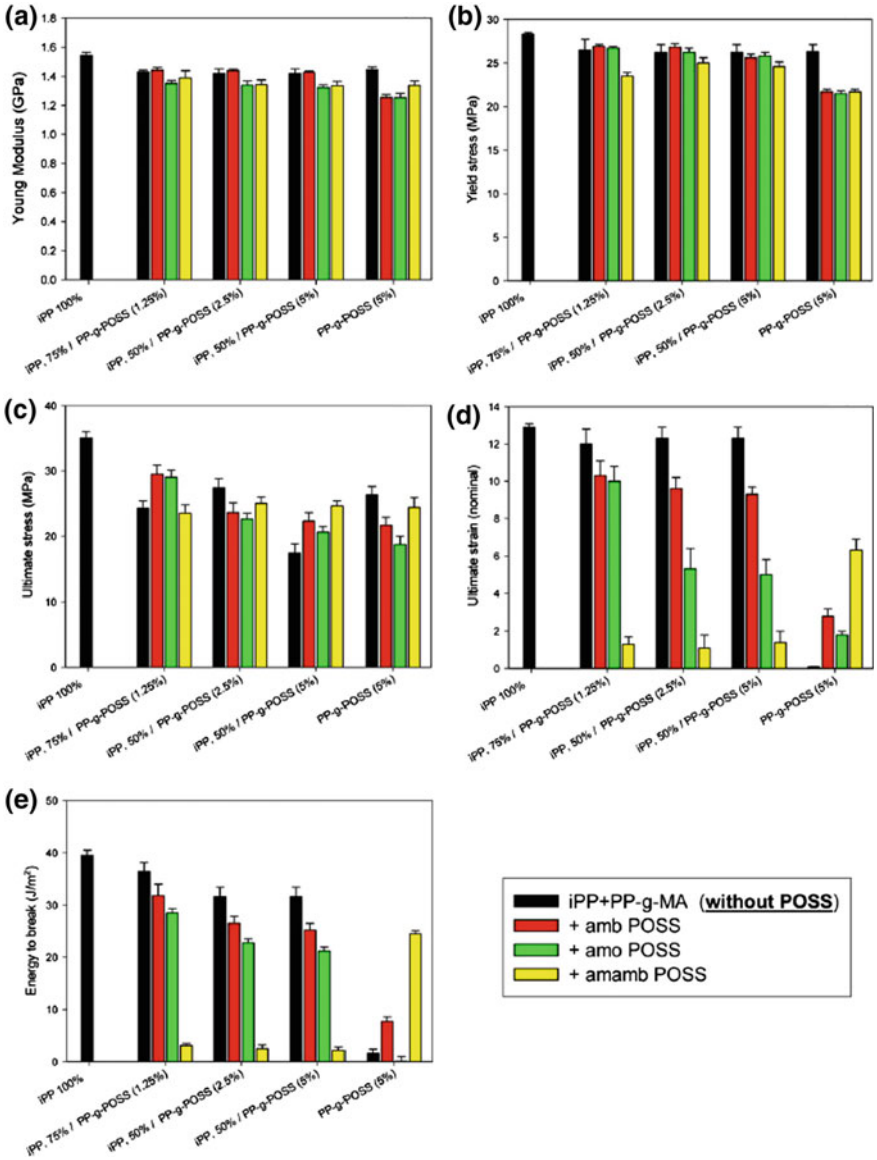

Fig. 26 Tensile properties of PP, PP-*g*-POSS hybrids and PP/PP-*g*-POSS blends. Reprinted from [40], Copyright 2013, with permission from John Wiley and Sons

concentration), as a consequence of the higher grafting degree of PP-*g*-am2bPOSS sample.

The energy dissipated by blend samples during tensile deformation is a measure of their toughness under conditions of slow deformation. Changes of the energy to

break (Fig. 26e) generally follow the already discussed trends in ultimate strain: the low-rate toughness of PP-*g*-POSS hybrids and their blends with PP is substantially reduced compared to plain PP. Concluding, the elastic modulus and the yield stress (both controlled primarily by properties of the crystalline phase) follow in PP-*g*-POSS hybrids and PP/PP-*g*-POSS blends the changes in crystallinity and crystal thickness, respectively. These changes in the properties of the crystalline phase were both induced by the presence of large quantity of PP-*g*-MA compatibilizer and by a relatively small fraction of POSS molecules grafted onto PP chains. Otherwise, ultimate properties of PP modified with either PP-*g*-MA or PP-*g*-POSS—controlled primarily by properties of the amorphous phase—are strictly influenced by PP-*g*-POSS since bulky POSS molecules grafted on PP chains lead to a large increase of the entanglement density and stiffening of the molecular network, which in turn result in significantly reduced deformability.

Izod impact tests demonstrated that the impact strength of PP/PP-*g*-POSS blends is slightly larger than that of plain PP, regardless of the type of POSS present. Such behaviour may suggest that toughness improvement of blends can be attributed primarily to smaller thickness of lamellar crystals in these blends as compared to plain PP. Thinner crystals start to deform earlier which allows for more energy being dissipated on plastic deformation before fracture. On the other hand, tensile results demonstrated a limited deformability of blends, probably related to larger stiffness of the more entangled amorphous phase containing PP-*g*-POSS hybrids.

The crystallization and rheological behaviours of nanocomposites of isotactic PP filled with octaaminophenyl-POSS (PP/oap-POSS) were compared with that of nanocomposites compatibilized with (10 wt%) maleic anhydride-grafted PP (PP/oap-POSS/PP-*g*-MA) [46]. It was found that PP-*g*-MA sharply improved the compatibility between polymer matrix and POSS inducing a fine dispersion of oap-POSS particles in PP, due to the reaction of amine groups of oap-POSS with maleic anhydride groups of PP-*g*-MA. DSC and POM analyses showed that oap-POSS retarded the crystallization of PP in non compatibilized system, whereas exhibited a nucleating effect in the presence of PP-*g*-MA. These findings were accounted for by the combination of retardation and nucleation effects of oap-POSS on PP chains: the nucleation effect of the oap-POSS-grafted PP (PP-*g*-POSS) would compensate and overlap the retardation effect when PP-*g*-MA was added. Rheological data indicated that the addition of PP-*g*-MA would decrease the viscosity of PP/oap-POSS composites probably due to the occurrence of weak particle–particle interaction and interface slipping. The results indicated that all the materials followed a power law relationship at low shear rate. The values of apparent shear viscosity η at the same shear rate increased with increasing oap-POSS content for PP/oap-POSS, while for the compatibilized system PP/PP-*g*-MA/oap-POSS, the reaction of POSS amino groups and PP-*g*-MA caused a lower viscosity, likely attributable to the larger number and smaller size of POSS particles after the addition of compatibilizer.

4 Applications

POSS molecules incorporated into polymer matrices, as well as hybrid polymers containing POSS, can find application in a wide variety of fields, ranging from high-performance materials to flame-resistant materials. The nanoscopic size and Si–O structure of POSS result in a significant improvement in the fire retardancy of polymer/POSS nanocomposites, generally accompanied by an increase in mechanical properties. POSS is considered as fire retardant whose main function involves the condensed phase with reduction of the rate of supply of polymer degradation combustible volatiles to the flame [1]. Such an improvement in fire retardancy is often found even at low POSS content. POSSs show a remarkable synergistic effect with traditional flame retardants: addition of POSSs can improve the flame retardancy of polymers in the presence of traditional flame retardants, or reduce the amount of flame retardants necessary for fire prevention, thus reducing their environmental impact. Many kinds of flame-retarding elements—such as P, N, S, B and catalytic metal elements—can be also incorporated into the POSS structures by chemical synthesis. Generally, a fine dispersion of these elements within the polymer matrix is obtained, owing to the good compatibility of POSS.

Lithographic applications of POSS-containing photoresist materials have been reported by Kuo and Chang [47]. They developed methacrylate-based photoresist materials containing POSS derivative for UV lithography with enhanced sensitivity, higher contrast and improved resolution due to the hydrogen bonding interactions between the siloxane units of the POSS moieties and the OH groups of methacrylate polymers. The strong hydrogen bonding interactions drew the methacrylate double bonds towards the POSS moieties, resulting in a higher concentration of these olefinic bonds around the POSS units that enhanced the rate of chemically crosslinking through photo-polymerization (Fig. 27) [48].

Further, POSS molecules have been employed in applications for photoluminescence (PL) and electroluminescence (EL) devices, since the POSS moiety can substantially suppress aggregation and improve quantum efficiency and thermal stability [49]. POSS-containing hybrid polymers have also been developed for applications in proton exchange membranes [50].

To decrease the dielectric constants of polymers, several research groups have explored the possibility of incorporating various nanoparticles into polymer matrixes to take advantage of the low dielectric constant of air ($k = 1$) [47]. Low dielectric constant materials have been prepared through dispersion of POSS molecules into polymer matrices, exploiting the hydrogen bonding interactions between the POSS moieties and the OH groups of the matrix to obtain homogenous nanocomposites, in which the POSS units also contributed to improve thermal and mechanical properties.

POSS-containing hybrid polymers can self-assemble into nanoscaled aggregates in selective solvents and form nanostructures in bulk [51]. Some of the interesting self-assembly morphologies are remarkably different from those formed from the conventional purely organic amphiphilic polymers. Well-defined POSS-containing hybrid polymers have shown unexpected properties, which lead to unlimited possi-

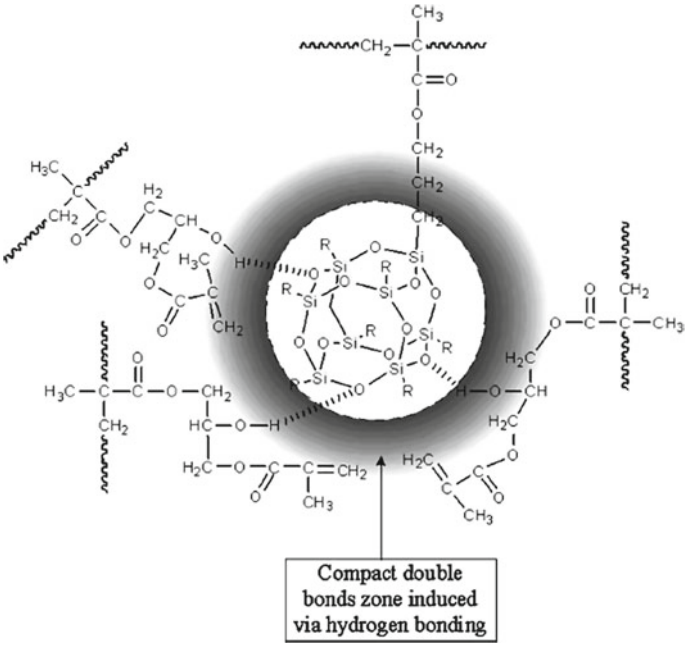

Fig. 27 Proposed microstructure via hydrogen bonding interaction of POSS with methacrylate polymer. Reprinted from [47], Copyright 2011, with permission from Elsevier

bilities for promising applications, such as biomedicine, electronic, optical, magnetic nanodevices, sensors and catalysts.

Self-organizing materials allow the development of simple and low-cost process for production of large periodic nanostructures from di-block copolymers or low molecular weight compounds by controlling their self-assembly. Zhu and coworkers [52] reported the self-assembly of a PEO-*b*-PE-POSS triblock copolymer, in which the POSS molecules crystallized prior to crystallization of PE, forming a well-defined lamellar structure. Hirai and coworkers [53] prepared POSS-containing di-block copolymers with PMMA and PS—PMMA-*b*-PMAPOSS and PS-*b*-PMAPOSS—through anionic living polymerization. These two kinds of block copolymers formed various self-assembled structures including spherical, cylindrical and lamellar morphologies.

POSS-containing hybrid polymers have been considered as very innovative materials in several biological fields, due to their excellent mechanical properties and biodegradability provided by Si–O–Si bonds. Novel tissue engineering materials based on POSS-containing polymers have been developed, which possess largely improved mechanical properties and extended service life, such as dental resins based on POSS [51].

5 Concluding Remarks

Polymeric nanocomposites represent a class of materials with high performance. The dispersion of POSS nanoparticles in polymeric matrices offers the opportunity of preparing advanced composite materials with high thermal, mechanical and oxidative performances. The presence of organic substituents at surface of POSS molecules can induce large effects on the nucleation and crystallization processes of the polymer, as well as on the compatibility of the composites by designed introduction of functional groups.

Compared with conventional polymeric blends or copolymers, nanocomposites exhibit dramatic improvement in thermal and mechanical properties at low loadings of the inorganic fillers. On the other hand, the properties are affected significantly by the processing conditions. It is well known the importance played by the morphology and the crystallinity degree on the final properties of the product, factors that substantially depend on the mutual interactions between polymers and inorganic fillers. From this point of view, the study of the effects of the inorganic particles on the polymeric chain dynamics is of fundamental importance in order to understand the way the crystalline phase develops during the solidification process, and in particular the distribution of crystallinity along the sample. In addition, a real-time monitoring of the changes in molecular dynamics during the solidification process provides information on the kinetics of the crystalline phase formation.

POSS molecules can be easily incorporated into many polymers, such as polyolefins, polyesters, polyacrylates, siloxanes for production of a variety of new materials with improved thermal, mechanical and transport properties. The final properties of these materials are strictly depending on the morphology generated during their processing, when the filler particle may act as nucleating agent and affect the crystallization behaviour. Therefore, the study of the crystallization processes and the interfacial interaction phenomena is of crucial importance for the optimization of the processing conditions and the property control of end products.

Polymer nanocomposites and hybrids reinforced with POSS can find application in many advanced sectors, such as aerospace, automotive, electronics; moreover, they can be employed for the production of films and membranes with tailored optical and transport properties. These materials display superstructural characteristics which are comparable to those of polymer-clay (or organosilicate) nanocomposites, but differently from these latter, they show a higher chemical versatility due to the possibility of modifying the POSS structure with functional groups, thus enhancing compatibility and processability. The research efforts in this field will contribute to expand the application potential and processing technologies of these materials.

Polyolefin/POSS hybrids based on PP-*g*-MA (or PP/PP-*g*-MA) matrix and amino-functionalized POSS, as dispersed component, display marked changes of morphology, structure and phase behaviour as compared to non-functionalized PP/POSS systems. Grafting reactions of amino-modified POSS onto maleated PP chains can be effectively exploited by melt mixing to promote the dispersion of POSS nanoparticles at molecular level, enhancing the properties and performances of these sys-

tems. The reported results pointed out that the crystallization behaviour and the crystal superstructure of the polyolefin matrix are strictly influenced by the POSS dispersion. Fully alkyl-substituted POSS in PP-*g*-MA (and PP) matrix gives rise to phase-separation phenomena and nucleating effects, increasing the overall crystallization rate of polypropylene, while in the reactive PP-*g*-MA/amb-POSS system, a marked decrease of the polymer crystallization rate is found as a consequence of the POSS grafting reactions. The molecular dispersion of grafted POSS is responsible for the neat improvement of thermal stability of the functionalized composites towards oxidative degradation.

References

1. Zhang W, Camino G, Yang R (2017) Polymer/polyhedral oligomeric silsesquioxane (POSS) nanocomposites: an overview of fire retardance. Prog Polym Sci 67:77–125
2. Li G, Wang L, Ni H, Pittman CU Jr (2001) Polyhedral oligomeric silsesquioxane (POSS) polymers and copolymers: A review. J Inorg Organomet Polym 11(3):123–154
3. Fu BX, Yang L, Somani RH, Zong SX, Hsiao BS, Phillips S, Blanski R, Ruth P (2001) Crystallization studies of isotactic polypropylene containing nanostructured polyhedral oligomeric silsesquioxane molecules under quiescent and shear conditions. J Polym Sci B Polym Phys 39:2727–2739
4. Joshi M, Butola BS (2004) Studies on nonisothermal crystallization of HDPE/POSS nanocomposites. Polymer 45:4953–4968
5. Zeng J, Kumar S, Iyer S, Schiraldi DA, Gonzalez RI (2005) Reinforcement of poly(ethylene terephthalate) fibers with polyhedral oligomeric silsesquioxanes (POSS). High Perform Polym 17:403–424
6. Li S, Simon GP, Matisons JG (2010) Morphology of blends containing high concentrations of POSS nanoparticles in different polymer matrices. Polym Eng Sci 50(5):991–999
7. Misra R, Fu BX, Plagge A, Morgan SE (2009) POSS-nylon 6 nanocomposites: influence of POSS structure on surface and bulk properties. J Polym Sci B Polym Phys 47:1088–1102
8. Ramasundaram SP, Kim KJ (2007) In-situ synthesis and characterization of polyamide 6/POSS nanocomposites. Macromol Symp 249–250:295–302
9. Cai H, Zhang X, Xu K, Liu H, Su J, Liu X et al (2012) Preparation and properties of polycarbonate/polyhedral oligomeric silsesquioxanes (POSS) hybrid composites. Polym Adv Technol 23:765–775
10. Zhao Y, Schiraldi DA (2005) Thermal and mechanical properties of polyhedral oligomeric silsesquioxane (POSS)/polycarbonate composites. Polymer 46:11640–11647
11. Matejka L, Strachota A, Plestil J, Whelan P, Steinhar M, Šlouf M (2004) Epoxy networks reinforced with polyhedral oligomeric silsesquioxanes (POSS): structure and morphology. Macromolecules 37:9449–9456
12. Strachota A, Kroutilova I, Kovarova J, Matejka L (2004) Epoxy networks reinforced with polyhedral oligomeric silsesquioxanes (POSS). Thermomechanical properties. Macromolecules 37:9457–9464
13. Liu L, Tian M, Zhang W, Zhang L, Mark JE (2007) Crystallization and morphology study of polyhedral oligomeric silsesquioxane (POSS)/polysiloxane elastomer composites prepared by melt blending. Polymer 48:3201–3212
14. Zheng L, Waddon AJ, Farris RJ, Coughlin EB (2002) X-ray characterizations of polyethylene polyhedral oligomeric silsesquioxane copolymers. Macromolecules 35:2375–2379
15. Blanco I, Bottino FA (2015) The influence of the nature of POSSs cage's periphery on the thermal stability of a series of new bridged POSS/PS nanocomposites. Polym Degrad Stab 121:180–186

16. Joshi M, Butola BS, Simon G, Kukaleva N (2006) Rheological and viscoelastic behaviour of HDPE/octamethyl-POSS nanocomposites. Macromolecules 39(5):1839–1849
17. Hato MJ, Ray SS, Luyt AS (2008) Nanocomposites based on polyethylene and polyhedral oligomeric silsesquioxanes, 1– microstructure, thermal and thermomechanical properties. Macromol Mater Eng 293(9):752–762
18. Niemczyk A, Dziubek K, Sacher-Majewska B, Czaja K, Dutkiewicz M, Marciniec B (2016) Study of thermal properties of polyethylene and polypropylene nanocomposites with long alkyl chain-substituted POSS fillers. J Therm Anal Calorim 125(3):1287–1299
19. Perrin FX, Panaitescu DM, Frone AN, Radovici C, Nicolae C (2013) The influence of alkyl substituents of POSS in polyethylene nanocomposites. Polymer 54:2347–2354
20. Heeley EL, Hughes DJ, El Aziz Y, Taylor PG, Bassindale AR (2013) Linear long alkyl chain substituted POSS cages: the effect of alkyl chain length on the self-assembled packing morphology. Macromolecules 46(12):4944–4954
21. Heeley EL, Hughes DJ, El Aziz Y, Taylor PG, Bassindale AR (2015) Crystallization and morphology development in polyethylene–octakis (*n*-octadecyldimethylsiloxy)-octasilsesquioxane nanocomposite blends. RSC Adv 5:34709–34719
22. Fina A, Tabuani D, Carniato F, Frache A, Boccaleri E, Camino G (2006) Polyhedral oligomeric silsesquioxanes (POSS) thermal degradation. Thermochim Acta 440:36–42
23. Frone AN, Perrin FX, Radovici C, Panaitescu DM (2013) Influence of branched or un-branched alkyl substitutes of POSS on morphology, thermal and mechanical properties of polyethylene. Composites Part B 50:98–106
24. Fu BX, Gelfer MY, Hsiao BS, Phillips S, Viers B, Blanski R, Ruth P (2003) Physical gelation in ethylene–propylene copolymer melts induced by polyhedral oligomeric silsesquioxane (POSS) molecules. Polymer 44:1499–1506
25. Fina A, Tabuani D, Frache A, Camino G (2005) Polypropylene-polyhedral oligomeric silsesquioxanes (POSS) nanocomposites. Polymer 46:7855–7866
26. Pracella M, Chionna D, Fina A, Tabuani D, Frache A, Camino G (2006) Polypropylene-POSS nanocomposites: morphology and crystallization behaviour. In: Pirozzi B, Roviello A (eds) Trends and perspectives in polymer science and technology. Macromol Symp 234:59–67
27. Chen JH, Yao BX, Su WB, Yang YB (2007) Isothermal crystallization behavior of isotactic polypropylene blended with small loading of polyhedral oligomeric silsesquioxane. Polymer 48:1756–1769
28. Fina A, Tabuani D, Camino G (2010) Polypropylene–polysilsesquioxane blends. Eur Polym J 46:14–23
29. Wunderlich B (1976) Macromolecular physics, crystal nucleation, growth, annealing, vol 2. Academic Press, New York, Chapter VI
30. Pracella M (2013) Crystallization of polymer blends. In: Piorkowska E, Rutledge G (eds) Handbook of polymer crystallization, Wiley, Hoboken, Chapter 10
31. Bartczak Z, Galeski A, Pracella M (1986) Spherulite nucleation in blends of isotactic polypropylene with high-density polyethylene. Polymer 27:537–543
32. Ozawa T (1971) Kinetics of non-isothermal crystallization. Polymer 12:150–158
33. Dobreva A, Vassilev T, de Saja JA, Rodriguez MA, Gutzow I (1999) Unified thermodynamic approach for describing the nucleating activity of substrates in the induced crystallization of undercooled glass-forming liquids. J Non Cryst Solids 253(1–3):157–162
34. Baldi F, Bignotti F, Ricco L, Monticelli O, Ricco T (2007) Mechanical characterization of polyhedral oligomeric silsesquioxane/polypropylene blends. J Appl Polym Sci 105:935–943
35. Dintcheva NT, Morici E, Arrigo R, La Mantia FP, Malatesta V, Schwab JJ (2012) UV-stabilisation of polystyrene-based nanocomposites provided by polyhedral oligomeric silsesquioxanes (POSS). Polym Degrad Stab 97(11):2313–2322
36. Pracella M (2017) Blends and alloys. In: Jasso-Gastinel CF, Kenny JM (eds) Modification of polymer properties, Elsevier, Oxford, Chapter 7
37. Waddon AJ, Zheng L, Farris RJ, Coughlin EB (2002) Nanostructured polyethylene-POSS copolymers: control of crystallization and aggregation. Nano Lett 2:1149–1155

38. Zhou Z, Cui L, Zhang Y, Zhang Y, Yin N (2008) Preparation and properties of POSS grafted polypropylene by reactive blending. Eur Polym J 44:3057–3066
39. Pracella M, Pancrazi C, Bartczak Z (2009) Reactive mixing of polypropylene/POSS nanocomposites. Crystallization, morphology and thermal properties. In: Proceedings 17th International Conference on Composite Materials, Edinbourgh, UK, 27–31 July
40. Grala M, Bartczak Z, Pracella M (2013) Morphology and mechanical properties of polypropylene-POSS hybrid nanocomposites obtained by reactive blending. Polym Compos 34(6):929–941
41. Wei Q, Chionna D, Galoppini E, Pracella M (2003) Functionalization of LDPE by melt grafting with glycidyl methacrylate and reactive blending with polyamide-6. Macromol Chem Phys 204:1123–1133
42. Hoyos M, Fina A, Carniato F, Prato M, Monticelli O (2011) Novel hybrid systems based on poly(propylene-*g*-maleic anhydride) and Ti-POSS by direct reactive blending. Polym Degrad Stab 96:1793–1798
43. Psarski M, Pracella M, Galeski A (2000) Crystal phase and crystallinity of polyamide-6/functionalized polyolefin blends. Polymer 41:4923–4932
44. Hoffmann JD, Davis GT, Lauritzen JI (1976) The rate of crystallization of linear polymers with chain folding. In: Hannay NB (ed) Treatise on solid state chemistry, Vol 3. Plenum Press, New York, Chapter 7
45. Bartczak Z, Kozanecki M (2005) Influence of molecular parameters on high-strain deformation of polyethylene in the plane-strain compression. Part I. Stress–strain behavior. Polymer 46:8210–8221
46. Zhou Z, Ouyang C, Zhang Y, Zhang Y, Yin N (2009) Crystallization and rheological behavior of POSS filled polypropylene. e-Polymers 9(1):036
47. Kuo SW, Chang FC (2011) POSS related polymer nanocomposites. Prog Polym Sci 36:1649–1696
48. Lin HM, Wu SY, Huang PY, Huang CF, Kuo SW, Chang FC (2006) Polyhedral oligomeric silsesquioxane containing copolymers for negative type photoresists. Macromol Rapid Commun 27:1550–1555
49. Xiao S, Nguyen M, Gong X, Cao Y, Wu HB, Moses D, Heeger AJ (2003) Stabilization of semiconducting polymers with silsesquioxane. Adv Funct Mater 13:25–29
50. Cheng CC, Yen YC, Ko FH, Chu CW, Fan SK, Chang FC (2012) A new supramolecular film formed from a silsesquioxane derivative for application in proton exchange membranes. J Mater Chem 22:731–734
51. Zhang W, Müller AHE (2013) Architecture, self-assembly and properties of well-defined hybrid polymers based on polyhedral oligomeric silsequioxane (POSS). Prog Polym Sci 38:1121–1162
52. Miao JJ, Cui L, Lau HP, Mather PT, Zhu L (2007) Self-assembly and chain-folding in hybrid coil-coil-cube triblock oligomers of polyethylene-b-poly(ethylene oxide)-b-polyhedral oligomeric silsesquioxane. Macromolecules 40:5460–5470
53. Hirai T, Leolukman M, Jin S, Goseki R, Ishida Y, Kakimoto M, Hayakawa T, Ree M, Gopalan P (2009) Hierarchical self-assembled structures from POSS-containing block copolymers synthesized by living anionic polymerization. Macromolecules 42:8835–8843

Polyurethane/POSS Hybrid Materials

Edyta Hebda and Krzysztof Pielichowski

Abstract Organic–inorganic hybrid materials, prepared via chemical synthesis or physical blending of functionalized nanofillers within polymer matrix, have gained an increased attention in the recent years. Polyhedral oligomeric silsesquioxane (POSS) nanoparticles, due to their nanometer size and functionalization possibilities, are applied as effective modifiers—both chemical and physical, for polymer matrices, including polyurethanes (PU). Research efforts focused on polymers incorporating polyhedral oligomeric silsesquioxane (POSS) have intensified in recent years, revealing new synthetic routes and interesting features of these composite materials. This chapter describes polyurethane/POSS systems with different architectures—with POSS molecules as pendant groups in the polyurethane chain, incorporated in the main chain and as cross-linking agents. The methods of incorporation of POSS into polymer matrices via covalent bonds or physical blending have been presented, and the influence of preparation conditions on the structure and properties of nanocomposites was discussed. Application fields, such as gas membranes or biomedical implants, have been outlined.

Keywords Polyurethane · POSS · Hybrid materials · Nanocomposites · Synthesis Modification · Properties

1 Introduction

Polyurethanes (PU) are an important group of polymers with a wide range of applications in industry and technology. They are obtained by polyaddition reactions of isocyanates with compounds containing reactive hydrogen atoms, such as alcohols or amines. The group of polyurethane materials includes foams, varnishes, adhesives, fibers, and elastomers [1, 2].

E. Hebda (✉) · K. Pielichowski
Department of Chemistry and Technology of Polymers, Cracow University of Technology, Ul. Warszawska 24, 31-155 Kraków, Poland
e-mail: ehebda@chemia.pk.edu.pl

S. Kalia and K. Pielichowski (eds.), *Polymer/POSS Nanocomposites and Hybrid Materials*, Springer Series on Polymer and Composite Materials,
https://doi.org/10.1007/978-3-030-02327-0_5

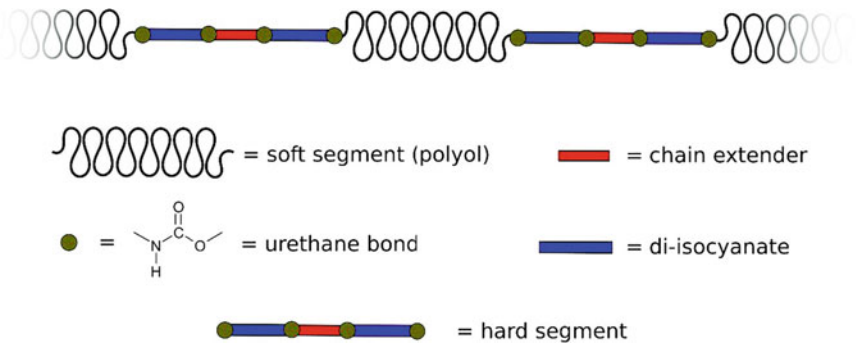

Fig. 5.1 Segmental construction of polyurethanes; adopted from [5]

Elastomers are characterized by a large modulus of longitudinal elasticity, tearing module, compressibility, very high resistance to scratches and attrition, and excellent elastic properties. They are resistant to aging, weathering, typical solvents, and oils. They can be manufactured in a very wide range of hardness, but—in contrast to hydrocarbon rubber—remain elastomers even at high hardness. Considering the processing, polyurethane elastomers can be divided into three main groups—cast, rolled, and thermoplast elastomers. Cast polyurethane elastomers are obtained with a ratio of isocyanate to hydroxyl and possibly amino groups nearing to stoichiometric. Because this provides the highest molecular weight of linear polyurethane, their physical properties are best among all polyurethanes [3].

Linear polyurethanes are segmented polymers consisting of rigid and flexible segments. There is a close relationship between the properties of segment polyurethanes and their chemical structure and physical structure. Rigid segments are formed by the reaction of isocyanate groups with chain extenders and consist of isocyanate residues, extenders, urethane, and possibly urea groups. On the other hand, the flexible segments are built from polyol chains and consist of methylene and ether groups or ester groups. Rigid segments are joined together via polyol flexible segments. The polyurethanes therefore resemble block copolymers with a structure of the type $(AB)_n$, which are constructed from alternating repetitive rigid and flexible blocks (Fig. 5.1). This type of segment construction is a key feature distinguishing polyurethane elastomers from other such materials and is the main reason for the favorable mechanical properties of these materials in a wide range of temperatures [4].

The polar and hard-to-melt rigid segments interact strongly with each other, in particular through hydrogen bonds between the NH groups and the oxygen atoms of the ether or ester group and usually do not mix homogeneously at temperatures below 120 °C with less polar, easily meltable flexible segments. This leads to their separation and formation of the so-called rigid domains, resulting in polyurethane becoming diphase and microheterogeneous. In polyurethanes with 10% of rigid segments, phase separation takes place before the start of the reaction. If the polymer is obtained below

the miscibility temperature with the chain extender—glycol, the resulting macromolecules show a higher degree of self-association than the polyurethane obtained in a homogeneous system or solution. In rigid domains, there is physical cross-linking; thus, they fulfill a function similar to the function of the polymer reinforcing filler. At room temperature, almost all NH groups in polyurethanes are bound by hydrogen bonds, therefrom only 30–60% with carbonyl groups of urethane groups. Rigid domains are the phase of ordered rigid segments, permeating with the phase (usually continuous) of flexible segments [3]. Even in the case of very good phase separation, interfacial areas can be distinguished which at the border between soft and hard domains. These areas have intermediate properties between flexible and rigid properties, and their dimensions are a measure of the degree of phase separation [1].

Due to stronger interaction with the urethane groups of segments of rigid ester groups of oligoester chains than with ether linkages of oligoether chains, the microphase separation takes place to a greater extent in polyetherurethanes than in polyesterurethanes. Flexible segments in the non-deformed state are distributed statistically, as a result of which the soft domains are isotropic and amorphous. The flexible segments are arranged approximately perpendicular to the longitudinal axis of the hard domains, which makes these domains locally anisotropic. Because rigid domains are also statistically arranged, the polymer as a whole exhibits mechanical isotropy and optical isotropy.

Rigid polyesterurethane domains are 3–10 nm in size and polyetherurethane 5–10 nm and consist of 2–4 repeating segments. Rigid domains both of polyether and polyesterurethane have a fringed-layered structure with a thickness equal to the length of the rigid segment, the average distance between the centers 10–25 nm and the width below several dozen nanometers. Such domains act as cross-linkers bond; they limit chain relaxation and allow crystallization of the segments after application of stress, thereby increasing the tensile strength of the polymer and its thermal resistance. In many polyurethane systems, in addition to the microphase structure, the oriented domains also form a super spherulitic structure. The spherulite radius is proportional to the size of the rigid segments, and the bigger is the radius, the larger the phase separation. In the center of the spherulite, the content of rigid segments is very large and decreases in the radial direction. The spherulites in polyetherurethanes made of 4,4′-methylenediphenyl diisocyanate (MDI) have a diameter of 1–10 μm and an open fiber structure [3].

The occurrence of a two-phase domain structure causes high strength of polyurethanes. The presence of resistant to sticky flow of rigid domains in which the rigid segments strongly interact with each other, in particular the formation of hydrogen bonds, reduces the intensity of the stress line due to domains deflection, forking of their cracks and their plastic deformation. The domains of the flexible segments additionally strengthen the polymer as a result of viscoelastic dissipation of energy in the immediate vicinity of the fractured blade, and thanks to the progressive ordering and crystallization during deformation. With the increase in the content of rigid segments, the degree of phase separation increases and the mechanical properties improve. The content and structure of flexible segments also significantly affect the properties of polyurethanes. Polyestroles provide excellent mechanical proper-

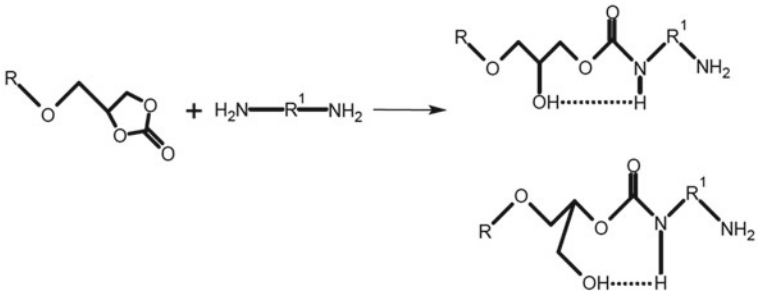

Fig. 5.2 Reaction of cyclic carbonate with amine; adopted from [9]

ties, while polyetheroles have better microbial resistance and hydrolysis. On the other hand, increasing the molecular weight of the elastic segment causes increase in the glass transition temperature of the obtained polyurethanes. Polyethers have poorer miscibility with MDI than polyesters; the elastomers obtained from them show a higher degree of phase separation, moreover the rigid domains forming in them are larger and their structure is more complex than in the case of polyestroles. The phase separation tendency also increases as the hydrocarbon chain length increases in polyetheroles and polyestroles due to the decreasing polarity of the polyol [4, 6].

As commonly used diisocyanates—(MDI) and toluene 2,4-diisocyanate (TDI) are reported to exert harmful effects if they enter the body through inhalation, skin (open wounds) or eye contact [7], and their production process is based on the reaction of toxic phosgene with amines, alternative synthetic routes have been proposed that do not require the use of diisocyanates. Three approaches have been applied for the synthesis of non-isocyanate PU (NIPU)—by step-growth polyaddition, polycondensation, and ring-opening polymerization. From industrial perspective, synthesis of polyurethanes in the reaction of multifunctional cyclic carbonates with aliphatic primary diamines or polyamines proceeding via step-growth polyaddition is the most viable option [8]. In the polyaddition reaction, two isomers are formed, one with a secondary β-hydroxyl group and the other possessing a methylol group, which form intramolecular hydrogen bonds with the urethane group—Fig. 5.2.

NIPU show relatively low sensitivity to moisture in the surrounding environment, and the hydroxyl groups formed at the β-carbon atom of the urethane group cause an increase in adhesion properties. The presence of intra and intermolecular hydrogen bonds [10] as well as the lack of unstable biuret and allophanate units [11] lead to an improved thermal stability and hydrolytic stability/chemical resistance of NIPU to nonpolar solvents, as compared to conventional PU.

The properties of polyurethanes can be changed by using different types of fillers that do not mix homogeneously with the polyurethane components. Classic powder or fibrous fillers increase the hardness and improve the mechanical properties of polyurethanes; however, they significantly increase the density of the material. In recent years, polyurethane/nanofiller composites have been extensively studied in which the particles of the reinforcing phase have nanometric dimensions. At

this length scale, significant improvements of some polymer properties with a relatively low content of the nanofiller can occur. As nanoadditives metal nanoparticles, organophilized layered silicates, including montmorillonite, zinc oxide, aluminum oxide, titanium oxide, silica or carbon nanotubes have been applied [12–16].

A new and promising group of materials are hybrid polyurethane/functionalized polyhedral oligomeric silsesquioxane (POSS) materials, which, due to the possibility of chemical bonding of nanoparticles with organic matrix, show improved properties compared to classical polymer/nanofiller systems.

The dimensions of POSS molecules do not exceed a few nm; therefore, they are classified as 0-D nanofillers with a spherical structure. Many POSS derivatives containing reactive functional groups attached to corners of Si-O cage have already been synthesized. The presence of such groups makes POSS capable of reacting with traditionally used monomers. Materials created in this way can be included in the group of (nano) hybrid materials in which oligosilsesquioxane molecules are covalently bound to organic polymers. POSS derivatives containing hydroxyl, amino, or isocyanate groups can be used for chemical modification of all kinds of polyurethane materials, such as elastomeric, foamed, and coating materials [17].

The number and functionality of the substituents attached to the POSS cage determine the way of incorporation of these compounds into the PUR structure as:

– a side group of the main chain or end group terminating the polymer chain (monofunctional POSS),
– a main chain fragment (di-functional POSS), or
– a network node (multifunctional POSS).

For the synthesis of hybrid polyurethanes, numerous POSS have been used, including POSS monofunctional compounds with isocyanate or amino substituents, POSS compounds with one dihydroxyalkyl and dihydroxyaryl reactive group, difunctional POSS compounds with two hydroxyl substituents, and multifunctional POSS with a partially caged structure or a fully condensed cage with isocyanate, hydroxyl, or amino substituents [17, 18].

2 Chemical Modifications

POSS molecules can be incorporated in the polymer matrix by copolymerization, grafting, or reactive blending. Numerous possibilities of chemical decoration of POSS molecules with organic substituents open up new perspectives for synthesis of organic–inorganic polyurethane hybrid materials in which silsesquioxanes can be incorporated in the macrochains as pendant groups, network nodes, or fragments of the main chain. This gives the opportunity to design novel materials with a broad spectrum of known and yet unknown properties [19]. Therefore, for several years, a significant increase in the use of POSS compounds as an inorganic nanoadditive in polymeric materials has been observed.

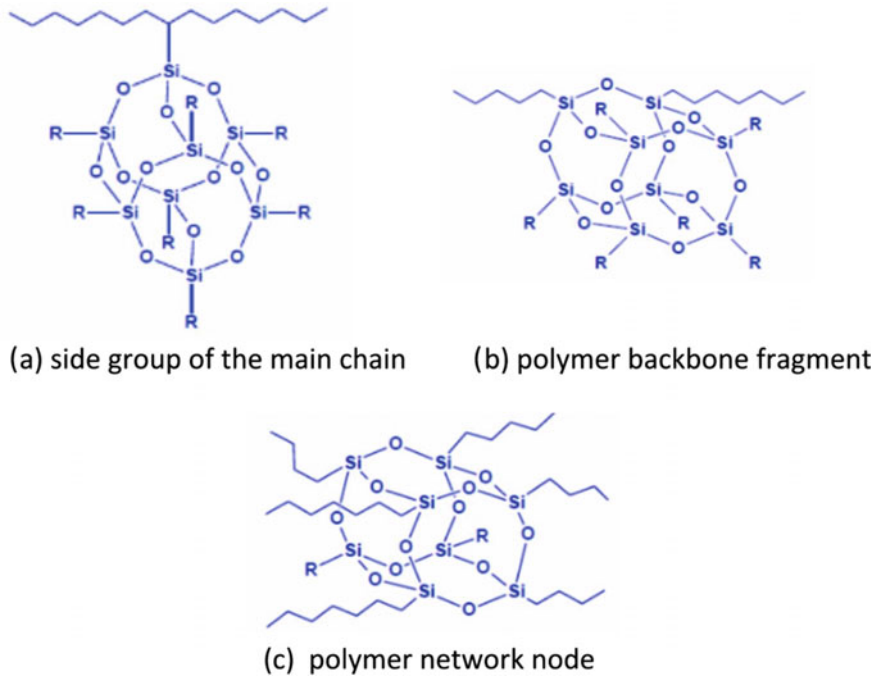

Fig. 5.3 Location of POSS moieties in the polymer structure

Polyhedral silsesquioxanes can be incorporated into the polymer chain chemically by several methods [18, 20–23]:

- copolymerization of organic monomers with POSS compounds having at least two reactive functional groups—hybrid polymers are obtained with covalently bound POSS nanoparticles as a side group of the macrochain (Fig. 5.3a), a polymer backbone fragment (Fig. 5.3b), or a polymer network node (Fig. 5.3c),
- chemical modification of polymers by grafting them with POSS molecules with one reactive group—systems with a covalently bond POSS molecule constituting a side group of the main chain of macromolecules or telechelic polymers terminated with POSS molecules are obtained.

2.1 POSS Molecules as Pendant Groups in the Polyurethane Chain

One of the first papers dealing with the subject of polyurethane hybrid materials, containing POSS compounds in their structure, were prepared by Schwab et al. [24, 25] Diol (bisphenol A—BPA)-POSS was used as a chain extender, the isocyanate

component was 4,4′-diphenylmethane diisocyanate (MDI), and soft segments were composed of flexible polyoxytetramethylene diol (PTMG) with an average molecular weight of 2000. The catalyst for the reaction between isocyanate and hydroxyl groups was dibutyltin dilaurate (DBTDL). Later, these studies were continued by Fu et al. who determined the influence of BPA-POSS on the structure and properties of polyurethane elastomers—Fig. 5.4 [26, 27].

The synthesized materials contained 21 and 34 wt% of BPA-POSS. Structural investigations using the WAXD and SAXS methods revealed that BPA-POSS creates crystallites in the polymer, whose presence is manifested by clear reflections on WAXD patterns. The formation of crystallites is most likely induced by polyurethane phase separation of rigid and elastic domains, which was confirmed by SAXS studies. The value of the great period was 111 Å for hybrids with 34 wt% of POSS and 164 Å for materials containing 21 wt% of POSS. The size of rigid domains determined by the SAXS method was 34 Å for both BPA-POSS loads. When polyurethane/POSS elastomers were subjected to uniaxial deformation, enhanced tensile modulus and strength of the hybrid polymers were recorded. TEM observations on a stretched and relaxed PUR/POSS materials indicated that tensile stretching broke the large hard segment domains into disk-like smaller domains with plane normals almost parallel to the stretching direction, as shown in Fig. 5.5.

Interesting research results were presented in the work of Hoflund and coworkers [28] on the resistance of PUR/POSS coatings used in space satellites for erosion caused by atomic oxygen. Polyurethane nanohybrid systems were prepared using MDI, polytetramethylene diol as an elastic component, and 1,4-butanediol and trimethylpropane substituted with a group containing heptacyclopentyl-POSS (TMP-POSS). XPS surface tests revealed that in the samples exposed to the oxygen atom stream for 63 h, the carbon content on their surface was reduced from 72.5 to 37.8%, while the concentration of oxygen and silicon on the surface increased with prolonged exposure time, from the initial value of 2.28–2.93%. The obtained data suggest that atomic oxygen destroys cyclopentyl rings in POSS-TMP, forming CO and/or CO_2 and H_2O that desorb from the material surface. Extended exposure time results in the formation of a silica layer on the surface of the sample, which favorably protects the inner polymer layers against the influence of atomic oxygen.

POSS nanohybrid polyurethanes for coatings, made of dihydroxy isobutyl-POSS (R = isobutyl), isophorone diisocyanate, dimethylolpropionic acid, and ethylenediamine as a chain extender, have been prepared by Turri [29, 30]. POSS particles easily integrated into the polyurethane structure, and the resulting materials formed stable aqueous dispersions if the POSS content did not exceed 10%. X-ray analysis showed the presence of crystallites in the obtained coatings even at low POSS content. The results of dynamic mechanical analysis show a reinforcing effect, mainly in the case of polytetramethylene diol with a molecular weight of 2000. In addition, polyurethanes with built-in POSS were characterized by lower surface wettability and lower value of the polar surface energy component than pure polymer, even with relatively low silsesquioxane content. This effect may be due to both a stratification of apolar components of the coating close to polymer–air interface and a topographical change of the surface due to formation of nanosized structures.

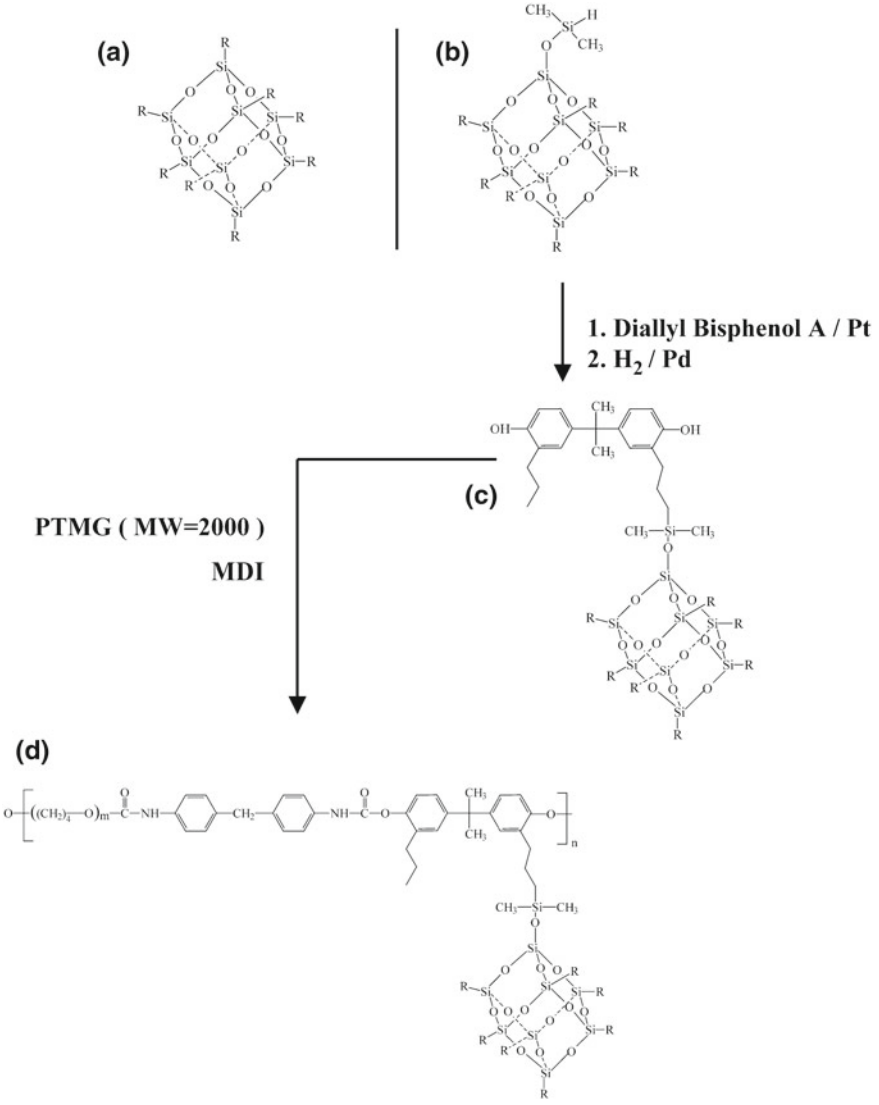

Fig. 5.4 Schematic diagram of the synthesis for POSS-polyurethane: **a** octacyclohexyl-POSS, with R = cyclohexyl; **b** hydrido-POSS; **c** BPA-POSS; and **d** POSS-PU [27]

The phenomenon of wetting the surface of polyurethane composites with 1-(2,3-propanediol)propoxy-3,5,7,9,11,13,15-heptaisobutylpentacyclo-POSS (PHI-POSS)was studied by Zhang et al. [31]. It was shown that the contact angle values increase with the increase of silsesquioxane content, whereas free surface energy decreases more than twice for a sample containing 8.5 wt% of PHI-POSS in oligoestrodiol, compared to unmodified polyurethane. As AFM studies showed, the

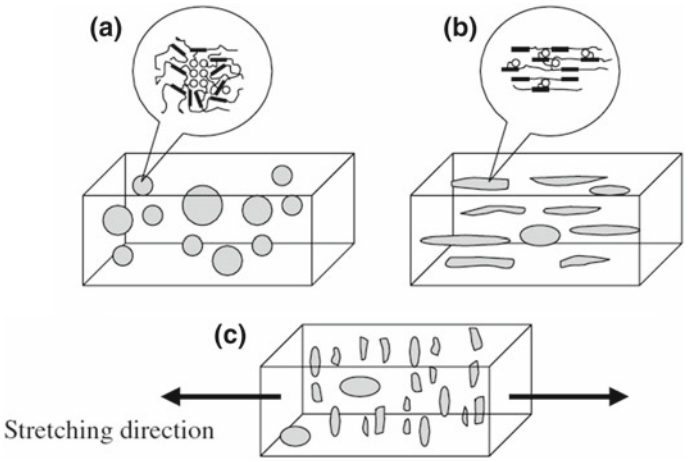

Fig. 5.5 Schematic diagram of microphase changes during stretching: **a** no deformation or low deformation (POSS molecules form nanocrystals in the hard segment domains); **b** intermediate deformation (e.g., 400%) (some POSS crystals are destroyed in the hard segment domains); and **c** large deformation after relaxation (e.g., 700%) as in TEM [27]

average surface roughness (Ra) increased with the increase of silsesquioxane content; however, Ra values were much lower than 100 nm, and thus the impact of roughness on the contact angle value was insignificant. As the reason for the reduction of surface energy of the materials studied, migration of the polyester segments toward the polimer surface was named. This effect intensifies after incorporation of silsesquioxane containing alkyl substituents which strengthen the migration effect of the elastic segments; it leads to a decrease in free energy and to an increase in the contact angle values. WAXD results showed that for lower PHI-POSS contents, the silsesquioxane nanoparticles are well dispersed in the polymer matrix, which limits the tendency to form crystallites. However, for hybrids containing 8.5 wt% of silsesquioxane, PHI-POSS forms crystallites, and there is a tendency for phase separation between the oligoester segments and silsesquioxane moieties. Besides, stiff POSS cages hinder crystallization of oligoestrodiol segments. The DMA analysis revealed an increase in the glass transition temperature of the elastic segments phase with an increase in silsesquioxane content, most likely due to limiting the mobility of oligoester chains by large silsesquioxane side groups. Thermal stability (decomposition onset temperature determined by TGA) under inert gas atmosphere was increasing with an increase of POSS content.

Surface roughness tests of coatings obtained from urethane cationomers synthesized from oligooxypropylene diol and modified PHI-POSS showed that at even a relatively small (1%) PHI-POSS content the roughness increases, as revealed by confocal laser microscopy results [32, 33]. Thermal and rheological properties of poly (urethane–urea) ionomers containing 3-(2-aminoethyl)amino)propylheptaisobutyl-POSS were discussed by Madbouly et al. [34, 35]. It was observed that the depen-

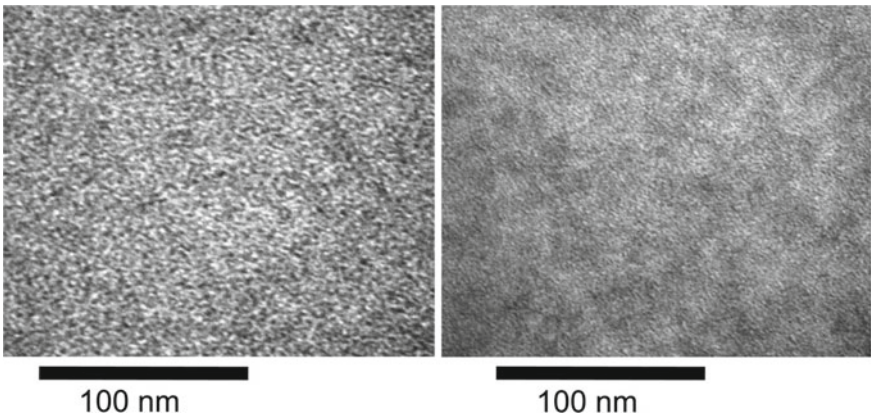

Fig. 5.6 TEM photographs for pure PU and PU/POSS composite (10 wt% POSS). The dark particles represent the hard segments, and the bright matrix represents the polyester soft segments. The sample of 10 wt% POSS shows finer morphology than that of pure PU [34]

dence of the imaginary component of the stiffness modulus versus the vibration frequency deviates from the straight line at 140 and 160 °C for a pristine polymer and polymer containing POSS, respectively. Such deviation indicates that above these temperatures the Williams–Landel–Ferry equation ceases to describe their viscoelastic properties due to the phase separation phenomena of rigid and elastic segments. The increase of this temperature value for nanohybrid polyurethane, as compared to the unmodified polyurethane, demonstrates that POSS has increased the miscibility between rigid and flexible segments, which leads to a material with a relatively higher homogeneity at elevated temperature. The increase in miscibility has also been confirmed by TEM microscopy—Fig. 5.6.

Thermogravimetric analysis of the obtained hybrid ionomers under inert atmosphere showed the beginning of the decomposition process at a temperature of 270 °C, regardless of the content of POSS in the polymer. The authors linked the first stage of thermal degradation of the material with the distribution of elastic segments, whereby in the second stage starting at ca. 350 °C, the rigid segments are decomposed. These results indicate that the presence of silsesquioxane in polyurethane does not significantly increase the polymer resistance to thermodegradation under inert conditions. In the oxidizing atmosphere, nanohybrid polyurethane is more stable at high temperatures compared to the unmodified polymer, and there is more solid (char) residue after decomposition.

Hybrid coatings based on polyurethanes/polyhedral oligomeric silsesquioxanes were investigated by Lai et al. [36]. Hydroxy-terminated polybutadiene (HTPB), isophorone diisocyanate (IPDI), and *trans*-cyclohexane diolisobutyl-POSS were used as precursors for the hybrid coatings which were spin-coated to form films. Electrochemical characteristics showed that the PU/POSS hybrids offer very good corrosion protection. In comparison with the value for the untreated aluminum alloy

(AA) ($2.48–8.22 \times 10^{-3}$ Acm^{-2}), the measured corrosion electric current (I_{corr}) value decreased significantly for the PU/POSS hybrids on the AA (1.24×10^{-6}–7.61×10^{-8} Acm^{-2}) and was lower than that of the PU film on AA ($1.32–1.37 \times 10^{-5}$ Acm^{-2}). The result obtained can be explained by the formation of denser hybrid films that were less susceptible to localized pitting.

Hu et al. [37] synthesized POSS molecule with two functional amino groups—3-(2-aminoethylamino)propylheptaphenylPOSS (AA-POSS). Incorporation of AA-POSS to polyurethane matrix causes changes in water uptake and contact angle. With an increase of AA-POSS content, the lower water uptake was observed from 13.6 to 3.2 wt% for pristine PU and PU/POSS (4 wt%), respectively. It was postulated that POSS migrates to the surface, thus preventing the solvent molecules to penetrate into the interior, as well as POSS molecules, as highly hydrophobic, lower the polymer surface–water interactions. DSC data showed increase of Tg from 75 °C (for reference PU) to 99 °C for PU containing 12 wt% of silsesquioxane; chemical incorporation of rigid POSS moieties effectively hinders the macrochains motions. The enhanced thermal stability of AA-POSS-modified polyurethanes, as found by TGA, could be caused by suppressing the molecular mobility of polyurethane chains by bulky POSS substituents which provide additional heat capacity, thereby stabilizing materials during the thermal degradation process.

Nanohybrid-segmented polyurethanes were obtained through solvent-free polymerization in mass by Janowski et al. [38]. 1-(1-(2,3-dihydroxypropoxy) butyl)-3,5,7,9,11,15-isobutyl-pentacyclo [9.5.1.1.(3.9).1(5.5).1(7,13)] octasiloxane (PHI-POSS), 4,4′-diphenylmethane diisocyanate (MDI), 1,4-butanediol (chain extender), and polyoxytetramethylene diol (PTMG) with an average molecular weight of 1000, 1400, and 2000 (soft segment) were used. Schematic route of polyurethane-/POSS-segmented elastomers synthesis is shown in Fig. 5.7.

Thermo (oxidative) stability of novel PU/POSS nanohybrids was investigated by thermogravimetry (TG) [39]—the highest thermal stability, both of inert and oxidative atmosphere, have the PU containing 4 and 6 wt% of PHI-POSS. Temperatures of maximum rate of degradation, defined as the first maximum in DTG curve (T_{DTGmax}), were shifted toward higher temperatures for polyurethanes containing 6 wt% of PHI-POSS (PTMG 1000) and for all nanohybrids based on PTMG 1400. In case of PTMG 2000, a slight decrease of T_{DTGmax} was observed. The results obtained suggest that there is a restricted molecular mobility of PU macrochains in the presence of POSS and reduction of rate of volatile products' emission. Lewicki et al. [40] investigated mechanisms by which POSS influences the molecular dynamics and phase separation behavior of both the hard- and soft-block segments. Different solid NMR techniques were used to probe the segmental dynamics of a model elastomeric system that incorporates POSS (at a range of loadings) into the elastomer hard block. NMR characterization of these novel systems has shown that the incorporation of POSS significantly alters the dynamical behavior of the soft-block interphase region and may be negatively impacting the crystalline order of the nanostructured hard-block domains. The obtained NMR data strongly suggest that at comparatively low polyol molecular weights, where overall phase separation is less favorable, there is an increase in the rigid domain fraction with increasing POSS loadings.

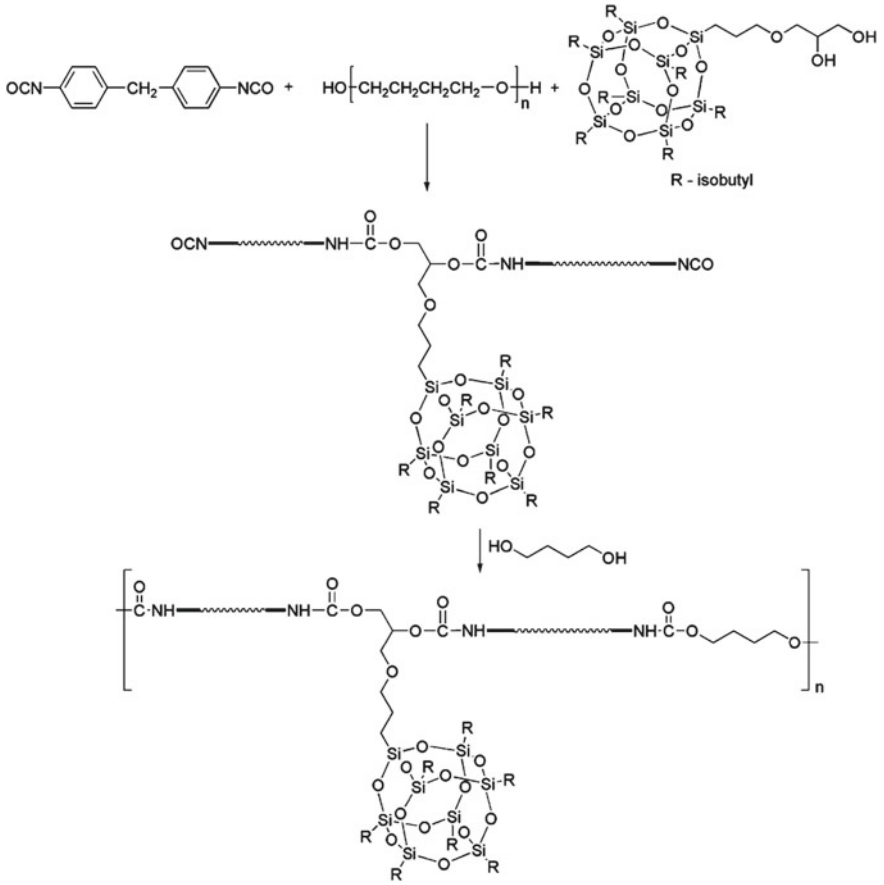

Fig. 5.7 Schematic presentation of the synthesis route for PU-/POSS-segmented elastomers [38]

Raftopoulos et al. [41–43] investigated morphology of a series of PHI-POSS/PU hybrid materials on the basis of poly (tetramethylene glycol) as the soft component, 4,4′-diphenylmethane diisocyanate and 1,4-butanediol as chain extender. AFM measurements indicate the formation of POSS crystallites in the PU matrix, with extended structures at low POSS content and more regular structures at higher POSS content. Figure 5.8 shows lateral force AFM images for polyurethanes with POSS content 4 and 10 wt%. For the PU hybrids with smaller filler content, the POSS molecules aggregate to nanometer-size longitudinal crystallites (about 60–70 nm in length) (Fig. 5.8, top), which form spherulites of several microns average sizes (Fig. 5.8, bottom left). At higher filler content (10 wt%), POSS forms more regular crystallites of ca. 120 nm size diameter (Fig. 5.8, bottom right). PHI-POSS displays tendency to form crystallites in the PU matrix, such as extended structures for lower POSS content and more regular structures for the higher silsesquioxane load (PU10).

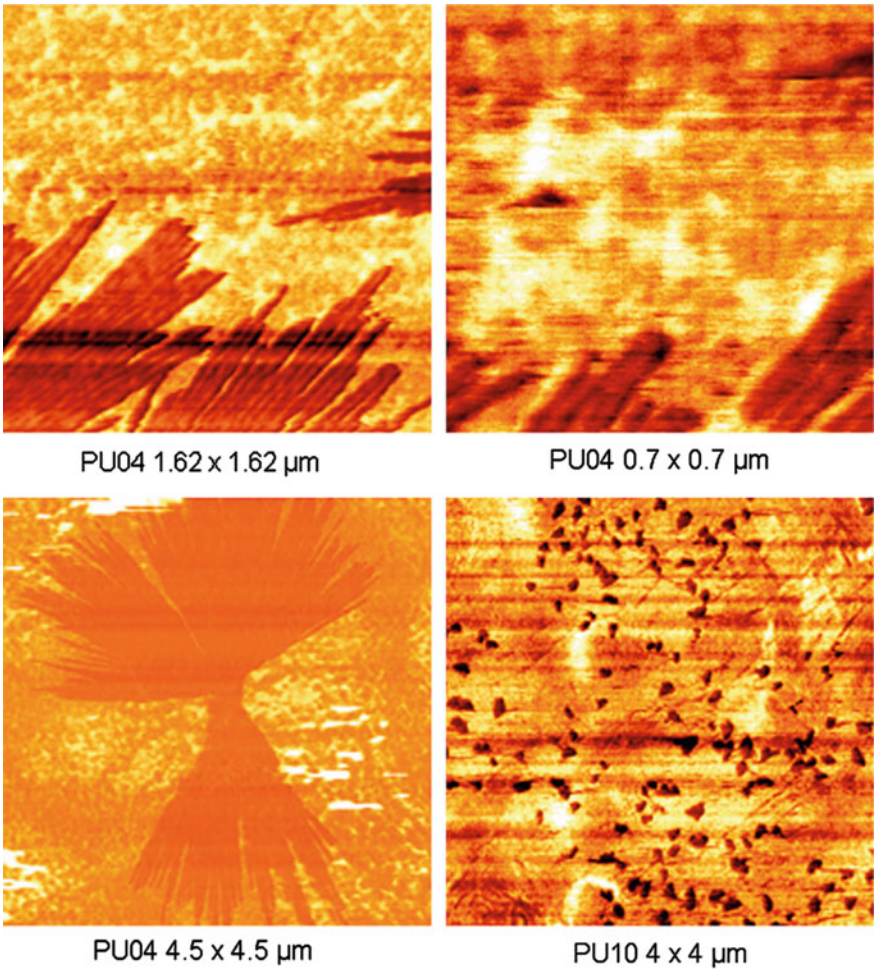

Fig. 5.8 Lateral force atomic force microscope images for PU04 (area 1.62 × 1.62 µm, top left; 0.7 × 0.7 µm, top right; 4.5 × 4.5 µm, bottom left) and for PU10 (4 × 4 µm, bottom right) [41]

The unique POSS cage structure, vast functionalization possibilities, and ease of their chemical incorporation into polymer matrices are the key factors deciding about silsesquioxanes application in the biomedical field. The main features that allow the medical use of POSS additives are biocompatibility, biodegradability, cytological compatibility, as well as no toxicity and thermodynamic stability [44–46].

Recently, numerous works have been devoted to polycarbonate-based materials with POSS molecules built in as pendant groups in the main chain [47–49]. The presence of POSS in the polymer chain results in increased mechanical strength and thermal stability [50]. The hybrid composites are also much more resistant to enzymatic and oxidative biodegradation [51]. Moreover, they suffer from calcination

to a much lesser extent than unmodified polycarbonate urethane [52]. Through the incorporation of POSS, a continuous, porous matrix is formed, with a pore size of 150–250 μm [53], which turns out to be an excellent substrate for propagation and cell differentiation [50]. Materials of this kind do not degrade in a living organism, so they can be a better substitute for silicones [54].

Kannan et al. patented a nanocomposite polymer based on poly(carbonate–urea)urethane (PCU) with *trans*-cyclohexanediolisobutyl-silsesquioxane as a pendant group [55]. Further developments include poly(carbonate–urea)urethane (PCU)/POSS hybrids for potential use in cardiovascular bypass grafts and as microvascular components of artificial capillary beds [56–58]. A POSS-PCU blood vessel implant with controlled porosity was obtained by foaming extrusion, applying $NaHCO_3$ as the blowing agent [59]. The obtained materials were found to show better resistance to hydrolysis and oxidative degradation, as well as viscoelasticity similar to that of the biological vessels [60, 61]. The PCU-POSS hemocompatibility was also tested, and it was found that silsesquioxane molecules repel platelet and fibrin adsorption because of their variable surface tension, and on a vascular interface, they would contribute to the increased thromboresistance [62–64]. Moreover, POSS cages are thought to exhibit optimal cytocompatibility [65].

Improved biocompatibility and biostability against oxidation, hydrolysis, and enzymatic attack under in vitro and in vivo conditions [66, 67] led to the design of the first artificial heart valve made of PCU-POSS nanocomposite [68]. Surface thrombogenicity and mechanical failure of polymeric heart valves are primarily associated with the choice of valve material. Polymer thicknesses of 100, 150, and 200 μm were selected to investigate the mechanical properties and the suitability of these nanocomposites for valve leaflet application. The mechanical test results (Table 5.1) showed that the tensile strength of POSS-PCU increased as compared to PCU. The Young's modulus of POSS-PCU was significantly greater in comparison with the control PCU for 100 μm thickness.

POSS-PCU showed no significant difference in tear strength compared to PCU. In addition, POSS-PCU demonstrated comparable tear strength to the commercially available PU materials (Table 5.2).

Since PCU/POSS nanocomposites possess excellent mechanical strength, good surface properties, and resistance to platelet adhesion, they were used to design prototype of an artificial heart valve—Fig. 5.9.

In the course of other studies, Ghanbari and colleagues [69] proved that the presence of POSS compounds in the PCU/POSS nanocomposite reduces the tendency of PCU to calcification and thus extends the duration of use of these materials in vivo.

PCU/POSS hybrid nanocomposites were utilized by Chaloupka et al. [70] for fabrication of lacrimal ducts. Different manufacturing techniques were applied to develop a small diameter conduit for the lacrimal duct reconstruction. The aim was to obtain a conduit with distinct outer and inner wall surfaces, characterized by controlled porosity forfacile integration and regeneration into native surrounding tissue.

Table 5.1 Summary of tensile strength, elongation at break, and tear strength for POSS-PCU (100, 150, and 200 μm thick) and control (100 μm thick PCU) at 25 and 37 °C [68]

Temperature (°C)	Thickness (μm)	Tensile strength (N mm^{-2})	Elongation at break (%)	Young's modulus (N mm^{-2})	Tear strength (N mm^{-1})
25	Control (100)	33.8 ±2.**1**	649.3 ±15	9.1 ±0.9	49.0 ± **1**.3
	100	53.6 ±3.4**	704.8 ± 38	25.9 ±1.9**	50.0 ± **1**.2
	150	54.0 ± 3.2	745.9 ± 10.7$^{\#}$	24.9 ± 0.4	55.6 ± 6.4
	200	55.7 ± 1.7$^{\#}$	745.8 ± 14.7$^{\#}$	17.3 ±0.3*	56.8 ± 3.5
37	Control (100)	24.8 ±3.4	683 ± 62.5	8.4 ±0.5	54.7 ± **1**.0
	100	55.9 ±3.9**	762.7 ± 19.3	26.2 ± 2.0**	50.9 ± 3.3
	150	55,6 ±2.4	845.4 ±21.0*	23.0 ±1.4	56.2 ± **1**.8
	200	31.0 ±0.6*	852.4 ± 4.7*	15.9 ±0.2*	63.4 ± **1**.5*

Data are presented as mean ± SEM, n = 5
*$P < 0.05$ compared to 100 μm thickness
**$P < 0.01$ compared to respective control
$^{\#}P < 0.01$ compared to respective thickness at 37 °C

Table 5.2 Mechanical properties of commercially available PU-based polymers and PCU/POSS [68]

Polymer	Hardness (Shore A)	Tear strength (N mm^{-1})	Tensile strength (N mm^{-2})	Elongation at break (%)
Estane® (PEU)	85	55	48.3	570
Chronoflex® C	80	45	37.9–45.5	400–490
Elasteon™	75–90	50–80	20–30	500–750
POSS–PCU	84	50 ± 1.2	53.6 ± 3.**4**	704.8 ± 38

It was found that by using cast PCU/POSS for the inner wall, formation of scar tissue is prevented and drainage is secured. This wall can thereafter be covered with a coagulated layer allowing suturing of the conduit to the residual lacrimal duct and preventing implant displacement.

The research on PCU/POSS nanocomposites was also carried out by Bakhshi et al. [71] As biocompatibility of PCU containing silsesquioxane is much better than this of nickel and titanium alloy used for shape-memory stents fabrication, an attempt was made to electrohydrodynamically sputter of organic–inorganic hybrids on metallic stents. The peel strength of the deposit was studied before and after degradation of the coating. It has been shown that the surface modification increases the peel strength by 300%. It was also shown how the adhesion strength of the PCU/POSS coating changes after exposure to physiological solutions composed of hydrolytic, oxidative, peroxidative, and biological media. Interestingly, it turned out that NiTi alloys coated with the PCU/POSS layer undergo integration with the stent after long-term (70 days) exposure to biological environments. The applied polymer coating also increases the corrosion resistance. Antithrombogenic properties have also been

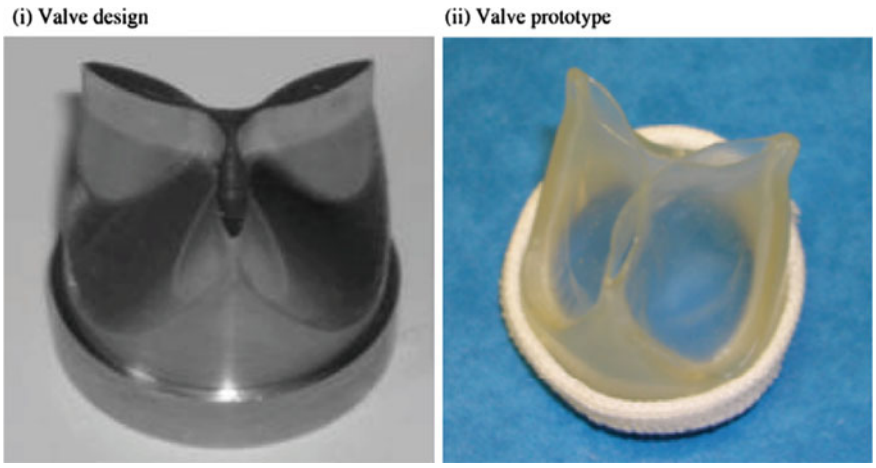

Fig. 5.9 Synthetic heart valve (i) design and (ii) prototype made with the POSS-PCU nanocomposite polymer developed at UCL and currently under investigation [68]

obtained, and facilitated endothelialization has been observed [72, 73]. Coating of NiTi alloys with poly(carbonate–urea)urethane/POSS layer extends the service life of metallic stents by about 10 years [74].

2.2 POSS Incorporated in the Main Chain

The process of obtaining polyurethanes with POSS cores incorporated in the main chain was studied by Oaten and Choudhury [75]. An open cage POSS with three functional hydroxyl groups (trisilanol) was used, and the synthesis of hybrid polyurethane relied on the direct reaction between an aliphatic diisocyanate (HDI) and trisilanolisobutyl-POSS in toluene, catalyzed by dibutyl tin dilaurate (DBTL). The transparent PU-POSS thin films obtained were used as a protective barrier to cover steel. The ^{29}Si NMR and angle-resolved (AR-XPS) investigations showed that PU-POSS forms a 3-D network which consists of polymer chains cross-linked through urethane bridges and due to condensation of free silanol groups from POSS units. Hydrogen bond interactions of the amide groups in the urethanes and the long-range hydrophobic interactions of the hexamethylene and isobutyl groups contribute to the lamellar structure formation—Fig. 5.10. Thermogravimetric studies revealed a three-stage decomposition of the polymers obtained. The first stage begins at a temperature of 200 °C and is related to the breakdown of urethane bonds and degradation of isobutyl groups of trisilanol. The second stage, starting at 415 °C, and the third stage, commencing at 470 °C, are related to the thermal degradation of the Si-O bonds of the silsesquioxane. DSC studies in combination with photoacoustic Fourier transform infrared spectroscopy (PA-FTIR) have revealed the formation of a silica

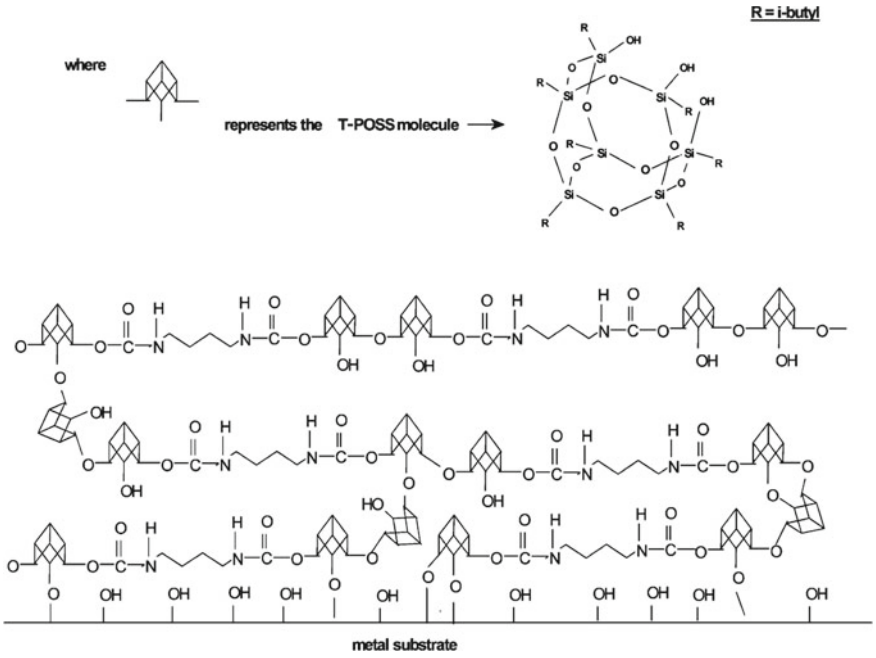

Fig. 5.10 Proposed structure of the hybrid thin film on steel [75]

layer that protects the material onto which the hybrid polyurethane was applied prior to thermal degradation.

Pistor et al. [76] described the effect of isobutyl trisilanol POSS on the crystalline structure of thermoplastic polyurethane. POSS nanocages introduced in the polyurethane matrix tended to form aggregates, and an increase in the rate of crystal formation was observed with the increase of POSS content in the PU matrix. At the content of 1.14 wt% of POSS, there was one crystallization stage, leading to formation of smaller crystals in the form of disks. With an increase of the POSS load, two stages of crystallization occurred. In the first stage, disks were created, while in the second stage, spherulites were formed—Fig. 5.11. The obtained results confirm that POSS nanoparticles have a strong influence on the crystallization mechanism.

Pan et al. [77, 78] obtained polyurethane/trisilanolisobutyl polyhedral oligomeric silsesquioxane (PU/TSI-POSS) hybrid composites using MDI and glycerol propoxylate as the PU components. The chemical structure of TSI-POSS and the synthesized hybrids are shown in Fig. 5.12.

X-ray diffractograms showed that by increasing the content of TSI-POSS in polyurethane matrix (above 22 wt%), larger cluster-like crystallites are formed in rigid segments, increasing thus their volume. Glass transition temperature of hybrid composites was found to increase with TSI-POSS content. Due to the presence of isobutyl groups in the TSI-POSS, which are sensitive to oxygen, a reduction in the

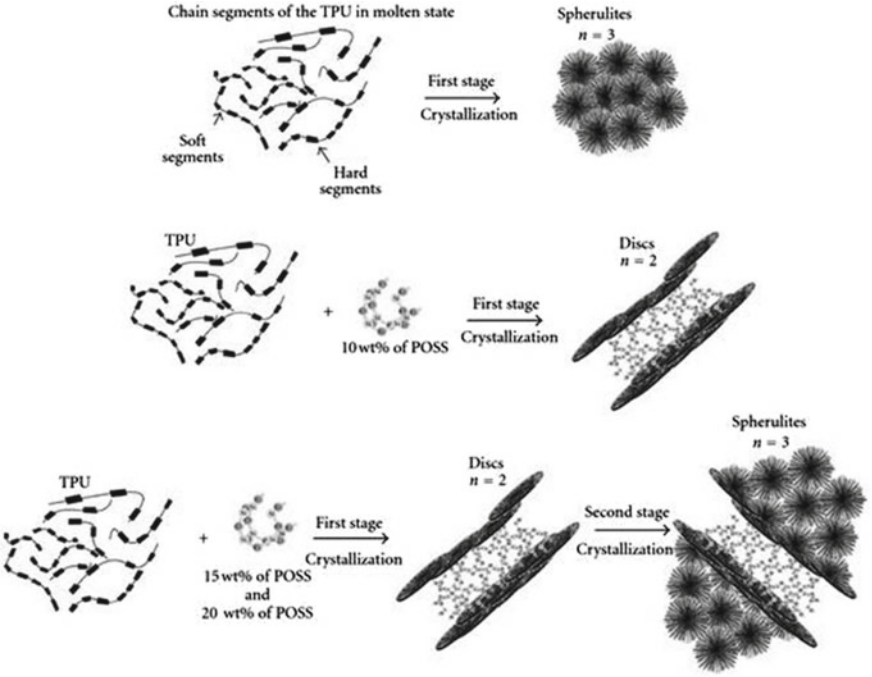

Fig. 5.11 Schematics for the PU and the nanocomposites nucleation and crystal growth phenomena [76]

decomposition temperature of the PU/TSI-POSS composites was observed with an increase of POSS content in the polymeric material [79, 80].

Our research group [81] incorporated disilanol isobutyl-POSS (DSI-POSS) in a PU synthesized using PTMG, MDI, and BD. The obtained hybrid materials were studied toward molecular dynamics behavior, and it was found that incorporation of DSI-POSS does not exert any significant effect on Tg, indicating that incorporation of POSS is practically not affecting the mobility of the soft phase. MDSC results revealed three distinct regions—the first weak and broad endotherm at ca. 70 °C has been associated with the disruption of ordering of short MDI-BD sequences or glass transition of hard segmental microdomains. The next endotherm around 170 °C was due to the main phase separation effect. The last peak commencing at ca. 250 °C was attributed to the thermal decomposition process. By utilizing pyrolysis-GC/MS and DSC methods, we have also studied the effects of DSI-POSS on the mechanisms of thermal degradation of polyurethane matrix [82]. The results of analytical pyrolysis assays of the polyurethane systems demonstrated that low levels of POSS substitution (<10 wt%) lead to a significant increase in both the onset temperature of thermal depolymerization and a reduction in the yield of volatile degradation products [83].

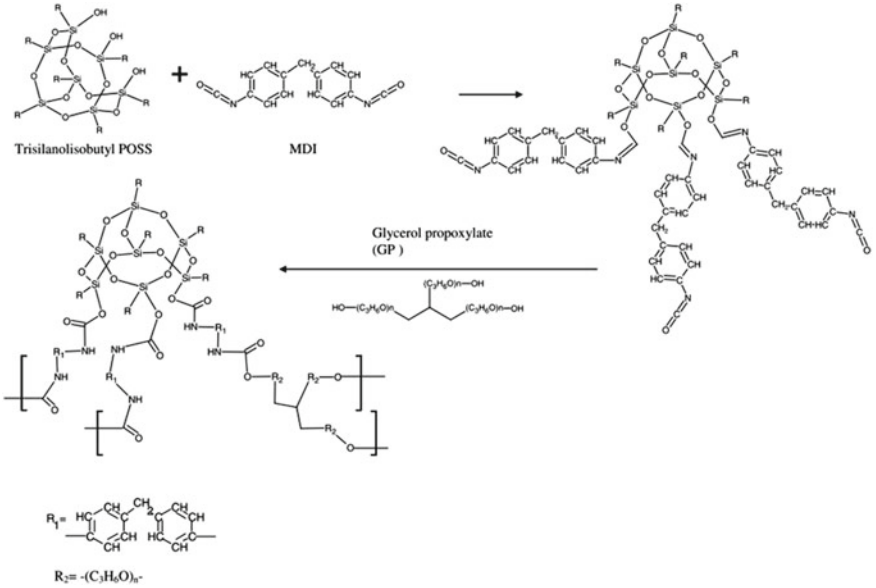

Fig. 5.12 Chemical structures of TSI-POSS monomer and PU/TSI-POSS–hybrid composites [77]

2.3 POSS in a Polyurethane Network Node

POSS can also be used as cross-linkers in polymeric systems. This is accomplished through the functionalization of POSS with eight identical groups that may react to form materials with a high cross-link density. Functional groups that have been employed in the preparation of cross-linked hybrid materials are epoxy, amine, methacryloyl, vinyl, alkyl halide, and hydroxyl groups. Neumann et al. [83, 84] synthesized POSS with eight –NCO groups, using hydrosilylation of octakis (dimethylsiloxy) octasilsesquioxane. As the cross-linking agent, POSS reacted with poly(ethylene glycol) to form cross-linked polyurethane. Nuclear magnetic resonance (^{29}Si NMR) showed that the cage structure of POSS was not damaged after chemical incorporation in the PU matrix [85].

Liu and Zheng [86, 87] used octaaminophenyl polyhedral oligomeric silsesquioxane as a cross-linking agent and 4,4′-methylenebis-(2-chloroaniline) to prepare polyurethane networks containing POSS. DMA investigations showed that in the glassy state ((−75)–(−25) °C), the dynamic storage moduli of all the POSS-containing hybrids are significantly higher than that of the control PU. The TGA results indicated that the thermal stabilities of the nanocomposites were improved, as evidenced by the rate of volatile release from the materials and the enhanced char yields together with ceramic yields. Moreover, contact angle measurements showed that the organic–inorganic nanocomposites with POSS displayed a significant enhancement in surface hydrophobicity. Significant nanoscale reinforcement

effect of the POSS cages on the polyurethane matrix and the formation of robust structure of the POSS-containing PU networks were postulated to be the main reasons for properties enhancements caused by silsesquioxanes moieties [88–90].

A functional N-phenylaminomethyl POSS was synthesized by Zhang and coworkers [91] and then used as a cross-linker for polyurethane elastomers—Fig. 5.13. The obtained PU-POSS elastomers showed no macrophase separation up to 52 wt% of POSS load. HRTEM images revealed a well-separated nanostructure of POSS with a typical phase size of 5–10 nm. The storage modulus (DMA), T_g, DSC, and Young modulus (tensile test) were increased with increasing POSS concentration. Thanks to good compatibility of POSS and PU, a cross-linker could be dispersed in PU matrix in nanoscale, restricting efficiently polyurethane chains mobility. As POSS concentration further increased, the cross-linking density also increased, and, when POSS concentration reached 26 wt%, a permanent network was formed.

The same authors studied the process of gelation of cross-linked PU-POSS composites at various curing temperatures, times, and POSS concentration [92]. After the completion of the curing reaction, the critical concentration of POSS beyond which the gelation of PU-POSS composites happens was found around 2.5 wt%. In the materials between 2.7 and 6 wt%, formation of self-similarity network near the critical gel occurred. This revealed that different structures were formed, which are shown in Fig. 5.14.

A new class of ester–amine-functionalized silsesquioxane macromers, synthesized by Madhavan et al. [93–96], was introduced into the polyurethane matrix. DSC showed that the glass transition temperature corresponding to the hard segment increases with an increase in the POSS-amine content as POSS rigid cubes restrict the free rotation of the macromolecular chains. The contact angle measurements revealed its increase with the increase of POSS-amine load for all hybrid materials. This was due to formation of granular POSS aggregates of highly hydrophobic nature on the PU surface. Moreover, permeability coefficient decreases with an increase the POSS concentration, and the selectivities of O_2/N_2 and CO_2/N_2 gas pairs increased with an increase in the POSS concentration.

Hu et al. [97, 98] used octa(aminopropyl) silsesquioxane (OapPOSS) for functionalization of graphene sheets (GO) via amide group formation between the amine groups at the eight vertices of POSS and the oxygen-containing groups of graphene oxide. The obtained functionalized graphene (OapPOSS-GO) was used to reinforce waterborne polyurethane (WPU) to obtain OapPOSS-GO/WPU nanocomposites by in situ polymerization. Morphological studies using field emission SEM (FESEM) showed a faster OapPOSS-GO development in the polyurethane matrix compared to GO and OapPOSS. It may be explained by a synergistic effect: The OapPOSS grafted onto the GO surface can lead to a large interlayer spacing, providing effective physical interactions such as van der Waals forces and hydrogen bonds, thus resulting in a better dispersion; on the other hand, OapPOSS-GO surface can provide abundant amine functional groups for grafting PU chains, thus introducing covalent bonds between OapPOSS-GO and PU chains through in situ polymerization. In addition, a significantly better hydrophobicity was achieved for OapPOSS-GO/WPU (contact angle values of ca. 94°) compared to the GO/WPU and OapPOSS/WPU matrix.

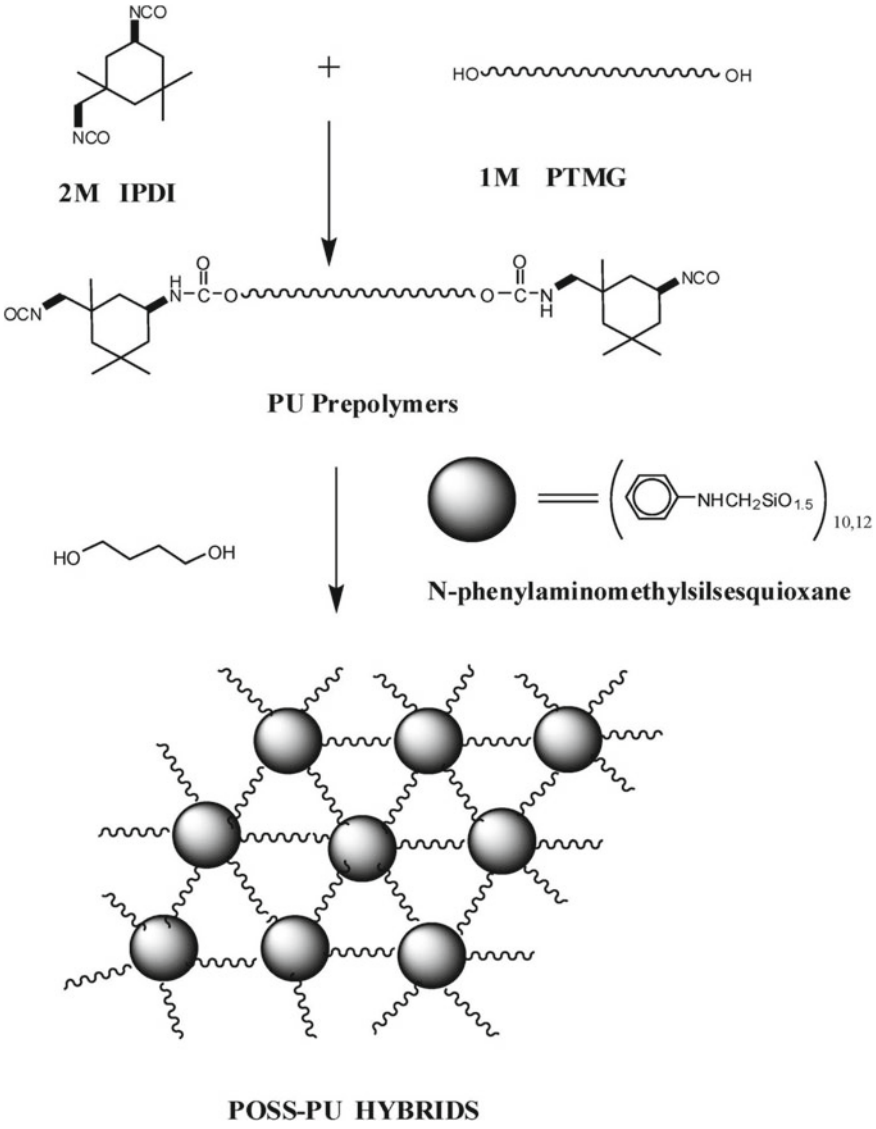

Fig. 5.13 Synthesis of PU-POSS hybrids [91]

Hybrid polyurethane elastomers with octakis [m-isopropyl-α, α'-dimethylbenzylisocyanatodimethylsiloxy]octa silsesquioxane (NCO-POSS) were synthesized by Prządka et al. [99] using IPDI and polyoxypropylene triol. The obtained polyurethane hybrids showed an increase in the M100 module (stress at 100% of the relative elongation) (Fig. 5.15) up to 2.5% mass of NCO-POSS and decrease above this concentration of silsesquioxane.

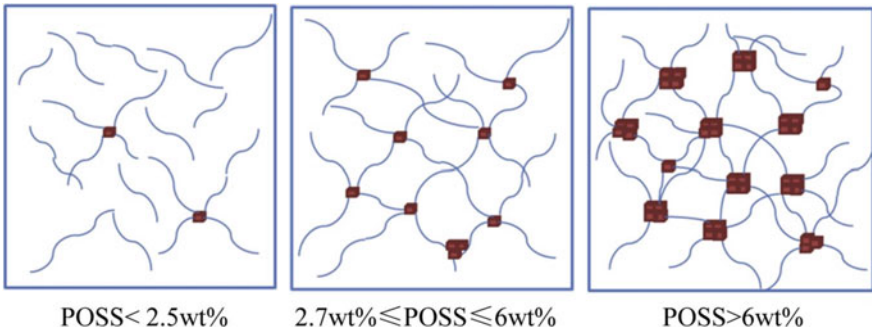

Fig. 5.14 Schematic diagram of PU-POSS composites at different POSS concentration. Cubics represent the POSS; lines represent the strands between POSS [92]

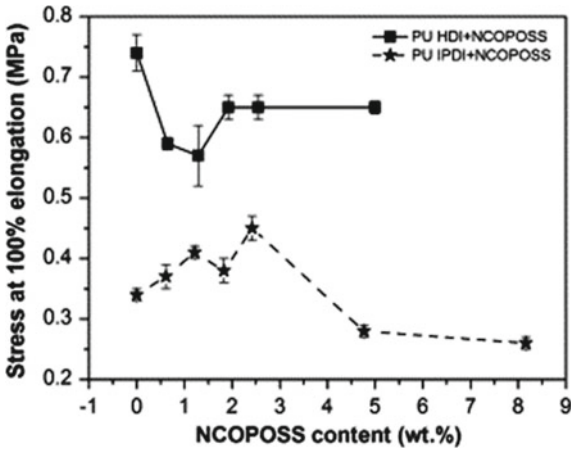

Fig. 5.15 Stress of hybrid polyurethane materials at 100% elongation as a function of NCO-POSS content [99]

NCO-POSS added in a small amount caused an increase in polyurethane stiffness, while its larger load led to excessive cross-linking, which disturbed the formation of hydrogen bonds with carbonyl groups, causing lower separation of rigid and soft segments and consequently reduction in the mechanical properties of polyurethane composites [100–103].

Star-shaped polyhedral oligomeric silsesquioxane-polycaprolactone-urethane hybrid materials were obtained by Teng et al. [104, 105] who used POSS with eight organic, functional arms chemically bonding to the polymer matrix. By incorporating organic groups in the core through extension with PCL and cross-linking with PU, organic–inorganic nanocomposites with enhanced cell attachment profile and biodegradability could be synthesized [106, 107]. The PCL-PU-POSS films revealed a high porosity of >75% and intrinsic nanoscale features that enhance cell attachment and growth. They exhibited negligible weight loss during the initial 24 weeks of degradation, followed by a large increase in the weight loss of 18% in the following 28 weeks. As cell viability is still maintained at >95%, even after 48 h of incubation

with the by-products of degradation, one can consider these hybrid materials to be promising candidates for scaffolds in tissue engineering.

Star-like PU hybrid films using functional cubic silsesquioxanes (CSSQ) (with up to eight reactive sites at the corner of POSS) were developed by Mya et al. [108, 109] Octakis-(dimethylsilyloxy) silsesquioxane isopropenyldimethylbenzylisocyanate (OS-PDBI), and octakis-(dimethylsilyloxy) hydroxypropyl silsesquioxane (HPS) were prepared by hydrosilylation reaction and used as nano-cross-linkers. Additionally, different types of PU hybrids were also prepared by using OS-PDBI macromonomer with hexane diol (HD) monomer. AFM images showed that no phase separation in the macroscopic level occurs for PU hybrid films and incorporation of CSSQ in PU structure provides enhanced thermal stability and increased cross-link density, as revealed by TGA and DMA results. Moreover, the presence of cage structure improved oxidation resistance and mechanical strength.

Pielichowski's group [110] incorporated into polyurethane elastomer octa-OH-functional POSS as a relatively massive and robust three-dimensional cross-linking core—Fig. 5.16. The influence of this cross-linking moiety on the morphology and molecular dynamics of the PU system was studied. AFM images for a polyurethane matrix showed numerous globules and spherulites of rigid segment domains dispersed in a flexible continuous phase with dimension 3–6 μm. After introducing the POSS molecules embedded as nodes of the polymer network, the globules sizes have decreased, and they assumed more spherical shapes ranging from 10 to 300 nm. On the phase images of hybrid elastomers with POSS, rigid spherical structures with softer center were observed. These new structures have been interpreted as forms consisting of POSS molecules connected to MDI, which have become soft cores surrounded by rigid segments. Additionally, despite extensive chemical cross-linking, the rubbery mechanical modulus decreased on addition of POSS, confirming that hard microdomains reinforce the matrix to a greater extent than chemical cross-links [111].

Blattmann and Mülhaupt [112] reported on the synthesis of novel multifunctional polyhedral oligomeric silsesquioxane (POSS) cyclic carbonates and their cure with diamines to produce POSS/NIPU nanocomposites with variable POSS content—-Fig. 5.17.

Authors found that Young's modulus and tensile strength were improved with an increase of POSS content as a result of higher cross-link density and silica content. Moreover, the incorporation of POSS considerably improved scratch resistance of optically transparent and colorless NIPU/POSS coatings as evidenced by the surface gloss and SEM images.

A series of NIPU coatings was prepared by Liu et al. through the ring-opening polymerization of rosin-based cyclic carbonate with amines, then the NIPUs were modified with epoxy and cyclic carbonate-functionalized POSS to form NIPU/POSS coatings [113]. Incorporation of POSS moieties into the NIPU networks caused an improvement in thermal stability, water tolerance, and pencil hardness of the hybrid coatings with an increase of the POSS content, whereby the impact strength, adhesion, and flexibility of the coatings were not observed to be affected to a significant extent. In an another development, this research group has obtained biomass-based

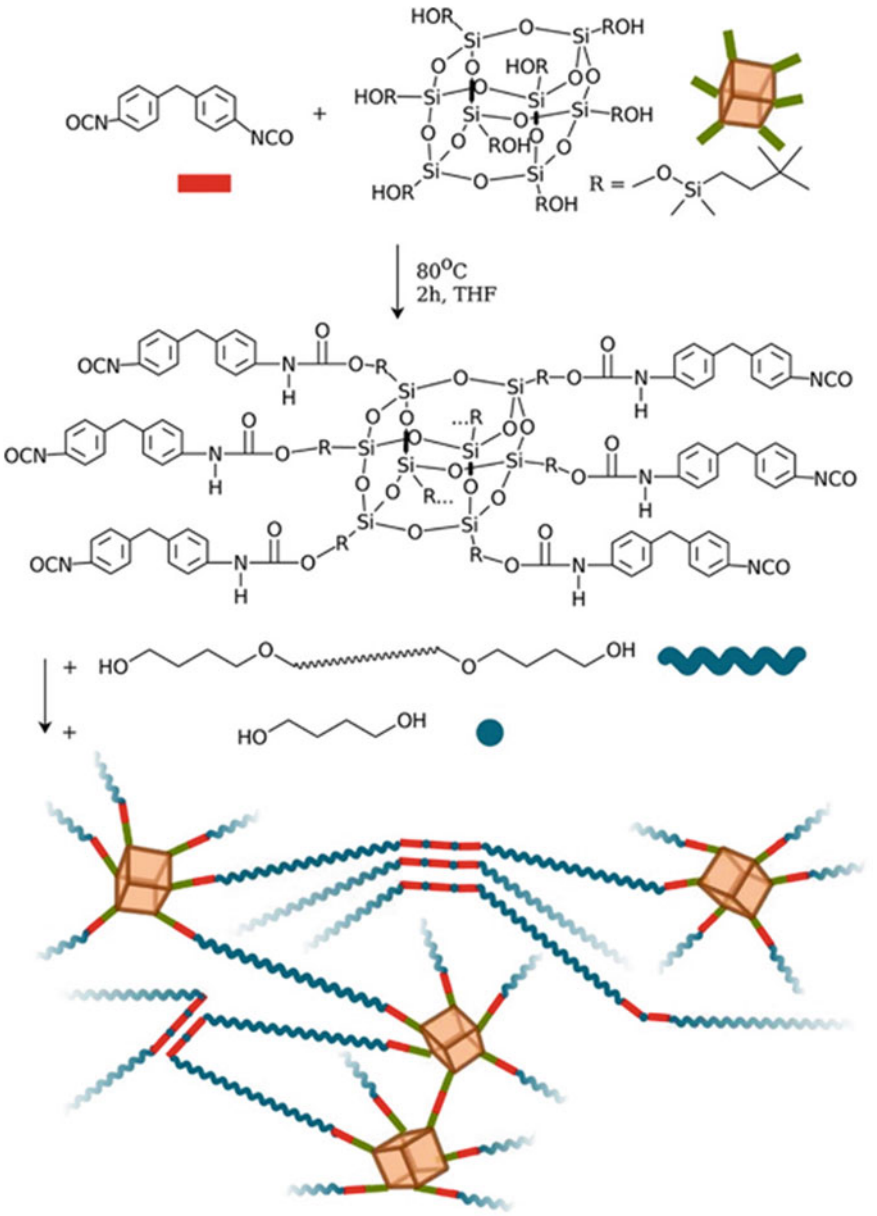

Fig. 5.16 Reaction route and sketch of the anticipated complex network. Some links have been omitted for clarity [110]

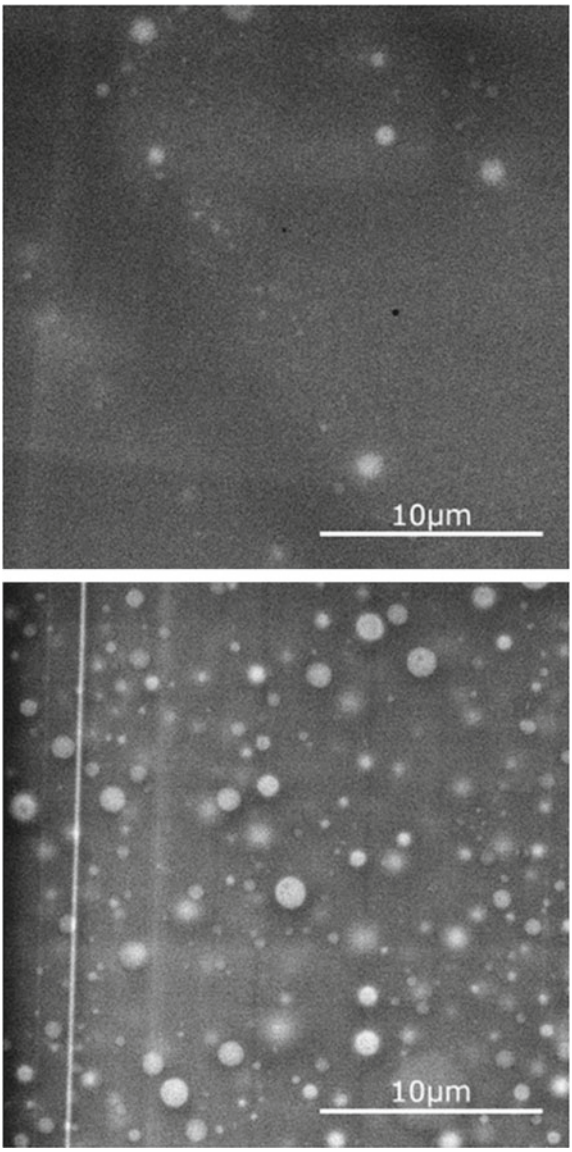

Fig. 5.17 SEM images of NIPU hybrid materials; SEM samples were obtained from NIPU specimens for tensile testing using the cryomicrotome technique [112]

NIPU coatings via the reactions of gallic acid-based cyclic carbonate with diamines which were then modified with epoxy-functionalized POSS to form NIPU/POSS coatings with chemically linked POSS groups [114]. The results revealed that the gallic acid-based NIPU coatings show excellent impact strength, adhesion, flexibility, pencil hardness, and thermal stability, but are suffering from low water resistance. Incorporation of POSS into the NIPU networks enhanced the pencil hardness, water

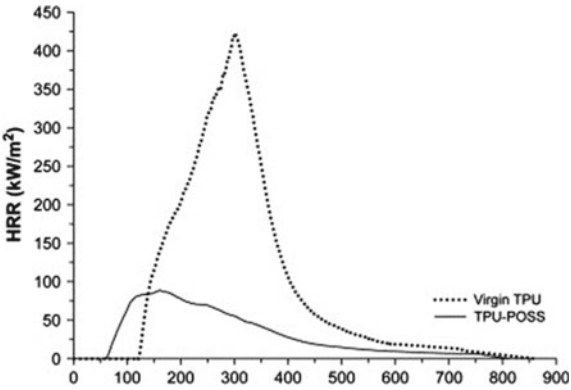

Fig. 5.18 Heat release rate (HRR) as a function of time of virgin TPU compared to TPU-POSS composite (external heat flux = 35 kW/m^2) [116]

resistance, and thermal stability of the NIPU/POSS coatings; however, the adhesion of the coatings was slightly decreased.

3 Physical Blending

Incorporation of POSS through physical blending offers several advantages, such as ease of processing, versatility, being fast, and cost-effective. The successful dispersion of POSS into polymeric matrices depends on the surface interactions of POSS, such as van der Waals and hydrogen bonding, with polymers [115–117]. However, interparticle interactions often result in the aggregation of POSS particles which may be a serious technological problem [118]. Polyurethane and POSS can be blended by using a solution or melt method [85].

Bourbigot et al. [119] reported on the preparation of POSS-containing composites based on PU by melt blending. Thermoplastic polyurethane was mixed with 10 wt% of poly(vinylsilsesquioxane) using a Brabender mixer running in nitrogen flow at 50 rpm for 10 min and at 180 °C. In the TEM image obtained at smaller magnification (17,000x), POSS particles were visible evenly dispersed in a thermoplastic polyurethane. At high magnification (30,000x), it turned out that POSS tended to create aggregates with micron size probably formed in the melt during processing. The silsesquioxane particle size was in the range of 200–400 nm, and the particles had an ellipsoidal shape.

Figure 5.18 shows a large reduction of the maximum peak of heat release rate (PHRR) in thermoplastic composites from 430 to 80 kW/m^2 as compared to pure TPU. The intumescent material has been found to be composed of ceramified char made of silicon network in a polyaromatic structure. This intumescent PU nanocomposite acts as a thermal barrier at the surface of the substrate limiting thus the heat and mass transfer as evidenced by lowered HRR [85, 120].

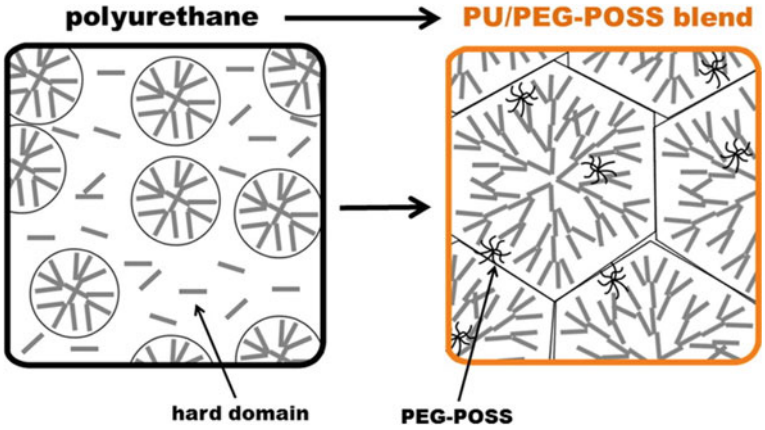

Fig. 5.19 Sketch of the mesostructure and organization of the microstructure of the reference polyurethane (left) and the PU/PEG-POSS blend (right) [120]

Reactive blending was applied by Montecelli et al. too [121]. to prepare polyurethane/POSS hybrids As a result of controlled scission of the thermoplastic polyurethane, isocyanate functional groups are formed during melt mixing, which react with OH groups in the functionalized POSS molecules: octaisobutyl POSS or *trans*-cyclohexanediolisobutyl POSS. These systems were prepared for mixing at 220 °C under the inert atmosphere for 10 min. The morphology studies using TEM microscopy revealed that there is no segregation or aggregation of POSS particles in TPU/POSS-OH (5 wt%), thus indicating that POSS-OH has chemically reacted with the polymer. DSC data showed an increase in glass transition temperature with increasing POSS content in TPU matrix from −48 °C for pristine TPU to −37 °C for TPU/POSS-OH (10 wt%).

Gu et al. [122] introduced octa(3-hydroxypropyl) polyhedral oligomeric silsesquioxane ($POSS\text{-}(OH)_8$) into ester-based thermoplastic polyurethane matrix by solution blending. The obtained composites displayed glass transition temperature around −25 °C, which can be used as trigger temperature of the shape-memory recovery. Moreover, they showed high shape fixity and shape recovery ratios with low trigger temperature.

Blended hybrid systems of PU with POSS having eight poly(ethylene glycol) (PEG) vertex groups (PEG-POSS) were prepared and characterized by Pielichowski's group [123]. The main change induced by the PEG-POSS is a plasticization effect which is observed by lowering the glass transition temperature. AFM and SEM analyses showed that hard segments form spherulites, and their size increases with the increase of POSS content. No POSS aggregates are observed while the storage modulus (DMA) in the rubbery phase decreases in the blends. This change in morphology, combined with the softening of the material on addition of POSS, suggests decreased microphase separation in polyurethane. Based on the results obtained, microstructure morphology development has been postulated—Fig. 5.19.

4 Application of PU-POSS Hybrid Materials

Hybrid materials by combining the features of organic and inorganic matter offer advantageous properties for different materials science applications. One of the application areas is polyurethane/POSS materials with controlled gas transport properties, as well as multilayer membranes [94, 124]. Specifically, by using amino-POSS to modify PU matrix, a reduction in permeability was achieved. The O_2/N_2 permeability and CO_2/N_2 permeability could be controlled by the POSS load and the PU structure [75]. It was postulated that bulky POSS moieties located on the polymer surface hinder transport of gas molecules. Moreover, POSS substituents influence formation of ordered crystalline structures [95, 124].

Hybrid thermally stable materials [38, 119, 125, 126], as well as materials with high dielectric constant, resistant to creeping currents [127], are considered as potential candidates for future applications. For instance, incorporation of PHI-POSS into polyurethane matrix composed of MDI and polytetramethylene glycol caused an increase in temperatures at which the degradation rate was the highest and a decrease in the intensity of emission of volatile decomposition products. This is most likely related to the reduced mobility of polymer chains in the presence of chemically linked POSS molecules [38]. Octaminophenyl-POSS (OapPOSS), added to epoxy-imine-polyurethane resins, caused an improvement in the heat resistance and in the Young's modulus values [125].

POSS nanoadditives were tested toward flame retardancy behavior of various polymers, and the best synergistic effects were found for a combination of conventional flame retardants with silsesquioxanes [126]. POSS mode of action includes preventing the fire by creation of ceramic, fire-resistant char layer on the surface of the burning material [116].

Special attention is focused on protective polymeric materials with POSS—due to good adhesion and improved durability, an effective protection against corrosion [128] and weathering effects has been reported [129]. Incorporation of POSS moieties into the polymer chain resulted in increased compressive strength [130], stretching [26], and improved thermoplasticity [128]. By using octaphenyl and glycidoxypropyl-POSS in the polyurethane matrix, glues with improved adhesion and shear strength could be obtained [131, 132]. Moreover, POSS nanofillers have been successfully used to obtain novel aerogels [130, 133] and shape-memory composites [134].

POSS modified polyurethane materials can also be used as high-strength coatings. The electrochemical and salt spray test evaluation of the PU films demonstrated the barrier and corrosion resistance properties improved by the POSS. The low current density over a wide potential indicated that the PU/POSS film provided an effective barrier to water. Additionally, the POSS components retain their partial cage structure, which give the product a high glass transition and enhanced thermal stability as compared to conventional polyurethanes, which is essential in their application as weatherable coatings [135, 136]. PU/POSS show also potential as flame retardants in textile coatings applications [137]. The unique POSS cage structure,

non-toxicity, and ease of properties control decided on the use of silsesquioxanes in the biomedical field. The main features that determine the medical applicability of POSS-containing materials are biocompatibility, biodegradability, cytological compatibility, and dimensional stability, as well as the already-mentioned no toxicity. Vast attention was paid to polycarbonate urethane-based (PCU) materials with POSS embedded in the main chain [138–140]. An increased mechanical strength and thermal stability [138], as well as better resistance to enzymatic and oxidative biodegradation, compared to pristine polymer, were reported [142]. Importantly, it was also found that PCU/POSS composites undergo calcination to a much lesser extent than non-modified polycarbonate urethane [69]. Through the incorporation of POSS, a continuous, porous matrix is formed, with a pore size of 150–250 μm [143], which turns out to be an excellent substrate for propagation and cell differentiation [141]. Materials of this type do not degrade inside mammalian organisms; therefore, they can be considered as a replacement for silicones [54, 144].

In general, research works on PCU/POSS hybrids are focused on three groups of biomaterials—blood vessel implants, lacrimal canal implants, and scaffolds that help regenerate tissues in the nervous system [142, 145]. As the fabrication route foaming extrusion proved to be a useful technique, enabling control of the porous structure formed [58].

Promising path is covering of shape-memory stents, made of nickel and titanium alloy (Nitinol), by electrohydrodynamic sputtering of PCU/POSS hybrids [70]. The layer formed shows antithrombogenic properties and facilitates endothelialization process [57, 71]. Noteworthy, Nitinol coating with POSS-containing polymer layer extends the usefulness of stents by about 10 years [74].

Another use of PCU/POSS materials in medicine is as scaffolds. These are mostly cell scaffolds capable of trapping cells and facilitating the creation of new tissues, such as RGD peptide (arginine-glycine-aspartic acid)-grafted PCU [146, 147]. The obtained materials are currently in the phase of clinical trials, and it is possible that they will initiate a new generation of scaffolds capable of regenerating nerves to a larger than 30 mm barrier. Using cell scaffolds, it is also possible to treat liver [148] and brain damages [149].

Materials containing POSS and nanotubes that can be used in the treatment of serious diseases are also of great interest. In this case, the nanotubes are coated with the PCL/POSS composite to ensure a biocompatible surface. Such materials exhibit strong near infrared absorption, emitting large amounts of thermal energy, and can be used for destruction of cancer cells [150].

5 Conclusions

In this work, diverse and significant research on polyurethane/POSS–hybrid materials has been presented. Two major routes of silsesquioxanes incorporation into polyurethane matrix—via chemical or physical path, leading to various organic–inorganic architectures, have been described. The crucial role of POSS functionalization

in the synthesis and during processing of polymers was highlighted. POSS moieties in nanohybrid polyurethanes influence the crystallization process of polymer matrix, leading to formation of stable morphological forms. The aggregation or crystallization behavior of POSS in nanocomposites plays an important role in manipulating the physical properties of materials, such as viscosity and melt elasticity. It is also important to limit the segment vibrations by large POSS substituents, which increases the glass transition temperature. There is also the possibility of occurrence favorable second-order interactions between macrochains containing POSS in their structure. The described polyurethane-POSS systems, due to their special properties, can find numerous applications, such as membranes, high-strength coatings and adhesives, aerogels, flame retardant materials, and shape-memory materials. The unique POSS cage structure, its non-toxicity, and broad functionalization possibilities make them useful modifiers for polyurethanes devoted to biomedical applications.

Acknowledgements Authors are grateful to the Polish National Science Center for support under Contract No. 2017/27/B/ST8/01584.

References

1. Florjańczyk Z, Penczek S (1998) Chemia polimerów, v.II, Oficyna Wydawnicza Politechniki Warszawskiej, Warszawa
2. Wirpsza Z (1991) Poliuretany: chemia, technologia, zastosowanie. Wydawnictwo Naukowo-Techniczne, Warszawa
3. Randall D, Lee S (2002) The polyurethane book. Wiley Ltd., New York
4. Szycher M (2003) Szycher's handbook of polyurethane. CRC Press, Taylor &Francis Group, Boca Raton
5. Prisacariu C (2011) Polyurethane Elastomers – from morphology to mechanical aspects. Springer Wien, New York
6. Prociak A, Rokicki G (2014) Materiały poliuretanowe. Polskie Wydawnictwo Naukowe, Warszawa
7. Allport DC, Gilbert DS, Outterside SM (2003) MDI and TDI: a safety Health and the environment. Wiley, Chichester
8. Rokicki G, Parzuchowski PG, Mazurek M (2015) Non-isocyanate polyurethanes: synthesis, properties, and applications. Polym Adv Technol 26:707–761
9. Kathalewar MS, Joshi PB, Sabnis AS et al (2013) Non-isocyanate polyurethanes: from chemistry to applications. RSC Adv 3:4110
10. Yaocheng H, Liyun L, Xu R et al (2011) Nonisocyanate polyurethanes and their applications. Prog Chem 23(6):1181–1188
11. Beniah G, Fortman DJ, Heath WH et al (2017) Non-Isocyanate polyurethane thermoplastic elastomer: amide-based chain extender yields enhanced nanophase separation and properties in polyhydroxyurethane. Macromolecules 50(11):4425–4434
12. Guo Z, Kim TY, Lei K, Pereira T et al (2008) Strengthening and thermal stabilization of polyurethane nanocomposites with silicon carbide nanoparticles by a surface-initiated-polymerization approach. Compos Sci Technol 62(1):164–170
13. Kuan HC, Ma CC, Chang WP et al (2005) Synthesis, thermal, mechanical and rheological properties of multiwall carbon nanotube/waterborne polyurethane nanocomposite. Compos Sci Technol 65(11):1703–1710

14. Koerner H, Liu W, Alexander M et al (2005) Deformation morphology correlations in electrically conductive carbon nanotube thermoplastic polyurethane nanocomposites. Polymer 46:4405–4420
15. Daniel MC, Astruc D (2004) Gold nanoparticles: assembly, supramolecular chemistry, quantum-size-related properties, and applications toward biology, catalysis, and nanotechnology. Chem Rev 104(1):293–346. https://doi.org/10.1021/cr030698+
16. Kuo SW, Chang FC (2011) POSS related polymer nanocomposites. Prog Polym Sci 36:1649–1696. https://doi.org/10.1016/j.progpolymsci.2011.05.002
17. Kickelbick G (2007) Hybrid materials. synthesis, characterization and application. Wiley-VCH, Weinheim
18. Markovic E, Constantopolous K, Janis G (2011) Polyhedral oligomeric silsesquioxanes: from early and strategic development through to materials application. In: Matisons Hartmann-Thompson C (ed) Applications of polyhedral oligomeric silsesquioxanes. Springer, New York, pp 1–46
19. Harrison PG (1997) Silicate cages: precursors to new materials. J Organomet Chem 542(2):141–183. https://doi.org/10.1016/S0022-328X(96)06821-0
20. Pielichowski K, Njuguna J, Janowski B, Pielichowski J (2006) Polyhedral oligomeric silsesquioxanes (POSS)-containing nanohybrid polymers. In: supramolecular polymers polymeric betains oligomers, Springer, Berlin, Heidelberg, pp 225–296. https://doi.org/10.1007/11614784
21. Pan G (2007) Polyhedral oligomeric silsesquioxane (POSS). In: Mark JE (ed) Physical properties of polymers handbook, Springer, New York, pp 577–584. https://doi.org/10.1007/978-0-387-69002-5
22. Janowski B, Pielichowski K (2008) Polimery nanohybrydowe zawierające poliedryczne oligosilseskwioksany. Polimery 53:87–98
23. Cordes DB, Lickiss PD, Rataboul F (2010) Recent developments in the chemistry of cubic polyhedral oligosilsesquioxanes. Chem Rev 110:2081–2173
24. Schwab JJ, Lichtenhan JD, Mather PT, Romouribe A et al, (1996) 21th meeting of the American Chemical Society, New Orleans, LA
25. Feher F, Schwab J, Tellers D, Burstein A (1998) A general strategy for synthesizing cubeoctameric silsesquioxanes containing polymerizable functional groups. Main Group Chem 2(3):169–181
26. Fu BX, Hsiao BS, White H, Rafailovich M et al (2000) Nanoscale reinforcement of polyhedral oligomeric silsesquioxane (POSS) in polyurethane elastomer. Polym Int 49:437–440
27. Fu BX, Hsiao BS, Pagola S, Stephens P et al (2001) Structural development during deformation of polyurethane containing polyhedral oligomeric silsesquioxanes (POSS) molecules. Polymer 42:599–611
28. Hoflund GB, Gonzalez RI, Philips SHJ (2001) In situ oxygen atom erosion study of a polyhedral oligomeric silsesquioxane-polyurethane copolymer. Adhesion Sci Technol 15:1199–1211. https://doi.org/10.1163/156856101317048707
29. Turri S, Levi M (2005) Preparation and characterization of polyurethane hybrids from reactive polyhedral oligomeric silsesquioxanes. Macromolecules 38:5569–5574
30. Turri S, Levi M (2005) Wettability of polyhedral oligomeric silsesquioxane nanostructured polymer surfaces. Macromol Rapid Commun 26:1233–1236. https://doi.org/10.1002/marc.200500274
31. Zhang S, Zou Q, Wu L (2006) Preparation and characterization of polyurethane hybrids from reactive polyhedral oligomeric silsesquioxanes. Macromol Mater Eng 291:895–901. https://doi.org/10.1002/mame.200600144
32. Król B, Król P (2010) Materiały powłokowe otrzymywane z kationomerów poliuretanowych modyfikowanych funkcjonalizowanym silseskwioksanem. Cz. I. Budowa chemiczna kationomerów. Polimery 55(6):440–451
33. Król B, Król P (2010) Materiały powłokowe otrzymywane z kationomerów poliuretanowych modyfikowanych funkcjonalizowanym silseskwioksanem. Cz. II. Właściwości użytkowe. Polimery 55(11–12):855–862

34. Madbouly SA, Otaigbe JU, Nanda AK et al (2007) Rheological behavior of POSS/polyurethane-urea nanocomposite films prepared by homogeneous solution polymerization in aqueous dispersions. Macromolecules 40:4982–4991
35. Madbouly SA, Otaigbe JU (2009) Recent advances in synthesis, characterization and rheological properties of polyurethanes and POSS/polyurethane nanocomposites dispersions and film. Prog Polym Sci 34:1283–1332. https://doi.org/10.1016/j.progpolymsci.2009.08.002
36. Lai YS, Tsai CW, Yang HW, Wang GP et al (2009) Structural and electrochemical properties of polyurethanes/polyhedral oligomeric silsesquioxanes (PU/POSS) hybrid coatings on aluminum alloys. Mater Chem Phys 117:91–98
37. Hu J, Li L, Zhang S, Gong L et al (2013) Novel phenyl-POSS-polyurethane aqueous dispersions and their hybrid coatings. J Appl Polym Sci 130:1611–1620. https://doi.org/10.1002/APP.39303
38. Janowski B, Pielichowski K (2008) Thermo(oxidative) stability of novel polyurethane/POSS nanohybrid elastomers. Thermochim Acta 478:51–53
39. Lewicki JP, Pielichowski K, TremblotDeLaCroix P, Janowski B et al (2010) Thermal degradation studies of polyurethane/POSS nanohybrid elastomers. Polym Degrad Stab 95(6):1099–1105. https://doi.org/10.1016/j.polymdegradstab.2010.02.021
40. Lewicki JP, Mayer BP, Pielichowski K, Janowski B et al (2010) Synthesis and characterization via solid state NMR of novel POSS-polyurethane nanohybrid elastomers. Polymer Preprints 51(2):343–344
41. Raftopoulos KN, Pandis Ch, Apekis L, Pissisa P et al (2010) Polyurethane–POSS hybrids: molecular dynamics studies. Polymer 51:709–718
42. Raftopoulos KN, Jancia M, Aravopoulou D, Hebda E et al (2013) POSS along the hard segments of polyurethane. Phase separation and molecular dynamics. Macromolecules 46:7378–7386. https://doi.org/10.1021/ma401417t
43. Raftopoulos KN, Janowski B, Apekis L, Pissis P et al (2013) Direct and indirect effects of POSS on the molecular mobility of polyurethanes with varying segment M_w. Polymer 54:2745–2754. https://doi.org/10.1016/j.polymer.2013.03.036
44. Cui D, Tian F, Ozkan CS, Wang M et al (2005) Effect of single wall carbon nanotubes on human HEK293 cells. Toxicol Lett 155(1):73–85. https://doi.org/10.1016/j.toxlet.2004.08.015
45. Kim SK, Heo SJ, Koak JY, Lee JH et al (2007) A biocompatibility study of a reinforced acrylic-based hybrid denture composite resin with polyhedraloligosilsesquioxane. J Oral Rehabil 34(5):389–395. https://doi.org/10.1111/j.1365-2842.2006.01671.x
46. Punshon G, Vara DS, Sales KM, Kidane AG et al (2005) Interactions between endothelial cells and a poly(carbonate-silsesquioxane-bridge-urea)urethane. Biomaterials 26(32):6271–6279. https://doi.org/10.1016/j.biomaterials.2005.03.034
47. Lakhani HA, Mel A, Seifalian AM (2015) The effect of TGF-β1 and BMP-4 on bone marrow-derived stem cell morphology on a novel bioabsorbable nanocomposite material. Artif Cells Nanomedicine Biotechnol 43(4):230–234. https://doi.org/10.3109/21691401.2013.856015
48. Maqsood A, Hamilton G, Seifalian AM (2010) Viscoelastic behaviour of a small calibre vascular graft made from a POSS-nanocomposite. In: 32nd annual international conference of the IEEE engineering in medicine and biology 251–254. https://doi.org/10.1109/iembs.2010.5627472
49. Kannan RY, Salacinski HJ, Sales KM, Butler PE et al (2006) The endothelialization of polyhedral oligomeric silsesquioxane nanocomposites: an in vitro study. Cell Biochem Biophys 45(2):129–136
50. Guo YL, Wang W, Otaigbe JU (2010) Biocompatibility of synthetic poly(ester urethane)/polyhedral oligomeric silsesquioxane matrices with embryonic stem cell proliferation and differentiation. J Tissue Eng Regen Med 4(7):553–564
51. Wu J, Gu X, Mather PT (2010) Biostable multiblock thermoplastic polyurethanes incorporating poly(ε-caprolactone) and polyhedral oligomeric silsesquioxane (POSS). Trans Annu Meet Soc Biomater 1(84)

52. Ghanbari H, Cousins BG, Seifalian AM (2011) A nanocage for nanomedicine: polyhedral oligomeric silsesquioxane (POSS). Macromol Rapid Commun 32(14):1032–1046. https://doi.org/10.1002/marc.201100126
53. Gupta A, Vara DS, Punshon G, Sales KM et al (2009) In vitro small intestinal epithelial cell growth on a nanocomposite polycaprolactone scaffold. Biotechnol Appl Biochem 54(4):221–229
54. Kannan RY, Salacinski HJ, Odlyha M, Butler PE et al (2006) The degradative resistance of polyhedral oligomeric silsesquioxane nanocore integrated polyurethanes: an in vitro study. Biomaterials 27(9):1971–1979
55. Salacinski HJ, Handcock S, Seifalian AM (2005) Polymer for use in conduits and medical devices. Patent Number: WO2005070998, 4 Aug 2005
56. Kannan RY, Salacinski HJ, Edirisinghe MJ, Hamilton G et al (2006) Polyhedral oligomeric silsequioxane-polyurethane nanocomposite microvessels for an artificial capillary bed. Biomaterials 27:4618–4626
57. Kannan RY, Salacinski HJ, Groot JD, Clatworthy I et al (2006) The antithrombogenic potential of a polyhedral oligomeric silsesquioxane (POSS) nanocomposite. Biomacromolecules 7:215–223
58. Ahmed M, Ghanbari H, Cousins BG, Hamilton G et al (2011) Small calibre polyhedral oligomeric silsesquioxane nanocomposite cardiovascular grafts: influence of porosity on the structure, haemocompatibility and mechanical properties. Acta Biomater 7(11):3857–3867
59. Ahmed M, Hamilton G, Seifalian AM (2014) The performance of a small-calibre graft for vascular reconstructions in a senescent sheep model. Biomaterials 35(33):9033–9040. https://doi.org/10.1016/j.biomaterials.2014.07.008
60. Tai NR, Salacinski HJ, Edwards A, Hamilton G et al (2000) Compliance properties of conduits used in vascular reconstruction. Br J Surg 87(11):1516–1524. https://doi.org/10.1046/j.1365-2168.2000.01566.x
61. Salacinski HJ, Tai NR, Carson RJ, Edwards A et al (2002) In vitro stability of a novel compliant poly(carbonate-urea)urethane to oxidative and hydrolytic stress. J Biomed Mater Res 59(2):207–218
62. Silver JH, Lin JC, Lim F, Tegoulia VA et al (1999) Surface properties and hemocompatibility of alkyl-siloxane monolayers supported on silicone rubber: effect of alkyl chain length and ionic functionality. Biomaterials 20(17):1533–1543
63. Park JH, Bae YH (2002) Hydrogels based on poly(ethylene oxide) and poly(tetramethylene oxide) or poly(dimethyl siloxane): synthesis, characterization, in vitro protein adsorption and platelet adhesion. Biomaterials 23(8):1797–1808. https://doi.org/10.1016/S0142-9612(01)00306-4
64. Kannan RY, Salacinski HJ, Butler PE, Seifalian AM (2005) Polyhedral oligomeric silsesquioxane nanocomposites: the next generation material for biomedical applications. Acc Chem Res 38(11):879–884. https://doi.org/10.1021/ar050055b
65. Kannan RY, Salacinski HJ, Sales K, Butler P et al (2005) The roles of tissue engineering and vascularisation in the development of micro-vascular net-works: a review. Biomaterials 26:1857–1875
66. Salacinski HJ, Tai NR, Punshon G, Giudiceandrea A et al (2000) Optimal endothelialisation of a new compliant poly(carbonate-urea)urethane vascular graft with effect of physiological shear stress. Eur J Vasc Endovasc Surg 20(4):342–352
67. Chawla R, Tan A, Ahmed M, Crowley C et al (2014) A polyhedral oligomeric silsesquioxane–based bilayered dermal scaffold seeded with adipose tissue–derived stem cells: in vitro assessment of biomechanical properties. J Surg Res 188(2):361–372. https://doi.org/10.1016/j.jss.2014.01.006
68. Kidane AG, Burriesci G, Edirisinghe M, Ghanbari H et al (2009) A novel nanocomposite polymer for development of synthetic heart valve leaflets. Acta Biomater 5(7):2409–2417. https://doi.org/10.1016/j.actbio.2009.02.025
69. Ghanbari H, Kidane AG, Burriesci G, Ramesh B et al (2010) The anti-calcification potential of a silsesquioxane nanocomposite polimer under in vitro conditions: potential material

for synthetic leaflet heart valve. Acta Biomater 6(11):4249–4260. https://doi.org/10.1016/j.actbio.2010.06.015
70. Chaloupka K, Motwani M, Seifalian AM (2011) Development of a new lacrimal drainage conduit using POSS nanocomposite. Biotechnol Appl Biochem 58(5):363–370. https://doi.org/10.1002/bab.53
71. Bakhshi R, Darbyshire A, Evans JE, You Z et al (2011) Polymeric coating of surface modified nitinol stent with POSS-nanocomposite polimer. Colloids Surf B 86(1):93–105. https://doi.org/10.1016/j.colsurfb.2011.03.024
72. Kannan RY, Salacinski HJ, De Groot J, Clatworthy I et al (2006) The antithrombogenic potential of a polyhedral oligomeric silsesquioxane (POSS) nanocomposite. Biomacromol 7(1):215–223. https://doi.org/10.1021/bm050590z
73. Farhatnia Y, Pang JH, Darbyshire A, Dee R et al. (2016) Next generation covered stents made from nanocomposite materials: a complete assessment of uniformity, integrity and biomechanical properties. Nanomed Nanotechnol Biol Med 12(1):1–12. https://doi.org/10.1016/j.nano.2015.07.002
74. Desai M, Bakhshi R, Zhou X, Odlyha M et al (2012) A sutureless aortic stent-graft based on a nitinol scaffold bonded to a compliant nanocomposite polymer is durable for 10 years in a simulated in vitro model. J Endovasc Ther 19(3):415–427. https://doi.org/10.1583/11-3740MR.1
75. Oaten M, Choudhury NR (2005) Silsesquioxane-urethane hybrid for thin film applications. Macromolecules 38(15):6392–6401. https://doi.org/10.1021/ma0476543
76. Pistor V, Conto D, Ornaghi FG, Zattera AJ (2012) Microstructure and crystallization kinetics of polyurethane thermoplastics containing trisilanol isobutyl POSS. J Nanomaterials 2012, Article ID 283031, 8 pages. https://doi.org/10.1155/2012/283031
77. Pan R, Shanks R, Kong I, Wang L (2014) Trisilanolisobutyl POSS/polyurethane hybrid composites: preparation, WAXS and thermal properties. Polym Bull 71:2453–2464. https://doi.org/10.1007/s00289-014-1201-7
78. Pan R, Shanks R, Wang L (2015) Crystallite cluster structure formation resulting from semi-enclosed cage interaction in TSI-POSS/PU hybrid composites. Adv Mater Res 1091:19–23
79. Pan R, Shanks R, Liu Y (2015) The effect of humping semi-enclosed cage structure on polymer chains characteristics of TSI-POSS/PU hybrid composites. Appl Mech Mater 751:30–34
80. Pan R, Wang LL, Shanks R, Liu Y (2016) The influence of trisilanolisobutyl POSS on domain microstructure of a polyurethane hybrid composite: A molecular simulation approach. Silicon. https://doi.org/10.1007/s12633-016-9463-3
81. Raftopoulos KN, Jancia M, Aravopoulou D, Hebda E et al (2013) POSS along the hard segments of polyurethane. Phase Sep Molecular Dyn Macromol 46(18):7378–7386. https://doi.org/10.1021/ma401417t
82. Lewicki JP, Pielichowski K, Jancia M, Hebda E et al (2014) Degradative and morphological characterization of POSS modified nanohybrid polyurethane elastomers. Polym Degrad Stab 104:50–56
83. Neumann D, Fisher M, Tran L, Matisons JG (2002) Synthesis and characterization of an isocyanate functionalized polyhedral oligosilsesquioxane and the subsequent formation of an organic-inorganic hybrid polyurethane. J Am Chem Soc 124(47):13998–13999. https://doi.org/10.1021/ja0275921
84. Markovic E, Nguyen K, Clarke S, Constantopoulos K et al (2013) Synthesis of POSS–polyurethane hybrids using octakis (m-isoprenyl-α, α′-dimethylbenzylisocyanato dimethylsiloxy) octasilsesquioxane (Q8M8TMI) as a crosslinking agent. J Polym Sci Polym Chem 51(23):5038–5045. https://doi.org/10.1002/pola.26934
85. Diao S, Mao L, Zhang L, Key YW (2015) POSS/Polyurethane hybrids and nanocomposites: a review on preparation, structure and performance elastomers and composites. 50(1):35–48
86. Liu H, Zheng S (2005) Polyurethane networks nanoreinforced by polyhedral oligomeric silsesquioxane. Macromol Rapid Commun 26:196–200
87. Liu H, Zheng S (2006) Polyurethane networks modified with octa(propylglycidyl ether) polyhedral oligomeric silsesquioxane. Macromol Chem Phys 207:1842–1851

88. Zhang Q, He H, Xi K, Huang X et al (2011) Synthesis of N-phenylaminomethyl POSS and its utilization in polyurethane. Macromolecules 44(3):550–557. https://doi.org/10.1021/ma101825j
89. Zhang Q, Huang X, Wang X, Jia X et al (2014) Rheological study of the gelation of cross-linking polyhedral oligomeric silsesquioxanes (POSS)/PU composites. Polymer 55:1282–1291
90. Zhang Q, Huang X, Meng Z, Jia X et al (2014) N-phenylaminomethyl hybrid silica, a better alternative to achieve reinforced PU nanocomposites. RSC Adv 4(35):18146–18156. https://doi.org/10.1039/C4RA01419G
91. Zhang Q, He H, Xi K, Huang X et al (2011) Synthesis of N-phenylaminomethyl POSS and its utilization in polyurethane. Macromolecules 44:550–557. https://doi.org/10.1021/ma101825j
92. Zhang Q, Huang X, Wang X, Jia X et al (2014) Rheological study of the gelation of cross-linking polyhedral oligomeric silsesquioxanes (POSS)/PU composites. Polymer 55:1282–1291. https://doi.org/10.1016/j.polymer.2014.01.040
93. Madhavan K, Reddy BSR (2009) Synthesis and characterization of polyurethane hybrids: influence of the polydimethylsiloxane linear chain and silsesquioxane cubic structure on the thermal and mechanical properties of polyurethane hybrids. J Appl Polym Sci 113:4052–4065
94. Madhavan K, Reddy BSR (2009) Structure–gas transport property relationships of poly(dimethylsiloxane–urethane) nanocomposite membranes. J Membr Sci 342(1–2):291–299
95. Madhavan K, Reddy BSR (2006) Poly(dimethylsiloxane-urethane) membranes: effect of hard segment in urethane on gas transport properties. J Membr Sci 283:357
96. Madhavan K, Gnanasekaran D, Reddy BSR (2011) Poly(dimethylsiloxane-urethane) membranes: effect of linear siloxane chain and caged silsesquioxane on gas transport properties. J Polym Res 18(6):1851–1861. https://doi.org/10.1007/s10965-011-9592-8
97. Hu L, Jiang P, Bian G, Huang M et al. (2017) Effect of octa(aminopropyl) polyhedral oligomeric silsesquioxane (OapPOSS) functionalized graphene oxide on the mechanical, thermal, and hydrophobic properties of waterborne polyurethane composites. J Appl Polym Sci 44440–44450. https://doi.org/10.1002/app.44440
98. Xue Y, Liu Y, Lu F, Qu J et al (2012) Functionalization of graphene oxide with polyhedral oligomeric silsesquioxane (POSS) for multifunctional applications. J Phys Chem Lett 3:1607–1612. https://doi.org/10.1021/jz3005877
99. Prządka D, Jęczalik J, Andrzejewska E, Marciniec B et al (2013) Novel hybrid polyurethane/POSS materials via bulk polymerization. React Funct Polym 73:114–121. https://doi.org/10.1016/j.reactfunctpolym.2012.09.006
100. Ti Y, Chen D (2008) Temperature dependence of hydrogen bond in Fe-OCAP/polyurethane blends. J Appl Polym Sci 130(4):2265–2271
101. Zhang J, Hu CP (2008) Synthesis, characterization and mechanical properties of polyester-based aliphatic polyurethane elastomers containing hyperbranched polyester segments. J Am Chem Soc 44:3708
102. Prządka D, Jęczalik J, Andrzejewska E, Dutkiewicz M (2013) Synthesis and properties of hybrid urethane polymers containing polyhedral oligomeric silsesquioxane crosslinker. J Appl Polym Scihttps://doi.org/10.1002/app.39385
103. Kim EH, Myoung SW, Jung YG, Paik U (2009) Polyhedral oligomeric silsesquioxane-reinforced polyurethane acrylate. Prog Org Coat 64(2–3):205–209. https://doi.org/10.1016/j.porgcoat.2008.07.026
104. Teng CP, Mya KY, Win KY, Yeo CC et al (2014) Star-shaped polyhedral oligomeric silsesquioxane-polycaprolactone-polyurethane as biomaterials for tissue engineering application. NPG Asia Mater 6:e142. https://doi.org/10.1038/am.2014.102
105. Liu Y, Yang X, Zhang W, Zheng S (2006) Star-shaped poly(ε-caprolactone) with polyhedral oligomeric silsesquioxane core. Polymer 47(19):6814–6825. https://doi.org/10.1016/j.polymer.2006.07.050
106. She MS, Lo TY, Hsueh HY, Ho RM (2013) Nanostructured thin films of degradable block copolymers and their applications. NPG Asia Mater 5:e42. https://doi.org/10.1038/am.2013.5

107. Wu J, Mather PT (2009) POSS polymers: physical properties and biomaterials applications. J Macromol Sci Polym Rev 49(1):25–63. https://doi.org/10.1080/15583720802656237
108. Mya KY, Wang Y, Shen L, Xu J et al (2009) Star-like polyurethane hybrids with functional cubic silsesquioxanes: preparation, morphology, and thermomechanical properties. J Polym Sci Part A Polym Chem 47:4602–4616. https://doi.org/10.1002/pola.23512
109. Mya KY, He CB, Huang J, Xiao Y et al (2004) Preparation and thermomechanical properties of epoxy resins modified by octafunctional cubic silsesquioxane epoxides. J Polym Sci Part A Polym Chem 42(14):3490–3503. https://doi.org/10.1002/pola.20168
110. Raftopoulos KN, Koutsoumpis S, Jancia M, Lewicki JP et al (2015) Reduced phase sparation and slowing of dynamics in polyurethanes with three-dimensional POSS-based cross-linking moieties. Macromolecules 48(5):1429–1441. https://doi.org/10.1021/ma5023132
111. Raftopoulos KN, Pielichowski K (2015) Segmental dynamics in hybrid polymer/POSS nanomaterials. Prog Polym Sci 52:136–187. https://doi.org/10.1016/j.progpolymsci.2015.01.003
112. Blattmann H (2016) Mülhaupt R (2016) Multifunctional POSS cyclic carbonates and non-isocyanate polyhydroxyurethane hybrid materials. Macromolecules 49(3):742–751. https://doi.org/10.1021/acs.macromol.5b02560
113. Liu G, Wu G, Chen J et al (2016) Synthesis, modification and properties of rosin-based non-isocyanate polyurethanes coatings. Prog Org Coat 101:461–467. https://doi.org/10.1016/j.porgcoat.2016.09.019
114. Liu G, Wu G, Chen J et al (2015) Synthesis and Properties of POSS-containing Gallic acid-based non-isocyanate polyurethanes coatings. Polym Degrad Stab 121:247–252. https://doi.org/10.1016/j.polymdegradstab.2015.09.013
115. Wu J, Mather PT (2009) POSS polymers: physical properties and biomaterials applications. Polym Rev 49(1):25–63 https://doi.org/10.1080/15583720802656237
116. Striolo A, McCabe C, Cummings PT (2005) Thermodynamic and transport properties of polyhedral oligomeric sislesquioxanes in poly(dimethylsiloxane). J. Phys. Chem. B 109(30):14300–14307. https://doi.org/10.1021/jp045388p
117. Striolo A, McCabe C, Cummings PT (2006) Organic-inorganic telechelic molecules: solution properties from simulations. J Chem Phys 125(10):104904. https://doi.org/10.1063/1.2348641
118. Ayandele E, Sarkar B, Alexandridis P (2012) Polyhedral oligomeric silsesquioxane (POSS)-containing polymer nanocomposites. Nanomaterials 2(4):445–475. https://doi.org/10.3390/nano2040445
119. Bourbigot S, Turf T, Bellayer S, Duquesne S (2009) Polyhedral oligomeric silsesquioxane as flame retardant for thermoplastic polyurethane. Polym Degrad Stab 94:1230–1237. https://doi.org/10.1016/j.polymdegradstab.2009.04.016
120. Majka TM, Raftopoulos KN, Pielichowski K (2018) The influence of POSS nanoparticles on selected thermal properties of polyurethane-based hybrids. J Therm Anal Calorim 133(1):289–301. https://doi.org/10.1007/s10973-017-6942-8
121. Monticelli O, Fina A, Cavallo D, Gioffredi E et al (2013) On a novel method to synthesize POSS-based hybrids: an example of the preparation of TPU based system. Express Polym Lett 7(12):966–973. https://doi.org/10.3144/expresspolymlett.2013.95
122. Gu SY, Jin SP, Liu LL (2015) Polyurethane/polyhedral oligomeric silsesquioxane shape memory nanocomposites with low trigger temperatur and quick response. J Polym Res 22:142. https://doi.org/10.1007/s10965-015-0779-2
123. Koutsoumpis S, Raftopoulos KN, Jancia M, Pagacz J et al (2016) POSS moieties with PEG vertex groups as diluent in polyurethane elastomers: morphology and phase separation. Macromolecules 49(17):6507–6517. https://doi.org/10.1021/acs.macromol.6b01394
124. Gnanasekaran D, Walter PA, Parveen AA, Reddy BSR (2013) Polyhedral oligomeric silsesquioxane-based fluoroimide-containing poly(urethane-imide) hybrid membranes: synthesis, characterization and gas-transport properties. Sep Purif Technol 111:108–118. https://doi.org/10.1016/j.seppur.2013.03.035
125. Song J, Chen G, Wu G, Cai C et al (2001) Thermal and dynamic mechanical properties of epoxy resin/poly(urethane-imide)/polyhedral oligomeric silsesquioxane nanocomposites. Polym Adv Technol 22(12):2069–2074

126. Bourbigot S., Duquesne S., Fontaine G., Bellayer S et al. (2008) Characterization and reaction to fire of polymer nanocomposites with and without conventional flame retardants. Mol Cryst Liq Cryst 486(1): 325/1367–339/1381
127. Fomenko AA, Gomza YP, Klepko VV, Gumenna MA et al (2009) Dielectric properties, conductivity and structure of urethane composites based on polyethylene glycol and polyhedral silsesquioxane. Polym J 31(2):137–143
128. Oaten M, Choudhury NR (2005) Synthesis and characterization of a POSS-urethane hybrid coating for use in the corrosion protection of metal. J Metastable Nanocrystalline Mater 23:231–234
129. Imai G, Inada Y, Matsuura Y, Nagai A (2013) Radiation-curable compositions with good curability under oxygen, and their coated scratch-resistant articles. JP Patent 2013018848
130. Hebda E, Ozimek J, Raftopoulos KN, Michałowski S et al (2015) Synthesis and morphology of rigid polyurethane foams with POSS as pendant groups or chemical crosslinks. Polym Adv Technol 26(8):932–940. https://doi.org/10.1002/pat.3504
131. Schwab J, Lichtenhan J, Carr M, Chaffee K et al (1997) Hybrid nanoreinforced polyurethanes based on polyhedral oligomeric silsesquioxanes. Polym Mater Sci Eng 77:549–550
132. Efrat T, Dodiuk H, Kenig S, Mccarthy S (2006) Nanotailoring of polyurethane adhesive by polyhedral oligomeric silsesquioxane (POSS). J Adhes Sci Technol 20(12):1413–1430
133. Jana SC, Duan Y, Wang X, Shinko A (2013) Chemical and engineering issues of functional polymer aerogels. In: Abstracts of papers of the American Chemical Society Spring Meeting, New Orleans, 7–11 April 2013
134. Xu J, Song J (2007) Biodegradable shape memory poly (ester-urethane) nanocomposites strengthened by polyhedral silsesquioxane (POSS) core. In: Abstracts of the 23th ACS National Meeting, Boston, 2007
135. Lai YS, Tsai CW, Yanga HW, Wang GP et al (2009) Structural and electrochemical properties of polyurethanes/polyhedral oligomeric silsesquioxanes (PU/POSS) hybrid coatings on aluminum alloys. Mater Chem Phys 117(1):91–98. https://doi.org/10.1016/j.matchemphys.2009.05.006
136. Wang X, Hu Y, Song L, Xing W et al (2011) UV-curable waterborne polyurethane acrylate modified with octavinyl POSS for weatherable coating applications. J Polym Res 18:721–729. https://doi.org/10.1007/s10965-010-9468-3
137. Devaux E, Rochery M, Bourbigot S (2002) Polyurethane/clay and polyurethane/POSS nanocomposites as flame retarded coating for polyester and cotton fabrics. Fire Mater 26(4–5):149–154. https://doi.org/10.1002/fam.792
138. Lakhani HA, Mel A, Seifalian AM (2015) The effect of TGF-β1 and BMP-4 on bone marrow-derived stem cell morphology on a novel bioabsorbable nanocomposite material. Artif Cells Nanomed Biotechnol 43(4):230–234
139. Maqsood A, Hamilton G, Seifalian AM (2010) Viscoelastic behaviour of a small calibre vascular graft made from a POSS-nanocomposite. In Abstracts 2010 annual international conference of the IEEE engineering in medicine and biology
140. Kannan R, Salacinski HJ, Sales KM, Butler PE et al (2006) The endothelialization of polyhedral oligomeric silsesquioxane nanocomposites: an in vitro study. Cell Biochem Biophys 45(2):129–136
141. Guo YL, Wang W, Otaigbe JU (2010) Biocompatibility of synthetic poly(ester urethane)/polyhedral oligomeric silsesquioxane matrices with embryonic stem cell proliferation and differentiation. J Tissue Eng Regen Med 4(7):553–564
142. Wu J, Gu X, Mather PT (2010) Biostable multiblock thermoplastic polyurethanes incorporating poly(ε-caprolactone) and polyhedral oligomeric silsesquioxane (POSS). Trans Annu Meet Soc Biomater 1(84)
143. Gupta A, Vara DS, Punshon G, Sales KM et al (2009) In vitro small intestinal epithelial cell growth on a nanocomposite polycaprolactone scaffold. Biotechnol Appl Biochem 54(4):221–229
144. Kannan RY, Salacinski HJ, Ghanavi JE, Narula A (2007) Silsesquioxane nanocomposites as tissue implants. Plast Reconstr Surg 119(6):1653–1662. https://doi.org/10.1097/01.prs.0000246404.53831.4c

145. Mel A, Chaloupka K, Malam Y, Darbyshire A et al. (2012) A silver nanocomposite biomaterial for blood-contacting implants. J Biomed Mater Res Part A 100(9)
146. Sedaghati T, Jell G, Seifalian A (2014) Investigation of Schwann cell behaviour on RGD-functionalised bioabsorbable nanocomposite for peripheral nerve regeneration. N Biotechnol 31(3):203–213
147. Mel A, Punshon G, Ramesh B, Sarkar S et al. (2009) In situ endothelialisation potential of a biofunctionalised nanocomposite biomaterial-based small diameter bypass graft. Biomed Mater Eng 19(4–5):317–331. https://doi.org/10.3233/bme-2009-0597
148. Adwan H, Fuller B, Seldon C, Davidson B et al (2013) Modifying three-dimensional scaffolds from novel nanocomposite materials using dissolvable porogen particles for use in liver tissue engineering. J Biomater Appl 28(2):250–261
149. Antoniadou EV, Ahmad RK, Jackman RB, Seifalian AM (2011) Next generation brain implant coatings and nerve regeneration via novel conductive nanocomposite development. In: 2011 annual international conference of the IEEE engineering in medicine and biology society, 2011
150. Tan A, Madani S, Rajadas J, Pastorin G et al (2012) Synergistic photothermal ablative effects of functionalizing carbon nanotubes with a POSS-PCU nanocomposite polimer. J Nanobiotechnology 10(1):34–42

POSS-Containing Polyamide-Based Nanocomposites

Biswajit Sarkar

Abstract Polyamide (PA) family of polymer is known as engineering plastics which are used in diverse industries such as synthetic fibers, automobiles, membranes. PA6 and PA66 are two major synthetic PAs that are widely used. Even though PAs possess several essential qualities, still some functional properties such as mechanical strength, rheological behavior, membrane permeability/permselectivity, flame retardancy need further improvement. Incorporation of POSS in PAs can improve those properties. In this chapter, we discussed POSS-containing PA nanocomposites. The influence of POSS on the structure and functional properties of PAs is discussed in particular.

Keywords Polyhedral oligomeric silsesquioxane (POSS) · Polyamides Nanocomposites · POSS-polyamide nanocomposites · Morphology Functional properties · Processing of nanocomposites

1 Introduction

Polymers possess several properties such as lightweight, ductile (easy to process), which make them highly valuable in various industrial applications as well as in our day-to-day life [1–4]. Compared to metals and ceramics, polymers lack sufficient mechanical properties such as Young's modulus and strengths which restrict their applications in many heavy-duty uses. The mechanical properties can be improved effectively by embedding a proper reinforcing material (filler) in polymer body. Various fillers are incorporated in polymer matrices such as fibers, platelets, nanoparticles. Based on the size, fillers can be broadly classified into two major categories,

B. Sarkar (✉)
Department of Chemical and Biological Engineering, University at Buffalo, Buffalo, NY 14260, USA
e-mail: bsarkar@buffalo.edu

B. Sarkar
Intel Corporation, Hillsboro, OR 97124, USA

S. Kalia and K. Pielichowski (eds.), *Polymer/POSS Nanocomposites and Hybrid Materials*, Springer Series on Polymer and Composite Materials,
https://doi.org/10.1007/978-3-030-02327-0_6

e.g., macrofillers and nanofillers. The improvement of mechanical properties by incorporating macroparticles often involves trade-offs of desirable properties, like stiffness can be improved at the cost of toughness. On the other hand, the incorporation of nanosized fillers (typical size 1–100 nm) into polymer matrices can improve desirable properties without harming other desired properties [5–8].

Nanofiller-containing polymers are known as polymer nanocomposite materials which are relatively new family of material. Nanofillers (nanoparticles) provide functional properties, and polymer provides processability. As a result, a family of processable functional hybrid materials with improved mechanical and functional properties can be produced. Polymer nanocomposite (clay/polyamide-6) was first commercially introduced by Toyota Motor Corp in the early 1990s [6]. Since then, substantial amount of work has been performed on polymer nanocomposites materials to improve various functional properties such as mechanical, electrical, thermal, membrane. Nanoparticles help in improving the properties of composites mainly in two ways: (i) by improving physical properties of polymer that depends on polymer–particle surface interactions and (ii) by embedding novel functional properties of nanoparticles.

1.1 POSS

Polyhedral oligomeric silsesquioxanes (POSS), also known as molecular silica, are nanoparticles (diameter in the range of 1–3 nm) with very well-defined organic–inorganic hybrid structure (see Fig. 1) [9–11]. POSS consists of inorganic silica (Si and O) core surrounded with organic ligands with empirical formula $(RSiO_{1.5})_n$ where R could be hydrogen or some organic ligands and $n = 4$ (T4), 6 (T6), 8 (T8, most common), 10 (T10), 12 (T12) (see Fig. 1). Surface properties of POSS particles depend on the properties of R which can vary from polar to nonpolar, reactive to nonreactive, and/or positively charged to negatively charge. A series of R ligands are presented in Table 1. Moreover, a range of POSS particles of various surface properties is commercially available. Depending on the nature of R, POSS can be classified into three types: (i) molecular silica (All R ligands are nonreactive), (ii) monofunctional POSS (one of the surface ligands is reactive), and (iii) multifunctional POSS (more than one surface ligands are reactive).

POSS can be incorporated into polymer matrices to improve various properties [12, 13]. For example, the incorporation of POSS into resin improved mechanical properties and surface finish. Depending on the nature of surface ligands, POSS particles can be incorporated into different polymer matrices [12]. The incorporation of POSS into polymer matrices can enhance various mechanical properties such as strength of modulus and rigidity, thermal stability without increasing weight of the materials (POSS-polymer composites remain lightweight). As a result, POSS-polymer nanocomposites are rapidly gaining interests in numerous commercial applications in the area of thermoplastics, thermosetting plastics, drug delivery, solid polymer electrolytes [14–17]. POSS are also used as additives to help other

Table 1 Various types of POSS surface ligands (R)

	R-type	Example of R
1	Acrylates	Acrylo
		Acryloisobutyl
2	Alcohols	Diol-isobutyl
		Cyclohexanediol
		Propanediol-isobutyl
3	Amines	Aminopropylisobutyl
		Aminopropylisooctyl
		Methyl-aminopropyl-isobutyl
4	Carboxylic acid	Maleamic acid isobutyl
		Octa maleamic acid
5	Epoxides	Epoxycyclohexyl
		Glycydyl
		Glycidyl isobutyl
6	Fluroalkyls	Trifluropropyl
		Trifluropropyl-isobutyl
7	Halides	Chlorobenzyl isobutyl
		Chlorobenzyl ethyl isobutyl
		Chloropropyl isobutyl
8	Methacrylates	Methacrylo isobutyl
		Methacrylate isobutyl
		Methacrylate ethyl
9	Alkane	Isooctyle
		Dodecaphenyl
		Phenylisobutyl
10	Olefins	Allylisobutyl
		Vinylisobutyl
11	PEG	PEG
12	Silanes	Octasilane
13	Silanol	Disilanol-isobutyl
		Trisilanolthyl
		Trisilanolisobutyl
14	Thyols	Mercaptopropylisobutyl
		Mercaptopropylisooctyl

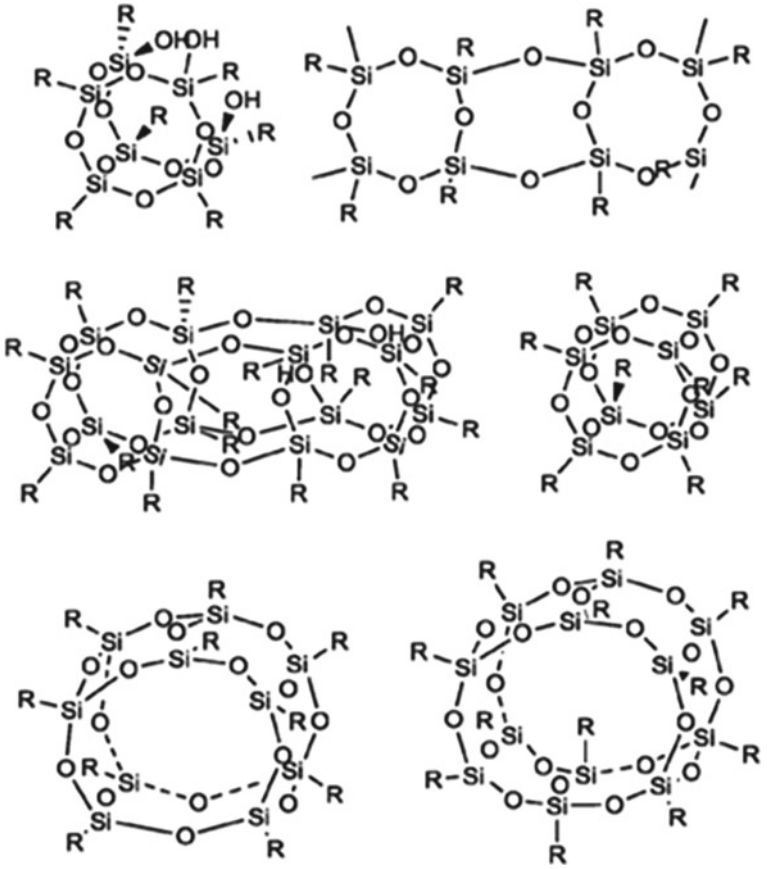

Fig. 1 Various chemical structure of polyhedral silsesquioxanes. Top left: partial cage structure; top right: ladder structure; middle left: random structure; middle right: T8; bottom left: T10; and bottom right: T12

nanoparticle dispersions in polymer matrices [18–20]. Moreover, POSS particles are environment-friendly, nonvolatile, and odorless, which are some additional benefits for using POSS.

The improvement of POSS-polymer composite properties lies in successful embodiment of POSS particles in polymer matrices without any macrophase separation. POSS can be incorporated in polymeric matrices in three different ways: (i) chemically cross-linking of POSS with polymer chains, (ii) in situ synthesis of POSS in side polymer matrices, and (iii) physical blending of POSS (synthesized ex situ) and polymer [12, 21]. Chemical cross-linking involves selective reaction between polymer chain and POSS active ligands and depends on active pair of polymer chain and POSS ligands. Therefore, the application of POSS is limited. On the other hand, in situ synthesis of POSS in polymeric matrices depends on the supply of chemical

which restricts amount of POSS particles in polymer matrices. For physical blending of POSS with polymer such restrictions do not exist. Physical blending depends on surface compatibility between POSS and polymers.

1.2 Polyamides

Polyamide (PA) is a family of polymers (also known as engineering plastics) which contain amide (–CONH) linkages along their molecular backbone. PA can broadly be classified into two types: (i) natural (various proteins) and (ii) artificial (nylon, aramide, etc.). Artificial PAs can be synthesized by condensation chemical reaction between and carboxylic acid group and amine group. Polyamide 6 (PA6) and polyamide 66 (PA 66) are two major types of commercial PAs (also known as nylon). PA6 is produced commercially by the polymerization of caprolactam. PA 66 is synthesized through polycondensation reaction of hexamethylene diamine and adipic acid. Several other commercial PAs are (i) PA 4,6 (poly(tetramethyleneadipamide)), (ii) PA 6.9 (poly(hexamethyleneazelamide)), (iii) PA 6.10 (poly(hexamethylenesebacamide)), (iv) PA 6.12 (poly(hexamethylenedodecanedioamide)), etc.

PA polymers possess various essential properties such as: (i) better chemical stability, (ii) good wear resistance, (iii) high strength. As a result, PAs are widely used in transport, automotive, textile, carpet, sportswear, etc., industries [22]. However, use of PAs without any modification is associated with many disadvantages such as (i) higher moisture absorption, (ii) poor notch toughness, (iii) bad dimensional stability. Therefore, the improvement of physical properties by incorporating nanosized filler POSS in PA matrices would be beneficial and attract significant attention of academics as well as industries. In this chapter, we discussed PA-POSS composite materials [23–26].

2 Polyamides-POSS Nanocomposites

2.1 Incorporation of POSS in Polyamides

Understanding the full potential of POSS-containing PA nanocomposites, the successful incorporation of POSS in PA matrices is needed without macrophase separation. POSS can be incorporated in PA matrices either by chemical cross-linking or by physical blending (melt blending or solvent blending). Incorporation by chemical cross-linking can be achieved via various complex polymer chemistries (such as coordination polymerization, ring-opening metathesis polymerization, free radical polymerization), and therefore, commercialization of such process is challenging. POSS particles are available with various surface properties, and the incorporation of

POSS in PA by physical blending is advantageous over chemical methods. However, the successful incorporation of POSS in PA matrices by physical blending without macrophase separation requires favorable POSS-PA surface interaction which is discussed in this section.

2.2 POSS-Polymer Interaction

For developing a suitable process for incorporation of POSS in PA or any other polymer matrices by physical blending (melt blending or solvent blending) without causing macrophase separation, it is critical to understand POSS-polymer surface interactions. In POSS-polymer systems, POSS-POSS, POSS-polymer, and polymer–polymer interactions are the three main surface interactions, which are present. The interplay of these three surface interactions determines the final POSS-polymer composites. Dominant POSS-POSS and polymer–polymer interactions would lead to aggregation of POSS particles and segregation of aggregated POSS particles toward the composite surface resulting macrophase separation. Favorable POSS-POSS interaction can lead to the formation of a network morphology [27, 28]. However, POSS-POSS interactions depend on their surface ligands. For example, triol-POSS forms dimer in solution through hydrogen-bonding interactions, whereas diol/monool-POSS did not form any dimer in solution [29].

Dominant POSS-polymer surface interactions result in successful incorporation of POSS in polymer matrices. The strength of POSS-polymer interactions determines the extent of reinforcement by POSS. For example, 10 wt% incorporation of more compatible trisilanolphenyl POSS in PA6 increased storage modulus from 1.3 GPa (neat polymer) to 1.96, while 10 wt% incorporation of less compatible octaisobutyl POSS in PA6 increased the storage modulus to 1.81 GPa [30]. Hydrogen-bonding interaction can increase the miscibility of POSS and results in successful incorporation of POSS in PA matrices. For example, octa-ammonimum POSS (OA-POSS) can form hydrogen bonds with N–H groups of PA6, and as a result, 5 wt% OA-POSS can be homogeneously dispersed in PA6 matrices [31].

POSS-PA surface interactions can be described by solubility parameters which are related to the enthalpy of mixing. A closer value of solubility parameters of POSS and PA indicates a favorable enthalpy of mixing. For example, a lower solubility parameter difference of 1.2 $(\text{cal/cm}^3)^{1/2}$ between PA6 and trisilanolphenyl POSS (Tsp-POSS) than that of PA6 and octaisobutyl POSS (Oib-POSS) (3.2 $(\text{cal/cm}^3)^{1/2}$) indicates that Tsp-POSS has better surface compatibility with PA6 than that of Oib-POSS. As a result, Tsp-POSS exhibited better dispersion in PA6 [30]. Therefore, solubility parameters can be used to determine the miscibility of POSS in PA and other polymers. Solubility parameters of PA6, aminopropylisobutyl POSS (apib-POSS), aminoisopropyl-isooctyl POSS (apio-POSS), and aminopropyl-phenyl POSS (app-POSS), and various other polymeric ligands and functional groups are presented in Table 2. Method for estimating solubility parameters was discussed elsewhere [32, 33]. POSS-polymer Flory–Huggins interactions parameter can also be used to

Table 2 Solubility parameters of PA and various POSS and POSS ligands

	δ_d ($J^{1/2}$ $cm^{-3/2}$)	δ_p ($J^{1/2}$ $cm^{-3/2}$)	δ_h ($J^{1/2}$ $cm^{-3/2}$)	δ ($J^{1/2}$ $cm^{-3/2}$)
PA6	15.9	34.6	13.4	18.0
Apib-POSS	17.5	0	0	17.5
Apio-POSS	18.6	0	0	18.6
App-POSS	19.2	1.5	0	19.3
-CH_3	19.49	0	0	19.49
-$C(CH_3)_3$	17.45	0	0	17.45
-$C(CH_3)_7$	18.59	0	0	18.59
-Phenyl	19.19	1.48	0	19.25
-$CH_{2\_}$)	17.36	0	0	17.36
-COO-	16.46	20.68	17.19	17.91
-CONH-	15.90	34.63	13.42	18.01

explain the surface compatibility and can help to determine whether a specific POSS will disperse in a particular polymer matrices or not. For example, aminopropyl-isobutyl POSS (AB-POSS) possess a more favorable surface interaction with PA6 (Flory–Huggins parameter $= -0.42$ cal/cm^3) and can be dispersed in PA6 uniformly up to 0.5 wt%. On the other hand, aminopropyl-isooctyl POSS (AO-POSS) and aminopropyl-phenyl POSS (AP-POSS) possess less attractive surface interactions with PA6 (Flory–Huggins parameters for PA6/AO-POSS and PA6/AP-POSS are -0.35 and -0.23 cal/cm^{-3}, respectively) and form POSS aggregates during melt mixing with PA6. Smaller Flory–Huggins interaction parameter suggests a more favorable thermodynamic favorable interaction.

3 PA-POSS Structure and Morphology

Physical properties of PAs and their composites are directly influenced by their microstructure and morphology. Therefore, it is important to understand how incorporation of POSS in PA can influence the structure and morphology of nanocomposites. Polyamide PA6 is a semi-crystalline polymer with two polymorphs: α and γ. α is thermodynamically stable phase and γ is kinetically trapped phase. The nature of hydrogen bonds between N–H and C=O is different for α and γ phases. Hydrogen bonds are formed between anti-parallel polymer chains in α phases, whereas in γ hydrogen bonds are formed between parallel chains. Also, lattice parameters are different for α and γ phases. For α phase, $a = 0.96$ nm, $b = 1.72$ nm, $c = 0.80$ nm, and $\beta = 67.5°$. For γ phase, $a = 0.93$ nm, $b = 1.69$ nm, $c = 0.48$ nm, and $\beta = 121.0°$. The incorporation of aminoisopropyle isobutyl POSS (APOSS) (0–5 wt%) by melt blending did not alter the crystal structure of α phase [31]. Similarly, the incorporation of glycidil-isobutyl POSS (G-POSS) in PA6 by melt blending did not show

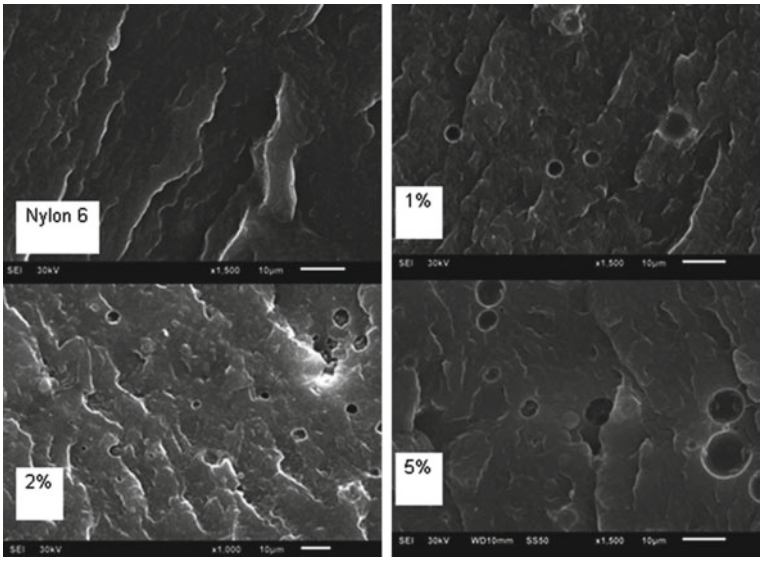

Fig. 2 SEM images of cross section of neat PA6 (top left), PA6 + 1% APOS (top right), PA6 + 2% APOSS (bottom left), and PA6 + 5% APOSS (bottom right). Images are adopted with permission from [37]. Copyright 2014 Elsevier

any significant influence on crystalline structure and degree of crystallinity [34]. On the other hand, the incorporation of POSS by chemical cross-linking in PA6 leads to crystalline phase transition from α to γ and degree of crystallinity decreased [35]. The incorporation of 5 wt% octaisobutyl POSS and trisilanolphenyl POSS in PA66 did not alter the polymer crystallinity [36]. The incorporation of OA-POSS in PA6 by solution blending also did not alter the crystalline structure (α phase) as well [31].

Morphology of melt blended PA6-aminopropylisobutyl POSS (AB-POSS) was studied using cross-sectional SEM [37]. AB-POSS phase separated and formed spherical aggregates in PA6 matrices (see Fig. 2). Number and size of phase-separated spherical aggregates increased with the increasing amount POSS in PA6. This phase separation suggests that AB-POSS is not very compatible with PA6, and at higher loading concentration, POSS formed spherical aggregates and phase separated. Different POSS with reactive and nonreactive side groups have been incorporated in PA6 matrices via synthetic methods where PA6 was synthesized in situ from ε-caprolactam in the presence of POSS [38]. In the presence of nonreactive apolar POSS, poor dispersion was obtained due to their poor interactions with polar PA6. In the case of POSS with reactive side groups, better dispersion of POSS in PA6 matrices was obtained where POSS was covalently bonded to PA6. POSS-containing PA6 composites were semi-crystalline, and degree of crystallinity decreases with increasing POSS content.

Uniform dispersion of POSS in PA or any other polymer matrices requires favorable surface compatibility. However, the surface compatibility is not sufficient which

can ensure the uniform dispersion of POSS in polymer matrices particularly when POSS is incorporated by melt blending due to higher viscosity of polymer melts. Depending on the processing type, POSS may disperse uniformly and form desired morphology which can provide better reinforcement or not. For example, the incorporation of AB-POSS in PA6 by injection molding could not provide better POSS dispersion in PA6 matrices; rather, it resulted in macrophase separation of spherical POSS aggregates (see SEM cross-sectional images Fig. 3, right) [39]. On the other hand, the incorporation of AB-POSS in PA6 by melt-spun technique provided better inclusion of POSS in PA6 matrix (see SME cross-sectional images Fig. 3, left). Composites fiber made by melt spun exhibited elongated POSS morphology in PA6 below 5 wt% POSS loading. However, above 5 wt% POSS loading, melt-spun technique could not provide better POSS dispersion. POSS particles formed spherical aggregates and macrophase separated above 5 wt% POSS loading. In melt-spun technique, a combination of shear and favorable PA6-POSS surface interactions helps forming elongated POSS structures inside amorphous POSS domain.

Polyamides are widely used as membranes materials, and therefore, it is important to investigate the thin-film surface and bulk structure. THF solvent cast PA6 film exhibited porous surface structure with microvoids (see Fig. 4) [40]. Film prepared under 55% relative humidity contains pores of diameter in the range of 5–7 μm. As RH increased, the pore size also increased. In the presence of moisture, water vapor condenses on PA6 film, coalesces, and forms a disordered array of droplets which resulted in the formation of disordered arrays of pores in PA6 film. At higher RH, water droplet size increased leading to larger pore size. When AB-POSS was incorporated in PA6 film, film surface becomes rougher (see Fig. 4 Bottom row). The presence of AB-POSS disrupts the water distribution resulting in an hetereogeneous smaller-sized pores. Introduction of AB-POSS also makes film more porous [40]. Similar impact of AB-POSS on pore film structure was visualized at cross-sectional SEM (see Fig. 5).

3.1 Morphology of POSS-Containing PA-Polymer Blends

To achieve desired polymer properties, PA often blends with another polymer. For example, PA is blended with methyl methacrylate-butadiene-styrene copolymer to achieve desired toughness [41]. Therefore, POSS-containing nanocomposites of PA6-polymer blend merit a discussion. The incorporation of epoxycyclohexyl-POSS in poly(2,6-dimethyl-1,4-phenylene-oxide)/PA6 (PdMPO/PA6) blends via melt mixing leads to morphological transformation from a droplet/matrix to co-continuous morphology [42] (see SEM images in Fig. 6). PdMPO phase (darker domains in SEM images) tends to coalesce during melt mixing due to their higher viscosity than PA6. As a result, equal mixture of PdMPO/PA6 blend exhibits a droplet–matrix morphology where PA6 formed the matrix and PdMPO formed the droplets (diameter ~0.67 μm) (see Fig. 6a). PdMPO droplet size decreases to 0.2 μm due to the incorporation of 2 wt% of POSS (see Fig. 6b). POSS particles localize at PdMPO-PA6

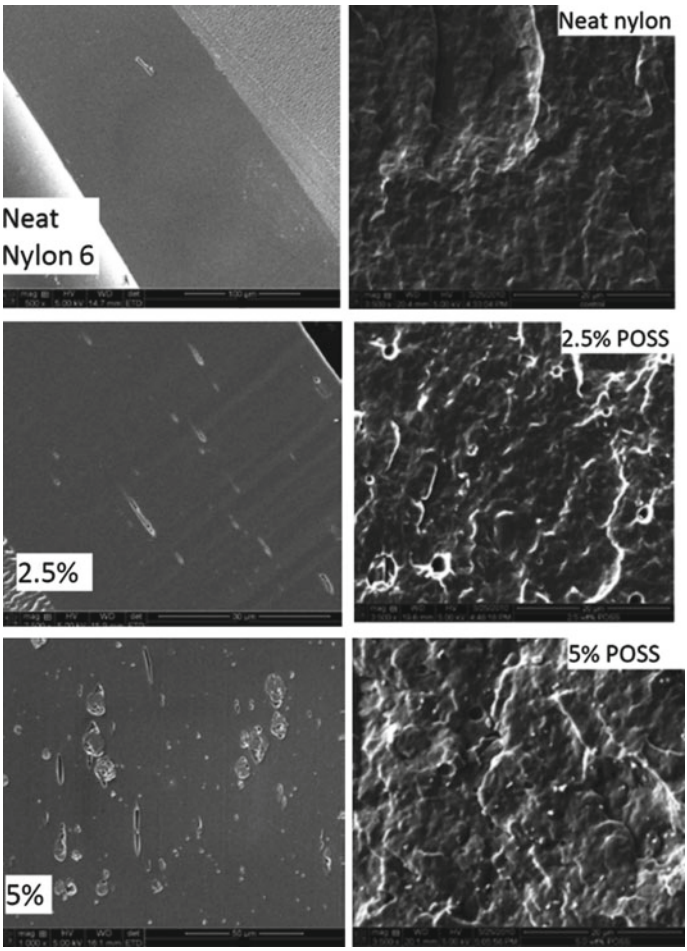

Fig. 3 Effect of processing and POSS loading on POSS dispersion. Aminopropylisobutyl-POSS was incorporated in PA6 by melt spin (left side) and by injection molding (right). SEM images are adopted with permission from [39]. Copyright 2012 American Chemical Society

interfacial regions, and as a result, PA6-PdMPO interfacial tension decreases leading to decrease in PdMPO droplet size.

As amount on POSS increased in PA6-PdMPO blend, more POSS particles localize in PA6-PdMPO interfacial region which further decreased the interfacial tension, break the complex cross-linked morphology, and generated new co-continuous morphology. 4 wt% POSS-containing PdMPO-PA6 blend composite exhibited a co-continuous morphology (see Fig. 6c) [42]. Further increase of POSS to 6 wt% in PA6-PdMPO blend, co-continuous morphology becomes coarse and rough (see Fig. 6d). On further increase of POSS content above 6 wt%, PA6 starts cross-linking to POSS, and melt viscosity of PA6 increased and becomes more viscous than PdMPO.

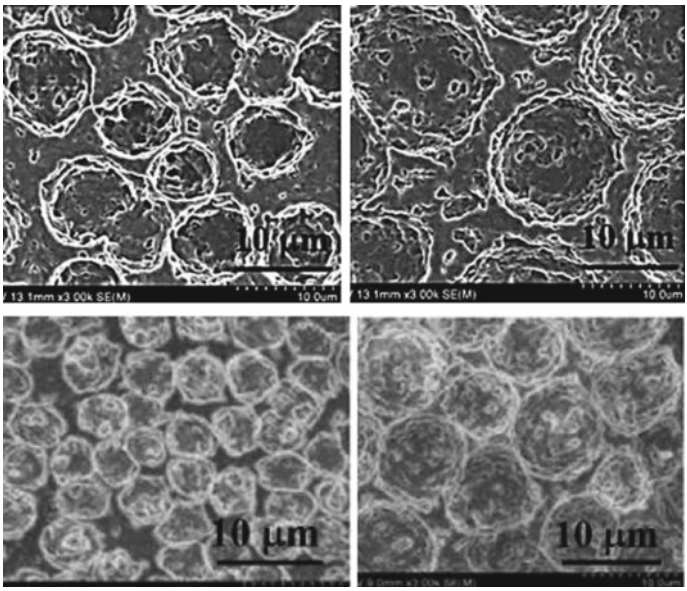

Fig. 4 Effect on AB-POSS incorporation of surface morphology of PA6 film under different relative humidity. Top left: PA6 film, 55% humidity; top right: PA6 film, 85% humidity, bottom, left: PA6 + AB-POSS film, 55% humidity, bottom, right: PA6 + AB-POSS film, 85% humidity. Images are adopted from [40]. Copyright 2016 Royal Society of Chemistry

As a result, PA6 starts coalescing during melt mixing at 8 wt% POSS loading to an inverse droplet–matrix morphology where PA6 formed dispersed droplets and PdMPO formed the matrix (see Fig. 6e). Note that POSS-containing PA6-PdMPO co-continuous morphology exhibits superior mechanical properties compared to droplet morphologies which is further discussed in next section.

4 PA-POSS Functional Properties

In the previous section, we discussed the structure and morphology of PA-POSS composites. In this section, we discuss different functional properties of PA-POSS composite materials.

4.1 Mechanical Properties

Mechanical properties (Young's modulus, tensile strength, elongation break, etc.) of PAs can be improved by incorporating POSS which can reinforce the polymers [41].

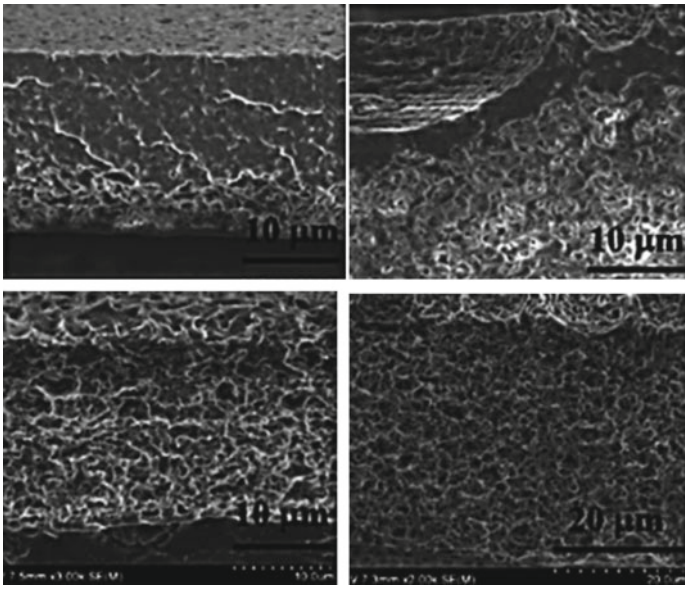

Fig. 5 Influence of AB-POSS incorporation on PA6 film cross-sectional morphology under different relative humidity. Top left: PA6 film, 55% humidity; top right: PA6 film, 85% humidity, bottom, left: PA6 + AB-POSS film, 55% humidity, bottom, right: PA6 + AB-POSS film, 85% humidity. Images are adopted from [40]. Copyright 2016 Royal Society of Chemistry

The mechanical property improvement of POSS-containing PA composites depends on several parameters such as (i) POSS surface property (that determine state of the POSS dispersion), (ii) POSS loading, (iii) morphology, (iii) shape and size of the aggregates, and (iv) processing type.

The POSS-PA surface interactions play a crucial role in improving mechanical properties. Favorable surface interaction can help successfully disperse POSS in PA matrices and reinforce mechanical properties of PA-POSS composites. On the other hand, unfavorable PA-POSS surface interactions can lead to POSS aggregation and phase separation.

Young's modulus of POSS-containing PA6 composites can increase up to 2 wt% POSS loading as shown in Fig. 7, left, and above 2.5 wt% POSS loading, Young's modulus starts decreasing. The mechanical property improvement below 2.5 wt% POSS loading is related to the longitudinal organization of POSS in PA6 fibers. Beyond 2.5% loading, POSS starts forming spherical aggregates. Elongated POSS aggregates reinforce polymer matrices and can change the flexibility of the polymer chains located along the particle assembly. As a result, Young's modulus of PA6-POSS composites starts to increase. However, the increase in Young's modulus is not equivalent to the arithmetic average of Young's modulus of PA6 and POSS. Similar increase in stress yield is also reported for aminoisopropyle-POSS-containing PA6 composites produced by melt-spinning process [39]. Incorporation of octaisobutyl

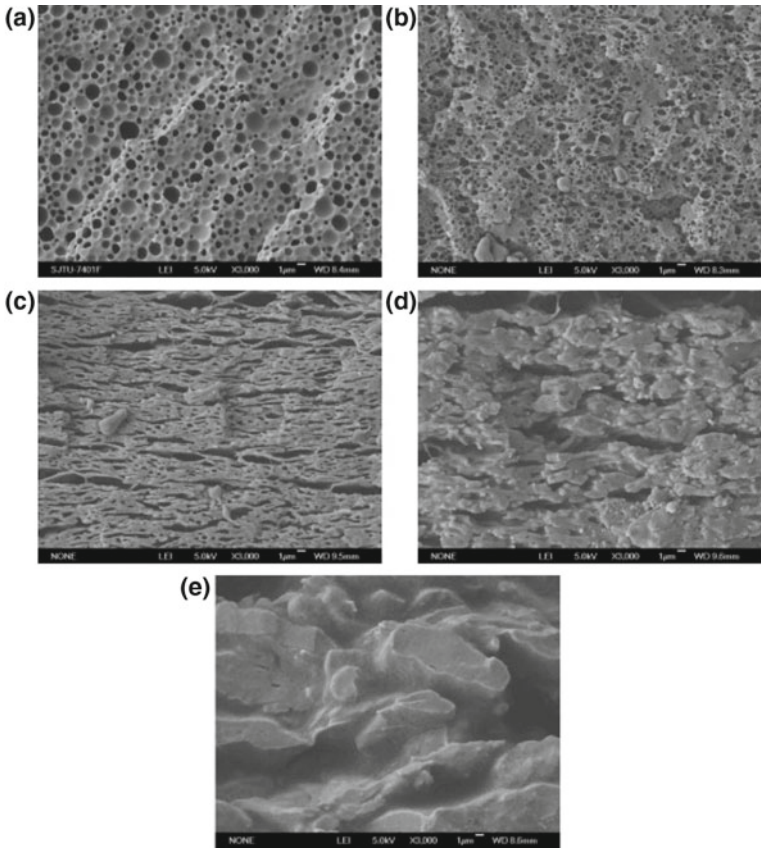

Fig. 6 Influence of POSS incorporation on 50:50 PA6-PdMPO blend (PA6 = polyamide 6 and PdMPO = poly(2,6-dimethyl-1-4-phenyl oxide). **a** 0 phr POSS, **b** 2 phr POSS, **c** 4 phr POSS, **d** 6 phr POSS, **e** 8 phr POSS. Reproduced with permission from [42]. Copyright 2009, Elsevier

POSS and trisilanol-phenyl POSS in PA66 enhances mechanical properties such as elongation at break and stiffness [36].

The processing condition can impact the degree POSS dispersion which influences the mechanical properties of nanocomposites. For example, the incorporation of aminoisopropyl-POSS in PA6 (nylon 6) by injection molding decreases mechanical properties (see Fig. 7), and thermal properties remained unchanged. The decrease in mechanical properties is attributed to spherical aggregates formation by POSS. On the other hand, incorporation of aminoisopropyl-POSS (up to 2.5% loading) in PA6 by melt-spinning process lead to an increase in mechanical properties (see Fig. 7) [39]. Chemical cross-linking of POSS to PA6 results to a decreases in the stiffness of PA6 due to decrease in degree of polymer crystallinity [35]. The increase in stiffness by POSS reinforce is overwhelmed by the loss of stiffness due to the decrease in degree of crystallinity.

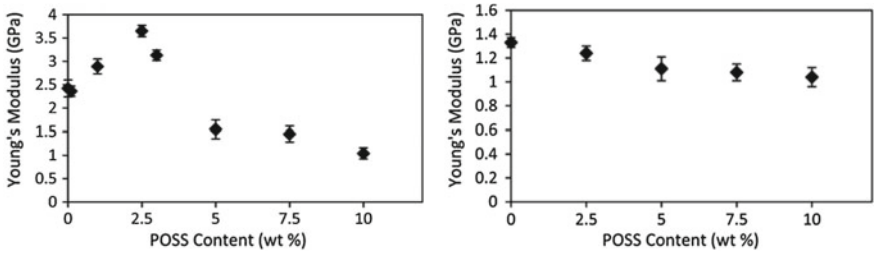

Fig. 7 Effect of processing and POSS loading on mechanical properties of PA6-POSS composites. Aminoisopropyl-POSS was incorporated in PA6 by melt spin (left side) and by injection molding (right). (Figures were reproduced from [39]. Copyright: American Chemical Society 2012.)

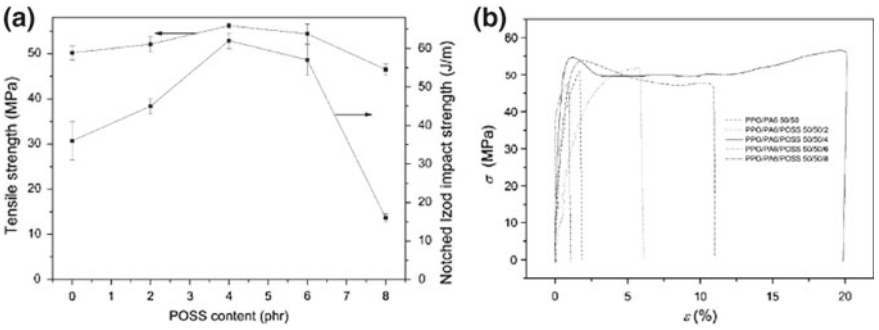

Fig. 8 Influence of POSS incorporation in PdMPO-PA6 polymer blends on mechanical properties: **a** tensile strength and notched izod impact strength; **b** stress–strain curve. Reproduced with permission from [42]. Copyright 2009, Elsevier

POSS-containing PA6-PdMPO composites possess superior tensile strength and notched izod impact strength (see Fig. 8a) [42]. Tensile strength and izod notched impact strength increase with increasing POSS concentration, and reach to maximum (55.2 MPa and 61 J/m, respectively) at around 4 wt% POSS loading, and above 4% POSS loading start decreasing. These variations in mechanical properties are related to the morphology of POSS-containing PA6-PdMPO campsites. At lower POSS loading, PA6-PdMPO form a droplet morphology (PdMPO droplets are dispersed in PA6 matrix). As POSS concentration increases, the drop morphology transforms to a co-continuous morphology which exhibits very high tensile strength and notch izod impact strength. On further increase in POSS concentration, co-continuous morphology transforms to inverse droplet morphology (POSS-containing PA6 formed droplets in PdMPO matrix). As a result, both tensile strength and notch izod impact strength decrease. The incorporation of POSS in PA6-PdMPO blends also help to increase elongation at break as suggested by stress–strain curve (see Fig. 8b) [42]. PA6-PdMPO blends show brittle break when no POSS is incorporated and more than 8 wt% POSS is incorporated.

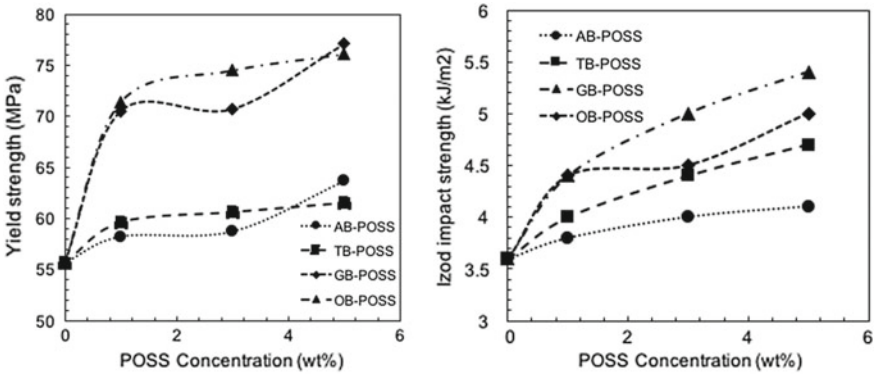

Fig. 9 Influence of amount and types of POSS on mechanical properties of PP-PA6 blends. Left: yield strength; right: izod impact strength. Data adopted from [43] and plotted

Incorporation of four different types of POSS (aminopropyl-isobuty POSS (AB-POSS), trisilanol-isobuty POSS (TB-POSS), glycidyl-isobuty POSS (GB-POSS), and octaisobuty POSS (OB-POSS)) in polypropylene (PP)-PA6 blend helps to improve the yield strength and izod impact strength irrespective of POSS types (see Fig. 9) [43]. General improvement in yield strength and izod impact strength due to the incorporation of POSS in PP-PA6 blends originates from the improvement of interfacial adhesion by POSS localization. PP-PA6 blends formed droplet-type morphology where larger PA6 droplets disperse in PP matrix. POSS particles localize at PP-PA6 interface and improvise interfacial adhesion, and PA6 droplet size decreases resulting in improved yield strength and izod impact strength. Yield strength and izod impact strength improvement depends on the POSS type and GB-POSS and OB-POSS exhibited higher improvement over AB-POSS and TB-POSS at a given POSS loading. This finding suggests that GB-POSS and OB-POSS are better candidates in providing PP-PA6 interfacial reinforcement over AB-POSS and TB-POSS.

4.2 Thermal Degradation

Poor thermal stability of polymeric materials often limits their applications to high-temperature applications due to their poor thermal stability. The incorporation of POSS nanofillers into polymeric matrices can enhance the thermal stability of polymeric materials due to the rigid POSS case. POSS-polymer interfacial interactions, cross-linking, and amount of POSS control the thermal stability of POSS-polymer thermal stability. For example, the incorporation of 0.5 wt% AB-POSS in nylon 6 increased the thermal decomposition temperature by about 10 °C (see Fig. 10) [44]. On further increase in AB-POSS, the thermal degradation temperature starts decreasing. When AB-POSS was replaced with less compatible AO-POSS or AP-POSS,

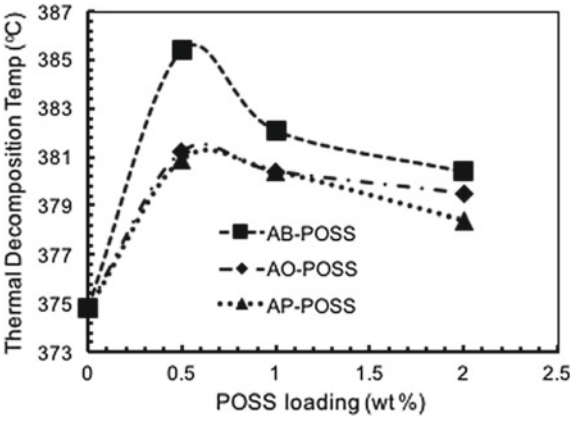

Fig. 10 Effect of various POSS on thermal degradation temperature of PA6-POSS composites. Data adopted from [44] and plotted

thermal degradation temperature increased by about 6 °C at 0.5 wt% POSS loading (see Fig. 10). On further increase in AO-POSS or AP-POSS, thermal degradation temperature starts decreasing similar to AB-POSS. The incorporation of octaphenyl POSS and octaamminophenyl POSS in PA66 also increases the decomposition temperature of PA66 [45].

4.3 Glass Transition Temperature

Glass transition temperature (T_g) is a characteristic of amorphous polymer or polymeric material above which hard glassy polymer turns into viscous or rubbery polymer. T_g is related to the rigidity of polymer chains and an important polymer property. PA is semi-crystalline polymer, and T_g is the property of disorder amorphous part of PA. The presence of nanoparticles in polymer matrices can influence the mobility of adjacent polymer chain and thus can influence the T_g. The incorporation of POSS that is attractive to the polymer surface can increase the glass transition (T_g) temperature as well as storage modulus [44]. T_g indicates the mobility of polymer chains, and an increase in T_g suggests that polymer becomes less mobile and more rigid. The incorporation of POSS particles, which are attractive to polymer, can interact favorably with polymer surface and arrest the mobility of polymer, and as a result, T_g increases. For example, incorporation of AB-POSS and AP-POSS in nylon 6 matrix increases the T_g as well as the storage modulus [44]. Also, the incorporation of AB-POSS and AP-POSS in nylon 6 increases the cross-linking density which also contributes partially to the storage modulus. T_g of a POSS-containing nanocomposites depends on several factors such as particle–polymer, particle–particle interactions, and amount of POSS. The incorporation of POSS in dimer fatty acid polyamide membrane prepared by solvent cast method exhibits an increase in T_g for 57 to 62 °C at about 20 wt% POSS loading [46].

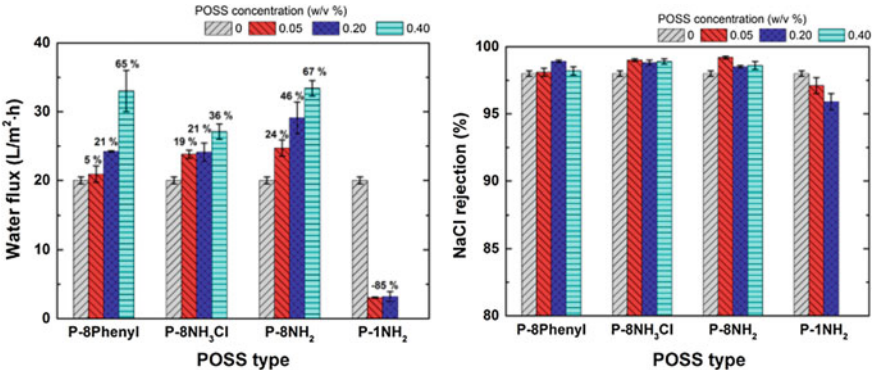

Fig. 11 Influence of 8Ph, $8NH_3Cl$, $8NH_2$, and $1NH_2$-POSS on water flux (left) and **b** NaCl rejection (right) of PA6 membranes. Figure adopted with permission from [53]. Copyright: Elsevier 2015

4.4 Membrane Properties

Polyamides and their composites are widely used in membrane technology which find many commercial applications in desalination [47–51], gas separation [52], biological applications [46], etc. Commercial reverse osmosis membranes consist of two major components: (i) active polyamide layer that is selective and (ii) pours support. The incorporation of POSS in PA layers could improve desired membrane properties and increased membrane performance (faster transport of desired material through the membrane and rejection of unwanted material). The incorporation of nanosized filler-like POSS into polyamide membranes can improve the water filtration performance of PA6 membranes. The incorporation of hydrophobic POSS (octaphenyl POSS (8Ph-POSS), octaammonium POSS ($8NH_3Cl$-POSS), octaaminophenyl-POSS ($8NH_2$-POSS), and aminopropylisobutyl POSS ($1NH_2$-POSS)) into PA6 thin-film membrane increased water flux and salt rejection (see Fig. 11) [53]. The incorporation of different hydropobic POSS in PA6 thin-film membranes increased free volume. Improved gas diffusivities were reported due to POSS incorporation in apliphatic polyamide membranes [52].

Fatty acid polyamides can be used in membrane applications. The incorporation of POSS in such biomembranes can improve bionanocomposite properties. A series (19) of bionanocomposite membranes which consist of dimer fatty acid polyamide in the presence of various POSS loading were investigated for structure, surface morphology (see Fig. 12), and membrane property (permeability) [46]. A series of characterization suggests that incorporation of POSS in PA nanobiocomposite membranes increased surface roughness, membrane density and decreased surface free energy and free volume. The incorporation of POSS in fatty acid polyamide membrane decreased permeability of various gases: N_2, O_2, and CO_2. In addition, the incorporation of POSS in PA membrane increased the permselectivity. This would

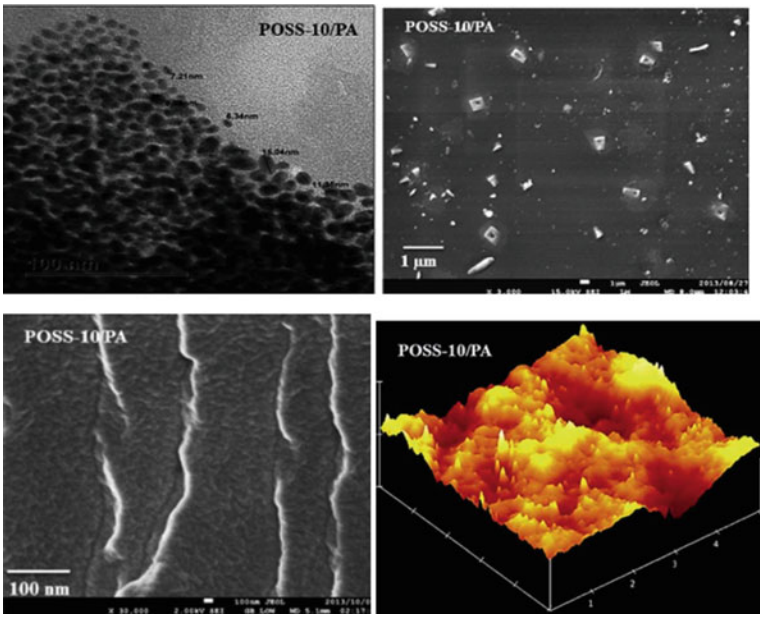

Fig. 12 10 wt% POSS-containing fatty acid polyamide bionanocomposite. Top left: TEM; top right: surface SEM; bottom left: cross-sectional SEM; bottom right: 3D AFM image. Images are adopted from [46]. Copyright 2015 Royal Society of Chemistry

enable POSS-containing nanocomposite membranes in various industrial applications such as food packaging.

4.5 Fire Retardancy

Successful application of POSS-containing PA composites requires superior fire retardant. This is particularly important for polyamide materials used for automobile parts such as tank, fuel line. Halogen is used as flame retardant, but due to environment regions, halogens are not useful as fire retardant. Si–O in POSS can provide flame retardancy, and therefore, POSS is a suitable candidate which can impart fire retardancy in POSS-containing PA composites [54–58]. The incorporation of 3.3 wt% in PA12 by melt compounding improved fire retardancy. Peak heat release rate decreases from 1635 to1521 kW/m^2 [56]. However, a combination of carbon nanotube and POSS incorporation in PA12 exhibited dramatic improvement in fire retardancy; peak heat release rate decreased from 1653 to 425 kW/m^2 [56]. 9,10-dihydro-9-oxa-10-phosphaphenanthrene-0-oxide POSS (DOPO-POSS) was incorporated in diglycide ether of bisphenol A (DGEBA) cured by PA650 or aromatic 4,4-diaminodiphenylsulphone (DDS) [57]. The heat release rate curve for

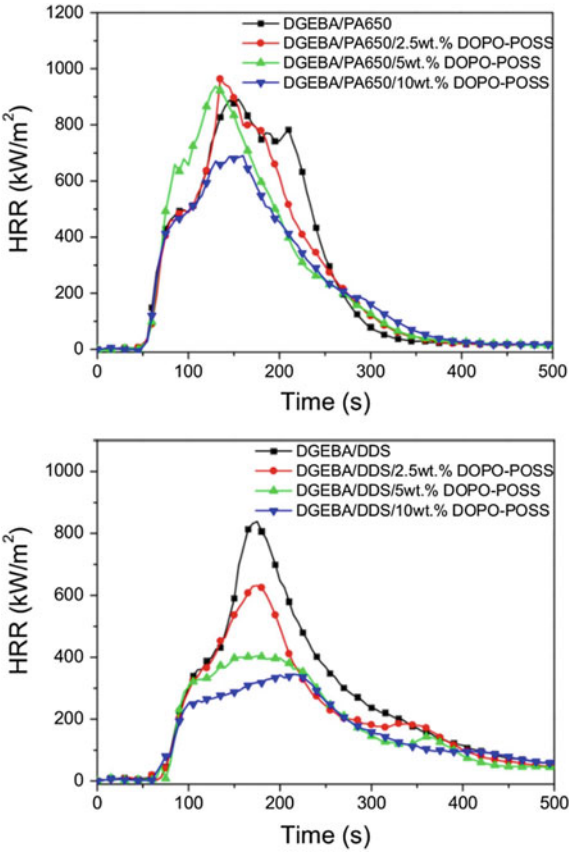

Fig. 13 Influence of DOPO-POSS on heat release rate of polyamide (top: PA650, bottom: DDS) cured DGEBA-DOPO-POSS nanocomposites. Reproduced with permission from [57]. Copyright 2012 Elsevier

these polyamide-cured nanocomposites (see Fig. 13) exhibits that peak heat release rate decreased with increasing amount of DOPO-POSS. The influence of PA650 cured composites is subtle. Also, incorporation of DOPO-POSS in polyamide-cured composites showed blowing out effect.

A combination of trisilanophenyl-POSS (T-POSS) and nanoclay inclusion in PA6 exhibits improved fire retardancy. In the presence of POSS, at higher temperature, POSS might transform to glassy material and can improve flame retardancy. Clay silicate can add further improvement on fire retardancy by adding an additional layer on silica glass. The incorporation of 15 wt% T-POSS in PA6-clay composites provides substantial fire retardancy improvement over PA6-clay composites. POSS provides a uniformly distributed composite (see the TEM image in Fig. 14) which helps improve fire retardancy [59]. POSS and clay seem to synergize their fire retardant properties. This idea was further taken a step forward where clay and POSS were combined and cross-linked to make clay-POSS surfactant line molecule. Further, the incorporation of POSS–montmorillonite clay surfactant in PA6 exhibits improved thermal and fire safety properties.

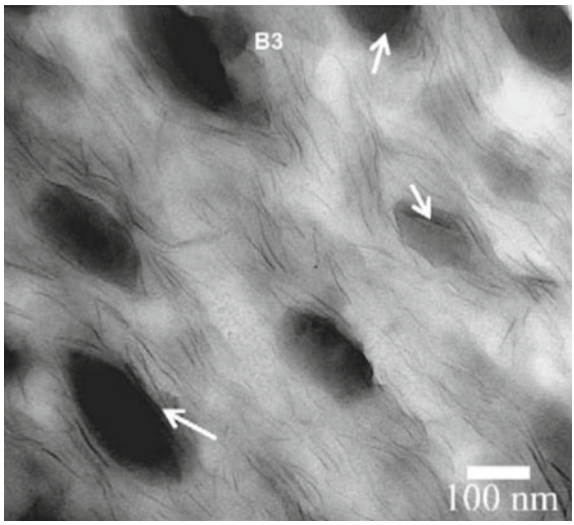

Fig. 14 Fine dispersion of T-POSS and clay in PA6 matrix. Adopted with permission from [59]. Copyright 2009 Elsevier

4.6 Rheological Properties

Rheological properties of polymer melt and POSS-containing polymer melts are crucial for processing. Therefore, it is essential to understand how POSS can be used to modulate rheological properties of polymer. Polymer viscoelastic properties are highly temperature dependent. At 225 °C, neat PA6 melt exhibits a constant dynamic modulus [60]. At higher temperature (285 °C), dynamic modulus changes with time. The incorporation of AB-POSS in PA6 increases the storage modulus with increasing AB-POSS concentration [60] (see Fig. 15). The plateau formation temperature also increased with AB-POSS incorporation. The tan δ is highly sensitive to POSS melting point ~267 °C where a second endothermic transition took place. At ~267 °C, slope of the tan δ decreases significantly for more than 1 wt% POSS-containing PA6 composites. This indicates that melting of POSS particles modifies the structure of PA6-POSS melt, and as a result, rheological properties changed. At lower POSS concentration (<3 wt%), POSS-polymer interactions lead to decrease the chain entanglement resulting in a lower viscosity of the composite. At relatively higher POSS loading (>3 wt%), the presence of solid POSS particles becomes significant, reinforces polymer, and as a result increases the storage modulus.

The rheological behavior of AB-POSS-containing PA6 multilayered film is similar to that of AB-POSS-containing PA6 blend. The influence of AB-POSS incorporation in PA6 think film was reported [61]. At lower temperature, the influence of AB-POSS on rheological properties is very subtle. At lower frequency, 5 wt% AB-POSS-containing PA6 film exhibited an increase in G′ and plateau which indicates the presence of POSS aggregates. At higher temperature and lower POSS loading (2.5 wt%), loss modulus of the film decreases. POSS particles interact favorably with PA6 resulting in a decrease in polymer entanglement and increase in free volume

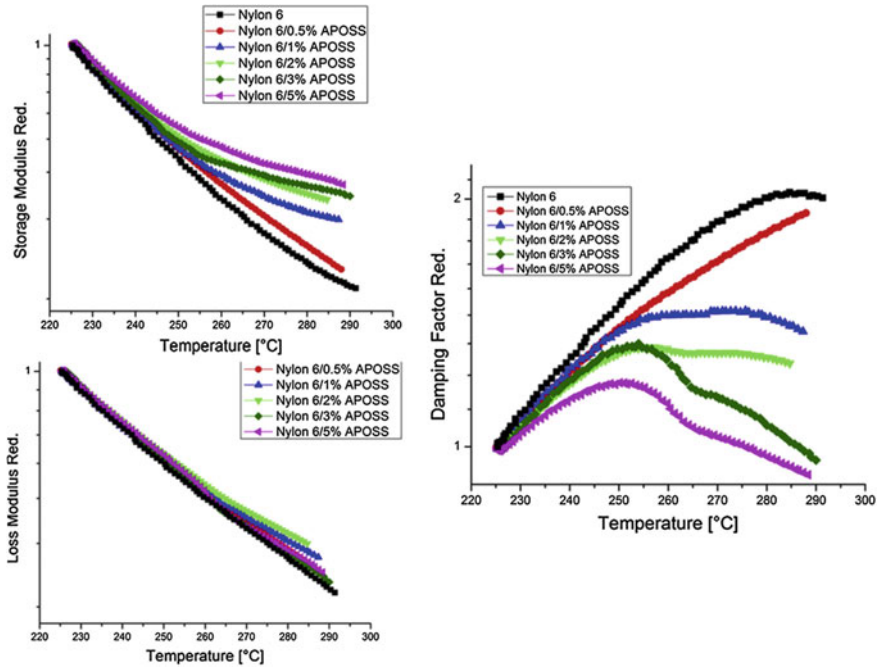

Fig. 15 Effect of POSS incorporation in PA6 on rheological properties. Reproduced with permission from [60]. Copyright 2014 Elsevier

which results in decreasing viscosity. At higher temperature and higher POSS loading (5 wt%), loss modulus increases. At higher concentration, POSS particles form aggregates which increased the G″.

5 Processing of POSS-Polymer Nanocomposites

In-depth understanding of the property improvement by POSS incorporation in polymers requires suitable processing method which can uniformly distribute POSS particle in desired location. POSS can be incorporated in polymer matrices by two ways: (i) chemical cross-linking and (ii) physical blending [12].

In the chemical cross-linking approach, POSS particles are covalently bonded with polymer either by grafting reaction or polymerization. Monofunctional POSS can bind covalently with polymer and form POSS-polymer nanocomposites. On the other hand, multifunctional POSS can react with reactive monomer and form network POSS-polymer composites. Chemical cross-linking provides precise control of nanoparticles distribution in polymer particles. However, chemical cross-linking

involves complex chemistry which can pose serious challenges for commercialization [13].

The incorporation of POSS in polymer by physical blending, on the other hand, is advantageous over chemical cross-linking. Physical blending processes are fast, versatile, cost-effective, and easy to handle. The incorporation of POSS particles in polymer by physical blending requires favorable POSS-polymer surface interactions which are noncovalent in nature (van der Waals, hydrogen-bonding, polar, electrostatic, etc.). Strong particle–particle interactions often lead to particle aggregation and macrophase separation. Therefore, proper processing for physical blending is essential. Physical blending is of two types: (i) melt blending and (ii) solvent blending.

Incorporation POSS by melt mixing requires melting of polymers and mixing by applying high shear. Twin-screw extruder is one of the melt compounding techniques used for processing of thermoplastics. However, polymer melt viscosity is very high, and movement of POSS particles in polymer melt is very slow, and equilibration is difficult. POSS forms aggregates and macrophase separates. Also, POSS-containing polymer nanocomposites end up with kinetically trapped condition due to slow equilibration.

In case of solvent blend process, both polymer and POSS particles are dissolved in a suitable solvent; for example, THF is widely used for PA6 [62]. Dissolved polymer is allowed to mix well with POSS dispersion. Once, polymer and POSS particles are mixed well, solvent cast leads to final POSS-containing polymer nanocomposites. The incorporation POSS in polymer by solvent blending has several advantages over chemical cross-linking and melt mixing such as very fast equilibration (no kinetically trapped product), ease of processing, no heat treatment (problem of thermal degradation is absent), and cost effectiveness. However, solvent cast has one disadvantage of remaining residual solvent.

6 Other Polymer-POSS Nanocomposites

6.1 POSS-Homopolymer Nanocomposites

In general, polymer lacks thermal stability and mechanical strengths which restricted their applications in severe conditions. Reinforcement of polymer by incorporating POSS can improve both mechanical strengths and thermal stability, which make them beneficial for several other severe conditions. Property enhancement of POSS-containing polymer composites depends on (i) polymer-POSS surface interactions, (ii) amount of POSS, (iii) cross-linking, (iv) special organization of POSS in polymer matrices such as elongated morphology. The incorporation of POSS in epoxy resins exhibits improved thermal stability [63]. The presence of POSS can hinder polymer chain mobility and increase glass transition temperature [64]. POSS incorporation in various polymers can improve Young's modulus, strain, stress,

elongation at break, izob impact strength, etc. POSS particles are inert in nature and are biocompatible which make them an ideal candidate for nanobiocomposites. POSS-containing nanobiocomposites can find applications in dental implant, drug delivery, tissue engineering, etc. [65, 66]. The incorporation of methyl functionalize POSS in polyvinyl chloride decreases the brittleness of the polymer [9]. Inclusion of POSS in poly(methyl methacrylate) helps improving their thermal stability [67]. POSS-containing polystyrene membranes show improved gas selectivity [68]. The incorporation of POSS in polyurethane provides superior mechanical behavior, hydrophobicity, and barrier property [69]. POSS-containing polymer nanocomposites possess several nanoscale structural and functional features which are not found in conventional composites.

6.2 POSS-Block Copolymer Nanocomposites

Amphiphilic block copolymer can self-assembled into order nanostructures which can be used for controlling POSS dispersion, location, and orientation in polymer matrices. Incorporation of octaphenol-POSS in ordered lamellar structure of poly(caprolactone)-poly(4-vinyl pyridine) (PCL-P4VP) block copolymer results order-to-order phase transitions such as cylindrical hexagonal-to-spherical cubic with increasing POSS loading [70]. The incorporation of octamaleamic acid and octaaminophenyl-POSS with solid poly(ethylene oxide)-poly(propylene oxide)-poly(ethylene oxide) PEO-PPO-PEO block copolymer causes disorder-to-order phase transition [71]. Depending on the amount of POSS, various ordered structures such as cylindrical hexagonal (50% POSS loading) and spherical cubic (70 wt% POSS loading) are observed. Similar disorder-to-order phase transition occurs when PEO-PPO-PEO block copolymer is dissolved in water.

PEO-functionalized POSS is incorporated in hexagonal structure of solvated PEO-PPO-PEO block copolymers. PEO-POSS has a favorable surface interaction with PEO-rich domains which help localization of PEO-POSS in PEO-rich domains. Hexagonal structure of solvated PEO-PPO-PEO remained stable up to 15 wt% of PEO-POSS loading [21]. Beyond 15 wt% PEO-POSS loading, structure transforms from hexagonal to lamellar order-to-order structural transition took place. The incorporation of tetramethylammonium-POSS in hexagonal structure of hydrated nonaethyl glycol dodecyl ether ($C_{12}EO_9$) remains stable up to 5 wt% POSS loading.

Chemical cross-linking of phenyl-POSS on polybutadiene block of polystyrene-polybutadiene-polystyrene (SBS) block copolymers led to decrease in the degree of block segregation [72]. This decrease in degree of block segregation results in a decrease in lattice parameter of ordered SBS structure. Phenyl-POSS displays a favorable surface interaction with polystyrene which decreases the incompatibility between polybutadiene and polystyrene; thus, degree of block segregation decreases. When phenyl-POSS is substituted by cyclopentyl-POSS or

cyclohexyl-POSS, or cyclohexenyl-POSS, effect of POSS on polybutadiene–polystyrene interface becomes insignificant.

7 Summary

This chapter presents the recent development of POSS-containing polyamide nanocomposites. POSS-PA nanocomposites exhibit improved structural and functional features which are not displayed by conventional PA composites. POSS particle possesses hybrid structure which contains a rigid silica core which is well defined and monodisperse. Diameter of POSS particles is typically in the range of 1–3 nm which is smaller than polymer radius of gyration.

Various POSS types and their influence on PA structure and functional properties were discussed with specific examples. POSS-containing PA composites can be obtained by chemical cross-linking, melt blending, or solvent casting method. Favorable interaction of POSS with PA enables physical blending (both melt mixing and solvent cast) feasible. POSS having surface functional group attractive to PA surface can distribute uniformly on PA matrices, and reinforces polymer. On the other hand, POSS with less attractive surface functional group can aggregate and cause macrophase separation without reinforcing polymer.

Incorporation of POSS in PA can improve several functional properties such as mechanical, rheological, thermal degradation, rheological, and membranes. Properties of POSS-containing PA nanocomposites depend on the state of POSS dispersion and composite structure. Further investigations on PA nanocomposites are required to gain deeper understanding of structure–property relations which will provide design rule for new materials. The incorporation of POSS would facilitate improved PA products in broad range of fields such as automobile, food packaging, reverse osmosis.

Acknowledgements Discussion and deliberation with Mr. Andrew Bodratti and Dr Swarup China during manuscript preparation were very helpful. Author gratefully acknowledges their contributions.

References

1. Sarkar B, Alexandridis P (2015) Block copolymer-nanoparticle composites: structure, functional properties, and processing. Prog Polym Sci 40:33–62
2. Balazs AC, Emrick T, Russel TP (2006) Nanoparticle polymer composites: where two small worlds meet. Science 314:1107–1110
3. Jancar J, Douglas JF, Starr FW, Kumar SK, Cassagnau P, Lesser AJ, Sternstein SS, Buehler MJ (2010) Current issues in research on structure–property relationships in polymer nanocomposites. Polymer 51:3321–3343
4. Paul DR, Robeson LM (2008) Polymer nanotechnology: nanocomposites. Polymer 49:3187–3204

5. Crosby AJM, Lee J-Y (2007) Polymer nanocomposites: the “nano” effect on mechanical properties. Polym Rev 47:217–229
6. Vaia RA, Giannelis EP (2001) Polymer nanocomposites: status and opportunities. MRS Bull 26:394–401
7. Winey KI, Vaia RA (2007) Polymer nanocomposites. MRS Bull 32:314–319
8. Alexandre M, Dubois P (2000) Polymer-layered silicate nanocomposites: preparation, properties and uses of a new class of materials. Mater Sci Eng Rep 28:1–63
9. Cordes DB, Lickiss PD, Rataboul F (2010) Recent developments in the chemistry of cubic polyhedral oligosilsesquioxanes. Chem Rev 110:2081–2173
10. Shea KJ, Loy DA (2001) Bridged polysilsesquioxanes. molecular-engineered hybrid organic – inorganic materials. Chem Mater 13:3306–3319
11. Lickiss PD, Rataboul F (2008) Fully Condensed polyhedral oligosilsesquioxanes (POSS): from synthesis to application. Adv Organomet Chem 57:1–116
12. Ayandele E, Sarkar B, Alexandridis P (2012) Polyhedral oligomeric silsesquioxane (POSS)-containing polymer nanocomposites. Nanomaterials 2:445–475
13. Kuo S-W, Chang F-C (2011) POSS related polymer nanocomposites. Prog Polym Sci 36:1649–1696
14. Milliman HW, Herbert MM, Schiraldi DA (2016) POSS® in tight places. Silicon 8:57–63
15. Raftopoulos KN, Pielichowski K (2016) Segmental dynamics in hybrid polymer/POSS nanomaterials. Prog Polym Sci 52:136–187
16. Pielichowski K, Njuguna J, Janowski B, Pielichowski J (2006) Polyhedral oligomeric silsesquioxanes (POSS)-containing nanohybrid polymers. supramolecular polymers polymeric betains oligomers. Adv Polym Sci 201:225–296
17. Zhao J, Fu Y, Liu S (2008) Polyhedral oligomeric silsesquioxane (POSS)-modified thermoplastic and thermosetting nanocomposites: a review. Polym Polym Comp 16:483–500
18. Zhao F, Bao X, McLauchlin AR, Gu J, Wan C, Kandasubramanian B (2010) Effect of POSS on morphology and mechanical properties of polyamide 12/montmorillonite nanocomposites. Appl Clay Sci 47:249–256
19. Wang SQ, Sharma M, Leong YW (2015) Polyamide 11/clay nanocomposite using polyhedral oligomeric silsesquioxane surfactants. Adv Mater Res 1110:65–68
20. Dintcheva NT, Arrigo R, Teresi R, Gambarotti C (2017) Silanol-POSS as dispersing agents for carbon nanotubes in polyamide. Polym Eng Sci 57:588–594
21. Sarkar B, Ayandele E, Venugopal V, Alexandridis P (2013) Polyhedral oligosilsesquioxane (POSS) nanoparticle localization in ordered structures formed by solvated block copolymers. Macromol Chem Phys 214:2716–2724
22. Feldman D (2017) Polyamide nanocomposites. J Macromol Sci A 54:255–262
23. Lu H, Xu X, Li X, Zhang Z (2006) Morphology, crystallization and dynamic mechanical properties of PA66/nano-SiO_2composites. Bull Mater Sci 29:485–490
24. Faridirad F, Ahmadi S, Barmar M (2017) Polyamide/carbon nanoparticles nanocomposites: a review. Polym Eng Sci 57:475–494
25. Huang JC, Zhu ZK, Yin J, Zhang DM, Qian XF (2001) Preparation and properties of rigid-rod polyimide/silica hybrid materials by sol–gel process. J Appl Polym Sci 79:794–800
26. Park S-Y, Cho Y-H, Vaia RA (2005) Three-dimensional structure of the zone-drawn film of the nylon-6/layered silicate nanocomposites. Macromolecules 38:1729–1735
27. Bizet S, Galy J, Gerard JF (2006) Structure-property relationships in organic-inorganic nanomaterials based on methacryl-POSS and dimethacrylate networks. Macromolecules 39:2574–2583
28. Huang JC, He C, Xian Y, Mya KY, Dai J, Siow YP (2003) Polyimide/POSS nanocomposites: interfacial interaction, thermal properties and mechanical properties. Polymer 44:4491–4499
29. Liu H, Kondo S, Tanaka R, Oku H, Unno M (2008) A spectroscopic investigation of incompletely condensed polyhedral oligomeric silsesquioxanes (POSS-mono-ol, POSS-diol and POSS-triol): hydrogen-bonded interaction and host–guest complex. J Organomet Chem 693:1301–1308
30. Misra R, Fu BX, Plagge A, Morgan SE (2009) POSS-nylon 6 nanocomposites: influence of POSS structure on surface and bulk properties. J Polym Sci B Polym Phys 47:1088–1102

31. Zhou Q, Pramoda KP, Lee JM, Wang K, Loo LS (2011) Role of interface in dispersion and surface energetics of polymer nanocomposites containing hydrophilic POSS and layered silicates. J Colloid Interface Sci 355:222–230
32. Lim SK, Hong EP, Song YH, Choi HJ, Chin I-J (2012) Thermodynamic interaction and mechanical characteristics of Nylon 6 and polyhedral oligomeric silsesquioxane nanohybrids. J Mater Sci 47:308–314
33. Milliman HW, Boris D, Schiraldi DA (2012) Experimental Determination of Hansen solubility parameters for select POSS and polymer compounds as a guide to POSS–polymer interaction potentials. Macromolecules 45(4):1931–1936
34. Yilmaz S, Yilmaz T (2014) Effect of POSS and chain extender on tensile and fracture properties of neat and short glass fiber reinforced polyamide 6 composites. Compos Part A-Appl S 67:274–281
35. Baldi F, Bignotti F, Ricco L, Monticelli O, Riccò T (2006) Mechanical and structural characterization of POSS-modified polyamide 6. J Appl Polym Sci 100:3409–3414
36. Andena L, Fajardo NC, Manarini F, Mercante L (2013) Scratch and wear characteristics of polyamide nanocomposites. World Tribology Cong Italy Sept 8–13:1–4
37. Andrade RJ, Weinrich ZN, Ferreira CI, Schiraldi DA, Maia JM (2015) Optimization of melt blending process of nylon 6-POSS: improving mechanical properties of spun fibers. Polym Eng Sci 55:1580–1588
38. Ricco L, Russo S, Monticelli O, Bordo A, Bellucci F (2005) ε-Caprolactum polymerization in presence of polyhedral olimeric silsesquioxanes (POSS). Polymer 46:6810–6819
39. Milliman HW, Ishida H, Schiraldi DA (2012) Structure property relationships and the role of processing in the reinforcement of nylon 6-POSS blends. Macromolecules 45:4650–4657
40. Zhou Q, Zhang J, Wang Y, Wang W, Yao S, Cong Y, Fang J (2016) Synergistic effects of filler-migration and moisture on the surface structure of polyamide 6 composites under an electric field. RSC Adv 6:95535–95541
41. Ding Y, Chen G, Song J, Gou Y, Shi J, Jin R, Li Q (2012) Properties and morphology of supertoughened polyamide 6 hybrid composites. J Appl Polym Sci 126:194–204
42. Li B, Zhang Y, Wang S, Ji J (2009) Effect of POSS on morphology and properties of poly(2,6-dimethyl-1,4-phenylene oxide)/polyamide 6 blends. Eur Polym J 45:2202–2210
43. Kodal M (2016) Polypropylene/polyamide 6/POSS ternary nanocomposites: effects of POSS nanoparticles on the compatibility. Polymer 105:43–50
44. Lim S-K, Lee JY, Choi HJ, Chin I-J (2015) On interaction characteristics of polyhedral oligomeric silsesquioxane containing polymer nanohybrids. Polym Bull 72:2331–2352
45. Koech J, Omollo E, Nzioka F, Mwasiagi J (2017) Thermal analysis of polyamide 66/POSS nanocomposite fiber. Int J Tech Res 7:35–40
46. Gnanasekaran D, Shanavas A, Focke WW, Sadiku R (2015) Polyhedral oligomeric silsesquioxane/polyamide bio-nanocomposite membranes: structure-gas transport properties. RSC Adv 5:11272–11283
47. Moon JH, Katha AR, Pandian S, Kolake SM, Han S (2014) Polyamide–POSS hybrid membranes for seawater desalination: effect of POSS inclusion on membrane properties. J Membrane Sci 461:89–95
48. Ridgway HF, Orbell J, Gray S (2017) Molecular simulations of polyamide membrane materials used in desalination and water reuse applications: recent developments and future prospects. J Membrane Sci 524:436–448
49. He Y, Tang YP, Chung TS (2016) Concurrent removal of selenium and arsenic from water using polyhedral oligomeric silsesquioxane (POSS)–polyamide thin-film nanocomposite nanofiltration membranes. Ind Eng Chem Res 55:12929–12938
50. Duan J, Pan Y, Pacheco F, Litwiller E, Lai Z, Pinnau I (2015) High-performance polyamide thin-film-nanocomposite reverse osmosis membranes containing hydrophobic zeolitic imidazolate framework-8. J Membrane Sci 476:303–310
51. Stevens DM, Shu JY, Reichert M, Roy A (2017) Next-generation nanoporous materials: progress and prospects for reverse osmosis and nanofiltration. Ind Eng Chem Res 56:10526–10551

52. Bandyopadhyay P, Banerjee S (2014) Synthesis, characterization and gas transport properties of polyamide-tethered polyhedral oligomeric silsesquioxane (POSS) nanocomposites. Ind Eng Chem Res 53:18273–18282
53. Duan J, Litwiller E, Pinnau I (2015) Preparation and water desalination properties of POSS-polyamide nanocomposite reverse osmosis membranes. J Membrane Sci 473:157–164
54. Markarian J (2005) Flame retardants for polyamides—new developments and processing concerns. Plastics Additives Comp 7:22–25
55. Qian Y, Wei P, Zhao X, Jiang P, Yu H (2013) Flame retardancy and thermal stability of polyhedral oligomeric silsesquioxane nanocomposites. Fire Mater 37:1–16
56. Gentiluomo S, Veca AD, Monti M, Zaccone M, Zanetti M (2016) Fire behavior of polyamide 12 nanocomposites containing POSS and CNT. Polym Degrad Stab 134:151–156
57. Zhang W, Li X, Yang R (2012) Blowing-out effect in epoxy composites flame retarded by DOPO-POSS and its correlation with amide curing agents. Polym Degrad Stab 97:1314–1324
58. Zhang W, Camino G, Yang R, Polymer/polyhedral oligomeric silsesquioxane (POSS) nanocomposites: an overview of fire retardance. Prog Polym Sci 67:77–125
59. Dasari A, Yu Z-Z, Mai Y-W, Cai G, Song H (2009) Roles of graphite oxide, clay and POSS during the combustion of polyamide 6. Polymer 50:1577–1587
60. Andrade RJ, Huang R, Herbert MM, Chiaretti D, Ishida H, Schiraldi DA, Maia JM (2014) A thermo-rheological study on the structure property relationships in the reinforcement of nylon 6–POSS blends. Polymer 55:860–870
61. Herbert MM, Andrade R, Ishida H, Maia J, Schiraldi DA (2013) Multilayered confinement of iPP/TPOSS and nylon 6/APOSS blends. Polymer 54:6992–7003
62. Zhou Q, Cong Y, Wu N, Loo LS (2015) The microstructure of polyamide 6 and polyamide 6/polyhedral oligomeric silsesquioxane nanocomposites synthesized by phase inversion procedure under electric field. Appl Surf Sci 357:1454–1462
63. Zhang Z, Gu A, Liang G, Ren P, Xie J, Wang X (2007) Thermo-oxygen degradation mechanisms of POSS/epoxy nanocomposites. Polym Degrad Stab 92:1986–1993
64. Mather PT, Jeon HG, Romo-Uribe A, Haddad TS, Lichtenhan JD (1999) Mechanical relaxation and microstructure of poly(norbornyl-POSS) copolymers. Macromolecules 32:1194–1203
65. Gao F, Tong YH, Schiricker SR, Culbertson BM (2001) Evaluation of neat resins based on methacrylates modified with methacryl-POSS, as potnetial organic-inorganic hybrids for formulating dental restoratives. Polym Adv Technol 12:355–360
66. Kannan RY, Salacinski HJ, Edirisnghe MJ, Hamilton G, Salacinski HJ (2006) Polyhedral oligomeric silsequioxane-polyurethane nanocomposite microvessles for an artificial capillary bed. Biomaterials 27:4618–4626
67. Jash P, Wilkie CA (2005) Effects of surfactants on the thermal and fire properties of poly(methyl methacrylate)/clay nanocomposites. Polym Degrad Stab 88:401–406
68. Rios-Dominguez H, Ruiz-Trevino FA, Contreras-Reyes R, Gonzalez-Montiel A (2006) Synthesis and evaluation of gas transport properties of polystyrene-POSS membranes. J Mater Sci 271:94–100
69. Devaux E, Rochery M, Bourbigot S (2002) Polyurethene/clay and polyurethane/POSS nanocomposites as flame retarded coating for polyester and cotton febrics. Fire Mater 26:149–154
70. Lu C-H, Kuo S-W, Chang W-T, Chang F-C (2009) The Self-assembled structure of the diblock copolymer PCL-*b*-P4VP transforms upon competitive interactions with octaphenol polyhedral oligomeric silsesquioxane. Macromol Rapid Commn 30:2121–2127
71. Daga VK, Anderson ER, Gido SP, Watkins JJ (2011) Hydrogen bond assisted assembly of well-ordered polyhedral oligomeric silsesquioxane–block copolymer composites. Macromolecules 44:6793–6799
72. Bai J, Shi Z, Yin J, Tian M (2014) A simple approach to preparation of polyhedral oligomeric silsesquioxane crosslinked poly(styrene-*b*-butadiene-*b*-styrene) elastomers with a unique micro-morphology *via* UV-induced thiol–ene reaction. Polym Chem 5:6761–6769

Dielectric Properties of Epoxy/POSS and PE/POSS Systems

Eric David and Thomas Andritsch

Abstract In many applications in electronic power, and high-voltage engineering, there is a need to improve the electrical properties of existing insulation systems and/or to develop novel insulation materials with properties more suitable with the changing requirements, particularly in the electrotechnical area. During the last few decades, a considerable attention has been given to the possible use of polymeric nanocomposites systems, usually a nonconductive polymer containing nanometric inorganic fillers, as a replacement to the neat polymers offering better electrical and thermal properties. There is almost, nowadays, a consensus among the scientific community that such property enhancements can only be achieved when the nano-fillers present a reasonably good size dispersion and spatial distribution within the host polymer. However, due to nano-fillers' strong tendency to agglomerate and their generally poor compatibility with commonly used polymers, to reach optimal dispersions has been found challenging in most cases. In order to improve the polymer/particles' compatibility and therefore to avoid agglomeration and poor-dispersion problems, polyhedral oligomeric silsesquioxanes (POSS) appear to be a filler of choice since they are by nature nanoscaled molecules bearing built-in functionalities which can be selected according to the chemical nature of the host polymer. This chapter summarizes the investigations that were reported so far on the electrical properties of epoxy/POSS, PE/POSS, and PP/POSS systems. The general conclusion is that in the case of polyolefin/POSS composites, nanoscale dispersion was found to be hard to reach despite the selection alkyl-type POSS and the dielectric properties were not found to be strongly improved while in the case of epoxy/POSS systems, the selection of appropriate POSS compounds and a carefully chosen resin/additive/hardener ratio allow nanoscale dispersion accompanied with noticeable improvements of the dielectric properties.

E. David (✉)
École de Technologie Supérieure, Montreal, Canada
e-mail: Eric.David@etsmtl.ca

T. Andritsch
University of Southampton, Southampton, UK

S. Kalia and K. Pielichowski (eds.), *Polymer/POSS Nanocomposites and Hybrid Materials*, Springer Series on Polymer and Composite Materials,
https://doi.org/10.1007/978-3-030-02327-0_7

Keywords POSS · Composites · Epoxy · Polyethylene · Polypropylene
Dielectric response · Erosion resistance · Breakdown strength

1 Introduction to Dielectric Properties of Polymeric Systems

Dielectric properties of polymers usually refer to polymer and their composites exhibiting very low conductivity (<10^{-12} S/m) under moderate electrical field and temperature conditions, which is the case for the overwhelming majority of natural and synthetic polymers. This means that when a step voltage is applied across such material, a decaying current will be monitored without reaching a steady-state level before hours with, often, this steady-state level being lower than the sensitivity of the measuring electrometer or amperemeter. Such typical curve is shown in Fig. 1a for cable-grade cross-linked polyethylene (XLPE). In the more general case where an arbitrary electrical field function is applied across the material, the observed current density (in 1D) is related to the material conductivity and its dielectric response function according to:

$$J(t) = \sigma E(t) + \varepsilon_0 \frac{\partial}{\partial t}\left[E(t) + \int_0^\infty f(\tau) E(t-\tau) \mathrm{d}\tau \right] \tag{1}$$

where *J(t)* is the current density, *E(t)* is the applied electrical field, σ the conductivity, and *f(t)* the dielectric response function. A more complete description of the above equation and its implications can be found in a number of well-known textbooks (see [1–3] for example, as these books are recent enough to not be plagued by the use of the Gaussian (cgs) system of units that was popular in older books on the theory of electric polarization and dielectrics). When an harmonic electrical field is applied, the use of the complex representation and the assumption of linearity allow simplifying Eq. (1). The relative complex dielectric permittivity is then related to the dielectric response function with:

$$\varepsilon^*(\omega) = \varepsilon_r'(\omega) - j\varepsilon_r''(\omega) = \int_0^\infty f(t) \exp(-j\omega t) \mathrm{d}t + 1 \tag{2}$$

where the negative sign between the real and the imaginary parts is the usual convention in electrical engineering (the current leading the voltage for a capacitive load). This expression does not include the contribution of the direct conduction to the imaginary part of the permittivity. In practice, since this contribution cannot be separated from the contribution to dielectric losses from relaxation mechanisms when a frequency-domain measurement is conducted, a $\sigma/\omega\varepsilon_0$ term should be added to the imaginary part of Eq. (2).

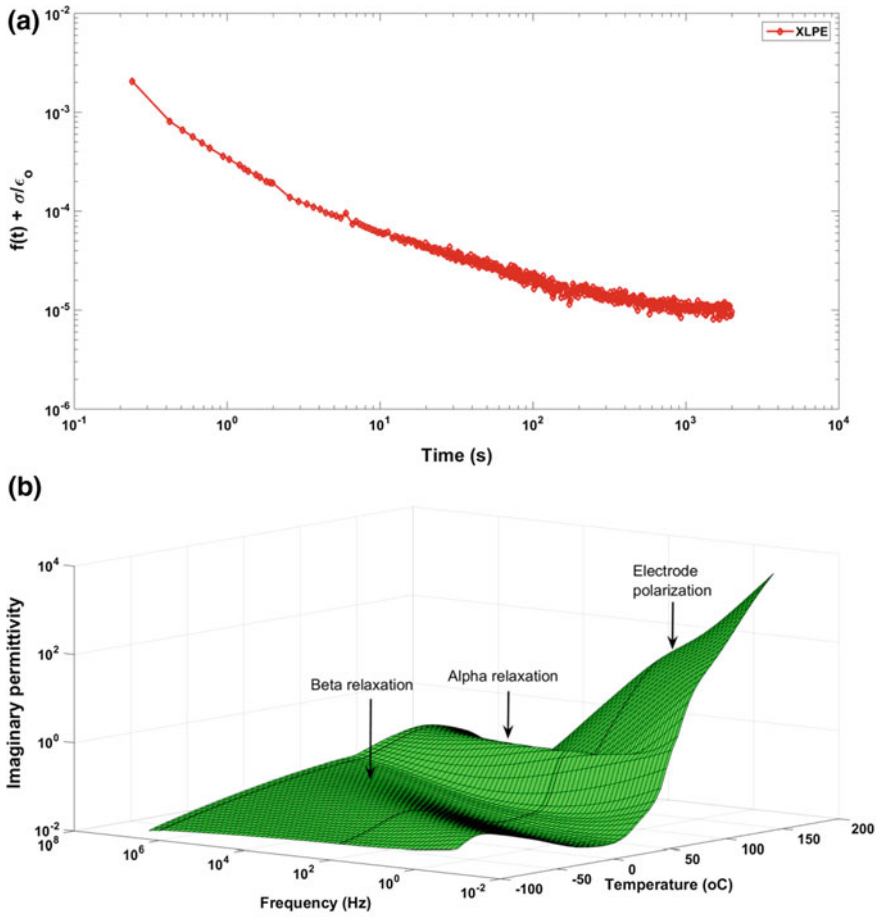

Fig. 1 **a** Contribution of the dielectric response function and the conductivity to the measured current as a function of time across XLPE after a voltage step; **b** imaginary permittivity of epoxy as a function of frequency and temperature showing several relaxation mechanisms

Polar polymers will exhibit a frequency-dependent complex permittivity according to their relaxation mechanisms that are conventionally labeled α, β, … as a function of their appearance from the highest to the lowest temperature. This appearance is characterized by a maximum value of the imaginary permittivity at a frequency corresponding to the reciprocal of the relaxation time. A good example of such typical relaxation mechanisms for an amorphous polymer is depicted in Fig. 1b. When a second phase, more usually inorganic or sometimes organic (for polymer blends, for example), is mixed with a nonconductive polymer forming a two-phase composite material, an additional relaxation mechanism is observed most of the time. This is essentially a result of the difference in the materials' conductivity, the inor-

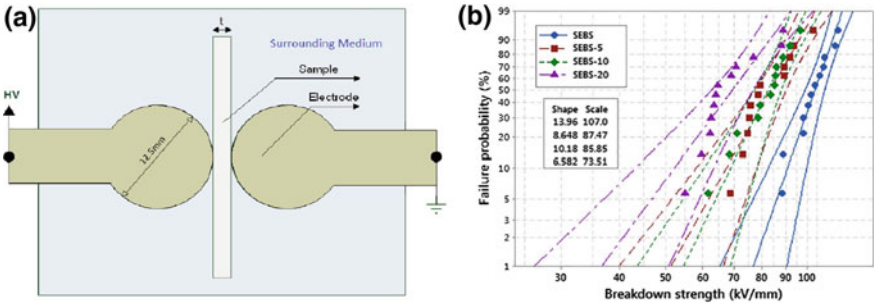

Fig. 2 **a** Typical dielectric breakdown measurement setup (© 2018 IEEE, reprinted, with permission, from [5]) and **b** typical results for SEBS/ZnO composites, showing the Weibull plots as well as the statistical shape and scale parameters of the Weibull function. The curve lines are the 95% confidence bounds. (Reprinted from [6], copyright 2018, with permission from Elsevier)

ganic phase being more conductive than the organic phase, leading to accumulation of charge carriers at the phases' boundary. Accordingly, this mechanism is called interfacial polarization or Maxwell–Wagner–Sillars (MWS) polarization. A similar mechanism, but at the macroscopic level, can occur near the electrodes, particularly when ionic conduction occurs, and accordingly is called electrode polarization, as shown in Fig. 1b.

For applications of polymeric systems as insulating material under moderate to high electrical field, one of the most critical dielectric properties are obviously the dielectric breakdown strength and the dielectric endurance. The breakdown strength usually refers to the highest electrical field that can be withstood before breakdown when the voltage, either AC or DC, across the insulating material is increased linearly, as defined in the ASTM D149 or the IEC Publication 60243-1 standards. A typical setup used for this type of measurement is illustrated in Fig. 2a. Since the experimental value of a breakdown field bears a statistical nature, the data from a set of breakdown tests on a given material is normally treated with statistical methods. These statistical methods are reviewed in details in the IEEE Std-930 [4]. Figure 2b is a typical example of a so-called Weibull plot of breakdown tests on four different materials, SEBS and SEBS-based composites containing 5, 10, and 20 wt% of zinc oxide.

2 PE/POSS and PP/POSS Systems

Various types of polyolefin-compatible POSS with favorable solubility parameters have been investigated as possible fillers to enhance the dielectric properties of either polyethylene or polypropylene. Figure 3 illustrates the chemical structure of some of the cage-structured POSS molecules that are possible candidates to be used for the fabrication of PE- or PP-based composites. These three POSS compounds, namely octamethyl-POSS (OmPOSS, Fig. 3a), octaisobutyl-POSS (OibPOSS, Fig. 3b) and

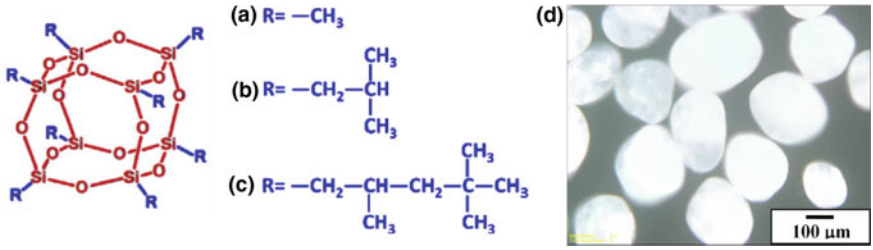

Fig. 3 **a** OmPOSS, **b** OibPOSS, and **c** OioPOSS cage structures (reprinted from [12], copyright 2018, with permission from Elsevier) and **d** photo of commercially available OibPOSS powder (reprinted from [13])

octaisooctyl-POSS (OioPOSS, Fig. 3c), bear in common alkyl-type radical groups that are expected to provide an adequate compatibility with an olefin host polymer. Accordingly, they have been investigated by several authors [7–18] as a potential enhancement additive to polyethylene or polypropylene. OmPOSS and OibPOSS are crystalline solids with densities of, respectively, 1.5 and 1.13 g/cm^3, and are commercially available in the form of a white powder (Fig. 3d), while OioPOSS is a viscous liquid having a density of 1.01 g/cm^3 [19].

2.1 Compounding Techniques and Microstructure

The most natural and industrially scalable method to compound solid, or liquid, fillers with either PE or PP is melt compounding using either an internal mixer or an extruder. Other compounding routes such as chemical blending and/or mechanical alloying have also been reported [9, 13, 14, 17]. Regardless of the chosen compounding technique, nanoscale dispersion of POSS, which basically means that all POSS molecules are separated from each other and uniformly dispersed within the host polymer, have been found very difficult to achieve in PP and particularly in PE, despite the apparent compatibility between the radical groups and the matrix.

In the case of PP matrices, the quality of the dispersion has been reported to increase with the increase of the length of the alkyl groups. SEM and TEM micrographs of PP/POSS composites prepared by melt mixing and containing either 3 or 10 wt% of POSS were reported in [7]. Figure 4 illustrates the fracture surface SEM micrographs of PP/OmPOSS (4a) and PP/OioPOSS (4b) composites, where 10–20 µm OmPOSS agglomerates are visible in Fig. 4a while no agglomerate was observed for 3wt% PP/OioPOSS composites as shown in Fig. 4b. Takala and coauthors [8] reported similar results with somewhat smaller aggregates when PP/OmPOSS composites were compounded with a twin-screw extruder rather than a mixer.

In the case of PE, good dispersion of POSS has been found even more difficult than in the case of PP. An extensive study on the effect of processing parameters and

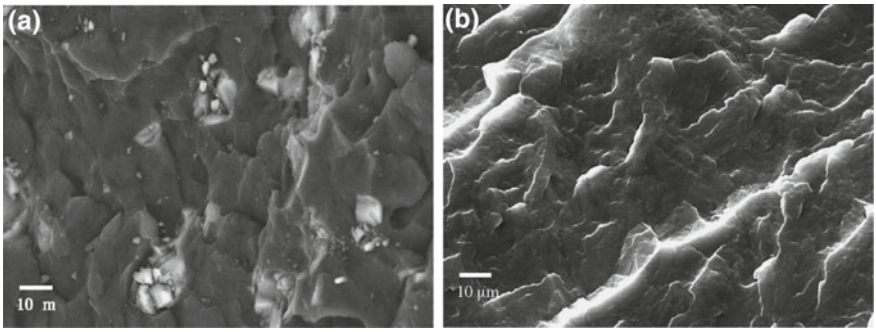

Fig. 4 PP/OmPOSS (**a**) and PP/OioPOSS (**b**) SEM micrographs in each case containing 3 wt% of POSS. (Reprinted from [7], copyright 2018, with permission from Elsevier)

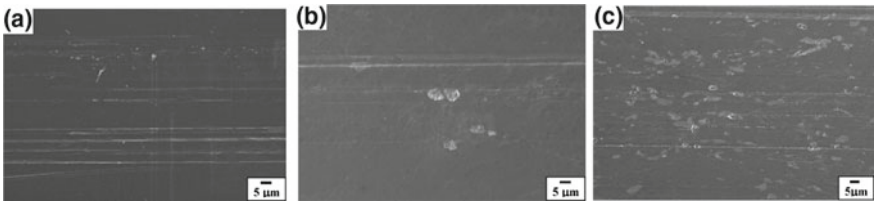

Fig. 5 SEM images of **a** UHMWPE, **b** UHMWPE/OibPOSS (99/1), and **c** UHMWPE/OibPOSS (95/5) (reproduced from [13])

processing techniques on the microstructure of PE/POSS composites has been conducted by Guo and coauthors [11–18]. Figure 5 illustrates the SEM micrographs of ultra-high-molecular-weight polyethylene (UHMWPE)/OibPOSS composites compounded by mechanical alloying. More details on this fabrication technique can be found in the literature [13, 20]. Microscale agglomerates were observed both at 1 and 5 wt% loadings. The use of chemical blending to fabricate PE/POSS composites was investigated in [9, 14, 17]. Submicrometric dispersion (~500 nm) was claimed in [9] as well as submicrometric and micrometric agglomerates in [14] when xylene dissolution was used for either OmPOSS, OibPOSS, or OioPOSS. POSS was found to crystallize in the case of OmPOSS and OibPOSS and to form droplets in the case of the liquid-type OioPOSS upon precipitation of the solution as shown in Fig. 6a, b, and c, respectively. However, when OibPOSS was treated by high-energy ball milling prior to chemical compounding with LDPE, an improved dispersion was reached [17] and that improved microstructure was found to lead to a significant enhancement of the dielectric properties [17], as shown in Fig. 13.

Solid OmPOSS and OibPOSS were also found to be hardly dispersed at nanoscale when melt compounding was used as the fabrication technique for PE-based composites. However, at low concentration, a nanoscale dispersion of OioPOSS was observed for LDPE composites prepared by twin-screw extrusion. Figure 7 is, particularly, good illustration of how the increase of the length of the alkyl groups

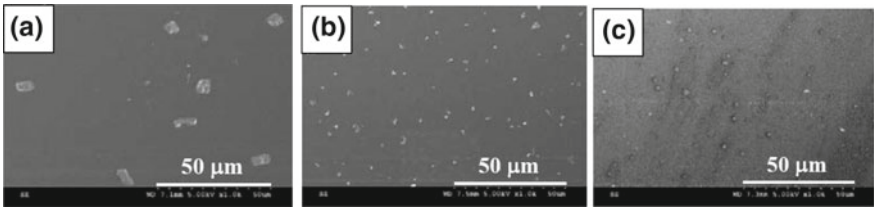

Fig. 6 SEM images of **a** LDPE/OmPOSS, **b** LDPE/OibPOSS and **c** LDPE/OioPOSS compounded by chemical blending and in each case containing 1 wt% of POSS (© 2018 IEEE, reprinted, with permission, from [14])

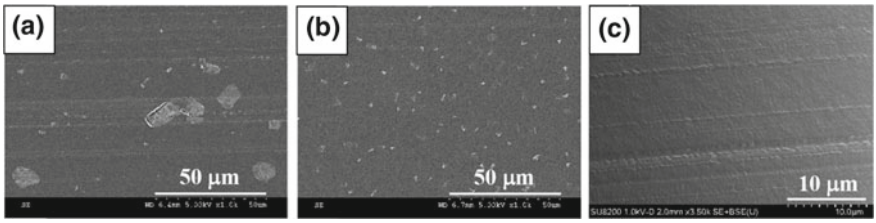

Fig. 7 SEM images of **a** LDPE/OmPOSS, **b** LDPE/OibPOSS and **c** LDPE/OioPOSS compounded by melt blending (extrusion) and in each case containing 1 wt% of POSS. (Reprinted from [12], copyright 2018, with permission from Elsevier)

increases the dispersion with the agglomerates changing from microsize (Fig. 7a) to submicrosize (Fig. 7b) and finally to nanosize (Fig. 7c) as the length of the POSS alkyl groups increases [12].

2.2 Breakdown Strength and Erosion Resistance

Data on the dielectric breakdown strength of PP/POSS or PE/POSS composites is mainly available for AC breakdown strength with the measurements conducted according to the short-term procedure described in the ASTM standard and with the use of an experimental setup similar to the one illustrated in Fig. 2a. The three main contributions regarding the data available in the literature are from Huang et al. [9], Takala et al. [8], and Guo et al. [11] with the most complete set of data being provided by Guo and coauthors who reported extensive investigations of the breakdown strength of LDPE/POSS composites as a function processing and microstructure. These results were somewhat disappointing as POSS was found to be barely able to improve the matrix dielectric breakdown strength and in fact in most of the cases a decrease was found, particularly when the microstructure exhibited microsize agglomerates, while in the best cases the dielectric breakdown strength of PE/POSS composites was similar or just slightly better to that of PE. Fabrication was found to significantly influence the breakdown strength through change in the filler disper-

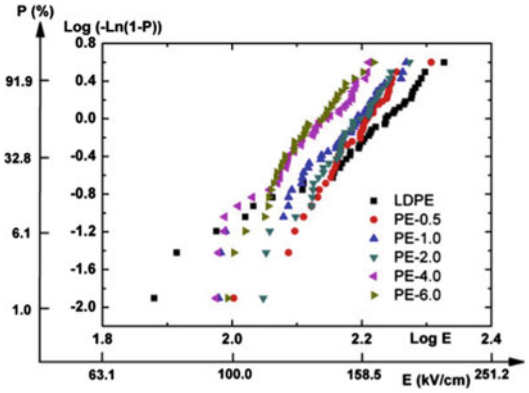

Material	ACBD (kV/mm)
LDPE	172 ± 1.3
LDPE/POSS-0.5 wt%	163 ± 0.6
LDPE/POSS-1.0 wt%	159 ± 0.8
LDPE/POSS-2.0 wt%	158 ± 0.6
LDPE/POSS-4.0 wt%	140 ± 0.8
LDPE/POSS-6.0 wt%	137 ± 0.7

Fig. 8 Weibull plots of the dielectric strength for LDPE and LDPE/POSS. The numerical values are the electrical field at percentile 63.2% of the Weibull cumulative probability function (this value is commonly referred as the material breakdown strength). (Reprinted from [9], copyright 2018, with permission from Elsevier)

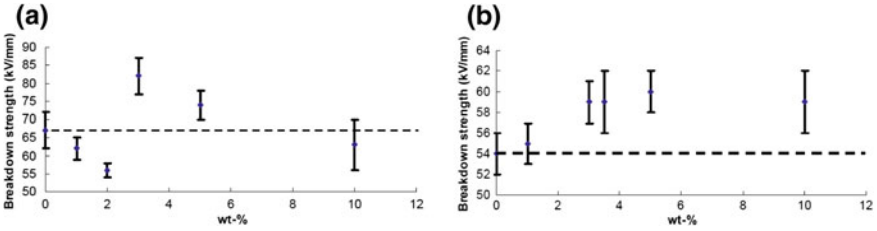

Fig. 9 AC breakdown strength of PP/POSS composites as a function of POSS content: **a** PP/OmPOSS and **b** PP/OioPOSS. © 2018 IEEE, reprinted, with permission, from [8]

sion, with good filler dispersions and relatively small POSS aggregates leading to the best results. Typical results (for an undisclosed type of POSS [9]) are illustrated in Fig. 8 showing a gradual decrease of breakdown strength as the concentration of POSS is increased with the almost inevitable simultaneous increase of agglomeration. Similarly, results reported by Takala et al. for PP/OmPOSS composites did not show any improvement of the AC breakdown strength of PP up to 10 wt% of loading. However, a slight improvement was observed by the same authors in the case of PP/OioPOSS composites for concentrations between 2 and 10 wt% (Fig. 9).

Much more detailed results were reported by Guo and coauthors in a series of paper [12–18], with [17] summarizing the main findings for the case of LDPE/OibPOSS composites. Figures 10 and 11 illustrate the variation of the AC breakdown strength of LDPE-based composites as a function of type and the amount of POSS when the composites were fabricated by chemical blending (Fig. 10) and melt compounding (Fig. 11). In all these data, the only case where a slight improvement of the ACBD was observed was for 1 wt% LDPE/OioPOSS composites either produced by chemical blending or extrusion. This was also the case for which the best dispersion was

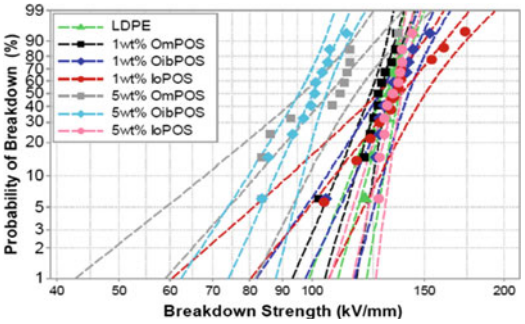

Samples	α (kV/mm)
LDPE	135.0 ± 3.8
1 wt% OmPOSS	129.7 ± 3.7
1 wt% OibPOSS	138.2 ± 6.5
1 wt% OioPOSS	144.8 ± 11.2
5 wt% OmPOSS	112.0 ± 9.8
5 wt% OibPOSS	102.9 ± 4.5
5 wt% OioPOSS	136.5 ± 3.0

Fig. 10 AC breakdown strength of PE/POSS composites compounded by chemical blending. IoPOS stands for Octaisooctyl-POSS. © 2018 IEEE, reprinted, with permission, from [14]

observed as shown in Figs. 6c (chemical blending) and 7c (melt blending). Despite an exhaustive investigation on various compounding methods, only microcomposites, not nanocomposites, were obtained in the case of the two solid POSS—OmPOSS and OibPOSS. However, when a reasonable, without any large agglomerates, dispersion of the POSS inclusions was achieved, the ACBD strength was maintained or did not suffer from a significant decrease. Figure 12 illustrates the case mentioned in the previous section of LDPE/OibPOSS composites compounded by chemical blending. At 5 wt%, large agglomerates were observed leading to a marked decrease of the ACBD (Fig. 12a). When ball milling was used prior to chemical blending, the agglomerates were reduced in size and the dielectric strength was maintained as shown in Fig. 12b.

2.3 Dielectric Response

Similarly to PP or PE, alkyl-type POSS are nonpolar and nonconductive in nature and accordingly their inclusion in a polyolefin matrix is not expected to increase significantly the material dielectric losses or its conductivity. Low-loss materials like PE and PP are characterized by nearly frequency-independent losses over several decades, typically between subaudio and microwave frequencies, where the dielectric losses reach very low values, in the vicinity of 10^{-4}, and does not vary by more than one or two decades for the whole measurable frequency range. A very good text describing such behavior can be found in one of the classic textbooks of the dielectric literature (see Chap. 4 of [21]). Figure 13 illustrates, for the temperature range from 20 to 80 °C, the typical spectrum of the real and imaginary parts of the relative permittivity of LDPE as measured by a modern frequency-domain dielectric spectrometer. The dielectric losses stay very low for the whole frequency range, often lower than the sensitivity of the measurement equipment which led to negative values for the intermediate frequency range (not plotted in the log–log graph). The real

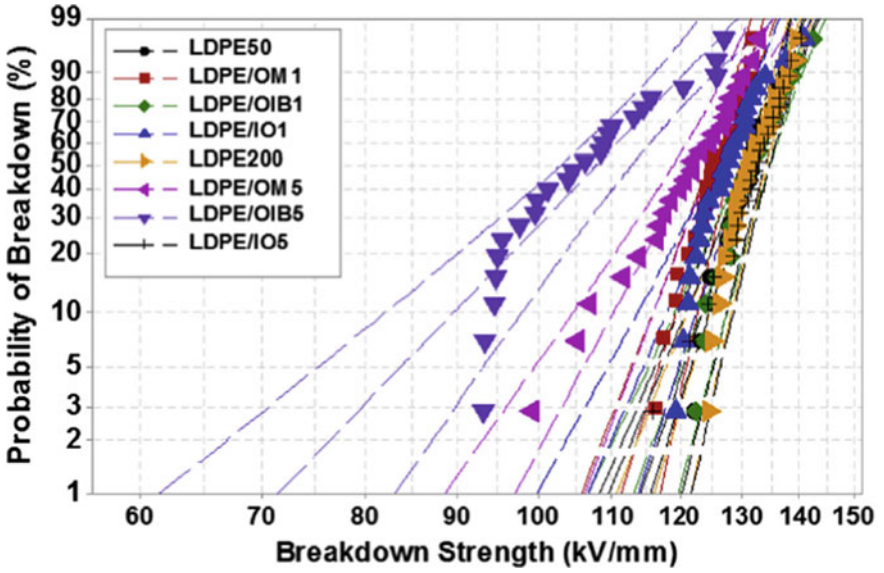

Samples	β	α (kV/mm)
LDPE50	29.3	133.5
LDPE/OM1	33.4	127.6
LDPE/OIB1	26.8	134.2
LDPE/IO1	23.0	130.2
LDPE200	32.5	133.7
LDPE/OM5	18.5	124.5
LDPE/OIB5	10.4	111.5
LDPE/IO5	30.7	134.2

Fig. 11 Weibull plot and Weibull parameters for the AC breakdown strength of PE/POSS composites compounded by melt blending. LDPE50 and LDPE200 mean LDPE that was extruded at 50 and 200 rpm, respectively. IO means octaisooctyl-POSS and the number at the end of the label is the weight concentration of POSS. (Reprinted from [12], copyright 2018, with permission from Elsevier)

part of the dielectric constant is frequency-independent and its value decreases with temperature as predicted by the Clausius–Mossotti equation [1, 2]. At room temperature, the inclusion of either type of POSS hardly affects the dielectric response of PE, at less up to 5 wt%. Figure 14 shows the frequency-domain dielectric response of various PE/POSS composites at room temperature. In every case, with the exception of the LDPE/OioPOSS at very low frequency, the dielectric losses for the whole frequency range remained very low, in fact at the limit the sensitivity of the measur-

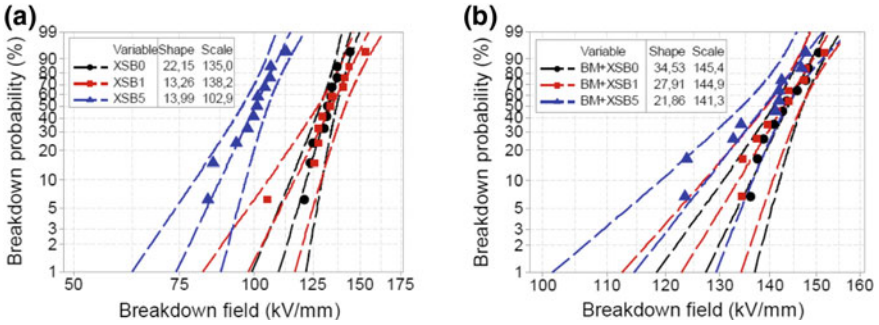

Fig. 12 AC breakdown strength of LDPE and LDPE/OibPOSS composites containing 1 and 5 wt% of POSS and compounded by chemical blending: **a** without ball milling prior to the chemical blending and **b** with ball milling prior to the chemical blending. The scale (α) and shape (β) parameter of the Weibull best fits are inserted in the figures. © 2018 IEEE, reprinted, with permission, from [17]

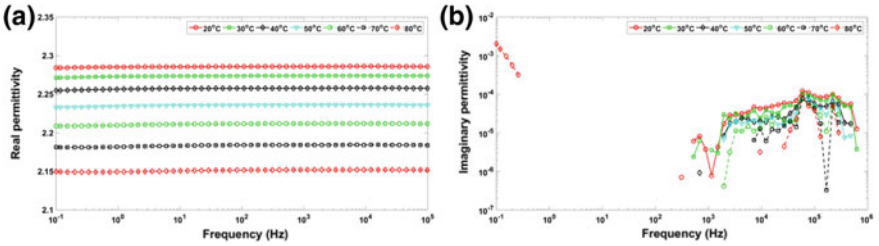

Fig. 13 Relative real permittivity (**a**) and relative imaginary permittivity (**b**) as a function of frequency and temperature for LDPE. © 2018 IEEE, adapted, with permission, from [15]

ing equipment. As the dielectric constant of POSS is higher than the one of LDPE, a slight increase of the dielectric constant of the composites can be expected. The dielectric constant of LDPE/OmPOSS and LDPE/OibPOSS was indeed found to increase compared to the neat polymer but it was not the case for LDPE/OioPOSS. The lowering, to a value lower than either the base polymer or the nanoparticle introduced into the matrix, of the dielectric constant when a nearly nanodispersion of the inclusions is reached, although in complete contradiction of the usual mixing laws, has been reported several times for various polymer/filler systems [22, 23]. Consequently, the fact that the system for which the best dispersion is observed, the LDPE/OioPOSS composites, shows the lowest dielectric constant seems to be in good agreement with the literature on the dielectric properties of nanocomposites. Using a different and less-sensitive equipment, Huang et al. [9] found similar results, measuring either an increase or a decrease of the dielectric constant for LDPE/POSS composites depending on the microstructure, and low dielectric losses in all cases.

Another impact of the state of dispersion of the POSS aggregates on the composite dielectric response can be observed at higher temperature as it can be shown in Fig. 15. The cases presented in this figure are 5 wt% LDPE/OmPOSS exhibiting

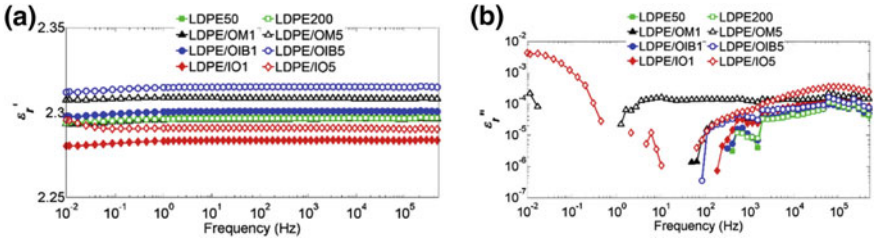

Fig. 14 Relative real permittivity (**a**) and relative imaginary permittivity (**b**) as a function of frequency and temperature for LDPE/POSS composites compounded by melt mixing. IO means octaisooctyl-POSS and the number at the end of the label is the weight concentration of POSS. (Reprinted from [12], copyright 2018, with permission from Elsevier)

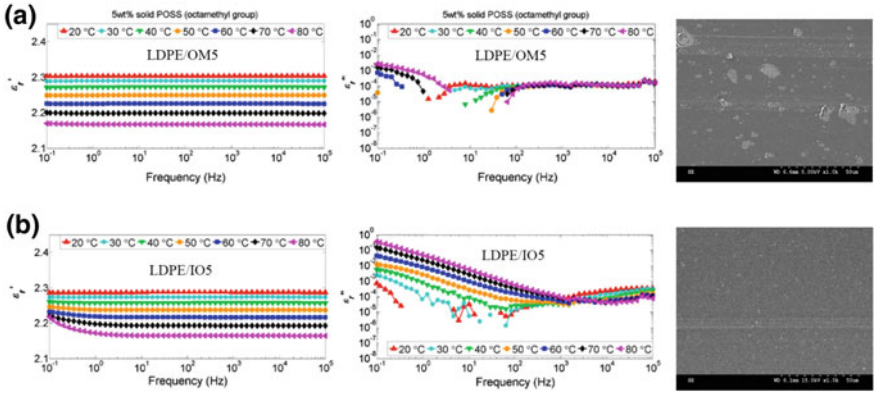

Fig. 15 Dielectric response and microstructure (SEM images of microtomed surfaces) of 5 wt% LDPE/OmPOSS (**a**) and 5 wt% LDPE/OioPOSS (**b**). In both cases, the compounding was conducted by melt mixing. © 2018 IEEE, reprinted, with permission, from [15, 16]

agglomerates of dozens of microns and 5% LDPE/OioPOSS having a much finer dispersion. In the latter case, a noticeable increase of the low-frequency losses, the so-called low-frequency dispersion (see Chap. 5 of [21]), due to charge fluctuations was observed at high temperature. This is related to the fact that nanoscale dispersion leads to lower percolation thresholds compared with microscale counterpart, which allows the onset of leakage current through the sample. A similar effect was observed in the case of zinc oxide containing dielectrics [24].

3 Epoxy/POSS Systems

3.1 Classification, Processing, and Additives

Epoxy resins (ER) are a common sight in polymer engineering. They typically consist of two components: the resin with at least one epoxide group within its molecular structure, and a hardener which interacts with the resin during a thermally accelerated curing process [25]. At the end of the curing process, they combined to a thermosetting material in a shape governed by a mold, usually made of stainless steel or similar metals. This process results in a complex 3D structure, which is made even more elaborate due to the use of a number of additives and stabilizers that can be found in commercially available epoxy resins. Without these additives, the polymer would degrade quickly due to oxidation, UV radiation and other influences, and added accelerants ensure that the curing time is in a range that allows timely manufacturing of mass market products. Additionally, release agents are often used at the interface between metallic mold and curing polymer, to ensure the complete product can be ejected without excessive use of mechanical forces. All these additives are trade secrets of the individual polymer suppliers, and information on them is rarely disclosed. This is compounded by the fact that ER classifications are not always distinctly clear in literature.

A broad classification of ER can be made based on the synthesis method used [26, 27]. Many engineering ER are based on variations of diglycidyl ether of bisphenol-A and novolac, depending on the operating temperatures the product needs to withstand. Much research is done on the former, mostly due to a combination of easy availability, cost, potting times and convenient processing temperatures. These can then be combined with a multitude of available hardeners, with amine or anhydrite-based systems being very common. All these elements need to be kept in mind when analyzing the response of ER as a result of adding additional elements like POSS into this mix, since the additives of one specific type of ER might interact with POSS in unpredictable ways. POSS can be considered a subset of reactive diluents.

Diluents are additives that have traditionally been used to control viscosity for easier processing, without major changes to the behavior of the cured ER system [27, 28]. Nonreactive diluents include solvents like toluene, acetone, and phenols among others, which cannot react with and therefore bond to the forming network, and are assumed to have negligible influence on the final properties of the ER [26, 29]. Due to the low boiling and flash points of such nonreactive diluents, they are assumed to leave the polymer matrix during degassing and curing, even though work has been published that showed some potential effects of diluents on properties of ER-based composites, but without giving explanation of the potential causes of said effects [30]. Further studies have shown that it is very likely that trace elements of nonreactive diluents can remain in such systems, which might affect dielectric properties [31, 32].

More interesting in the context of this work are reactive diluents. These are solvents or chemicals that can become part of the ER network during the curing process,

and therefore have the potential to directly affect physical properties of the ER system. These can contain an epoxy themselves, or be nonepoxy-based, like phenols, lactone compounds, divinyl ethers, polyols, lauric acid, or polyurethanes [33–36]. Epoxy-based reactive diluents are chemicals with one or more epoxide groups as part of their molecular structure, with most POSS used falling in the category of polyepoxies [37], compared to monoepoxies like glycidyl hexadecyl ether, which would have only a single epoxy group [38]. Although there are monoepoxide POSS variations available, they tend to be outperformed by their polyepoxy alternatives, not just in terms of dielectric properties [39]. The subsequent sections will focus on measured effects on a number of dielectric parameters as a result of the use of POSS as an additive to ER.

3.2 Breakdown Strength and Erosion Resistance

While there is a wealth of literature regarding thermal and mechanical properties of POSS-modified epoxies, surprisingly little work has been done on the electrical properties. One of the first publications focusing on the dielectric properties was by Horwath et al. in 2005, where they showed a five times increase of time to failure when subjected to corona, compared to unmodified epoxy [40]. They were, like many others afterward, considering POSS as the smallest possible silica-type nanoparticle, instead of treating them as molecules. Hence there was an attempt on explaining the results using the same theories as established for nanodielectrics at the time [41]. It took almost eight years until these early results were independently confirmed by other research groups [42, 43]. Further work followed, all results showing a significant impact of POSS on the corona resistance of ER [37, 44]. In the case of polyepoxy POSS containing only three reactive groups, microsize agglomerates were found to occur when the load was increased above 2.5 wt% and at the same time, the corona resistance was found to decrease from an optimal value at low concentration, as illustrated in Fig. 16 and discussed in more details in [44]. When polyepoxy POSS containing eight reactive groups were used instead, it was possible to maintain a dispersion of the POSS particles at nanosize level up to 10 wt% and the erosion resistance was found to continuously increase with the load level as illustrated in Fig. 17 and discussed in more details in [37]. Similarly, it was also found by Bocek and coauthors [45] that a good and homogeneous dispersion of POSS up to 36 wt% can be achieved when octaepoxy POSS was used. While the fact that additional load content leads to diminishing returns when agglomerates start to form was not surprising, that the best-performing ER composites were those with the lowest amount of additives was. But these results are a clear indication that the amount of assumed "nanoparticles" have little effect on the corona resistance, and that the change to the ER structure is the main driver for the observed improvements. This is in line with observations on the effect of POSS as flame retardant additive in ER, where the improved resistance to thermal decomposition is attributed to restrictions

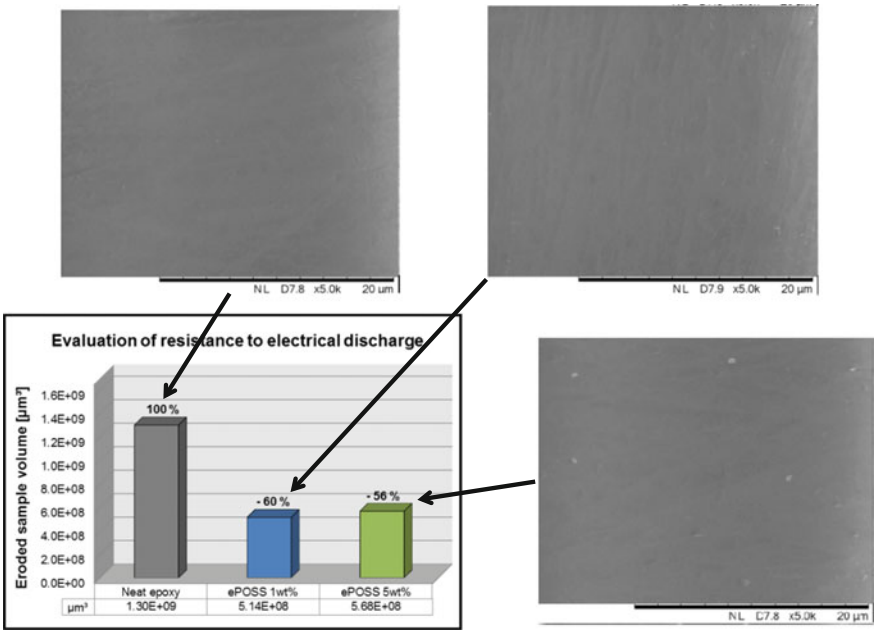

Fig. 16 Evaluation of resistance to electrical discharge by comparison of eroded sample volume after 30 h under corona exposure for ER containing POSS with three reactive groups. Values of eroded volume and SEM pictures are reprinted, with permission, from [44, 49], respectively (© 2018 IEEE)

in the degree of freedom of chain motions as direct result of increased POSS content [46, 47].

An important measure for electrical applications is the maximum value to the electrical field that an insulating polymer can withstand without long-term damage. Methods of assessing this are AC, DC, and impulse voltage breakdown tests. Even though the value of short-term breakdown data for practical engineering purposes is debatable, due to the simplicity of the test it is a popular technique. For material designers the results are very useful to gauge if changes to the material lead to improvements, compared to the reference material they started with. The investigations on POSS-modified ER show no significant change in breakdown data for most research groups that measured them [43, 48], while others showed that there is the tendency of POSS–ER to have improved breakdown strength [49]. For data shown with no change in breakdown strength, the authors did not confirm how they adjusted the epoxy–hardener ratio to account for the additional epoxides in the ER system. The materials sections in [43, 48] do indicate the epoxy–hardener ratio was not adjusted, which would of course mean the resulting samples would not have been mixed with the stoichiometric ratio, which in turn could have affected the breakdown strength negatively. Looking at the Weibull parameters available for samples where the stoichiometry was considered [42, 49], an increase can be observed not only of

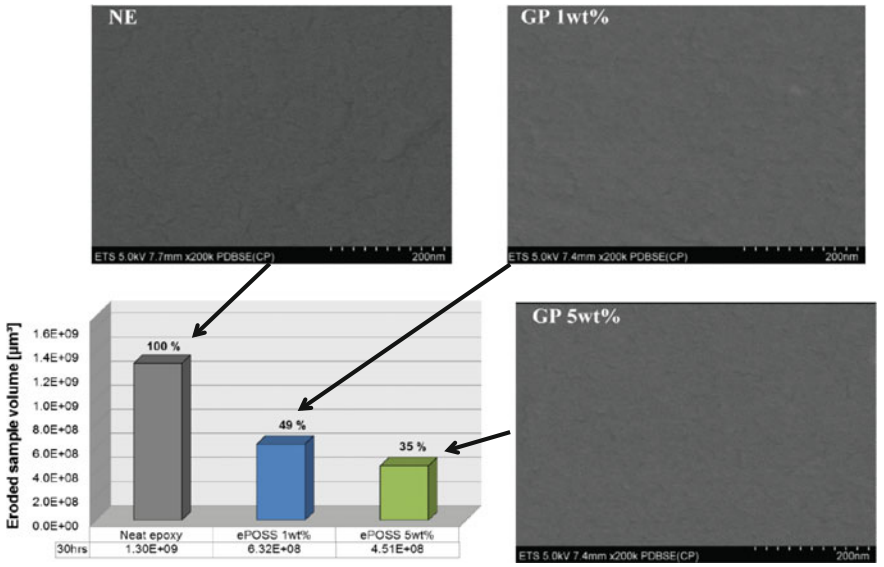

Fig. 17 Evaluation of resistance to electrical discharge by comparison of eroded sample volume after 30 h under corona exposure for ER containing POSS with eight reactive groups. Values of eroded volume and SEM pictures are reprinted, with permission, from [37, 42], respectively (© 2018 IEEE)

the scale, but also the shape parameter. This is particularly interesting, since that would indicate a material which has a more reliable long-term performance, which is in line with the corona resistance results above. Actually, quite similar results than in the case of corona resistance were reported [37, 44] for the AC breakdown strength as measured by the short-term procedure. Indeed, as illustrated in Fig. 18, the breakdown strength was found to initially increase at low concentration and then to decrease when agglomeration started to occur, while it was found to remain at a higher value than the neat polymer when the eight reactive groups POSS was used up to 20 wt%. However, since there is no experimental long-term data regarding withstand voltage available at the time of writing, these results need to be considered carefully. The correct mixture of resin, hardener, and POSS needs to be considered, since it has been shown that changes of the ratio away from the stoichiometric ratio do affect the breakdown strength significantly [38].

3.3 Glass Transition Temperature of POSS/Epoxy Resins

The glass transition temperature in epoxies is linked with the structure of the cross-linked 3D network established during curing. Accordingly, the measurement of the T_g as function of POSS content is a good indicator if there are widespread changes to

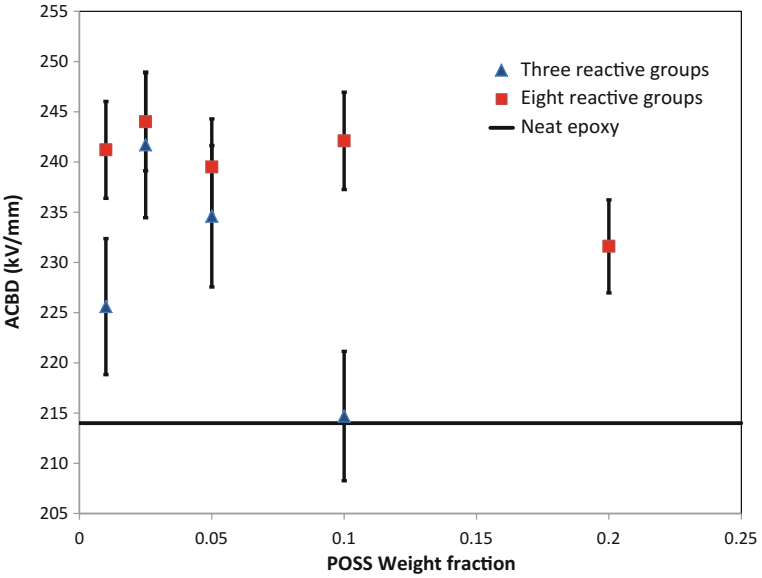

Fig. 18 AC breakdown strength for ER/POSS composites for two different type of POSS. The breakdown strength of the unload neat epoxy was 214 ± 5.0 kV/mm. The absolute values of breakdown strength have to be considered carefully as they are dependent on many experimental parameters (reported in [37, 44]). The error bars are the 90% confidence bounds calculated according to [4]

the amorphous structure of the polymer, which might help explaining the observed dielectric behavior. The glass transition temperature established via DMA indicates an increase with increased POSS content up to about 10%, with a slower increase after this threshold [50]. Zhang et al. relate this behavior to two separate causes: the increase of rigid silica-like structure to replace soft polymer chains, which require increased energy to move, thus increasing T_g; secondly, the increased amount of potentially unreacted POSS once the additive content is too high, leading to diminishing returns with increased amounts of POSS. Villanueva et al. found similar increase of T_g up until 10% when measuring with DSC, but a drastic drop of the glass transition temperature once they exceeded this amount when a short-curing cycle was used [51]. With a long-curing cycle, a monotonic decrease of the T_g as function of POSS content was observed in the same study, along with increased activation energies for all POSS samples when compared to reference ER systems. Complementary to these results, Takala et al. used DSC to establish T_g in their composites with a long-curing cycle and noticed a reduction in line with results discussed above [48]. Samples investigated by other groups have not seen any significant change of T_g, which was there attributed to the correct stoichiometry [42, 44].

3.4 Dielectric Response

The dielectric response of fully cured ER features a main relaxation peak related to the glass transition (α) and a subglassy secondary relaxation peak (β) as well as contributions from charge carriers at low frequencies/high temperatures as illustrated in Fig. 1b. When the dispersion of POSS remains at the nanoscale level, the inclusion of POSS does not change significantly the epoxy dielectric response, even for concentration as high as 20 wt%, as illustrated in Fig. 19a. However, as soon as microsize agglomeration occurs, an additional relaxation mechanism, originating from the accumulation charge carriers at the agglomerates/polymer boundaries, is observed as illustrated in Fig. 19b. At high temperature, the addition of POSS was found to slightly increase the losses due to low-frequency dispersion while it did not affect significantly the behavior of the α relaxation process, except for high loads (~20 wt%), for which cases the glass temperature was also found to be affected [37]. The dielectric response of both monoepoxy and octaepoxy POSS composites is also reported in [45] in the form of isochronal plots of the dissipation factor at power frequency for two different curing temperatures. These results seem to be somewhat in agreement with those illustrated in Fig. 19, with the dielectric loss of the epoxy matrix not being significantly affected when the dispersion remained homogenous while a noticeable increase was observed at high temperature, including the occurrence of an interfacial relaxation peak, for the composites for which agglomerations were found (composites containing monoepoxy POSS or high concentration of octaepoxy POSS). A detailed report on the frequency-domain dielectric response of rubbery epoxy network containing covalently bonded POSS groups is provided by Kourkoutsaki and coauthors [52]. Although this system is quite different from the POSS composites previously presented, it was also observed in that case that the inclusion of POSS in the formulation of rubbery epoxy networks leads to practically no change in the magnitude and frequency localization of the secondary relaxation processes, similarly to what is shown in Fig. 19.

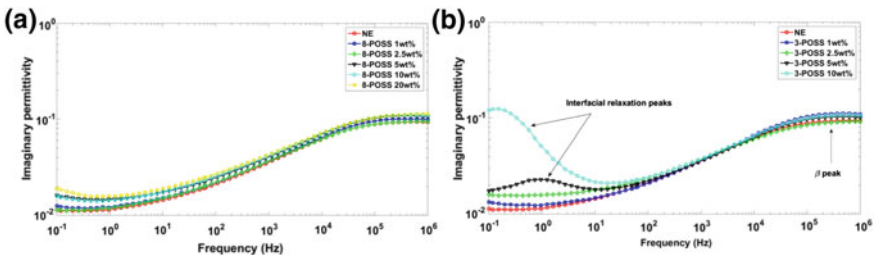

Fig. 19 Imaginary part of the complex permittivity at 40 °C for neat epoxy (NE) and its POSS composites with **a** eight reactive groups and **b** three reactive groups. (**a**, **b**) are adapted, with permission, from [37, 44], respectively (© 2018 IEEE)

4 Conclusions

A number of favorable results reported in the literature related to the dielectric properties of polymeric nanocomposites [53, 54] were also observed in the case of POSS-based composites. One of them, the resistance to erosion due the exposure to corona discharge, is probably the most significant improvement as it was found to be sharply enhanced both in the cases of PE/POSS and ER/POSS composites. This is quite significant as this parameter is probably more related to the long-term performance of high-voltage insulation systems since many degradation processes, such as electrical treeing, involve the action of partial discharges. In the case of ER/POSS composites, the short-term AC breakdown strength was also found to be noticeably improved as long as the dispersion of the POSS particles remains at the nanoscale level. This was possible up to 20 wt% when POSS with eight reactive groups was used and when a careful attention was paid to keep the right resin/hardener stoichiometric ratio, taking into account the additive's reactive groups. In the case of PE/POSS composites, whatever the type of POSS or the processing technique, nanoscale dispersion was found to be very difficult to reach, being reported only in the case of POSS with longest alkyl groups (OioPOSS) at low concentration. This also coincides with the case for which the most favorable results were reported.

The dielectric response of PE/POSS and ER/POSS composites remained essentially unchanged most of the time when compared with the neat polymer. In the case of PE-based composites, when nanoscale dispersion was obtained, low-frequency dispersion due to charge fluctuation was observed at temperature above 30 °C. All the other cases were characterized by only a slight increase of the dielectric constant with no significant changes of the dielectric losses. For ER/POSS composites, agglomeration of the POSS molecules was found to lead to an interfacial relaxation process located between the α and β processes. When nanoscale dispersion was reached, no change in the dielectric response was observed for the ER/POSS composites as compared with the neat polymer. As a concluding remark, both in the case of PE and ER, actually more particularly in the case of ER, as long as a reasonable dispersion is achieved, POSS has shown the potential to enhance the polymer dielectric properties in the context of its usage as an insulating material.

References

1. Kremer F, Schönhals A,(eds) (2003) Broadband dielectric spectroscopy. Springer-Verlag, Berlin
2. Jonscher AK (1983) Dielectric relaxation in solids. Chelsea Dielectrics Press, London
3. Runt, JP Fitzgerald JJ (eds) (1997) Dielectric Spectroscopy of Polymeric Materials: Fundamentals and Applications. ACS, Washington D.C
4. IEEE Standard 930 (2005) IEEE guide for the statistical analysis of electrical insulation breakdown data. IEEE Dielectrics and Electrical Insulation Society

5. Daran-Daneau C, David E, Fréchette MF, Savoie S (2012) Influence of the surrounding medium on the dielectric strength measurement of LLDPE/clay nanocomposites. In: IEEE international symposium on electrical insulation, pp 654–658
6. Helal E, David E, Fréchette M, Demarquette NR (2017) Thermoplastic elastomer nanocomposites with controlled nanoparticles dispersion for HV insulation systems: correlation between rheological, thermal, electrical and dielectric properties. Eur Polymer J 94:68–86
7. Fina A, Tabuani D, Frache A, Camino G (2005) Polypropylene–polyhedral oligomeric silsesquioxanes (POSS) nanocomposites. Polymer 46:7855–7866
8. Takala M, Karttunen M, Salovaara P, Kortet S, Kannus K, Kalliohaka T (2008) Dielectric properties of nanostructured polypropylene-polyhedral oligomeric silsesquioxane compounds. IEEE Trans Dielectr Electr Insul 15:40–51
9. Huang X, Xie L, Jiang P, Wang G, Yin Y (2009) Morphology studies and ac electrical property of low density polyethylene/octavinyl polyhedral oligomeric silsesquioxane composite dielectrics. Eur Polymer J 45:2172–2183
10. Horwath, J, Schweickart D (2009) Inorganic fillers for corona endurance enhancement of selected polymers. In: IEEE international power modulator and high voltage conference (IPMHVC), pp 644–647
11. Guo M (2017) Polyethylene/polyhedral oligomeric silsesquioxanes composites: electrical insulation for high-voltage power cables, Ph.D. thesis, École de Technologie Supérieure
12. Guo M, David E, Fréchette M, Demarquette NR (2017) Polyethylene/polyhedral oligomeric silsesquioxanes composites: dielectric, thermal and rheological properties. Polymer 115:60–69
13. Guo M, Fréchette M, David E, Demarquette NR (2015) Polyethylene-based dielectric composites containing polyhedral oligomeric silsesquioxanes obtained by ball milling. Trans Electr Electron Mater 16:53–61
14. Guo M, Fréchette M, David E, Demarquette NR, Daigle JC (2017) Polyethylene/polyhedral oligomeric silsesquioxanes composites: electrical insulation for high voltage power cables. IEEE Trans Dielectr Electr Insul 24:798–807
15. Fréchette M, Guo M, David E, Min D, Li S (2017) The dielectric response of polyethylene/polyhedral oligomeric silsesquioxanes composites at various temperatures. IEEE conference on electrical insulation and dielectric phenomenon, pp 501–504
16. Guo M, David E, Fréchette M, Demarquette NR (2016) Low-Density Polyethylene/Polyhedral Oligomeric Silsesquioxanes Composites Obtained by Extrusion. In: IEEE conference on electrical insulation and dielectric phenomena, pp 647–650
17. Guo M, Fréchette M, David E, Demarquette NR (2016) Influence of fabrication techniques on the dielectric properties of PE/POSS polymeric composites. In: IEEE electrical insulation conference, pp 297–300
18. Guo M, Fréchette M, David E, Demarquette NR Daigle JC (2014) Polyethylene-based nanodielectrics containing octaisobutyl polyhedral oligomeric silsesquioxanes obtained by solution blending in xylene. In: IEEE conference on electrical insulation and dielectric phenomena, pp 731–734
19. DeArmitt C (2013) Polyhedral oligomeric silsesquioxane handbook http://phantomplastics.com/wp-content/uploads/2013/08/POSS-Handbook.pdf
20. Suryanarayana C (2001) Mechanical alloying and milling. Prog Mater Sci 46:1–184
21. Jonscher AK (1996) Universal relaxation law. Chelsea Dielectrics Press, London
22. Roy M, Nelson JK, MacCrone RK, Schadler LS, Reed CW, Keefe R, Zenger W (2005) Polymer nanocomposite dielectrics—the role of the interface. In: IEEE Trans. on dielectrics and electrical insulation, vol 12. pp 629–643
23. Tsekmes IA, Morshuis PHF, Smit JJ, Kochetov R (2015) Enhancing the thermal and electrical performance of epoxy microcomposites with the addition of nanofillers. IEEE Electr Insul Mag 31(3):32–42
24. Helal E, Pottier C, David E, Fréchette M, Demarquette NR (2018) Polyethylene/thermoplastic elastomer/Zinc Oxide nanocomposites for high voltage insulation applications: dielectric, mechanical and rheological behavior. Eur Polymer J 100:258–269
25. Nicholson JW (2012) The chemistry of polymers, Royal Society of Chemistry, London

26. Lee H, Neville K (1967) Handbook of Epoxy Resins, McGraw Hill, New York
27. Tesoro G (1988) In: May CA(ed) Epoxy resins-chemistry and technology, 2nd edn. Marcel Dekker, New York
28. Mustata F, Bicu I, Cascaval CN (1997) Rheological and thermal behaviour of an epoxy resin modified with reactive diluents. J Polym Eng 17:491–506
29. Wang RM, Zheng SR, Zheng YP (2011) Polymer matrix composites and technology, Woodhead Publishing, Cambridge
30. Liao YH, Marietta-Tondin O, Liang ZY, Zhang C, Wang B (2004) Investigation of the dispersion process of SWNTs/SC-15 epoxy resin nanocomposites. Mater Sci Eng A 385:175–181
31. Hong SG, Wu CS (1998) DSC and FTIR analysis of the curing behaviors of epoxy/DICY/solvent open systems. Thermochim Acta 316:167–175
32. Loos MR, Coelho LAF, Pezzin SH, Amico SC (2008) The effect of acetone addition on the properties of epoxy. Polimeros-Ciencia E Tecnologia 18:76–80
33. Bakar M, Duk R, Przybylek M, Kostrzewa M (2009) Mechanical and thermal properties of epoxy resin modified with polyurethane. J Reinf Plast Compos 28:2107–2118
34. Harani H, Fellahi S, Bakar M (1999) Toughening of epoxy resin using hydroxyl-terminated polyesters. J Appl Polym Sci 71:29–38
35. Suprapakorn N, Dhamrongvaraporn S, Ishida H (1998) Effect of $CaCO_3$ on the mechanical and rheological properties of a ring-opening phenolic resin: polybenzoxazine. Polym Compos 19:126–132
36. Tang B, Liu XB, Zhao XL, Zhang JH (2014) Highly efficient in situ toughening of epoxy thermosets with reactive hyperbranched polyurethane, J Appl Polym Sci, 131
37. Heid T, Fréchette M, David E (2016) Enhanced electrical and thermal performances of nanostructured epoxy/POSS composites. IEEE Trans Dielectr Electr Insul 23:1732–1742
38. Saeedi IA, Vaughan AS, Andritsch T (2016) On the dielectric performance of modified epoxy networks. In: IEEE international conference on dielectrics
39. Saeedi IA, Andritsch T, Vaughan AS (2017) Modification of resin/hardener stoichiometry using POSS and its effect on the dielectric properties of epoxy resin systems. In: International symposium on electrical insulating materials (ISEIM), pp 366–369
40. Horwath J, Schweickart D, Garcia G, Klosterman D, Galaska M (2005) Improved performance of polyhedral oligomeric silsesquioxane epoxies. In: IEEE conference on electrical insulation and dielectric phenomena, pp 155–157
41. Horwath JC, Schweickart DL, Garcia G, Klosterman D, Galaska M, Schrand A, Walko LC (2006) Improved electrical properties of epoxy resin with nanometer-sized inorganic fillers. In: Conference record of the 2006 twenty-seventh international power modulator symposium, pp 189–191
42. Heid T, Fréchette M, David E (2014) Nanostructured epoxy/POSS composites: high performance dielectrics with improved breakdown strength and corona resistance. In: IEEE conference on electrical insulation and dielectric phenomena, pp 659–662
43. Huang X, Li Y, Liu F, Jiang P, Iizuka T, Tatsumi K, Tanaka T (2014) Electrical properties of epoxy/POSS composites with homogeneous nanostructure. IEEE Trans Dielectr Electr Insul 21:1516–1528
44. Heid T, Fréchette M, David E (2015) Nanostructured epoxy/POSS composites: enhanced materials for high voltage insulation applications. IEEE Trans Dielectr Electr Insul 22:1594–1604
45. Bocek J, Matejka L, Mentlik V, Trnka P, Slouf M (2011) Electrical and thermomechanical properties of epoxy-POSS nanocomposites. Eur Polym J 47:861–872
46. Lin Z, Lau S, Moon KS, Wong CP (2012) Polyhedral oligomeric silsesquioxanes (POSS)-filled underfill with excellent high temperature performance. In: IEEE electronic components and technology conference, pp 1599–1604
47. Mya KY, He CB, Huang JC, Xiao Y, Dai J, Siow YP (2004) Preparation and thermornechanical properties of epoxy resins modified by octafunctional cubic silsesquioxane epoxides. J Polym Sci Part a-Polym Chem 42:3490–3503
48. Takala M, Karttunen M, Pelto J, Salovaara P, Munter T, Honkanen M, Auletta T, Kannus K (2008) Thermal, mechanical and dielectric properties of nanostructured epoxy-polyhedral oligomeric silsesquioxane composites. IEEE Trans Dielectr Electr Insul 15:1224–1235

49. Heid T, Fréchette M, David E (2014) Nanostructured epoxy/POSS composites: high performance dielectrics with improved corona resistance and thermal conductivity. In: IEEE electrical insulation conference, pp 316–319
50. Zhang ZP, Liang GZ, Wang XL (2007) The effect of POSS on the thermal properties of epoxy. Polym Bull 58:1013–1020
51. Villanueva M, Martin-Iglesias JL, Rodriguez-Anon JA, Proupin-Castineiras J (2009) Thermal study of an epoxy system DGEBA (n = 0)/MXDA modified with POSS. J Therm Anal Calorim 96:575–582
52. Kourkoutsaki Th, Logakis E, Kroutilova I, Matejka L, Nedbal J, Pissis P (2009) Polymer dynamics in rubbery epoxy networks/polyhedral oligomeric silsesquioxanes nanocomposites. J Appl Polym Sci 113:2569–2582
53. Nelson JK (ed) (2010) Dielectric polymer nanocomposites. Springer Science + Business Media, New York, NY
54. David E, Fréchette M (2013) Polymer nanocomposites—major conclusions and achievements reached so Far. IEEE Electr Insul Mag 29(6):29–36

Porous Hybrid Materials with POSS

Sasikumar Ramachandran and Alagar Muthukaruppan

Abstract Massive applications and advantages of porous hybrid materials based on polyhedral oligomeric silsesquioxane (POSS) have generated enormous research interest in the development of porous POSS hybrid materials in both the industries and the academics. POSS, a well-known nanoporous inorganic building block materials with the formula $(RSiO_{1.5})_n$, $(n \geq 6)$ including definite cage-shaped three-dimensional structures is surrounded by organic functional groups, which were utilized to produce porous hybrid materials with organic molecules via copolymerization, grafting, and blending and also with metals by coordination. This chapter reviews the properties and importance of porosity of POSS and POSS hybrid materials.

Keywords POSS · Porosity · Polymer · Hybrid material · Low-*k* dielectric Catalyst

1 Introduction

The combination of organic and inorganic materials in a single chemical entity was prepared few decades ago to achieve improved properties for high-performance industrial and engineering applications. For example, in an old house construction, they have used combination of straw materials of an organic fiber and inorganic clay as a thermal insulator. We would not really call this material a hybrid material in a scientific context, more likely it would count to the composite materials. But the

S. Ramachandran (✉)
PICM, Ecole Polytechnique, Palaiseau, France
e-mail: rskmsc@gmail.com

A. Muthukaruppan
Centre of Excellence in Advanced Materials, Manufacturing, Processing and Characterization (COExAMMPC), Vignan's University, Vadlamudi, Guntur 522213, India
e-mail: muthukaruppanalagar@gmail.com

S. Kalia and K. Pielichowski (eds.), *Polymer/POSS Nanocomposites and Hybrid Materials*, Springer Series on Polymer and Composite Materials,
https://doi.org/10.1007/978-3-030-02327-0_8

other case, a mixture of a clay mineral and the organic dye indigo called Maya blue dye shows significantly high stability than that of the indigo alone; this material is often mentioned as hybrid material. Recently, the development of porous materials is considered as an important part of the present research for various applications in the area of energy and medicine. The homogeneous porous materials can be prepared through solgel method by self-assembling of surfactant molecules as templates. Usually, amphiphilic surfactants are used as a template in this procedure, in which the templates are removed by thermal process after the network formed. The resulting mesoporous materials possess pores with diameters between 2 and 10 nm which depends on the templates. The porous system consisted only of a purely inorganic silica network when it was discovered. The reactive organic functionalization of mesoporous materials made it possible to extend their potential applications. The following methods can be used to prepare organic–inorganic hybrid mesoporous materials: (i) the cocondensation of trialkoxysilanes in specific conditions and (ii) the surface functionalization of purely inorganic porous materials using monofunctional silane coupling agents [1].

The development of porous hybrid materials by hybridization of polymers with porous inorganic materials such as silsesquioxanes/POSS, MCM-41, SBA-15, and Zeolite, via grafting, blending, and copolymerization methods and hybrid POSS–metal coordination polymers has potential features [2–4]. Porous hybrid materials having POSS moieties are an emerging class of new materials that hold significant promise applications in catalysis, gas storage, separation, energy, and electronics. POSS/silsesquioxanes, a class of unique porous inorganic materials with the generic formulas $(RSiO_{1.5})_n$, where R is hydrogen or any alkyl, alkenyl, and aryl groups. These groups are extremely useful as platforms for assembling organic/inorganic hybrid materials via covalent bonds and are directly attached to silicon in the silane and typically do not react during the process of hydrolysis and condensation of trialkoxysilanes [5]. POSS/silsesquioxanes can be synthesized from chlorosilanes, silanols, silanolates, tetraalkoxysilanes, and organotrialkoxysilanes by hydrolysis/condensation process [6].

The term silsesquioxanes refers each silicon (sil) atom is bound to an average of one and a half (sesqui) oxygen (oxane) atom and to one hydrocarbon group/hydrogen atom (ane) which indicates that 1:1:1.5 ratio of hydrocarbon:silicon:oxygen atoms [7]. The silsesquioxane building blocks can be classified as non-caged and caged structure; the non-caged molecular structure can be further classified into partial cage structure (a), ladder structure (b), and random structure (c) (Fig. 1a), and the cage-like silsesquioxanes are usually called as polyhedral oligomeric silsesquioxanes (POSS) which are also denoted by the letters T_6, T_8, T_{10}, and T_{12} (Fig. 1b) based on the siloxane unit [8].

The IUPAC name of silsesquioxanes is complicated, and so the compounds are more conveniently named using the number of silsesquioxane linkages present in a molecule and substituents attached to the silicon atom. For example, $(HSiO_{1.5})_8$ is named as octa(hydridosilsesquioxane) or octasilsesquioxane. Further, these names are more simplified by letters using the siloxane chemistry, one to four oxygen bonds attached to silicon atoms referred as D, M, T, and Q, respectively, and the numerical

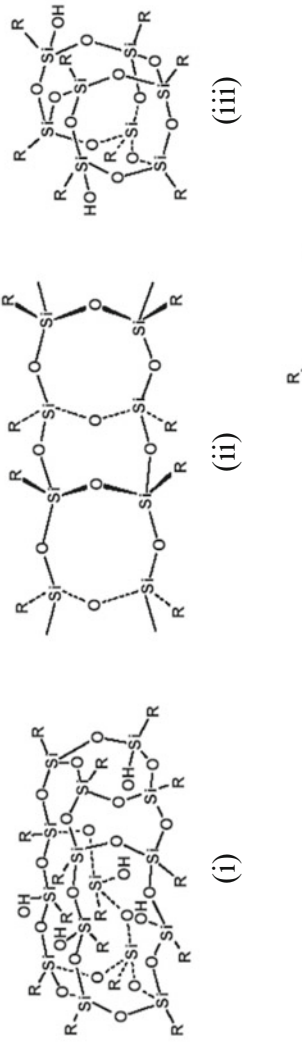

Fig. 1 Chemical structures of silsesquioxanes. **a** Non-caged silsesquioxanes: (i) random, (ii) ladder, (iii) partial caged structures, and **b** caged silsesquioxanes: (i) T_8, (ii) T_{10}, (iii) T_{12} structures. Reprinted from [8], © 2016 with permission from Royal Society of Chemistry

subscript states that the number of silicon atoms in the molecule and the superscripts denoting the number of oxygen atoms further attached to the other silicon atoms. Accordingly, $(HSiO_{1.5})_8$ is named as $(HT^3)_8$ or H_8T_8 or simply T_8 where an octameric cage structure was constructed by connecting each silicon atom to three oxygen atoms and hydrogen atom [9]. Among the polyhedral silsesquioxanes, octahedral cages (T_8) have been widely studied, and they are constructed with the rigid silica core (0.53 nm diagonal) and eight organic groups tethered to the silicon atoms which forms unique sphere like molecules with volumes less than 2 nm^3 and 1–3 nm in diameter [10]. The defined chemical structure and pore size of the octahedral/polyhedral cages offer a wide range of porous POSS hybrid materials.

Porous structured cross-linked polymers possess intrinsic physicochemical properties and have potential applications with the limited thermomechanical properties since that have attracted research interest in recent years by the scientific researchers in the development of porous structured covalently bonded organic–inorganic hybrid polymer nanocomposites [11]. The organics tethered inorganic POSS materials can be well dispersed in hybrid polymers through covalent bonds which can provide well-defined porous structure including excellent thermal and mechanical properties. Also POSS is a non-volatile, lightweight, odorless, nanoporous, and environmentally friendly material. The homogeneous arrangement of POSS units in the hybrid polymer nanocomposite materials can be stabilized by different polymerization techniques. The reinforcement of POSS nanoparticles into a polymer matrix increases the porosity, strength, modulus, and rigidity and reduces the flammability, heat discharge, and viscosity of the polymer. Despite the properties of polymer nanocomposites depend on the method of incorporation of POSS particles. There are two methodologies adopted for the dispersion of POSS into a polymer; (i) physical blending and (ii) chemical cross-linking. In the first approach, POSS nanoparticles are physically blended with polymer by melt mixing or solvent casting methods whereas in the second approach, POSS nanoparticles are bonded covalently with polymer. Various ranges of porous hybrid materials can be prepared from POSS and polymer materials by chemical cross-linking methods using different organic groups anchoring on POSS. Further, POSS can be divided into monofunctional POSS, multifunctional POSS, and molecular silica which refers the presence of only one of the reactive organic groups, more than one reactive organic groups, and non-reactive organic groups, respectively.

POSS molecules have been used to develop well-defined POSS–polymer hybrid porous structured films. These films can be prepared by directly blending/chemical cross-linking of POSS molecules and polymers. For example, octa(3-aminopropyl)-POSS was used to construct multilayered thin films via self-assembly approach with polyanion, which can be potentially applied in designing porous ceramic membranes. Further, the POSS-containing block copolymers could be self-assembled into thin films with a well-ordered structure by varying the parameters of the annealing process such as solvents and temperature [12]. By varying the functionalities of POSS building blocks, reaction conditions and cross-linkers could build porous structured hybrid networks. This chapter mainly devoted to discuss the construction of different

sizes of porous hybrid materials with POSS and concurrently examine the properties and applications of the porosity of POSS hybrids.

2 POSS Materials

POSS is one of the familiar 3D building blocks which are used to construct new porous materials to alternate porous activated carbon, zeolites, metal–organic frameworks, porous organic polymers, etc. Their unique star-shaped nanostructures , physical and chemical properties, such as facile chemical modification, good pH tolerance, high temperature and oxidation resistance properties, specific reactivity, unique morphology and diverse porosity, make POSS an excellent building block for constructing multi-functional materials. In 1946, Scott discovered the first oligomeric organosilsesquioxanes, $(CH_3SiO_{1.5})_n$, by the cocondensation of methyltrichlorosilane and dimethylchlorosilane in specific reaction conditions. In 1995, Baney et al. reviewed the preparation, properties, structures, and applications of silsesquioxanes, especially those of ladder-like polysilsesquioxanes. However, in the past few years, much more attention has been paid to the silsesquioxanes with specific cage structures. However, the POSS is one of the well-known cage-structured porous molecules which can be embedded with mono-, di-, and multi-functional reactive sites that are naturally compatible with organic hosts and can be utilized to incorporate POSS into the polymeric materials through polymerization or grafting. In this manner, a large variety of POSS–polymer nanocomposites have been prepared as high-performance materials. Porous hybrid materials based on POSS precursors have been developed by various chemical methods including copper-mediated coupling, Friedel–Crafts reaction, Yamamoto reaction, Sonogashira cross-coupling, Suzuki coupling, hydrosilylation, solgel chemistry, thermolysis, self-assembly, Schiff base chemistry, radical polymerization, and electro-spinning. The formation of porous hybrid materials is subjected to the precursor of monomer and functional groups of POSS.

2.1 Organic Functional POSS Cages

In principle, the selected organic functional cubic POSS could offer access to the polymerization of organic–inorganic hybrids with controlled porosity, surface area and functionality via non-aqueous methods. It follows that the main aspects of POSS-nanobuilding blocks porosity characteristics include control over the porosity, pore size, and pore template. Design of the materials with the appropriate functional groups is important goal in the development of hybrid materials with high surface areas and controlled pore size. The ability to bridging the non-porous POSS building blocks might be useful for fabricating dense membranes, chemical barriers, and optical coatings. For example, POSS with non-reactive groups (Fig. 2a) has been used in polymer host in a molecular-level dispersion via physical blending and are studied as

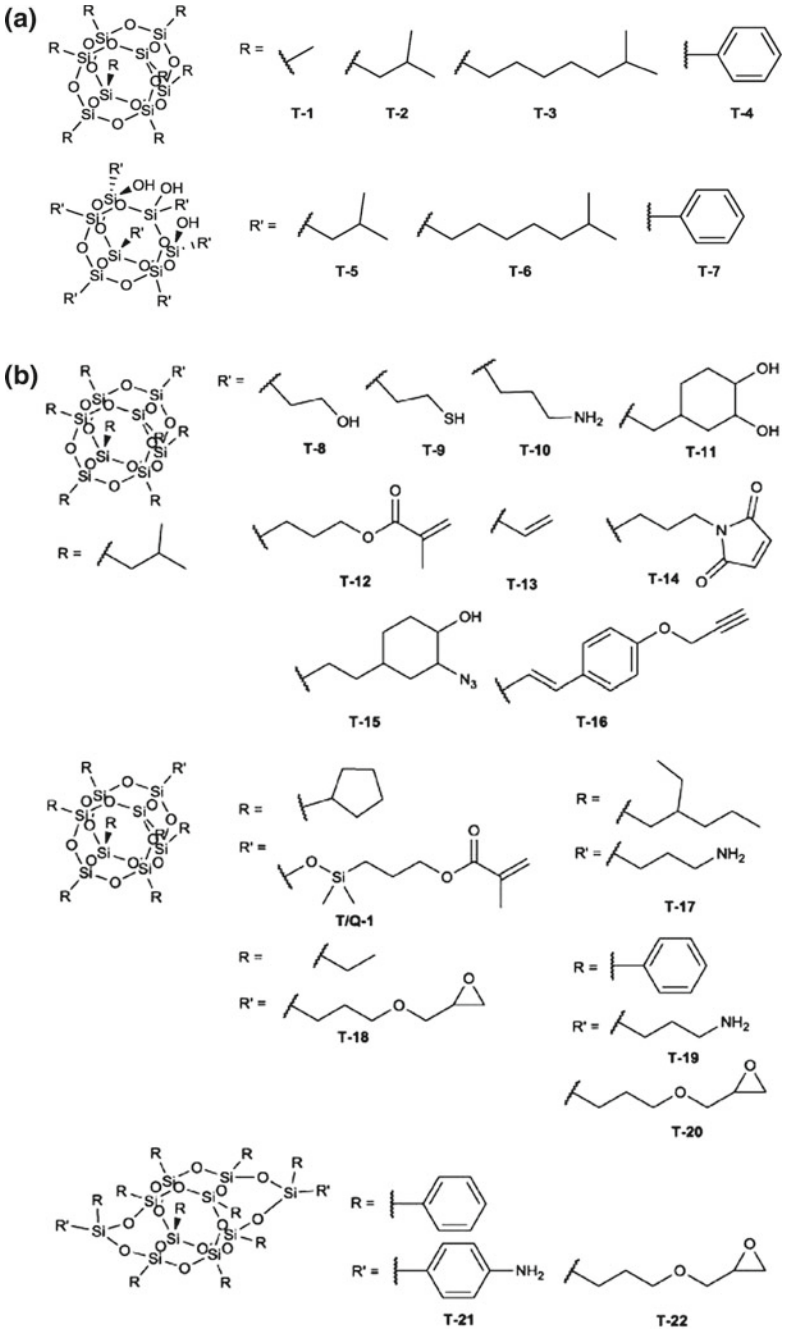

Fig. 2 Non-reactive organofunctional POSS (**a**), Mono- and di-functional POSS (**b**), Octa-functional POSS (**c**). Reprinted from [8], © 2016 with permission from Royal Society of Chemistry

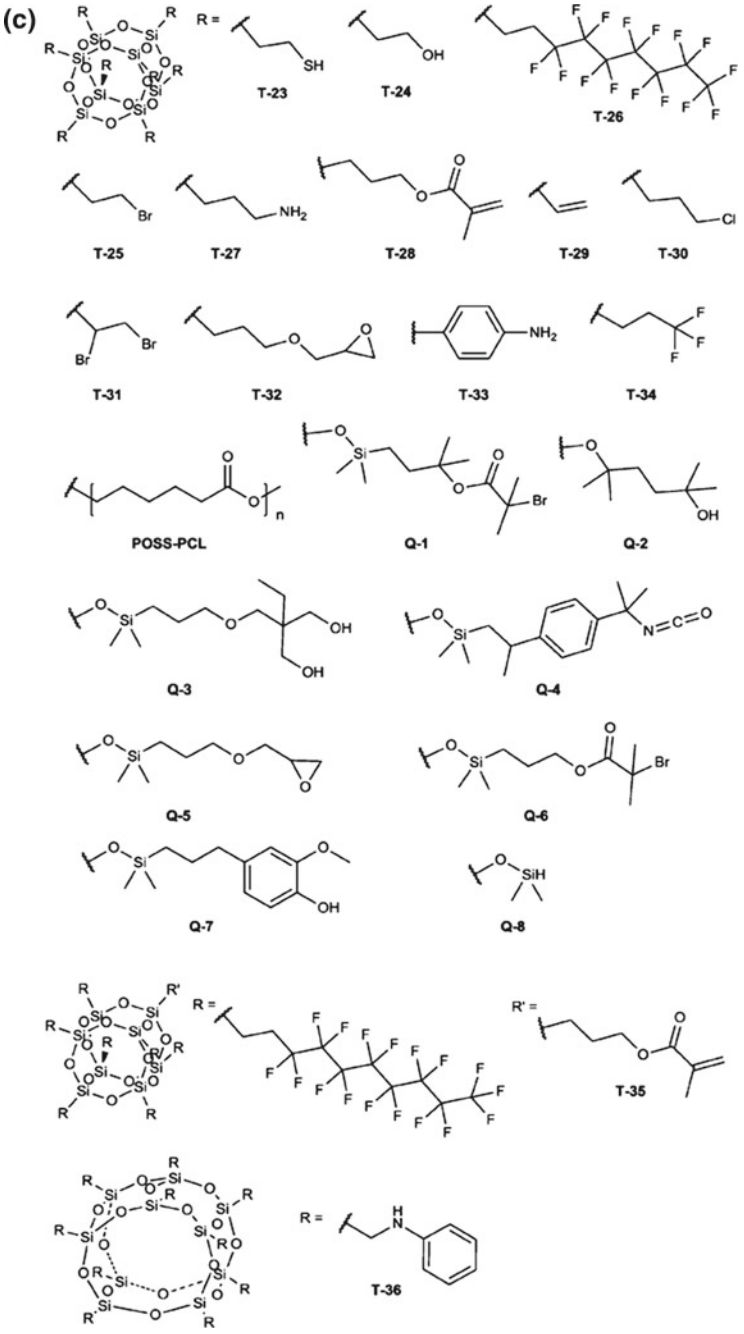

Fig. 2 (continued)

nanoscopic fillers. Further, mono- and di-functional reactive vertex groups of POSS (Fig. 2b) are used to cross-link covalently with the polymer matrix by polymerization or grafting. Most significantly, octa-functional reactive tether groups of POSS (Fig. 2c) were utilized to prepare different pore size of porous POSS hybrid materials, which would be homo-/copolymerization of POSS cages or POSS–polymer hybridization. The selectivity of incorporation of POSS functional reactive groups is associated with the polymer precursors that must be able to react with the polymer precursor otherwise it would be present as a blend; these reactive abilities of the organics can be by thermal, light, and catalyst. Multi-functional POSS gives a star-like macromolecule by initiating polymerization from the surface of the POSS, while the multi-reactive groups anchored POSS produce a heavily cross-linked polymer network. The well-ordered POSS–polymer hybrid matrix can be more precisely prepared via controlled polymerization, such as ATRP and RAFT. A large variety of POSS–polymer porous hybrids are possible to build up with these advanced polymerization strategies.

3 Porous Hybrid Materials with POSS

Organic–inorganic hybrid materials have long been known to play a major role in developing high-performance materials. Those hybrid materials are expected to exhibit new characteristics and both the advantages of organic and inorganic materials. In addition, hybrid materials have unique features which are not shown in the independent organic and inorganic materials. Thus, the hybrid materials have great interest to exploit their potential applications in the fields of mechanics, sensors, catalyst, medical, optical and electronic devices. Inorganic POSS is one of the versatile starting platforms which have one or more reactive sites, such as epoxy, thiol, amine, methacrylate, acrylate, styrene, norbornene, alcohol, and phenol, that provide ease compatibility of POSS with polymeric materials through the formation of strong covalent bonds. In this manner, a large diversity of POSS–polymer nanocomposites has been designed; they have many advantages in industrial appliances. Recently, benzoxazine-functionalized POSS has great attention in the development of hybrid polybenzoxazine thermosetting resins for high-performance and electrical applications. Lee et al. [13] reported the synthesis of a monofunctional POSS-benzoxazine which was used to incorporate into the polybenzoxazine system. Also, Zhang et al. [14] and Ariraman et al. [15] have been reported octahedral benzoxazine-functionalized POSS which was copolymerized with conventional benzoxazine results in the formation of porous structured POSS–polybenzoxazine matrix. They have been used as an interlayer low-k dielectric in microelectronics devices with good thermomechanical properties. Also the construction of porous POSS-based hybrids with those properties could be used to fabricate advanced devices. The rigid and cubic POSS with different functional groups has been well explored to construct three-dimensional porous hybrid polymer materials. Functional

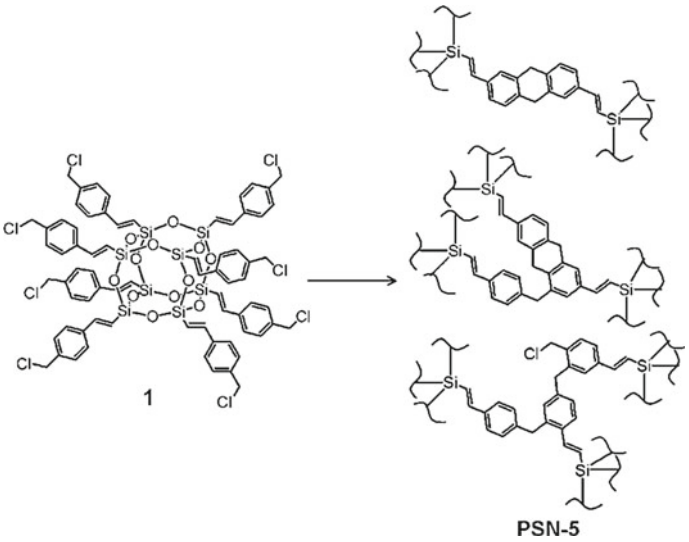

Fig. 3 Synthesis of PSN-5 by Friedel-Crafts Self-Condensation of 1. Reprinted from [16], © 2011 with permission from American Chemical Society

porous materials have diverse applications, such as gas storage, dielectric, sensor, gas separation, and heterogeneous catalysis.

Chaikittisilp et al. [16] offered porous hybrid polymers via Friedel–Crafts alkylation polymerization of a benzyl chloride-terminated POSS monomer (Fig. 3) which shows Brunauer–Emmett–Teller (BET)-specific surface area of $2509 + 59$ m^2 g^{-1} and a large total pore volume of $3.28 + 0.10$ cm^3 g^{-1}. Further, acrylo-isobutyl-POSS and tetraphenylethene-containing acrylate-based copolymer (thickness of 560 nm) with uniform porous fiber-structured (~300 nm diameters) films have been developed by electro-spinning as an aggregation-induced emission (AIE)-active material, which shows significantly enhanced sensitivity to explosive vapors than the more thickness films, where the POSS cages are assisting in the formation of porous structures and subsequently increasing response to explosive vapors. The surface area of electro-spun thin film (S_{BET} 170 m^2 g^{-1}) is higher than that of the drop-cast thin films (S_{BET} 4 m^2 g^{-1}) [17]. Similarly, octa-tetraphenylethene-POSS-based microporous hydrogen-bonded organic framework (HOF) was developed via amide linkages [18], which shows a porosity of 101.9 m^2/g S_{BET}. The HOF exhibits a high fluorescence quenching effect with copper ion, and also the fluorescence of HOF has been recovered by cyanide. Also, a hybrid porous material was obtained via AIBN radical polymerization of octavinylsilsesquioxane (OVPOSS) with high S_{BET} of 1080 m^2 g^{-1} and 2 wt% hydrogen uptake [19].

Zhang et al. [20] offered a new approach to synthesis of mesoporous POSS hybrid materials with ordered structure, co-assembly of octa-ethyltriethoxysilyl-POSS around the P123 micelles and following condensation of triethoxysilyl and

extraction of the obstructed P123 was generated mesoporous POSS network with uniform pore size, which exhibits a S_{BET} of 960 $m^2\ g^{-1}$ with a total pore volume of 0.91 $cm^3\ g^{-1}$. Likewise, Li et al. [21] fabricated a series of ordered mesoporous silica and organosilicates using Pluronic F127 as a template via evaporation-induced self-assembly method. The weight ratios of tetraethyl orthosilicate (TEOS) and octaethyltriethoxysilyl-POSS precursors determined the mesophases, where the TEOS alone exhibits an ordered body-centered cubic (bcc) structure and was changed to ordered face-centered cubic (fcc) structure for 10 and 20 wt% of POSS and above 30 wt% of POSS showed disordered spherical pores. The porosity of the resulting hybrids was decreased from 831 to 537 $m^2\ g^{-1}$ while increasing the POSS content from 0–50 wt%, respectively.

Alves et al. [22] developed hybrid porous materials from OVPOSS via radical polymerization and thiol-ene click reaction using porogenic diluents such as tetrahydrofuran and polyethylene glycols. Highly porous monolithic building blocks with S_{BET} 700 $m^2\ g^{-1}$ or more and mesopore volumes of up to 2 $cm^3\ g^{-1}$ were prepared by choosing proper porogenic solvents and initiator. This approach explores a new route to derive porous hybrid adsorbents for a wide variety of applications.

Flexibility and length of the linking moieties and polycondensation reaction efficiency were determined the degree of porosity. Pawlak et al. [23] offered the hybrid porous structured frameworks, which were synthesized via hydrosilylation reactions of flexible linear siloxane spacers of 1,1,3,3-tetramethyldisiloxane (S-1) and 1,1,3,3,5,5,7,7-octamethyltetrasiloxane (S-2) with octa(vinyl)-POSS using Pt(dvs) catalysts. The pore sizes of these two hybrid polymers were measured by positron annihilation lifetime spectroscopy. The S-1 exhibits a shorter linker with the free volume diameters of 5.32 ± 0.06 Å (POSS cages), 8.28 ± 0.05 Å, and 10.42 ± 0.05 Å (linker spacing), whereas S-2 has a longer linker with the diameters of 4.96 ± 0.04 Å (POSS cages) and 7.96 ± 0.06 Å (linker spacing). Further, based on the cross-linkers' length, the pores' shapes have shown as an ellipsoidal shape, and the S-1 and S-2 have similar pore sizes of 8–12 Å and 8–15 Å, respectively (Fig. 4). These pore sizes were related to the lengths of the cross-linkers.

Moreover, the PALS measurements revealed that the larger pore sizes of the polymers are not depending on the longer spacers. The S-1 shows a significant disorder and scatter in pore size, whereas the S-2 exhibits well-ordered POSS cages which were connected by the longer space linkers. Studies on the host–guest interactions of the complexes suggested that the presence of organic solvents strongly influenced on the molecular motion of the POSS units of S-2, whereas the S-1 remains rigid. This type of porous materials can be used for gas carriers and as containers for small organic compounds.

3.1 POSS–Polymer Hybrids

Polymers have widely been used as an adhesive in the preparation of composite films through covalent bonding and/or physical blending with inorganic species, includ-

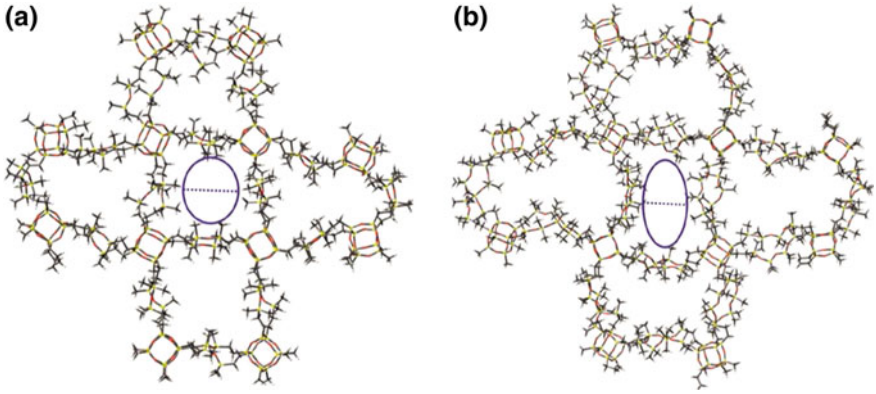

Fig. 4 Theoretical model of 1 (**a**) and 2 (**b**) with a pore size of 8–12 Å and 8–15 Å, respectively. Reprinted from [23], © 2015 with permission from American Chemical Society

ing silica. The incorporation of nanoparticles into the polymer thin films is useful to control porosity and permeability. The construction of thin films using large silica compounds has some limitations such as porosity, thickness, and strength of the film which are mainly defined by the size and stability of the silica species. Further, the liquid crystals or micelles are used as a template to attain nanometer-sized mesoporous silica films from a soluble silica source (e.g., TEOS) under hydrothermal or acidic conditions, despite problems arise from the limited stability of silica sols with <5 nm particles size. To overcome these limitations, the silica species are stabilized with organic molecules, for example, nanoporous POSS materials could be used as a nanosized building block with enhanced physical and chemical properties. The layer-by-layer self-assembly of octa(aminophenyl)silsesquioxane (OAPS) and poly-(styrene-4-sulfonate) (PSS) on the planar substrates and polystyrene particles formed as a multilayer thin film. The OAPS has adsorbed on PSS by promoting acid–base interactions between amine groups of OAPS and sulfonate groups of the PSS. Similarly, thin films have been constructed with alkylamines/amine-bearing organometallics and Bronsted acids, R-M(IV)$(HPO_4)_2$, H_2O (M = Zr, Ti, Sn, etc.), $HTiNbO_5$, and $HTaWO_6$, nH_2O [24]. OAPS is a prominent building block in the construction of ceramic membranes and different size and shape of siliceous capsular colloids and hybrid porous films on planar and spherical supports (Fig. 5).

Ye et al. [25] recently demonstrated POSS cross-linked polyimide (PI) aerogels, and OAPS was used to cross-link oligomers made from 3,3′,4,4′-biphenyltetracarboxylic dianhydride and bisaniline-p-xylidene; the resulting hybrids exhibit high thermal stability with 2% wt loss at 400 °C and low thermal conductivity of 14 mW$(mK)^{-1}$ at 760 Torr. SEM images of aerogels showed the porous morphology in which polymer fibers with diameters in the range of 15–50 nm tangled together and the S_{BET} of the aerogel was 240–260 $m^2\ g^{-1}$. Furthermore, the reinforcement method of POSS cages into the polymer matrix is an important in the hybridization, because the physical properties of the hybrid materials were attributed

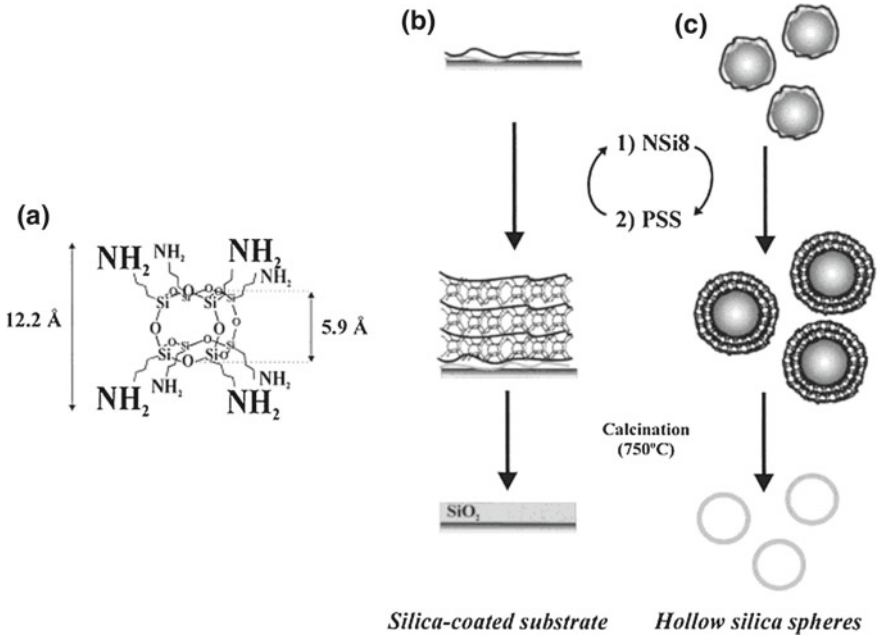

Fig. 5 Schematic diagrams of the LbL assembly of NSi8 molecules (**a**), with PSS on planar substrates (**b**), and on PS particles (**c**). Subsequent calcination results in supported thin silica films (**b**) or hollow silica spheres (**c**). Reprinted from [24], © 2002 with permission from American Chemical Society

to the homogeneous dispersion of POSS cages. Cozza et al. [26] demonstrated the homogeneous dispersion of POSS at a nanometric level into a polymer matrix by electro-spinning approach. Cellulose acetate was dissolved in the mixture of acetone/DMAc solvents with different weight percentages of epoxycyclohexylisobutyl-POSS and was used for the electro-spun and cast film preparation. This approach obliges in the molecular-level/nanosized clusters dispersion of POSS to develop alternative approaches capable to promote POSS distribution in the film. In addition, the hybrid micelles are derived from the combination of the hydrophobic segment of 3-iodopropyl-hepta(cyclopentyl)-POSS and hydrophilic part of polyoxazolines (POZO), where the micelle formation relies on the concentration of POSS incorporated into the POZO [27]. Consequently, the octa(isobutyl)-POSS is a non-amphiphilic and forms aggregates at all surface concentrations at the air/water interface; subsequently, the aggregation was dramatically decreased by blending with polydimethylsiloxane (PDMS) used as an amphiphilic (>10 wt% PDMS) which were studied by Brewster angle microscopy (BAM) [28]. Also, elastomers were developed from PDMS and POSS cages, the resulting POSS–PDMS nanocomposite elastomers show an improved thermal and mechanical properties, due to increase in the free volume of the final matrix [29].

Xiu Qiang et al. [30] demonstrated a series of star-shaped POSS-fluorinated acrylate copolymers, which are used to produce hydrophobic honeycomb-patterned micro-/nanoscale porous films via breath figure (BF) method, which depends on the influences of fluorine-based polymers and POSS cages, solvents utilized, and solution concentrations. These kinds of porous films could be retained after longtime preservation in an acid–base condition and show a great potential in cell culture, filtration, and tissue engineering applications. Likely, Hong et al. [31] reported POSS-fluorinated polyacrylates, which were synthesized by atom transfer radical polymerization. The hybrid porous films were optimized by varying the solution concentrations and solvents, and then the surface morphology of the porous films was evaluated which revealed that the amphiphilic-structured block copolymers are capable of forming well-organized porous films in a wide range of concentration, while star-shaped polymer without amphiphilic structure could only form regular porous array in some specific conditions. The ratios of pore diameter (D) and rim width (W), D/W, for the porous films were determined from SEM images and defined as fa. The influence of chemical composition and morphology on the surface hydrophobicity can be separated by the investigation of the correlation between fa and surface water CAs for the polymer films. The advantages of amphiphilic-structured block copolymers for porous films preparation are the ability to form hydrophobicity surface with much higher fa than those from hydrophobic polymer. The BF film with superhydrophobic surface was obtained by stripping the surface of the porous films, and the resulted films with pincushion-like structure show a high fa value.

A series of amphiphilic poly(vinyl alcohol)-POSS (PVA-POSS) hybrids have been synthesized via urethane linkage formation between the hydroxyl groups of PVA and the mono-isocyanate group of POSS macromers [32]. The electro-spun PVA-POSS fibers with highly porous crystalline structure show enhanced/controlled water resistance without the covalent cross-linking. The incorporation of POSS dramatically altered the solubility of the PVA-POSS hybrids, and hydrophobicity of PVA-POSS could be varied by controlling the concentration of POSS cages. Also, hybrid three-dimensional thermosetting resin of resol-type POSS–polymer ablative heat shielding material was produced from resorcinol formaldehyde (RF) and octa(phenyl)-POSS (OP-POSS) via facile in situ polymerization technique for thermal protection system (TPS) [33]. Further, POSS and 2-oxazoline-benzoxazine-based hybrids were prepared in one-pot reaction by the functionalization of OAPS via the formation of benzamidine structure by ring-opening and addition reactions between oxazoline and amino phenyl group at room temperature and subsequently the polymerization of benzoxazine at higher temperature [34]. However, higher content of OAPS may reduce the thermal properties of the nanocomposites. It is wondered that the introduced OAPS decreased the packing density and increased rigidity of the polymer matrix. OAPS may increase free volume by its nanoporous structure, and the Si–O core in OAPS leads to a plasticization of polymers, which decreases the Tg of the polymers. At high POSS content, the polymer matrix aggregation of POSS usually occurs, which is not advantageous for the thermal properties of the polymer. Therefore, particular concentration of POSS only can be utilized to enhance the thermal properties of the nanocomposites.

Hybrid mesoporous materials are synthesized from OAP-POSS and di-aldehyde through Schiff base chemistry; these hybrid materials show uniform mesoporous size and high specific surface areas. The molar ratio of POSS and aldehyde affects the porosity of the resultant POSS hybrid materials, where 1:0.7, 1:1, and 1:1.2 ratios show the S_{BET} of 637, 617, and 1103 $m^2\ g^{-1}$, respectively, and beyond this ratio of 1:1.5 shows reduced S_{BET} [35]. Further, the condensation of OAPS and glutaraldehyde provides hybrid mesoporous networks via the formation of Schiff base. The material shows uniform mesoporous size and have S_{BET} of 641–1103 $m^2\ g^{-1}$ and pore volumes of 0.47–0.53 mL g^{-1} [35]. In addition, Liu et al. [36] fabricated the similar amine-terminated OAPS-glutaraldehyde hybrid networks with a specific surface area of 42.8 $m^2\ g^{-1}$ via modified reaction conditions, for the removal of acidic dye from wastewater. As a novel solid-phase adsorbent, these POSS nanohybrids possess selective adsorption properties for acidic dyes (e.g., methyl orange (MO). The strong electrostatic interactions between MO species and the amine groups of the nanohybrid are the main driving forces for MO adsorption, and the hybrid shows a maximum adsorption capacity of 237.5 mg g^{-1}. The adsorbed MO species could be effectively recovered by using the mixture of methanol/NaOH (9/1, v/v, 0.1 mol L^{-1} NaOH) as eluent. The cross-linked POSS nanohybrid appears to be a promising material in dye removal field which can be potentially applied for textile wastewater treatment.

Flexible polyurethane foams (PUFs) were largely used in mattresses, upholstered furniture, seats, etc., and needed to improve the quality of polyurethane foam which has been increased by adding POSS materials into the polyurethane foam via cross-linking. Recently, high compressive strength, thermally stable, and less water-absorbing polyurethane foams were constructed with defined cell structure and density by using 0–15 wt% of 1,2-propanediolisobutyl POSS (PHI-POSS) as a pendant group and octa (3-hydroxy-3-methylbutyldimethylsiloxy) POSS (OCTA-POSS) as a chemical cross-linker in the polyurethane polymer matrix. The addition of PHI-POSS into PUF significantly increased the number of foam cells with reduced average area of cells, whereas the OCTA-POSS decreased the number of foam cells and increased the average area of cells. Moreover, POSS cages form different sizes of lamellae-shaped crystals, distributed homogeneously in the bulk (PHI-POSS) or close to the self surfaces (OCTA-POSS). POSS-reinforced PUF hybrid foams possess greater compressive strength than the reference foam in the direction parallel and perpendicular to the direction of foam rise. The largest increase in compressive strength is observed for the 5 wt% OCTA-POSS/PUF hybrid, and it is about 192 kPa in a perpendicular direction and 189 kPa in the parallel direction, but further loading reverses the phenomenon. This is due to the crystalline nature of OCTA-POSS retained up to a particular concentration beyond that the PU closed cell structure was damaged. But, the compressive strength increases steadily with increasing PHI-POSS content in the PUF matrix, in all three directions is observed as compared with the reference foam. Also, due to increasing foam density, the PUF/POSS hybrids absorb less water than the pristine foam [37].

A sorbitol-based polyether polyol, polymeric 4,4′-diphenylmethane diisocyanate and dimethyl propane phosphonate (DMPP), PHI-POSS, and OCTA-POSS were

used to prepare hybrid foam materials as a flame retardant. The incorporation of the POSS cages influences the cellular structure of PU as evidenced by a change in anisotropy index of the cross section parallel to the growth direction. The flammability results and thermogravimetric data suggest that the formation of char as a layer at the surface acts as an insulating barrier limiting heat and mass transfer with flame retardant and thus leading to decreased heat release rate, especially for systems containing OCTA-POSS. This is due to the formation of denser network by cross-linking of OCTA-POSS, whereas the pendant PHI-POSS cage does not impose such a prominent effect owing to its more loose arrangement in the PU matrix [38].

A high internal phase emulsion (HIPE) has been defined as an emulsion in which the internal phase occupies more than 74% of the volume. The porous structured polyHIPE nanocomposite with densities of around 1.5×10^2 kg/m^3 has been synthesized by cross-linking of 2-ethylhexyl acrylate (EHA) with vinyl silsesquioxane (VSQ) reinforcement. PolyEHA has a glass-transition temperature (T_g) of −50 °C and is flexible, and so EHA is often used as a cross-linked and reinforced elastomer. With increasing VSQ content, tan δ peak temperature, tan δ full width at half-maximum, room-temperature modulus, and stress at 40% strain all increased in a linear fashion, reflecting the increase in cross-linking through reaction with the reinforcing Si-O network. The VSQ-containing polyHIPE was compared to polyHIPE based on EHA cross-linked with divinylbenzene (DVB) and reinforced by reaction with a one vinyl tethered POSS, the tan δ peak temperature and modulus increased with increasing DVB content, reflecting the increase in cross-link density and in backbone rigidity [39]. In addition, polyHIPE nanocomposite with about 0.13 g/cm^3 densities was synthesized from EHA, DVB, organic cross-linker, and either methylsilsesquioxane (MSQ) or vinylsilsesquioxane (VSQ, SSQ cross-linker) [40]. The POSS-containing polyHIPE had significantly higher tan δ peak temperatures and moduli for similar Si contents. These properties were significantly larger for VSQ-based polyHIPE than for MSQ-based polyHIPE. Porous inorganic monoliths were produced on pyrolysis of these VSQ-containing polyHIPE. The most thermally stable polyHIPE nanocomposites were produced by the formation of SSQ-organic interconnected networks through VSQ and DVB cross-linking.

3.2 POSS–Metal Hybrids

POSS derivatives have been introduced into inorganic minerals to tune their physical properties. Kataoka et al. developed layered organic–inorganic hybrid perovskites with high crystallinity by self-assembling of metal halides ($CuCl_2$, $PdCl_2$, $PbCl_2$, and $MnCl_2$) and octa(Propylammonium)-POSS [41]. The presence of POSS as an interlayer between the metal halide perovskite layers producing the micropores enhances the low-dimensional properties of the materials. Also it has some magnetic ordering (CuPOSS and MnPOSS) and excitonic absorption/emission (PbPOSS) properties. The producing micropores in the perovskite materials by inserting POSS cages rendered a new approach the physical properties of the perovskite materials (Fig. 6).

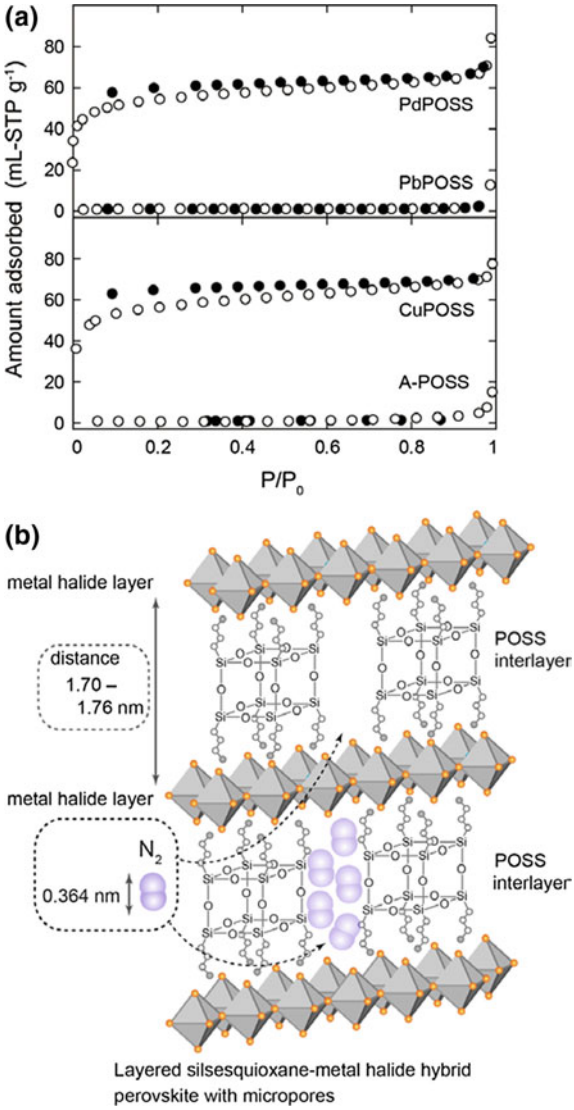

Fig. 6 **a** N_2 sorption isotherms of silsesquioxane−metal halide complexes at 77 K (open circles, adsorption; filled circles, desorption). **b** Schematic diagram of layered POSS−inorganic hybrid perovskites with N_2 adsorbed between layers. Reprinted from [41], © 2015 with permission from American Chemical Society

Another approach has been made for the construction of dumbbell-shaped hybrid organic–inorganic molecules based on polyoxometalates (POM) and POSS with hierarchical supramolecular nanostructures [42]. A highly ordered lamellar morphology of POM-organic-POSS cocluster represents a strong thermodynamic force driving a nanoscale phase separation of the POM and POSS blocks. Further, coordination polymer networks have developed with ordered porous structure from eight carboxylic terminated POSS (S-POSS) and copper ions. The S-POSS was prepared by

the treatment of octa(aminopropyl)-POSS with succinic anhydride; subsequently, the S-POSS was used as a ligand for making a network with metal centers [43].

Similarly, Hay et al. [44] reported linear titanium(IV)-POSS coordination polymer. Also, Sanil et al. [45] demonstrated a new method for the adsorption and separation of gases in the presence of relatively large amounts of moisture by enhancing the stability of $Cu_3(BTC)_2$ against moisture. To this, a metal–organic framework (MOF) was constructed by the functionalization of octa(aminopropyl)-POSS (O-POSS) with copper trimesate ($Cu_3(BTC)_2$) with enhanced hydrophobicity and stability against humidity. POSS modification was also successfully applied to other MOFs such as MOF-74 and MIL-100. $Cu_3(BTC)_2$ and O-POSS@$Cu_3(BTC)_2$ showed a S_{BET} of 1661 and 1514 $m^2\ g^{-1}$, respectively. After the modification of $Cu_3(BTC)_2$ with O-POSS, there was no considerable decrease in the surface area. Due to the smaller window size of $Cu_3(BTC)_2$ (ca. 0.9 nm), it prevents the penetration of the larger size of O-POSS through the micropores of $Cu_3(BTC)_2$. After exposure to 90% relative humidity (RH), the S_{BET} of $Cu_3(BTC)_2$ drastically decreased from 1661 to 81 $m^2\ g^{-1}$, whereas the S_{BET} of O-POSS@$Cu_3(BTC)_2$ slightly decreased from 1514 to 1476 $m^2\ g^{-1}$. Also the SEM image of O-POSS@$Cu_3(BTC)_2$ showed there was no change in the morphology, but the morphology of $Cu_3(BTC)_2$ changed from cubic particles to agglomerated particles having an undefined shape. These results suggest that the surface modification of $Cu_3(BTC)_2$ with O-POSS dramatically enhances the stability of $Cu_3(BTC)_2$ against humidity.

Significant ion-exchanging capacity of the ionic-based porous materials shows important applications in various fields. Ionic liquids (ILs) often obtained from quaternization of N-heterocyclic compounds and alkyl halides, and also the POSS-based ILs were prepared by using the functional POSS moieties as cations or anions. However, Chen et al. [46] demonstrated the POSS-based porous cationic frameworks (PCIF-n), synthesized from octakis(chloromethyl)silsesquioxane (ClMePOSS) and N-heterocyclic cross-linkers [4,4′-bipyridine (4,4′-bpy), 1,2-bis(4-pyridyl)ethylene (bpe), N,N,N′,N′-tetramethylethylenediamine (tmeda), 1,3-bis(4-pyridyl) propane (bppa), 1,2-bis(4-pyridyl)ethane (bpea), bis(1-imidazolyl)methane (bim), and 1,4-diazabicyclo[2.2.2]octane (dabco)] as shown in Fig. 7. Hydrophobicity, mesoporosities with enhanced poly(ionic liquid)-like cationic structures, high surface areas (1025 $cm^3\ g^{-1}$), and larger pore volumes (0.90 $cm^3\ g^{-1}$) are the main advantages of the PCIF-n. Moreover, the most rigid molecule 4,4′-bpy shows the highest surface area of 1025 $m^2\ g^{-1}$, whereas the less rigid bpe possesses lowered surface area of 396 $m^2\ g^{-1}$ and contrarily the flexible molecules bppa and bpea exhibit very low surface area ($\leq$40 $m^2\ g^{-1}$), while the rigid cross-linkers of non-pyridine-based N-bearing organic molecules (bim, dabco, and tmeda) showed considerably high surface areas (183 ~ 729 $m^2\ g^{-1}$) and also attained micro-/mesoporous frameworks. The resulting data revealed that the rigid structures of both POSS and N-bearing organic cross-linkers are the important prerequisites in the development of POSS-based porous cationic polymeric frameworks. Also, the PCIF-n materials were used as the supports for loading guest species ($PMo_{10}V_2O_{40}{}^{5-}$) to obtain the porous POSS–metal hybrid material denoted as PMoV@PCIF-1 as a potent heterogeneous catalyst for oxidation of cyclohexane and benzene.

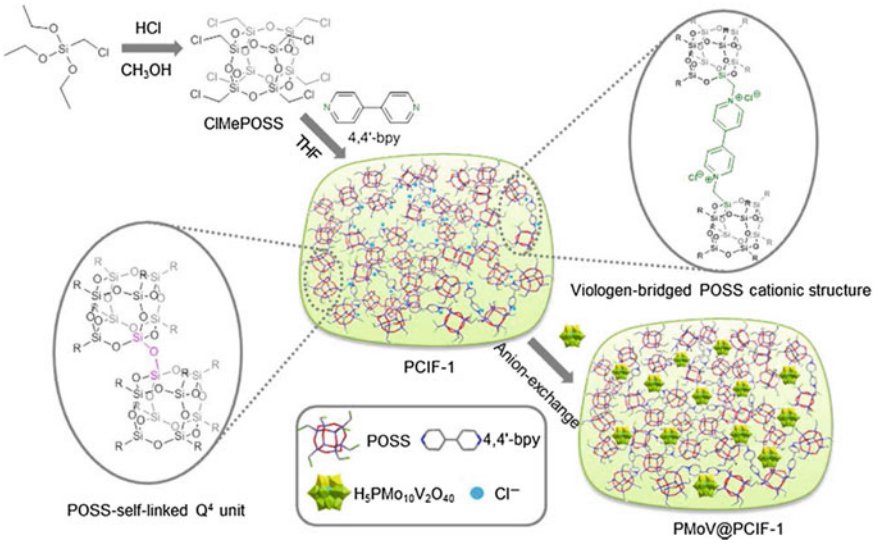

Fig. 7 Synthetic procedure of POSS-based porous cationic framework PCIF-1. From original synthesis of a new octakis(chloromethyl)silsesquioxane (ClMePOSS) monomer to the successive quaternization reaction of ClMePOSS with 4,4′-bipyridine (4,4′-bpy) to form PCIF-1. Then, bulky $PMo_{10}V_2O_{40}^{5-}$ (PMoV) anions are loaded into PCIF-1 to obtain the PMoV@PCIF-1 catalyst via anion-exchange process. Reprinted from [46], © 2015 with permission from Springer Nature

4 Properties of POSS Hybrid Porous Materials

Porous hybrids with pore properties such as pore size, pore volume, surface area, and pore geometry as well as shapes of materials (monoliths, films, and particles) including thermal and mechanical properties are technologically important materials especially in the field of adsorption, catalysis, and separation [47]. Well-defined POSS-based hybrid polymers with a variety of architectures have been developed including telechelic polymer, block copolymer, and star-shaped polymer hybrids by using variety of POSS precursors and unique living polymerization techniques, such as ring-opening/addition polymerization, free radical polymerization, coupling reactions, such as click chemistry and hydrosilylation reactions. Also, POSS nanoparticles have been self-assembled into aggregates in a selective solvents and form nanostructures in bulk [12]. The high compatibility of trisilanolphenyl-POSS/polycarbonate composites possesses significant transparency and crystallinity along with enhanced thermal and mechanical properties [48]. Also, Crowley et al. [49] reported POSS–poly(carbonate-urea)urethane (POSS-PCU) nanocomposites as a bio-scaffold for tissue engineering, which was optimized by dispersion of porogens (sodium chloride, sodium bicarbonate, and sucrose) onto the material surface to increase the surface porosity, thus providing additional opportunities for improved cellular and vascular ingrowth. The surface porosity of the composites relies on the

size of porogens and larger porogens provided improved porosity. The larger pore sizes of these scaffolds favor for cellular integration and vascular ingrowth.

Brigo et al. [50] offered porous inorganic thin films from phenyl-bridged-POSS via sol-gel process. The structural and optical properties of the films were assessed and the formation of the porous system was investigated, after deposition and thermal treatments at increasing temperatures in the range of 60–800 °C. The spectral data indicate that the completely inorganic silica-based network at curing temperatures is higher than 500 °C, at which temperature the organic components of the hybrid film were eliminated and an elevated residual porosity was observed with a pore volume fraction of 35%. The films cured at 700 °C exhibited very low refractive index of 1.244 at 600 nm. Those micro- and mesoporous POSS hybrid thin films differentiate in pore dimension, dispersion, and connectivity from wide-spread developed mesoporous thin films for which large pores are produced by the removal of self-assembled polymeric units at higher temperature. The well-constructed porous structured hybrid POSS materials have shown significant properties, which lead to unlimited potentials for promising applications, such as biomedicine, electronic, sensors, optical, magnetic nanodevices, gas storage, and stimulated catalysts.

4.1 Porosity/Surface Area

More recently, porous materials with controlled porosity have been developed by the connection of inorganic building blocks themselves or with organics through the bridging groups, where the size of pores is controlled through the choice of the organic bridging groups that are capable of selective adsorption or catalysis. Copolymerization of hydride-terminated silyl POSS and alkene functionalized POSS through hydrosilylation process using Karstedt's catalyst offered porous materials [2]. The homogeneous porous materials have been developed by template synthesis method; organic templates are used during polymerization or cocondensation process which will be self-assembled uniformly, after that the templates are removed by the process of calcination, chemical oxidation or hydrolysis, whose pores size are roughly resembles to the size of the template. Accordingly, the acetylene-bridged POSS materials are allowed to the thermolysis process to burn away the acetylene template for obtaining the porous silica material. Also an alternative approach used low-temperature, inductively coupled plasma to eliminate organic bridging groups in cross-linked POSS xerogels and resulted in porous silica gels which pores size is larger than that of xerogels. The mesoporous silica gels can be obtained by treating non-porous alkylene-bridged POSS xerogels. The size of the pores can be increased by increasing the length of the bridging group.

The solgel process for the preparation of porous hybrid materials is sensitivity to the factors such as pH, aging time, catalyst, temperature, and solvent which are significantly controlled to permit the structure–property effects of the bridging group to be determined reproducibly. Many kinds of porous materials with different pore size have been prepared by changing the organic bridging groups. For example,

arylene- and ethenylene-bridged POSS give rise to microporous materials with high surface areas of 1800 m^2/g including the mean pore diameters of <2 nm, whereas the alkylene-bridged POSS–polymer matrix with the bridging groups up to 10 carbons in length possess mesoporous xerogels. Despite, some of the literature suggested that the materials only with five- or six-atom bridges would be porous, while shorter or longer than that bridges led to be non-porous materials. But, another prepared porous hybrids exhibited high specific surface areas even with bridge lengths of two to four atoms. However, it has been suggested that the length of the organic bridges between the POSS cages is a critical factor in determining porosity. The length of the bridging groups is roughly proportional to the mean pore diameter of the hybrid material. Presence of unsaturated functional groups like aromatic and olefinic in the organic bridges could increase the rigidity and prevent the collapse of the formed pores during thermal process.

The condensation of metal alkoxides or alkoxysilanes has been mostly explored via solgel approach. The synthesis conditions such as concentrations of catalyst, type of catalyst, choosing solvent, temperature of the medium and also the drying circumstances of the materials are playing vital role in the formation of porous materials. Controlled processes of silane condensation under acidic or basic conditions offer gels which can be air-dried to get xerogels or supercritically dried to produce aerogels. For instance, POSS aerogels have been prepared as micro-/mesoporous materials based on organics-bridged bis(trialkoxy)silanes with surface areas up to 1000 m^2/g, pore volumes up to 0.6 mL/g. The further investigations on the synthesis of porous POSS–polymer hybrids offered types of pores generated during the condensation and cross-linking process with controlled surface area, porosity, and functionality. The positron annihilation lifetime spectroscopy (PALS) permitted to identify pores size of the cubic rigid POSS core (~0.3 nm) and in between of the POSS cubes (1–1.1 nm), while S_{BET} provided a view of the pore sizes in the range of 1–50 nm, whereas SAXS gives the overlapping confirmation of the two methods. The irreversible adsorption phenomena was happening at particular experimental conditions due to the presence of flexible linkages and micropores as well as mesopores in the hybrid polymers, which might be related to the swelling of a non-rigid porous structure.

4.2 Morphology

Liu et al. [51] reported the organic–inorganic mesoporous hybrid; the hybrid was prepared by two steps from octa-anionic-POSS and cationic surfactant: (i) lamellar precursor made of POSS and surfactant was prepared by template-directed synthesis; (ii) mesoporous structure was obtained via the reformation of lamellar precursor to hexagonal mesophase under hydrothermal treatment. The transformation can be illustrated by four stages, as (Fig. 8): (1) original lamellar structure, (2) corrugation of the lamellar sheets, (3) primary mesoporous structure, and (4) ordered mesoporous structure.

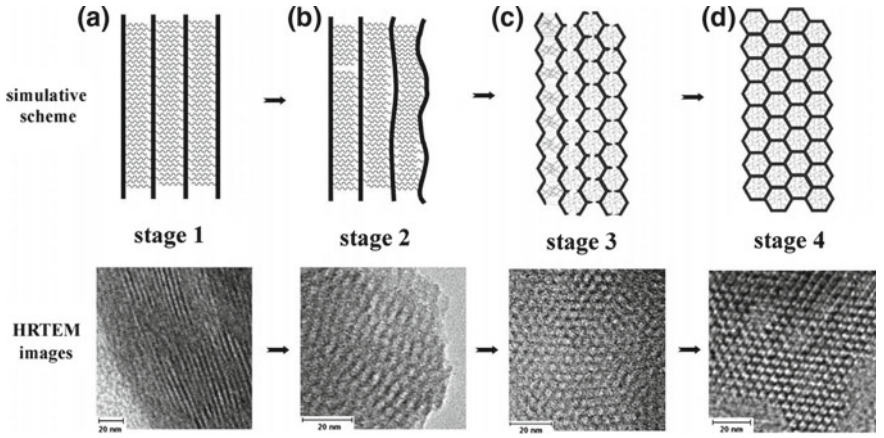

Fig. 8 Lamellar-to-hexagonal transformation process and corresponding HR-TEM images. **a** Original lamellar structure; **b** corrugation of the lamellar sheets; **c** primary mesoporous structure; **d** ordered mesoporous structure. Reprinted from [51]], © 2010 with permission from Elsevier

4.3 Thermal Properties

Incorporation of POSS molecules into the polymer system by blending/chemical cross-linking significantly enhances the thermal stability and porosity of the resulting POSS–polymer hybrid network. Alagar and coworkers [52] demonstrated the different functionalities of POSS reinforcement into the different kind of polymer materials and the thermal properties of resulting hybrid polymer materials with POSS. For example, a series of four different linear aliphatic ether-linked aromatic bismaleimides (AEBMIs) were synthesized, and then different ratios of POSS-AEBMI nanocomposites were prepared by Michael addition reaction. Data from thermal studies revealed that the particular ratios of POSS-AEBMI nanocomposites exhibit higher glass-transition temperature (T_g), thermal stability, limiting oxygen index, and lower dielectric constant when compared to that of neat AEBMI. Similarly, octa(maleimide)-POSS (OMPS), bisphenol-A-based cyanate ester (CE) and diaminodiphenylmethane (DDM) acting as a coupling agent were used to prepare CE-POSS hybrid network via in situ polymerization method by thermal curing [53], where the 5 wt% OMPS-incorporated nanocomposite shows higher glass-transition temperature than those of nanocomposites filled with a lower percentages of OMPS and neat amine-CE system. Also, Octakis(dimethylsiloxypropylglycidylether)silsesquioxane (OG-POSS)-reinforced polybenzoxazine nanocomposites exhibit significantly improved thermal stability and reduced dielectric constant [54]. Moreover, OAPS-incorporated epoxy-amine nanocomposites based on diglycidyl ether of bisphenol-A (DGEBA) and tetraglycidyl diamino diphenyl methane (TGDDM) were prepared and studied using differential scanning calorimetry (DSC) and dynamic mechanical analysis (DMA), indi-

cate that the glass-transition temperatures of POSS (63 wt%) containing nanocomposites are higher than that of the corresponding neat epoxy systems [55]. Besides, the thermogravimetric analysis (TGA) shows that the POSS–epoxy nanocomposites exhibit high ceramic yields, suggesting that the improved flame retardant property. Similarly, the various compositions of OAPS-PI hybrids were prepared and thermal and dielectric properties of the nanocomposites were studied, higher content of POSS (15 wt%) in the nanocomposites substantially enhanced the glass-transition temperature (T_g), and thermal stability and char yield decreased the value of dielectric constant when compared to neat PI matrix [56].

4.4 Mechanical Properties

The nanoporous POSS cages' reinforcement into the polymer matrix by chemical cross-linking considerably increased the mechanical properties of the polymer hybrid system. In the glass state (−75 to −25°C), POSS–polymer hybrids exhibit higher value of dynamic storage moduli than that of the polymers. For example, 2 wt% of POSS cages introduced polyurethane (PU) polymer hybrids possessing significantly increased dynamic storage modulus [57]. However, the higher concentration of POSS-containing hybrids was showing less storage modulus than that of the PU. Due to the decreasing cross-linking densities of the hybrids with increasing concentration of POSS, the decreased densities could be attributed to an increase in the porosity of the POSS hybrids. The porosity of the matrix will rise by insertion of POSS cages which arises from the external porosity via increasing free volume of the nanocomposites and the nanoporosity of the POSS core with diameter of 0.54 nm. OAPS-incorporated epoxy-amine nanocomposites shows improved tensile, impact and flexural strength including thermal stability than that of the neat epoxy-amine system [58]. The OG-POSS and OAPS were used as a building block in the cyanate ester–epoxy nanocomposites; thermal, mechanical, and dielectric studies indicate the influences of POSS macromer existing in the nanocomposites, where the thermal stability and mechanical properties were enhanced significantly with increasing POSS content but decreased the value of dielectric constant and dielectric loss of the hybrid polymer system [59]. DDM and structurally modified diamines, namely bisphenol-A-based ether diamine, octane-diol-based ether diamine, and capron-based diamine, were used to cure DGEBA epoxy resin and were reinforced with different weight percentages of OAPS to obtain OAPS-epoxy-amine nanocomposites, where the epoxy-capron-based diamine cured matrix shows better improvement in tensile strength and impact strength of 39.8 and 137.0%, respectively, than those of epoxy-DDM system [60]. Additionally, the OAPS incorporation further improved the mechanical and thermal properties and also lowers the value of dielectric constant.

4.5 Catalytic Properties

Well-designed porous structured hybrid materials with POSS showed an excellent catalytic properties, Leng et al. [61] have been constructed porous amphiphilic polyoxometalate-paired ionic hybrids POSS–DIM_x–CIM_y–PW via free radical polymerization and ion exchange reaction using octavinyl-POSS and ionic liquids as building blocks. The POSS-free polymeric hybrid DIM_3–CIM_5–PW is a non-porous material with a surface area of only 6.2 $cm^2\ g^{-1}$. POSS-containing polymer hybrid shows optimum specific surface area of 24.2 $cm^2\ g^{-1}$ and pore volume of 0.175 $cm^3\ g^{-1}$ and are found to be highly efficient catalysts for epoxidation of alkenes with H_2O_2 as oxidant. POSS–polymer hybrids show increasing relative pressure of $0.8 < P/P0 < 1$, indicating the presence of porous structures. This proves that the POSS plays an important role in the pore formation. Further, Scholder and Nischang [62] demonstrated the preparation of highly efficient and robust capillary flow reactors based on large surface area, hierarchically structured porous hybrid material constructed in situ from vinyl POSS. Functional variants of vinyl POSS show an excellent catalytic performance in Suzuki and carbon–carbon cross-coupling reactions. Also, Sangtrirutnugul et al. [63] reported POSS-based materials, poly-POSS-Tn ($n = 8$, 10, 12, and mix), were prepared in high yields via free radical polymerization of corresponding pure forms of methacrylate functionalized POSS monomers, MMA-POSS-Tn ($n = 8$, 10, 12), and the mixture form, MMA-POSS-Tmix (Fig. 9). The S_{BET} of the POSS hybrids decreased from 839 to 683 $m^2\ g^{-1}$ in the following trend: poly-POSS-T12 > poly-POSS-T10 > poly-POSS-Tmix > poly-POSS-T8. Also, the Barrett–Joyner–Halenda (BJH) analysis represents highest mesopores of poly-POSS-T12. The Pd nanoparticles immobilized on poly-POSS-Tn ($n = 8$, 10, 12, and mix) are well dispersed with 4–6 wt% Pd content and similar average particle sizes of 6.2–6.5 nm with the S_{BET} ranges of 521–850 $m^2\ g^{-1}$. The stabilized POSS-based Pd nanoparticles catalyzed aerobic oxidation of benzyl alcohol to benzaldehyde in the reaction conditions of 90 °C, 6 h and a mixture of a H_2O/Pluronic (P123) solution, 72–100% yield. The PdNp@poly-POSS-T8 catalyst indicated the lowest catalytic activity, as a result of its lowest surface areas, total pore volumes, and amounts of mesopores. However, the PdNp@poly-POSS-Tmix catalyst showed an excellent catalytic activity in the conversion of various benzyl alcohol derivatives to the corresponding aldehydes in good to excellent yields.

4.6 Dielectric Properties

Dielectric properties of the materials can be improved by the incorporation of nano-sized filler-like POSS into polymeric matrices. The porous structured materials produced by POSS template or nanoporous POSS can generate air/vacuum in the hybrid materials which would help in the reduction of dielectric constant (κ) value of that materials [64]. Lee et al. [65] explained the reduction of κ value of PI/POSS hybrids

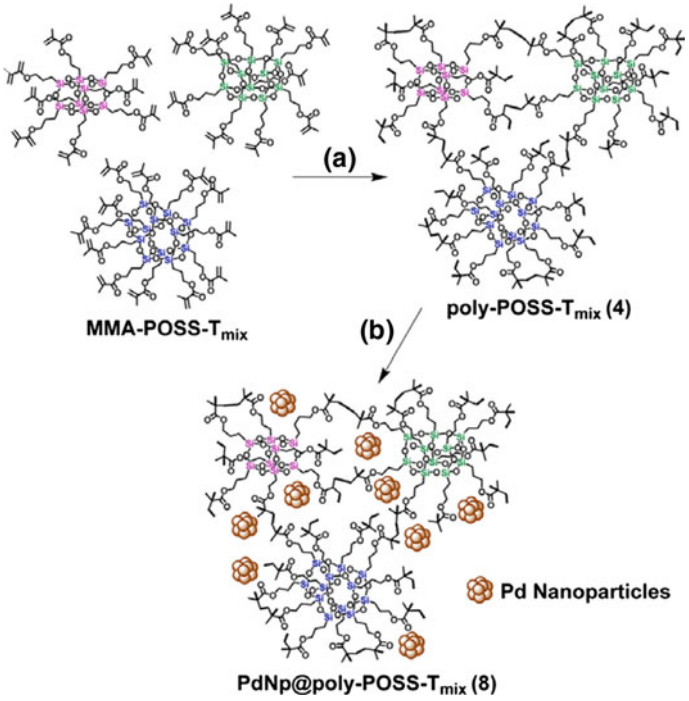

Fig. 9 A Representative Example for the Synthesis of Poly-POSS-Tmix and PdNp@poly-POSS-Tmix [**a** AIBN, PEG-200:THF (1:3 w/w), 60 °C, 24 h; **b** $Pd(OAc)_2$, NaBH4, CH3 OH, rt, 24 h]. Reprinted from [63]], © 2017 with permission from American Chemical Society

in terms of creating the porous silsesquioxane nanocores of the POSS and the free volume increase by the presence of the rigid and large POSS structure resulting in a loose polyimide (PI) network. The porosity of these nanocomposites is difficult to measure, and so they have adopted to measure the density to compare the relative porosity of these films. The density of pure PI and POSS are 1.38 and 1.10 g/cm^3, respectively. The measured dielectric constant of the PI is 3.22, whereas the PI/10 wt% epoxy—POSS is 2.65. However, OAPS/PI hybrid nanocomposites possess the lower value of κ (2.35) than that of PI ($\kappa = 4.45$) which inferred that the introduction of free volume into the hybrid matrix via restricted rotation of POSS by multiple point attachment to the PI backbone [66]. Accordingly, the proper insertion of POSS into a PI backbone can give rise to a reduction in the material's dielectric constant along with improved thermal and mechanical properties.

Leu et al. [67] reported porous POSS/PI nanocomposites as a low-κ dielectrics; nanoporous POSS-containing monoreactive amine group materials were reacted with poly(amic acid) having anhydride end groups. Polyimide chain-end tethered POSS can self-assemble into zigzag-shaped cylinders or lamellae by van der Waals force, 60–70 nm long and 5 nm wide. The resultant dielectric constant of the PI nanocomposite was reduced from 3.40 for the pure PI to 3.09 by incorporating 2.5 mol% of

POSS molecules. The PI/OAPS-POSS nanocomposites also exhibit a tunable dielectric constant with the change of content of OAPS-POSS, and the lowest value of 2.29 was observed 24.8 wt% of OAPS-POSS content. The reduction of dielectric constant was attributed to the POSS-induced external porosity and nanoporosity of POSS [68]. The low-κ nanoporous POSS-PI hybrid films could be developed by the incorporation of monoreactive functional group tethered octasilsesquioxanes into polymers via covalent bond [69]. Kuo and Chang [70] reported the grafting of a POSS derivative to POSS-PI hybrids having well-defined architectures. The presence of POSS molecules in a polymer matrix resulted in a nanoporous crystalline structure has both lower and tunable dielectric constants and controllable mechanical properties. Based on this approach, by controlling the amount of added POSS can be altered the dielectric constant of the film. Similarly, POSS-PI nanocomposites prepared by a graft polymerization of methacrylcyclopentyl-POSS (MA-POSS) with ozone-pretreated poly[N,N-(1,4-phenylene)-3,3,4,4-benzophenonetetra-carboxylic amic acid] (PAA), followed by thermal imidization which shows lower value of κ (2.2) than that of neat PI ($\kappa = 3.0$). The insertion of POSS cages into the side chain of PI films retained the nanoporous crystalline structure of the resulting matrix [71].

With minimal mole (2%) percentage of POSS-incorporated PI nanocomposites shows reduced κ value from 3.4 to 3.09 with retaining their tensile strength. The hybrid system self-assembled as lamellae or zigzag-shaped cylinders with 60–70 mm long and 5 mm wide, due to the formation of polar interactions between imide and van der Waal's forces between POSS cages [72]. Similarly, incorporation of 24.8 wt% OAPS into PI containing fluorine yielded 23% reduction in κ value, whereas 15 wt% Octakis(dimethylsiloxyhexafluoropropylglycidyl ether)silsesquioxane (OFG-POSS) in PI exhibits a 28% decrease in κ [73]. Moreover, the system retains high cross-link density, Young's modulus, porosity, and hydrophobicity but low polarizability. It is demonstrated that OFG-POSS efficiently reduces κ of PIs compared to other POSS derivatives.

Also, a nanoporous additive of fluorine-rich POSS cages (OF) were used to blend with UV-cured epoxy resin to decrease the κ value of the system by reducing polarizability, 10 wt% of OF reduces the κ value from 3.71 (plain epoxy) to 2.65 [74]. A poly(acetoxystyrene-co-octavinyl-POSS) (PAS–POSS) was developed as a low-κ organic–inorganic hybrid nanocomposites. The dielectric constant of PAS–POSS ($\kappa = 2.48$) is lowered than that of neat PAS ($\kappa = 2.81$), due to the increased relative porosity of the nanocomposite which arises from the intrinsic nanoporosity of POSS cages and the external porosity caused by the diluent effect of POSS [75].

Periodic mesoporous organosilica (PMO) is a distinct class of hybrid materials; POMs have shown diverse applications such as interconnect dielectrics for enabling smaller, faster, more powerful computer chips. Hybrid POSS-PMO thin film has been prepared using octa(triethoxysilylethyl)POSS by a template-directed, evaporation-induced, self-assembly (EISA) spin coating procedure, and the POSS-PMO thin film shrinks during those process. However, the POSS cage structure within the pore walls is retained and the mesoporous structure of the resulting POSS-PMO composites with ~1.5 nm pore size is maintained. Around 40% porosity of the hybrid POSS-PMO network was increased when compared to a reference POSS film, providing

a reduced κ value from 2.03 (POSS-PMO) to 1.73 (POSS film) [76]. Joseph et al. [77] demonstrated the homogeneously dispersed hybrid syndiotactic polystyrene-POSS composites which exhibit low-κ value of 1.95 and loss of 10^{-4} at 5 GHz, with high thermal and mechanical properties. Moreover, POSS-based polybenzoxazine nanocomposites were prepared by the copolymerization of furan-containing benzoxazine compounds and methylmethacrylate-POSS (MMA-POSS). The dielectric constants of the nanocomposites reduced to 2.3 up to 0–70 wt% of POSS. Also the POSS orientation into lamellar structures in nanometer sizes further reduced the κ value of the nanocomposites to about 1.9 [78]. Thus, the structural arrangements are also significantly involved in the reduction of κ value of the nanocomposites.

Similarly, Alagar and coworkers [15] demonstrated a new class of lamellar structured POSS/bisphenol Z (POSS/BPZ) polybenzoxazine (PBz) nanocomposites with low-κ dielectrics. The BPZ-PBz and POSS-PBz layers were self-assembled by intermolecular hydrogen bonding in such a way as to form the lamellar structure during ring-opening polymerization. An advantage of this lamellar structure is that 30% POSS/BPZ polybenzoxazine nanocomposite exhibits an ultralow-κ value of 1.7 at 1 MHz as well as high thermal stability. Further, the combination of octa(glycidylether)-POSS, benzoxazine, and DGEBA-based low-κ materials developed with enhanced porosity or free volume; higher content of POSS (5.0 wt%) in PBZ/EP nanocomposites showed the lower values of κ (2.54) when compared to that of neat PBZ/EP ($k = 4.72$) [79]. However, POSS-reinforced polyurethane (PU)-based polybenzoxazine (PBz) nanocomposites demonstrated as an interlayer low-κ dielectric material based on the concept of polarization and porosity of the composite. Different weight ratios of hydroxyl terminated nanoporous POSS (OH—POSS) material and hydroxyl terminated benzoxazine (OH–Bz) materials containing a less polar long aliphatic chain were copolymerized with hexamethylenediisocyante (HMDI) to obtain POSS–Bz–PU nanocomposites. The κ value of the nanocomposites decreased with increasing aliphatic chain length and concentrations of POSS, but it is limited up to 30 wt% POSS–PU–PBz ($k = 1.94$), and beyond this concentration the reverse trend was observed which might be due to increasing density of the resulting nanocomposites by agglomeration of POSS nanoparticles [80]. The SEM images of 40% POSS–PU–PBz composites evidently support that the agglomerate formation of POSS particles. Also, two types of polybenzoxazine (PBZ) nanocomposites were prepared from benzoxazine monomer (BZ-Cy-OH) and organomodified MMT clay (OMMT) and OG-POSS (up to 7.5 wt%). The dielectric studies of these polybenzoxazine nanocomposites reveal that the POSS-reinforced nanocomposites have lower value of κ, whereas the OMMT clay possesses high-κ. This is due to changing the polarization of the resulting polymer nanocomposite matrix [81]. The biomaterial euginol-based POSS-OCN was hybridized in different ratios with bisphenol-A cyanate ester (BACY) to obtain porous structured BACY/POSS-OCN nanocomposites. The reinforcement of POSS-OCN significantly reduced the value of dielectric constant and dielectric loss as well; 30 wt% POSS-OCN/BACY nanocomposite possesses the lowest value of dielectric constant of 1.81 at 1 MHz [82]. Then different composition of OG-POSS and a flexible linear aliphatic alkoxy core-bridged bisphenol cyanate ester (AECE) nanocomposites demonstrated for low-

κ dielectrics; 10 wt% POSS-$AECE_4$ exhibits higher thermal stability and lower κ value of 2.4 when compared to that of neat AECE ($\kappa = 4.2$) [83]. The increasing contact angle value and lowering surface free energy with POSS content inferred that the increasing hydrophobicity also contributes to the reduction of κ value.

A new approach has developed based on POSS-dendrimer hybrids to ultralow dielectric thin films for advanced microelectronics. This would be of particular interest to obtain nanoporous materials because they may avoid the porogen agglomeration and porogen matrix phase separation problems encountered with the so-called templating technique, where the thermally volatile dendrimer core is first added to the matrix and then removed from a two-component system by controlled temperature to produce well-defined voids in the remaining matrix. For example, hybrid materials having POSS cages and polyamidoamine dendrimer core were prepared and then allowed for the thermal treatment to create 3D nanodomained films or coatings as a low-κ material by removing thermally volatile dendrimer cores [84]. For example, a hybrid PEO-POSS template was used to prepare porous polyimide films, and thermally labile PEO-POSS nanoparticles would undergo oxidative thermolysis after blending with PI and to release small molecules as byproducts that diffuse out of the matrix to leave voids with the pore sizes of 10–40 nm into the polymer matrix which would efficiently reduce the value of κ (from 3.25 to 2.25) of the hybrid materials [85].

5 Applications of Porous POSS Hybrid Materials

POSS-based hybrid polymers have shown high glass-transition temperature, high decomposition temperature, and excellent oxygen permeability and also possess atomic oxygen resistance properties; they form a SiO_2 passivation layer during the thermal/UV treatment that prevents further decay of the underlying polymer [86]. Also those hybrids exhibit excellent flame-retardant properties and are used as a film coating for cabin items during space missions.

POSS-based epoxy resins can be used as an insulating glue to hold several metal layers of substrate in the printed circuit boards, which minimize shear stress with coefficients of thermal expansion between the circuit board and the Si chip [87].

The well-known binding properties of proteins to the silicone surfaces create more attention in the development of the biomedical devices. In addition, deposition of protein on silicone-based contact lenses is known to reduce both their medical performance and comfort. To overcome these drawbacks, POSS/silicone–protein interactions were studied which offered potential applications in biomedical fields [88].

Significant thermal and mechanical properties of POSS bring forward to the industries to solve the problem of higher temperature and oxidation resistance materials. POSS cages offer a simple alternative to rigid and high-resistant hybrid materials. POSS monomers can be easily soluble in most the organic solvents and are thermally

stable which offered easy to blend or react with the organic molecules resulting hybrid polymers via radical, condensation, ring-opening polymerizations.

Highly porous three-dimensional array of cubes could offer excellent catalytic activities. POSS-based metal–organic frameworks are being explored as a catalyst for their ability to participate in chemical reactions [89].

Additionally, POSS-based metal–organic frameworks offered extensive applications in gas sorption, gas storage, and separation [90, 91]. The hybrid POSS-MOFs based materials sorption rate may be promising, but their structural, mechanical, and thermal stability needs to be improved.

Due to the presence of high porosity and stability of the Si-O cages in the hybrid matrix, coordination and hydrogen-bonded POSS–polymeric materials [92] might produce high-efficient gas storage materials.

POSS-based porous hybrid polymers and frameworks could be potentially applied for the fabrication of membranes, interlayer dielectrics, capacitors, insulators, monolithic columns, and medical devices.

Hybrid porous POSS–polymers can be applied as a promising material for H_2 and CO_2 storage; also those kinds of hybrids show selective CO_2 adsorbents rather than CH_4. These polymers are also show luminescent properties (maximum emission at ca. 420 nm), and they could be potentially applied as a blue light-emitting material [93].

5.1 Monolithic Columns

The monolithic column is being considered as a new-generation column for the chromatographic separation techniques; a novel organic–inorganic hybrid monolithic column was obtained by the cross-linking of inorganic octa-methacryl-POSS and organic long-chain quaternary ammonium methacrylate of *N*-(2-(methacryloyloxy)ethyl)-dimethyloctadecylammonium bromide via thermal initiated free radical copolymerization. Moreover, the permeability and porosity of the hybrid materials could be altered by varying the polymerization reagent composition. The incorporation of nanosized rigid POSS cages would be the responsible for thermal and mechanical properties of the POSS-based monolithic columns [94]. This work is enthused to develop various organic–inorganic hybrid monoliths through the copolymerization between organics and various POSS reagents for different applications. Later, organic–inorganic hybrid monolithic materials have been reported based on OVPOSS and appropriate multi-functional thiols as a linker [95]. Lin et al. [96] developed a series of epoxy–POSS and amine-based hybrid polymer monoliths with well-defined 3D skeletal and high-ordered microstructure (Fig. 10). These kinds of monoliths based on column chromatography exhibit high efficiency for the separation of small molecules, and this approach is versatility for the preparation of series of ordered porous hybrid monoliths with high surface area. Similarly, they were prepared by hybrid monoliths via thiol-methacrylate click polymerization reaction from methacrylate-POSS and multi-thiol cross-linkers such

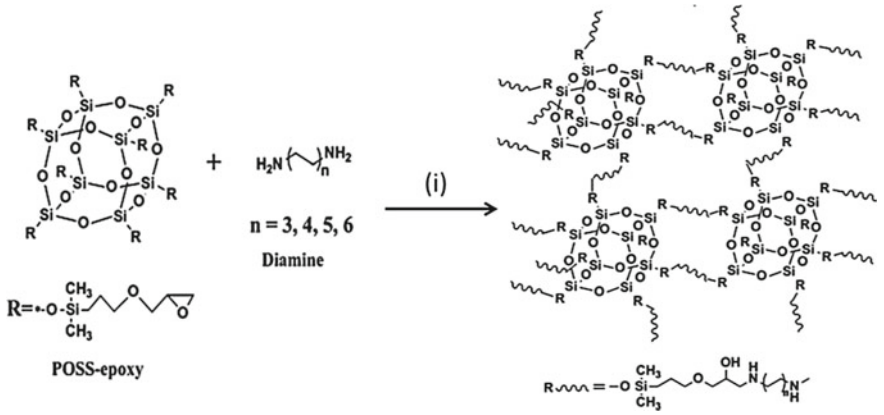

Fig. 10 Preparation of the hybrid monoliths via ring-opening polymerization of POSS–epoxy with different diamines. (i) PEG 10 000, propanol, 1,4-butanediol, 50 °C, 24 h. Reprinted from [96], © 2012 with permission from Royal Society of Chemistry

as trimethylolpropane tris(3-mercaptopropionate), 1,6-hexanedithiol, and pentaerythritol tetrakis(3-mercaptopropionate). These kinds of hybrid monoliths show high efficiency, and it can be used for the separations of polycyclic aromatic hydrocarbons, phenols, anilines, etc. [97].

Nischang and coauthors [98] reported two new hybrid monolithic columns based on OVPOSS, which were prepared by the copolymerization of vinylPOSS with pentaerythritol tetra (3-mercaptopropionate) or 2,20-(ethylenedioxy) diethanethiol via one-pot thiol-ene click reaction (Fig. 11), which monoliths show nanoscale network structures in an appropriate reaction conditions, and they were potentially used for the separation of uracil, benzyl alcohol, benzene, and alkylbenzenes.

Zhang et al. [99] reported new type of POSS-based hybrid monolithic column which prepared by thiol-acrylate click reaction using acryl-POSS as the cross-linker and sodium 3-mercapto-1-propanesulfonate as the monomer. The acryl-POSS cages were first constructed by self-polymerization and are polymerized with thiol monomer in one-pot and two-step approaches (Fig. 12). The one-pot approach has several potential applications in the separation of compounds, such as alkylbenzenes, basic compounds, phenolic compounds, a-casein or model proteins, and myoglobin. The efficiency of columns could be 60,000–73,500 plates/m for alkylbenzenes.

OG-POSS and polyethyleneimine (PEI)-based hybrid monolithic column was prepared by ring-opening polymerization; excess of unreacted amino groups on monolithic columns were treated chemically with g-gluconolactone or 1,2- epoxyoctadecane and physically coated with cellulose tris(3,5-dimethylphenyl-carbamate) (CDMPC) to obtain two different monolithic columns as shown in Fig. 13. High efficiencies (110,000 plates/m) of POSS-PEI hybrid monolithic column prepared for alkylbenzenes separation. The efficiency of g-gluconolactone-modified hybrid monolithic column could reach 60,000–80,000 plates/m for phenols, and also this

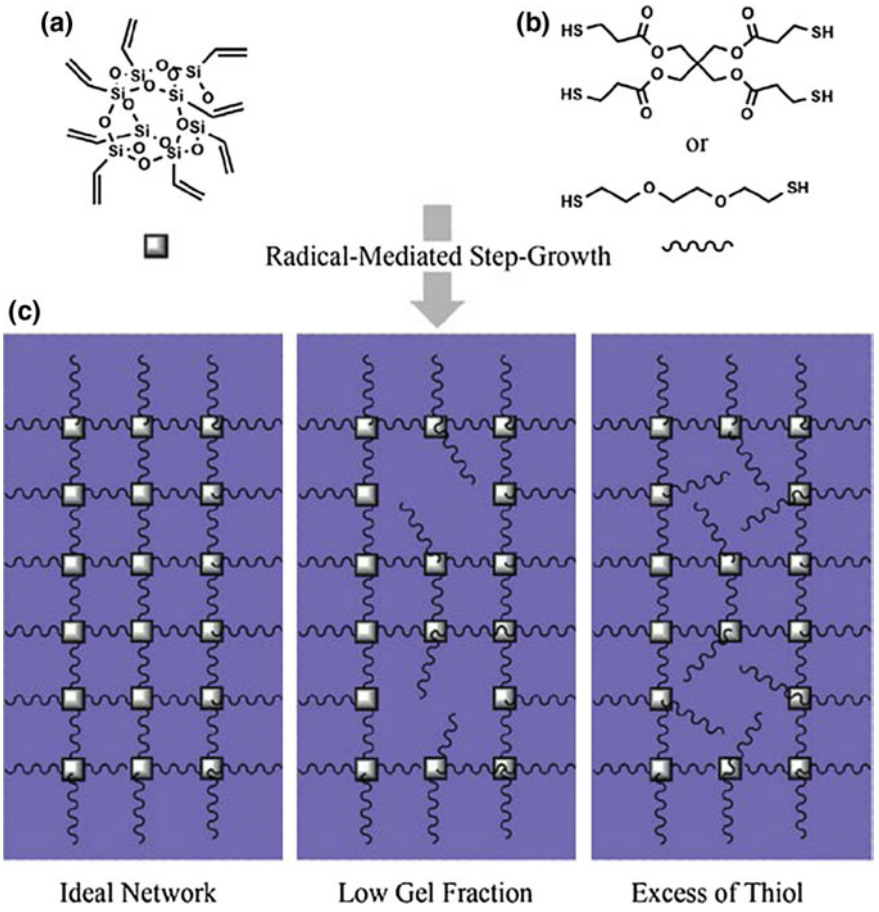

Fig. 11 Schematic diagram for the fabrication of POSS-PETMP and POSS-EDDT hybrid monolithic columns through the thiol-ene click reaction. Reprinted from [98], © 2015 with permission from Elsevier

column has high hydrophilicity which can potentially applied for the hydrophilic interaction liquid chromatography separation of phenols, small peptides, pyrimidines, purines, and nucleosides, with excellent peak shapes. Similarly, the CDMPC-modified column was used for the separation of basic racemates [100].

5.2 Biological Uses

The surface roughness and porosity have significant effect on hemocompatibility of blood-contacting biomaterials; porosity of POSS-PCU compromises its hemo-

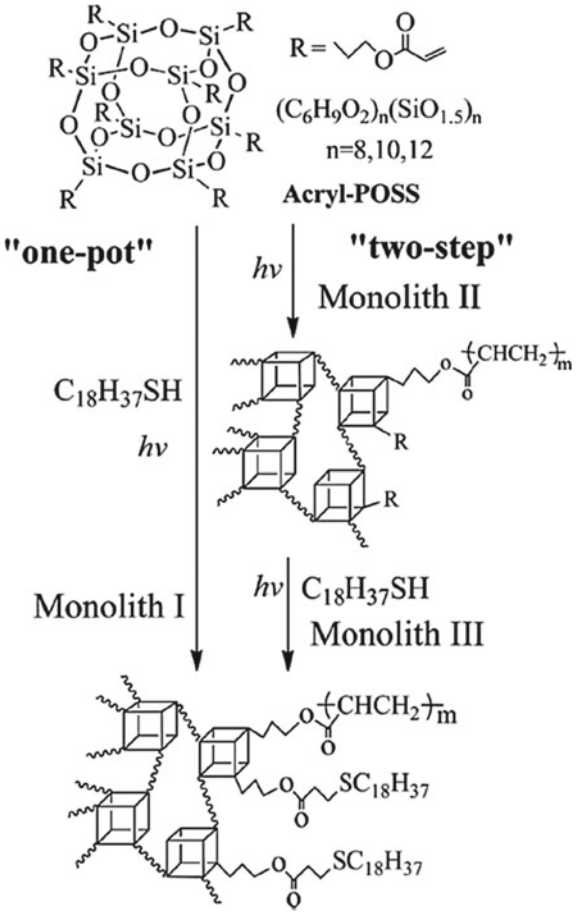

Fig. 12 "One-pot" and "two-step" methods for the preparation of C18-functionalized POSS-based hybrid monolithic columns through the thiol-acrylate click reaction. Reprinted from [99], © 2015 with permission from American Chemical Society

compatibility. The hemocompatibility of these materials was studied with different pore size of POSS-PCU films with PTFE as a control. Both tensile stress and strain decreased as the pores size of POSS-PCU increased, whereas the water contact angle (WCA) increased with the pore size of the film. However, when compared to PTFE, POSS-PCU showed both higher tensile stress and strain. Further, in whole-blood reactions, around 2–5 um pores size of POSS-PCU showed superior whole-blood compatibility index (BCI) than plain films and those with pores size around 35–45 um. Compared to porous PTFE, POSS-PCU showed lower thrombogenicity and higher hemocompatibility on the aspects of platelet activation, adhesion, and whole-blood reaction [101].

Teng et al. [102] reported highly porous star-shaped POSS–polycaprolactone-polyurethane (POSS-PCL-PU) films with improved mechanical and biological properties for tissue engineering. The high porosity, excellent biocompatibility, cell-substrate affinity, and unique surface nanotopography of the star-shaped POSS-PCL-

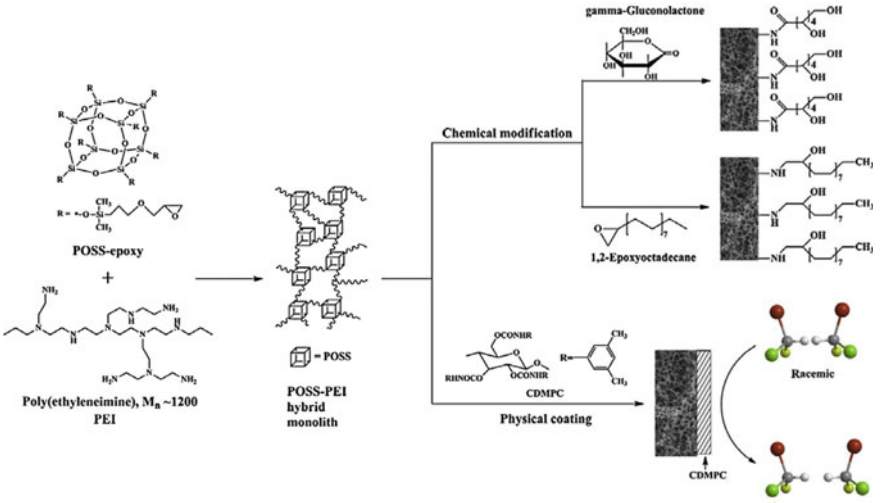

Fig. 13 Schematic diagram for the fabrication and post-modification of POSS-PEI hybrid monolithic column. Reprinted from [100], © 2013 with permission from Elsevier

PU film make it a great candidate as a tissue engineering scaffold biomaterial. The POSS-PCL-PU films have a high porosity of >75% and intrinsic nanoscale features that enhance cell attachment and growth. Compared to the porosity of the linear PCL-PU films of $43.1 \pm 4.4\%$, star-shaped POSS-PCL-PU films exhibit a higher porosity of $75.7 \pm 7.4\%$. The higher porosity with greater interconnectivity of pores enables more efficient transport of nutrients in the scaffolds without compromising the mechanical stability.

Janeta et al. [103] developed a macroporous scaffold through the reaction of 3-(trimethoxysilyl)propyl methacrylate-POSS (pTMSPMA–POSS) (Fig. 14) and the trifluoromethanesulfonate-POSS salt for sophisticated bone replacement, avoiding a long-lasting and complex methodology. The chemical composition, structural dimensions, topography, and microstructural properties of the hybrid macroporous scaffold fulfill the potential requirements for hard-tissue engineering.

He et al. [104] reported molecularly imprinted hybrid porous nanomagnetic-POSS-based materials for the determination of antibiotic residues in milk samples, which were constructed from nanomagnetic-OVPOSS (Fe_3O_4@POSS), methacrylic acid, and enrofloxacin via copolymerization. Compared to non-imprinted POSS nanoparticles (Fe_3O_4@NI-POSS), molecularly imprinted nanoparticles (Fe_3O_4@MI-POSS) showed higher adsorption and selectivity toward enrofloxacin template. The larger surface area and pore volume of MI-material would be responsible for its larger adsorption capacity than that of NI-material, S_{BET} of Fe_3O_4@POSS, Fe_3O_4@MI-POSS, and Fe_3O_4@NI-POSS are 625.96, 357.06, and 294.75 $m^2\ g^{-1}$, respectively. Three fluoroquinolones (FQs) such as ofloxacin, enrofloxacin, and danofloxacin were selectively extracted from the milk simples

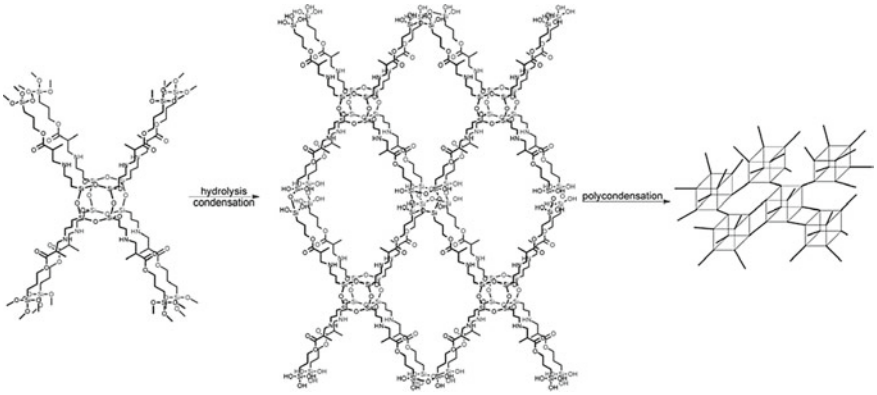

Fig. 14 General idea of the formation of the pTMSPMA–POSS network. Reprinted from [103], © 2016 with permission from Royal Society of Chemistry

through the Fe_3O_4@MI-POSS material which was combined with HPLC-UV detection. This technique would support to develop POSS-based molecularly imprinted porous hybrid materials with high efficiency for the analysis of complicated biological samples.

5.3 Gas Storage/CO_2 Adsorption

Wang et al. [105] have been prepared hybrid porous polymers via Heck reaction using octavinylsilsesquioxane and different tetrahedral silicon-centered precursors containing di-, tri-, or tetrabromophenyl groups. Their porosities have been tuned in the range of almost no porosity and to high porosity by altering the number of the connecting sites of silicon-centered units; POSS-silicon-centered tetrabromophenyl (HPP-5) hybrids possess high porosities with a maximum S_{BET} of 875 $m^2\ g^{-1}$ and total pore volume of 0.56 $cm^3\ g^{-1}$. For gas storage applications, HPP-5 exhibits the following properties: a high H_2 uptake of 7.76 mmol g^1 (1.56 wt%) at 77 K and 1.01 bar; a moderate CO_2 uptake of 1.04 mmol g^1 (4.58 wt%) at 298 K and 1.04 bar; and a low CH_4 uptake of 0.28 mmol g^1 (0.45 wt%) at 298 K and 1 bar. Similarly, cubic octavinylsilsesquioxane with planar tri-halogenated benzene shows tunable porosities with S_{BET} ranging from 479 to 805 $m^2\ g^{-1}$ and with the total pore volume ranging from 0.33 to 0.59 $cm^3\ g^{-1}$ [106].

Petit et al. [107] described the ionic grafting of polymer chains onto POSS cages to obtain liquid-like nanoparticles organic hybrid materials relevant to CO_2 capture. Increasing POSS units significantly enhance the thermal stability and porosity of the hybrid materials and CO_2 capture as well. Also, a series of POSS-based luminescent hybrid porous polymers were synthesized by Heck coupling reaction from octa(vinyl)-POSS and halogenated triphenylamine (TPA), porous and luminescent

properties of those POSS hybrids were tuned by altering TPA species and reaction condition. The optimized tris(4- bromophenyl)amine-based POSS–polymer hybrid exhibits high porosity with a S_{BET} of 680 $m^2\ g^{-1}$ and pore volume of 0.41 $cm^3\ g^{-1}$ and also possesses reasonable CO_2 uptake of 1.44 mmol g^{-1} at 273 K and 0.77 mmol g^{-1} at 298 K at 1.01 bar and emits high yellow luminescence [108]. In addition, luminescence of these hybrids could be quenched by nitroaromatic explosives; thus, it can be used as chemical sensors for explosives detection. Excellent luminescent performance was obtained for the highest porous POSS–polymer hybrid which infers that the increased porosity can enhance the luminescence due to the interwoven porous network.

Similarly, Wang et al. [109] reported the octa(vinyl)-POSS and 2,7-dibromo-9-fluorenone-based hybrid porous polymer (HPP-1) as an eminent material for post-functionalization of amine by conversion of ketone moieties into amine functionalities. The HPP-1-amine shows enhanced CO_2 uptake than that of HPP-1, from 0.63 mmol g^{-1} (HPP-1) to 1.01 mmol g^{-1} (HPP-1-EDA, EDA = ethylenediamine) and 0.72 mmol g^{-1} (HPP-1- HDA, HDA = hexamethylenediamine) at 298 K and 1 bar. Further, the porosity of HPP-1-amine is not compromised, but the S_{BET} increased from 529 $m^2\ g^{-1}$ (HPP-1) to 651 $m^2\ g^{-1}$ (HPP-1-EDA) and 615 $m^2\ g^{-1}$ (HPP-1-HDA). Also by altering the monomer species and reaction conditions can increase the porosity of the HPP-1 containing POSS units and CO_2 uptake as well. Furthermore, the hybrid porous materials were synthesized using octa(phenyl)-POSS and formaldehyde dimethyl acetal via Friedel–Crafts (POPS-1) and Scholl coupling (POPS-2) reactions to obtain two different porous POSS hybrid materials. These materials are predominantly microporous and mesoporous with S_{BET} of 795 and 472 $m^2\ g^{-1}$ for POPS-1 and POPS-2, respectively. Moreover, POPS-1 can reversibly adsorb 9.73 wt% CO_2 (1 bar and 273 K) and 0.89 wt% H2 (1.13 bar and 77 K), and POPS-2 shows moderate gas uptake with 8.12 wt% CO_2 (1 bar and 273 K) and 0.64 wt% H_2 (1.13 bar and 77 K) [110].

5.4 Energy Storage

Tang et al. [111] demonstrated the nitrogen-doped carbon materials with well-defined nanoporous structure (Fig. 15) for the electrochemical energy conversion and storage devices. Different weight ratios of OAPS/resol were mixed and cured at 100 °C for 24 h, and then it was crushed and allowed to pyrolysis at 900 °C under nitrogen atmosphere for 3 h; the resulting powder was washed with 10 wt% of HF solution to remove silica moieties and was dried at 120 °C, and the obtained powder was denoted as *N*-doped nanoporous carbon (NNC). The NNC from OAPS to resol ratio of 95:5 showed adjustable nitrogen content (3.63–5.37%), large surface area (1942 $m^2\ g^{-1}$), uniform and well-defined nanopores (0.85–1 nm), high nanopore volume (0.53–0.88 $cm^3\ g^{-1}$) and also have high specific capacitance of 230 Fg^{-1} at 1 Ag^{-1}.

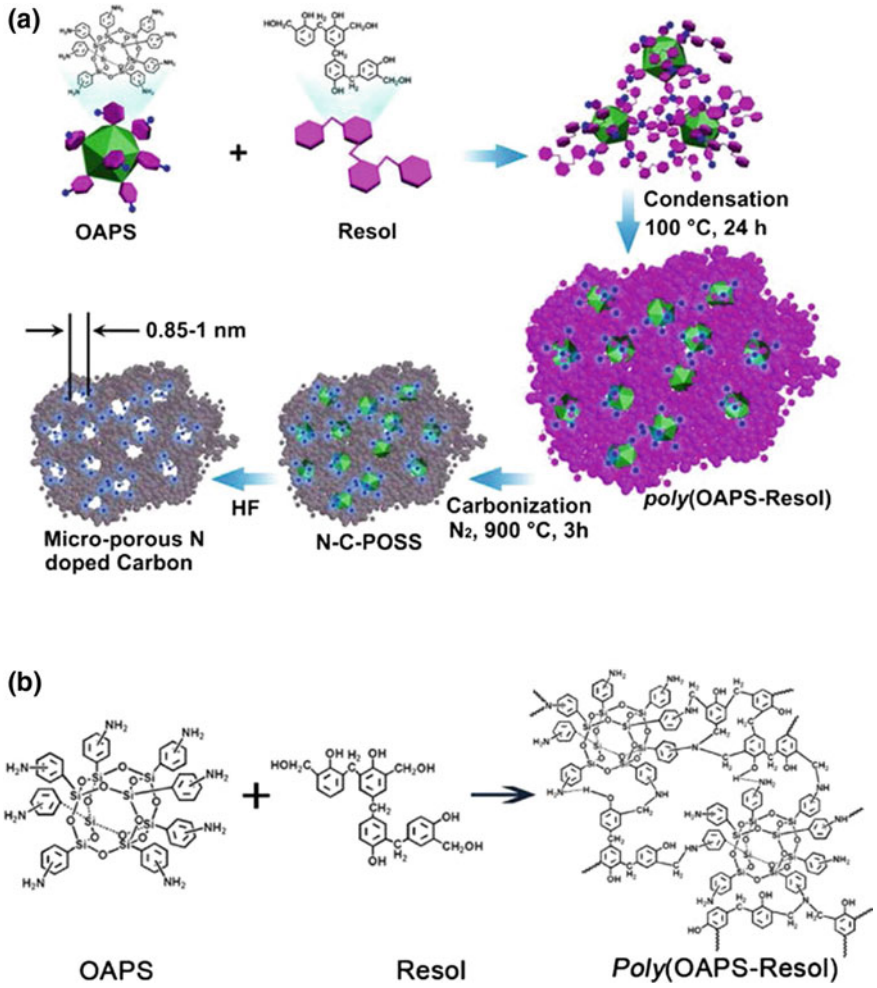

Fig. 15 **a** Schematic illustration of synthesis of OAPS-derived nitrogen-doped nanoporous carbon materials and **b** formation of poly(OAPS-resol) between OAPS and resol cross-linker via hydrogen bonding. Reprinted from [111], © 2016 with permission from Elsevier

Liu et al. [112] fabricated hierarchically porous structured carbon materials on the basis of self-assembly of POSS and amphiphilic triblock copolymers (PEO-PPO-PEO), where the POSS acts both as the carbon source and the self-template for producing uniform micropores while the block copolymers act as the soft templates for producing ordered mesopores. The obtained carbon materials with high specific surface area of over 2000 $m^2\ g^{-1}$ and large pore volume of over 1.19 $cm^3\ g^{-1}$ possess both quite uniform micropores with the size of 1 nm and highly ordered mesopores with the size of 4 nm, owing to the molecular-scale templating effect of POSS silox-

ane cages as well as the good assembly compatibility between the block copolymers and the aminophenyl-POSS. Galvanostatic charge/discharge test results show that their maximum specific capacitance can reach 163 Fg^{-1} in ionic liquid electrolyte and 216 Fg^{-1} in aqueous H_2SO_4 electrolyte, when measured in a symmetrical two-electrode cell. The advantage of the hierarchical micro-/mesoporous carbons over the strictly microporous carbons lies in their outstanding rate performance, due to dramatically reduced charge transfer resistance. The sample with the highest mesoporosity demonstrates a best rate capability with 94 and 97% of capacitance retention when the current density is increased from 0.25 to 10 A g^{-1} in ionic liquid and 1 M H_2SO_4, respectively.

5.5 Membranes

Only limited articles reported on porous POSS–polymer membranes; Dasgupta et al. [113] reported that the POSS–polyimide membranes for gas (H_2, N_2, CH_4, O_2, and CO_2) separation. Masakoto et al. reported the synthesis of inter- and intra-cubic porous structured homogeneous POSS-derived silica membranes and their single gas permeation characteristics. The amorphous silica structured membranes have a negligible number of pores larger than 0.35 nm and are appropriate to separate organic gas mixtures [73]. The controlled pore size of the silica networks was prepared by organic-template method, organotrialkoxysilanes are copolymerized with tetralkoxysilane, and the organic portion will burn out after pyrolysis and leave pores homogeneously where the size and shape of the organic groups determine the size and shape of the pores.

The homogeneous (HOMO)-POSS-derived silica membranes were prepared by the solgel method, and their single gas permeation characteristics were studied in the temperature range of 100–500 °C. Normalized Knudsen-based permeance (NKP) was applied for quantitative evaluation of membrane pore sizes less than 1 nm. By changing the calcination temperatures, pore size of the HOMO-POSS membranes was successfully tuned and the membrane shows loose amorphous silica structures compared to TEOS membranes, due to the difference in the minimum unit of silica networks. Compared to tetraethoxysilane (TEOS)-derived silica membranes HOMO-POSS membranes showed superior CO_2/CH_4 separation performance with a CO_2 permeance of 1.1×10^{-7} mol m^{-2} s^{-1} Pa^{-1} with a CO_2/CH_4 permeance ratio of 131 at 100 °C. Membranes fired at 300 °C showed high hydrogen permeance of 2.0×10^{-6} mol m^{-2} s^{-1} Pa^{-1} with a high H_2/SF_6 permeance ratio of 1200 and a low H_2/N_2 permeance ratio (20) at 200 °C. HOMO-POSS-derived membranes fired at 550 °C showed uniform pore size of 0.42 nm with much higher activation energy and larger He/H_2 permeance ratios [114]. Also, a series of aminoethylaminopropylisobutyl functionalized POSS-based POSS–polyimide (POSS-PI) nanocomposite membranes shows unique gas transport properties; these POSS–polyimide membranes have a significant increase in permeability of gas compared to the pure polyimide membranes. The permeability order of membranes for four gas is

as $P(CO_2) > P(O_2) > P(N_2) > P(CH_4)$. The PI-POSS-II has max CO_2 permeability (128%), whereas the PI-POSS-III shows high O_2 permeability (143%) [113]. The diverse characteristics of permeability coefficients of the different membranes can be explained by the variation of free volume, caused by the bulky nanoporous POSS cages exhibited within the polymer network.

6 Conclusion

Different approaches were demonstrated for diversity of porous structured POSS-based hybrid materials; the nanoporous POSS tethered with different organic functional groups were applied. In this chapter, the importance of porosity and the method of pores construction by using the combination of POSS and organics/metal ions were provided with their dielectric, catalytic, adsorption, thermal, and mechanical properties. The alignment of POSS by self-polymerization or copolymerization with organic polymers determined the formation of pores in the resulting hybrid POSS–polymer networks, where the arrangement varies with varying POSS functional groups. The largest porous POSS hybrid polymers with BET surface area of $2509 + 59$ m^2 g^{-1} and a large total pore volume of $3.28 + 0.10$ cm^3 g^{-1} were synthesized via Lewis acid-assisted Friedel–Crafts alkylation polymerization of benzyl chloride-terminated POSS. POSS-based catalysts have potential applications for epoxidation of alkenes, Suzuki and carbon–carbon cross-couplings, and aerobic oxidation of benzyl alcohol to benzaldehyde. Moreover, POSS-based organic–inorganic hybrid porous materials could be applied for a wide variety of gas storage, membranes, foams, chromatogram, biomedical, energy storage, and engineering applications.

Acknowledgements The authors thank Dr. Mathivathanan Ariraman, Department of Chemical Engineering, National Chung Hsing University, Taichung, Taiwan for his support.

References

1. Kickelbick G (2014) Hybrid materials–past, present and future. Hybrid Mater 1
2. Pielichowski K, Njuguna J, Janowski B, Pielichowski J (2006) Polyhedral oligomeric silsesquioxanes (POSS)-containing nanohybrid polymers. In: supramolecular polymers polymeric betains oligomers. Springer Berlin Heidelberg, Berlin, Heidelberg, pp 225–296. https://doi.org/10.1007/12_077
3. Seçkin T, Köytepe S, Adıgüzel Hİ (2008) Molecular design of POSS core star polyimides as a route to low-κ dielectric materials. Mater Chem Phys 112:1040–1046
4. Zhang C, Babonneau F, Bonhomme C, Laine RM, Soles CL, Hristov HA, Yee AF (1998) Highly porous polyhedral silsesquioxane polymers. Synth charact J Am Chem Soc 120:8380–8391
5. Bassindale AR, Gentle TE (1993) Siloxane and hydrocarbon octopus molecules with silsesquioxane cores. J Mater Chem 3:1319–1325

6. Feher FJ, Budzichowski TA, Blanski RL, Weller KJ, Ziller JW (1991) Facile syntheses of new incompletely condensed polyhedral oligosilsesquioxanes:[(c-C5H9) 7Si7O9 (OH) 3],[(c-C7H13) 7Si7O9 (OH) 3], and [(c-C7H13) 6Si6O7 (OH) 4]. Organometallics 10:2526–2528
7. Ro HW, Soles CL (2011) Silsesquioxanes in nanoscale patterning applications. Mater Today 14:20–33
8. Zhou H, Ye Q, Xu J (2017) Polyhedral oligomeric silsesquioxane-based hybrid materials and their applications. Mater Chem Front 1:212–230
9. Hurd CB (1946) Studies on siloxanes. I. the specific volume and viscosity in relation to temperature and constitution. J Am Chem Soc 68:364–370
10. Wu J, Mather PT (2009) POSS polymers: physical properties and biomaterials applications
11. Wang F, Lu X, He C (2011) Some recent developments of polyhedral oligomeric silsesquioxane (POSS)-based polymeric materials. J Mater Chem 21:2775–2782
12. Zhang W, Müller AH (2013) Architecture, self-assembly and properties of well-defined hybrid polymers based on polyhedral oligomeric silsequioxane (POSS). Prog Polym Sci 38:1121–1162
13. Lee J, Cho H-J, Jung B-J, Cho NS, Shim H-K (2004) Stabilized blue luminescent polyfluorenes: introducing polyhedral oligomeric silsesquioxane. Macromolecules 37:8523–8529
14. Zhang K, Zhuang Q, Liu X, Yang G, Cai R, Han Z (2013) A new benzoxazine containing benzoxazole-functionalized polyhedral oligomeric silsesquioxane and the corresponding polybenzoxazine nanocomposites. Macromolecules 46:2696–2704
15. Ariraman M, Alagar M (2014) Design of lamellar structured POSS/BPZ polybenzoxazine nanocomposites as a novel class of ultra low-k dielectric materials. Rsc Adv 4:19127–19136
16. Chaikittisilp W, Kubo M, Moteki T, Sugawara-Narutaki A, Shimojima A, Okubo T (2011) Porous siloxane–organic hybrid with ultrahigh surface area through simultaneous polymerization–destruction of functionalized cubic siloxane cages. J Am Chem Soc 133:13832–13835
17. Zhou H et al (2014) Electrospun aggregation-induced emission active POSS-based porous copolymer films for detection of explosives. Chem Commun 50:13785–13788
18. Zhou H et al (2015) A thermally stable and reversible microporous hydrogen-bonded organic framework: aggregation induced emission and metal ion-sensing properties. J Mater Chem C 3:11874–11880
19. Wei Z, Luo X, Zhang L, Luo M (2014) POSS-based hybrid porous materials with exceptional hydrogen uptake at low pressure. Microporous Mesoporous Mater 193:35–39
20. Zhang L et al (2007) Mesoporous organic–inorganic hybrid materials built using polyhedral oligomeric silsesquioxane blocks. Angew Chem 119:5091–5094
21. Li J-G, Chu W-C, Kuo S-W (2015) Hybrid mesoporous silicas and microporous POSS-based frameworks incorporating evaporation-induced self-assembly. Nanomaterials 5:1087–1101
22. Alves F, Scholder P, Nischang I (2013) Conceptual design of large surface area porous polymeric hybrid media based on polyhedral oligomeric silsesquioxane precursors: preparation, tailoring of porous properties, and internal surface functionalization. ACS Appl Mater Interfaces 5:2517–2526
23. Pawlak T, Kowalewska A, Be Zgardzińska, Potrzebowski MJ (2015) Structure, dynamics, and host-guest interactions in POSS functionalized cross-linked nanoporous hybrid organic-inorganic polymers. J Phys Chem C 119:26575–26587
24. Cassagneau T, Caruso F (2002) Oligosilsesquioxanes as versatile building blocks for the preparation of self-assembled thin films. J Am Chem Soc 124:8172–8180
25. Ye Q, Zhou H, Xu J (2016) Cubic polyhedral oligomeric silsesquioxane based functional materials: synthesis, assembly, and applications. Chem–An Asian J 11:1322–1337
26. Cozza ES, Monticelli O, Marsano E (2010) Electrospinning: a novel method to incorporate POSS into a polymer matrix. Macromol Mater Eng 295:791–795
27. Kim K-M, Keum D-K, Chujo Y (2003) Organic−inorganic polymer hybrids using polyoxazoline initiated by functionalized silsesquioxane. Macromolecules 36:867–875
28. Hottle JR, Deng J, Kim H-J, Farmer-Creely CE, Viers BD, Esker AR (2005) Blends of amphiphilic poly (dimethylsiloxane) and nonamphiphilic octaisobutyl-POSS at the air/water interface. Langmuir 21:2250–2259

29. Baumann TF, Jones TV, Wilson T, Saab AP, Maxwell RS (2009) Synthesis and characterization of novel PDMS nanocomposites using POSS derivatives as cross-linking filler. J Polym Sci, Part A: Polym Chem 47:2589–2596
30. Qiang X, Ma X, Li Z, Hou X (2014) Synthesis of star-shaped polyhedral oligomeric silsesquioxane (POSS) fluorinated acrylates for hydrophobic honeycomb porous film application. Colloid Polym Sci 292:1531–1544
31. Hong Q, Ma X, Li Z, Chen F, Zhang Q (2016) Tuning the surface hydrophobicity of honeycomb porous films fabricated by star-shaped POSS-fluorinated acrylates polymer via breath-figure-templated self-assembly. Mater Des 96:1–9
32. Kim C-K, Kim B-S, Sheikh FA, Lee U-S, Khil M-S, Kim H-Y (2007) Amphiphilic poly (vinyl alcohol) hybrids and electrospun nanofibers incorporating polyhedral oligosilsesquioxane. Macromolecules 40:4823–4828
33. Gupta R, Kandasubramanian B (2015) Hybrid caged nanostructure ablative composites of octaphenyl-POSS/RF as heat shields. RSC Adv 5:8757–8769
34. Cao H, Yan D, Sun X, Xu R, Yu D (2009) Synthesis and characterization of a novel 2-oxazoline-benzoxazine compound with incorporated polyhedral oligomeric silsesquioxane. Des Monomers Polym 12:565–578
35. Qin Y, Ren H, Zhu F, Zhang L, Shang C, Wei Z, Luo M (2011) Preparation of POSS-based organic–inorganic hybrid mesoporous materials networks through Schiff base chemistry. Eur Polym J 47:853–860
36. Liu J, Yu H, Liang Q, Liu Y, Shen J, Bai Q (2017) Preparation of polyhedral oligomeric silsesquioxane based cross-linked inorganic-organic nanohybrid as adsorbent for selective removal of acidic dyes from aqueous solution. J Colloid Interface Sci 497:402–412
37. Hebda E, Ozimek J, Raftopoulos KN, Michałowski S, Pielichowski J, Jancia M, Pielichowski K (2015) Synthesis and morphology of rigid polyurethane foams with POSS as pendant groups or chemical crosslinks. Polym Adv Technol 26:932–940. https://doi.org/10.1002/pat.3504
38. Michałowski S, Hebda E, Pielichowski K (2017) Thermal stability and flammability of polyurethane foams chemically reinforced with POSS. J Therm Anal Calorim 130:155–163. https://doi.org/10.1007/s10973-017-6391-4
39. Normatov J, Silverstein MS (2007) Silsesquioxane-cross-linked porous nanocomposites synthesized within high internal phase emulsions. Macromolecules 40:8329–8335
40. Normatov J, Silverstein MS (2008) Interconnected silsesquioxane—organic networks in porous nanocomposites synthesized within high internal phase emulsions. Chem Mater 20:1571–1577
41. Kataoka S et al (2015) Layered hybrid perovskites with micropores created by alkylammonium functional silsesquioxane interlayers. J Am Chem Soc 137:4158–4163
42. Hu M-B et al (2013) POM–organic–POSS cocluster: creating a dumbbell-shaped hybrid molecule for programming hierarchical supramolecular nanostructures. Langmuir 29:5714–5722
43. Banerjee S, Kataoka S, Takahashi T, Kamimura Y, Suzuki K, Sato K, Endo A (2016) Controlled formation of ordered coordination polymeric networks using silsesquioxane building blocks. Dalton Trans 45:17082–17086
44. Hay MT, Seurer B, Holmes D, Lee A (2010) A Novel Linear Titanium (IV)-POSS Coordination Polymer. Macromolecules 43:2108–2110
45. Sanil E et al (2015) A polyhedral oligomeric silsesquioxane functionalized copper trimesate. Chem Commun 51:8418–8420
46. Chen G et al (2015) Construction of porous cationic frameworks by crosslinking polyhedral oligomeric silsesquioxane units with N-heterocyclic linkers. Sci Rep 5:11236
47. Kanamori K, Nakanishi K (2011) Controlled pore formation in organotrialkoxysilane-derived hybrids: from aerogels to hierarchically porous monoliths. Chem Soc Rev 40:754–770
48. Zhao Y, Schiraldi DA (2005) Thermal and mechanical properties of polyhedral oligomeric silsesquioxane (POSS)/polycarbonate composites. Polymer 46:11640–11647
49. Crowley C et al (2016) Surface modification of a POSS-nanocomposite material to enhance cellular integration of a synthetic bioscaffold. Biomaterials 83:283–293

50. Brigo L, Faustini M, Pistore A, Kang HK, Ferraris C, Schutzmann S, Brusatin G (2016) Porous inorganic thin films from bridged silsesquioxane sol–gel precursors. J Non-Cryst Solids 432:399–405
51. Liu L, Hu Y, Song L, Gu X, Chen Y, Ni Z (2010) Mesoporous hybrid from anionic polyhedral oligomeric silsesquioxanes (POSS) and cationic surfactant by hydrothermal approach. Microporous Mesoporous Mater 132:567–571
52. Devaraju S, Vengatesan M, Selvi M, Alagar M (2014) Thermal and dielectric properties of newly developed linear aliphatic-ether linked bismaleimide-polyhedral oligomeric silsesquioxane (POSS-AEBMI) nanocomposites. J Therm Anal Calorim 117:1047–1063
53. Jothibasu S, Devaraju S, Venkatesan MR, Chandramohan A, Kumar AA, Alagar M (2012) Thermal, thermoechanical and morphological behavior of Octa (maleimido phenyl) silsesquioxane (OMPS)-cyanate ester nanocomposites. High Perform Polym 24:379–388
54. Chandramohan A, Devaraju S, Vengatesan M, Alagar M (2012) Octakis (dimethylsiloxypropylglycidylether) silsesquioxane (OG-POSS) reinforced 1, 1-bis (3-methyl-4-hydroxymethyl) cyclohexane based polybenzoxazine nanocomposites. J Polym Res 19:9903
55. Nagendiran S, Alagar M, Hamerton I (2010) Octasilsesquioxane-reinforced DGEBA and TGDDM epoxy nanocomposites: characterization of thermal, dielectric and morphological properties. Acta Mater 58:3345–3356
56. Devaraju S, Vengatesan M, Alagar M (2011) Studies on thermal and dielectric properties of ether linked cyclohexyl diamine (ELCD)-based polyimide POSS nanocomposites (POSS-PI). High Perform Polym 23:99–111
57. Liu H, Zheng S (2005) Polyurethane networks nanoreinforced by polyhedral oligomeric silsesquioxane. Macromol Rapid Commun 26:196–200
58. Chandramohan A, Alagar M (2013) Preparation and characterization of cyclohexyl moiety toughened POSS-reinforced epoxy nanocomposites. Int J Polym Anal Charact 18:73–81
59. Chandramohan A, Dinkaran K, Kumar AA, Alagar M (2012) Synthesis and characterization of epoxy modified cyanate ester POSS nanocomposites. High Perform Polym 24:405–417
60. Sethuraman K, Prabunathan P, Alagar M (2014) Thermo-mechanical and surface properties of POSS reinforced structurally different diamine cured epoxy nanocomposites. RSC Adv 4:45433–45441
61. Leng Y, Zhao J, Jiang P, Wang J (2015) Amphiphilic porous polyhedral oligomeric silsesquioxanes (POSS) incorporated polyoxometalate-paired polymeric hybrids: Interfacial catalysts for epoxidation reactions. RSC Adv 5:17709–17715
62. Scholder P, Nischang I (2015) Miniaturized catalysis: monolithic, highly porous, large surface area capillary flow reactors constructed in situ from polyhedral oligomeric silsesquioxanes (POSS). Catal Sci Technol 5:3917–3921
63. Sangtrirutnugul P et al (2017) Tunable porosity of cross-linked-polyhedral oligomeric silsesquioxane supports for palladium-catalyzed aerobic alcohol oxidation in water. ACS Appl Mater Interfaces 9:12812–12822
64. Ayandele E, Sarkar B, Alexandridis P (2012) Polyhedral oligomeric silsesquioxane (POSS)-containing polymer nanocomposites. Nanomaterials 2:445–475
65. Lee Y-J, Huang J-M, Kuo S-W, Lu J-S, Chang F-C (2005) Polyimide and polyhedral oligomeric silsesquioxane nanocomposites for low-dielectric applications. Polymer 46:173–181
66. Song L, He Q, Hu Y, Chen H, Liu L (2008) Study on thermal degradation and combustion behaviors of PC/POSS hybrids. Polym Degrad Stab 93:627–639
67. Leu C-M, Reddy GM, Wei K-H, Shu C-F (2003) Synthesis and dielectric properties of polyimide-chain-end tethered polyhedral oligomeric silsesquioxane nanocomposites. Chem Mater 15:2261–2265
68. Huang J, Lim PC, Shen L, Pallathadka PK, Zeng K, He C (2005) Cubic silsesquioxane–polyimide nanocomposites with improved thermomechanical and dielectric properties. Acta Mater 53:2395–2404
69. Leu C-M, Chang Y-T, Wei K-H (2003) Polyimide-side-chain tethered polyhedral oligomeric silsesquioxane nanocomposites for low-dielectric film applications. Chem Mater 15:3721–3727

70. Kuo S-W, Chang F-C (2011) POSS related polymer nanocomposites. Prog Polym Sci 36:1649–1696
71. Chen Y, Chen L, Nie H, Kang E (2006) Low-κ nanocomposite films based on polyimides with grafted polyhedral oligomeric silsesquioxane. J Appl Polym Sci 99:2226–2232
72. Joshi M, Butola BS (2004) Polymeric nanocomposites—Polyhedral oligomeric silsesquioxanes (POSS) as hybrid nanofiller. J Macromol Sci Part C: Polym Rev 44:389–410
73. Zhao J, Fu Y, Liu S (2008) Polyhedral oligomeric silsesquioxane (POSS)-modified thermoplastic and thermosetting nanocomposites: a review. Polym Polym Compos 16:483
74. Wang YZ, Chen WY, Yang CC, Lin CL, Chang FC (2007) Novel epoxy nanocomposite of low Dk introduced fluorine-containing POSS structure. J Polym Sci, Part B: Polym Phys 45:502–510
75. Zhang C, Xu HY, Zhao X (2010) Structure and properties of low-dielectric-constant poly (acetoxystyrene-co-octavinyl-polyhedral oligomeric silsesquioxane) hybrid nanocomposite. Chin Chem Lett 21:488–491
76. Seino M, Wang W, Lofgreen JE, Puzzo DP, Manabe T, Ozin GA (2011) Low-k periodic mesoporous organosilica with air walls: POSS-PMO. J Am Chem Soc 133:18082–18085
77. Joseph AM, Nagendra B, Surendran K, Bhoje Gowd E (2015) Syndiotactic polystyrene/hybrid silica spheres of POSS siloxane composites exhibiting ultralow dielectric constant. ACS Appl Mater Interfaces 7:19474–19483
78. Tseng M-C, Liu Y-L (2010) Preparation, morphology, and ultra-low dielectric constants of benzoxazine-based polymers/polyhedral oligomeric silsesquioxane (POSS) nanocomposites. Polymer 51:5567–5575
79. Selvi M, Devaraju S, Vengatesan M, Go J, Kumar M, Alagar M (2014) The effect of UV radiation on polybenzoxazine/epoxy/OG-POSS nanocomposites. RSC Adv 4:8238–8244
80. Alagar M (2015) Dielectric and thermal behaviors of POSS reinforced polyurethane based polybenzoxazine nanocomposites. RSC Adv 5:33008–33015
81. Vengatesan M, Devaraju S, Dinakaran K, Alagar M (2011) Studies on thermal and dielectric properties of organo clay and octakis (dimethylsiloxypropylglycidylether) silsesquioxane filled polybenzoxazine hybrid nanocomposites. Polym Compos 32:1701–1711
82. Ariraman M, Sasikumar R, Alagar M (2016) Cyanate ester tethered POSS/BACY nanocomposites for low-k dielectrics. Polym Adv Technol 27:597–605
83. Alagar M, Devaraju S, Prabunathan P, Selvi M (2013) Low dielectric and low surface free energy flexible linear aliphatic alkoxy core bridged bisphenol cyanate ester based POSS nanocomposites. Front Chem 1:19
84. Dvornic PR, Hartmann-Thompson C, Keinath SE, Hill EJ (2004) Organic−inorganic polyamidoamine (PAMAM) dendrimer−polyhedral oligosilsesquioxane (POSS) nanohybrids. Macromolecules 37:7818–7831
85. Lee Y-J, Huang J-M, Kuo S-W, Chang F-C (2005) Low-dielectric, nanoporous polyimide films prepared from PEO–POSS nanoparticles. Polymer 46:10056–10065
86. Schwab JJ, Lichtenhan JD (1998) Polyhedral oligomeric silsesquioxane (POSS)-based polymers. Appl Organometal Chem 12:707–713
87. Gong D, Long J, Jiang D, Fan P, Zhang H, Li L, Zhong M (2016) Robust and stable transparent superhydrophobic polydimethylsiloxane films by duplicating via a femtosecond laser-ablated template. ACS Appl Mater Interfaces 8:17511–17518
88. Bassindale AR, Codina-Barrios A, Frascione N, Taylor PG (2008) The use of silsesquioxane cages and phage display technology to probe silicone–protein interactions. New J Chem 32:240–246
89. Qiu LG, Xie AJ, Zhang LD (2005) Encapsulation of catalysts in supramolecular porous frameworks: size-and shape-selective catalytic oxidation of phenols. Adv Mater 17:689–692
90. Bordiga S et al. (2004) Electronic and vibrational properties of a MOF-5 metal–organic framework: ZnO quantum dot behaviour. Chem Commun 2300–2301
91. Collins DJ, Zhou H-C (2007) Hydrogen storage in metal–organic frameworks. J Mater Chem 17:3154–3160

92. Sun D et al (2003) Novel silver-containing supramolecular frameworks constructed by combination of coordination bonds and supramolecular interactions. Inorg Chem 42:7512–7518
93. Ahmad N, Noh AM, Leo C, Ahmad A (2017) CO_2 removal using membrane gas absorption with PVDF membrane incorporated with POSS and SAPO-34 zeolite. Chem Eng Res Des 118:238–247
94. Wu M, Ra Wu, Li R, Qin H, Dong J, Zhang Z, Zou H (2010) Polyhedral oligomeric silsesquioxane as a cross-linker for preparation of inorganic−organic hybrid monolithic columns. Anal Chem 82:5447–5454
95. Alves F, Nischang I (2013) Tailor-made hybrid organic-inorganic porous materials based on polyhedral oligomeric silsesquioxanes (POSS) by the step-growth mechanism of thiol-ene "click" chemistry. Chem-A Eur J 19:17310–17313
96. Lin H, Ou J, Zhang Z, Dong J, Zou H (2013) Ring-opening polymerization reaction of polyhedral oligomeric silsesquioxanes (POSSs) for preparation of well-controlled 3D skeletal hybrid monoliths. Chem Commun 49:231–233
97. Lin H, Ou J, Liu Z, Wang H, Dong J, Zou H (2015) Facile construction of macroporous hybrid monoliths via thiol-methacrylate Michael addition click reaction for capillary liquid chromatography. J Chromatogr A 1379:34–42
98. Alves F, Nischang I (2015) Radical-mediated step-growth: preparation of hybrid polymer monolithic columns with fine control of nanostructural and chromatographic characteristics. J Chromatogr A 1412:112–125
99. Zhang H, Ou J, Liu Z, Wang H, Wei Y, Zou H (2015) Preparation of hybrid monolithic columns via "one-pot" photoinitiated thiol-acrylate polymerization for retention-independent performance in capillary liquid chromatography. Anal Chem 87:8789–8797. https://doi.org/10.1021/acs.analchem.5b01707
100. Lin H, Ou J, Tang S, Zhang Z, Dong J, Liu Z, Zou H (2013) Facile preparation of a stable and functionalizable hybrid monolith via ring-opening polymerization for capillary liquid chromatography. J Chromatogr A 1301:131–138
101. Zhao J, Farhatnia Y, Kalaskar DM, Zhang Y, Bulter PE, Seifalian AM (2015) The influence of porosity on the hemocompatibility of polyhedral oligomeric silsesquioxane poly (caprolactone-urea) urethane. Int J Biochem cell Biol 68:176–186
102. Teng CP, Mya KY, Win KY, Yeo CC, Low M, He C, Han M-Y (2014) Star-shaped polyhedral oligomeric silsesquioxane-polycaprolactone-polyurethane as biomaterials for tissue engineering application. NPG Asia Mater 6:e142
103. Janeta M, Rajczakowska M, Ejfler J, Łydżba D, Szafert S (2016) Synthesis and microstructural properties of the scaffold based on a 3-(trimethoxysilyl) propyl methacrylate–POSS hybrid towards potential tissue engineering applications. RSC Adv 6:66037–66047
104. He H-B et al. (2014) Fabrication of enrofloxacin imprinted organic–inorganic hybrid mesoporous sorbent from nanomagnetic polyhedral oligomeric silsesquioxanes for the selective extraction of fluoroquinolones in milk samples. J Chromatogr A 1361:23–33
105. Wang D, Yang W, Li L, Zhao X, Feng S, Liu H (2013) Hybrid networks constructed from tetrahedral silicon-centered precursors and cubic POSS-based building blocks via Heck reaction: porosity, gas sorption, and luminescence. J Mater Chem A 1:13549–13558
106. Wang D, Yang W, Feng S, Liu H (2014) Constructing hybrid porous polymers from cubic octavinylsilsequioxane and planar halogenated benzene. Polym Chem 5:3634–3642
107. Petit C, Lin K-YA, Park A-HA (2013) Design and characterization of liquidlike POSS-based hybrid nanomaterials synthesized via ionic bonding and their interactions with CO_2. Langmuir 29:12234–12242
108. Wang D, Li L, Yang W, Zuo Y, Feng S, Liu H (2014) POSS-based luminescent porous polymers for carbon dioxide sorption and nitroaromatic explosives detection. RSC Adv 4:59877–59884
109. Wang D, Yang W, Feng S, Liu H (2016) Amine post-functionalized POSS-based porous polymers exhibiting simultaneously enhanced porosity and carbon dioxide adsorption properties. RSC Adv 6:13749–13756
110. Wang S, Tan L, Zhang C, Hussain I, Tan B (2015) Novel POSS-based organic–inorganic hybrid porous materials by low cost strategies. J Mater Chem A 3:6542–6548

111. Tang H et al (2016) Octa (aminophenyl) silsesquioxane derived nitrogen-doped well-defined nanoporous carbon materials: synthesis and application for supercapacitors. Electrochim Acta 194:143–150
112. Liu D et al (2016) Self-assembly of polyhedral oligosilsesquioxane (POSS) into hierarchically ordered mesoporous carbons with uniform microporosity and nitrogen-doping for high performance supercapacitors. Nano Energy 22:255–268
113. Dasgupta B, Sen SK, Banerjee S (2010) Aminoethylaminopropylisobutyl POSS—Polyimide nanocomposite membranes and their gas transport properties. Mater Sci Eng: B 168:30–35
114. Kanezashi M, Shioda T, Gunji T, Tsuru T (2012) Gas permeation properties of silica membranes with uniform pore sizes derived from polyhedral oligomeric silsesquioxane. AIChE J 58:1733–1743

Rubbers Reinforced by POSS

Anna Kosmalska and Marian Zaborski

Abstract In this chapter, a brief account of the recent researches on the properties of POSS-containing polymeric materials, i.e., polyurethanes, resins, and thermoplastics, has been done. On this background, rubbers, generally known as elastomers, have been presented as an important class of polymers and a very essential material in industry due to their unique properties. The general characteristics of elastomers and the common classification of different types, including general-purpose, special-purpose, and specialty elastomers, together with the relevant examples, have been described. To extend service life, reduce cost and therefore improve service efficiency of elastomeric materials, various fillers have always been extensively used in the rubber industry and are addressed in the chapter. Particular attention has been given to POSS. The influence of POSS moieties in rubber matrix on the functional properties of the composites fabricated is discussed. Attempt has been made to explain the role of POSS surface functional groups in controlling the properties of POSS-containing materials, and the reinforcement mechanism is presented.

Keywords Rubber · Elastomer · Reinforcement · Filler · Silsesquioxanes · POSS

1 Introduction

Polyhedral oligomeric silsesquioxane (POSS) nanoparticles have attracted much attention recently due to their nanometer size, the ease of which these particles can be incorporated into polymeric materials and the unique capability to reinforce polymers. Summing up briefly the literature review, it follows that research on the use of silsesquioxanes to obtain polymeric materials with interesting and valuable properties is largely related to polyurethanes (PUs), as well as resins and thermoplastics, mainly polyethylene (PE), polypropylene (PP), polystyrene (PS), polyamide-6

A. Kosmalska (✉) · M. Zaborski
Faculty of Chemistry, Lodz University of Technology, Institute of Polymer and Dye Technology, Stefanowskiego 12/16, 90-924 Lodz, Poland
e-mail: anna.kosmalska@p.lodz.pl

S. Kalia and K. Pielichowski (eds.), *Polymer/POSS Nanocomposites and Hybrid Materials*, Springer Series on Polymer and Composite Materials,
https://doi.org/10.1007/978-3-030-02327-0_9

[1–6]. In such systems, silsesquioxanes usually play the role of nanofillers, cross-linking coagents or compatibilizers, and the materials obtained with their use show improved mechanical and thermal properties.

Silsesquioxanes, depending on the structure and functional groups, change the surface properties of these materials. Due to small amounts of POSS in polyurethanes (3%), a significant increase in surface hydrophobicity and reduction of surface energy was observed [7]. Such behavior may contribute to corrosion protection of POSS-modified polymers or influence the adhesion forces with other materials [8]. In the case of polyurethanes (PUs), modification with POSS, both through chemical reactions and physical mixing of the components, leads to polymer strengthening at the molecular level. As a result, the obtained composite materials are characterized by better hardness than the base polymer and resistance to scratches, tensile strength, heat resistance, gloss, and quality (in the case of coatings) [9]. The reduction in the emission of volatile degradation products clearly demonstrates the increased thermal stability of polyurethanes, as well as other hybrid polymeric materials containing POSS [10].

Another group of materials showing significant improvement of properties, due to the POSS addition, are resins. A clear increase in the thermal stability of epoxy resins can be considered as the result of two main elements coupling: achievement of the degree of POSS dispersion at the nanometric scale and interactions between the matrix and POSS cages to form the aromatic structure [11]. The structures of the obtained hybrid polymers were characterized with Fourier-transformed infrared spectroscopy (FT-IR) and transmission electron microscopy (TEM). According to Liu and coworkers [12, 13], the FT-IR spectra suggested successful bonding between POSS molecules and methyl silicone resin, followed by TEM microscopic analysis which showed the very good solubility of silsesquioxanes in the resin, at the molecular level. Furthermore, the increase of decomposition temperature and oxidation resistance in these materials is related to the formation of an inorganic layer of SiO_2 (also called in the literature as the "ceramic layer") preventing further degradation of the resin.

Polymeric materials based on thermoplastics are also characterized by new or improved physicochemical parameters. In such systems, the modification of the matrix is usually carried out using conventional processing techniques, such as mechanical melt blending or by in situ polymerization [14, 15]. In thermoplastics, especially polystyrene (PS), poly(vinyl chloride) (PVC), and poly(methyl methacrylate) (PMMA), silsesquioxanes are often used as effective and efficient plasticizers [15]. Though, the effect depends, among others, on the type of POSS functionalization, the amount in which it is incorporated into the polymer matrix, as well as the nature of the host chains. Hence, POSS has been also proved to be effective nucleating agents of isotactic polypropylene (iPP) and high-density polyethylene (HDPE). A number of studies have been published revealing, that the inclusion of octamethyl-POSS at different loadings, depending on the host, can significantly promote nucleation rate of iPP or HDPE to increase (or retard) the crystallization processes, that were tested under various conditions, such as isothermal or non-isothermal cooling, quiescent or shear states [16–19].

Typically, mixing POSS into a thermoplastic polymer affects the increase in hardness and the mechanical properties are generally improved as well. An increase in the glass transition temperature may be also observed, probably resulting from segmental mobility reduction due to relatively large POSS molecules. Furthermore, decomposition temperature and resistance to oxidation, as well as the network density, are also increased [20]. Studies describing the effect of POSS on flame retardancy of PP [21] and reduction of viscosity of HDPE under processing conditions have been published as well [22].

Also, research on the effect of silsesquioxanes in the field of modeling the surface character of thermoplastic nanocomposites obtained with their participation was described. As a rule, POSS molecules, especially POSS functionalised with fluorine or containing nonpolar groups, increase hydrophobicity. However, nanocomposites based on polyamide-6 (PA6) were also obtained, in which silsesquioxanes used in higher concentrations, act as surfactants, and, on the contrary, increase the hydrophilicity of the surface of the hybrid materials obtained [23].

The scope of research involving the use of POSS in order to modify and improve the properties of elastomers is somewhat less diverse and extensive than in the case of the polymers mentioned above. The patented results largely concern the use of silsesquioxanes in elastomers for needs of the tire industry and to a lesser extent the use of POSS to modify the properties of common synthetic elastomers. Among the available literature of the subject, there are a significant number of papers describing a positive influence of POSS on the polysiloxane characteristics, which due to their unique properties have found broad application in many branches of industry. In most cases, however, available data concern silicone rubbers cross-linked at room temperature (RTV type) [24, 25], showing the features and range of applications different to a large extent than high-temperature cross-linked silicone elastomers.

Different example may be, for example, new hybrid materials based on thermoplastic elastomers (TPEs), which are also readily described recently. Combining nanometer POSS molecules with such copolymers, of multifunctional properties and showing advantages typical of both rubbery and plastic materials, may result in the novel inorganic–organic materials with a unique combination of properties and thus being useful in a variety of demanding technological fields. These hybrid materials may gain many unique advantages by bridging the space between inorganic materials (rigidity, high thermal stability, and unique optical, electronic or magnetic properties) and organic matrix (flexibility, strength, and processibility) [26–28]. More detailed description of POSS-containing thermoplastic elastomers (TPE/POSS) is given in the further section of the chapter.

Nonetheless, the research area regarding developing of POSS-containing elastomeric materials and their properties remains therefore interesting, both from a scientific and application point of view, and still encourages the intensification of research in this area.

2 Elastomers and Rubber—General Characteristics

Elastomers are a group of polymers that, over a wide range of temperatures, usually from about −70 °C up to 60 °C, exhibit the ability to large deformations of a reversible nature, reaching up to 1000%, i.e., they are in the so-called state of high flexibility. According to the standards, "*elastomer*" is defined as a macromolecular substance, which undergoes significant deformation under considerable stress and, after its removal, returns quickly to the initial dimensions and shape [29]. The proposed definition is not strict, especially that elastomers commonly include rubbers, cross-linked rubbers, and rubber mixtures (rubber compounds), as well as cross-linked rubber compounds, commonly referred to as "*rubber*" (in the common sense as "*gum*"). And so, the terms rubber and elastomer may be used interchangeably. As in the case of the terms, rubber composition (or mixture), compounded rubber, and rubber compound, that are used interchangeably as well, to refer to rubber which has been blended or mixed with various ingredients and materials.

Non-cross-linked block copolymers, containing rigid domains of one of the components, show the state of high elasticity, fixed in elastomers as a result of the spatial network formation. From the aforementioned materials, primarily the following reveal the technical significance: "*rubber*" and thermoplastic rubbers (TPE), while the cross-linked rubbers and latexes—to a lesser extent.

There are plenty of different rubber types available but still the largest single type used is natural rubber (NR) produced of latex from the tree *Hevea Brasiliensis*. The synthetic types of polymers, mainly manufactures from oil, have been developed either to replace or to be used together with NR or to make polymers with properties superior of NR in special areas, typically with better high-temperature resistance, better outdoor resistance and/or resistance to fuels and oils. A common classification of different types of rubber includes general-purpose elastomers, special-purpose elastomers, specialty elastomers. Each type comprises the rubbers presented in Table 1.

General-Purpose Rubbers mean polymers which, in their processability and mechanical properties, meet the requirements of the main application areas and which are also sufficiently cheap. Therefore, they have good physical properties, good processability, and compatibility, are generally economical, and are typical polymers used in tires and mechanical rubber goods with demand for good abrasion resistance and tensile properties. They constitute the largest volume of polymer used [30]. Today inexpensive hydrocarbon rubbers belong to the group of general-purpose rubbers, including both polymers and copolymers of butadiene, isoprene and styrene (SBR, NR, BR, IR). The hydrocarbon rubbers EPDM and IIR are classified among rubbers for special purposes.

Special-Purpose Rubbers have all unique properties which cannot be matched by the general-purpose types and are very important for manufacturing of industrial and automotive rubber products. Table 2 shows the classification of rubbers according to their distinct properties through which they surpass the general-purpose rubbers.

Table 1 Common classification of different types of rubber

General-purpose rubbers	Natural rubber (NR) Polyisoprene rubber (IR) Styrene-butadiene rubber (SBR) Butadiene rubber (BR)
Special-purpose rubbers	Ethylene propylene rubber (EPM and EPDM) Butyl rubber (IIR) Chloroprene rubber (CR) Acrylonitrile-butadiene rubber or nitrile rubber (NBR) Polysulphide rubber (T)
Specialty rubbers	Chlorosulfonated polyethylene (CSM) Acrylic rubber (ACM) Silicone rubber (MPQ/MPVQ/MQ/MVQ) Fluorosilicone rubber (MFQ) Fluorocarbon elastomers (FPM/FFKM/FEPM, CFM) Polyurethane rubber (AU/EU/PUR) Epichlorohydrine rubber (CO/ECO/GECO)

Table 2 Classification of rubbers according to their specific feature

Description/special-purpose	Rubber
Oils and hydrocarbon liquid-resistant	NBR, CO, ECO CR, CSM ACM, T FKM, CFM
Chemical-resistant	CR, CSM IIR, EPDM, EPM FKM, CFM
Heat-resistant	CSM, NBR (up to 120 °C) IIR(vulcanized with resins), EPDM, EPM (140-150 °C) ACM (150–170 °C) MQ, FKM, CFM (above 200 °C)
Low temperature-resistant	EPDM, BR MPQ
Ozone-resistant	IIR, EPDM, EPM CR, NBR/PVC CSM, CO, ECO, ACM MQ, FKM, CFM

The *Speciality Rubbers* are a great number of polymers with very special properties, in many cases of great importance for the automotive-, aircraft-, space-, and offshore industries, as well as for medicine.

Thus, rubbers, generally known as elastomers, have been an extremely useful and essential class of materials since time immemorial. Typical properties of pre-cross-linked elastomers are low glass transition temperatures and low secondary forces.

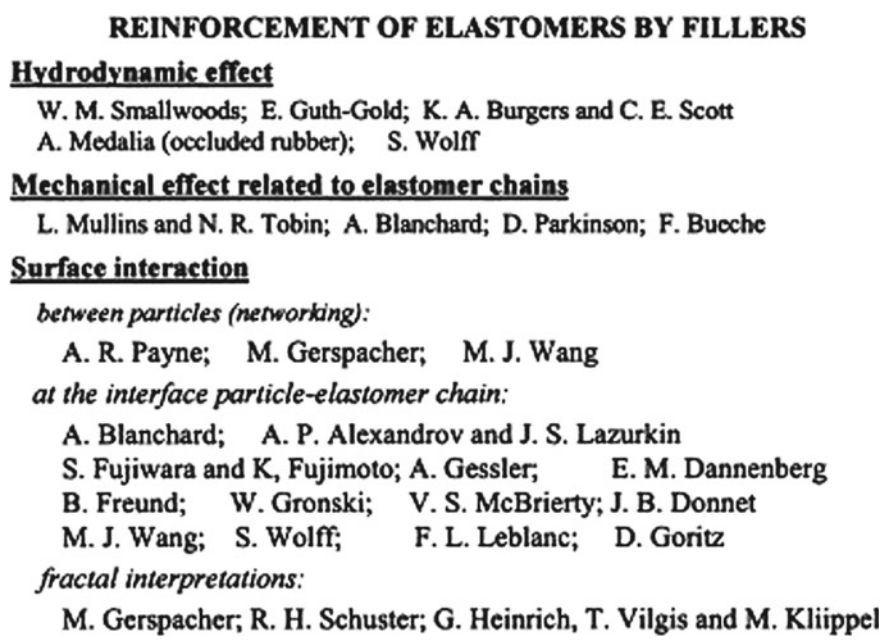

Fig. 1 Reinforcement of elastomers by fillers. Reprinted from [57], © 2003 with permission from Elsevier

These polymers, to behave as "*rubber,*" require macromolecular chains to be partially interconnected by chemical bonds and to the most extent conformationally entangled.

They are then chemically cross-linked, most frequently by sulfur or peroxides. Cross-linking gives elastomers their strong mechanical and elastic properties. However, a cross-linked elastomer in its own does not qualify to the accurate performance requirements for many applications. To meet these requirements and reveal its valuable and unique functional properties, particularly viscoelasticity, it must be homogeneously blended with comparatively rigid components offering high surface to volume ratio, known as "reinforcing fillers" [29, 31, 32]. The phenomenon of "*reinforcement,*" which is related to very important properties in the practice, may thus be defined by the improvement of mechanical properties of the compounds, notably the strength properties, hardness and stiffness, abrasion and tear resistance and hence improvement of their service life. Although the theories of the reinforcement have been diverging and Fig. 1 recalls the main proposals considered in this matter, it is usual to accept the Payne proposals illustrated in Fig. 2.

Fillers are therefore used to make the elastomers applicable in various fields and to result in the manufacture of varieties of composites. They impart high elastic moduli and durability for the elastomers, which were always limiting their practical usage. Fillers, generally, improve the poor mechanical condition of neat elastomers. The exception is natural and chloroprene rubber, which even when not filled are characterized by good strength.

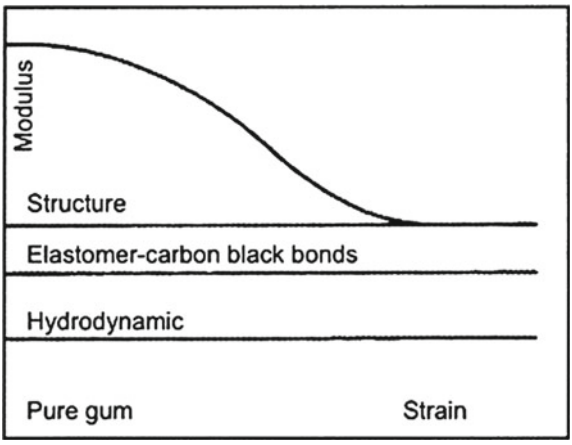

Fig. 2 Contributions to the stiffening effect. Reprinted from [57], © 2003 with permission from Elsevier

A whole range of substances, organic or inorganic, characterized by an appropriate degree of disintegration, has been used for this purpose. They exhibit different reinforcing capacity in relation to the rubber, depending on the size of rubber–filler interactions, measured by the size of the solid-phase surface and interactions at the interface.

A brief overview of the fillers used for elastomers is presented in the following section.

3 Fillers for Elastomers—General Characteristics

As it was mentioned above, a large number of diverse substances, both organic and inorganic, are added to the elastomers as the fillers. Particulate of them is added for mechanical reinforcement, the others for electrical or thermal conductivity modification, and ease of processing. Mineral fillers are known to improve the strength and stiffness of rubbers. However, the extent of property enhancement depends on various factors, such as the size and shape of the particles, filler aspect ratio, degree of dispersion and orientation of particles in the matrix and the interfacial adhesion between filler and polymer chains [33]. In general, it is said that the filler–filler [34–36] and the filler–rubber interactions [37] cause better reinforcement.

The most important group of fillers for elastomers consists of various types of carbon black (CB), followed by synthetic silicas and silicates. However, CB remains the predominant reinforcing filler, especially for high-performance elastomers (which means a type of elastomers, which are characteristic of high tensile strength, high tear strength, and low abrasion). Therefore, CB finds the leading application in the production of rubber goods, accounting for more than 90% of total carbon black consumption. In 2010, use in tires accounted for 73% of world consumption, with other rubber goods (hoses, belts, etc.) accounting for an additional 19% [38].

Other substances that have been used in the rubber technology are also such as kaolin, calcium carbonate, talc, magnesium carbonate, barium sulfate, diatomaceous earth, ebonite dust and some polymers, such as novolak phenolic resins, styrene-butadiene resins, polystyrene, polyethylene, isotactic polypropylene or emulsion polyvinyl chloride. The attempts have been made to synthesize hybrid carbon–silica fillers that combine the advantages of carbon black and silica [39].

Since the most conventional filler used for elastomer reinforcement, which is carbon black, is entirely dependent on the non-renewable petroleum resource, there is a growing interest and demand for research in the field of using substances derived from renewable sources as fillers for elastomers. Thus, a separate group is such fillers, which include starch, vegetable fibers, and wood flour, as well as recycled products (reclaimed rubber, or rubber powder, granulate and scrap) and products of elastomers pyrolysis (mainly carbon black).

Starch is of great potential due to its limitless source and friendly environmental processing. But the basic problem is its destructuring, and unfortunately, the previous research indicates an unsatisfied reinforcement by starch [40–45]. Buchanan et al. prepared styrene-butadiene rubber (SBR) composites by a co-precipitation procedure, but the mechanical property improvement was not as good as expected (the tensile strength was only improved from 2.6 to 6.3 MPa with 10 phr of zinc starch). Nevertheless, some patents in this area have been used in the technology of tread compound production [46, 47] and recent research shows different approaches to overcome this problem [48–51]. According to Qi et al. [52], starch will become an effective filler if modified properly. They described a novel starch modification for filler-reinforced elastomer, using two types of modifiers, i.e., resorcinol–formaldehyde (RF) and a silane surfactant (S). Originally used as a curing agent for rubber vulcanization, the RF was applied to interact with starch and rubber and thus improved the interface.

Recently, some interest was also aroused by the natural hybrid, containing in its composition also fullerenes and carbon nanotubes, called *shungite*. Shungite is a mineral consisting of silicate particles (60%) and amorphous shungite carbon (30%) with the addition of inorganic substances; it is low in cost and high in ecological safety. Usually, microdispersed (5 μm) shungite is used as a non-reinforcing filler for elastomeric materials (up to 60%) or as an additive (3–15%) to standard compositions. However, from the research published it follows, it is also of interest to investigate the possibility of using shungite, of a greater degree of dispersion, as the main filler for elastomeric materials [53–56].

Meanwhile, the most commonly and conventionally used fillers for the reinforcement of rubbers still remain particulate fillers, such as carbon black and silica [57]. Their primary particles are in the nanometer range, but they also reveal a strong tendency to form aggregates and agglomerates having size in the micrometer range. This provides a problem to overcome and often becomes a challenge when preparing rubber (and generally polymer) composites since one of the crucial factors in controlling the reinforcing effect on rubbers is the filler dispersion degree. For this reason, nanofillers, due to the small size and increased surface area, have emerged as promising fillers for improving polymer properties with only low filler loadings.

With average particle size in the range of 1–100 nm, the nanomaterials are extremely useful polymeric reinforcing agents [58].

Several types of nanofillers with different geometry, such as nanosilica, carbon nanotubes, layered silicates, graphene, metallic nanoparticles, metal oxides, and polyhedral oligomeric silsesquioxane (POSS) are used extensively in rubber composites.

Among the 1D (one dimensional, i.e., plates or layered type) fillers, the predominant role is played by montmorillonite and other natural aluminosilicates with a layered structure and products of their chemical modification (i.e., organophilization). In the case of montmorillonite, the thickness of a single plate is about 1 nm, and the remaining dimensions are in the range of 200–1000 nm. Since the clays are highly hydrophilic, as resulted from the surface charges, they show poor compatibility with a wide range of nonpolar elastomers, which subsequently causes inferior filler–polymer interaction. As a consequence, clay-filled composites reveal impaired mechanical properties when compared to the carbon black fillers. In many examples, however, the presence of nanoplatelets has a very beneficial effect on reducing the flammability of the filled material. They impede heat transfer into the composite much more efficiently than conventional fillers, increasing the initial temperature of the composite decomposition. Furthermore, clay composites exhibit improved gas barrier properties and therefore are used in many applications where they are helpful in reducing the air permeability, e.g., in tire inner liners. It is believed that the basic mechanism limiting the permeability is the increase in the so-called *path tortuosity* of fluids through the structure of the polymer nanocomposite, in relation to the corresponding microcomposite. Then, the penetrating molecules must bypass physical obstacles in the form of impermeable filler particles or polymer crystallites, which both the orientation and morphology are determined by specific interaction with the surface of the modifier. That way, the permeability of small molecules (O_2, H_2O, He, CO_2) in the polymer nanocomposite may be reduced several times with relatively low filler content, resulting in the permeability coefficient lower by approximately 60–90%. There are numerous studies on the incorporation of nanoclays into natural rubber, styrene-butadiene rubber, ethylene-propylene-diene rubber, epoxidized natural rubber, and blends thereof [58, 59].

The best-known 2D (two dimensional, i.e., nanotubes and nanofibres) fillers are carbon nanotubes and nanofibers. Carbon nanotubes (CNT) made of cylindrical graphitic sheets with fullerene end cups, depending on the structure may be single-walled (SWCNT) and multi-walled (MWCNT) carbon nanotubes, having diameter ranging from 1 to 100 nm and the length up to several mm. The basic problems occurring in the synthesis of rubber nanocomposites with CNT are the tendency of nanotubes to agglomerate and create entangled, multi-fiber strands, as well as weak interactions at the interphase between CNT and the matrix. For this reason, systems containing unmodified CNTs are relatively rare. Nevertheless, the CNTs are also considered as an attractive nanofillers which add the valuable properties to elastomers. The published results indicate that the homogeneous dispersion of MWCNT throughout styrene-butadiene rubber (SBR) matrix and strong interfacial adhesion between oxidized MWCNT and the matrix are responsible for the considerable enhancement

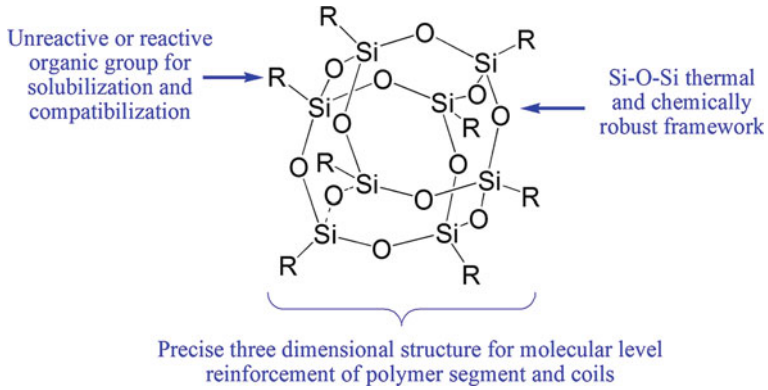

Fig. 3 POSS features. Reprinted from [65], © 2016 with permission from Elsevier

of mechanical properties of the composites. A comparison with carbon black filled SBR showed the significant improvement in Young's modulus and tensile strength by incorporating scarcely 0.66 wt% of the filler without forfeiture of SBR elastomer high elongation at break [60]. Additionally, CNTs improve the thermal as well as electrical conductivity of elastomers, that is very important in the tire industry, for example, regarding the static charge dissipation. Moreover, they provide better skid resistance and reduced tire abrasion.

Recently, graphite and its derivatives are also distinguished for their valuable properties like transparency superior barrier properties and excellent conductivity (both thermal and electrical) that make these materials a great substrate, e.g., for the production of touch screens, new generation batteries that are able to recharge within of seconds, or photovoltaic cells. High conductivity of these fillers makes them applicable in electronics for instance in sensor skins, flexible display, and in dielectric actuators.

On the background of the mentioned fillers, polyhedral oligomeric silsesquioxanes (POSS), being an example of 3D (three dimensional, i.e., nanogranules, nanocrystals, and spherical type) fillers, are excellent, high-performance materials used to modify many polymer properties, including rubbers [58, 59, 61]. They reveal combined organic–inorganic properties and are included in the group of reactive fillers, i.e., those that can be compounded with a polymer matrix by covalent or ionic bonds. This type of nanocomposites is called nanohybrid materials (Fig. 3).

Unlike most nanofillers (carbon nanotube or nanoclay), POSS molecules contain organic constituents on their external surface, which create their peculiar tailormade peripheral organic functionality that enables the preferential interactions with a variety of matrices and makes POSS nanofillers compatible with many polymers. As a result, having 1–3 nm diameter, POSS generally can enhance the service temperatures providing improved thermal stability and modifying the polymer glass transition temperature as well as decomposition temperatures. Moreover, incorporation of POSS molecules influences the rate of combustion in the event of fire,

flame retardancy, heat evolution, and oxidation resistance. It is also responsible for improved dielectrical properties, surface hardening, mechanical properties, etc., to a great extent. More detailed description of diverse rubbers composites with POSS will be presented in the following sections of the chapter.

The preparation methods of polymer/POSS materials are mainly dependent on the chemical structures of POSS and polymer. Two approaches have been adopted to incorporate POSS particles into polymer matrices: chemical reactions in the molten state (melt reactive blending) and physical interactions (simple melt blending). In the chemical reaction approach, POSS nanoparticles are bonded covalently with the polymer backbone, which obviously requires a chemical reaction to occur. Then, radical grafting reaction may be applied, which is widely used especially for compatibilization of immiscible polymer blends as well as functional polymers or polymerization [6, 61–64]. Chemical reactions between POSS and polymer chains are considered to be very appealing method of new materials synthesis with controlled structure and properties, being fast, inexpensive, and environmentally friendly. There are some examples of POSS grafted with polymer chains by atom transfer radical polymerization, reversible addition fragmentation chain transfer polymerization, ring-opening polymerization, anionic polymerization, and click chemistry technique [84–90]. However, it is thought that due to the complicated synthesis and purification procedures POSS grafted with polymer chains is not expected for massive production. Farther, POSS grafted α-olefins, for example, may be good filler choice for natural rubber composites on account of molecular polarity; however, POSS grafted α-olefins are very difficult to obtain [91].

In the physical blending approach, POSS nanoparticles are physically blended with the polymer by melt mixing or solvent casting methods. The physical blending, which is more typical for preparation of rubber composites, presents several advantages as well, being the same inexpensive, fast, and versatile technology. Indeed, standard equipment used for polymer and rubber compounding, such as twin screw extruders or internal mixers, is generally suitable for the processing of nanostructured thermoplastic polymers, for example, and/or rubber composites [14, 65]. Compared to the chemical reaction approach, however, aggregation of POSS during the extrusion process is difficult to control that influences the final dispersion of POSS nanoparticles [66]. It requires the strict control of the balance between polymer and POSS interactions, as well as POSS–POSS self-interactions. Thus, to provide effective interactions, the organic groups which are chemically similar to the polymer and long enough are needed.

Although POSS nanoparticles could be incorporated into almost all the polymers by chemical reaction or physical blending, the difficulties in obtaining molecular dispersion of POSS still remain open challenge. A major role seems to be played by the balance between interactions (van der Waals forces, hydrogen bonding, etc.) between POSS and the polymer, as well as the POSS–POSS self-interactions. By the same token, the control of nanostructure and location of nanoparticles, responsible, and crucial for reinforcing effect in polymer—and/or rubber-POSS nanocomposites—is not an obvious achievement and results to be challenging issue.

4 General-Purpose Rubbers/POSS

As it was briefly mentioned in the Introduction, often the patented results concern the use of silsesquioxanes (POSS) in elastomers for needs of the tire industry [67–70].

Silsesquioxanes containing alkoxysilane groups, that can interact with silica, behave then as silica dispersing agents in the rubber. Additionally, these compounds are useful in compounding, processing, cure, and storage of silica-reinforced rubbers, especially for a pneumatic tire production, because they contain low levels of volatile organic compounds (VOC) [69]. The patent describes a modification with this type of POSS [70]. The alkoxy-modified silsesquioxane (AMS) compounds contain the alkoxysilane group that participates in alkoxysilane–silica reaction, with the release of zero to about 0.1% by weight of the rubber of VOC during compounding and further processing. Particularly, suitable rubbers for use in the vulcanized elastomeric compound of the invention, mainly include of natural rubber (NR), butadiene rubber (BR), styrene-butadiene rubber (SBR), and combinations thereof.

As a result, the vulcanized rubber compounds containing the alkoxy-modified POSS revealed enhanced rubber reinforcement, increased polymer–filler interaction and lower compound viscosity. Such alkoxy-modified silsesquioxane compounds may be successfully applied in the production of tires having improved wet and snow traction, lower rolling resistance, increased rebound, and decreased hysteresis [70].

The usefulness of using similar POSS compounds, namely amino alkoxy-modified silsesquioxanes as adhesion promoters in rubber, has been also demonstrated and patented. Amino alkoxy-modified silsesquioxanes (amino AMS) and/or amino co-AMS compounds, that also comprise a mercaptosilane or a blocked mercaptosilane, have proven to be an excellent adhesives for coating the conductive and non-conductive wires for adherence to a rubber stock. These adhesives can be used with all types of rubbers. Additionally, what is valued and important, and there is no requirement for the use of special adhesive additives to the rubber vulcanizate.

In particular, the use of amino AMS and amino/mercaptan (co-AMS) compounds as adhesives for bonding wire to the rubber also improves the adherence performance of the reinforcement. It is possible then to obtain sufficient bonding that is resistant to degradation, especially to the thermal and thermo-oxidizing aging, in particular corrosion in the presence of water [71].

The use of POSS to modify the properties of common synthetic elastomers for ordinary applications is patented to a lesser extent. An example is an invention that contains the results of research on the use of one or more polyhedral oligomeric silsesquioxanes in butadiene (BR) and styrene-butadiene rubber (SBR) [72]. The POSS compounds under study may be included in the rubber composition during mixing, as a part of the rubber compound masterbatch, or alternatively after production of the rubber compound masterbatch, as an additive. The amount of POSS, preferably included in or added, was 1–10 parts per hundred rubber (phr), more preferably 1–6 parts phr, and most preferably 2–4 parts phr.

The addition of POSS, in particular trisilanol isobutyl polyhedral oligomeric silsesquioxane, affected the cure characteristics of the rubber compositions and caused rise to a decrease in optimum cure time (T_{90}). In other words, the rubber compounds may reach 90% of cure in a shorter time and by the same token spend a shorter time in the mold before they can be removed. The obtained rubber compositions revealed improved hysteresis and physical properties after vulcanisation. The point at which the polyhedral oligomeric silsesquioxane additive is added in the mixing cycle was also important to the hardness of the compound obtained. Furthermore, the results showed also that POSS, in particular the same trisilanol isobutyl polyhedral oligomeric silsesquioxane, has the ability to modify the viscoelastic properties [72].

Nevertheless, the number and scope of patents dealing with the use of silsesquioxanes in elastomeric composites further encourage the intensification of research in this field.

Another example dealing with the application of POSS compounds to the general-purpose rubbers, concern studies on natural rubber (NR). The NR-based nanocomposites were prepared using POSS-intercalated rectorite (POSS-REC), as the nanofiller [73]. Such elastomer composites have not been studied before. Rectorite (REC) is a type of regularly interstratified clay mineral which reveals larger interlayer distance, higher aspect ratio, and better separable layer thickness compared with montmorillonite, especially organomodified rectorite (OREC). The unique structure of the filler translates into better properties of the composites produced with its use, i.e., higher thermostability, barrier property, and better dispersion in polymer matrix [74–76, 79–82]. Nevertheless, as layered silicates, in general, which are hydrophilic, likewise REC needs to be modified to improve its affinity with organic polymers. Since POSS compounds have been considered as a type of promising surfactant, they have been employed readily and widely to modify layered silicates [77, 78].

Thus, POSS with amino group was intercalated into REC to obtain POSS-REC nanofiller, which was then dispersed into NR matrix [73]. The obtained material was investigated via X-ray diffraction (XRD) and transmission electron microscopy (TEM) which revealed that the composites were obtained successfully, with a relatively even dispersion and no serious agglomeration was observed. However, due to the difference in the polarities as well as the limited shear forces, the POSS-REC nanofiller was present both in intercalated and in exfoliated state. Measurements of thermal properties indicated that the presence of POSS-REC improved thermostability of the composites. SEM observations of fracture surfaces showed that POSS-REC nanofiller could prevent primary crazes from developing into macroscopic cracking, as well as absorb energy through inducing new smaller crazing in the composites. Mechanical tests proved that the presence of POSS-REC brought about remarkable increase in the tensile strength and elongation at break. Maximum mechanical properties were at 4% content of POSS-REC nanofiller and then reduced. To conclude, according to the authors a new type of the nanocomposites obtained may have excellent prospects in the fields demanding high performances, including high-speed train and aircraft [73]. However, the amino-POSS-REC nanofiller showed relatively weak influence on the thermostability of NR composites.

Better results in this field were noted by Zhao et al. [83] and presented very recently. In this case, octavinyl-polyhedral oligomeric silsesquioxane (OV-POSS) was applied and incorporated into NR matrix. It is thought so far that OV-POSS is the most representative member of POSS family containing multiple vinyl groups. Further, it has been produced industrially for many years providing its price very attractive for engineering applications.

It was expected that as a result of POSS incorporation into NR, the co-cross-linking reaction could be triggered between NR and OV-POSS, after vulcanization, and hence, macroscopic phase separation via POSS agglomeration would be hindered [83]. Thereby, both the mechanical properties and thermostability of the vulcanizates should be improved. The co-cross-linking between OV-POSS and NR matrix may reduce the stress of the molecular chains around OV-POSS particles and increase the entropy elasticity of the macromolecular chains [92].

Morphologies of the resulted OV-POSS/NR vulcanizates, investigated with the use of scanning electron microscopy (SEM), revealed that with a relatively low loading of OV-POSS (i.e., less than 10 wt%), no distinguishable OV-POSS aggregates were detected in the NR matrix, indicating that the macroscopic phase separation can be strangled owing to the co-cross-linking reaction (Fig. 4). With OV-POSS content more than 10 wt%, some agglomerated domains with the size of 340–620 nm, attributable to POSS crystals, appeared (Fig. 4c) or even some large and vesicle-like features with the size of 4–6 μm, indicating poor miscibility, when the OV-POSS content was higher than 15 wt% (Fig. 4d, e).

The morphology and structure of the obtained vulcanizates influenced their mechanical properties, such as tensile strength, tearing strength, hardness and elongation at break. Generally, compared to the unmodified (i.e., neat) NR, the mechanical properties of the OV-POSS/NR vulcanizates were improved. Both, tensile and tearing strength were slightly enhanced with the addition of OV-POSS. The highest elongation at break was obtained at 5 wt% loading of OV-POSS, which increased by about 25% compared to that of pristine NR, however apparently decreasing with higher OV-POSS loading. Accordingly, the agglomeration of OV-POSS tends to reduce tensile and tearing strength acting as strong stress concentrators [83] (Fig. 5).

Similar relationships were observed in the case of hardness which is, in general, proportional to the cross-linking density of natural rubber vulcanizates. Thus, due to the rigid character of OV-POSS, as well as co-cross-linking reaction between OV-POSS and NR matrix, the increase of OV-POSS loading almost resulted in increase of hardness of the vulcanizates. Nevertheless, cavities of the vesicle-like aggregates could decrease hardness and at the relatively high OV-POSS loading (i.e., more than 15 wt%) hardness of the vulcanizates decreased slightly [83].

Lastly, advantageous results were achieved in the range of thermal stability of NR composites. Thermogravimetric analysis (TGA) revealed significant increase, of about 27 °C, in the onset degradation temperature (T_{onset}) for the vulcanizates modified with OV-POSS compared to the plain NR sample. With the loading of 5–20 wt% OV-POSS, the observed increase in T_{onset} was from 317 to 344 °C (Table 3). In summary, based on the properties presented in the work, the OV-POSS/NR vulcanizates could be adopted as a heat-resistant elastomeric material.

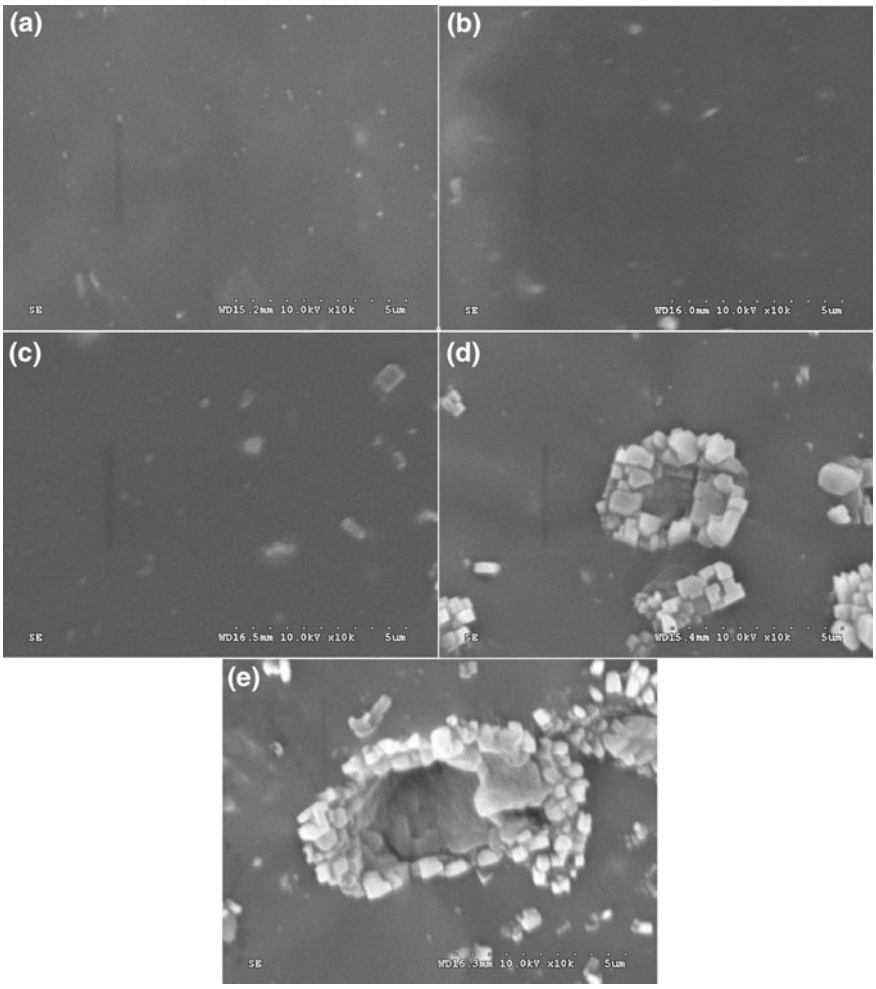

Fig. 4 SEM images of the natural rubber (NR) vulcanizates with different octavinyl-polyhedral oligomeric silsesquioxane (OV-POSS) loading (**a**) 0 wt%; (**b**) 5 wt%; (**c**) 10 wt%; (**d**) 15 wt%; (**e**) 20 wt%. Reprinted from [83], © 2017 with permission from Elsevier

5 Special-Purpose Rubbers/POSS

As mentioned at the beginning, rubbers for special purposes reveal one or more definite properties that exceed the general-purpose rubbers. The particularly relevant examples may be heat-resistant rubbers and rubbers resistant to swelling in oils and other liquids that comprise the most important subgroups of specialty rubbers (Table 2). In addition to C and H atoms in their chain, most special-purpose rubbers contain, then, other atoms, such as N, O, S, Si, Cl, Br, and F. The hydrocarbon

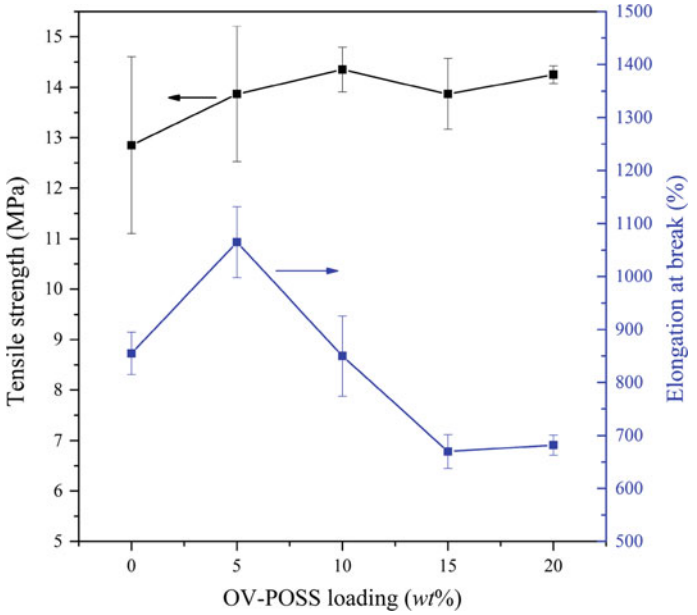

Fig. 5 Effect of OV-POSS loading on the tensile properties of OV-POSS/NR vulcanizate. Reprinted from [83], © 2017 with permission from Elsevier

Table 3 Thermal properties of the OV-POSS/NR vulcanizates. Reprinted from [83], © 2017 with permission from Elsevier

Sample	T_g (°C)	T_{onset} (°C)	Char yield at 800 °C (wt%)
Plain NR	−60.4	317	8
5% OV-POSS/NR	−59.9	343	12
10% OV-POSS/NR	−59.8	340	18
15% OV-POSS/NR	−59.6	343	20
20% OV-POSS/NR	−58.3	343	23

polymers are the cheapest, while on introduction of O, N, S, and Cl atoms the price increases. Ultimately, the two polymers containing Si (silicone, MQ rubbers) and F (fluorocarbon, FKM rubber) are the most expensive [30]. Special-purpose rubbers have been developing with progress of automotive technology and their consumption rises with the expansion of the world automotive market. However, they have many other applications, in addition to tires, which we may not even notice, as they for example are hidden in various devices.

In the past few years, POSS has been incorporated into some polymeric elastomeric materials including polydimethylsiloxane (PDMS), polystyrene-block-polybutadiene-block-polystyrene (SBS), polyurethane (PU), and ethylene-propylene-diene-monomer (EPDM) rubber to improve the comprehensive perfor-

mance of the materials. The effect of POSS particles on many properties of silicone rubber, for example, primarily thermal and oxidative stabilities and mechanical behavior, has been investigated by number of researchers in the literature [93–99]. As it was mentioned in the Introduction, a large number of scientific papers often concern silicone rubbers cross-linked at room temperature (RTV type), showing the features and range of applications quite different than high-temperature cross-linked silicone elastomers.

Recently, however, the number of publications regarding composites with POSS molecules dispersed in high-temperature vulcanized (HTV) silicone rubber also has been increasing (Table 4). When compared to most organic elastomers, silicone rubbers owe its popularity to better and longlasting functional properties at elevated temperatures. At room temperature, they are almost equal with good electro-insulating materials, while at elevated temperatures these properties are much better than in most materials. Due to high hydrophobicity of silicone rubber, moisture and water do not significantly affect these properties. A further advantageous feature, among the many other properties, is the puncture resistance during a fire, as a result of the outer silica layer on the surface of silicone rubber that provides good electrical insulation. In addition, silicone rubbers are characterized by an extremely high gas permeability, which is due to the large free volume as a result of free space presence between macromolecules. Unfortunately, this feature, as well as weak intermolecular interactions caused by, for example, the Si–O bond length, results in poor mechanical behavior. This is why, in general, the scientific research focuses mostly on the topic of improving mechanical properties of silicone rubber. More examples on this subject, showing the influence of POSS as modifying agents in the composites filled with silica as a reinforcing filler, will be given later in the chapter.

Apart from typical studies, on thermal and mechanical properties influenced by POSS, equally important and interesting is the impact of POSS molecules on added and specific properties, e.g., the adhesive properties of POSS-incorporated rubber to any reinforcing fibers. According to a recent paper quoted here, for the first time in the literature octamaleamic acid-POSS (OM-POSS), having reactive polar groups, was used to improve the adhesive properties of silicone rubber compounds [100]. Earlier some studies on adhesion, as well as flocculation and dispersibility in different elastomers, were reported with the use of new classes of nanosized substances other than POSS, namely organophilic clay or carbon nanotubes in combination with carbon black or silica [101]. According to Sirin et al. [100], the advantage of this POSS type (i.e., OM-POSS) is the presence of double bonds on the side chains (Fig. 6). It provides grafting of POSS onto silicone rubber molecules during cross-linking, which can be carried out in high temperature (HTV) with dicumyl peroxide (DCP). Additionally, the -COOH groups, present in this POSS-type nanoparticle, are supposed to play the role of an adhesion promoter in potential industrial applications, such as fiber-reinforced hoses.

In the studies, the silicone composites containing POSS were compared with the reference, which was a 5-phr silica-filled silicone rubber compound. The added value of elastomeric composites with POSS has been demonstrated based on H-adhesion test, measuring the interfacial properties of the rubber. It was shown that

Table 4 Some examples of POSS beneficial influence on rubber properties

Rubber/POSS	Characteristic	Additional benefit/Ref.
HTV silicone rubber/OM-POSS (octamaleamic acid-POSS)	– Adhesion force vs. reference sample: 1,5 fold greater (at 3 phr OM-POSS) – Thermal stability vs. reference sample: T_{d5} = 442 °C vs. 400 °C; T_{d10} = 494 °C vs. 434 °C (at 3 phr OM-POSS)	– Possible to decrease dicumyl peroxide (DCP) amount and to avoid the adverse effects of DCP decomposition products – Possible to eliminate the usage of toxic adhesives, e.g., resorcinol formaldehyde latex (RFL)Ref. [100]
HTV silicone rubber/amine-functionalized-POSS (OAPS—octa(aminophenyl)silsesquioxane; NPAMS—N-phenylaminomethylsilsesquioxane)	– Enhanced mechanical properties, especially tear strength: TS = 9,8 MPa; T_R = 42,3 kN/m (OAPS) TS = 9,9 MPa; T_R = 48,1 kN/m (NPAMS) – Markedly better thermal stability, resistant to oxidation up to 400 °C	Ref. [102]
HTV silicone rubber/vinyl-,carboxyl-, amine-functionalized-POSS	– Enhanced mechanical properties vs. reference sample: TS = 11,7 MPa vs. 6,8 MPa (at 5 phr POSS)	– Better damping properties – Higher relaxation rates Ref. [112] – Possible to obtain materials with increased surface hydrophobicity and barrier properties, as well as self-healing after damage Ref. [113]
HNBR/MV-POSS (monovinylisobutyl-POSS); OV-POSS (octavinyl-POSS); MM-POSS (methacryloisobutyl-POSS); OM-POSS (octamethacryl-POSS)	– Higher modulus (SE300) and tensile strength (TS) vs. reference sample: TS = 26,7 MPa (OV-POSS); TS = 32,7 MPa (OM-POSS) vs. 19,6 MPa	– stabilizing effect and improved aging resistance Ref. [123]

T_{d5}, T_{d10}—decomposition temperatures at 5 and 10% weight loss, respectively; TS—tensile strength; T_R—tear resistance

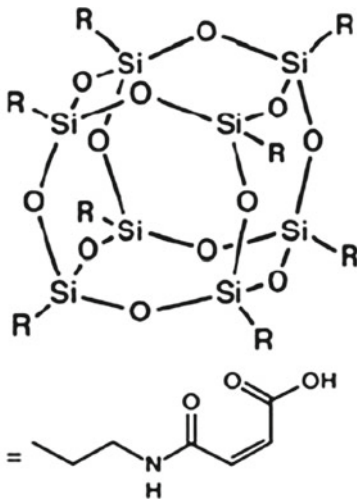

Fig. 6 Chemical structure of octamaleamic acid-POSS (OM-POSS). Reprinted from [100], © 2016 with permission from Elsevier

the application of OM-POSS in the silicone rubber composites improved the adhesion of the matrix to the reinforcing fiber, which was regenerated cellulose fiber (Rayon fiber), used to reinforce rubbers mostly in continuous woven or braid form. The typical application is the technical hoses. As a result of OM-POSS application as the adhesion enhancer, the OH groups of the Rayon interact with the –COOH groups of OM-POSS during the cross-linking process. The interaction may be either a condensation reaction yielding an ester bonding or hydrogen bonding. In this way, by the usage of OM-POSS as the adhesion enhancer, it is possible to eliminate the application of toxic adhesives such as resorcinol formaldehyde latex (RFL).

Sirin et al. [100] revealed also the different mechanism of silicone rubber cross-linking in the presence of OM-POSS and demonstrated some interesting findings of the chemical interaction between OM-POSS and the peroxide radicals. Based on DSC analysis, they showed that in the presence of OM-POSS and depending on its concentration, the cross-linking reaction in silicone rubber matrix started at lower temperatures. In the presence of OM-POSS, the radicals from DCP decomposition react preferentially with the C=C groups of OM-POSS, than taking hydrogen from the main chain of silicone rubber, what may have an obvious effect on the cross-linking density decrease. The cross-linking peak temperature of silicone rubber without OM-POSS showed an exothermic peak at 189 °C, whereas in the presence of POSS the cross-linking exotherm was obtained around 150 °C. This lowering in cross-linking onset temperatures can be associated with the dominating reaction between OM-POSS and DCP, as mentioned above.

On the basis of conducted studies, Sirin et al. [100] draw attention to the additional application of practical importance. By the introduction of OM-POSS as the main cross-linker, it is possible to decrease the amount of dicumyl peroxide (DCP) and therefore to avoid the adverse effects of DCP decomposition products in the composites. The obtained results are also valuable in order to evaluate the cross-linking

temperature to be applied in compression molding and rheology. It was revealed from the curves that the curing temperature in compression molding and in rheological analysis can be taken as 160 °C for all the compounds. At this temperature, cross-linking starts for all of the compounds, regardless the OM-POSS loadings.

Other measurements, commonly carried out for POSS-filled composites and obtained from TGA analysis, also revealed apparently improved thermal stability of the silicone composites, induced by the presence of OM-POSS. For instance, decomposition temperature at 5% weight loss increased from 400 to 441 °C with only 1 phr OM-POSS loading, whereas the maximum thermal stability was obtained at 3 phr OM-POSS [100].

Another example of the very recent studies on POSS-incorporated special-purpose rubbers concern application of amine-functionalized POSS with polysiloxane containing γ-chloropropyl groups [102]. Polysiloxane containing γ-chloropropyl groups (CPPS) is an important group of functional polysiloxanes containing halogen groups, recently used as key chemical intermediates or additives to prepare advanced functional materials [103, 104]. In order to produce a heat-curable silicone rubber based on CPPS, namely methyl chloropropyl silicone rubber (MCSR), an innovative curing system has been developed [105–107] that offers many advantages over the conventional one (e.g., peroxide curing system). Among others, the resulting vulcanizates obtained by the application of novel curing system exhibits excellent mechanical properties and thermal stability; moreover, the by-product can be easily eliminated. Many compounds containing amino groups can be chosen as cross-linkers in this curing system, as well, e.g., functionalized POSS nanoparticles with highly reactive amine groups at the corners of their cage structures [108–110]. Thus, it can be considered as a promising technique for the preparation of a heat-curable silicone rubber with improved performance as a result of chemical reaction between amino and γ-chloropropyl groups. The most recent paper, mentioned above [102], deals with these compounds, i.e., octa(aminophenyl)silsesquioxane (OAPS), an aromatic amine-functionalized POSS exhibiting a T_8 cage structure, and N-phenylaminomethylsilsesquioxane (NPAMS), another aromatic amine-functionalized POSS, which is a mixture of T_{10} and T_{12} cage structures (Fig. 7).

Typical procedure and technology for rubber (elastomer) compounds were used, i.e., the materials and other ingredients were mixed on a two-roll mill. The mixtures were then cured, typically for HTV rubbers, in a mold under pressure and high temperature of 160 °C. In order to obtain final samples for testing, the post-curing procedure was carried out in oven with air circulation, at 180 °C for 4 h.

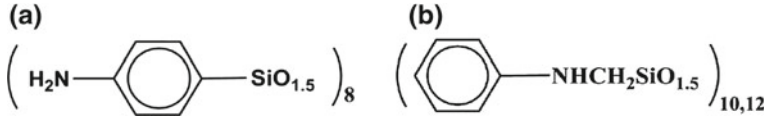

Fig. 7 Structures of amine-functionalized POSS: A) octa(aminophenyl)silsesquioxane (OAPS); B) *N*-phenylaminomethylsilsesquioxane (NPAMS). Reprinted from [102], © 2018 with permission from Elsevier

As a result, the vulcanizates cross-linked with the amine-functionalized POSS (OAPS or NPAMS) exhibited enhanced mechanical properties, especially tear strength (Fig. 8 and Table 5). The obtained effect was compared with other possible cross-linkers for silicone rubber, i.e., amine-functionalized silicone oils. Compared to them, when amine-functionalized POSS particles were used as cross-linkers of CPPS, more efficient concentrative cross-linking network could be formed and distribute stress to many adjacent and more cross-linked chemical bonds. The results indicate that the amine-functionalized POSS used as cross-linkers in the novel curing system can lead to more effective concentrative cross-linking compared with other cross-linkers. Thus, higher mechanical properties of the vulcanizates were obtained.

In addition, the results of thermal analysis showed that the cross-linked networks built by OAPS and NPAMS revealed markedly better thermal stabilities. It can be attributed to the presence of functional corner groups of aromatic structures, present in OAPS and NPAMS, which, thus, delay the decomposition of MCSR/POSS. Hence, according to the paper, the MCSR/POSS composites remained resistant to oxidation at temperatures up to 400 °C [102].

Different examples of using POSS molecules to reinforce silicone rubber matrix, which due to very weak intermolecular interactions results in a poor network structure and the composites showing much worse mechanical properties than other synthetic rubbers, deal with POSS functionalized with vinyl-, carboxyl, or amine- groups [111, 112]. They were applied as modifying agents toward methyl vinyl silicone

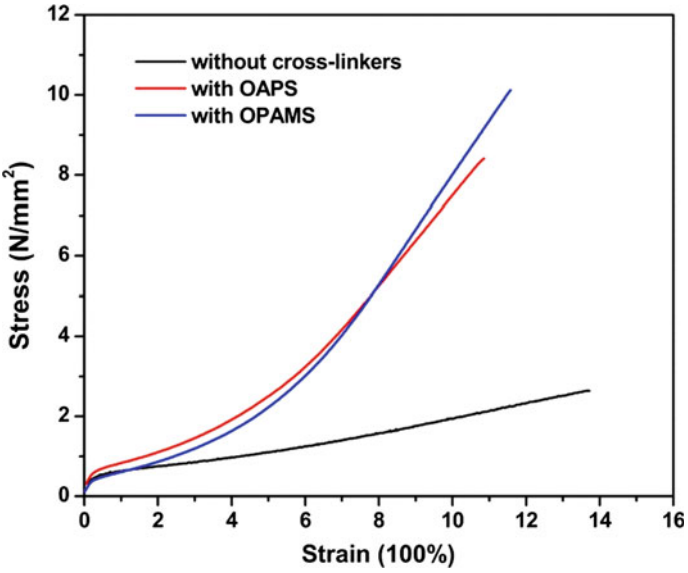

Fig. 8 Stress–strain relations of model specimens of heat-curable silicone rubber (MCSR—methyl chloropropyl silicone rubber) filled and unfilled with cross-linkers. Reprinted from [102], © 2018 with permission from Elsevier

Table 5 Mechanical properties of MCSR (methyl chloropropyl silicone rubber) cured with linear silicone oil or amine-functionalized POSS concentrative cross-linkers

Mechanical properties	Linear silicone oil		Amine-functionalized POSS	
	APPS	AEAPPS	OAPS	NPAMS
Tensile strength (MPa)	9.8	9.3	9.8	9.9
Tear strength (kN/m)	41.1	38.6	42.3	48.1

Reprinted from [102], © 2018 with permission from Elsevier
APPS—(poly(dimethyl-*co*-3-aminopropylmethyl) silicone oil; AEAPPS—poly(dimethyl-*co*-3-(2-aminoethylamino)propyl) silicone oil; OAPS—octa(aminophenyl)silsesquioxane; NPAMS—N-phenylaminomethylsilsesquioxane

rubber (MVQ). Additionally, oxazoline derivative and itaconic acid were used as the coupling agents. As a result, the most significant effect was observed for the composite obtained with vinyl-isobutyl-POSS, which resulted in twice the tensile strength, compared to the reference sample, and good rubber damping properties [111].

From the point of view of silicone rubber special applications, some interesting results were also obtained in reduced temperature, e.g., the temperature of silicone rubber crystallization. The studied silicone rubber composites with monovinyl(isobutyl)-POSS exhibited then very good mechanical properties; at temperature of −50 °C, tensile strength was over 17 MPa. The studies also revealed that suitably functionalized POSS could reduce the aging effect and increase the surface hydrophobicity, while at the same time influencing oxygen barrier properties. Moreover, the addition of POSS, containing acidic or basic groups, to the silicone rubber resulted in the material with self-healing properties after damage [112].

The literature review shows also the examples of rubber nanocomposites preparation using non-reactive POSS particles [113]. In such a case, lack of polymer–filler bonding available through chemical cross-linking can be overcome by using a coupling agent that could increase the polymer–filler interaction. Thus, in the case of non-reactive particles, the hydrodynamic reinforcement that results from the incorporation of rigid particles can be obtained.

According to a paper, fumed silica was functionalized by aliphatic and aromatic groups by silane coupling agents and then used in combination with non-reactive POSS particles, namely octamethyl-POSS and octaphenyl-POSS, to obtain heat-curable silicone elastomer nanocomposites.

TEM analysis showed a good dispersion in the matrix, however, only in the composites having silica and POSS fillers with similar modifications. Moreover, aliphatic POSS owing to the small size and good compatibility, acted as a lubricant, reducing the polymer–silica filler interaction and also the filler–filler interaction within fumed silica. According to the authors of the published studies, there will be a competition between the POSS and fumed silica fillers in interacting with the silicone rubber

matrix and this destroys the existing filler–filler interaction within silica, which was actually responsible for the strength of the material and forming new POSS–silica interactions as well as resulting in the aggregates [113].

As it was emphasized, interfacial adhesion between polymer and nanoparticles is one of the key factors to prepare polymer nanocomposites with excellent performances [114–117]. It can be realized then by introducing strong interactions facilitating an easy and homogeneous dispersion of nanoparticles in the polymer matrix, leading eventually to a great improvement in mechanical properties [116]. Based on these concepts, there are many studies on POSS application in carboxylated nitrile rubber (XNBR) by means of the interactions between organofunctional groups of POSS, such as epoxycyclohexyl [118, 119], glycidyl [120] or hydroxyl groups [121], and carboxyl groups of XNBR.

Studies on acrylonitrile-butadiene rubber (NBR), which is a kind of polar rubber and one of the most extensive synthetic rubbers, have been reported less often, mainly due to the absence of carboxyl groups in NBR molecular chain, thereby because of the lack of intermolecular interactions. However, some recent studies [122] reveal the application of a novel kind of POSS derivate, octa-(polyethylene glycol)-POSS (PEG-POSS—Fig. 9) to prepare NBR/POSS nanocomposites based on the nature coordination ability of electron-rich groups (–CN and –C–O–C- groups) with metal (Li^+) cations. Considering the results, the possible microstructure has been proposed to express the experimental observation and relationship between mechanical properties obtained (Fig. 10).

According to the authors, a novel network structure consists of several kinds of effective cross-links, which facilitates strong interface cohesion between POSS and NBR matrix and effective dispersion of POSS. The addition of POSS not only increased the cross-linking density of NBR/$LiClO_4$/PEG-POSS nanocomposites, but also improved the 300% modulus and tensile strength greatly. It was observed, that at 20 wt% of POSS loading, the 300% modulus and tensile strength are about 4 and 13 times in comparison with the pristine NBR, respectively, with almost the same elongation at break (Table 6).

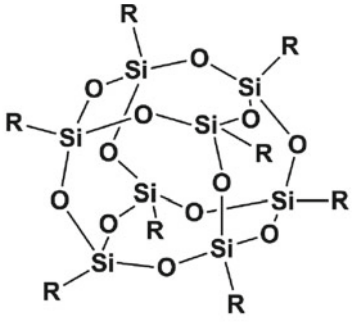

Fig. 9 Chemical structure of octa-(polyethylene glycol)-POSS (PEG-POSS). Reprinted from [122], © 2016 with permission from Elsevier

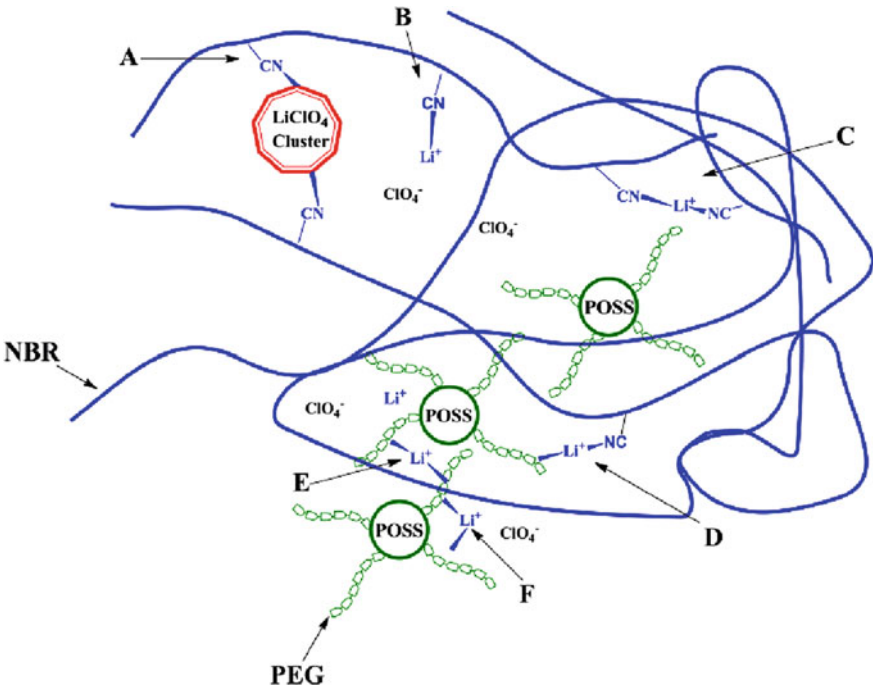

Fig. 10 Fig. 10. Possible microstructure in NBR/$LiClO_4$/POSS nanocomposites. Reprinted from [122], © 2016 with permission from Elsevier

Since the most important properties of rubbers are closely in association with the network structure, the stress–strain behavior is not only controlled by chemical cross-

Table 6 Mechanical parameters of NBR and NBR/$LiClO_4$/PEG-POSS nanocomposites.

Sample	300% modulus (MPa)	Tension strength (MPa)	Elongation at break (%)	G_c	G_e
NBR	0.40	0.57	910	0	0.53
NBR-Li-10 wt% POSS	0.97	2.68	921	0.096	0.67
NBR-Li-20 wt% POSS	1.85	7.17	865	0.15	1.43
NBR-Li-30 wt% POSS	0.98	4.29	681	0.14	0.55

Reprinted from [122], © 2016 with permission from Elsevier
where G_c represents the cross-link contribution and G_e represents the constraint contribution

linkages, but also by the contributions of confinement, where G_c represents the cross-link contribution and G_e—the constraint contribution. According to the published paper, only the topological confinement (G_e), particularly the chain entanglement, contributes to the stress–strain behavior of neat NBR, whereas the G_c value is zero. Higher values of G_c and G_e indicate that the addition of $LiClO_4$/POSS can bring cross-links to NBR matrix, implying PEG-POSS is a potential cross-linking candidate for NBR/$LiClO_4$/POSS nanocomposites. The network structure could relax then to a more perfect regime by applied stress distribution with the aid of the effective NBR-POSS cross-linking network (G_c and G_e), which was good for the mechanical properties of the rubber nanocomposites (Table 6).

The possibility of using POSS as nanofillers or modifying additives to elastomers was also reported for Hydrogenated Acrylonitrile Butadiene Rubber (HNBR) [123]. The POSS used in the study were vinylisobutyl-POSS (MV-POSS), octavinyl-POSS (OV-POSS), methacryloisobutyl-POSS (MM-POSS), and octamethacryl-POSS (OM-POSS). According to the paper, it follows that they were successfully incorporated into silica-filled HNBR matrix as modifying agents, since they enhanced cross-link density and improved properties of the resulting network. Especially, larger POSS molecules, with eight reactive groups at the vertices (e.g., OV-POSS or OM-POSS), considerably increased interfacial interactions in studied HNBR matrix thus leading to a rigid and robust elastomeric composites, as evidenced by much higher modulus (SE300) and tensile strength (TS) in comparison with vulcanizates filled with silica, without the presence of POSS molecules.

Therefore, it was concluded that octafunctional POSS molecules could be successfully used as cross-linking species, what could allow to reduce loading levels of traditional chemical cross-linkers. It is also worth noting that the incorporation of POSS molecules into silica-filled HNBR matrix resulted in stabilizing effect against adverse changes induced by both the climatic and UV radiation aging [123].

6 Thermoplastic Elastomers/POSS

Where conventional elastomers cannot provide the range of physical properties needed in the product then thermoplastic elastomers (TPEs) are used. These materials find large application in the automotive sector and in household appliances sector. About 40% of all TPE products are used in the manufacturing of vehicles. They are sometimes referred to as thermoplastic rubbers, being a class of copolymers or a physical mix of polymers, which consist of materials with both thermoplastic and elastomeric properties. Thus, they show advantages typical of both rubbery and plastic materials. The principal difference between thermoset elastomers and thermoplastic elastomers is the type of cross-linking bonds in their structures. In fact, cross-linking is a critical structural factor which imparts high elastic properties. Nowadays, many types of injection-moldable thermoplastic elastomers (TPEs) are replacing traditional rubbers.

TPEs are characterized, hence, by intermediate properties between cross-linked rubber and a thermoplastic material, and they reveal the ability of large reversible deformations in a certain temperature range, although they are not chemically cross-linked. TPEs are the only class of elastomers that do not require chemical cross-links, as they gain their strength from physical interactions between polymer components [124, 125].

Following the various nanosized fillers, mainly layered silicates, polyhedral oligomeric silsesquioxanes were also incorporated in these types of block copolymers. Some examples of POSS chemically incorporated into TPEs may be studies dealing with a novel hybrid organic–inorganic triblock copolymer of polystyrene-butadiene-polystyrene (SBS) containing POSS molecules grafted onto 1,2-butadienes in the polybutadiene soft block by hydrosilylation method [126–128]. Unlike typical free radical copolymerizations (generally one-pot copolymerization methods) commonly used for POSS incorporations, the applied method of synthesis allowed POSS molecules to be selectively grafted to the copolymer segments without introducing other effects that might arise from changes to the molecular structure of the main SBS backbone. As a result, X-ray diffraction analysis revealed that the grafted POSS molecules were very well dispersed in the matrix of the hybrid polymer. The presence of POSS in the soft segments of SBS enhanced the value of T_g for the polybutadiene block, and according to the authors, an interesting effect has been observed, mainly an improved load carrying capability for the POSS-modified SBS triblock copolymer at temperatures where the styrene block begins to soften [127].

Another example of interest in thermoplastic elastomers that contain POSS are the studies referring to the POSS molecules chemically incorporated into ethylene–propylene copolymers [129, 130]. These novel thermoplastic elastomers, ethylene–propylene-POSS (EP-POSS) terpolymers, were synthesized as a result of polymerization using a hafnium-based metallocene catalyst [130]. This method was applied in contrast to the traditional one, which uses vanadium-based Ziegler–Natta catalysts. According to the authors of the paper, the applied metallocene polymerization offers advantages over the traditional one, giving unimodal polymer distributions with sufficiently high molecular weights, good propylene and diene incorporation, relatively low polydispersities, and easier removal of cocatalysts.

An important feature of POSS is the ability to aggregate in copolymers, thereby creating physical interactions between polymer chains, where POSS can act as a physical cross-link. The published studies revealed that POSS particles aggregation is strongly dependent on the nature of the POSS peripheral group off each silicon atom. It was thus shown, based on X-Ray studies, that aggregation of POSS in the EP-POSS elastomer did not occur with isobutyl and ethyl peripheries, as they disperse well within the polymer matrix. The obtained results suggest that such POSS particles can act as a plasticizer. In contrast, nanoparticles of POSS with the phenyl periphery showed a tendency to aggregation and the formation of POSS nanocrystals increased the mechanical properties of these thermoplastic elastomers, leading as a result to mechanically robust material [130]. Therefore, the storage modulus of the terpolymer increased significantly with increasing POSS loading in the rubbery plateau region, as compared to the ethylene–propylene parent polymer. Tensile studies revealed also an

increase in the elastic modulus with increasing POSS with the phenyl periphery (EP-PhPOSS) loading, as well as elongations at break as high as 720% for EP-PhPOSS sample, with the others between 400 and 500%.

Other examples of research may concern tetrafluoroethylene–propylene copolymer (TFE/P) which is a type of elastomer with a unique combination of high-temperature, electrical, and chemical resistance properties [131, 132]. In general, TFE/P elastomers emerged also in chemical, agrichemical, automotive, and aerospace industries [133–135]. Because of the superior advantages of chemical stability and better mechanical properties, TFE/P elastomers have found wide industrial applications in corrosive oilfield environments, such as the fabrication material for O-rings, seals, and gaskets.

TFE/P copolymer cannot be cured by most cross-linking agents, it is only slightly susceptible to peroxide at high temperatures. It has been demonstrated that POSS compounds, functionalized with appropriate groups, may function as auxiliary cross-linking agents in the peroxide vulcanization of the copolymer [131]. Octavinyl-polyhedral oligomeric silsesquioxane was therefore used in the studies, as a type of POSS providing eight vinyl double bonds at every corner that can react with the TFE/P molecular chain to form a cross-link structure with the help of dicumyl peroxide (DCP).

The obtained results showed that the incorporation of octavinyl-POSS significantly enhanced the mechanical property and elevated the glass temperature of the composites. However, the thermal endurance properties were only improved slightly [131].

Accordingly, another paper of the same authors presents the results of the same TFE/P and octavinyl-POSS composites on account of improving the working performance of the composites under special working conditions, i.e., under conditions that cause the material aging [132]. The composites were aged in a 10 wt% hydrochloric acid solution for 2, 4, and 6 days at 140 °C. Combining the results of the XRD and SEM with ^{29}Si NMR and XPS analyses, it was determined that there are two types of changes that occur during the aging process of the examined composites. During the initial degradation period, the crystalline structure of the octavinyl-POSS aggregates was partly damaged (but still existed). Later in the degradation process, the POSS aggregates converted into certain Si–OH compounds and gradually disappeared. Meanwhile, the cross-links between the POSS and TFE/P chains were also damaged. Consequently, the cross-link density decreased, leading to deterioration in the mechanical and thermal properties.

Next examples of the novel hybrid materials obtained with use of different thermoplastic elastomers refer to poly(styrene-b-(ethylene-co-butylene)-b-styrene) (SEBS) triblock copolymer which is a kind of useful commercial thermoplastic elastomer [136–140]. It is characterized by excellent resistance to thermal degradation and ultraviolet irradiation, owing to the rubbery nature of the inner blocks, and mechanical strength, offered by polystyrene hard block domains that act in similar way to physical cross-linkings [141–143]. Thus, SEBS has been widely used as biomimetic gels, shock absorbing materials, adhesives, sensors, sealants, coatings and wire insulation,

etc. [144, 145]. Besides, the hard segments (S blocks) in SEBS may be functionalized to improve the performance of thermoplastic elastomer.

Various studies have been reported on the SEBS chloromethylation of styrene units in polystyrene segments [137, 138]. Based on the advantages of hybrid inorganic–organic materials, increasing number of functional nanomaterials were grafted onto the side phenyl group in SEBS; worth mentioning here, multi-walled carbon nanotubes or graphene oxide sheets, for example [139, 140].

The click coupled bonding of nanoadditives with SEBS can be considered as an efficient and facile method for controlling the resulting properties and achieving high-performance materials. Such materials are believed to offer possibilities to fully combine the extraordinary performances of the applied nanoadditives with multifunctional properties of block copolymers and thus be useful in a variety of technological fields.

The click coupling chemistry was employed in order to introduce alkyne-functionalized POSS molecules into the hard polystyrene segments in SEBS thermoplastic elastomer to improve its mechanical and thermal properties [136]. As a result, based on FT-IR, ^{1}H NMR, and GPC measurements, it was proved that POSS was quantitatively bonded onto the polystyrene hard segments in SEBS via clicking chemical reaction. TEM images showed clearly that self-aggregates inorganic phase (of around 30 nm in size, originating from POSS) was formed and homogeneously dispersed in organic SEBS matrix, resulting in the SEBS-g-POSS hybrid material. No separated phase could be observed in the SEBS without staining of phenyl groups in hard segments (Fig. 11).

The resulting SEBS-g-POSS copolymer revealed interesting surface characteristic, which was a great increase of hydrophobicity due to low surface energy of cage-like nanostructure of POSS [146, 147]. POSS would like to migrate to the surface in POSS-containing hybrid polymers, leading to a remarkable hydrophobic change on the polymer surface performance. As a result, the contact angle of SEBS-g-POSS increased to 94,8°, which is larger than that of SEBS (86,7°)—see Fig. 12.

Moreover, valuable properties in the range of thermal stability have been obtained. The final decomposition temperature was increased by c.a. 20 °C in comparison with that of SEBS, and it was attributed to heatproof of Si–O–Si framework of POSS.

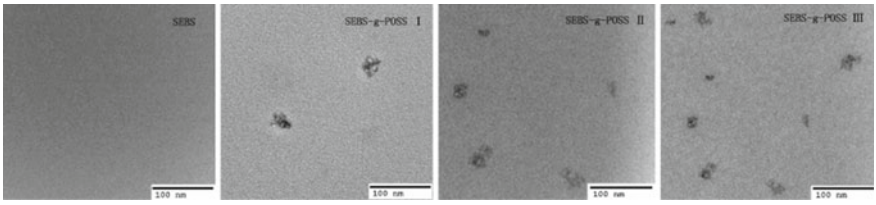

Fig. 11 TEM images of thermoplastic elastomer of SEBS poly(styrene-*b*-(ethylene-*co*-butylene)-*b*-styrene) and SEBS-*g*-POSS hybrid copolymers without any staining (I, II, and III). Reprinted from [133], © 2013 with permission from Elsevier

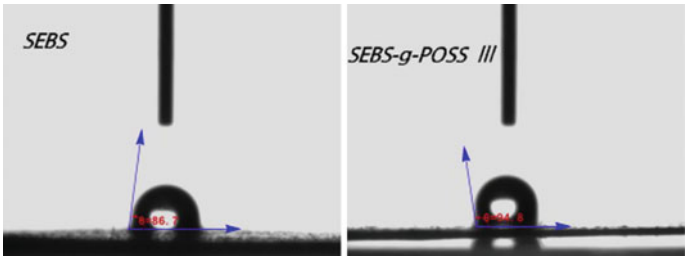

Fig. 12 Water contact angles images of neat SEBS and SEBS-*g*-POSS. Reprinted from [133], © 2013 with permission from Elsevier

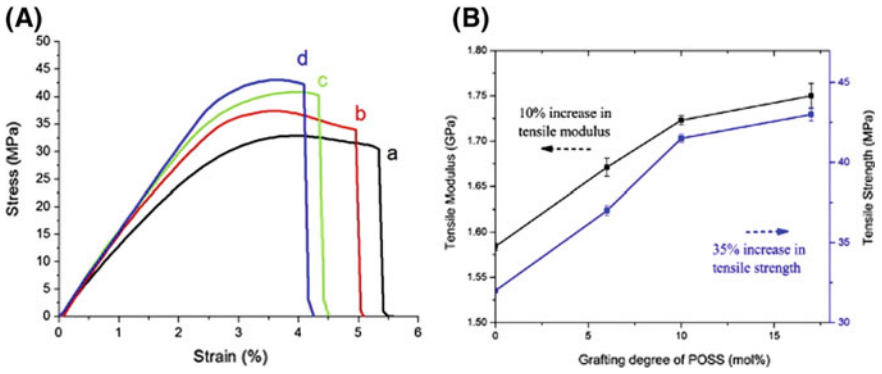

Fig. 13 (A) Stress–strain curves and (B) mechanical properties of PS/SEBS (a) and PS/SEBS-*g*-POSS composites (b: SEBE-*g*-POSS I; c: SEBE-*g*-POSS II; d: SEBE-*g*-POSS III). Reprinted from [133], © 2013 with permission from Elsevier

In addition, SEBS-g-POSS makes a contribution to tensile stress and modulus improvements of PS/SEBS-g-POSS composites due to the hard core with Si–O–Si inorganic structure of POSS and its nanoscaled aggregates. Compared to parallel PS/SEBS composite without any inorganic phase, tensile strength and modulus of PS/SEBS-g-POSS (90/10) blend could be increased by 35% and by 10%, respectively (Fig. 13).

Lastly, there are also researches on POSS application in block copolymers in order to obtain novel elastomer dye-functionalised nanocomposites [148]. It has been shown that preparing dye-functionalised POSS nanoparticles, with the purpose of further dispersing them throughout a polymer, provides many advantages over conventionally colored polymers that can fade, lose color or undergo unexpected color changes. The reported studies concern a popular choice of block copolymer which is polystyrene-butadiene-polystyrene elastomer, i.e., SBS, already mentioned at the beginning of the chapter [127]. The applied POSS molecules were functionalised with two dichlorotriazine reactive dyes, and next SBS-POSS nanocomposites were prepared using a solvent dispersion technique. The obtained results showed

that hybrid-pigment encouraged dispersion, allowing a degree of control over the functionality and producing a more uniform, stable, and visually pleasing material. Additionally, functionalised POSS improved thermal stability by imparting restrictions on SBS chain motions. Tensile stress–strain analysis revealed an increase in modulus with filler concentration. Storage modulus, loss modulus, and glass transition temperature increased with filler content due to effective SBS-POSS interaction [148].

7 Summary and Perspectives

Since the first *Polyhedral Oligomeric Silsesquioxanes* (POSS) application to polymer modifications, there has been a huge increase in interest in this type of compounds. Despite the lapse of years, research on materials containing POSS derivatives continues to develop dynamically.

Application possibilities of POSS compounds are very broad, including resistors used to obtain new materials in lithography, high-temperature lubricants or low-dielectric constant materials or pigments and dyes carriers. POSS can be used in biomaterials (drug delivery systems, antibacterial coatings, dental nanocomposites), optics and electronics (materials exhibiting properties of quantum dots, OLED diodes, electrolytes, fuel cells, lasers) and in space industry (fire-resistant materials and resistant to conditions prevailing in outer space). Polyhedral silsesquioxanes can also be used in cosmetics, printing inks or to modify the surface of materials in order to obtain hydrophobic, self-cleaning properties and increased abrasion resistance. POSS compounds, however, find the greatest application in the production of new polymer hybrid materials that combine both the properties of inorganic materials and organic polymers, Unlike most fillers, POSS molecules contain organic constituents on their external surface, which can make them compatible with many polymers.

The focus of this chapter was to discuss the influence of POSS incorporation into rubber matrix on functional properties of their composites. The POSS surface functional groups play a crucial role in controlling properties of POSS-containing materials and their reinforcement. Generally, the properties of hybrid polymeric materials mainly depend on the methods of their synthesis, the amount of POSS introduced and physical properties, and chemical substituents attached to the polyhedral cage of silsesquioxane. POSS compounds can be dispersed at the molecular level, and they can form aggregates, amorphous, or crystalline phase. POSS having surface functional groups that have favorable surface interactions can disperse uniformly in the matrix and uniform dispersion helps to improve physical properties of the nanocomposites. On the other hand, POSS having surface functional groups not compatible with the polymer matrix leads to phase-separated systems with POSS-rich domain and polymer-rich domains. Such microphase separated systems cannot provide proper reinforcement and may even lead to a decrease in desired properties.

The reinforcement mechanisms in the rubber nanocomposites are complicated and still remain an open question. The complications of a heterogeneous system

very often present in rubber composites and cross-linking structure of the rubber cause that the observed effective enhancement of the properties cannot be explained by one simple theory.

The main challenge restricting the commercial POSS applications in polymer nanocomposites is the cost. However, POSS has obtained practical application in the military field, aviation and aerospace fields, and some other high-performance materials where the cost is not relevant. On the other hand, cost of POSS is not the right issue when developing the novel materials having an excellent physical properties or niche applications where POSS can deliver what no other additive is able to. Some promising areas for POSS, that would potentially increase the market for POSS particles, are therefore probably related to biomedical applications and may include bone growth or tissue healing, for example.

References

1. Prządka D, Jęczalik J, Andrzejewska E, Szłapka M, Marciniec B, Dutkiewicz M (2013) Novel hybrid polyurethane/POSS materials via bulk polymerization. React Funct Polym 73(1):114–121. https://doi.org/10.1016/j.reactfunctpolym.2012.09.006
2. Bourbigot S, Turf T, Bellayer S, Duquesne S (2009) Polyhedral oligomeric silsesquioxane as flame retardant for thermoplastic polyurethane. Polym Degrad Stab 94:1230–1237
3. Pellice SA, Fasce DP, Williams RJJ (2003) Properties of epoxy networks derived from the reaction of diglycidyl ether of bisphenol A with polyhedral oligomeric silsesquioxanes bearing OH-functionalized organic substituents. J Polym Sci B Polym Phys 41:1451–1461 https://doi.org/10.1002/polb.10494
4. Matejka L, Strachota A, Plestil J, Whelan P, Steinhart M, Slouf M (2004) Epoxy networks reinforced with polyhedral oligomeric silseqioxanes (POSS). Struct Morphol Macromol 37:9449–9456
5. Zhou Z, Cui L, Zhang Y, Zhang Y, Yin N (2008) Preparation and properties of POSS grafted polypropylene by reactive blending. Eur Polym J 44:3057–3066
6. Waddon A, Zheng L, Farris R, Coughlin EB (2002) Nanostructured polyethylene-POSS copolymers: control of crystallization and aggregation. Nano Lett 2(10):1149–1155. https://doi.org/10.1021/nl020208d
7. Turri S, Levi M (2005) Wettability of polyhedral oligomeric silsesquioxane nanostructured polymer surfaces. Macromol Rapid Commun 26:1233–1236
8. Tao W, Zhou H, Zhang Y, Li G (2008) Novel silsesquioxane mixture-modified high elongation. polyurethane with reduced platelet adhesion. Appl Surf Sci 254:2831–2836
9. Mirchandani G, Waghoo G, Parmar R, Haseebuddin S, Ghosh SK (2009) Oligomeric silsesquioxane reinforced polyurethane with enhanced coating performance. Prog Org Coat 65(4):444–449. https://doi.org/10.1016/j.porgcoat.2009.03.009
10. Lewicki JP, Pielichowski K, Tremblot De La Croix P, Janowski B, Todd D, Liggat JJ (2010) Thermal degradation studies of polyurethane/POSS nanohybrid elastomers. Polym Degrad Stab 95(6):1099–1105
11. Ni Y, Zheng S, Nie K (2004) Morphology and thermal properties of inorganic–organic hybrids involving epoxy resin and polyhedral oligomeric silsesquioxanes. Polymer 45(16):5557–5568. https://doi.org/10.1016/j.polymer.2004.06.008
12. Liu YR, Huang YD, Liu L (2006) Effects of TriSilanolIsobutyl-POSS on thermal stability of methylsilicone resin. Polym Degrad Stab 91(11):2731–2738. https://doi.org/10.1016/j.polymdegradstab.2006.04.031

13. Liu YR, Huang YD, Liu L (2007) Thermal stability of POSS/methylsilicone nanocomposites. Comp Sci Tech 67:2864–2876
14. Fina A, Monticelli O, Camino G (2010) POSS-based hybrids by melt/reactive blending. J Mater Chem 20:9297–9305. https://doi.org/10.1039/C0JM00480D
15. Zhao J, Fu Y, Liu S (2008) Polyhedral Oligomeric Silsesquioxane (POSS)-modified thermoplastic and thermosetting nanocomposites: a review. Polym Polym Comp 16(8):483–500
16. Chen JH, Yao BX, Su WB Yang YB (2007) Isothermal crystallization behavior of isotactic polypropylene blended with small loading of polyhedral oligomeric silsesquioxane. Polymer 48(6):1756–1769
17. Chen JH, Chiou YD (2006) Crystallization behavior and morphological development of isotactic polypropylene blended with nanostructured polyhedral oligomeric silsesquioxane molecules. J Polym Sci Part B Polym Phys 44:2122–2134
18. Joshi M, Butola BS (2004) Studies on nonisothermal crystallization of HDPE/POSS nanocomposites. Polymer 45(14):4953–4968
19. Fu BX, Yang L, Somani RH, Zong SX, Hsiao BS, Philips S, Blanski R, Ruth P (2001) Crystallization studiem of isotactic polypropylene containing nanostructured polyhedral oligomeric silsesquioxane molecules under quiescent and shear conditions. J Polym Sci Part B: Polym Phys 39:2727–2739
20. Huang JC, He CB, Xiao Y, Mya KY, Dai J, Siow YP (2003) Polyimide/POSS nanocomposites: interfacial, interaction, thermal properties and mechanical properties. Polymer 44:4491–4499
21. Fina A, Abbenhuis HCL, Tabuani D, Camino G (2006) Metal functionalized POSS as fire retardants in polypropylene. Polym Degrad Stab 91:2275–2281
22. Joshi M, Butola BS, Simon G, Kukaleva N (2006) Rheological and viscoelastic behavior of HDPE/Octamethyl-POSS nanocomposites. Macromolecules 39(5):1839–1849. https://doi.org/10.1021/ma051357w
23. Zhou Q, Pramoda KP, Lee JM, Wang K, Loo LS (2011) Role of interface in dispersion and surface energetics of polymer nanocomposites containing hydrophilic POSS and layered silicates. J Colloid Interface Sci 355(1):222–230. https://doi.org/10.1016/j.jcis.2010.12.010
24. Chen D, Yi S, Fang P, Zhong Y, Huang C, Wu X (2011) Synthesis and characterization of novel room temperature vulcanized (RTV) silicone rubbers using octa[(trimethoxysilyl)ethyl]-POSS as cross-linker. React Funct Polym 71:502–511
25. Chen D, Yi S, Wu W, Zhong Y, Liao J, Huang C (2010) Synthesis and characterization of novel room temperature vulcanized (RTV) silicone rubbers using vinyl-POSS derivatives as cross-linking agents. Polymer 51:3867–3878
26. Schubert U, Huesing N, Lorenz A (1995) Hybrid inorganic-organic materials by sol-gel processing of organofunctional metal alkoxides. Chem Mater 7(11):2010–2027. https://doi.org/10.1021/cm00059a007
27. Joshi M, Butola BS (2004) Polymeric nanocomposites—Polyhedral oligomeric silsesquioxanes (POSS) as hybryd nanofillers. J Macromol Sci Part C Polym Rev 44(4):389–410. https://doi.org/10.1081/MC-200033687
28. Phillips S, Haddad T, Tomczak S (2004) Developments in nanoscience: polyhedral oligomeric silsesquioxane (POSS)-polymers. Curr Opin Solid State Mater Sci 8:21–29. https://doi.org/10.1016/j.cossms.2004.03.002
29. Bhowmick AK, Stephens HL (2001) Handbook of elastomers, 2nd edn. Marcel Dekker Inc, New York
30. Franta I (ed) Elastomers and rubber compounding materials. Manufacture, properties and applications, ISBN 9780444601186, Elsevier, 2012
31. Paul DR, Mark JE (2010) Fillers for polysiloxane ("silicone") elastomers. Prog Polym Sci 35:893–901
32. Mark JE, Erman B (2007) Rubber-like elasticity: a molecular primer, 2nd edn. Cambridge University Press, Cambridge
33. Bokobza L (2007) Polymer 48(17):4907–4920
34. Payne AR, Whittaker RE (1971) Rubber Chem Technol 44:440
35. Waddell WH, Beauregard PA, Evans LR (1995) Tire Technol Int 1995:24

36. Wang MJ (1999) Rubber Chem Technol 72:430
37. Pliskin I, Tokit NJ (1972) Appl Polym Sci 16:173
38. http://carbonblacksales.com/carbon-black-reinforcing-agent/the access date: 30 January 2018
39. Rattanasom N, Saowapark T, Deeprasertkul C (2007) Reinforcement of natural rubber with silica/carbon black hybrid filler. Polym Testing 26(3):369–377
40. Buchanan RA, Weislogel OE, Russell CR, Rist CE (1968) Starch in rubber. Zinc starch xanthate in latex masterbatching. Prod Res Dev 7(2):155–158. https://doi.org/10.1021/i360026a013
41. Buchanan RA, Kwolek WF, Katz HC (1971) Die Starke 23:350
42. Buchanan RA, Katz HC, Russell CR, Rist CE (1971) Rubber J 10:28
43. Buchanan RA (1974) Peoria Illinois Die Starke 26(5):165
44. Buchanan RA, Doane WM, Russel CR, Kwolek WF (1975) Elastomers Plast 7:95
45. Abbott TP, Doane WM, Russell CR (1973) Rubber Age 8:43
46. Rubber containing starch reinforcement and tire having component thereof. EP1074582 A1 (2001)
47. Farm tire with tread of rubber composition containing starch/plasticizer composite. EP1514900 A1 (2005)
48. Rouilly A, Rigal L, Gilbert RG (2004) Polymer 45:7813
49. Wu CS (2005) Macromol Biosci 5:352
50. Wang S, Yu J, Yu J (2005) Polym Degrad Stab 87:395
51. Patel NK, Pandya PD, Kehariya H, Patel H, Sinha VK (2005) Int J Polym Mater 54:985
52. Qi Q et al (2006) Modification of starch for high performance elastomer. Polymer 47:3896–3903
53. Gura DV, Sokolova LA, Ovcharov VI, Soroka PI (2015) Assessing the properties of elastomer composites filled with hybrid filler. Int Polym Sci Technol 42(3):T23–T25
54. Barashkova II, Komova NN, Motyakin MV, Potapov EE, Wasserman AM (2014) Shungite-elastomer interface layers. In: Doklady Physical Chemistry, vol 456. Pleiades Publishing, pp 83–85
55. Barashkova II et al (2015) EPR Spin Probe Study of Local Mobility at the Shungite/Elastomer Interface. Appl Magn Reson 46(12):1421–1427
56. Kornev YuV et al (2013) Investigating the influence of the degree of dispersion of mineral shungite on the properties of elastomeric materials based on butadiene-styrene rubber. Int Polym Sci Technol 40(3):T27–T32
57. Donnet JB (2003) Nano and microcomposites of polymers elastomers and their reinforcement. Compos Sci Technol 63(8):1085–1088. https://doi.org/10.1016/S0266-3538(03)00028-9
58. Ponnamma D, Maria HJ, Chandra AK, Thomas S (2013) Rubber Nanocomposites: latest trends and concepts. Adv Elastomers II 12:69–107. https://doi.org/10.1007/978-3-642-20928-4_3
59. Thomas S, Maria HJ (eds) Progress in rubber nanocomposites, Woodhead Publishing, Cambridge 2016
60. De Falco A, Goyanes S, Rubiolo GH, Mondragon I, Marzocca MA (2007) Carbon nanotubes as reinforcement of styrene-butadiene rubber. Appl Surf Sci 254(1):262–265
61. Cardoen G, Coughlin EB (2004) Hemi-telechelic polystyrene-POSS copolymers as model systems for the study of well-defined inorganic/organic hybryd materials. Macromolecules 37:5123–5126
62. Tan BH, Hussain H, Leong YW, Lin TT, Tjiu WW, He C (2013) Tuning self-assembly of hybrid PLA-P(MA-POSS) block copolymers in solution via stereocomplexation. Polym Chem 4:1250–1259
63. Bliznyuk V, Tereshchenko T, Gumenna M, Gomza YP, Shevchuk A, Klimenko N et al (2008) Structure of segmented poly (ether urethane)s containing amino and hydroxyl functionalized polyhedral oligomeric silsesquioxanes (POSS). Polymer 49:2298–2305
64. Kuo SW, Chang FC (2011) POSS related polymer nanocomposites. Prog Polym Sci 36:1649–1696

65. Zhang W, Camino G, Yang R (2017) Polymer/polyhedral oligomeric silsesquioxane (POSS) nanocomposites: An overview of fire retardance. Prog Poly Sci 67:77–125. https://doi.org/10.1016/j.progpolymsci.2016.09.011
66. Laik S, Galy J, Gérard JF, Monti M, Camino G (2016) Fire behaviour and morphology of epoxy matrices designed for composite materials processed by infusion. Polym Degrad Stab 127:44–55
67. Rubber compound containing a polyhedral oligomeric silsesquioxanes. Pat. US 6852794 B2 (2005)
68. Method for making alkoxy-modified silsesquioxanes. Pat. US 7915368 B2 (2011)
69. Amino alkoxy-modified silsesquioxane and method of preparation. Pat. US 8513371 B2(2013)
70. Compouding silica-reinforced rubber with low volatile organic compounds (VOC) emission. Pat. US9403969 B2(2016)
71. Amino alkoxy-modified silsesquioxane adhesives for improved metal adhesion and metal adhesion retention to cured rubber. Pat. US 8794282 B2(2014)
72. Rubber composition comprising a polyhedral oligomeric silsesquioxane additive. Pat. WO 2006027618 A1(2006)
73. Zhao Y, Jiang X, Zhang X, Hou L (2017) Toughened elastomer/polyhedral oligomeric silsesquioxane (POSS)-intercalated rectorite nanocomposites: preparation, microstructure, and mechanical properties. Polym Compos 38:E443–E450. https://doi.org/10.1002/pc.23784
74. Deng H et al (2012) Quaternized chitosan-layered silicate intercalated composites based nanofibrous mats and their antibacterial activity. Carbohydr Polym 89(2):307–313
75. Wang X et al (2010) Preparation and characterization of new quaternized carboxymethyl chitosan/rectorite nanocomposite. Compos Sci Technol 70(7):1161–1167
76. Li W et al (2013) Poly(vinyl alcohol)/sodium alginate/layered silicate based nanofibrous mats for bacterial inhibition. Carbohydr Polym 92(2):2232–2238
77. Fox DM, Maupin PH, Harris RH Jr, Gilman JW, Eldred DV, Katsoulis D, Trulove PC, De Long HC (2007) Use of a polyhedral oligomeric silsesquioxane (POSS)-imidazolium cation as an organic modifier for montmorillonite. Langmuir 23:7707–7714
78. Fox DM, Harris RH Jr, Bellayer S, Gilman JW, Gelfer MY, Hsaio BS, Maupin PH, Trulove PC, De Long HC (2011) The pillaring effect of the 1,2-Dimethyl-3(benzyl ethyl iso-butyl POSS) imidazolium cation in polymer/montmorillonite nanocomposites. Polymer 52:5335–5343
79. Wan C, Yu J, Shi X, Huang L (2006) Preparation of poly(propylene carbonate)/organophilic rectorite nanocomposites via direct melt intercalation. Trans Nonferrous Metals Soc Chin 16:s508–s511. https://doi.org/10.1016/S1003-6326(06)60245-8
80. Li B, Dong FX, Wang XL, Yang J, Wang DY, Wang YZ (2009) Organically modified rectorite toughened poly(lactic acid): nanostructures, crystallization and mechanical properties. Eur Polym J 45(11):2996–3003. doi.org/https://doi.org/10.1016/j.eurpolymj.2009.08.015
81. Ma XY, Liang GZ, Lu HJ, Liu HL, Huang Y (2005) Novel intercalated nanocomposites of polypropylene, organic rectorite, and poly(ethylene octene) elastomer: morphology and mechanical properties. J Appl Polym Sci 97:1907–1914. https://doi.org/10.1002/app.21931
82. Ma XY, Liang GZ, Liu HL, Fei JY, Huang Y (2005) Novel intercalated nanocomposites of polypropylene/organic-rectorite/polyethylene-octene elastomer: rheology, crystallization kinetics, and thermal properties. J Appl Polym Sci 97:1915–1921. https://doi.org/10.1002/app.21938
83. Zhao L et al (2018) Morphology and thermomechanical properties of natural rubber vulcanizates containing octavinyl polyhedral oligomeric silsesquioxane. Compos Part B 139:40–46. https://doi.org/10.1016/j.compositesb.2017.11.052
84. Tanaka K, Chujo Y (2012) Advanced functional materials based on polyhedral oligomeric silsesquioxane (POSS). J Mater Chem 22(5):1733–1746
85. Ghanbari H, Cousins BG, Seifalian AM (2011) A nanocage for nanomedicine: polyhedral oligomeric silsesquioxane (POSS). Macromol Rapid Commun 32(14):1032–1046
86. Li YW, Dong XH, Guo K, Wang Z, Chen ZR, Wesdemiotis C et al (2012) Synthesis of shape amphiphiles based on POSS tethered with two symmetric/asymmetric polymer tails via sequential "Grafting-from" and thiol–ene "click" chemistry. ACS Macro Lett 1(7):834–839

87. Wei K, Wang L, Li L, Zheng SX (2015) Synthesis and characterization of bead-like poly(Nisopropylacrylamide) with double decker silsesquioxanes in the main chains. Polym Chem 6(2):256–269
88. Alvarado-Tenorio B, Romo-Uribe A, Mather PT (2015) Nanoscale order and crystallization in POSS–PCL shape memory molecular networks. Macromolecules 48(16):5770–5779
89. Franczyk A, He H, Burdyńska J, Hui C, Matyjaszewski K, Marciniec B (2014) Synthesis of high molecular weight polymethacrylates with polyhedral oligomeric silsesquioxane moieties by atom transfer radical polymerization. ACS Macro Lett 3(8):799–802
90. Zhang WA, Muller AHE (2013) Architecture, self-assembly and properties of well-defined hybridpolymers basedonpolyhedraloligomericsilsesquioxane (POSS) Prog Polym Sci 38(8):1121–62
91. Shockey EG, Bolf AG, Jones PF, Schwab JJ, Chaffee KP, Haddad TS et al (1999) Functionalized polyhedral oligosilsesquioxane (POSS) macromers: new graftable POSS hydride, POSS a-olefin, POSS epoxy, and POSS chlorosilane macromers and POSS-siloxane triblocks. Appl Organomet Chem 13(4):311–327
92. Sun DX, Li XJ, Zhang YH, Li YW (2011) Effect of modified nano-silica on the reinforcement of styrene butadiene rubber composites. J Macromol Sci B 50(9):1810–1821
93. Chen D, Liu Y, Huang C (2012) Synergistic effect between POSS and fumed silica on thermal stabilities and mechanical properties of room temperature vulcanized (RTV) silicone rubbers. Polym Degrad Stab 97:308–315. https://doi.org/10.1016/j.polymdegradstab.2011.12.016
94. Shi Y, Huang G, Liu Y, Qu Y, Zhang D, Dang Y (2013) Synthesis and thermal properties of novel room temperature vulcanized (RTV) silicone rubber containing POSS units in polysioxane main chains. J Polym Res 20(9):245. https://doi.org/10.1007/s10965-013-0245-y
95. Zhang Y, He J, Yang R (2016) The effects of phosphorus-based flame retardants and octaphenyl polyhedral oligomeric silsesquioxane on the ablative and flame-retardation properties of room temperature vulcanized silicone rubber insulating composites. Polym Degrad Stab 125:140–147. doi.org/https://doi.org/10.1016/j.polymdegradstab.2015.12.007
96. Liu L, Tian M, Zhang W, Zhang LQ, Mark JE (2007) Crystallization and morphology study of polyhedral oligomeric silsesquioxane (POSS)/polysiloxane elastomer composites prepared by melt blending. Polymer 48:3201–3212
97. Meng Y, Wei Z, Liu L, Liu L, Zhang L, Nishi T, Ito K (2013) Significantly improving the thermal stability and dispersion morphology of polyhedral oligomeric silsesquioxane/polysiloxane composites by in-situ grafting re action. Polymer 54:3055–3064
98. Chen DZ, Nie JR, Yi SP, Wu WB, Zhong YL, Liao J, Huang C (2010) Thermal behaviour and mechanical properties of novel RTV silicone rubbers using divinylhexa[(trimethoxysilyl)ethyl]-POSS as cross-linker. Polym Degrad Stab 95:618–626
99. Chen DZ, Liu Y, Huang C (2012) Synergistic effect between POSS and fumed silica on thermal stabilities and mechanical properties of room temperature vulcanized (RTV) silicone rubbers. Polym Degrad Stab 97:308–315
100. Sirin H, Kodal M, Karaagac B, Ozkoc G (2016) Effects of octamaleamic acid-POSS used as the adhesion enhancer on the properties of silicone rubber/silica nanocomposites. Composites Part B 98:370–381. https://doi.org/10.1016/j.compositesb.2016.05.024
101. Stockelhuber KW, Das A, Jurk R, Heinrich G (2010) Contribution of physico-chemical properties of interfaces on dispersibility, adhesion and flocculation of filler particles in rubber. Polymer 51(9):1954–1963
102. Dong F, Zhao P, Dou R, Feng S (2018) Amine-functionalized POSS as cross-linkers of polysiloxane containing γ-chloropropyl groups for preparing heat-curable silicone rubber. Mater Chem Phys 208:19–27. https://doi.org/10.1016/j.matchemphys.2018.01.024
103. Madsen FB, Yu L, Daugaard AE, Hvilsted S, Skov AL (2015) A new soft di electric silicone elastomer matrix with high mechanical integrity and low losses. RSC Adv 5:10254–10259
104. Madsen FB, Yu L, Mazurek P, Skov AL (2016) A simple method for reducing inevitable dielectric loss in high-permittivity dielectric elastomers. Smart Mater Struct 25:075018–075032
105. Diao S, Dong FY, Meng J, Ma PQ, Zhao YY, Feng SY (2015) Preparation and properties of heat-curable silicone rubber through chloropropyl/amine crosslinking reactions. Mater Chem Phys 153:161–167

106. Dong FY, Diao S, Ma DP, Zhang SY, Feng SY (2015) Preparation and characterization of 3-chloropropyl polysiloxane-based heat-curable silicone rubber using polyamidoamine dendrimers as cross-linkers. React Funct Polym 96:14–20
107. Dong FY, Ma DP, Feng SY (2016) Aminopropyl-modified silica as cross-linkers of polysiloxane containing chloropropyl groups for preparing heat-curable silicone rubber. Polym Test 52:124–132
108. Choi J, Tamaki R, Kim SG, Laine R (2003) Organic/inorganic imide nanocomposites from aminophenylsilsesquioxanes. Chem Mater 15:3365–3375
109. Iyer P, Iyer G, Coleman MC (2010) Gas transport properties of polyimide-POSS nanocomposites. J Membr Sci 358:26–32
110. Zhang QH, He H, Xi K, Huang X, Yu XH, Jia XD (2011) Synthesis of N-phenylaminomethyl POSS and its utilization in polyurethane. Macromolecules 44:550–557
111. Strąkowska A, Kosmalska A, Zaborski M (2012) Silsesquioxanes as modifying agents of methylvinylsilicone rubber. Mater Sci Forum 714:183–189. https://doi.org/10.4028/www.scientific.net/MSF.714.183
112. Zaborski M, Strąkowska A, Kosmalska A, Maciejewski H, Michał Dutkiewicz (2013) POSS compounds as modifiers and additives for elastomeric composites. Polimery 58:772–782. https://doi.org/10.14314/polimery.2013.772
113. Joshi V, Srividhya M, Dubey M, Ghosh AK, Saxena A (2013) Effect of functionalization on dispersion of POSS-silicone rubber nanocomposites. J Appl Polym Sci 130:92–99. https://doi.org/10.1002/app.39112
114. Yang Z, Liu J, Liao R, Yang G, Wu X, Tang Z, Guo B, Zhang L, Ma Y, Nie Q, Wang F (2016) Rational design of covalent interfaces for graphene/elastomer nanocomposites. Compos Sci Technol 132:68–75
115. Zhong B, Jia Z, Luo Y, Jia D (2015) A method to improve the mechanical performance of styrene-butadiene rubber via vulcanization accelerator modified silica. Compos Sci Technol 117:46–53
116. Rooj S, Das AStockelhuber KW, Wießner S, Fischer D, Reuter U, Heinrich G (2015) Expanded organoclay assisted dispersion and simultaneous structural alterations of multiwall carbon nanotube (MWCNT) clusters In natural rubber. Compos Sci Technol 107:36–43
117. Le H, Parsaker M, Sriharish M, Henning S, Menzel M, Wiessner S, Das A, Do Q, Heinrich G, Radusch H (2015) Effect of rubber polarity on selective wetting of carbon nanotubes in ternary blends. Express Polym Lett 9(11):960–971
118. Liu Q, Ren W, Zhang Y, Zhang Y (2012) A study on the curing kinetics of epoxycyclohexyl polyhedral oligomeric silsesquioxanes and hydrogenated carboxylated nitrile rubber by dynamic differential scanning calorimetry. J Appl Polym Sci 123(5):3128–3136
119. Liu Q, Ren W, Zhang Y, Zhang Y (2011) Curing reactions and properties of organicinorganic composites from hydrogenated carboxylated nitrile rubber and epoxycyclohexyl polyhedral oligomeric silsesquioxanes. Polym Int 60(3):422–429
120. Konnola R, Nair CPR, Joseph K (2016) Cross-linking of carboxyl-terminated nitrile rubber with polyhedral oligomeric silsesquioxane. J Therm Anal Calorim 123(2):1479–1489
121. Sahoo S, Bhowmick AK (2007) Polyhedral oligomeric silsesquioxane (POSS) nanoparticles as new crosslinking agent for functionalized rubber. Rubber Chem Technol 80(5):826–837
122. Yang S, Fan H, Jiao Y, Cai Z, Zhang P, Li Y (2017) Improvement in mechanical properties of NBR/$LiClO_4$/POSS nanocomposites by constructing a novel network structure. Compos Sci Technol 138:161–168. https://doi.org/10.1016/j.compscitech.2016.12.003
123. Kosmalska A, Strąkowska A, Zaborski M (2012) Properties of POSS/HNBR elastomer nanocomposites. Mater Sci Forum 714:175–181. https://doi.org/10.4028/www.scientific.net/MSF.714.175
124. Sperling L (2001) Physical polymer science, 3rd edn. Wiley Interscience and Sons Inc, New York
125. Odian G (2001) Principles of polymerization, 3rd edn. Wiley Interscience and Sons Inc, New York

126. Drazkowski DB, Lee A, Haddad TS, Cookson DJ (2006) Chemical substituent effects on morphological transitions in styrene – butadiene – styrene triblock copolymer grafted with polyhedral oligomeric silsesquioxanes. Macromolecules 39(5):1854–1863
127. Fu BX, Lee A, Haddad TS (2004) Styrene – butadiene – styrene triblock copolymers modified with polyhedral oligomeric silsesquioxanes. Macromolecules 37(14):5211–5218. https://doi.org/10.1021/ma049753m
128. Drazkowski DB, Lee A, Haddad TS (2007) Morphology and phase transitions in styrene – butadiene – styrene triblock copolymer grafted with isobutyl-substituted polyhedral oligomeric silsesquioxanes. Macromolecules 40(8):2798–2805. https://doi.org/10.1021/ma062393d
129. Salamore J (1996) Polymeric materials encyclopedia. CRC Press, New York, pp 2264–2271
130. Seurer B, Coughlin EB (2008) Ethylene–propylene–silsesquioxane thermoplastic elastomers. Macromol Chem Phys 209(12):1198–1209
131. Cong C, Cui C, Meng X, Zhou Q (2013) Structure and property of tetrafluoroethylene-propylene elastomer-OVPOSS composites. J Appl Polym Sci 130(2):1281–1288. https://doi.org/10.1002/app.39223
132. Cong C, Cui C, Meng X, Zhou Q (2014) Stability of POSS crosslinks and aggregates in tetrafluoroethylene-propylene elastomers/OVPOSS composites exposed to hydrochloric acid solution. Polym Degrad Stab 100:29–36. https://doi.org/10.1016/j.polymdegradstab.2013.12.032
133. Kostov GK, Chr PetrovP (1992) Study of synthesis and properties of tetrafluoroethylene-propylene copolymers. J Polym Sci Part A Polym Chem 30:1083–1088
134. Aminabhavi TM, Harlapur SF, Balundgi RH, Dale Ortego J (1998) Theoretical and experimental investigations of molecular migration and diffusion kinetics of organic esters into tetrafluoroethylene/propylene copolymer membranes. Can J Chem Eng 76:104–112
135. Kulkarni SB, Kariduraganavar MY, Aminabhavi TM (2003) Sorption, diffusion, and permeation of esters, aldehydes, ketones, and aromatic liquids into tetrafluoroethylene/propylene at 30, 40, and 50 °C. J Appl Polym Sci 89(12):3201–3209. https://doi.org/10.1002/app.2376
136. Niu M et al (2013) Novel hybrid copolymer by incorporating POSS into hard segments of thermoplastic elastomer SEBS *via* click coupling reaction. Polymer 54:2658–2667. https://doi.org/10.1016/j.polymer.2013.02.042
137. Zeng QH, Liu QL, Broadwell I, Zhu AM, Xiong Y, Tu XP (2010) Anion-exchange membranes based on quaternized polystyrene-block-poly(ethylene-ran-butylene)-block-polystyrene for direct methanol alkaline fuel cells. J Membr Sci 349:237–243. https://doi.org/10.1016/j.memsci.2009.11.051
138. Xu W, Cheng Z, Zhang Z, Zhang L, Zhu X (2011) Modification of SEBS rubber via iron-mediated AGET ATRP in the presence of limited amounts of air. React Funct Polym 71(6):634–640. https://doi.org/10.1016/j.reactfunctpolym.2011.03.008
139. Yadav SK, Mahapatra SS, Cho JW, Lee JY (2010) Functionalization of multiwalled carbon nanotubes with poly(styrene-b-(ethylene-co-butylene)-b-styrene) by click coupling. J Phys Chem C 114(26):11395–11400. https://doi.org/10.1021/jp1028382
140. Cao Y, Lai Z, Feng J, Wu P (2011) Graphene oxide sheets covalently functionalized with block copolymers via click chemistry as reinforcing fillers. J Mater Chem 21(25):9271–9278. https://doi.org/10.1039/C1JM10420A
141. Allen NS, Edge J, Wilkinson A, Liauw CM, Mourelatou D, Barrio J et al (2001) Degradation and stabilisation of styrene-ethylene-butadiene-styrene (SEBS) block copolymer. Polym Degrad Stab 71:113–122
142. Allen NS, Luengo C, Edge M, Wilkinson A, Parellada MD, Barrio JA et al (2004) Photooxidation of styrene-ethylene-butadiene-styrene (SEBS) block copolymer. J Photochem Photobiol A Chem 162:41–51. https://doi.org/10.1016/S1010-6030(03)00311-3
143. Darling SB (2007) Directing the self-assembly of block copolymers. Prog Polym Sci 32(10):1152–1204. https://doi.org/10.1016/j.progpolymsci.2007.05.004
144. Shankar R, Krishnan AK, Ghosh TK, Spontak RJ (2008) Triblock copolymer organogels as high performance dielectric elastomers. Macromolecules 41(16):6100–6109. https://doi.org/10.1021/ma071903g

145. Ganguly A, Bhowmick AK (2009) Quantification of surface forces of thermoplastic elastomeric nanocomposites based on poly(styrene-ethylene-co-butylene-styrene) and clay by atomic force microscopy. J Appl Polym Sci 111:2104–2115. https://doi.org/10.1002/app.29268
146. Koh K, Sugiyama S, Morinaga T, Ohno K, Tsujii Y, Fukuda T et al (2005) Precision synthesis of a fluorinated polyhedral oligomeric silsesquioxane-terminated polymer and surface characterization of its blend film with poly(methyl methacrylate). Macromolecules 38(4):1264–1270. https://doi.org/10.1021/ma047636l
147. Tuteja A, Choi W, Ma M, Mabry JM, Mazzella SA, Rutledge GC et al (2007) Designing superoleophobic surfaces. Science 318(5856):1618–1622. https://doi.org/10.1126/science.1148326
148. Spoljaric S, Shanks RA (2012) Novel elastomer dye-functionalised POSS nanocomposites: enhanced colourimetric, thermomechanical and thermal properties. Express Polymer Letters 6(5):354–372. https://doi.org/10.3144/expresspolymlett.2012.39

POSS as Fire Retardant

Ming Hui Chua, Hui Zhou and Jianwei Xu

Abstract Many common petroleum-based polymeric materials used in our daily life are highly flammable and thus essential for introduction of fire-retardant properties for a greater safety purpose. Recently, polyhedral oligomeric silsesquioxanes (POSS) have received great attention in the application of fire-retardant materials by incorporating proper POSS compounds either physically or chemically into common polymer systems to offer hybrid composites with improved fire-retardant properties. This chapter will summarize the latest development on the POSS-based fire-retardant polymer composite materials mainly in terms of the class of polymers including epoxy resins, polycarbonates, polyesters, polyolefins, polystyrene, polyurethanes, vinyl esters, acrylics, and cotton fabrics. Not only will the effects of POSS on the fire-retardant properties, for example, the peak heat release rate, the total heat release, the time of ignition, and the fire ratings, obtained from key flammability tests such as cone calorimetry and UL94 testing be reviewed, but the structural diversity of POSS, process of making composites as well as mechanism for improvement in fire-retardant properties will also be holistically discussed. Finally, perspectives on potentials, challenges, and further development of POSS as fire-retardant additives are commented.

Keywords POSS · Fire retardant · Flammability, polymer composites
Hybrid composites

1 Introduction

Fire safety is an important aspect for consideration in the manufacturing of consumer products and construction of buildings and physical infrastructures. Therefore, much

M. H. Chua · H. Zhou · J. Xu (✉)
Institute of Materials Research and Engineering (IMRE),
Agency for Science, Technology and Research (A*STAR), 2 Fusionopolis Way,
Innovis, #08-03, Singapore 138634, Singapore
e-mail: jw-xu@imre.a-star.edu.sg

S. Kalia and K. Pielichowski (eds.), *Polymer/POSS Nanocomposites and Hybrid Materials*, Springer Series on Polymer and Composite Materials,
https://doi.org/10.1007/978-3-030-02327-0_10

focus has been invested in the development of materials with fire-retardant properties for greater safety assurance against fire hazards to the general public. In the present context, commercial products such as fire-proof fabrics or fire-proof paints and coatings are readily available as a result of intense research in this area. It is well known that three important components, i.e., fuel, ignition source (heat), and oxygen, must be concurrently present to sustain the process of combustion. These three components form the "fire triangle" where the removal of any one component will prevent or effectively extinguish a fire. This fundamental concept is effectively applied in the development of fire-retardant materials. As such, many fire-retardant materials work via the formation of a protective "char layer" at initial ignition, effectively protecting the inner bulk material from burning by preventing oxygen from diffusing in. These are known as intumescent materials [1].

Petroleum-based organic polymers such as polyolefins and polyesters form the bulk of materials in our everyday lives. Unfortunately, these polymers are highly flammable, restricting their scope of applications and posing a safety risk to consumers at large. The polymers burn in a very complex process, often involving free radicals, resulting in chemical degradation and decomposition and the release of smoke and gases [2]. There are several approaches to improve fire retardancy in such polymers. These include the introduction of halogens into the polymeric framework, as well as the addition of phosphorus-based or inorganic oxide additives in the form of polymer nanocomposites [3–5]. While improvement in fire retardancy was generally observed, several setbacks were experienced in such approaches. These include the release of harmful substances into the environment as well as compromising the mechanical properties of the polymers, if added in too large an amount [6, 7].

Polyhedral oligomeric silsesquioxane (POSS) is a type of inorganic–organic hybrid materials, often with cage-like three-dimensional nanostructures, chemically comprising silicon and oxygen atoms with possible organic groups attached to the former. POSS as a material has received considerable attention for its several desirable properties such as improved mechanical strength, heat resistance, and lightweight [8–10]. It is noteworthy to mention that studies have shown that incorporating POSS into polymeric materials, particularly as an additive, brings about tremendous improvement in fire-retardant properties without compromising the mechanical properties of the polymers [11, 12]. To date, a wide range of polymer/POSS nanocomposites has been reported with different extent of fire-retardant improvement. As reports are too many, it would not be possible to cover every single one of them. This chapter thus seeks to highlight some of the key findings and progress in the development of POSS-based fire-retardant polymer composite materials. In this general review, methods of incorporating POSS into polymers will be introduced, as well as the mechanisms of fire retardancy in these polymer composites. With the promising results reported, it was envisaged that polymer/POSS composites will be an outstanding candidate for fire-retardant materials with commercial and widespread use in the near future.

2 Parameters in Flammability Testing

Before we begin looking into various examples of POSS-based fire-retardant materials, it would be useful to briefly introduce some key parameters and techniques of flammability testing which are commonly used to quantify the performance of these materials in fire retardancy. Several common flammability testing techniques are currently employed to determine the extent of fire retardancy in materials. Prior to any flammability testing, thermal gravimetric analysis (TGA) can be performed to study the thermooxidative behavior of the materials, particularly, to determine the decomposition temperature and hence understand the thermal stability of materials [13].

The limiting oxygen index (LOI) test determines the minimum concentration of oxygen (in a mixture of oxygen and nitrogen) required to support combustion of the materials [4]. Any materials with LOI equal or less than 21%, which is the approximate amount of oxygen in air, are classified flammable, while any with LOI above are classified self-extinguishing. The LOI is measured by passing a different concentration of oxygen and nitrogen into a glass chamber together with a vertically standing sample that is ignited at the top and is allowed to burn downwards with the proportion of oxygen that is gradually reduced until the critical concentration is reached. In general, a material with a higher LOI value exhibits a better flame-retardant property.

Cone calorimetry is an essential technique used to quantify the flammability of materials [14–16]. In a standardized cone calorimeter, the sample is placed on a load cell which is capable of determining the evolution of mass loss during combustion. With uniform heat radiation from vertically below, combustion is triggered by an electric spark. The gas produced during combustion is captured by an exhaust placed vertically above, which is channeled to a gas analyzer capable of determining the level of smoke and the concentration of oxygen, carbon monoxide (CO), and carbon dioxide (CO_2). Making use of Huggett's principle, the decreasing oxygen concentration monitored during combustion is translated to heat release by the material during combustion. A continuous plot of heat release rate (HRR) versus time will be given from a typical cone calorimetry test. Using this plot, several parameters can be determined: the peak heat release rate (pHRR), total heat release (THR), time of ignition (TTI), time of flameout (TOF) [16]. An improvement in fire-retardant property can be verified in terms of an increase in TTI and a decrease in both pHRR and THR. Also, cone calorimetry provides the peak release rates of CO (pCORR), smoke production rate (SPR), total smoke release (TSR), and mass loss rate (MLR). Ideally, a good fire-retardant material should have low pCORR, SPR, and TSR.

Similar to cone calorimetry, the pyrolysis combustion flow calorimetry (PCFC) can also be used to determine the heat release of materials during combustion by monitoring oxygen consumption. The setup of a typical PCFC is, however, different from that of cone calorimetry. To summarize, the PCFC measures the maximum specific heat release rate at a particular heating rate, THR, and temperature at the maximum pyrolysis rate [17]. The advantage of PCFC over cone calorimetry is

that it allows us to characterize materials in a small quantity (5–50 mg). Similar to cone calorimetry, both techniques have been accredited to a set of national and international standards.

Characterization of the char layer was also an important aspect to study in fire retardancy or flammability of materials. The char yield determines what is left after a material undergoes complete combustion. As previously discussed, intumescent materials form a protective layer of char at the beginning of combustion. It is also of great importance to study the structure and morphology of this char layer to better understand the mechanism and rationalize the extent of fire retardancy in certain materials. These studies often involve electron spectroscopy of chemical analysis (ESCA) and are usually done on the residue obtained after cone calorimetry testing.

Finally, the Underwriters Laboratory 94 (UL94) testing serves as an internationally standardized method to classify polymeric materials on their extent of fire retardancy [18, 19]. UL94 tests seek to assess the ignitability, spread of flame, and/or self-extinguish ability of materials upon the removal of ignition flame. UL94 tests include horizontal and vertical burning tests to find out how well the small flame spreads across the bulk materials in various orientations. The dripping of burning materials, particularly that will ignite cotton placed below the sample, is also an important parameter included in UL94 tests, with the higher UL94 ratings not allowing any dripping of flaming materials. The UL94 tests categorize materials into three ratings: V-0 (best), V-1 (good), and V-2 (drips). No dripping is allowed for V-0 and V-1 ratings. V-0 requires a duration of flaming for each horizontal and vertical flame application to be below 10 s, and the total duration of flaming for five specimens is to be below 50 s. In contrast, V-1 and V-2 require the former criteria to be less than 30 s, and the latter criteria to be less than 250 s. Anything beyond these requirements would have deemed the material to have failed the UL94 tests.

3 Fire Retardancy of Polymer/POSS Composites

With numerous reports of polymer/POSS composites exhibiting improved fire-retardant properties, it would be useful for us to identify certain general trends and parameters across all the reports before looking into individual examples.

3.1 General Trends and Parameters

3.1.1 Chemical Structures of POSS Additives

Structural diversity exists in the POSS additives incorporated into polymer composites for the development of fire-retardant materials. While most POSS additives exist as cage structures, there were also reports of POSS with ladder structure and partial cage structure incorporated into polymer matrices for such a purpose [10]. Also,

POSS with cage structures may differ in cage size, with the smallest T8 cage being the most common. Finally, silicone atoms of POSS additives are functionalized with either different unreactive or reactive organic groups. These organic groups serve different purposes as they can be used to tune its solubility, improve compatibility with organic polymer matrices, or participate in co-polymerization reactions. POSS structures may also contain fire-retardant elements such as P, N, S, B, and halogens. They may also contain metal atoms which exhibit catalytic effect on thermal behavior and fire retardancy. Synthesis and functionalization of POSS additives generally take place before incorporating them into polymer matrices.

3.1.2 Preparation of Polymer/POSS Materials

POSS can be incorporated into polymer matrices by either chemical reaction or physical blending. For the former, POSS may be covalently attached to polymeric materials by chemically grafting onto existing polymeric networks or by co-polymerization involving a POSS-containing monomer with one or more reactive functional arms such as epoxy, amino or terminal vinyl groups. For the latter, POSS may be physically blended into matrices via melt-mixing or solvent casting. POSS may also be physically mixed with monomers to prepare thermosetting polymers via mechanical stirring prior to curing. Such physical means are usually deemed to be easier, cheaper, and more versatile compared to counterparts that adopt chemical methods. In addition to these two methods, POSS may also be loaded onto polymeric fabrics or textiles via layer-by-layer deposition methods [20]. This can simply be done by recurrently immersing the fabric materials into aqueous ionic POSS solution, followed by immersing into aqueous ionic co-additives solution or another oppositely charged POSS species. The bilayers with alternating cationic and anionic species are held strongly together by electrostatic forces of attraction.

3.1.3 POSS Loading and Co-additives

Loading refers to how much POSS additives was added into polymer matrices, which is typically expressed as weight percentage (wt%). Ideally, significant improvement in fire retardancy can be achieved with a very low POSS loading. Most polymer/POSS composites involved a POSS loading of less than 10 wt%. POSS may be added as the sole additive, or added with another co-additive, usually a traditional flame retardant. In the latter, synergistic effect with traditional fire retardant in improving flame retardancy is often observed at a very low POSS loading.

3.1.4 Dispersion of POSS in Polymer Matrices

Although POSS may have tendency to aggregate during physical blending, it is desirable to achieve good POSS dispersion at a low loading within the polymer matrices

to improve fire-retardant performance and even enhance mechanical properties. As such, compatibility between POSS (affected by the organic groups attached) and the polymer matrices is crucial in achieving good dispersion. The dispersion of POSS within polymer matrices may be assessed via scanning electron microscopy (SEM) or transmission electron microscopy (TEM).

3.1.5 Mechanism of Fire Retardancy

In general, polymer/POSS materials exhibit fire-retardant properties by undergoing initial decomposition and forming a timely protective char layer that serves as a barrier which insulates the bulk materials beneath from heat and gas transfer necessary for continual combustion. The char layer may also reduce the amount of smoke and harmful gases released during burning. During initial ignition, POSS were reported to migrate to the surface and undergo degradation via the homolytic cleavage of Si–C bonds (between POSS cage and the organic substituents). What was left was the ceramic layer of char composed of thermally and oxidatively stable Si–O bonds fused together, thus forming a reinforced char layer that better protects the material from further combustion. As previously discussed, the side groups, metal atoms, and heteroatoms present in the POSS chemical structures, as well as co-additives, may also have effect on the forming and physical structure of the char layer which may improve fire-retardant properties. Finally, it was reported that polymer/DOPO-POSS composite materials exhibited a "blowing-out" effect in which the pyrolytic gas produced during initial burning jetted outwards from the condensed-phase surface, thus effectively extinguishing the flame and resulting in dramatic improvement in fire-retardant properties. The specific mechanisms toward improving fire retardancy in different polymer/POSS composite materials will be further discussed.

3.1.6 Parameters of Assessing Fire-Retardant Properties

Improvement in fire-retardant properties of polymer/POSS materials was assessed by a common set of parameters discussed in the previous section: LOI, UL94 tests, and findings from cone calorimetry analysis, particularly plots of heat release rates (HRR). In addition, physical analysis of the char layer formed was also performed to rationalize the effects of POSS and other co-additives on fire-retardant properties of the materials.

Having understood the main key aspects of developing fire-retardant polymer/POSS composites, key examples from several common categories of polymers will be discussed in the following part of this chapter.

3.2 Examples of Fire Retardant Polymer/POSS Composites

3.2.1 Epoxy Resins

Epoxy resins (EP) are important thermosetting plastic materials used in the manufacturing of a wide range of products, particularly electronics. EPs exhibit desirable properties such as high tensile strength and modulus, as well as chemical and corrosion resistivity. Unfortunately, like most other organic polymers, EPs are flammable and this draws attention to develop EP-based materials with improved fire-retardant properties. Among these, there were a considerable number of reports on the development of EP/POSS materials. POSS with different structures was incorporated into EP as the sole additive as well as with other co-additives such as phosphate fire retardants, aluminum catalyst, boron and halogen compounds. We herein introduce some key examples of EP/POSS-based materials with improved fire-retardant properties.

To begin with, Lu et al. reported the preparation of hybrid resin materials involving partially caged POSS, SDOH, and STOH, in diglycidyl ether of bisphenol A (DGEBA) and 4,5-epoxyhexyl-1,2-dimethyl acid diglycidyl ester (TDE-85) matrices, respectively, using 4,4-diaminodiphenylsulphone (DDS) as curing agent [21, 22]. The silanol groups (Si–OH) on SDOH and STOH were able to chemically react with oxirane rings of DGEBA and TDE-85, forming Si–O–C bonds. Reaction of DGEBA with SDOH in the presence of cobalt naphthenate catalyst afforded EP-SDOH hybrid resins. On the other hand, EP-STOH hybrid resins were prepared by blending STOH into preheated TDE-85 epoxy liquids until transparent solution was formed and then followed by curing with DDS. The structures of the compounds were given in Fig. 1a. It was found that LOI for EP-SDOH resins was increased steadily from 22.6 to 32.8% as SDOH loading was increased from 0 to 25 wt%, whereas LOI for EP-STOH was increased from 22.6 to 32.8% as STOH loading was increased from 0 to 5 wt%, reflecting an increase in fire-retardant property.

Wu et al. reported the synthesis of multifunctional NPOSS from TPOSS and triglycidyl isocyanurate (TGIC) as shown in Fig. 1b. EP-NPOSS composites were then prepared by dispersing NPOSS in DGEBA at 60 °C (10 wt% loading) followed by the addition of curing agent *m*-phenylenediamine for curing process to take place. Both fire retardancy and thermal stability were found to be enhanced after incorporation of NPOSS, with sharply reduced peak HRR (first peak HRR = 13.8, second peak HRR = 368.8 w/g for EP/NPOSS versus peak HRR = 553.5 w/g for neat EP) [23]. TPOSS (10 wt%) and TGIC were also incorporated into an aerospace-grade epoxy resin (1,4-butanediol diglycidyl ether) with modified cycloaliphatic amines (HY5052) hardener [24]. Cone calorimetry analysis of this hybrid material showed a decrease more than by 53% in peak HRR and more than by 28% THR as compared to neat epoxy resin. In both cases, POSS helps in forming a stable char, exhibiting good thermal insulation properties, and hence better fire retardancy with respect to neat EP. It was also proposed that in the case of EP-NPOSS composite, NPOSS can slow down the movement and scission of the EP backbone during thermal degradation process as well as trap both hydrogen and hydroxyl radicals and form a stable

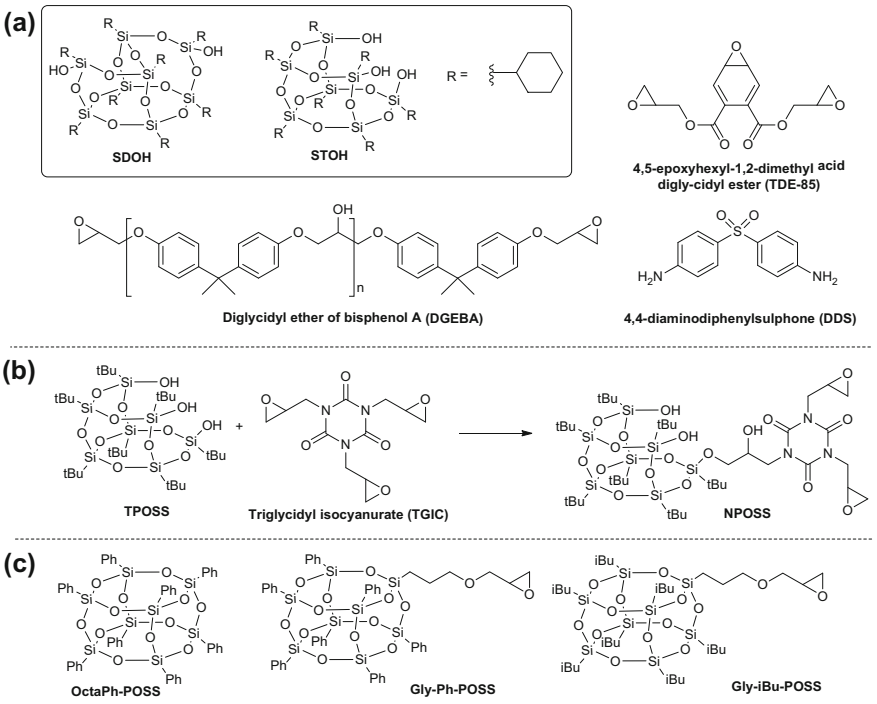

Fig. 1 **a** Chemical structures of SDOH, STOH, DGEBA, DDS, and TDE-85. **b** Synthesis of NPOSS from TPOSS. **c** Chemical structures of OctaPh-POSS, Gly-Ph-POSS, and Gly-iBu-POSS

charred layer in the condensed phase, thus preventing the underlying materials from further destruction during combustion [24].

Franchini et al. developed a series of EP-POSS hybrid materials based on non-functional OctaPh-POSS, and monofunctional Gly-Ph-POSS and Gly-iBu-POSS, whose structures are shown in Fig. 1c. The epoxy resin used was DGEBA while 4,4-methylene bis(2,6-diethylaniline) (MDEA) was used as curing agent. At 3.7 wt% of POSS loading, there was significant improvement (up to 40% reduction) in the peak HRR obtained from cone calorimetry analysis. Neat EP had a peak HRR of 1040 KW/m^2, whereas the peak HRRs for hybrids containing OctaPh-POSS, Gly-Ph-POSS, and Gly-iBu-POSS were 689, 622, and 782 KW/m^2, respectively [25]. It was suggested that phenyl-containing POSS nanoclusters were responsible for tremendous reduction in peak HRR. In addition, monofunctional Gly-Ph-POSS can form covalently bonded network resulting in a more homogenous dispersion in the EP matrix as compared to OctaPh-POSS. This favors the formation of rigid and spongy post-combustion char that improves fire retardancy.

9,10-dihydro-9-oxa-10-phosphaphenanthrene-10-oxide (DOPO) is a cyclic biphenyl phosphate which attracts a lot of interest due to its high thermal stability, thus serving as a good alternative to halogen-containing fire-retardant properties'[26,

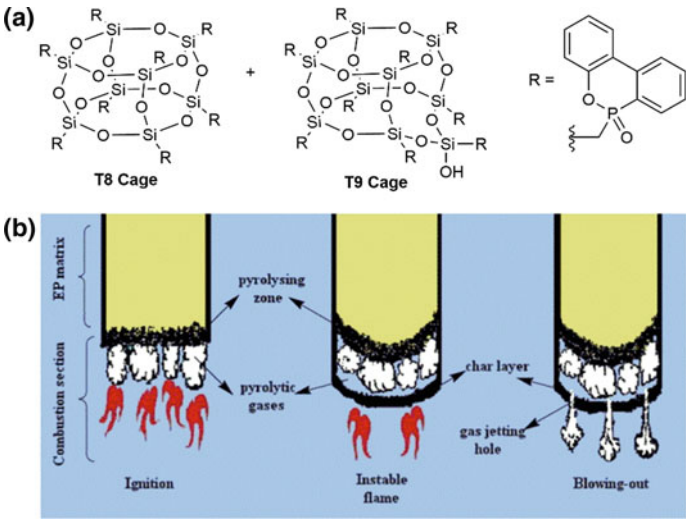

Fig. 2 **a** Chemical structures of DOPO-POSS. **b** Model of the blowing-out effect [34]. Copyright 2012. Reproduced with permission from Elsevier Ltd.

27]. Epoxy resins containing DOPO showed improvement in fire-retardant properties [28–31]. As such, Zhang et al. intelligently functionalized a POSS cage with DOPO substituents (Fig. 2a) which were then incorporated into DGEBA EP by mechanical stirring at different loadings, with *m*-phenylenediamine as curing agent [32, 33]. Cone calorimetry analysis showed that, compared to neat EP, TTI of EP/DOPO-POSS composite at 5 and 10 wt% DOPO-POSS loadings was increased from 45 to 58 and 61 s, respectively, peak HRR was reduced significantly from 855 to 588 and 483 kW/m^2, respectively, and THR was reduced from 122 to 92 and 85 MJ/m^2, respectively. EP/DOPO-POSS at 1.5 to 3.5 wt% POSS loading received a V-1 rating in UL94 tests [33]. When DOPO-POSS was incorporated into DGEBA EP by mechanical stirring with polyamide 650 (PA650) as curing agent, cone calorimetry showed that peak HRR was reduced significantly from 892 to 690 kW/m^2 at 10 wt% DOPO-POSS loading. When incorporated into DGEBA EP with DDS as curing agent, the peak HRR was reduced even more from 839 to 404 and 346 kW/m^2 at 5 and 10 wt% DOPO-POSS loadings, respectively [34].

Studies in mechanism of fire retardancy of EP/DOPO-POSS composite materials suggested that on top of the formation of a reinforced char layer, "blowing-out" effect was also responsible for the great improvement in fire-retardant properties [34, 35]. The "blowing-out" effect is as shown in Fig. 2b: The ignited sample initially showed unstable flame for a few seconds, after which pyrolytic gaseous products jetted outwards from the condensed-phase surface. The blowing-out of gas not only decelerated the transfer of heat from flame to unburnt matrix, but also removed some heat from the burning surface, hence effectively extinguishing the flame outside.

Interestingly, it was observed that such "blowing-out" effect was weakened with increase of DOPO-POSS loading as evident in LOI and UL94 ratings.

As mentioned, POSS was also incorporated into EP matrices with co-additives such as traditional phosphate fire retardants, metallic and non-metallic compounds. Synergistic effects between POSS additive and phosphate fire retardants in EP composites were investigated. Gerard et al. reported a reduction of peak HRR from cone calorimetry analysis of DGEBA EP composite, using diethylenetriamine as hardener, containing octamethyl-POSS (OM-POSS) and ammonium polyphosphate (APP) at 1 and 4 wt%, respectively [36]. Peak HRR for pure EP, EP + APP (5 wt%) and EP + OM-POSS (5 wt%) was 1077, 536, and 582 kW/m^2, respectively. The peak HRR of 326 kW/m^2 for EP + APP (4 wt%) + OM-POSS (1 wt%), however, was significantly lower. As previously mentioned, DOPO is a phosphate-containing organic fire retardant. Similarly, Zhang et al. reported a series of DGEBA EP composites incorporated with DOPO and phenylated-POSS [37–39]. Figure 3a shows the preparation of OPS and OAPS additives. As compared to pure EP, EP composite incorporated with DOPO and octaphenyl-POSS (OPS) experienced a reduction in peak HRR from 855 to 557 kW/m^2, whereas EP composite incorporated with DOPO and octaaminophenyl-POSS (OAPS) also has a reduced peak HRR of 645 kW/m^2 as shown in Fig. 3b. The UL94 ratings were also found to be improved from no ratings to V-1 and V-0 ratings, respectively [37]. The improvement in fire retardancy was attributed to the formation of –P(=O)–O–Si– linkages connecting the three-dimensional reinforced network of Si(–O)$_4$ and polyaromatic carbon structures as shown in Fig. 3c.

Wu et al. reported the addition of aluminum triacetylacetonate ([Al]) latent catalyst (0.6 wt%) to DGEBA/TPOSS (10 wt%) EP composite, which effectively reduced the peak HRR from 883 to 590 kW/m^2. Without [Al], the composite has a peak HRR of 777 kW/m^2 [38]. Smoke, CO, and CO_2 production rates were decreased as well. It was rationalized that the presence of [Al] could reduce the POSS particle size from the micron to submicron scale in the epoxy matrix and hence improve the fire-retardant properties via higher efficiency in insulating char formation [40].

Yang et al. reported a series of flame-retardant DGEBA EP containing boron and silicon prepared via a cross-linking reaction, using tris (2-hydroxypropyl) borate (THPB) together with octaaminophenyl-POSS (OAPS) as curing agents [41]. Synergistic effect between THPB and OAPS was observed in these composite materials as evident in the reduction of the peak HRR from 478 kW/m^2 (of pure EP) to as low as 148 kW/m^2 at 2.57 wt% OAPS loading and 32.19 wt% THPB loading. Without either THPB or OAPS, the peak HRR was slightly higher at 175.1 and 172.7 kW/m^2, respectively. THR was also reduced from 21.7 to 11.8 kJ/g for the EP/OAPS/THPB composite. The improvement in fire retardancy was attributed to THPB and OAPS catalyzing the degradation of EP during initial ignition forming a heat-resistant char layer, which reduced the emission of the flammable gas products and thus retard the combustion [41].

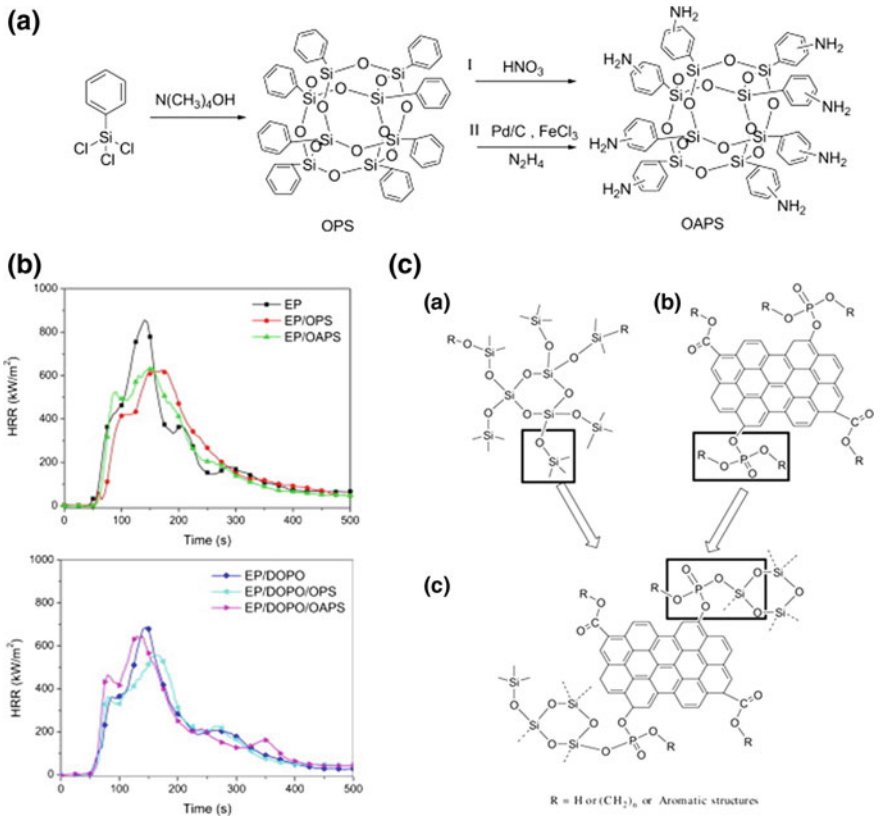

Fig. 3 **a** Synthesis of OPS and OAPS [37]. **b** HRR curves of the flame-retarded EP composites [37]. **c** Chemical structure of the chars of the EP composites [37]. Copyright 2012. Reproduced with permission from Elsevier Ltd

3.2.2 Polycarbonates

Like epoxy resins, bisphenol A polycarbonate (PC) is an extremely useful thermosetting plastic widely used in the manufacturing of a range of products, including electronic components, construction materials, automotive and aircraft, and even water bottles. In comparison to EP, pure PC exhibits slightly better fire retardancy with a UL94 rating of V-2 due to flame dripping [42]. Nonetheless, efforts were still made to enhance the fire-retardant properties of PC, of which one of the strategies is to incorporate POSS into PC composites.

Li et al. reported incorporating ultrafine OPS (Fig. 4) into PC via melt blending, with the addition of 0.3% polytetrafluoroethylene (PTFE) and a small amount of antioxidant 1010 and 168. The LOI of the composite materials was improved from 26.0% for pure PC to 31.8% and 33.8% for PC/OPS with 3 and 6 wt% OPS loadings, respectively. UL94 ratings were also improved from V-2 to V-1 and V-0,

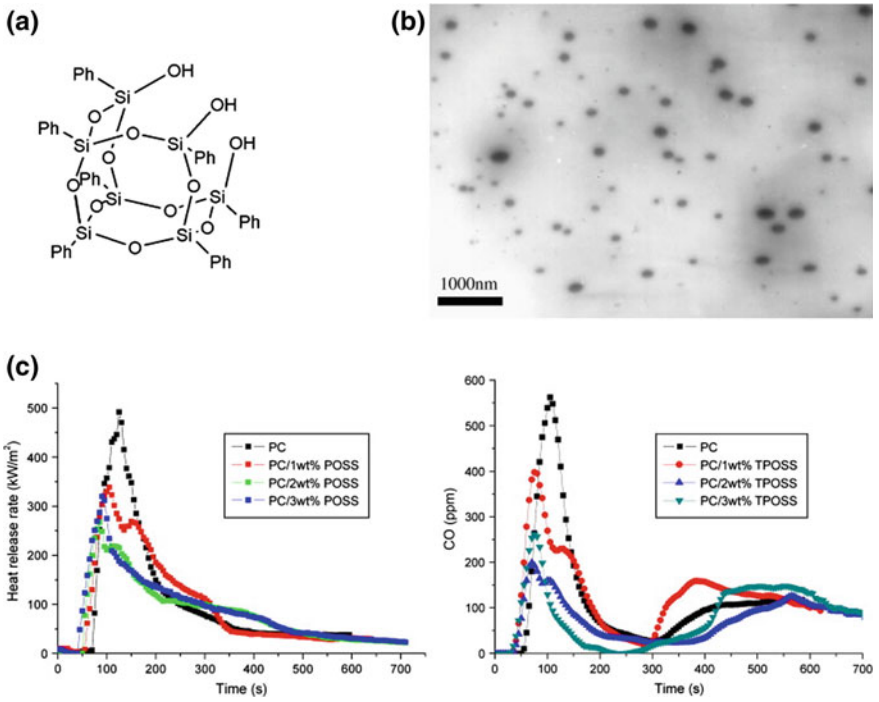

Fig. 4 **a** Chemical structure of TPOSS [44]. **b** TEM image of the PC/3 wt% TPOSS hybrid [44]. **c** HRR and COC plots of the PC, PC/1 wt% TPOSS, PC/2 wt% TPOSS, and PC/3 wt% TPOSS [44]. Copyright 2008. Reproduced with permission from Elsevier Ltd

respectively [43]. It was rationalized that ultrafine OPS accelerated the formation of compact and homogeneous char that is effective in preventing heat transfer. Similarly, Song et al. reported preparation of PC composites with trisilanolphenyl-POSS (TPOSS, Fig. 4a) of different loadings (0–3 wt%) via melt blending at 290 °C [44]. There were no chemical reactions between TPOSS and PC during the process. A homogenous blend was achieved for PC/TPOSS (3 wt%) composite as evident in TEM characterization shown in Fig. 4b. Cone calorimetry analysis of the composites (Fig. 4c) showed general improvement in fire retardancy compared to pure PC, with the peak HRR from 492 to 267 kW/m^2 and peak CO concentration from 562.3 to 199.3 ppm for composite with 2 wt% POSS loading. Studies found that thermal-oxidative degradation of the PC/TPOSS composites proceeded via a complicated process involving hydrolysis of carbonate linkage, chain scission of the isopropylidene linkage, the free radical oxidative chain degradation, the reformation, the branching and cross-linking reactions.

Following the similar method [45–47], Zhang et al. reported DOPO-POSS-PC composites. PC was blended with different levels of DOPO-POSS (0–6 wt%), 0.3% PTFE, and a small amount of antioxidant using an SJ-20. Significant improvement

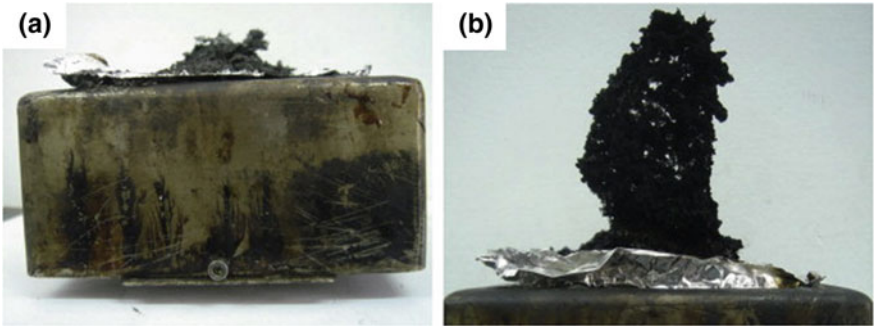

Fig. 5 Photographs of char from cone calorimeter testing: **a** PC, **b** 4 wt% DOPO-POSS/PC [46]. Copyright 2010. Reproduced with permission from Elsevier Ltd

in fire retardancy was observed with the incorporation of DOPO-POSS with LOI increasing from 24.1% in pure PC to 25.5, 30.5, and 31.3% in PC/DOPO-POSS composites with 2, 4, and 6 wt% loadings, respectively. Similarly, UL94 tests showed an improvement in rating from V-2 to V-0 with no flame dripping observed [46]. The char of PC/DOPO-POSS composite was observed to be firm, and its shape was retained while the char of PC collapsed readily as shown in Fig. 5. PC composites were also prepared with DOPO-POSS which is added as a co-additive (0 to 10 wt%) with acrylonitrile–butadiene–styrene (ABS) (15%) to inhibit the notch sensibility and improve melt processability and impact toughness which can decrease radically with PC aging. Fire retardancy of PC/ABS composite was improved with the addition of DOPO-POSS with UL94 rating from no rating to V-0 and LOI improving from 23.7 to 26.0% for composite with 10 wt% DOPO-POSS loading [47].

Attempts were also made to incorporate POSS additives to PC composites together with organophosphate flame retardants such as oligomeric bisphenyl A bis(diphenyl phosphate) (BDP) and resorcinol bis(diphenyl phosphate) (RDP). He et al. developed a series of flame-retardant PC hybrids incorporating TPOSS (0–3 wt%) and BDP (0–5 wt%, Fig. 6b) by melt blending method [48]. Significant enhancement in flame retardancy was observed with the co-incorporation of TPOSS and BDP as compared to incorporating either additives alone into PC matrix, with the decreased peak HRR of pure PC from 451.7 to 256.5 kW/m^2 in PC/3 wt% BDP/1 wt% POSS composite, as shown in Fig. 6c, d. The synergistic effect of POSS and BDP was attributed to the formation of SiO_2 residue from TPOSS reacting with phosphate groups in the char layer (from BDP) to form silico-phosphate that stabilized the phosphate species and char layer. It was also reported that SiO_2 could further enhance the char layer's viscosity and thermal-oxidative stability which developed on the burning polymer surface. This provided insulation to the PC matrix from heat and oxygen transfer into underlying polymeric substrate and also prevented the emission of volatile species from the underlying polymeric substrate of the matrix [48].

Similarly, Vahabi et al. reported blending TPOSS and RDP (0 or 5 wt% each) into PC matrices and the resulting composite exhibited improved fire retardancy due

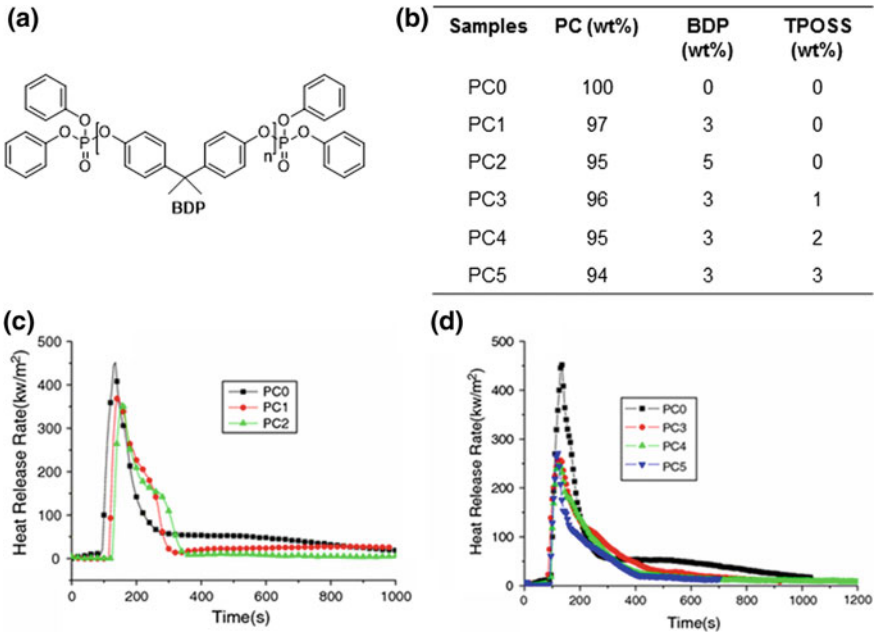

Samples	PC (wt%)	BDP (wt%)	TPOSS (wt%)
PC0	100	0	0
PC1	97	3	0
PC2	95	5	0
PC3	96	3	1
PC4	95	3	2
PC5	94	3	3

Fig. 6 **a** Chemical structures of organophosphate flame-retardant BDP. **b** Chemical compositions of PC/BDP/TPOSS hybrids [48]. HRR plots of **c** PC and PC/BDP series hybrids and **d** PC/BDP/TPOSS series hybrids [48]. Copyright 2009. Reproduced with permission from Springer Nature

to the synergistic effect of POSS and RDP [49]. Cone calorimetry analysis shows that the series of composites exhibit two peak HRRs as shown in Fig. 7b. The peak HRRs for pure PC were 439 and 431 kW/m^2. These were improved to 322 and 266 kW/m^2 for PC/POSS (5 wt%) composite, and 322 and 461 kW/m^2 for PC/RDP (5 wt%) composite. The PC/POSS (5 wt%)/RDP (5 wt%), however, showed even greater decrease in peak HRRs, at 284 and 144 kW/m^2. THR was also reduced from 82 MJ/m^2 for pure PC to 64 MJ/m^2 for PC/POSS/RDP composite [49]. The improved fire retardancy was attributed to RDP which improved the dispersion of POSS in PC.

3.2.3 Polyesters

Polyesters are an important and common class of materials commonly used in textile fabrics, plastic bottles, consumer electronic parts, etc. There are several types of commonly used polyesters, such as polyethylene terephthalate (PET), polybutylene terephthalate (PBT), and polybutylene succinate (PBS). There were several reported attempts to incorporate POSS into different polyesters composites in order to improve their fire-retardant properties, frequently with phosphorus-containing compounds as co-additives, although reports that are successful synergy between POSS and phosphorus compounds were few.

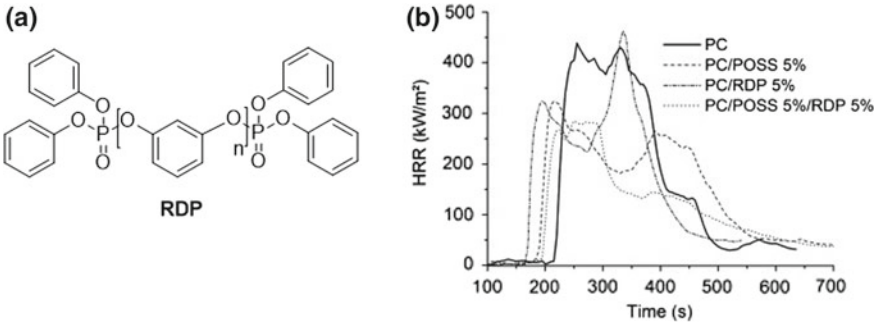

Fig. 7 **a** Chemical structure of organophosphate flame-retardant RDP, **b** HRR curves for PC, PC/POSS, PC/RDP, and PC/POSS/RDP [49]. Copyright 2012. Reproduced with permission from Elsevier Ltd

Fig. 8 Chemical structure of AEAPI-POSS

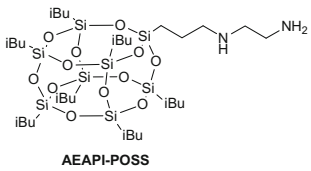

Wang et al. reported melt blending PBS with the environmentally friendly fire-retardant melamine phosphate (MP), using octaaminophenyl-POSS (OAPS) at low concentrations ($\leq$2 wt%) as synergists [50]. Unfortunately, no additional improvement to flame retardancy was observed with the addition of POSS when compared to PBS/MP composites in terms of LOI, UL94, and cone calorimetry, indicating no synergistic effect between OAPS and MP. This is due to the formation of the cracked char layer with poor thermal-oxidative resistance, thus less effectively insulating the bulk PBS from combustion.

Louisy et al. explored the possible synergistic effect of three different POSS, octamethyl-POSS (OM-POSS), trisilanol phenyl POSS (TPOSS), and amino-ethyl-amino-propyl-isobutyl POSS (AEAPI-POSS, Fig. 8), with either aluminum diethylphosphinate (OP1240) or a combination of melamine cyanurate and aluminum diethylphosphinate (OP1200), in PBT composites. The hybrid materials were prepared via melt blending. UL94 testing showed that while no synergistic effect was observed with the addition of OM-POSS and TPOSS, with rating remaining at V-0, antagonistic effect was observed for the addition of TPOSS with a rating of V-1. Cone calorimetry, however, showed a decrease in peak HRR for the addition of OM-POSS and TPOSS in the presence of both OP1200 and OP1240 co-additives [51].

Didane et al. developed a series of PET composites containing different POSS additives, in the presence of different phosphate compounds, and studied the possible synergistic effects between the POSS additives and phosphate compounds [52–54]. Firstly, three different POSS additives (at 1 wt%), OM-POSS, poly(vinylsilsesquioxane) also known as fire quencher POSS (FQ-POSS), and dode-

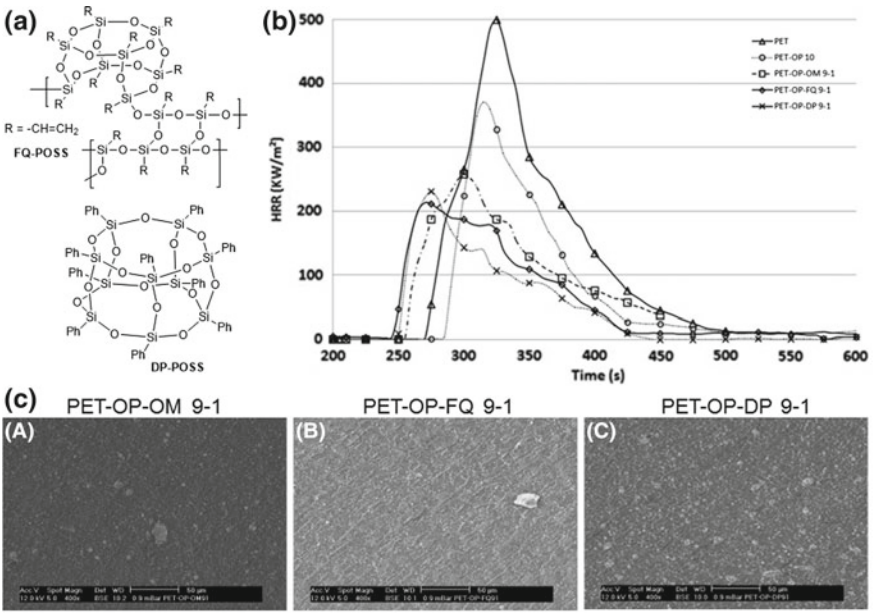

Fig. 9 **a** Chemical structures of FQ-POSS and DP-POSS. **b** HRR curves of the PET hybrids with OM-POSS (OP), FQ-POSS (FQ), and DP-POSS (DP) [52]. **c** SEM images of sheets (A) PET-OP-OM 9-1; (B) PET-OP-FQ 9-1; (C) PET-OP-DP 9-1 [52]. Copyright 2011. Reproduced with permission from Elsevier Ltd.

caphenyl POSS (DP-POSS), were added into PET composites via melt blending in the presence of zinc phosphinate compound, Exolit OP950 (at 9 wt%) [52]. Pure PET had a peak HRR of 500 kW/m^2. With only OP950, it fell to 365 kW/m^2. In the presence of OM-POSS, FQ-POSS, and DP-POSS, together with OP950, however, the peak HRR decreased even more to 244, 214, and 226 kW/m^2, respectively, as shown in Fig. 9b. The THR, however, was not decreased significantly in the presence of OP-POSS and FQ-POSS (25 and 26 MJ/m^2, respectively, compared to 27 MJ/m^2 for PET/OP950 composite) but decreased to 18 MJ/m^2 in the presence of DP-POSS. As such, synergistic effects were most prominent between DP-POSS and Exolit OP950, contributing to the resultant composite's high thermal stability and processability [52]. This was because DP-POSS was better dispersed than OM-POSS and FQ-POSS in the composites as reflected by SEM images shown in Fig. 9c. In addition, benzene was released from DP-POSS, which reportedly reacted with aromatic radicals during burning to form a stable polyaromatic char. On the other hand, OM-POSS and FQ-POSS contribute to intumescence by producing volatile species that caused the resultant structure to swell [52].

Replacing zinc phosphinate with aluminum phosphinate (OP1230), PET fabrics containing OM-POSS and DP-POSS were prepared by melt-spinning with a POSS loading of 1 wt% and an OP1230 loading of 9 wt% [53]. Synergy was observed for

PET fabrics treated with OM-POSS and DP-POSS. The peak HRR of PET fabrics decreased slightly from 321 to 300 kW/m^2 in the presence of only OP1230. This was further decreased to 163 and 258 kW/m^2 in the presence of OM-POSS and DP-POSS, respectively. THR of PET/OP1230/DP-POSS fabrics was not improved compared to PET/OP1230 (21 and 23 MJ/m^2, respectively, compared to 26 MJ/m^2 for pure PET), but reduced more for PET/OP1230/OM-POSS fabrics (16 MJ/m^2). Thus, OM-POSS presented better fire retardance performances than DP-POSS with OP1230 in a fibrous PET textile, and this was reasoned due to the former showing the earliest ignition time, which allowed for the formation of an effective insulating barrier protecting the bulk material from the external heat and reducing the emission of pyrolytic gaseous by-products [53].

In a separate work, Carosio et al. deposited α-zirconium phosphate nanoplatelets in combination with cationic octa-*n*-propylammonium chloride POSS on PET fabrics via a layer-by-layer (LbL) deposition method consisting of repeated soaking and washing steps [55]. Fire retardancy performance was reported to improve as evident in the reduction of the peak HRR of PET from 340 to 252 and 273 kW/m^2 with 5 and 10 bilayers of POSS deposited. Also, thermal and thermos-oxidative stability was improved on the LbL deposition, together with decrease in heat, smoke, and CO release. It was believed that the assembly of ZrP nanoplatelets and POSS nanocages form an inorganic protective layer that physically protected PET fibers from heat and oxygen transfer [55].

3.2.4 Polyolefins

Polyolefins are polymers made from simple olefins monomers, with applications ranging from plastic toys, furniture, fabric, bottles, and transparent wraps. Polypropylene (PP) is perhaps the most commonly used polyolefins, and therefore improvement in fire-retardant properties of PP by incorporating POSS additives would be of interest.

Fina et al. blended a series of polysilsesquioxane (PSS) (Fig. 10a) with PP and studied their mechanical, thermal, and flame retardancy properties [56]. Among the PP/PSS composites, those composites containing vinyl-substituted (Vi-PSS) and phenyl-substituted PSS (Ph-PSS) experienced a general decrease in peak HRR. The composite containing Vi-PSS (5 wt%) showed the most significant drop from 968 to 616 kW/m^2, while those containing methylated-PSS (Me-PSS) gave an increased peak HRR to 1023 kW/m^2 at 1.5 wt% loading, but it decreased to 786 kW/m^2 at 5 wt% loading. There were no significant improvements in LOI and THR, while TTI of PP/Vi-PSS (5 wt%) was increased to the most from 60 to 72 s. Overall, both thermal analyses and combustion tests showed improved performances for the PP/PSS in terms of the higher thermal stability and the lower combustion rate because of the formation of a ceramic superficial layer protecting underlying material from further degradation [56]. The best result from incorporation of Vi-PSS was due to homogenous dispersion of Vi-PSS and the polymerization of vinyl groups upon heating to produce cross-linked ceramic phase.

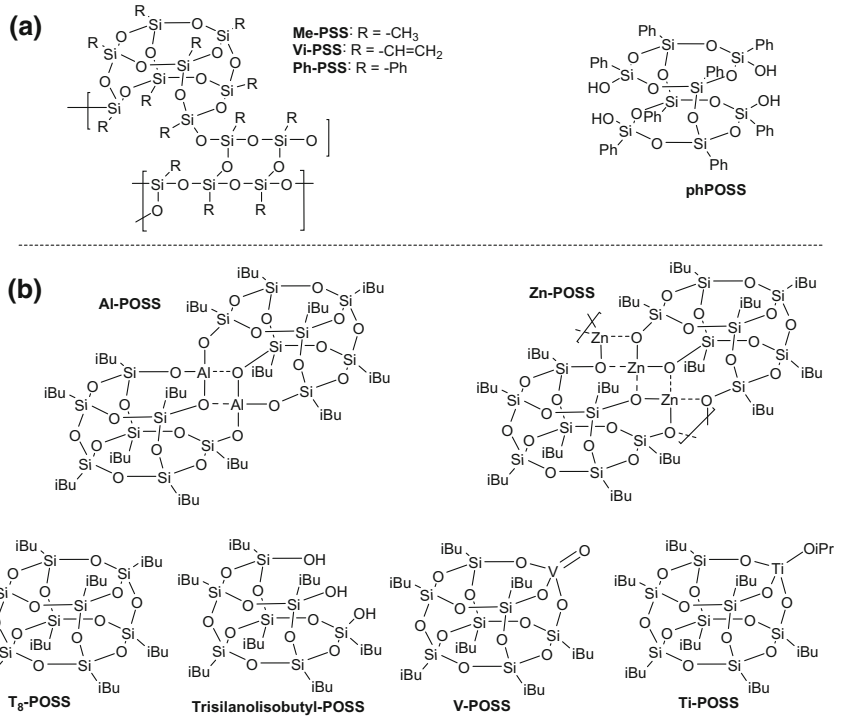

Fig. 10 Chemical structures of **a** methyl-, vinyl-, and phenyl-polysilsesquioxane (PSS), as well as tetrasilanolphenyl POSS (phPOSS); **b** T_8-POSS, trisilanolisobutyl-POSS, and POSS-containing metal centers (Al-POSS, Zn-POSS, V-POSS, Ti-POSS)

Barczewski et al. investigated the effect on thermal stability and flammability of composites formed by blending isostatic polypropylene (iPP) with partially caged tetrasilanolphenyl POSS (phPOSS) (Fig. 10a) at 0 to 10 wt% loadings [57]. TGA studies showed samples containing 5 and 10 wt% of phPOSS experienced an increase in thermal stability in comparison with pure iPP. UL94 horizontal burning tests suggested that the burning rate decreased in the presence of 2 wt% or more phPOSS, which was attributed to the migration of inorganic parts of phPOSS into the materials surface during decomposition, hence causing a shielding effect that greatly reduces burning. Moreover, no flame dripping was observed in iPP composite with 10 wt% phPOSS loading. A "boiling effect" was observed at the burning surface caused by water released from the POSS structure, which helped reduce the burning rate and spread of flame [57].

Camino et al. reported composites fabricated from metal-chelated POSS and PP (Fig. 10) [58, 59]. Among PP composites containing octaisobutyl-POSS (T_8-POSS), aluminum-containing Al-POSS, and zinc-containing Zn-POSS, only PP/Al-POSS composites exhibited improved fire-retardant properties as evidenced by cone calorimetry analysis. Peak HRR was improved from 1103 kW/m^2 of pure PP to

624 kW/m^2 for PP/Al-POSS (10 wt%), THR was reduced from 111 to 98 MJ/m^2 and the average CO release yield decreased from 43 to 35 g/kg [58]. The improved fire retardancy in PP/Al-POSS is probably due to Al moieties catalyzing secondary reactions during polymer degradation, resulting in partial PP charring, instead of complete volatilization. Figure 11a–c shows the char residues after cone calorimetry. Ramen spectroscopy analysis of char residues showed the evidence of the formation of a graphenic phase from the presence of two bands at ca. 1359 and 1607 cm^{-1} (Fig. 11d), evidencing an aromatization effect induced by the Al moieties [58]. The catalytic effect of metal centers in POSS additives to PP on the char formation during degradation was also evident in the studies of a series of PP composites comprising of PP melt-blended with trisilanolisobutyl-POSS, vanadium-containing V-POSS, and titanium-containing Ti-POSS (Fig. 10) at 3 wt% loading [59]. TGA analysis showed that the post-thermal degradation residue yields of PP/V-POSS and PP/Ti-POSS were higher by 6 and 20% than those of pure PP and PP/trisilanolisobutyl-POSS, respectively. Although no cone calorimetry was performed in the report, studies suggested that metal-bearing POSS nanofillers could result in PP matrix undergoing completely different chemical degradation processes under high temperature during burning, which eventually resulted in the formation of thermally stable charring products [59].

3.2.5 Polystyrenes

Polystyrenes (PS) are polymerized form of styrene monomers and are widely used in disposable containers and consumer products. Liu et al. prepared PS incorporated with octa(tetramethylammonium)-POSS (OctaTMA-POSS, Fig. 12a) by a mix-melting method at different loadings. Figure 12b, c shows the HRR and CO release rate curves of PS/OctaTMA-POSS hybrid materials, respectively. A general improvement in fire retardancy properties of PS composites with OctaTMA-POSS was observed with the improved peak HRR, peak CORR and LOI from 882.9 kW/m^2, 252.6×10^{-4} μg/s and 17.0%, respectively, for pure PS, to as low as 401.4 kW/m^2, 85.7×10^{-4} μg/s and 23.0%, respectively, for PS/OctaTMA-POSS at 30 wt% loading. The enhancement in fire retardancy was attributed to increase in char residue. The decomposition of OctaTMA-POSS was also reported to absorb heat, which slowed down the temperature rise and delay combustion of the composite. The degradation of OctaTMA-POSS produced inert gas to dilute flammable gases and oxygen, taking away heat from the burning system as well [60].

Further cutting down the loading of OctaTMA-POSS, Liu et al. prepared OctaTMA-POSS-based lamellar hybrids using cetrimonium bromide surfactant, which were then incorporated into PS by mix-blending to achieve a very finely and homogenously dispersed composite [61]. Cone calorimetry showed that the peak HRR dropped by 50.6, 48.9, 45.2, and 51.3% for composite with 1, 3, 5, and 10 wt% of POSS-based lamellar hybrid loadings, when compared to pure PS. More impressively, the CO release rate of PS composites was found to drastically and correspondingly drop by 74.4, 73.3, 68.4, and 73.6% [61]. Using a similar strategy, Liu

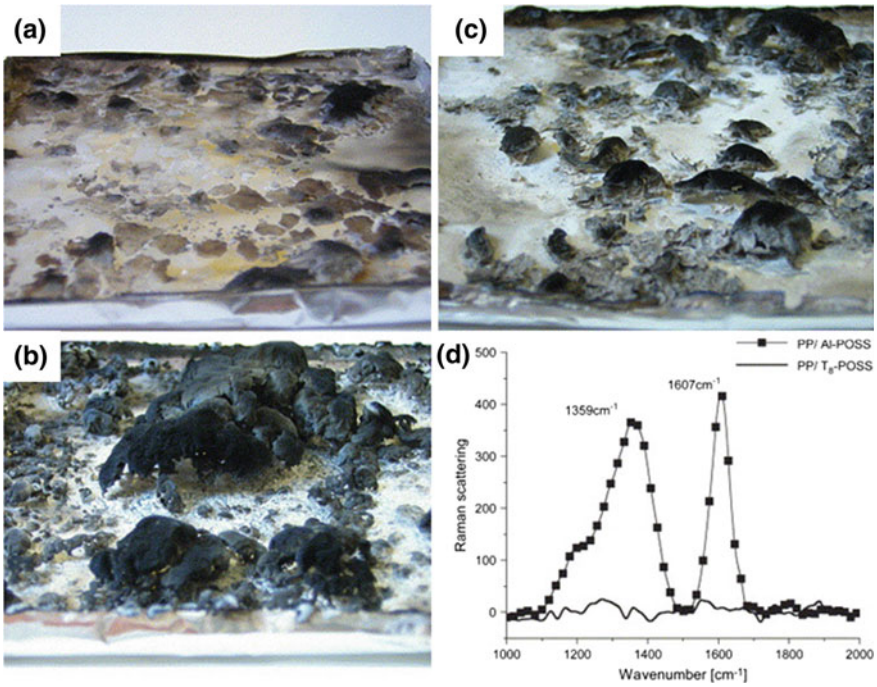

Fig. 11 Char residue obtained from cone calorimeter tests, **a** PP/T8-POSS, **b** PP/Al-POSS, **c** PP/Zn-POSS [58]. Neat PP: residue not present. **d** Raman spectroscopy on PP/Al-POSS versus PP/T_8-POSS [58]. Copyright 2006. Reproduced with permission from Elsevier Ltd.

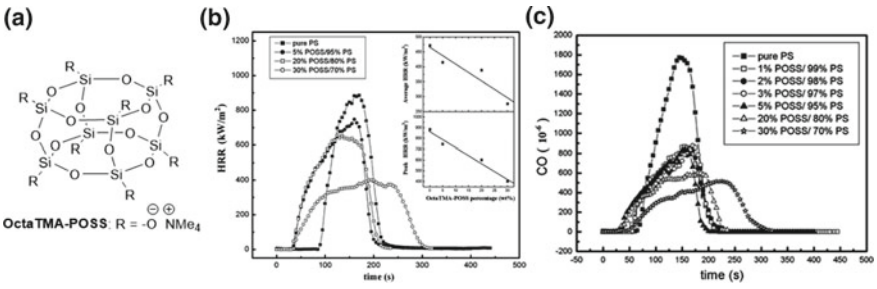

Fig. 12 **a** Chemical structures of OctaTMA-POSS. **b** HRR results of OctaTMA-POSS/PS composites with POSS weight ratios from 5 to 30%. The radiant power is 35 kW/m^2 [60]. **c** CO release rate curve in the combustion of OctaTMA-POSS/PS composites [60]. Copyright 2007. Reproduced with permission from Springer Nature

et al. further prepared POSS-based lamellar hybrids using octa(chloroamino-propyl) POSS (OCAP-POSS) with dodecyl benzene sulfonic acid sodium salt surfactant (DBSS) (Fig. 9), which were incorporated in PS composites and were found to exhibit improved fire-retardant property as well. The peak HRR decreased by 51.4,

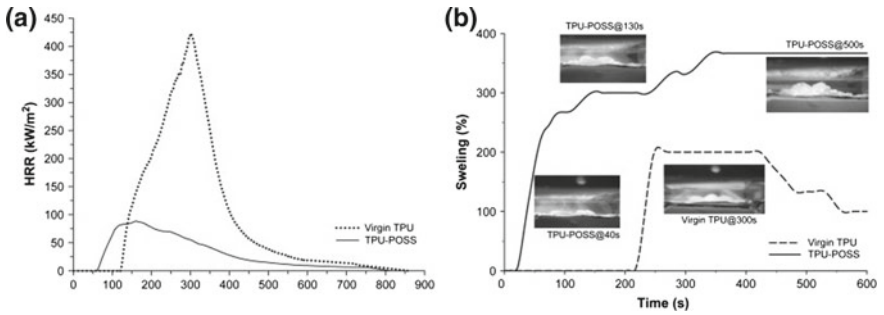

Fig. 13 **a** HRR versus time of virgin TPU compared to TPU–POSS composite [63]. **b** Swelling versus time of virgin TPU [63]. Copyright 2009. Reproduced with permission from Elsevier Ltd.

49.0, 47.1, and 50.6% for composite with POSS-based lamellar hybrid loading of 1, 3, 5, and 10 wt%, respectively, while the peak CORR decreased by 62.6, 59.7, 57.8, and 61.9%, respectively [62]. TEM analysis showed homogenous dispersion of the POSS-based lamellar hybrid at as low as 1 wt% loading. Similarly, the reinforced ceramic layer produced during the degradation of organic parts of OCAP-POSS shielded the inner layer of the composite from heat and oxygen, resulting in better flame retardancy.

3.2.6 Polyurethanes

Polyurethanes (PU) exhibit desirable mechanical properties including high tensile strength, tear strength, good flexibility, and high abrasion resistance. Depending on the denseness and stiffness of PU, they are often utilized in building and constructions, transportations, furniture and beddings, as well as coatings for textile. PU/POSS hybrid materials were reported to exhibit enhanced fire-retardant properties.

Bourbigot et al. reported the preparation of thermoplastic polyurethane (TPU) hybrids with addition of Vi-PSS (Fig. 10a) at 10 wt% loading, which led to a remarkable 80% decrease in peak HRR in comparison to virgin TPU (80 vs. 430 kW/m^2), as shown in Fig. 13a [63]. In addition, TTI of the composite (60 s) is twice shorter than that of virgin TPU (120 s), though there is no considerable improvement to LOI and UL94 ratings. The improvement was likely due to the formation of ceramic char of silicon and polyaromatic network structure, due to TPU-POSS degradation. The swelling of TPU and TPU-POSS hybrid over time on heating was monitored as shown in Fig. 13b. Under an external flux, the viscous char paste formed was subjected to expansion and swelling because of the partial volatilization of the organic component of POSS as well as evolving degrading products of TPU [63]. This served as an effective insulation barrier against mass and heat transfer, thus leading to a lower HRR and TTI.

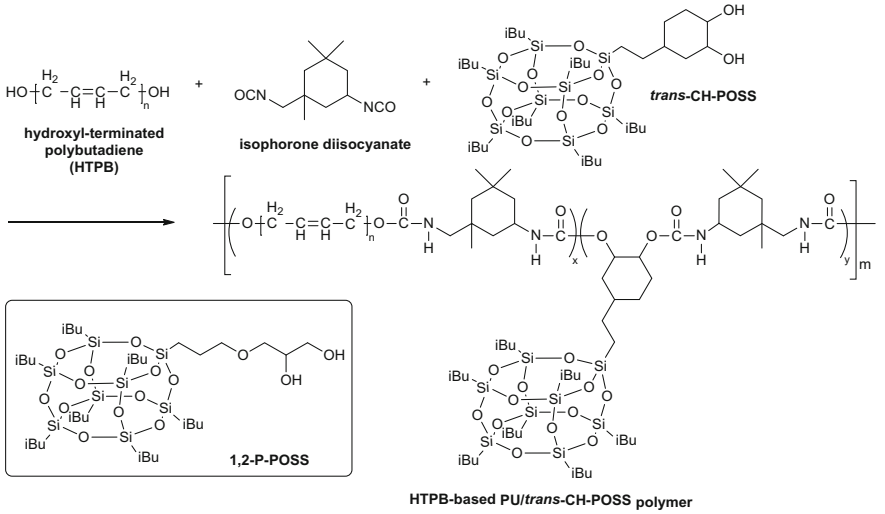

Scheme 1 Preparation of HTPB-based PU containing *trans*-CH-POSS and 1,2-P-POSS via one-pot PU reaction

In addition to this, Bourbigot et al. also prepared PU composites by introducing 10 wt% Vi-PSS or OM-POSS at different stages of PU synthesis, which were subsequently coated onto the knitted PET textile serving to enhance the textile's fire-retardant properties [64]. It was observed that TTI for Vi-PSS-containing material was increased and the HRR dropped by as much as 55%. No significant improvements in fire-retardant properties were observed for OM-POSS-containing composites. TGA studies showed that textile treated with PU/OM-POSS exhibited a higher degradation rate than textile treated with virgin PU, whereas textile treated with PU/Vi-PSS presented a similar initial degradation pattern up to 400 °C, but after which it was stabilized [64].

Kim et al. reported hydroxyl-terminated polybutadiene (HTPB)-based PU with *trans*-cyclohexanediol isobutyl POSS (*trans*-CH-POSS) and 1,2-propanediol isobutyl POSS (1,2-P-POSS) chemically grafted onto the polymer chain, via a one-step reaction as shown in Scheme 1 [65]. Compared to pure PU, cone calorimetry showed significant improvement in fire-retardant properties for the POSS-grafted PU with the reduced peak HRR from 1037.0 to 632.5 and 709.9 kW/m^2 for PU/trans-CH-POSS and PU/1,2-P-POSS composites, respectively. Similarly, THR reduced from 135.1 to 119.0 and 109.8 MJ/m^2, respectively. Compared to pure PU, the LOI values of PU/POSS composites were also found to be 1.9 times higher. These improvements were due to the formation of more compact nanospherical SiO_2 protective droplet layers, which were more insulating than the carbon-based char layer formed over pure PU [65].

3.2.7 Vinyl Esters

Vinyl ester resins (VE) are mechanically strong and resistant to chemicals, corrosion, and water absorption. They are commonly used in marine industry and also manufacturing of military vehicles. Vinyl ester resins are nonetheless flammable, which is why they are important to develop VE with enhanced fire-retardant properties.

Glodek et al. physically blended three different POSS, Vi-PSS, methacrylisobutyl POSS (MI-POSS), and methacryl POSS (OMA-POSS), at 0 to 30 wt% loading, to fatty acid vinyl esters (FAVEs) made up of bisphenol A vinyl ester, styrene (20 wt%) and methacrylated lauric acid (MLau, 15 wt%), with or without brominated vinyl ester [66]. The respective chemical structures are shown in Fig. 14a. It was found that only OMA-POSS is completely soluble in all the resins even up to 30 wt% loading. This was due to chemical reaction between OMA-POSS and the VE resins. UL94 testing showed that VE composites containing Vi-PSS and MI-POSS failed UL94 testing with a burning time lasting longer than 30 s, while VE composites containing OMA-POSS improved the flammability to a class of V-2, with a significant reduction in average burning time. The improved results were attributed to the good dispersion of OMA-POSS [66].

Chigwada et al. evaluated the flammability of a series of bisphenol A and novolac epoxy-based poly(vinyl esters) (PVE) composites containing octavinyl-POSS (OV-POSS), with and without the addition of phosphate-containing fire retardant, tricresylphosphate (TCP), as a co-additive. The chemical structures of the respective compounds are shown in Fig. 14b [67]. At 4 and 5 wt% OV-POSS loadings and 4 to 30 wt% TCP loadings, the PVE composites containing both additives were found to exhibit much lower peak HRR and THR compared to PVE containing solely OV-POSS or TCP. Introduction of 5 wt% OV-POSS and 30 wt% TCP led to a remarkable reduction in the peak HRR by 68% from 1197 to 384 kW/m^2, and meanwhile, the THR was reduced from 80 to 32 MJ/m^2 correspondingly [67]. However, no further mechanistic studies, especially into char composition, was provided in this report to elucidate the synergy between POSS and TCP as a combination of other additives was explored to reduce flammability.

3.2.8 Acrylics and Cotton Fabrics

Most of the examples we have discussed so far employed physical blending and chemical grafting methods to incorporate POSS additives into polymer matrix. These methods served their purposes for moldable polymers and polymers in pre-casted forms, where the major aim is to achieve composite hybrid materials with POSS homogenously dispersed across all directions. However, these methods may not be feasible for ready-made textiles and fabrics. POSS additives may still be loaded onto the surface of the fabric via a layer-by-layer (LbL) deposition method such that ionic

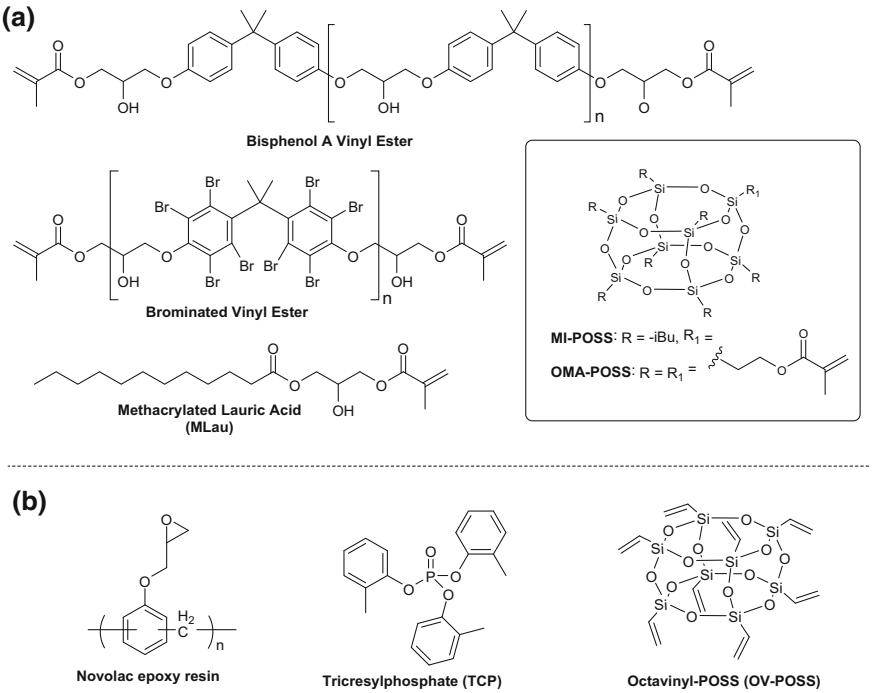

Fig. 14 **a** Chemical structures of bisphenol A vinyl ester, brominated vinyl ester, and methacrylated lauric acid used in the synthesis of fatty acid vinyl esters, as well as MI-POSS and OMA-POSS. **b** Chemical structures of novolac epoxy resin, tricresylphosphate, and octavinyl-POSS

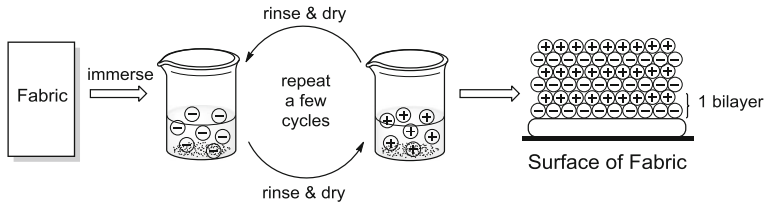

Fig. 15 Schematic of layer-by-layer deposition/coating of additives onto fabric surfaces

POSS and other ionic co-additives dissolved in solution are coated onto the fabric surface by repeated cycles of immersing, rinsing and drying, and eventually holding strongly together by electrostatic forces of attraction as shown in Fig. 15. This shall be discussed with the use of the following two examples.

Carosio and Alongi coated an acrylic fabric consisting of 90% of polyacrylonitrile and 10% methyl acrylate, with octa(*n*-propylammonium chloride)-POSS (OCAP-POSS, Fig. 9) and ammonium polyphosphate (APP) using the LbL method, by repeatedly immersing fabric into separate solutions containing two additives, forming

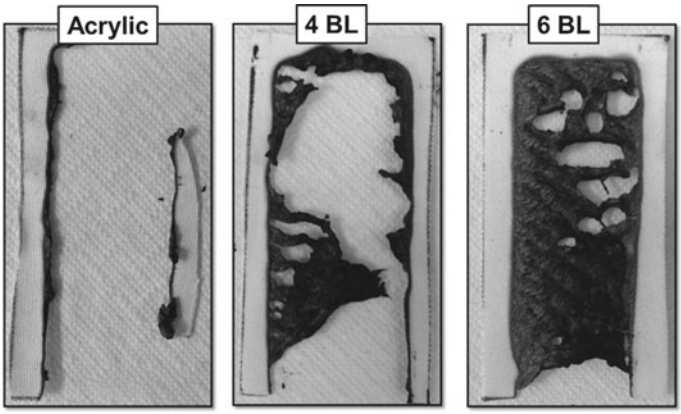

Fig. 16 Untreated and LbL-treated residues at the end of horizontal flame spread tests [68]. (BL stands for bilayer) Copyright 2016. Reproduced with permission from Elsevier Ltd.

4 to 6 bilayers [68]. SEM analysis of the post-treated fabric confirmed homogenous coating of the bilayers. On exposing the POSS-coated fabric to a 20 mm methane flame or a heat flux of 35 kW/m^2, the phenomenon of melt dripping was not observed, and combustion rate was tremendously reduced. LOI was increased from 20.5% for uncoated fabrics to 22.0% for fabrics coated with 4 and 6 bilayers, respectively. Figure 16 shows fabrics both treated and untreated with POSS after the end of horizontal flame test. No residue was found for untreated fabric but fabric treated with 6BL showed the residue which appears almost completely intact [68]. Analysis of the char residue suggested that thermal degradation and thermos-oxidation process of the fabric were significantly modified by the coating, with the improvement to fire-retardant properties. Such improvement was attributed to the formation of thermal insulating barrier reinforced by the respective chars formed from both APP and POSS in the LbL assembly [68].

Similarly, Li et al. coated cotton fabric with alternate layers of cationic octa(*n*-propylammonium)-POSS ((+)POSS) and anionic pentacyclo-[9.5.1.1^{3,9}.1^{5,15}.1^{7,13}] octasiloxane 1,3,5,7,9,11,13,15-octakis-(cyloxide)hydrate ((−)POSS) using the LbL deposition method [69]. The two ionic POSS species prevailed when OCAP-POSS and OctaTMA-POSS were dissolved in water. Separately, cotton fabric was also coated with amino-propyl silsesquioxane oligomer (AP) (as an alternate cationic species) and (−)POSS via the LbL method as well. All fabrics were coated with 5, 10, and 20 bilayers. Microscale combustion calorimetry results showed that all treated cotton fabric experienced an increase in char yield and a decrease in THR. Such a trend became more prominent when a greater number of bilayers were coated. Slight reduction of the peak HRR was also observed for cotton treated with 10 and 20 bilayers of AP/(−)POSS and cotton treated with 20 bilayers of (+)POSS/(−)POSS.

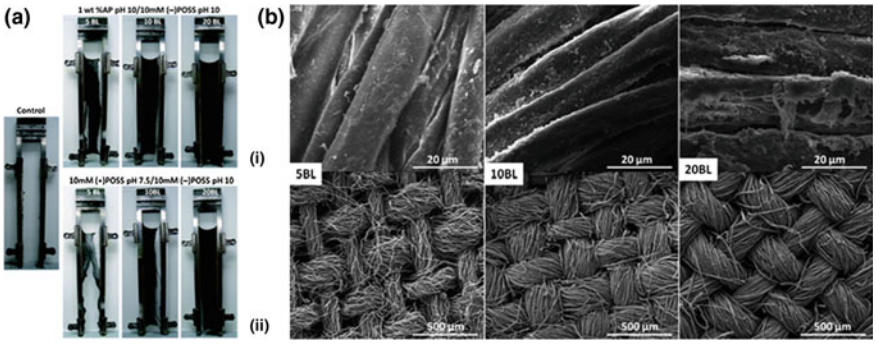

Fig. 17 **a** Residue images of control cotton fabric, as well as fabrics coated with 5, 10, and 20 BL of AP/(−)POSS (i), and (+)POSS/(−)POSS (ii) after vertical flame test [69]. **b** SEM images of 5, 10, and 20 BL of AP/(−)POSS-coated fabrics before (top) and after (bottom) the vertical flame test [69]. The SEM images of (+)POSS/(−)POSS-coated fabrics were also similar to that shown in (**b**). Copyright 2011. Reproduced with permission from the Royal Society of Chemistry

The maximum reduction in total HR (23%) and peak HRR (20%) compared to the control was observed for cotton treated with 20 bilayers of AP/(−)POSS. Furthermore, cotton fabric coated with 10 and 20 bilayers of AP/(−)POSS and 20 bilayers of (+)POSS/(−)POSS did not ignite during a vertical flame test (pill test) but only smoldered and charred. The rest including untreated cotton, however, was thoroughly burnt out, as shown in Fig. 17a. SEM analysis showed that the weaved structure of cotton was still observable in POSS-treated fabrics after burning (Fig. 17b), and it was thought that the AP and POSS species underwent bond dissociation and formation to re-establish a ceramic network of continuous hollow structures over burnt-out cellulosic cotton fiber [69].

4 Conclusions and Perspectives

In this chapter, we have provided a summary of research findings and progress in the field of POSS-based fire retardants by providing many typical examples of polymer/POSS hybrid materials from the different categories of commonly used polymers in our daily lives. It has been evident that in these reports, the incorporation of POSS into a variety of polymer systems by either a physical or a chemical method has resulted in reasonable improvement in fire-retardant property as experimentally proven in the common set of tests performed. Due to a sheer number of reports on POSS-based fire-retardant materials, particularly polymer/POSS hybrid materials,

we are unable to discuss every single one of them, but it is envisaged that through these representative examples provided (Table 1), we can clearly demonstrate the usefulness and potential of POSS in developing excellent fire-retardant materials.

Briefly recapping the main points, whatever POSS additives are pre-synthesized, pre-modified, or commercially purchased, they could be readily incorporated into polymer matrices via common methods such as physical blending, chemical grafting, co-polymerization, or even layer-by-layer deposition. POSS may be added as the sole additive or with other co-additives, such as traditional phosphate fire retardants, which potentially cause a synergistic effect on fire retardancy. Ideally, a low POSS loading is desired to achieve promising outcome in fire-retardant properties. Homogenous dispersion of POSS additives within the polymer matrices, which is verifiable via SEM or TEM analysis, is beneficial for better fire-retardant properties, and this can be achieved by choosing or modifying POSS with compatible side chains and proper functional groups. POSS aided in fire retardancy by reinforcing the char layer formed by the polymers during initial burning. This is possible from the chemical degradation of POSS cage, which resulted in the formation of a thermally and oxidatively stable silicon-oxycarbide "ceramic" surface that enables to insulate the inner bulk material from heat and gas transfer, thus slowing down the burning process. Some examples of polymer/POSS hybrid materials, for example, those containing DOPO-POSS can even exhibit a "blowing-out" effect, in which pyrolytic gaseous products formed jetted outwards from the condensed-phase char surface, hence effectively extinguishing the flame outside. The fire-retardant properties of these POSS-incorporated materials can be assessed by a category of standard tests and parameters, including LOI test, UL94 testing, cone calorimetry, and PCFC. TGA can also be performed prior on the prepared materials to preliminarily determine the thermal and thermooxidative stability, while the post-burning char residue of the materials can be further studied to rationalize the mechanism of fire-retardant properties.

POSS-based materials are promising alternatives to traditional fire-retardant materials, but one practical limitation to their commercial adoption and production is the relatively high cost of POSS starting materials. Nonetheless, it is envisaged that such a problem may be overcome with greater demand for POSS-based materials and POSS starting materials which can drive chemical plants and vendors to reap economies of scale from a large-scale production. Furthermore, it was proven that improved fire-retardant properties can be achieved with a very low loading of POSS at 1 wt% or less, and this can hopefully be improved on with further research in this field.

Table 1 Summary of key examples of polymer/POSS composites fire retardants

Primary polymer	POSS additive	Co-additive	Method of incorporation	Effects on fire retardancy	Proposed mechanism	References
EP	SDOH and STOH	NIL	Chemical reaction	Increase in LOI	Char reinforcement	[21, 22]
EP	NPOSS	NIL	Chemical reaction	Reduction in peak HRR and THR	Capturing of formed radicals; char reinforcement	[23, 24]
EP	OctaPh-POSS; Gly-Ph-POSS; Gly-iBu-POSS	NIL	Chemical reaction	Reduction in peak HRR	Char reinforcement	[25]
EP	DOPO-POSS	NIL	Mechanical stirring	Reduction in peak HRR and THR	Blowing-out effect	[33, 34]
EP	OM-POSS	APP	Mechanical stirring	Reduction in peak HRR	Synergistic effect between POSS and co-additives	[36]
EP	OPS and OAPS	DOPO	Mechanical stirring	UL94 ratings improvements	Char reinforcement	[37]
EP	TPOSS	Aluminum triacetylacetonate ([Al])	Mechanical stirring	Decrease in smoke, CO and CO_2 production rates	[Al] reduces dispersed POSS particle size; hence char reinforcement	[40]
EP	OAPS	THPB	Mechanical stirring	Reduction in peak HRR and THR	EP degradation catalyzed during initial ignition, hence forming char layer	[41]

(continued)

Table 1 (continued)

Primary polymer	POSS additive	Co-additive	Method of incorporation	Effects on fire retardancy	Proposed mechanism	References
PC	Ultrafine OPS	PTFE	Melt blending	Improvement in LOI and UL94 ratings	Accelerated char formation	[43]
PC	TPOSS	NIL	Melt blending	Reduction in peak HRR and CO concentrations	Thermal-oxidative degradation of the PC/TPOSS composites proceeded via complicated chemical process	[44]
PC	DOPO-POSS	PTFE and SJ-20	Melt blending	Improvement in LOI and UL94 ratings	Char reinforcement	[46]
PC	DOPO-POSS	ABS	Melt blending	Improvement in LOI and UL94 ratings	Char reinforcement	[47]
PC	TPOSS	BDP	Melt blending	Reduction in peak HRR	Char reinforcement through reaction of POSS with BDP	[48]
PC	TPOSS	RDP	Blending	Reduction in peak HRR and THR	RDP improves dispersion of POSS	[49]
PBS	OAPS	Melamine phosphate	Melt blending	No improvements in fire retardancy	Cracks in char resulted in less effective insulation	[50]
PBT	OM-POSS, TPOSS and AEAPI-POSS	Aluminum diethylphosphinate and melamine cyanurate	Melt blending	Decrease in peak HRR (OM-POSS and TPOSS); No change in UL94 rating	No synergy between POSS and co-additives observed	[51]

(continued)

Table 1 (continued)

Primary polymer	POSS additive	Co-additive	Method of incorporation	Effects on fire retardancy	Proposed mechanism	References
PET	OM-POSS, FQ-POSS and DP-POSS	Zinc phosphinate (exolit OP950)	Melt Blending	Great decrease in peak HRR, slight decrease in THR	Formation of stable and reinforced polyaromatic char	[52]
PET fabric	OM-POSS and DP-POSS	Aluminum phosphinate (OP1230)	Melt-spinning	Reduction in both peak HRR and THR	Early ignition time allowed formation of insulating barrier	[53]
PET Fabric	Octa-n-propylammonium chloride POSS	α-zirconium phosphate nanoplatelets	Layer-by-layer (LbL) Deposition	Reduction of peak HRR, THR, smoke and CO release	Inorganic protective layer formed from assembly of ZrP	[55]
PP	Me-PSS, Vi-PSS and Ph-PSS	NIL	Blending	Reduction of peak HRR with no improvement to LOI and THR	Char reinforcement	[56]
iPP	phPOSS	NIL	Blending	Decrease in horizontal burning rate; no flame dripping	Char reinforcement and "boiling effect" at burning surface	[57]
PP	OI-POSS, and Zn-POSS	NIL	Blending	No improvement	–	[58]
	Al-POSS			Reduction in peak HRR, THR and CO release yield	Catalytic effect of Al promoting formation of char with graphenic phase	
PP	V-POSS and Ti-POSS	NIL	Melt blending	Higher post-thermal degradation residue yield	Catalytic effect of V and Ti affect degradation pathway	[59]

(continued)

Table 1 (continued)

Primary polymer	POSS additive	Co-additive	Method of incorporation	Effects on fire retardancy	Proposed mechanism	References
PS	OctaTMA-POSS	NIL	Mix-melting	Reduction in peak HRR and peak CORR and increase in LOI	Increase in char residue, heat absorption by POSS decomposition, and dilution of flammable gas from inert gas generated	[60]
PS	OctaTMA-POSS	Cetrimonium bromide surfactant	Mix-blending	Decrease in peak HRR and drastic decrease in CORR	Homogenous dispersion of POSS aid in better char formation	[61]
PS	OCAP-POSS	DBSS surfactant	Mix-blending	Decrease in peak HRR and CORR	Char reinforcement	[62]
TPU	Vi-PSS	NIL	Melt-mixing	Drastic decrease in peak HRR and halving of TTI, but no improvements to LOI and UL94 ratings	Formation of viscous char paste that served as effective insulation barrier	[63]
PU	Vi-PSS and OM-POSS	NIL	Reaction	Increase in TTI and reduction of HRR for PU/Vi-PSS composites	Degradation rate stabilized after initial degradation stage	[64]
PU	*trans*-CH-POSS and 1,2-P-POSS	NIL	Chemical grafting	Reduction in peak HRR and THR	Char reinforcement	[65]
PVE	Vi-POSS, MI-POSS, and OMA-POSS	NIL	Physical blending	UL94 ratings of VE/OMA-POSS composites improved	Good dispersion of OMA-POSS leads to better char formation	[66]

(continued)

Table 1 (continued)

Primary polymer	POSS additive	Co-additive	Method of incorporation	Effects on fire retardancy	Proposed mechanism	References
PVE	OV-POSS	TCP	Mechanical stirring	Reduction in peak HRR and THR	–	[67]
Acrylic fabric	OCAP-POSS	APP	Layer-by-layer (LbL) deposition	Melt dripping suppressed and LOI increased	Char reinforcement	[68]
Cotton fabric	Cationic and anionic POSS derived from OCAP-POSS and OctaTMA-POSS, respectively, and aminopropyl silsesquioxane oligomer (AP)	NIL	Layer-by-layer (LbL) deposition	Increase in char yield and decrease in THR. Reduction in peak HRR also observed. Fabric coated with 20 bilayers did not catch fire but only smolder	Reinforcement and re-establishment of weaved network structure through chemical reaction of POSS species	[69]

References

1. Alongi J, Han Z, Bourbigot S (2014) Intumescence: tradition versus novelty. a comprehensive review. Prog Polym Sc 51:28–73. https://doi.org/10.1016/j.progpolymsci.2015.04.010
2. Price D (2001) Introduction: polymer combustion, condensed phase pyrolysis and smoke formation. In: Fire retardant materials. Woodhead Publishing, pp 1–30
3. Georlette P, Simons J, Costa L (2000) Halogen-contining fire-retardant compounds. In: Grand AF, Wilkie CA (eds) Fire retardancy of polymeric materials. Marcel Dekker Inc, Basel, New York, pp 245–284
4. Scharte B (2010) Phosphorus-based flame retardancy mechanisms-old hat or a starting point for future development? Mater Basel 3:4710–4745. https://doi.org/10.3390/ma3104710
5. Brown SC (1998) Flame retardants: inorganic oxide and hydroxide systems. In: Pritchard G (ed) Plastics additives. Springer, Dordrecht, Netherlands, pp 287–296
6. Wei G-L, Li D-Q, Zhuo M-N, Liao Y-S, Xie Z-Y, Guo T-L, Li J-J, Zhang S-Y, Liang Z-Q (2015) Organophosphorus flame retardants and plasticizers: Sources, occurrence, toxicity and human exposure. Environ Pollut 196:29–46. https://doi.org/10.1016/j.envpol.2014.09.012
7. Shaw SD, Blum A, Weber R, Kannan K, Rich D, Lucas D, Koshland CP, Dobraca D, Hanson S, Birnbaum LS (2010) Halogenated flame retardants: do the fire safety benefits justify the risks? Rev Environ Health 25:261–305. https://doi.org/10.1515/REVEH.2010.25.4.261
8. Gnanasekaran D, Madhavan K, Reddy BSR (2009) Developments of polyhedral oligomeric silsesquioxanes (PaSS), pass nanocomposites and their applications: a review. J Sci Ind Res 68:437–464

9. Kuo SW, Chang FC (2011) POSS related polymer nanocomposites. Prog Polym Sci 36:1649–1696. https://doi.org/10.1016/j.progpolymsci.2011.05.002
10. Kausar A (2017) State-of-the-Art overview on polymer/POSS nanocomposite. Polym—Plast Technol Eng 56:1401–1420. https://doi.org/10.1080/03602559.2016.1276592
11. Qian Y, Wei P, Zhao X, Jiang P, Yu H (2013) Flame retardancy and thermal stability of polyhedral oligomeric silsesquioxane nanocomposites. Fire Mater 37:1–16. https://doi.org/10.1002/fam.1126
12. Zhang W, Camino G, Yang R (2017) Polymer/polyhedral oligomeric silsesquioxane (POSS) nanocomposites: an overview of fire retardance. Prog Polym Sci 67:77–125. https://doi.org/10.1016/j.progpolymsci.2016.09.011
13. Bottom R (2008) Thermogravimetric analysis. Principles and applications of thermal analysis. Blackwell Publishing Ltd, Oxford, pp 87–118
14. Mngomezulu ME, John MJ, Jacobs V, Luyt AS (2014) Review on flammability of biofibres and biocomposites. Carbohydr Polym 111:149–182. https://doi.org/10.1016/j.carbpol.2014.03.071
15. Carvel R, Steinhaus T, Rein G, Torero JL (2011) Determination of the flammability properties of polymeric materials: A novel method. Polym Degrad Stab 96:314–319. https://doi.org/10.1016/j.polymdegradstab.2010.08.010
16. Schartel B, Hull TR (2007) Development of fire-retarded materials—Interpretation of cone calorimeter data. Fire Mater 31:327–354. https://doi.org/10.1002/fam.949
17. Lyon RE, Walters RN (2004) Pyrolysis combustion flow calorimetry. J Anal Appl Pyrol 71:27–46. https://doi.org/10.1016/S0165-2370(03)00096-2
18. Laoutid F, Bonnaud L, Alexandre M, Lopez-Cuesta JM, Dubois P (2009) New prospects in flame retardant polymer materials: from fundamentals to nanocomposites. Mater Sci Eng R Reports 63:100–125. https://doi.org/10.1016/j.mser.2008.09.002
19. Dupretz R, Fontaine G, Duquesne S, Bourbigot S (2015) Instrumentation of UL-94 test: understanding of mechanisms involved in fire retardancy of polymers. Polym Adv Technol 26:865–873. https://doi.org/10.1002/pat.3507
20. Qiu X, Li Z, Li X, Zhang Z (2018) Flame retardant coatings prepared using layer by layer assembly: a review. Chem Eng J 334:108–122. https://doi.org/10.1016/j.cej.2017.09.194
21. Lu T, Chen T, Liang G (2007) Synthesis, thermal properties, and flame retardance of the epoxy-silsesquioxane hybrid resins. Polym Eng Sci 47:225–234. https://doi.org/10.1002/pen.20676
22. Lu T, Liang G, Peng Y, Chen T (2007) Blended hybrids based on silsesquioxane–OH and epoxy resins. J Appl Polym Sci 106:4117–4123. https://doi.org/10.1002/app.26974
23. Wu K, Song L, Hu Y, Lu H, Kandola BK, Kandare E (2009) Synthesis and characterization of a functional polyhedral oligomeric silsesquioxane and its flame retardancy in epoxy resin. Prog Org Coatings 65:490–497. https://doi.org/10.1016/j.porgcoat.2009.04.008
24. Wu K, Kandola BK, Kandare E, Hu Y (2011) Flame retardant effect of polyhedral oligomeric silsesquioxane and triglycidyl isocyanurate on glass fibre-reinforced epoxy composites. Polym Compos 32:378–389. https://doi.org/10.1002/pc.21052
25. Franchini E, Galy J, Gérard J-F, Tabuani D, Medici A (2009) Influence of POSS structure on the fire retardant properties of epoxy hybrid networks. Polym Degrad Stab 94:1728–1736. https://doi.org/10.1016/j.polymdegradstab.2009.06.025
26. Schartel B, Braun U, Balabanovich AI, Artner J, Ciesielski M, Döring M, Perez RM, Sandler JKW, Altstädt V (2008) Pyrolysis and fire behaviour of epoxy systems containing a novel 9,10-dihydro-9-oxa-10-phosphaphenanthrene-10-oxide-(DOPO)-based diamino hardener. Eur Polym J 44:704–715. https://doi.org/10.1016/j.eurpolymj.2008.01.017
27. Qian X, Song L, Jiang S, Tang G, Xing W, Wang B, Hu Y, Yuen RKK (2013) Novel flame retardants containing 9,10-dihydro-9-oxa-10-phosphaphenanthrene-10-oxide and unsaturated bonds: synthesis, characterization, and application in the flame retardancy of epoxy acrylates. Ind Eng Chem Res 52:7307–7315. https://doi.org/10.1021/ie400872q
28. Artner J, Ciesielski M, Walter O, Döring M, Perez RM, Sandler JKW, Altstädt V, Schartel B (2008) A novel DOPO-Based diamine as hardener and flame retardant for epoxy resin systems. Macromol Mater Eng 293:503–514. https://doi.org/10.1002/mame.200700287

29. Ciesielski M, Schäfer A, Döring M (2008) Novel efficient DOPO-based flame-retardants for PWB relevant epoxy resins with high glass transition temperatures. Polym Adv Technol 19:507–515. https://doi.org/10.1002/pat.1090
30. Perret B, Schartel B, Stöβ K, Ciesielski M, Diederichs J, Döring M, Krämer J, Altstädt V (2011) Novel DOPO-based flame retardants in high-performance carbon fibre epoxy composites for aviation. Eur Polym J 47:1081–1089. https://doi.org/10.1016/j.eurpolymj.2011.02.008
31. Schartel B, Balabanovich AI, Braun U, Knoll U, Artner J, Ciesielski M, Döring M, Perez R, Sandler JKW, Altstädt V, Hoffmann T, Pospiech D (2007) Pyrolysis of epoxy resins and fire behavior of epoxy resin composites flame-retarded with 9,10-dihydro-9-oxa-10-phosphaphenanthrene-10-oxide additives. J Appl Polym Sci 104:2260–2269. https://doi.org/10.1002/app.25660
32. Zhang W, Li X, Yang R (2011) Pyrolysis and fire behaviour of epoxy resin composites based on a phosphorus-containing polyhedral oligomeric silsesquioxane (DOPO-POSS). Polym Degrad Stab 96:1821–1832. https://doi.org/10.1016/j.polymdegradstab.2011.07.014
33. Zhang W, Li X, Yang R (2011) Novel flame retardancy effects of;DOPO-POSS on epoxy resins. Polym Degrad Stab 96:2167–2173. https://doi.org/10.1016/j.polymdegradstab.2011.09.016
34. Zhang W, Li X, Yang R (2012) Blowing-out effect in epoxy composites flame retarded by DOPO-POSS and its correlation with amide curing agents. Polym Degrad Stab 97:1314–1324. https://doi.org/10.1016/j.polymdegradstab.2012.05.020
35. Zhang W, Li X, Yang R (2013) Blowing-out effect and temperature profile in condensed phase in flame retarding epoxy resins by phosphorus-containing oligomeric silsesquioxane. Polym Adv Technol 24:951–961. https://doi.org/10.1002/pat.3170
36. Gérard C, Fontaine G, Bourbigot S (2011) Synergistic and antagonistic effects in flame retardancy of an intumescent epoxy resin. Polym Adv Technol 22:1085–1090. https://doi.org/10.1002/pat.1996
37. Zhang W, Li X, Fan H, Yang R (2012) Study on mechanism of phosphorus e silicon synergistic flame retardancy on epoxy resins. Polym Degrad Stab 97:2241–2248. https://doi.org/10.1016/j.polymdegradstab.2012.08.002
38. Zhang W, Li X, Jiang Y, Yang R (2013) Investigations of epoxy resins flame-retarded by phenyl silsesquioxanes of cage and ladder structures. Polym Degrad Stab 98:246–254. https://doi.org/10.1016/j.polymdegradstab.2012.10.005
39. Zhang W, Li X, Li L, Yang R (2012) Study of the synergistic effect of silicon and phosphorus on the blowing-out effect of epoxy resin composites. Polym Degrad Stab 97:1041–1048. https://doi.org/10.1016/j.polymdegradstab.2012.03.008
40. Wu Q, Zhang C, Liang R, Wang B (2010) Combustion and thermal properties of epoxy/phenyltrisilanol polyhedral oligomeric silsesquioxane nanocomposites. J Therm Anal Calorim 100:1009–1015. https://doi.org/10.1007/s10973-009-0474-9
41. Yang H, Wang X, Yu B, Song L, Hu Y, Yuen RKK (2012) Effect of borates on thermal degradation and flame retardancy of epoxy resins using polyhedral oligomeric silsesquioxane as a curing agent. Thermochim Acta 535:71–78. https://doi.org/10.1016/j.tca.2012.02.021
42. Levchik SV, Weil ED (2005) Overview of recent developments in the flame retardancy of polycarbonates. Polym Int 54:981–998. https://doi.org/10.1002/pi.1806
43. Li L, Li X, Yang R (2012) Mechanical, thermal properties, and flame retardancy of PC/ultrafine octaphenyl-POSS composites. J Appl Polym Sci 124:3807–3814. https://doi.org/10.1002/app.35443
44. Song L, He Q, Hu Y, Chen H, Liu L (2008) Study on thermal degradation and combustion behaviors of PC/POSS hybrids. Polym Degrad Stab 93:627–639. https://doi.org/10.1016/j.polymdegradstab.2008.01.014
45. Zhang W, Li X, Yang R (2012) Flame retardant mechanisms of phosphorus-containing polyhedral oligomeric silsesquioxane (DOPO-POSS) in polycarbonate composites. J Appl Polym Sci 124:1848–1857. https://doi.org/10.1002/app.35203
46. Zhang W, Li X, Guo X, Yang R (2010) Mechanical and thermal properties and flame retardancy of phosphorus-containing polyhedral oligomeric silsesquioxane (DOPO-POSS)/polycarbonate composites. Polym Degrad Stab 95:2541–2546. https://doi.org/10.1016/j.polymdegradstab.2010.07.036

47. Zhang W, Li X, Yang R (2012) Flame retardancy mechanisms of phosphorus-containing polyhedral oligomeric silsesquioxane (DOPO-POSS) in polycarbonate/acrylonitrile-butadiene-styrene blends. Polym Adv Technol 23:588–595. https://doi.org/10.1002/pat.1929
48. He Q, Song L, Hu Y, Zhou S (2009) Synergistic effects of polyhedral oligomeric silsesquioxane (POSS) and oligomeric bisphenyl a bis(diphenyl phosphate) (BDP) on thermal and flame retardant properties of polycarbonate. J Mater Sci 44:1308–1316. https://doi.org/10.1007/s10853-009-3266-5
49. Vahabi H, Eterradossi O, Ferry L, Longuet C, Sonnier R, Lopez-Cuesta J-M (2013) Polycarbonate nanocomposite with improved fire behavior, physical and psychophysical transparency. Eur Polym J 49:319–327. https://doi.org/10.1016/j.eurpolymj.2012.10.031
50. Wang X, Hu Y, Song L, Yang H, Yu B, Kandola B, Deli D (2012) Comparative study on the synergistic effect of POSS and graphene with melamine phosphate on the flame retardance of poly(butylene succinate). Thermochim Acta 543:156–164. https://doi.org/10.1016/j.tca.2012.05.017
51. Louisy J, Bourbigot S, Duquesne S, Desbois P, König A, Klatt M (2013) Novel synergists for flame retarded glass-fiber reinforced poly(1,4-butylene terephthalate). Polim Polym 58:403–412. https://doi.org/10.14314/polimery.2013.403
52. Didane N, Giraud S, Devaux E, Lemort G (2012) A comparative study of POSS as synergists with zinc phosphinates for PET fire retardancy. Polym Degrad Stab 97:383–391. https://doi.org/10.1016/j.polymdegradstab.2011.12.004
53. Didane N, Giraud S, Devaux E, Lemort G (2012) Development of fire resistant PET fibrous structures based on phosphinate-POSS blends. Polym Degrad Stab 97:879–885. https://doi.org/10.1016/j.polymdegradstab.2012.03.038
54. Didane N, Giraud S, Devaux E, Lemort G, Capon G (2012) Thermal and fire resistance of fibrous materials made by PET containing flame retardant agents. Polym Degrad Stab 97:2545–2551. https://doi.org/10.1016/j.polymdegradstab.2012.07.006
55. Carosio F, Alongi J, Malucelli G (2011) [small alpha]-Zirconium phosphate-based nanoarchitectures on polyester fabrics through layer-by-layer assembly. J Mater Chem 21:10370–10376. https://doi.org/10.1039/C1JM11287B
56. Fina A, Tabuani D, Camino G (2010) Polypropylene–polysilsesquioxane blends. Eur Polym J 46:14–23. https://doi.org/10.1016/j.eurpolymj.2009.07.019
57. Barczewski M, Chmielewska D, Dobrzyńska-Mizera M, Dudziec B, Sterzyński T (2014) Thermal stability and flammability of polypropylene-silsesquioxane nanocomposites. Int J Polym Anal Charact 19:500–509. https://doi.org/10.1080/1023666X.2014.922268
58. Fina A, Abbenhuis HCL, Tabuani D, Camino G (2006) Metal functionalized POSS as fire retardants in polypropylene. Polym Degrad Stab 91:2275–2281. https://doi.org/10.1016/j.polymdegradstab.2006.04.014
59. Carniato F, Boccaleri E, Marchese L, Fina A, Tabuani D, Camino G (2007) Synthesis and Characterisation of Metal Isobutylsilsesquioxanes and Their Role as Inorganic-Organic Nanoadditives for Enhancing Polymer Thermal Stability. Eur J Inorg Chem 2007:585–591. https://doi.org/10.1002/ejic.200600683
60. Liu L, Hu Y, Song L, Nazare S, He S, Hull R (2007) Combustion and thermal properties of OctaTMA-POSS/PS composites. J Mater Sci 42:4325–4333. https://doi.org/10.1007/s10853-006-0470-4
61. Liu L, Hu Y, Song L, Ni Z (2011) Preparation and characterizations of novel PS composites containing octaTMA-POSS-based lamellar hybrids. Int J Polym Mater Polym Biomater 60:947–958. https://doi.org/10.1080/00914037.2010.551373
62. Liu L, Hu Y, Song L, Ni Z (2011) Novel PS Composites by Using Artificial Lamellar Hybrid from Octa(γ-chloroaminopropyl) POSS and Surfactant. Polym Plast Technol Eng 50:73–79. https://doi.org/10.1080/03602559.2010.512353
63. Bourbigot S, Turf T, Bellayer S, Duquesne S (2009) Polyhedral oligomeric silsesquioxane as flame retardant for thermoplastic polyurethane. Polym Degrad Stab 94:1230–1237. https://doi.org/10.1016/j.polymdegradstab.2009.04.016

64. Devaux E, Rochery M, Bourbigot S (2002) Polyurethane/clay and polyurethane/POSS nanocomposites as flame retarded coating for polyester and cotton fabrics. Fire Mater 26:149–154. https://doi.org/10.1002/fam.792
65. Kim H-J, Kim CK, Kwon Y (2014) Ablation and fire-retardant properties of hydroxyl-terminated polybutadiene-based polyurethane-g-polyhedral oligomeric silsesquioxane composites. High Perform Polym 27:749–757. https://doi.org/10.1177/0954008314559554
66. Glodek TE, Boyd SE, McAninch IM, LaScala JJ (2008) Properties and performance of fire resistant eco-composites using polyhedral oligomeric silsesquioxane (POSS) fire retardants. Compos Sci Technol 68:2994–3001. https://doi.org/10.1016/j.compscitech.2008.06.019
67. Chigwada G, Jash P, Jiang DD, Wilkie CA (2005) Fire retardancy of vinyl ester nanocomposites: Synergy with phosphorus-based fire retardants. Polym Degrad Stab 89:85–100. https://doi.org/10.1016/j.polymdegradstab.2005.01.005
68. Carosio F, Alongi J (2016) Influence of layer by layer coatings containing octapropylammonium polyhedral oligomeric silsesquioxane and ammonium polyphosphate on the thermal stability and flammability of acrylic fabrics. J Anal Appl Pyrol 119:114–123. https://doi.org/10.1016/j.jaap.2016.03.010
69. Li Y-C, Mannen S, Schulz J, Grunlan JC (2011) Growth and fire protection behavior of POSS-based multilayer thin films. J Mater Chem 21:3060–3069. https://doi.org/10.1039/C0JM03752D

POSS Hybrid Materials for Medical Applications

Hossein Yahyaei, Mohsen Mohseni and H. Ghanbari

Abstract Medical application is one of the most important issues in the field of material science and has found very high level of attention. During the last decades, the development of new methods or materials which can improve the quality of medical services has been very intense. Using nanotechnology provides new rooms to enhance this field. Polyhedral oligomeric silsesquioxane (POSS) is a new generation of nanostructures showing the properties of nanoparticles and molecules at the same time. Improving thermal and mechanical properties and enhanced solubility are interesting characteristics found in these materials. POSS can be used in medical applications, broadly. It can improve mechanical properties of biomaterials that are very important in tissue engineering. Also, it can improve the resistance of biomaterials against degradation. Today, dental materials use POSS as a key component. Drug delivery and bioimaging are other examples that use POSS as discussed in this chapter.

Keywords Bioimaging · Biomaterial · Dental nanocomposite · Drug delivery POSS · Tissue engineering

Biomaterials play an important role to improve the quality of mankind life. The acceptance or rejection of biomaterials depends on the behavior of body environment with the biomaterial. In this regards, chemistry of biomaterial, physical and chemical properties of surface, and mechanical properties of biomaterials govern this behavior.

Polymers are one of the most important types of biomaterials which have found many applications in this field. Chemically, polymers are long-chain molecules of very high molecular weight, often measured in the hundreds of thousands. For this reason, the term "macromolecules" is frequently used when referring to polymeric

H. Yahyaei · M. Mohseni (✉)
Department of Polymer Engineering and Color Technology, Amirkabir University of Technology, P.O. Box 15875-4413, Tehran, Iran
e-mail: mmohseni@aut.ac.ir

H. Ghanbari
Department of Medical Nanotechnology, School of Advanced Technologies in Medicine, Tehran University of Medical Sciences (TUMS), Tehran, Iran

S. Kalia and K. Pielichowski (eds.), *Polymer/POSS Nanocomposites and Hybrid Materials*, Springer Series on Polymer and Composite Materials,
https://doi.org/10.1007/978-3-030-02327-0_11

materials [1]. Polymers can be synthesized by using variety of monomers and different methods and conditions. Therefore, due to the ability to design and synthesis of polymers desired properties are possible.

The first polymers which used were natural products, such as proteins, wool, starch, cotton. Beginning early in the twentieth century, synthetic polymers were made. The first polymers of importance, Bakelite and Nylon, showed the tremendous possibilities of the new materials. By progressing in science, synthesis of more polymers was possible and new polymers were created. Polyethylene, polypropylene, polyacrylate, polyamide, polyurethane, and polysiloxane are non-degradable polymers that commonly use as medical polymers.

New polymers would provide better properties, but in some applications (like medical applications) the demand was more. Therefore, composites and nanocomposites were invented. These materials broadly refer to composite components with nanoscale dimensions. Nanostructure materials are materials by at least one dimension between 1 and 100 nm and have attracted steadily growing interest by providing unique properties and novel applications. Polymeric nanocomposites are matrices containing fillers in mentioned dimension. By the incorporation of nanofillers into polymer matrix, the beneficial features of both can be combined. Nanofillers provide mechanical properties (such as strength, modulus, and hardness), chemical and thermal resistance, electrical and magnetic properties. Polymer matrix provides flexibility, lightweight, optical properties. It is important to emphasize that these properties not only combined in one material, but also synergistic effect will be obtained. The good interaction between nanophase and polymeric matrix provides better properties and this good interaction is depended on good dispersion of disperse phase in continuous phase. Top down and bottom up are two main strategies to prepare nanomaterials. In top-down approaches, a bulk material is restructured (i.e., partially dismantled, machined, processed, or deposited) to form nanomaterials. In bottom-up approaches, nanomaterials are assembled from basic building blocks, such as molecules or nanoclusters. The basic building blocks, in general, are nanoscale objects with suitable properties that can be grown from elemental precursors.

Nanomaterials classified based on their number of dimensions that are not confined to the mentioned limit of the nanoscale range.

- Three-dimensional (3D) nanomaterials
- Two-dimensional (2D) nanomaterials
- One-dimensional (1D) nanomaterials
- Zero-dimensional (0D) nanomaterials

1 Three-Dimensional (3D) Nanomaterials

Bulk nanomaterials are materials that are not confined to the nanoscale in any dimension. These materials are thus characterized by having three arbitrary dimensions above 100 nm. Materials possess a nanocrystalline structure or involve the presence

of features at the nanoscale. In terms of nanocrystalline structure, bulk nanomaterials can be composed of a multiple arrangement of nanosize crystals, most typically in different orientations.

2 Two-Dimensional (2D) Nanomaterials

Two-dimensional nanomaterials are plate-like shapes. In these nanomaterials, one dimension is in the nanoscale, and two dimensions are not confined to the nanoscale. Platelets, including layered silicates or layered double hydroxides (LDHs), are examples of two-dimensional nanomaterials, which the thickness is lower than nanometer range and the dimensions in length and width far exceeding the particle thickness.

3 One-Dimensional (1D) Nanomaterials

1D materials include nanotubes, nanorods, and nanowires. Two dimensions are in the nanorange, but one dimension is outside the nanoscale. Carbon nanofibers, carbon nanotube (CNT), and halloysite nanotubes (HNTs) are examples of 1D nanomaterials.

4 Zero-Dimensional (0D) Nanomaterials

Materials in which all the dimensions are measured within the nanoscale (no dimensions, or 0D) are larger than 100 nm. The most common representation of zero-dimensional nanomaterials is nanoparticles. Nanoparticles of metal oxides are common example of zero-dimensional nanomaterial. However, silsesquioxanes are new generation of zero-dimensional nanomaterials. Silsesquioxane is composed of silicon and oxygen atoms with empirical formula of $RSiO_{1.5}$, which R can be hydrogen, carbon chain with or without functional groups. Silsesquioxane can be in random or regular shapes. The most common types of silsesquioxane which has found many applications in the researches are a cage-like molecule, and polyhedral oligomeric silsesquioxane is known as POSS.

POSS consists of an inner inorganic framework of silicon and oxygen atoms that is externally covered by organic groups (R). This structure makes a cage-like molecule in nano-dimensions with special and strange properties. The most common structure with stoichiometric formula composed of an inner inorganic framework of molecular silica comprised of 8 silicon atoms, 12 oxygen atoms, and 8 organic chains (R) which merged together and form a cage-like molecule. Hence, each silicon atom is surrounded by three oxygen atoms and one organic chain which may be either inert or reactive. These molecules are highly symmetric and in nanoscale size. Their

size is of approximately 1.5 nm in diameter, including the R groups, and can be considered as the smallest achievable silica particles [2]. POSS contains three special elements in which oxygen and silicon are third- and fourth-abundant element in the universe. However, silicon is the eighth abundant element in the universe and second one in the earth after oxygen. The combination of these provides special physic-chemical properties that are the main reason of popularity of silsesquioxanes. The electronegativity of the oxygen atom confers a degree of polarity on each siloxane bond, and the bond energy of Si–O is relatively high.

Si–O bond is a special bond which provides special properties for compounds containing this bond. Materials containing Si–O bond usually are biocompatible due to chemical stability and surface properties (low surface energy and hydrophobicity). However, polydimethyl siloxane polymers despite high biocompatibility showed weak mechanical properties. High ultimate elongation, low hardness and low modulus, low-to-moderate tensile strengths are properties of silicon materials have caused dilemma which use them or no. The best way to overcome this difficulty is addition of POSS into other appropriate polymers that with the same chemistry not only provide biocompatibility but also improve mechanical properties.

Actually, in the bulk POSS influences on mechanical, thermal, and other similar properties. But, at the same time POSS incorporation can affect surface properties of nanocomposites and hybrid materials. Deng and coworkers [3] showed that partial cage POSS can form stable Langmuir–Blodgett (LB) monolayers at the air/water interface because of their amphiphilic nature. The migration of POSS and its surface segregation has been confirmed in other studies [4, 5]. The existence of cytocompatible and non-toxic POSS on the surface motivated the biomaterial researchers to use POSS in medical applications. In the next part, the application of POSS in polymeric materials like dental materials, drug delivery, and biomedical devices will be discussed.

5 Dental Materials

For many decades, dental amalgams were used to fill tooth. For more than four decades, dental composites were emerged. In comparison with amalgams, the composites have better esthetic feature without some concern about safety and toxicity. Generally, the composites contain organic matrix composing acrylate resin and glass or ceramic as an inorganic phase. Due to double bond on acrylic functional groups, composites cured by free radical polymerization that is initiated by light and named photopolymerization. Viscosity, hydrophilicity, double bond conversion, shrinkage, and mechanical properties (modulus, abrasion resistance, and strength) are important issues which should be considered in preparation of dental composites. POSS with acrylate function is a good choice to add into acrylate monomer to get a robust dental composite. Using acrylate functional POSS provides an inorganic cage composing Si–O bonds and acrylate functional groups that can react with double bonds in matrix. The inorganic cage has substantial strength which donates to composite

and covalent interaction with matrix providing compatibility and preventing phase separation.

Also, the incorporation of POSS can improve biocompatibility and reduce inflammation and hypersensitivity reactions to denture materials. Sellinger and Laine [6] for the first time proposed to incorporate POSS into dental materials to enhance properties of dental restorative. The goal of Gao and coworkers [7] was exploring that how the methacrylate POSS could be applied into formulation and preparation of hybrid dental restorative. They used three methods to incorporate a methacrylate POSS (MA-POSS) into polymeric matrix. In the first method, bisphenol A glycol dimethacrylate (bis-GMA), diluent monomers, and MA-POSS were mixed and copolymerized in one pot. In the second method, MA-POSS and 2-hydroxylethyl methacrylate (HEMA) with an equal weight ratio were reacted and then hydroxyl groups were converted into methacrylate groups, and finally, the resulted macromonomer was copolymerized with bis-GMA and diluents. In the third method, the copolymer of MA-POSS and t-butyl methacrylate (t-BMA) or 2-ethylhexyl methacrylate (EHMA) was prepared and then was added into the mixture of bis-GMA and diluents. The final amount of POSS in the system was controlled as 5, 10, and 15 by weight percent. About formulation in the first method, it was found that the viscosity and double bond conversion (DC) increased by addition of MA-POSS. The decrease of shrinkage is attributed to the presence of POSS cage that does not collapse or shrink during polymerization. They found that the miscibility and well blending of POSS with monomer and oligomer is a key factor which determines the effect of POSS in the mechanical properties and shrinkage. This is the reason that the incorporation of MA-POSS more than 10 wt% decreased the mechanical properties.

In the second series, POSS–HEMA macromonomer showed better compatibility with oligomer/diluent system, where by increasing POSS content double bond conversion and mechanical properties improved along with reduction of polymerization shrinkage.

Despite improving mechanical properties in series II, the synthesis of macromonomer has been a difficult path and the authors sought to find another way to improve compatibility of POSS and polymeric matrix. In formulation series III, a copolymer of MA-POSS with t-BMA or EHMA was prepared and dissolved into bis-GMA/t-BMA or EHMA. In this method, double bond conversion increased, shrinkage decreased significantly, and mechanical properties especially compressive strength improved.

Fong and coworkers [8] used a liquid methacrylate POSS and substituted it with 2,2′-bis-[4-(methacryloxypropoxy)-phenyl]-propane (Bis-GMA). Concerning the role of compatibility between POSS and monomers in improving properties of dental restorative, they have chosen a liquid POSS to be sure about compatibility. Bis-GMA and TEGDMA monomer were used as organic phase in 50/50 wt% that MA-POSS was replaced by bis-GMA in 2, 10, 25, and 50%. Camphorquinone (CQ) and co-initiator ethyl-4 (N,N′-dimethylamino) benzoate (4EDMAB) were selected to cure it by visible light. The results showed that the addition of POSS in all loadings did not affect volumetric shrinkage and no significant difference was observed. Small-angle X-ray scattering (SAXS) was used to study the phase separation and

mixing of POSS and monomers. No long-range ordering in SAXS implied that the three monomers were well mixed and formed a homogenous network. Wide-angle X-ray scattering (WAXS) indicated that all POSS composites were amorphous. Even in high loading of POSS, no POSS crystal peaks was identified, which further confirmed that the POSS-MA was not segregated. The substitution of Bis-GMA with POSS-MA affected both the methacrylate double bond conversion and the photopolymerization rate. They conclude that increasing of POSS content decreased double bond conversion and reduced the rate of polymerization. Young's modulus, Flexural strength, and diametral tensile strength (DTS) were measured as mechanical properties. At the low content of POSS, moderate improvement in mechanical properties was observed, while in higher loading of POSS the mechanical properties decreased dramatically.

Soh and coworkers [9] synthesized POSS with different functionalities. POSS with code A was contained 8 acrylate groups, POSS B included 6 acrylate groups and 2 epoxy groups, POSS C contained 4 acrylate and 4 epoxy groups, and POSS D contained 2 acrylate and 6 epoxy groups. The POSS materials were added into organic part (mixing bisphenol A glycerolate (1 glycerol/phenol) dimethacrylate (Bis-GMA) and tri(ethylene glycol) dimethacrylate (TEGDMA) in a weight ratio of 1:1. The amount of POSS in polymeric matrix was adjusted as 5, 10, 20, and 50 wt%.

They found that increasing of POSS concentration decreased shrinkage as at 50 wt% POSS it was about 0.06%. POSS with 8 methacrylate groups (A) showed the highest shrinkage in comparison to B, C, and D. Results revealed that POSS with lower acrylate groups provided lower shrinkage. This has been expressed that these cubes restrict the movement of the methacrylate groups and hence act as a hindrance. This steric hindrance may increase coincident with network formation and force the unreacted methacrylate groups to re-adjust their conformations and limit the approach of reactive species. Thus, the mutual accessibility of two functionalities, rather than their chemical reactivities, governs the rate and degree of crosslinking in copolymerizations. Hardness and elastic modulus were measured by indentation and result showed that the addition of POSS decreased both. This reduction at 5 wt% addition of POSS was not significant, but hardness and modulus of all formulated neat resins were found to be significantly softer than the control at 10, 20, and 50 wt%. Compound D was found to be significantly harder and more rigid than compounds A–C at 10 wt%.

In general, both hardness and modulus were found to decrease with a decrease in methacrylate chains, except for compound D, which has six short chains of epoxy groups attached and has been shown to have better mobility and flexibility for crosslinking compared with compounds A, B, and C, as evidenced by the higher hardness and modulus values.

Wu et al. [10] prepared a mixture of bis-GGMA and TEGDMA and added 2, 5, 10, and 15 wt% a multi-acrylate functional POSS into it. Barium oxide dispersed in the matrix in 60 wt%. To evaluate double bond conversion, the absorption of C=C at 1635 cm^{-1} in FTIR analysis was monitored. The results showed the sample containing 2 wt% POSS had better double bond conversion than sample without POSS.

X-ray diffraction indicated that all POSS nanocomposites were amorphous, even when the mass fraction of the methacryl POSS monomers in the resin mixture was as high as 15%, no POSS crystal peaks could be identified, which confirmed that the multifunctional POSS had polymerized within the resin matrix.

Shrinkage was from 3.53 to 3.10% when only 2 wt% POSS was incorporated, and it reduced from 3.53 to 2.18% when 15 wt% POSS was used. The results proved that multifunctional methacryl POSS can effectively reduce the shrinkage of resins and that shrinkage is reduced with the increasing percentage of POSS. They believed that the MA-POSS limited the changing of free volume after curing and therefore reduced shrinkage.

The incorporation of POSS could improve mechanical properties of nanocomposites. By addition of 2 wt% POSS, the nanocompsite's flexural strength increased 15%, compressive modulus increased 4%, compressive strength increased 12%, and flexural modulus showed no change. The incorporation of 5 wt% POSS increased compressive strength from 192 to 251 MPa. Compressive modulus increased from 3.93 to 6.62 GPa and flexural strength decreased from 87 to 75 MPa. The decline of mechanical properties after 10 wt% addition of POSs has been attributed to the lower mobility and lower conversion of double bond by increasing of POSS loading. The surface hardness of nanocomposites has been tested, and the hardness of sample containing 2 wt% POSS increased from 350 MPa (without POSS) to 400 MPa. Higher amount of POSS decreased the surface hardness of nanocomposites. The addition of 2 wt% of POSS was helpful to improve toughness as 57% increment was observed in the fracture energy of nanocomposites.

Beigi Burujeny and coworkers [11] functionalized a POSS with a bactericidal compound to and added into formulation of a nanocomposite dental material. Actually using ionic bactericidal compounds into dental composites causes deterioration of mechanical strength. This problem is originated from the reduction of the intermolecular interaction of polymeric network due to plasticization effect of absorbed water molecules penetrated between the chain segments. They have chemically anchored the bactericidal 1, 2, 3-triazolium functional groups on the surface of hydrophobic POSS and was added into the formulation of dental composite including ternary thiol-allyl ether-methacrylate resin and glass fillers. The synthesis of POSS derivatives was checked by 1HNMR and FTIR spectra. Transmission electron microscopy (TEM) image showed roughly spherical particles with average size about 80 nm which themselves composed of aggregated Triazolium-POSS cages.

The water uptake of nanocomposites containing Triazolium-POSS was measured and compared with corresponding formulations containing a common bactericidal monomer with active QAS moieties (DMAEMA-BC). They have expressed that the hydrophobicity of POSS has caused the lower water uptake of sample containing Triazolium-POSS in comparison with common bactericidal. Composite containing Triazolium-POSS showed more than 60% bacterial reduction while the control sample with the same concentration of antibacterial materials did not showed significant bactericidal activity. As the concentration of antibacterial material increases in the control sample although bacterial reduction up to 30% was detected but mechanical properties dropped and water uptake increased. No significant impact on shrinkage

has been reported for addition of POSS, but sample containing Triazolium-POSS showed higher double bond conversion compared with neat composite. Also, the cytocompatibility was investigated by of L929 mouse fibroblast cells and no significant of cell viability was observed for neat composite and composite include Triazolium-POSS compared to control.

Zelmer et al. [12] synthesized POSS-co-acrylic acid star copolymers. The as-prepared star copolymers were mixed with the glass powder to prepare glass ionic cement (GIC).

When aqueous solutions of POSS-(PAA) eight copolymers were mixed with glass powder, they formed rigid GICs. The tensile compression stress and toughness of these GICs were found to be less than that of a commercial resin-reinforced material.

Rizk and coworkers [13] used multifunctional POSS into dental adhesives to provide a bioactive potential without changing material properties adversely. The degree of conversion, water sorption, and sol fraction showed a maintained or improved network structure and properties when filled with multifunctional POSS; however, less polymerization was found when loading a monofunctional POSS.

6 Drug Delivery

Efficient drug delivery plays an important role in disease treatment and is a crucial challenge in medicine. Drug delivery has the potential to have a tremendous impact on treatment of diseases. There are a large number of drugs that are reasonably effective to treat disease, but those drugs are limited by delivery issues. The challenges of having drugs at a physiologically relevant concentration for extended periods or in a localized delivery system are challenges that can be solved with drug delivery technology, whether it is using cellular delivery systems, microelectromechanical (MEM)-based devices, polymer matrices, or gene delivery systems [14].

Drug delivery is the method or process of administering a pharmaceutical compound to achieve a therapeutic effect in humans or animals. A drug delivery system (DDS) is defined as a formulation or a device that enables the introduction of a therapeutic substance into the body and improves its efficacy and safety by controlling the rate, time, and place of release of drugs in the body [15].

Physic-chemical properties of drug delivery system determine drug absorption, distribution, and elimination in the human body. Therefore, nanosystem due to huge surface which can provide is a good option to use in drug delivery system.

The hybrid material based on silica could share the significant area of nanoscience and technology. Actually, the susceptibility of the presence of organic moieties and inorganic silica at the same time in hybrid silica provides the possibility to use it in interesting applications. In this regard, POSS materials have shown a great capability to use in drug delivery system (Fig. 1).

McCusker et al. [16] reported the ability of polycationic amine-functionalized polyhedral oligomeric silsesquioxanes (Octa-ammonium–POSSH), to serve as carriers and potential drug delivery agents. They neutralized the ammonium sites on the

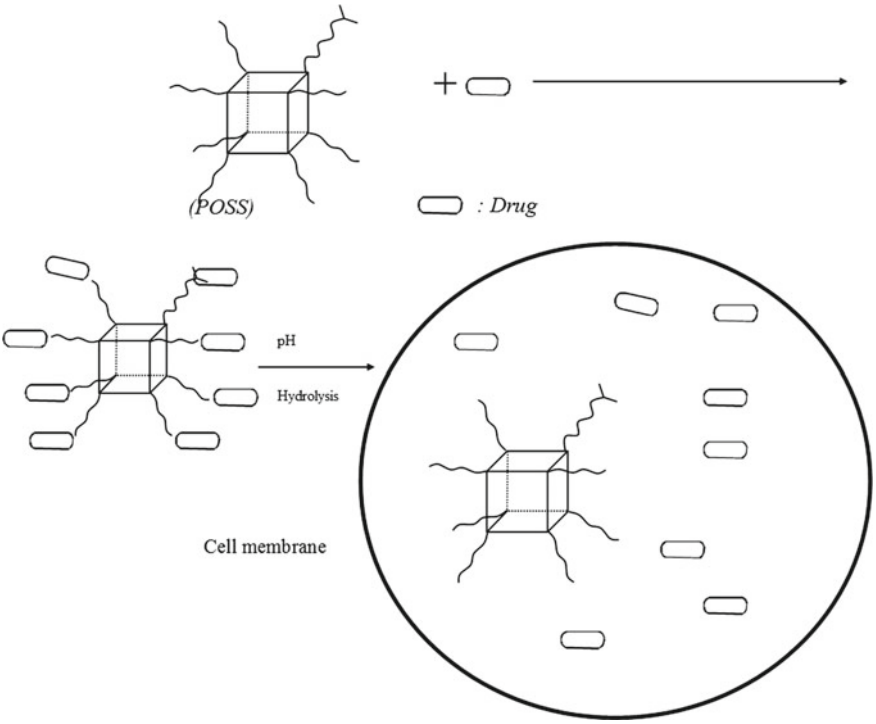

Fig. 1 Schematic diagram of drug delivery system by using POSS. Molecules of drug can be released under physiological conditions and then the POSS-based carrier will be hydrolyzed (pH = 7.40) to a proper non-toxic functional groups (like carboxylic acid salt) and a water-soluble polyhedral oligomeric silsesquioxane

Octa-ammonium–POSS units with triethylamine and labeled with a fluorescent dye (Fig. 2). Subsequently, the structure is substituted with a succinimidyl ester derivative of the BODIPY dye. BODIPY is a commonly employed fluorescent cellular membrane marker, which can be readily conjugated to various systems in order to track cellular migration patterns.

The remaining ammonium groups on the POSS–BODIPY conjugate had positive charge and provide solubility in aqueous media and increased cellular uptake. As a control, a similar amine-terminated BODIPY dye was used.

Live fluorescence confocal images effectively demonstrated that the POSS–BODIPY units became localized in the intracellular regions, mainly in the cytosol.

Control microscopy images with the amine-terminated BODIPY showed no cellular uptake of the dye in the absence of POSS. The results of MTT assay showed no affection of cells by POSS–BODIPY and the morphology of cells was intact.

Pu and coworkers [17] by using ring-opening polymerization of b-benzyl L-aspartate-N-carboxyanhydride (BLA–NCA) with a-methoxyv-aminopoly(ethylene glycol) (mPEG–NH2) synthesized poly(benzyl L-aspartate)-

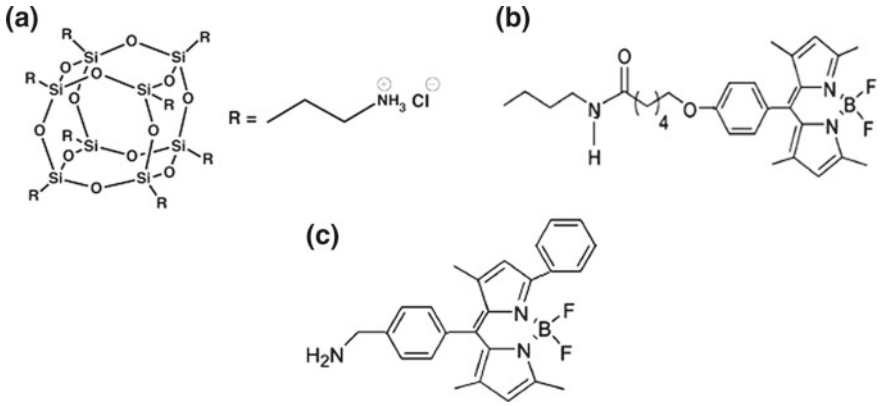

Fig. 2 **a** Octa-ammonium–POSS **b** fluorescent labeled BODIPY (POSS–BODIPY) **c** control amine-terminated BODIPY

b-PEG (PBLA-b-PEG) and grafted it onto 8 carbocxyl groups of POSS to provide amphiphilic star-shaped copolymers (POSS-g-(PBLA-b-PEG)). The final product was characterized by FTIR, proton NMR, and GPC. The solution of (POSS-g-(PBLA-b-PEG)) in DMSO solvent was added dropwise into distilled water. It was lyophilized and the micelle powder was received. Finally, (POSS-g-(PBLA-b-PEG)) and quercetine (5 to 1 ratio by weight) were dissolved in DMSO and stirred for 1 h. The DLCs of quercetin in POSS-g-(PBLA15-b-PEG) and POSS-g-(PBLA30-b-PEG) micelles were 4.55 and 9.82% and the EEs were 27.2 and 58.8%, respectively. Both the DLC and EE of POSS-g-(PBLA30-b-PEG) micelles were higher than those of POSS-g-(PBLA15-b-PEG), which is probably attributable to the longer hydrophobic blocks which result in stronger interactions between quercetin and the PBLA blocks.

The in vitro quercetin release from drug-loaded star-shaped polymeric micelles was investigated in PBS (pH 7.4, 0.01 M) at 37 °C.

A burst release in the first 10 h and about 20% of quercetin was observed. The drug was released nearly in a zero-order style after burst release. The accumulated release rates of drug-loaded POSS-g-(PBLA15-b-PEG) and POSS-g-(PBLA30-b-PEG) micelles were 86 and 70% for 160 h of release. Comparing with POSS-g-(PBLA30-b-PEG) micelles, the quercetin released from POSS-g-(PBLA15-b-PEG) micelles was faster, and they have attributed it to the stronger hydrophobic interactions between quercetin and the hydrophobic blocks in the POSS-g-(PBLA30-b-PEG) micelles.

Another important matter about drug carrier is cytotoxicity. The MTT assay results showed about 100% cell viability which approved its biocompatibility.

Fan et al. [18] reacted hydroxyl groups on (3-hydroxy-3-methylbutyldime thylsiloxy)-polyhedral oligomeric silsequioxane (POSS-8OH) with the combination of repetitive ring-opening polymerization (ROP) of L-lactide and branching reactions and synthesized POSS-(G3-PLLA-OH)8. It was followed by esterification coupling

between allyl-PEO-COOH chains and POSS-(G3-PLLA-OH)8, and the peripheral allyl groups reacting with 3-mercaptopropionic acid (MPA). It was trepan to the amphiphilic copolymer POSS-(G3-PLLA-b-PEO-COOH)8. Dynamic light scattering (DLS) and TEM results showed a unimolecular micelles with a unique core–shell structure and uniform size distribution (99.9–102.5 nm). An anticancer drug, Doxorubicin (DOX), was encapsulated into the POSS-(G3-PLLA-b-PEO-COOH)8 micelles to evaluate the drug release profile. POSS-(G3-PLLA-b-PEO-COOH)8 unimolecular micelles possess an inner hydrophobic PLLA core and an outer hydrophilic PEO shell. Herein, DOX, a hydrophobic anticancer drug, was encapsulated into the PLLA core.

Loading dosage of 18.5 ± 2.3 w/w% DOX-loaded micelles showed controlled release of up to 39% loaded drug over a time period of 80 h. About 27% DOX was released in first 24 h with a slight burst and then it slowly rose to 39% in the followed 56 h. In contrast, nearly all free DOX had released relatively faster into the medium with 8 h.

These results revealed that the structurally stable unimolecular micelles from POSS-(G3-PLLA-b-PEO-COOH)$_8$ have potential applications as controlled drug delivery nanocarriers.

Li and coworkers [19] used different PCL segments and thiol-ene click reaction, ring-opening polymerization (ROP), and atom transfer radical polymerization (ATRP) to synthesis poly(ε-caprolactone)-poly(2-(dimethylamino)ethyl methacrylate)-*co*-poly(ethylene glycol) methacrylate) (POSS-PCL-P(DMAEMA-*co*-PEGMA))$_{16}$.

FTIR, H NMR, GPC, XPS, and TGA were used to confirm synthesis. DLS, UV–visible spectroscopy, and TEM were used to investigate the ability of self-assembly into micelles in aqueous solution. The sizes of the micelles were about 150 and 200 nm with spherical shapes. The pH-responsive self-assembly behavior of these triblock copolymers in water was studied at different pH values of 5.0 and 7.4 for controlled doxorubicin release, it was indicated that the release rate of DOX could be effectively controlled by changing the pH, and the release of drug loading efficiency (DLE) was up to 82% (w/w). The DOX-loaded micelles could easily enter the cells and produce the desired pharmacological action and minimize the side effect of free DOX.

By increasing the PCL segments, the DOX loading contents were increased. The release of DOX from the micelles was significantly accelerated by decreasing pH from 7.4 to 5.0 at 37 °C, and after 55 h for DOX-loaded micelles, the cumulative release was about 82% (w/w), which could be provided sustained drug delivery behavior after the DOX-loaded micelles entered into blood circulation by endocytosis.

John et al. [20] believed that there is a high probability that some of the drug molecules can be completely trapped inside the ramified structures and are a good option to use as drug delivery system. They synthesized an amido-functionalized POSS (Fig. 3) and entrapped ibuprofen and acetaminophen by dissolving the drugs and POSS in ethanol and stirring.

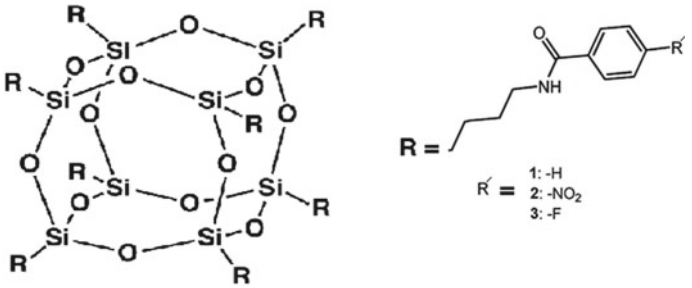

Fig. 3 Octa propyl benzamido silsesquioxane chemical structure

The structures of both the carrier molecules and drug molecules allowed at the interface of pharmacologically active compounds and the network's POSS side arms attachment occurred. They have proposed that it can be due to the affection of hydrogen bond or halogen/phenyl supramolecular interactions.

Nanoparticle acetaminophen entrapment efficiency equal values for sample 1 was measured 64 and 39% for samples 2 and 3. About ibuprofen, it was 63% for sample 1 and 39% for 2 and 3. They have studied the release of acetaminophen by UV–Vis spectroscopy and drug release of sample 1 was more (40%), whereas about samples 2 and 3 it was about 18%. It has been attributed to the less interaction of sample 1 with drug and just breaking of hydrogen bonding has been enough for realizing of drug, while about 2 and 3 samples 2 and 3 had additional groups (NO_2 and F) which could form extra interactions. About ibuprofen 40, 25, and 20 mg of drug was released for compounds 1, 2, and 3, respectively. In vitro degradation of nanoparticles was investigated in acidic, neutral, and basic environments. At pH 4–7 only released drug molecules are observed, whereas at pH = 7.4 (normal tissue has a pH of around 7.40) hydrolysis of amide bond occurs.

They have concluded that the POSS-based carrier is able to hydrolyze (at pH = 7.40) to non-toxic carboxylic acid salts and water-soluble polyhedral oligomeric silsesquioxanes containing aminopropyl groups which products can be safely removed from the organism.

Naderi and coworkers [21] oxidized single-walled carbon nanotubes (SWCNTs) and reacted with Octa-ammonium polyhedral oligomeric silsesquioxanes (Octa-ammonium POSS) to render them biocompatible and water dispersable. It was used as targeted delivery of paclitaxel (PTX) to cancer cells. Figure 4 shows the chemical structure of paclitaxel, single-walled carbon nanotube, and Octa-ammonium POSS.

To study the effect of PTX-POSS-SWCNTs Nanocomposites complexes by MCF-7 and HT-29 cell lines and to investigate the suitability of functionalized SWCNTs as a DDS, HT-29 and MCF-7 cells were incubated with the nanotube-drug complexes for 24, 48, and 72 h. In Alamar blue assay, three different concentrations were used for each nanocomposite and free PTX, and –COOH-functionalized SWCNTs. There was no statistical difference in cell viability between the different concentrations of the nanocomposites and controls at any time point. In both cell lines, increased cell

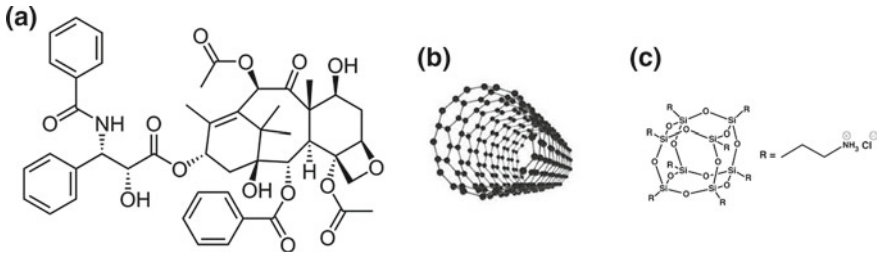

Fig. 4 Chemical structure of **a** paclitaxel **b** single-walled carbon nanotube **c** Octa-ammonium POSS

death was observed with free PTX and PTX containing nanocomposites compared to nanocomposites not containing PTX, cell-only controls, and –COOH-functionalized SWCNT at 48 and 72 h time points. They have concluded that POSS, SWCNT, and PTX as a conjugate can be a novel strategy for cancer drug delivery and therapy and can deliver PTX to cancer cells. More importantly, the covalent bonding of SWCNT-PTX still preserves its anticancer activities.

Jiang et al. [22] used POSS in gen delivery systems. Atom transfer radical polymerization (ATRP) method used to synthesize a series of novel hybrid amphiphilic copolymers consisting of dimethylaminoethyl methacrylate (DMAEMA), polyhedral oligomeric silsesquioxane (POSS), poly(ethylene glycol) methacrylate (PEGMA), and glycidyl methacrylate (GMA) monomeric segments. MTT assay showed relatively low cytotoxicity. The copolymer could successfully condense the plasmid DNA (pDNA) into nanoparticles. Owing to the incorporation of POSS and PEGMA, the POGED copolymers displayed better gene transfection efficiencies compared to the PDMAEMA homopolymer control.

7 Tissue Engineering of POSS

Professor Seifalian and his team in University College London synthesized a nanocomposite based on polyhedral oligomeric silsesquioxane and polyurethane and found the potential of using in medical applications (biocompatibility, hemocompatibility, antithrombogenic effect, endothelization, etc.). They found that polyurethane based on polycarbonate polyol has the best biostability in comparison with polyester and polyether polyol. Although their poly (carbonate-urea) urethane (PCU) was thrombogenic, it was lesser than the other polyurethanes which the soft segments were composed polyether or polyester. It was required to modify the surface thrombogenicity. Also, anti-platelet and protein inhibitory qualities coupled with the ability to demonstrate cytocompatibility allowing cells to grow on its surface could be as good achievements. According to the literature, incorporating silicon, which repels platelet and fibrin adsorption because of its variable surface tension, onto a vas-

cular interface would confer to it increased thromboresistance, but silicon had its own disadvantages too. The incorporation of POSS and synthesis a hybrid material (poly(carbonate-silsesquioxanebridge-urea)urethane) could be a good idea.

Being inorganic in nature silsesquioxanes negated the problems and complexities associated with the incorporation of drugs and biomolecules such as heparin into the matrix of the material. POSS due to its surface tension could segregate on the surface and permit the anti-platelet and anti-coagulant function but prevents the cytotoxic effects associated with materials containing silicon.

Both the direct and indirect effects of POSS-PCU on human umbilical vein endothelial cells (HUVEC) have been explored [23]. Actually, as the first step the cytocompatibility of the new polymer and any potential cytotoxic effects were investigated. Human umbilical vein cells (HUVEC) were used as cell to test cell viability and growth by using Alamar blue TM, lactate dehydrogenase, and Pico green assays, and morphology was studied by Toluidine blue staining and SEM images. It was observed that viable cells were present on the surface of POSS-PCU sample after 16 days seeded. The SEM images demonstrated that the surface of hybrid materials was uniform and endothelial cells were present on the surface at both 24 and 96 h post-seeding.

The cell proliferation study revealed that HUVEC can be maintained on POSS-PCU for an extended period (16 days) and that the growth pattern was similar to that for HUVEC grown on a surface of glass.

The antithrombogenic potential of POSS-PCU hybrids was investigated in another study [24]. TEM and EDXA combined to map morphology of hybrid and distribution of POSS in PCU. Three specific regions were distinguished. A silicon-oxygen rich area immediately surrounded by urethane linkage rich which together constitutes the hard segment. Carbon-rich region related to the polycarbonate soft segment was another phase which was observed. Distribution of silicon (POSS) throughout the hard segment of PU evenly was another data that obtained from TEM images. The dynamic water contact angle measurement has been performed to investigate surface hydrophobicity of nanocomposite. POSS-PCU containing 2% POSS showed advance contact angle about 81 degree and receding contact angle about $36 \pm 5°$. The large difference between receding and advancing contact angle causes of a large hysteresis loop include surface roughness, microscale chemical heterogeneity, and surface fabrication in an aqueous environment. They have concluded that the large hysteresis was due to the chemical heterogeneity which was revealed in TEM images, and the advanced angle is thought to be typical of the low-energy surface component and the receded angle typical of the high-energy surface component. Atomic force microscopy showed that three phases had formed on the surfaces of POSS-PCU containing 2 wt% POSS.

A crystalline-like phase and a two-phase "pebble stone" were blended. The smooth crystalline phase consisted of domains that were 5–20 μm in size with a height of 1–6 μm compared to base level. The pebble-stone blend could only be observed at higher magnifications and consisted of elevated domains that were 200–500 nm in size and 100–200 nm in height.

Thromboelastography has used as a sensitive indicator of thrombogenicity. They found that the polymer had lower maximum amplitude (MA) value(s) indicative of decreased platelet bonding strength as compared to control polystyrene and PCU. In addition, it was also found that the clots which formed on POSS-PCU were significantly unstable and lysed by 60 min compared to PCU or the control polystyrene polymer. These results have been attributed to either decreased fibrin binding strength to the polymer or lower fibrin adsorption to the TEG cup or a combination of both. A significantly decreased fibrinogen adsorption to the polyurethanes (POSS-PCU and PCU) as compared to PTFE was observed in direct ELISA fibrinogen adsorption analyses. The lower fibrinogen adsorption of POSS-PCU again has been related to the existence of POSS in the hybrid polyurethane which caused variable surface tension and hence reduced both platelet and protein adsorption. This POSS presence caused that the weaker the strength of the fibrin clot in POSS-PCU as compared to PCU.

Factor X has been considered as an important function that affects both the extrinsic and intrinsic coagulation pathways. By increasing POSS loading (2–6 wt%), the anti-FXa activity of the copolymer as compared to both PCU and PTFE increased, significantly. These findings indicate that POSS-PCU nanocomposites inactivate FXa to a greater extent than PTFE and PCU.

Platelet adsorption on the surface of POSS-PCU was significantly less than PCU and PTFE. It was indicated that POSS-PCU repels platelet adsorption with increasing time to its surface to a greater extent compared to PTFE and PCU. In conjunction with the lower MA values obtained on TEG, this suggested that POSS-PCU had an anti-platelet effect by both repelling their surface adsorption and lowering the binding strength of platelets to the polymer which corresponded to the poor adsorption characteristics exhibited toward fibrinogen.

The endothelialization was an important issue that was concentrated in an independent study [25]. No significant difference between cell viability in standard culture media and POSS-PCU was observed. Endothelial cells were adhered to the polymer within 30 min of contact with no difference between POSS-PCU and control cell culture plates. Good cell proliferation POSS-PCU was also observed for up to 14 days even from low seeding densities (1.0×103 cells/cm^2) and reaching saturation by 21 days. Microscopic analysis showed evidence of optimal endothelial cell adsorption morphology with the absence of impaired motility and morphogenesis. It was concluded that POSS-PCU had potential to use as a suitable biomaterial scaffold in bio-hybrid vascular prostheses and biomedical devices. In this regard, the POSS-PCU was used as microvessels for an artificial capillary bed [26]. By changing the concentration of POSS-PCU in the solvent, the appropriate homogeneity and viscosity were obtained for dip coating.

In the second phase, the polymer-coated mandrels were coagulated in a variety of solutions to achieve ideal compliance and porosity characteristics.

They found that it was possible to mimic the hydraulic conductivity and pressure-responsive radial compliance characteristics of biological microvessels.

This would allow nutrient exchange across its walls as well as minimize compliance mismatch throughout the physiological pressure range, thus reducing intimal

hyperplasia in the long term. They concluded that this microvessel would have the following implications: (1) as a microvascular substitute to vein grafts and (2) in the future as a component of a microvascular network. In real terms, these microvessels could serve as an effective alternative to vein grafts in microsurgery while in the long term, allow the construction of more complicated microvascular networks.

In another study [27], POSS-PCU nanocomposite was used as coating of metallic stent. Nitinol (alloy of nickel and titanium) is a metal with shape memory properties that could be a very good alloy to use as a self-expandable stent. But, in vivo studies of NiTi stent have shown that deleterious nickel (Ni) ions can release because of corrosion. The corrosion products can provoke an inflammatory response and induce thrombus formation. Also, better biocompatibility and hemocompatibility are another matter that should be paid attention. It was considered that non-biodegradable polymer coatings may provide a solution for both of these problems as they can serve as a shield against corrosion and also as a platform for improving the biocompatibility of the device.

The development of protocols with the potential for effective bonding of the polymer to NiTi in the development of small diameter stents; including coronary or peripheral stents was studied by using POSS-PCU as coating.

In the first step, anodizing the Ti alloy in a methanolic electrolyte on the NiTi was performed. In the second step, 3-Aminopropyltriethoxysilane (γ-APS) was applied to the surface as the coupling agent to chemically improve the adhesion between NiTi substrate and POSS–PCU film. The alkoxide groups on (γ-APS) were hydrolysis and found the potential to react with groups on the anodize coating. The authors believed that amine group on the (γ-APS) can react with isocyanate groups in POSS-PCU.

In the last step, the solution of POSS-PCU (15%) was applied on the stent by using electrospray method. In corrosion resistance test, the Ni releasing from bare NiTi and NiTi coated with POSS-PCU with (γ-APS) treatment and without treatment was measured.

The Ni release experiments showed the effect of coating NiTi samples with POSS–PCU, after one hour. Ni release was much greater compared with the bare NiTi samples, reaching 1784 ng/mL in DMEM after 3 days in comparison with to 4.16 ng/mL, respectively, for surface treated coated NiTi samples.

In addition, there was also a difference between untreated POSS–PCU-coated NiTi samples and surface-treated samples. After 3 h, the amount of Ni released from untreated coated samples was more than the amount released from surface-treated samples, 13.77 ng/mL released from untreated NiTi samples in DMEM, respectively, compared with 4.163 from surface-treated samples. Also, it was observed that more over the reduction of Ni release, the rate of Ni releasing was reduced by applying the coating.

This was of great importance as the release of Ni from NiTi could result in tissue damage and therefore delay healing and increase of the risk of thrombus formation. Another important issue which should be considered in the designing and using biomaterials is biodegradation and biostability of product. Fragmentation or delamination of thin coating from the strut surface during degradation process may present safety concerns. The coated samples were immersed in the test solutions and

results showed no cracks or failure of the coatings were also observed for the polymer coating subjected to hydrolysis. However, pores or surface cracking was visible on the surface of the nanocomposite exposed to oxidative degradation. Therefore, the nanocomposite coating incubated in H_2O_2 solution did not exhibit the required resistance to oxidative environment. This effect was even more pronounced with the t-butyl peroxidation systems. Despite the weakness in oxidative environment, peel strength analysis showed no significant difference in adhesion properties between the control, hydrolytic, and plasma-degraded nanocomposites. The biostability and derivative resistance of POSS-PCU have been focused on another paper [28]. Their results revealed that POSS can play the role of shielding for the soft segment which is responsible for its compliance and elasticity and save it against all forms of degradation, principally oxidation and hydrolysis. Stress–strain curves performed on the polymers which were most affected physically as well as chemically showed that no significant difference in stress–strain behavior existed.

Heart valve was another device that was prepared by the POSS-PCU nanocomposite [29]. About heart valve, the mechanical properties are very important and it has been focused in their study. POSS–PCU (hardness 84 ± 0.8 Shore A) measured significantly higher tensile strength (53.6 ± 3.4 and 55.9 ± 3.9 N mm^{-2} at 25 and 37 °C, respectively) than PCU (33.8 ± 2.1 and 28.8 ± 3.4 N mm^{-2} at 25 and 37 °C, respectively). Tensile strength and elongation at break of POSS–PCU were significantly higher than PCU at both 25 and 37 °C. POSS–PCU showed a relatively low Young's modulus (25.9 ± 1.9 and 26.2 ± 2.0 N mm^{-2}) which was significantly greater in comparison with control PCU (9.1 ± 0.9 and 8.4 ± 0.5 N mm^{-2}) at 25 and 37 °C, respectively, with 100 μm thickness. There was no significant difference in tear strength between POSS–PCU and PCU at 25 °C. However, tear strength increased significantly (at 37 °C) as the thickness increased from 100 μm (51.0 ± 3.3 N mm^{-1}) to 200 μm (63 ± 1.5 N mm^{-1}). The surface of POSS–PCU was significantly less hydrophilic than that of PCU.

Yahyaei and coworkers studied biocompatibility of hybrid polyurethane coating. A POSS with the potential to react with organic phase and another one that just physically blended with PU were compared [4].

Results revealed that the incorporation of an open cage POSS by physical mixing caused segregation of POSS at the surface, while by addition of a POSS-containing hydroxyl functional group, it distributed in bulk and surface uniformly. The migration of POSS on the surface decreased water contact angle and increased hydrophobicity of surface. Viability of endothelial cells on the polymers was investigated by MTT assay. Physically blended sample with lower surface energy showed significant improvement in cell viability and biocompatibility. In another study, polyhedral oligomeric metalized silsesquioxane (POMS) was synthesized [5]. The silanol groups on the corner of an open cage POSS were reacted with titanium alkoxide to end cap the POSS molecule with titanium atom. The structure of POMS was studied by FTIR, RAMAN, and UV–visible spectroscopy as well as ^{29}Si NMR. MALDI-TOF revealed that POMS formed in monomeric molecule instead of dimeric. The synthesized POMS and pristine POSS were added into polycarbonate urethane polymer. FE-SEM images from cross section of hybrid showed compatibility between

POMS and PU system while incompatibility of pristine POSS and PU was obvious. In comparison to pristine POSS hybrid, the POMS based hybrid showed higher hydrophobicity. HUVEC and MRC-5 were cells that used to study cell viability of hybrid. Although the cell viability of sample containing POSS was higher than control, the sample containing POMS showed the highest cell viability in MTT assay and no cytotoxicity in LDH assay.

8 Bioimaging

During recent years, bioimaging could find many popularity. Bioimaging techniques such as fluorescent imaging, magnetic resonance imaging (MRI), and X-ray tomography (CT) can label targeted object and prepare information of the anatomic structure of tissues. In comparison with the conventional biological labels, such as organic dyes and quantum dots, nanotechnology possesses superior physicochemical features, including low auto-fluorescence, large anti-Stokes shifts, low toxicity, high resistance to photobleaching, and high penetration depth.

Liu et al. [30] grafted Gd complex on POSS (POSS–HPG–Gd) that was applied to fluorescence and magnetic resonance dual modal imaging due to their low cytotoxicity, good water solubility, and high biocompatibility (Fig. 5).

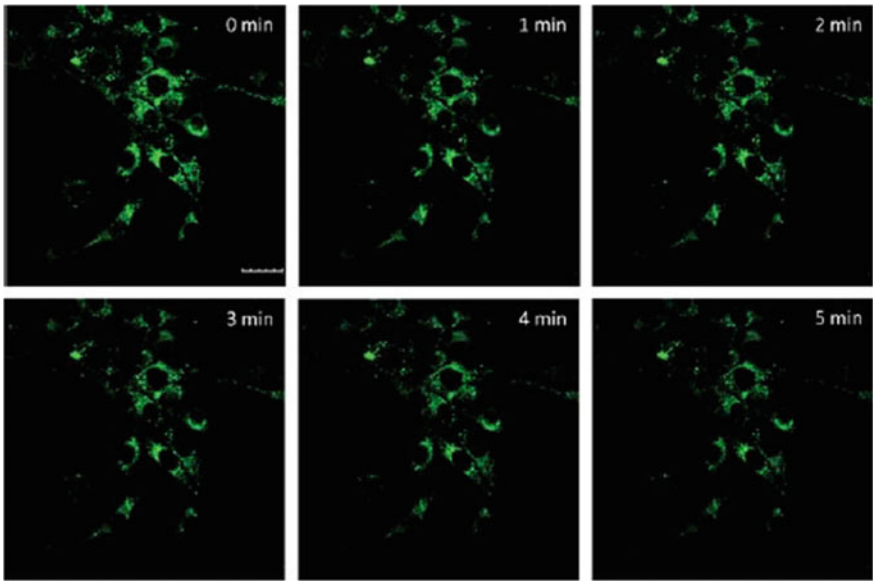

Fig. 5 CLSM fluorescence images of MCF-7 cells upon continuous laser excitation at 405 nm with a laser power of 3.75 mW for 0–5 min. The MCF-7 cells were incubated with 62.5 mg mL_1 POSS–HPG–Gd for 2 h. The scale bar is 30 mm (reported in Ref. [30])

Zhu and coworkers [31] believed that most photodynamic therapy (PDT) suffer from insufficient drug loading capacity, severe self-quenching effect, premature release of drugs and/or potential toxicity. In this regards, they used an amino functional cage-like POSS and crosslinked with chlorin e6 (Ce6), a carboxyl-containing photosensitizer, by the amine–carboxyl reaction. To enhance the aqueous dispersibility and prolong the circulation time of the final nanoconstruct, polyethylene glycol (PEG) polymers were further modified on the surface of the nanoparticle. They expected high drug loading capacity and superior chemical stability for enhanced PDT from POSS-Ce6-PEG.

Singlet oxygen generation, desirable fluorescence emission, and high (19.8 wt%) loading rate of Ce6 have been reported. Also, it showed improved cellular uptake and favored intracellular accumulation within mitochondria and endoplasmic reticulum, resulting in high anticancer efficiency under light irradiation. The side effect and cytotoxicity were investigated, and negligible undesirable effect was reported. The effective tumor targeting and ablation ability of POSS-Ce6-PEG were the results that obtained from in vivo imaging-guided PDT.

Wang et al. [32] synthesized star polymers with POSS core which had partly fluorinated arms.

Octavinyl POSS used as starting material, the eight vinyl groups converted to hydroxyl via UV-induced thiol-ene reaction. In the next step, by esterification reaction between hydroxyl functionalized POSS and a carboxyl-terminated chain transfer agent (CTA) a macroCTA with eight CTA moieties on the POSS core was obtained. The macroCTA was used for the RAFT polymerization of a fluorinated monomer and poly(ethylene glycol) (PEG)-based oligomer, affording star polymers with a POSS core. Star polymers with different arm lengths were synthesized by varying the feed ratio of monomer to CTA and were purified by extensive dialysis in water. The well-defined fluorine chemical environment was confirmed by observation of a single peak in the 19F NMR spectra. The T2 relaxation times increased with the arm length due to enhanced segmental chain flexibility. The 19F MRI intensity was calculated from measured relaxation parameters and the known chemical structure and confirmed that the star polymers have greater potential for use as 19F MRI agents with high imaging intensity.

Ge et al. [33] used POSS to transfer upconversion-luminescent nanoparticles from hydrophobic to hydrophilic. The POSS modified upconversion nanoplatforms [POSS-UCNPs(Er), POSS-UCNPs(Tm)] exhibited favorable monodispersion in water and good water solubility, while their particle size did not change substantially. The POSS modified upconversion nanoplatforms were successfully applied to upconversion luminescence imaging of living cells in vitro and nude mouse in vivo (upon excitation with 980 nm). In addition, the doped $Gd3+$ ion endows the POSS-UCNPs with effective T1 signal enhancement and the POSS-UCNPs were successfully applied to in vivo magnetic resonance imaging (MRI) for Kunming mouse, which affords them as potential MRI positive-contrast agent.

9 Conclusion

The application of POSS in medical application has been discussed. Studied showed that POSS can improve mechanical properties of dental composite while reduces volume shrinkage in many cases. POSS naturally is biocompatible, and by adding POSS into polymers, cell viability improved. POSS by affecting of surface properties reduces adsorption of protein on the surface of biomaterials which are in contact with blood and improved blood compatibility. Drug delivery system was another field that used functional POSS to serve as carriers and potential drug delivery agents. POSS has the superior physicochemical features, and bioimaging is another field that can use POSS.

References

1. Sperling LH (2005) Introduction to physical polymer science. Wiley
2. Li GZ, Wang LC, Toghiani H, Daulton TL, Koyama K, Pittman CU (2001) Viscoelastic and mechanical properties of epoxy/multifunctional polyhedral oligomeric silsesquioxane nanocomposites and epoxy/ladderlike polyphenylsilsesquioxane blends. Macromolecules 34(25):8686–8693
3. Deng JJ, Viers BD, Esker AR, Anseth JW, Fuller GG (2005) Phase behavior and viscoelastic properties of trisilanolcyclohexyl-POSS at the air/water interface. Langmuir 21:2375–2385
4. Yahyaei Hossein, Mohseni Mohsen, Ghanbari Hossein (2015) Physically blended and chemically modified polyurethane hybrid nanocoatings using polyhedral oligomeric silsesquioxane nano building blocks: surface studies and biocompatibility evaluations. J Inorg Organomet Polym Mater 25(6):1305–1312
5. Yahyaei Hossein, Mohseni Mohsen, Ghanbari Hossein, Messori Massimo (2016) Synthesis and characterization of polyhedral oligomeric titanized silsesquioxane: a new biocompatible cage like molecule for biomedical application. J Mater Sci Eng C 61:293–300
6. Sellinger A, Laine, RM (1996) Silsesquioxanes as synthetic platforms. 3. Photocurable, liquid epoxides as inorganic/organic hybrid precursors. Chem Mater 8:1592–1593
7. Gao F, Tong Y, Schricker SR, Culbertson BM (2001) Evaluation of neat resins based on methacrylates modified with methacryl-POSS, as potential organic–Inorganic hybrids for formulating dental restoratives. Polym Adv Technol 12(6):355–360
8. Fonga Hao, Dickens Sabine H, Flaim Glenn M (2005) Evaluation of dental restorative composites containing polyhedral oligomeric silsesquioxane methacrylate, Physicomechanical evaluation of low-shrinkage dental nanocomposites based on silsesquioxane cores. Dent Mater 21:520–529
9. Soh MS, Yap AUJ, Sellinger A (2007) Physicomechanical evaluation of low-shrinkage dental Nanocomposites based on silsesquioxane cores. Eur J Oral Sci 115:230–238
10. Wua X, Sun Y, Xie W, Liu Y, Song X (2010) Development of novel dental nanocomposites reinforced with polyhedral oligomeric silsesquioxane (POSS). Dent Mater 26:456–462
11. Burujeny SB, Yeganeha H, Ataia M, Gholami H, Sorayy M (2017) Bactericidal dental nanocomposites containing1,2,3-triazolium-functionalized POSS additive prepared through thiol-ene click polymerization. Dent Mater 33(1):119–131
12. Zelmer C, Wang DK, Keen I, Hill DJT, Symons AL, Walsh LJ, Rasoul F (2016) Synthesis and characterization of POSS-(PAA)8starcopolymers and GICs for dental applications. Dent Mater 32:e82–e92

13. Rizka M, Hohlfeld L, Thanh LT, Biehl R, Lühmann N, Mohn D, Wieganda A (2017) Bioactivity and properties of a dental adhesive functionalized with polyhedral oligomeric silsesquioxanes (POSS) and bioactive glass. Dent Mater 33(9):1056–1065
14. Lavik EB, Kuppermann BD, Humayun MS (2013) Retina, vol. 1, 5th edn (Chapter 38). In: Drug delivery, pp 734–745
15. Bruschi ML (2015) Modification of drug release. In: Strategies to modify the drug release from pharmaceutical systems, pp 15–28
16. McCusker C, Carroll JB, Rotello VM (2005) Cationic polyhedral oligomeric silsesquioxane (POSS) units as carriers for drug delivery processes. Chem Commun:996–998
17. Pu Y, Zhang L, Zheng H, He B, Gu Z (2014) Synthesis and drug release of star-shaped poly(benzyl L-aspartate)-block-poly(ethylene glycol) copolymers with POSS cores. Macromol Biosci 14:289–297
18. Fan X, Hu Z, Wang G (2015) Synthesis and unimolecular micelles of amphiphilic copolymer with dendritic poly(L-lactide) core and poly(ethylene oxide) shell for drug delivery. RSC Adv 5:100816–100823
19. Li L, Lu B, Fan Q, Wu J, Wei L, Hou H, Guo X, Liu Z (2016) Synthesis and self-assembly behavior of pH-responsive star-shaped POSS-$(PCLP(DMAEMA\text{-}co\text{-}PEGMA))_{16}$ inorganic/organic hybrid block copolymer for the controlled intracellular delivery of doxorubicin. RSC Adv 6:61630–61640
20. John Ł, Malik M, Janeta M, Szafert S (2017) First step towards a model system of the drug delivery network based on amide-POSS nanocarriers. RSC Adv 7:8394–8401
21. Naderi N, Madani SY, Mosahebi A, Seifalian AM (2015) Octa-ammonium POSS-conjugated single-walled carbon nanotubes as vehicles for targeted delivery of paclitaxel. J Nano Rev 6:28297–28307
22. Jiang S, Poh YZ, Loh XJ (2015) POSS-based hybrid cationic copolymers with low aggregation potential for efficient gene delivery. RSC Adv 5:71322–71328
23. Punshona G, Vara DS, Sales KM, Kidane AG, Salacinski HJ, Seifalian AM (2005) Interactions between endothelial cells and a poly(carbonate-silsesquioxane-bridge-urea)urethane. Biomaterials 26:6271–6279
24. Kannan RY, Salacinski HJ, De Groot J, Clatworthy I, Bozec L, Horton M, Butler PE, Seifalian AM (2006) The antithrombogenic potential of a polyhedral oligomeric silsesquioxane (POSS) nanocomposite. Biomacromolecules 7:215–223
25. Kannan RY, Salacinski HJ, Sales KM, Butler PE, Seifalian AM (2006) The endothelialization of polyhedral oligomeric silsesquioxane nanocomposites an in vitro study. Cell Biochem Biophys 45(2):129–136
26. Kannana RY, Salacinskia HJ, Edirisingheb MJ, Hamilton G, Seifalian AM (2006) Polyhedral oligomeric silsequioxane–polyurethane nanocomposite microvessels for an artificial capillary bed. Biomaterials 27:4618–4626
27. Bakhshi R, Darbyshire A, Evans JE, You Z, Lu J, Seifalian AM (2011) Polymeric coating of surface modified nitinol stent with POSS-nanocomposite polymer. Colloids Surf B: Biointerfaces 86:93–105
28. Kannan RY, Salacinski HJ, Odlyha M, Butlerc PE, Seifalian AM (2006) The degradative resistance of polyhedral oligomeric silsesquioxane nanocore integrated polyurethanes: an in vitro study. Biomaterials 27:1971–1979
29. Kidane AG, Burriesci G, Edirisinghe M, Ghanbari H, Bonhoeffer P, Seifalian AM (2009) A novel nanocomposite polymer for development of synthetic heart valve leaflets 5(7):2009–2017
30. Liu J, Li K, Geng J, Zhou L, Chandrasekharan P, Yang C-T, Liu B (2013) Single molecular hyperbranched nanoprobes for fluorescence and magnetic resonance dual modal imaging. Poly Chem 4:1517–1524
31. Zhu Y-X, Jia H-R, Chen Z, Wu F-G (2017) Photosensitizer (PS)/polyhedral oligomeric silsesquioxane (POSS)-crosslinked nanohybrids for enhanced imaging-guided photodynamic cancer therapy. Nanoscale 9(35):12874–12884
32. Wang K, Peng H, Thurecht KJ, Whittaker AK (2016) Fluorinated POSS-star polymers for 19F MRI. Macromol Chem Phys 217:2262–2274

33. Ge X, Dong L, Sun L, Song Z, Wei R, Shi L, Chen H (2015) New nanoplatforms based on UCNPs linking with polyhedral oligomeric silsesquioxane (POSS) for multimodal bioimaging. Nanoscale 7(16):7206–7215

Organic–Inorganic Hybrid Materials with POSS for Coatings

Hossein Yahyaei and Mohsen Mohseni

Abstract Surface coatings are important in terms of aesthetic and protection against the environmental and harsh conditions such as corrosion, erosion, abrasion, mechanical forces. Importance of coating is due to this fact that by use of a sub-micrometer film special substrates can be protected and find an appropriate role in the application sought. However, improvement in properties of coating is so important and one of the best methods to improve their properties is using nanotechnology. Polyhedral oligomeric silsesquioxane (POSS) is a special type of silica family with the imperial structure of $RSiO_{1.5}$. This is a cage-like molecule that has been able to take on a special space in coating industry. It can affect mechanical properties (modulus, elongation at break, yield strength, impact resistance), surface properties (hydrophilicity, hydrophobicity, surface friction, and surface roughness), thermochemical properties (curing time and curing behavior), rheological properties, chemical resistance, and permeability. In this chapter, the effect of POSS addition on the mechanical properties, surface properties, flame retardant effect, and corrosion resistance has been studied.

Keywords Coating · Hybrid · Nano · POSS · Silica

1 Coating Properties

Surface coatings intended to provide special functions for different applications. Requirements for use of coatings include science and technology backing the development, production, and use of these materials. Surface coating is known as any material that may be applied as a film to a surface. The huge surface-to-volume ratio has caused many complicated matters in designing and producing coating. In coating industry, many special properties should be provided by this layer. The film should

H. Yahyaei · M. Mohseni (✉)
Department of Polymer Engineering and Color Technology, Amirkabir University of Technology, P.O. Box 15875-4413, Tehran, Iran
e-mail: mmohseni@aut.ac.ir

S. Kalia and K. Pielichowski (eds.), *Polymer/POSS Nanocomposites and Hybrid Materials*, Springer Series on Polymer and Composite Materials,
https://doi.org/10.1007/978-3-030-02327-0_12

protect the structure against attacking the environmental conditions such as mechanical and thermal shocks, UV and light as well as chemical attacks and humidity, exhibiting decorative properties. Furthermore, coatings can play an important role to provide some special function. Actually, in many cases, the coating may be not used to protect the substrate but to fulfill some functions. These functions are: hygienic, water preservation, insulating of heat and sound, hydrophobicity and hydrophilicity (self-cleaning and anti-graffiti), electromagnetic interference shielding (EMI), fire retarding, and fireproofing.

To design these coatings, many parameters should be considered to do it well.

What is the substrate?

Which type of surface preparation should be performed on the substrate before applying of coating?

How coating should be applied?

What is the film formation mechanism and condition?

What is the main duty of coating?

- Paints and coatings play a key role in today's life and include everything we use, e.g., household appliances, structures, cars, ships. Today, coatings not only preserve and beautify the substrate. They also have functional properties: They are used as anti-skid surfaces, they can save energy or act as a conductor, they can reflect or absorb light, etc.

Therefore, it needs to use new materials and improve properties of coatings by utilizing new science and technology.

As an old challenge in developed industry, human being always has attempted to combine the properties of organic and inorganic simultaneously in one material. Mollusk shells and bone were the first natural materials that inspired scientist. The most important goal to preparation of hybrid materials is not only saving the properties of each component but also enhancement of these properties and eliminating weak points. Actually, the properties of hybrid materials are not the combination of each property and novel results are always considered. These materials have been defined in different ways, but one definition could be as nanocomposites containing organic and inorganic moieties which combined at scales ranging from molecular (angstroms) to a few tens of nanometers.

2 Organic–Inorganic Coatings

Many hybrid organic–inorganic materials have been developed, to access to new area in materials science. The progress of these materials has a major effect on future applications in the fields of coating. Depending on the structures, the required properties may be easily tuned. Different possibilities and structure of hybrid materials are therefore imaginable. Actually, by choosing precursors and controlling preparation method, the interaction of phases governed the final properties of hybrid materials.

The interaction between phases is so important that the nature of the interface is utilized to divide hybrid materials into two classes.

The first includes inorganic and organic embedded by weak bonds (hydrogen, van der Waals, or ionic bonds). In the second class, two phases are connected through chemical bonds (covalent or iono-covalent bonds) [1].

To prepare hybrid materials, "top-down" or "bottom-up" method can be used. In top-down method, usually inorganic phase is ground to a nanoscale phase and then is dispersed in an organic media. The dispersion of inorganic phase in organic media is a real challenge that should overcome. Another problem in this method is preparing a hybrid with strong interaction between components; although surface treatment of nanobuilding blocks could create strong interaction, it costs energy and time. However, in bottom-up method, the disperse phase is grown by organic phase. Sol–gel processing is a versatile method to prepare hybrid materials by bottom-up method. This process is composed of two reactions: hydrolysis and condensation of precursors. Sol–gel method is very popular due to low-temperature condition and easy preparation of hybrids, but the problem is the unpredictable structure of the final product.

3 POSS-Containing Coatings

Silsesquioxane is nanobuilding blocks which caused a revolution in hybrid materials by providing its special properties. Actually, the special properties of these materials stem from its special structure. "$RSiO_{1.5}$" is the general formula of silsesquioxane and explains molar ratio of the oxygen to silicon. Silsesquioxane comes from this chemical structure; sesqui means one and half and mentions O to Si ratio. "sil" is related to silicone, and "ane" shows connection of Si to hydrocarbon.

In the formulation of silsesquioxane, R could be hydrogen or an organic substituent attached to the inorganic framework of Si–O–Si. Different organic groups or functionalities like alkyl, alkylene, aryl, arylene, or organo-functional derivatives such as vinyl, acrylate, epoxy, amine, isocyanate can be attached to the inorganic framework. Silsesquioxanes can be in different architectures like random, ladder, and cage.

Polyhedral oligomeric silsesquioxane is a cage-like structure which is the most famous structure that is used in the silsesquioxane family. Cage-like structures are in two categories: partially condensed and completely condensed form of caged structure (Fig. 1).

As shown above, $(RSiO_{1.5})_n$ is the general formula of complete condensed cages where n could be 8, 10, and 12. According to the terminology of silicon compounds, they are T_8, T_{10}, and T_{12}, respectively. Partial cage POSS contains seven silicon atoms, and this makes them different in terms of the existence of silanolic groups (SiOH) on one corner of cage and gives them special properties.

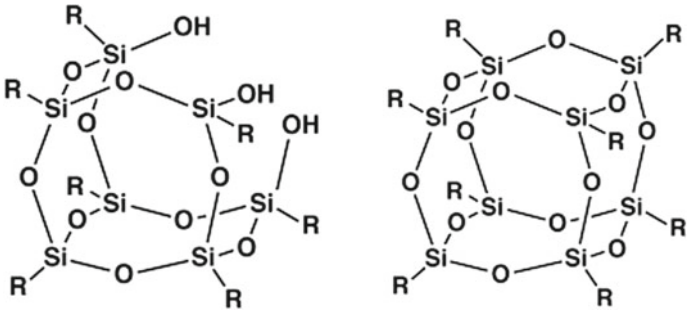

Fig. 1 Partially condensed and complete cage-like structure of silsesquioxane (POSS)

Unlike molecules in classical chemistry that usually are linear or branched, POSS molecules are cage-like. This is the main complexity of POSS that everyone can ask is it molecule or particle?

POSS analysis has shown some properties that are just for molecules:

- POSS can be dissolved in an appropriate solvent or polymer.
- It is possible to perform some characterization experiment on its structure (^{1}H or ^{29}Si NMR; mass spectroscopy and dielectric spectroscopy).
- POSS may be liquid at room temperature or solid.
- POSS can be melted and recrystallized.
- POSS can be recrystallized from a solution.
- So, POSSs are molecules that just resemble particles. When trying to determine POSS applications, it could be appropriate to look at the unusual and unique function based on the molecular structure. These can be summarized as follows where each of the features results in consequences in terms of properties:
- Complete adjustable reactivity (functional groups on the cage can react with appropriate functional groups on the polymers)
- Relatively high molecular weight
- Highly adjustable solubility
- High thermal resistance
- Rigid cage structure

These properties and many others can provide special benefits for hybrids containing POSS. The solubility is the most interesting property that POSS has. By dissolving the POSS in the solvents or polymers, the main difficulty is that using inorganic nanoparticles is eliminated. Also, the high reactivity of POSS functional groups on its corner is another important property that increases interaction of polymers with inorganic POSS structure. One of the most important concerns in utilizing hybrid coating is clarity and transparency. Compatibility between two phases causes high transparency and solubility, and reaction between two phases increases compatibility. Furthermore, POSS addition to organic coatings is robust and improves mechanical properties of coating (abrasion resistance, scratch resistance, hardness,

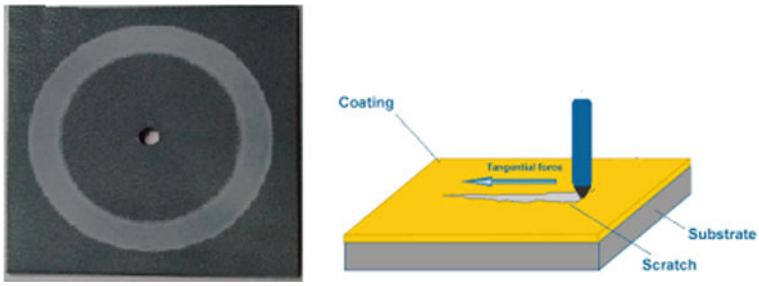

Fig. 2 Abrasion and scratch of coatings

etc). Heat resistance, hydrophobicity, permeability, and many other properties are provided by POSS that are very important issues in coating, and it is worthy to have a look at organic–inorganic hybrid materials with POSS for coatings in a different perspective.

4 Mechanical Properties

Obviously, one of the most important requirements for coating is mechanical properties. POSS with its natural stiff structure is a good candidate to improve tensile strength, elastic modulus, hardness and wear, abrasion, and scratch resistance of organic coatings (Fig. 2).

Gao et al. [2] by using a two-step approach synthesized a ladderlike polyphenylsilsesquioxane and then by nitration and reduction reaction modified to ladderlike poly(nitrophenyl)silsesquioxane (LPNPSQ) and poly(aminophenyl)silsesquioxane (LPAPSQ). Characterization by FTIR, NMR, and XRD confirmed ladderlike structure of polysilsesquioxanes (LPSQs). Also, it was confirmed that chemical modifications reduced the regularity of LPSQs. Then, the modified silsesquioxanes were incorporated into polyimide (PI) matrix. The XRD and SEM micrograph results indicated that different functional groups in LPSQs had an impaction on the interfacial interactions and the properties of the hybrids. LPNPSQ showed better dispersion. The sample containing LPAPSQ showed a better distribution of inorganic phase. This interaction between phases in hybrid affected mechanical properties. In comparison with pure PI, the tiny changes in T_g and tan δ max of PI/LPPSQ were explained by the weak hydrogen bonding. The distinct phase separation and weak interfacial interactions in PI/LPPSQ hybrid film were said the most significant reasons for the relatively low T_g. However, the physical entanglement networks in PI/LPNPSQ film lead to an enhancement of T_g and a depreciation of tan δ_{max}. Their results suggested the physical interactions were high enough to limit the motion of PI. However, chemical interactions of amino groups in LPAPSQ with the PI matrix led to significant changes in tan δ peak. The cross-linking in LPAPSQ lowering of tan δ_{max} was due

to restriction of PI chain movement. This increasing in rigidity increased T_g nearly 50 °C. The tensile experiment confirmed mechanical improvement by increasing interaction. PI/LPPSQ showed a beat lower Young's modulus (1.9 Gpa) in comparison with PI (2 Gpa). Modified LPSQs showed improvement in Young's modulus (2.3 Gpa for LPNPSQ and 2.8 Gpa for LPAPSQ) significantly.

Wang et al. [3] reported the preparation of epoxy acrylate/POSS (EA/POSS) coatings via thiol–ene photopolymerization. They modified UV cure epoxy acrylate resin by adding octamercaptopropyl polyhedral oligomeric silsesquioxane (OMP-POSS) (Fig. 3).

The conversion study showed that the addition of POSS into EA could enhance the double-bond conversion. After 1980s, the sample without POSS had 86.8% conversion, while samples containing 10 and 20 weight percent of POSS showed 91.3 and 98.4% double-bond conversion, respectively. They explained that the quicker thiol–ene reaction prefers to react with double bonds, and then the residual acrylates begin to homopolymerize, both contributing to the consumption of double bonds. The ^{1}H NMR was used and confirmed this hypothesis. TEM and XRD are utilized to study the morphology of hybrid coatings. The X-ray diffraction showed no crystallization of POSS in hybrid coatings. No phase separation and well homogenous dispersion of POSS in the epoxy acrylate resins were indicated in TEM images.

In order to investigate mechanical properties, DMTA has been used. Significant decreasing of T_g was reported by increasing POSS content. This phenomenon has been explained that mercapto groups around POSS cages onto acrylates were flexible, which greatly reduce the stiffness of the polymer chains and contributed to the chain motion at a lower temperature. The decrease in storage modulus was explained in this point, as well.

Thermal degradation of samples was investigated by using thermogravimetric analysis (TGA), and the result showed better heat resistance of hybrids. The blank epoxy acrylate coating presented only one degradation stage with the temperature at its maximum mass loss rate at 439 °C. The sample containing 20% POSS the early decomposition of EA was 418 °C, but retarded the degradation of some moieties in EA

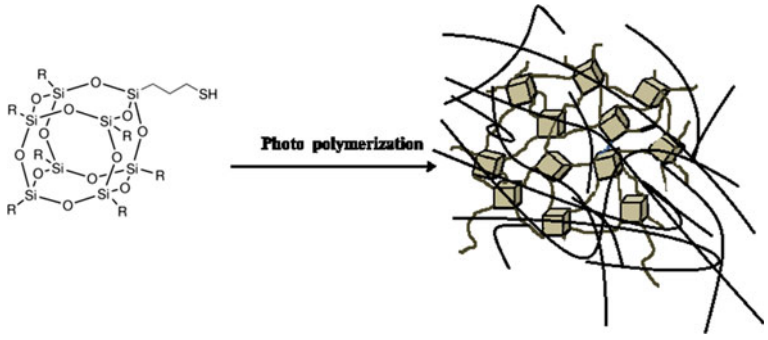

Fig. 3 Formation of hybrid coating by photopolymerization of epoxy acrylate/POSS (EA/POSS)

in the high temperature range of 480–600 °C. It was found that OMP-POSS revealed a double effect on the thermal stability of EA/POSS hybrid networks: The weak thioether linkages led to the premature degradation of EA/POSS nanocomposites, while POSS cage could give a well protective effect on the aromatic groups and on carbonaceous char. The XPS was used to analyze the residue of sample containing 20 wt% of POSS at various temperatures, and POSS could well support the carbonaceous char from thermal-oxidative degradation at 600 °C.

Gao et al. [4] modified a waterborne epoxy acrylate (EA) coating modified with methylacryloylpropyl polyhedral oligomeric silsesquioxanes (MAP-POSSs). DSC and FTIR were used to study the curing reaction and non-isothermal cure kinetics of the EA coating containing different amounts of MAP-POSS. These results showed that it is possible to describe of the non-isothermal curing process by Kissinger method and a two-parameter autocatalytic ˇSesták–Berggren (S–B) model. The UV-curing property of nanocomposite coating containing POSS was higher than that of pure polymeric coating. In DMTA, it was observed that addition of 12 wt% MAP-POSS increased T_g about 9.5 °C in comparison with pure epoxy acrylate coating. The addition of MAP-POSS increased the heat resistance of hybrid coatings. Furthermore, the residual rates of the nanocomposites at high temperature were more than that of pure epoxy acrylate coating.

Yari and coworkers [5, 6] studied the effect of POSS on thermal, rheological, and mechanical properties of an automotive acrylic/melamine coating. They used eight hydroxyl functional POSSs in different loadings that can react with melamine component and form a covalent bond with organic phase (Fig. 4).

They reported that POSS could effectively enhance the total cross-linking of the clearcoat when it was incorporated into the clearcoat. They observed that POSS at lower loadings enhanced cross-link density slightly, but a significant enhancement was observed at 15 at a higher percent of POSS. These results have been contributed to higher curing degree of clearcoat in the presence of POSS which was confirmed in FTIR study. Good correlation between total intensity of ether and methylene bridges with cross-linking density was found and confirmed that POSS via easing the curing reactions intensifies the cross-linking density. They supposed that the higher conversion and cross-link density could be due to the affection of POSS on viscosity. Therefore, viscosity at different shear rates was measured and it was seen that addition of POSS is highly pronounced to decrease the viscosity. As the POSS loading increased, the viscosity regularly decreased. It was explained that the more compact structure of POSS relative to the long linear chains of acrylic resulted in less chain entanglements in the formulation, leading to a higher level of chain flexibility and thus a significant decrease in viscosity. ‘Also, it was observed that by adding 5 and 10% POSS, glass transition temperature decreased and at higher POSS loadings T_g behaved inversely and increased. The addition of POSS in 5 and 10% increased storage modulus at glassy region slightly (8.003, 8.13, and 9.26 MPa for blank and hybrid containing 5 and 10 wt% POSS, respectively), but addition of POSS in higher loadings (15 and 25 wt%) storage modulus increased significantly (24.87 and 3.1 MPa). The dispersion of POSS in the acrylic/melamine matrix was studied by TEM. It was revealed that POSS building blocks have been dispersed on a molecular

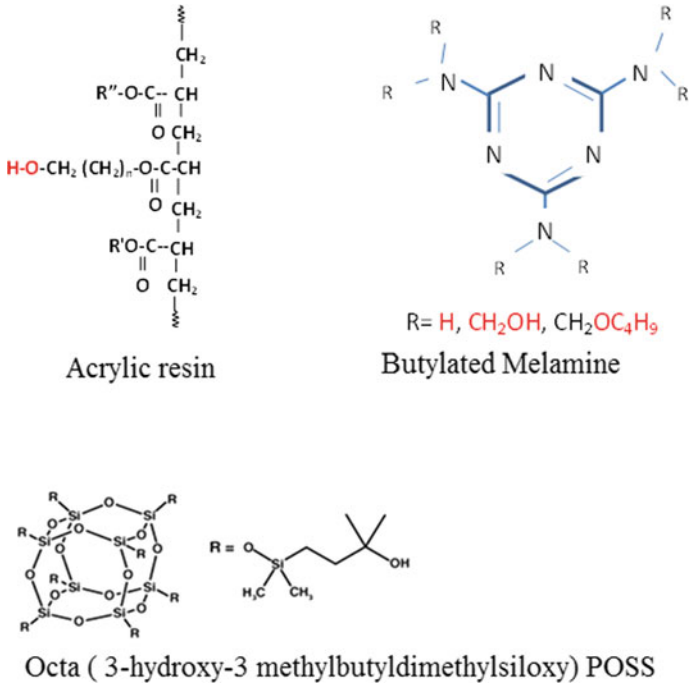

Fig. 4 Chemical structure of acrylic resin, butylated melamine, and POSS

level and no trace of POSS aggregation was observed. Molecular dispersion of POSS was occurred then due to the high compatibility of POSS and the acrylic/melamine matrix. The hydroxyl groups on the pendant organic chains on the corner of POSS as well as covalent bonding of POSS to the matrix helped compatibility and prevented POSS aggregation. In a tensile experiment, it was observed that addition of POSS increased elastic modulus from 2.04 GPa for blank sample to 2.4 GPa for sample containing 25% POSS. Elongation at break showed a maximum amount in 10% POSS. By addition of POSS up to 10% elongation at break increased and then it depreciated. The similar behavior was observed for toughening. It was mentioned that free volume and flexibility increasing were the main mechanism to improve toughening of acrylic/melamine matrix.

Ghermezcheshme et al. [7] studied the role of hydroxyl functionality of POSS and polyol in hardness and scratch improvement of 2 k polyurethane coating. They used a two-functional and an eight-functional POSS (Fig. 5) and added them into two polyester polyol resins with 3.4 and 5.7 hydroxyl percent and cured coating by a biuret polyisocyanate.

Their results showed that strong chemical interaction between POSS and organic phase is a necessary requirement to achieve transparent hybrid clearcoat. They support this idea by FTIR and UV–Visible spectrophotometry. The indentation and nanoscratch experiment showed that addition of a two-functional POSS reduced

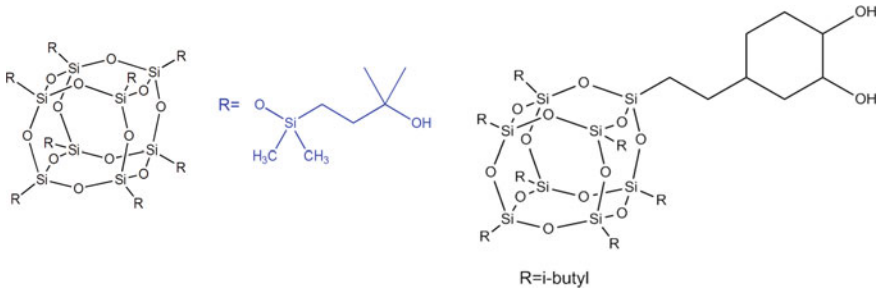

Fig. 5 Chemical structure of 2 and 8 hydroxyl functional POSS

mechanical properties like scratch resistance and hardness due to lower cross-link density and increased free volume. Although the addition of an eight-functional hydroxyl could increase in elastic modulus of low hydroxyl percent sample, the elastic modulus of high hydroxyl polyol reduced by addition of two- and eight-functional hydroxyl POSS.

Liu et al. [8] modified a non-isocyanate polyurethane by adding POSS. They prepared a series of bio-based non-isocyanate polyurethane (NIPU) coatings by the ring-opening polymerization of rosin-based cyclic carbonate with amines. The NIPUs were modified with epoxy and cyclic carbonate-functionalized polyhedral oligomeric silsesquioxanes (POSSs) to make NIPU/POSS coatings, respectively.

The thermal stabilities, hardness, and water tolerance of the NIPU/POSS coatings were enhanced by increasing of the POSS dosage. However, in comparison with the neat NIPU coatings without POSS, flexibility, adhesion and the impact strength of NIPU/POSS coatings were not influenced significantly.

Ma and He [9] by combining atom transfer radical polymerization (ATRP) technique, epoxy opening reaction, and free radical polymerization grafted a nanoscaled methacrylisobutyl polyhedral oligomeric silsesquioxane (MA-POSS) onto glycidyl methacrylate (GMA) and prepared organic–inorganic hybrid. In this paper, it was expected to improve the thermal stability of prepared PGMA-g-P(MA-POSS) hybrid by the insertion of MA-POSS into PGMA matrix and by the formation of the cross-linking network developed via curing reaction to inhibit the movements of chains. Differential scanning calorimetry (DSC) showed glass transition temperature increase to 135 °C for hybrid in comparison to pure PGMA (T_g = 76 °C) in was about two folds. Therefore, the incorporation of MA-POSS with the large bulky side will slow the polymer mobility and therefore resulted in higher T_g. Also, the hybrid provided films with surface roughness about 0.19–14.4 nm, a significant water resistance (static contact angle about 113–123°), high thermal stability (Td = 300–600 °C), and strong adhesive strength (216–333 N).

5 Surface Properties

Physical chemistry of surfaces is very important which is adjustable by using surface coatings. Hydrophilicity and hydrophobicity are two important features of surfaces that are determined by water contact angle experiment. The contact angle higher than 90° shows hydrophobic surface, while the surface with contact angle lower than 90° is a hydrophilic surface (Fig. 6).

POSS molecules have this ability to segregate into the surface and govern surface properties of hybrid coating (Fig. 7). This migration depends on compatibility of POSS with matrix and quiddity of groups connected to the corner and concentration of POSS. Therefore, POSS has been used in many researches to achieve preferential surface properties.

Li et al. [10] used reversible addition–fragmentation chain transfer (RAFT) polymerization to synthesis fluorosilicone block copolymers containing polyhe-

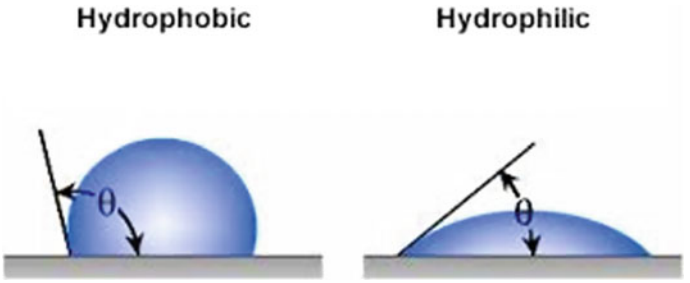

Fig. 6 Hydrophobic and hydrophilic surfaces

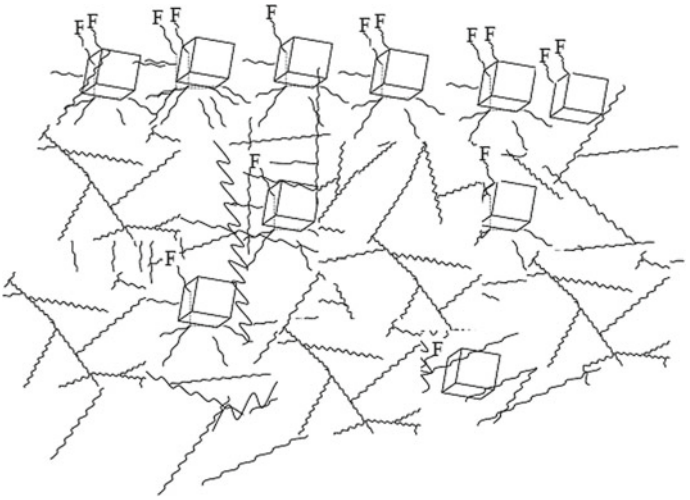

Fig. 7 POSS migration on the surface of coatings

dral oligomeric silsesquioxane (POSS) and used polydimethylsiloxane (PDMS) macrochain transfer agent with trithiocarbonate groups at both ends. Acryloisobutyl POSS (APOSS) and 2,2,3,4,4,4-hexafluorobutyl acrylate (HFBA) were sequentially introduced into the copolymers. At the first 6 h of polymerization, triblock copolymer exhibited a low polydispersity index (PDI) of less than 1.42, but due to the configuration of the POSS macromere the broader PDI value was observed, increased PDI up to about 2, and showed clear microphase separation. It was sought that the POSS-containing fluorosilicone block copolymers can combine the advantages of PDMS and poly(fluoroalkyl acrylate), and that the incorporation of APOSS can modify the topological surfaces. Characterizations of the prepared copolymers were performed to confirm the macromolecular structure, microphase separation structure, and the surface topology of the coatings. The XRD experiment showed that by increasing of POSS content in polymer, diffraction peaks at $\theta = 8.3°$, 10.6°, and 18.6° that correspond to the diffraction pattern of the rhombohedral unit cell due to crystallization of the POSS structure were appeared. The SEM micrographs showed globular pits in the range of 200–300 nm due to the different migration velocities of the PDMS and fluorine blocks to air during solvent annealing, as well as the block fractions of both components. Because of its lower surface energy compared with that of PDMS, the fluorine block migrated easier to the air side during the drying process. The roughness data (R_q) from AFM analysis was also obtained and increased by increasing POSS content. The POSS units were prone to make a cluster in the polymer blocks and migrated to the polymer surfaces and increased surface roughness.

The purpose of their study was preparation of a low surface energy coating with hydrophobic microphase domains that could be used as anti-icing, anti-frosting, and other non-wetting applications. For this purpose, water contact angle was measured to check water wettability and hydrophobicity. Static and dynamic contact angle was measured. Because of the presence of POSS, water contact angle increased. As mentioned in AFM images, the more presence of POSS increased surface roughness and it caused a significant increase in the receding angle value. It has been suggested that the increased surface roughness generated by POSS had a more important effect on water contact angle than surface composition does like fluorine material. It was found that the higher content of the fluorine blocks is not suitable for anti-icing because it can enhance the interaction between the polymer surface and water. Consequently, the ice shear strength has a direct relationship with the chemical structure and surface morphology. Introducing POSS could possibly improve the anti-icing and anti-frosting properties of a polymer film by decreasing its water receding angle or its contact angle hysteresis.

Yang et al. [11] synthesized a novel hybrid of PDMS-b-PMMAm-b-P(MA-POSS)$_n$ by linear polydimethylsiloxane (PDMS) macro-initiator initiating methyl methacrylate (MMA) and caged methacrylisobutyl polyhedral oligomeric silsesquioxane (MA-POSS) via a two-step ATRP technique. The different polymers were synthesized by different permutations of monomers and macromers. SEC-MALLS instrument equipped with a viscometer was used to measure molecular weight, and it showed molecular weight of 50,090–58,650 g mol^{-1} and poly disparity index of 1.215–1.391. With the increase of P(MA-POSS)$_n$ content to 23.93% wt, the

glass transition temperature of polymers was increased from 95 °C to 137 °C, and the corresponding storage modulus of mechanical property was raised from 579 ± 3 MPa to 902 ± 5 MPa. It was revealed that the surface roughness and water contact angle were dependent on solvent of polymer solution. It was observed that by using $CHCl_3$ as solvent the water contact angle was higher when THF was used as solvent. The reason is that core/shell micelles of PMMA core and PDMS/P(MA-POSS) shell formed in $CHCl_3$ solution are likely migrated. PDMS and P(MA-POSS) come onto film surface, improve the surface roughness (2.480 nm), and form silicon-rich domain on the surface (14.62%) than 220 nm P(MA-POSS) core/PMMA shell/PDMS-corona micelles formed in THF solution (0.906 nm, 7.86%). It was concluded that THF is better to obtain PDMS-rich surface, and $CHCl_3$ is suitable for the migration of P(MA-POSS) onto the film surface.

Chen et al. [12] reacted poly(1,4-butylene adipate) end-capped diol (PBAD) and 2,2-bis(hydroxymethyl) butyric acid (DMBA) with isophorone diisocyanate (IPDI) and synthesized a diisocyanate-terminated PU prepolymer. Then, monofunctional aminopropyl isobutyl POSS (AIPOSS) and with (3-aminopropyl) triethoxysilane (APTES) were used together to block the PU chain. Thus, waterborne polyurethane (WPU) hybrid coatings modified with 2–8 wt% POSS were obtained.

The XRD experiment showed a peak at 8.1° belongs to POSS and by increasing of POSS content the intensity of this peak increased. Scherrer rule was used, and the crystalline grain thickness was estimated about 3 nm. It was distinguished that 3 nm is significantly smaller in comparison with PU/POSS prepared with other methods in the literature which can be corresponded to the kinetic limitation, possibly because of the existence of the chemical cross-linking network. Furthermore, the film formation process of particle coalescence typical in polymer dispersions is also not favored for the production of large crystalline domains. The nanoreinforcement of the POSS cages on PU was confirmed by increasing elastic modulus and tensile strength, where the tensile strength increased from 12.9 MPa to 22.9 MPa and the elastic modulus increased from 12.9 MPa to 51.1 MPa for PU and PU containing 8 wt% POSS, respectively.

The surface composition of the hybrid films is demonstrated by XPS data. The Si-to-N ratio was chosen as criteria, and the higher ratio for sample containing 8 wt% POSS was corresponded to the self-stratification of the Si moieties. This emigration of POSS on the surface should increase hydrophobicity and decrease surface energy. Therefore, water contact angle was used and it revealed surface hydrophobicity of coating which water contact angle increased from 92° for PU without POSS to 104° for sample containing 8 wt% POSS.

Chouwatat et al. [13] prepared UV-cured hybrid coating and applied on polymethyl methacrylate as substrate. They used pentaerythritol triacrylate (PETA), trimethylolpropane ethoxylate triacrylate as organic phase that 1-hydroxycyclohexyl phenyl ketone (photo-initiator) was used as photo-initiator. Multifunctional methylmethacrylate-POSS (MA8POSS) was used as inorganic phase and in different loadings. The introduction of MA8POSS loadings less than 10 wt% showed low surface segregation led to a superior scratch resistance, whereas the films containing high load of MA8POSS showed poor scratch resistance. Water and diiodomethane

were used to measure static contact angle. Addition of POSS in 3 wt% increased water contact angle of blank sample from 61.9° to 69.8°. The water contact angle increased to 72.2° in 10 wt% POSS sample, but more loadings of POSS did not have a significant effect on water contact angle. The similar trend was observed for diiodomethane contact angle. Actually, POSS addition decreased total surface energy, especially polar component of surface energy decrease.

Zhang et al. [14] used a methacrylated POSS and perfluorooctyl methacrylate (13FMA) or 2-perfluorooctyl ethyl methacrylate (17FMA). The dithioester ends of the copolymers were converted to thiol groups and then mixed with vinyl-functionalized PDMS (PDMS-V) and thiol-functionalized PDMS (PDMS-SH). Fluorinated methacrylate block copolymers were synthesized by reversible addition–fragmentation chain transfer polymerization and transformed into thiolated copolymers by aminolysis to control the self-assembly and modify surface morphology. TEM was used to investigate bulk morphology, and 500-nm aggregate diameter of POSS was observed. In AFM images and XPS, results confirmed that the longer fluorinated side chains in S17F provided greater hydrophobic performance than the shorter one in S13F because of the lower surface energy and the limited surface mobility that prevented local remodeling of the surface. Also, in AFM images, it was mentioned that POSS did not have any significant effect on roughness. Static, receding, and advancing contact angle and hysteresis were measured to assess surface properties of coatings. All the UV-cured coatings exhibited WCA above 102°. As compared with S13F-containing coatings, S17F-containing coatings presented higher WCA (113–116.5°), enhanced receding contact angles (100–113°), lower hysteresis as well as lower surface energies. Also, it was confirmed that samples containing longer fluorinated chains showed better iceophobic properties. They concluded that the UV-curable POSS-fluorinated diblock copolymers can be a good alternative for ice phobic coating.

Pan et al. [15] synthesized linear/star-shaped fluoropolymer coating containing POSS. It was revealed that surface composition and self-assembled micelles of coatings are dependent on solvent and in consequence surface hydrophobicity is influenced.

Ma et al. [16] investigated the effect of two different POSSs on properties of poly glycidyl methacrylate (PGMA) matrix and compared the effect of a cage-like structure of POSS with a linear polysiloxane. Methacrylisobutyl polyhedral oligomeric silsesquioxane (MA-POSS) via free radical polymerization was added to glycidyl methacrylate (GMA), and P(GMA/MA-POSS) copolymer was prepared.

Aminopropyllsobutyl POSS (NH_2-POSS) was another cage-like POSS that was added into PGMA and PGMA/NH2-POSS prepared. The last hybrid which was synthesized (PGMA/NH_2-PDMS) was prepared by addition of NH_2-PDMS into PGMA. The results revealed that based on the tendency of POSS to agglomerate on the surface of coating, the samples containing POSS showed more heterogeneous surfaces than PGMA/NH_2-PDMS coating. MA-POSS showed better compatibility with matrix and higher transmission (98%), while PMGA/NH_2-POSS showed lower transmission (24%) and it was similar to PGMA/NH_2-PDMS film (27%) that is signed which revealed incompatibility of NH_2-POSS and NH_2-PDMS with matrix.

P(GMA/MA-POSS) showed high adhesive strength (1113 N) and thermos-stability ($T_g = 282$ °C). However, flexible PDMS improves PGMA/NH_2-PDMS hybrid with much higher storage modulus (519 MPa) than PGMA/NH_2-POSS (271 MPa), which indicated that PDMS is an advantage in enhancing the film stiffness than POSS cages. Also, samples containing cage-like POSS showed higher permeability in comparison with linear PDMS.

PGMA/NH_2-PDMS coating showed the highest water contact angle of ca. 109.1°. PGMA/NH_2-PDMS showed 104.4°, and it was about 94.8° for P(GMA/MA-POSS). It can be related to the surface segregation of NH_2-POSS and PDMS because of incompatibility with matrix as it was observed in transparency.

One of the most important challenges of using nanoparticles in polymeric coatings is dispersion of nanoparticle in matrix. Surface treatment or surface modification can improve dispersibility of pigment in the polymeric matrix. Surface modification can be performed by polymeric surfactant that interacts with inorganic filler by non-covalent interaction. This surfactant becomes attached to the particle surface by presumed adsorption of the polar groups via electrostatic interactions or by stronger interactions between most common alkoxysilanes and the particle surface. The functionalization of TiO_2 nanoparticles by grafting amino propyl trimethoxy silane is an example of the use of silane for modification of the particle in order to prepare stable non-agglomerated dispersion of nanoparticles. Actually, silanol on the organosilane materials can react with M-OH (M shows the metal element of inorganic fillers) and Si-OH on the open-cage POSS can react with M-OH as well. Organosilane could self-condense together, and this reaction competes compared to reaction onto the metal or filler surface. The trisilanol bonds the POSS to the surface, and the –R groups on the POSS are selected because it is compatible with (similar polarity to) organic coating. Thus, alkyl –R groups are convenient for polyolefins like PE, PP, and COC, whereas for more polar polymers a more polar –R group may be beneficial. For reactive coatings and thermosets, a reactive –R group on the POSS is better. The dispersion imparted by the POSS is impressive. The particle size of the TiO_2 is reduced from 100 to 30 nm. This results in better impact resistance in the pigmented system, and less TiO_2 is needed to achieve the desired whiteness. Only a few reports exist on trisilanol POSS molecules as dispersants.

Godnjavec et al. [16] used POSS to treated surface of TiO_2. They prepared rutile crystal structure of TiO_2 nanoparticles by using sulfate process and surface treated by precipitation with Al_2O_3. The aqueous dispersion of Al_2O_3 treated TiO_2 was in weight ratio of 10 to 1 related to POSS was added into solution of HCl in water and shake for 2 min. Then, the mixture was agitated for 6 h at 70 °C. The TiO_2–Al_2O_3 and TiO_2–Al_2O_3–POSS were added into a water-based acrylic 0.6 wt% and stirred for 20 min and 1000 rpm. The FTIR and TGA analysis were used to characterize TiO_2–Al_2O_3–POSS. In FTIR band corresponding to CH_3 at 2950 and 1230 cm^{-1} indicated the free sites on the TiO_2 surface by POSS. POSS, TiO_2–Al_2O_3, and TiO_2–Al_2O_3–POSS were characterized by TGA. Decomposition of POSS started at 190 °C and finished at 520 °C. The weight loss of untreated TiO_2–Al_2O_3 has been attributed to the absorbed organic surface-active compounds. The weight loss of POSS-treated sample was about 0.97% which was attributed to organic groups

of POSS on the surface of TiO_2–Al_2O_3. Zeta potential of POSS-treated and POSS-untreated TiO_2–Al_2O_3 was measured and showed different values. The zeta potential for untreated sample was −29.9 mV and for POSS-treated sample −39.8 mV. The particle size was measured by dynamic light scattering (DLS). The average particle size of untreated sample was 736.9 nm and POSS-treated sample was 274.9 nm. Also, particle size distribution of samples was compared and observed that the sample TiO_2–Al_2O_3 contained two different scattering centers, whereas monodisperse particle size for sample TiO_2–Al_2O_3–POSS was observed that was attributed to lower agglomeration tendency.

Mihelčič et al. [17] treated the surface of anatase with heptaisobutyl silsesquioxane dispersant (trisilanol POSS) in butanol and hexane. Adsorption of trisilanol POSS on the surface of the pigment particles was determined from the FTIR. Vibrational bands of trisilanol POSS and trisilanol POSS adsorbed on pigment were determined and their changes attributed to the H bond interactions of the SiOH groups. Direct evidence of the formation of a dispersant layer on the pigment surface was obtained from TEM and EDAX measurements. The pigment coatings prepared from dispersions of trisilanol POSS dispersant showed much lower haze than coatings without them.

6 Flame Retardancy Effect of POSS

Polymeric coatings have a special role to protect and aesthetic aspect of substrate. But, they are flammable and this behavior to ignite and/or burn restricted their application (Fig. 8).

Halogens are a good option to use as a fire retardant, but the environmental issues are important and it is not rational to avoid a presumptive risk by a decisive risk. Using heat-resistant inorganic materials could be a good idea. This inorganic material does not have any bad effect on the environment, improves mechanical properties, and at the same time increases heat resistance and fire retardancy. Some inorganic

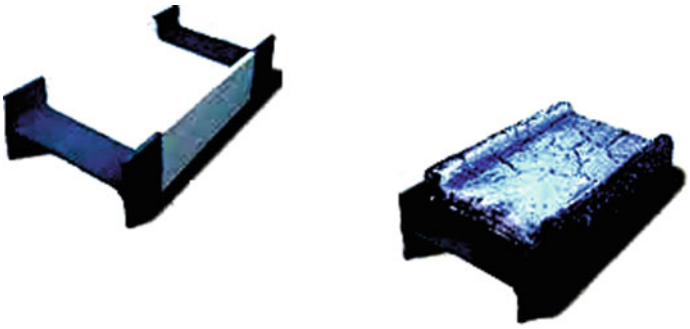

Fig. 8 Fire exposure of coatings

oxide like antimony trioxide cannot improve fire retardancy individually and just can have some synergistic effect if used with bromine or intumescent fire retardants [18]. However, nanosized inorganic fillers showed fire retardant effect even in low dosages, while improving mechanical properties. In this regard, POSS is a good choice due to the environmental neutrality, good heat resistance as well as high thermoxidative stability.

Wu et al. [19] improved flame retardancy of epoxy coating by POSS. The silanol group of an open-cage POSS (trisilanolisobutyl-POSS) was reacted with epoxy group of triglycidyl isocyanurate (TGIC) in the presence of tin chloride as catalyst, and a two epoxy functional POSS (NPOSS) was obtained.

Ten wt% of NPOSS was dispersed in DGEBA, and m-phenylenediamine was added as curing agent. FTIR and ^{29}Si NMR were used to characterize the structure of NPOSS.

Microscale combustion calorimeter (MCC) uses thermal analysis methods to measure chemical properties needed for fire resistance. The heat release rate (HRR) and total heat release (THR) for epoxy coating were 553.5 w/g and 24.6 kJ/g., respectively. Two overlapping peaks in HRR curve of NPOSS/EP were observed: first peak HRR = 13.8, and second peak HRR = 368.8 w/g, THR = 24.7 kJ/g. Though the addition of NPOSS does not significantly change the THR, the peak HRR is sharply reduced. It was concluded that the incorporation of NPOSS into the EP had been preferred for improving the flame retardancy of epoxy coating. DSC experiment showed a higher glass transition temperature of NPOSS/EP (166 °C) than neat epoxy coating (145 °C). TGA experiment showed that the thermal-oxidative degradation process of NPOSS is composed of three steps and their corresponding T_{max} was between 192 and 517 °C, respectively. During thermal degradation, EP is easily broken and releases material containing small molecules, such as CO_2 and CO. However, EP/NPOSS releases mainly methyl-substituted, carbonyl, and aromatic ring compounds with greater molecular weight compared with that of EP.

Cakmakc [20] investigated the synergistic effect of a nitrogen and phosphorus containing reactive monomer, allylamino diphenylphosphine oxide (AADPPO or allyl phosphinic amide-APA) and octamercaptopropyl polyhedraloligomeric silsesquioxane (POSS-8SH) on the flame retardancy of photocured epoxy acrylate-based coatings. The addition of POSS-8SH improved double-bond conversion significantly and in consequence affected mechanical properties. For example, pendulum hardness trend was 136, 141, and 154 for sample containing 2.5, 5, and 10 wt% POSS, respectively. Tensile modulus, tensile strength, and elongation at break were increased by increasing POSS content. The char at 700 °C was reported, 0.8 for sample without POSS and 4.8, 11, and 12.5 for samples containing 2.5, 5, and 10% POSS. The addition of APA improved the thermal properties and the flame retardancy of the coatings, but decreased the modulus and the tensile strength. POSS-8SH was found to adversely affect the flame resistance of the coatings.

7 Corrosion-Resistant Coating Containing POSS

Corrosion is an important phenomenon, and one of the most important duties of coating is protection of metallic surfaces against the corrosive environments. Different materials have been used to improve corrosion resistance of organic coatings. Corrosion inhibitor and different types of pigment and fillers were used to confront with corrosion. POSS due to the mentioned properties could be a good idea to incorporate into the organic coating and improve corrosion resistance of coatings.

Lai et al. [21] added trans-cyclohexane diolisobuty-POSS into a polyurethane consisting of hydroxyl terminated polybutadiene (HTPB) and isophorone diisocyanate (IPDI). The hybrid coatings were applied by spin coating onto an aluminum alloy sheet in order to improve the corrosion protection. Gel permeation chromatography (GPC) was used to investigate molecular weight of hybrid coatings. GPC showed lower molecular weight of hybrids than pure PU, and it decreased by increasing POSS content. It was attributed to the steric hindrance arising from POSS when polymerized. FTIR analysis confirmed that the curing reactions in the hybrids were carried out to completion. T_g, hardness, and heat resistance increased with increasing POSS content.

Bode plots of log Z–log Freq revealed high impedance at low frequency for PU and PU/POSS and reflected capacitive behavior.

In comparison with the value for the untreated aluminum samples ($2.48–8.22 \times 10^{-3}$ Acm^{-2}), the measured corrosion electric current (I_{corr}) value decreased significantly for the PU/POSS hybrids on the AA (1.24×10^{-6}–7.61×10^{-8} Acm^{-2}) and was lower than that of the PU film ($1.32–1.37 \times 10^{-5}$ Acm^{-2}).

The result was due to the production of denser films that were correspondingly less susceptible to localized pitting.

Rodošek et al. [22] added POSS into polydimethylsiloxane (PDMS) and applied it on Aluminum 2024 to protect it against corrosion. The coatings were subjected to ex situ and in situ vibrational spectroscopies to follow the changes in the bands of protective coatings during forced anodic polarization. The ex situ IR RA bands of coatings with 0.2 POSS did not reveal any intensity decrease up to potential _0.1 V/Ag/AgCl/KClsat, while the intensity of PDMS bands of coatings without POSS decreased by about 16%, up to the same potential. On average, the coatings revealed only slight decrease in intensity of bands during anodic polarization, but the areas at which the pitting corrosion started became characterized by a significant decrease in the bands' intensity.

8 Conclusion

In this study, the impact of POSS addition on the different properties of coating has been studied. It was found that the addition of POSS could improve mechanical properties of coatings. This enhancement depends on quality of dispersion, functionality

of POSS, and POSS polymeric matrix interaction. Depending on the POSS–matrix interaction and functionality of POSS, cross-link density and glass transition temperature increase or decrease. POSS with fluorinated moieties can increase water contact angle and hydrophobicity. Also, POSS can improve thermal resistance of coating and the ability of POSS for fire retardancy has been reported. Using of POSS in corrosion protective coatings was a promising experience. The addition of POSS can reduce corrosion electric current.

References

1. Sanchez C, Julia´n B, Belleville P, Popall M (2005) Applications of hybrid organic–inorganic Nanocomposites. J Mater Chem 15:3559–3592
2. Gao Q, Qi S, Wu Z, Wu D, Yang W (2011) Synthesis and characterization of functional ladder-like polysilsesquioxane and their hybrid films with polyimide, Thin Solid Films 519:6499–6507
3. Wang X, Wang X, Song L, Xing W, Tang G, Hu W, Hu Y (2013) Preparation and thermal stability of UV-cured epoxy-based coatings modified with octamercaptopropyl POSS. Thermochimica Acta, 568:130–139
4. Gao J, Lv H, Zhang X, Zhao H (2013) Synthesis and properties of waterborne epoxy acrylate nanocomposite coating modified by MAP-POSS. Prog Org Coat 76:1477–1483
5. Yari H, Mohseni M (2015) Curing and thermo-mechanical studies of a modified thermosetting clearcoat containing OH-functional POSS nanocages. Prog Org Coat 87:129–137
6. Yari H, Mohseni M, Messori M (2015) Toughened acrylic/melamine thermosetting clear coats using POSS molecules: mechanical and morphological studies. Polymer 63:19–29
7. Ghermezcheshme H, Mohseni M, Yahyaei H (2015) Use of nanoindentaion and nanoscratch experiments to reveal the mechanical behavior of POSS containing polyurethane nanocomposite coatings: the role of functionality, Tribol Int 88:66–75
8. Liu G, Guomin W, Chen J, Kong Z (2016) Synthesis, modification and properties of rosin-based non-isocyanatepolyurethanes coatings. Prog Org Coat 101:461–467
9. Ma Y, He L (2017) POSS-pendanted in epoxy chain inorganic-organic hybrid for highly thermomechanical, permeable and hydrothermal-resistant coatings. Mater Chem Phys 201:120–129
10. Li B, Li X, Zhang K, Li H, Zhao Y, Ren L, Yuan X (2015) Synthesis of POSS-containing fluorosilicone block copolymers viaRAFT polymerization for application as non-wetting coating materials. Prog Org Coat 78:188–199
11. Yang S, Pan A, He L (2015) Organic/inorganic hybrids by linear PDMS and caged MA-POSS for coating. Mater Chem Phys 153:396–404
12. Chen S, Guo L, Du D, Rui J, Qiu T, Ye J, Li X (2016) Waterborne POSS-silane-urethane hybrid polymer and the fluorinated films. Polymer 103:27–35
13. Chouwatat P, Nojima S, Higaki Y, Kojio K, Hirai T, Kotaki M, Takahara A (2016) An effect of surface segregation of polyhedral oligomeric silsesquioxanes on surface physical properties of acrylic hard coating materials Polymer 84:81–88
14. Zhang K, Li X, Zhao Y, Zhu K, Li Y, Tao C, Yuan X (2016) UV-curable POSS-fluorinated methacrylate diblock copolymers for icephobic coatings. Prog Org Coat 93:87–96
15. Pana A, Hea L, Wangb L, Xi N (2016) POSS-based diblock fluoropolymer for self-assembled hydrophobic coatings. Mater Today Proc 3:325–334
16. Godnjavec J, Znoj B, Veronovski N, Venturini P (2012) Polyhedral oligomeric silsesquioxanes as titanium dioxide surface modifiers for transparent acrylic UV blocking hybrid coating. Prog Org Coat 74:654–659
17. Mihelčič M, Francetič V, Pori P, Gradišar H, Kovač J, Orel B (2014) Electrochromic coatings made of surface modified rutile and anatase pigments: influence of trisilanol POSS dispersant on electrochromic effect. App Surf Sci 313:484–497

18. Zhang W, Camino G, Yang R (2017) Polymer/polyhedral oligomeric silsesquioxane (POSS) nanocomposites: an overview of fire retardance. Prog Polym Sci 67:77–125
19. Wu K, Song L, Hu Y, Lu H, Kandola BK, Kandare E (2009) Synthesis and characterization of a functional polyhedral oligomeric silsesquioxane and its flame retardancy in epoxy resin. Prog Organic Coatings 65:490–497.
20. Cakmakc E (2017) Allylamino diphenylphosphine oxide and poss containing flameretardant photocured hybrid coatings. Prog Org Coat 105:37–47
21. Lai YS, Tsai CW, Yang HW, Wang GP, Wu KH (2009) Structural and electrochemical properties of polyurethanes/polyhedral oligomeric silsesquioxanes (PU/POSS) hybrid coatings on aluminum alloys. Mater Chem Phys 117:91–98
22. Rodošek M, Rauter A, Perše LS, Kek DM, Vuk AŠ (2014) Vibrational and corrosion properties of poly(dimethylsiloxane)-based protective coatings for AA 2024 modified with nanosized polyhedral oligomeric silsesquioxane, 85:193–203

Decomposition and Ageing of Hybrid Materials with POSS

Ignazio Blanco

Abstract The use of polyhedral oligomeric silsesquioxanes (POSSs), as reinforcing agent for making polymer composites and nanocomposites, recorded an exponential grown in the last two decades. Differently to the other most used fillers POSSs are molecules, thus combining their nanosized cage structures that have dimensions comparable with those of most polymer segments and a particular and exclusive chemical composition. These characteristics linked with their hybrid (inorganic–organic) nature allow the researchers to obtain multifunctional materials with intermediate properties between those of organic polymers and ceramics. In this chapter, the most common POSS–polymer composites, namely epoxies, polypropylene, polystyrene, polylactide, polyimides and polyurethane, were analysed in their thermal behaviour.

Keywords POSS · Thermal stability · Nanocomposites · Thermogravimetry Hybrid materials · Ageing

1 Introduction

Composite can be considered as the well-defined platform materials of the twenty-first century and represent today an important slice of the market in the production of modern plastics. The principle of their design is based on the adding of a second component to polymeric materials with the aim to enhance, primarily, thermal stability and/or mechanical strength. It is widely recognized in the literature that among composites, organic–inorganic hybrid materials offer advantageous performance relative to either of the non-hybrid counterparts. Many studies have shown dramatic improvement of physical properties, compared with pure materials, when inorganic particles or nanoparticles are inserted into an organic polymeric matrix. This behaviour, probably due to the interfacial interaction among nanoparticles and polymer seg-

I. Blanco (✉)
Department of Civil Engineering and Architecture and INSTM UdR,
University of Catania, V.le a. Doria 6, 95125 Catania, Italy
e-mail: iblanco@unict.it

S. Kalia and K. Pielichowski (eds.), *Polymer/POSS Nanocomposites and Hybrid Materials*, Springer Series on Polymer and Composite Materials,
https://doi.org/10.1007/978-3-030-02327-0_13

ments, provides nanocomposites the potential to bridge the gap between ceramics and polymers [1]. In this context, the use of polyhedral oligomeric silsesquioxanes (POSSs) has grown exponentially in recent years. Differently to the other most used fillers POSSs are molecules, thus combining their nanosized cage structures that have dimensions comparable with those of most polymer segments and a particular and exclusive chemical composition. These characteristics linked with their hybrid (inorganic–organic) nature allow the researchers to incorporate POSS reagents into polymer chains and modify the local polymeric structure and chain mobility, thus obtaining multifunctional materials with intermediate properties between those of organic polymers and ceramics [2, 3]. In the last 25 years, there was an increasing interest in the use of POSSs as building blocks for inorganic–organic hybrid materials, in which the incorporated organic moiety is expected to ensure compatibility with the matrix whilst the inorganic one to contribute to the improving of properties, such as thermal stability, abrasion and oxidation resistance, reduction of polymer flammability [4–7]. The incorporation of inorganic building blocks into organic polymers, to improve its properties, continues to be a driven force for the development of new materials and one of the other reasons of choice POSS for this purpose is that are typically stable up to 300 °C, which is higher than the thermal degradation temperatures of most organic molecules [8–10]. Besides high-temperature stability, POSS nanoparticles, unlike other fillers such as organoclay, offer also other advantages like mono-dispersibility, low density and non-presence of trace metals [1]. The preferred method for introducing POSS cages into polymer systems is via copolymerization, which is an efficient approach to POSS-containing nanocomposites due to the formation of chemical bonds between POSS and polymer matrices [11]. Copolymerization is generally preferred to the nanocomposite preparations via physical blending, due to possibly unfavourable miscibility (or solubility) of POSS within the polymers, anyway following the functionalization of the organic vertices of the cage (e.g. alkyl, alkylene, acrylate, hydroxyl or epoxide groups), POSS molecules acquire good solubility, compatibility and reactivity with other materials compared to inorganic silica nanoparticle [12]. In fact, the typical POSS monomers are characterized by a cubic structure with eight organic corner groups, one or more of which reactive or polymerizable, thus leading to an easily functionalization of organic periphery with facile tuning of the silsesquioxane properties [13, 14]. As far as we have written above, in most cases the functionalized POSSs are covalently bound to the matrix, leading to reinforcement of the system on molecular level. Therefore, a correct balance of POSS–POSS and POSS–polymer interactions is the key factor for the resulting improved thermal performance. The increase in functionality of nanoparticles leads to steric restrictions around the forming POSS junction, thus reducing the degree of POSS aggregation. On the contrary, strong aggregation and crystallization can occur in the case of POSS pendant on the polymer chain [15]. Furthermore, it is possible to obtain copolymers, where POSS becomes part of the polymer chemical structure, by the insertion of polymerizable substituents on the cages. Reactive functional groups can also bond POSS to resin molecules, which subsequently cure into thermoset matrices. However, in both of these situations, tiny POSS domains often form as nanoparticles undergo self-aggregation in competition with both chemical bonding

Table 1 Popular techniques of thermal analysis

Technique	Principle	Abbreviation
Differential scanning calorimetry	Heat flux difference	DSC
Differential thermal analysis	Temperature difference	DTA
Dynamic mechanical analysis	Oscillating force @ given T	DMA
Thermogravimetric analysis	Mass loss	TGA
Thermal volatilization analysis	Volatilization rate	TVA

and molecular dispersion in the matrix [16]. The tendency to aggregation is not only determined by the POSS compatibility with the polymer matrix, which depend by the organic substituents, but also by the symmetry/asymmetry of POSSs molecules [17, 18]. In other words, the favourable combination of properties between POSS and polymers requires the optimum dispersion of POSSs in polymeric matrix, which can be set by controlling type and reactivity of organic groups in POSS cubes [11]. Thermal stability is an important characteristic of POSS compounds, which improves the thermal properties of the resultant polymer nanocomposites and hybrids, and different thermal analysis methods are used to investigate the thermal degradation of POSS-based materials. With the term thermal analysis (TA), we mean the whole of various measuring techniques that share a common feature: the measure of the material response when heated or cooled (or, in some cases, held isothermally). TA goal is to establish a connection between temperature and specific physical properties of materials [19]. The most popular techniques are reported in Table 1 where they are classified by the physical property measured.

TA, that is recognized as one of the most important research and quality control methods in the development and manufacture of polymeric materials, is used not only for measuring the actual physical properties of materials but also for clarifying their thermal and mechanical histories, for characterizing and designing processes used in their manufacture and for estimating their lifetimes. The most employed parameters to test the thermal performance of POSS–polymer composites are undoubtedly the onset decomposition temperature or initial decomposition temperature (T_i) and the temperature at 5% mass loss ($T_{5\%}$). Generally, this latter is considered more reliable than initial decomposition temperature, because, especially when more than one stages of degradation are detected, T_i largely depends on the slope of the descending piece of thermogravimetric (TG) curve. In order to establish the mechanism of degradation and to make prevision on the materials lifetime, kinetics studies are carried out and the obtained kinetic parameters allow to the researcher to make their hypothesis. Among these, the degradation activation energy (E_a) is the most used. The molecular level reinforcement provided by the POSS cages can significantly retard the physical aging process in the glassy state, thus another important parameters used in the material thermal characterization is the glass transition temperature (T_g), determined both with Differential Scanning Calorimetry (DSC) and Differential Thermal Analysis (DTA) and Dynamic mechanical analysis (DMA).

2 Epoxies–POSSs Composites

Among the various classes of polymers, epoxies consolidated their position as one of the most versatile ones. They are employed in different applications, such as metal coatings, automotive primer, printed circuit boards, semiconductor encapsulants, adhesives and aerospace composites. Therefore, based on their commercial applications, they can be categorized for non-structural or low-temperature applications and structural or high-temperature applications [20, 21]. Because of problems in their engineering applications like low stiffness and strength, and in processing due to the exothermic heat generated by their curing, the use of additives in their formulation has always been widely exploited [22, 23]. Silicon compounds are widely added in epoxy, resulting in high flame-retardant efficiency and good thermal stability [24, 25], among them the incorporation of POSS nanoparticles into epoxy resins has been shown to improve their thermomechanical properties.

At first, Laine and his collaborators by comparing the behaviour of nanocomposite epoxy resins based on octaglycidyl (OG) and octaethylcyclohexenyl epoxide (OC) cubic silsesquioxanes with a common organic epoxy resin—diglycidyl ether of bisphenol A (DGEBA) with diaminodiphenyl methane (DDM)—showed that small changes in organic nanoarchitecture can be important in changing or manipulating nanocomposite properties [26].

The thermomechanical properties of various formulation ratios of organic–inorganic hybrid composites (OG/DDM) have been reported by Choi et al., showing that OG/DDM composites offer better thermal stability than the standard DGEBA/DDM system [27]. Contrary to the thermal stabilities of pure DGEBA and OG, the 5% mass loss temperatures for these composites are almost identical at about 340 °C, and this was expected since that the organic tethers determine the thermal stability. However, the half decomposition temperature for OG/DDM composites is higher than that of DGEBA/DDM by ~50 °C and the char residue, in inert environment, for OG/DDM (~40%) is also higher than DGEBA/DDM (17%) as expected because of the high silica content. This difference in half decomposition temperatures was considered significant by Choi and his collaborators, because it may be construed as an effect of creating a nanocomposite. The doubt, instilled by the same authors, is that, in the nanocomposites, tether thermal motion is restricted thereby reducing the organic decomposition pathways accessible to the tether. It is likely that the inorganic component provides additional heat capacity, thereby stabilizing the bulk material against thermal decomposition except at surfaces where the decomposition would be expected to start. Moreover, they argued that the somewhat lower than expected char yield in air may be ascribed to volatilization.

Lee and Lichtenhan [28] studied the thermal behaviour of DGEBA incorporated with mono-functional epoxy-substituted POSS–Jeffamine D230 (diamine-terminated polypropylene oxide) curing agent (Fig. 1).

An increase of the glass transition temperature (T_g) as a function of the weight fraction of the mono-functional POSS–epoxy was observed. In addition, they also examined the viscoelastic response, at temperatures below T_g, correlating it to a stretched

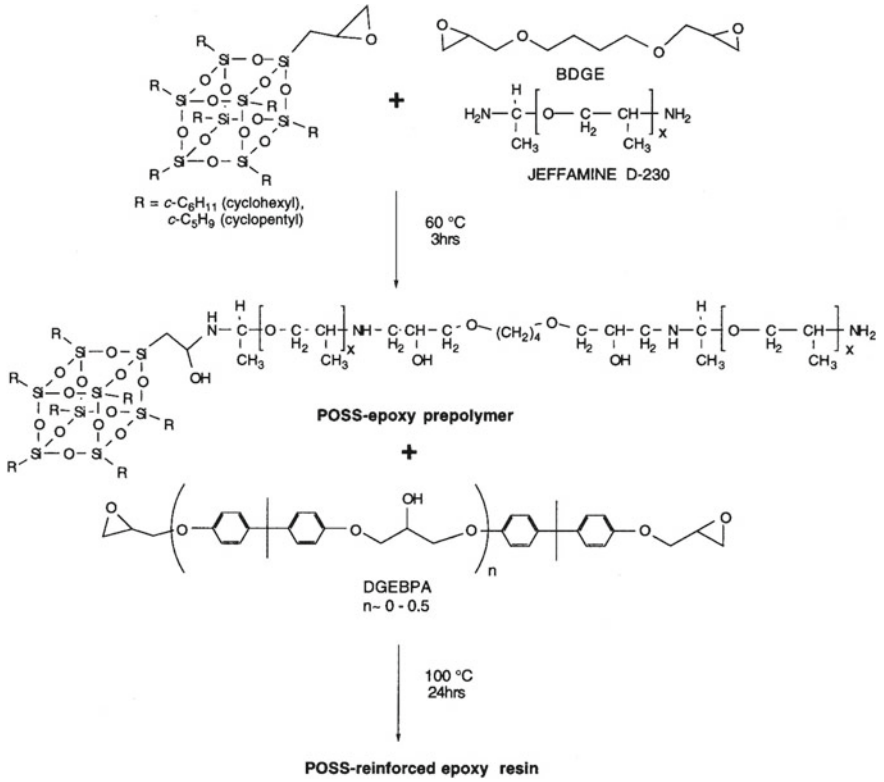

Fig. 1 Curing cycle of the POSS–epoxy system. Reprinted from [28], © 1998 with permission from ACS Publications

exponential relaxation function. The instantaneous modulus was not observed to be affected by incorporation of the POSS nanoparticles, on considering that time—aging time-superposition were found to be applicable to the data under all test conditions used. This finding suggested to the two authors that whilst POSS cages influence polymer chain motions, including the motion of the molecular junctions, they did not participate in the overall deformation of the chains. Finally, experiments performed under the same thermodynamic states revealed that the molecular-level reinforcement provided by the POSS cages also retarded the physical ageing process in the glassy state. Allowing the two scientists to conclude that the time required to reach a structural equilibrium was dependent to the POSS reinforcement level in epoxy and anyway was longer than for those of the neat resins.

Li et al. studied aliphatic epoxy composites with multifunctional polyhedral oligomeric silsesquioxane (POSS) (Fig. 2), $(C_6H_5CHCHO)_4(Si_8O_{12})(CHCHC_6H_5)_4$ nanophases (epoxy/POSS 95/5 and 75/25) and epoxy blends with the pre-polymer of ladderlike polyphenylsilsesquioxane (PPSQ) (95/5, 90/10 and 85/15) by dynamic

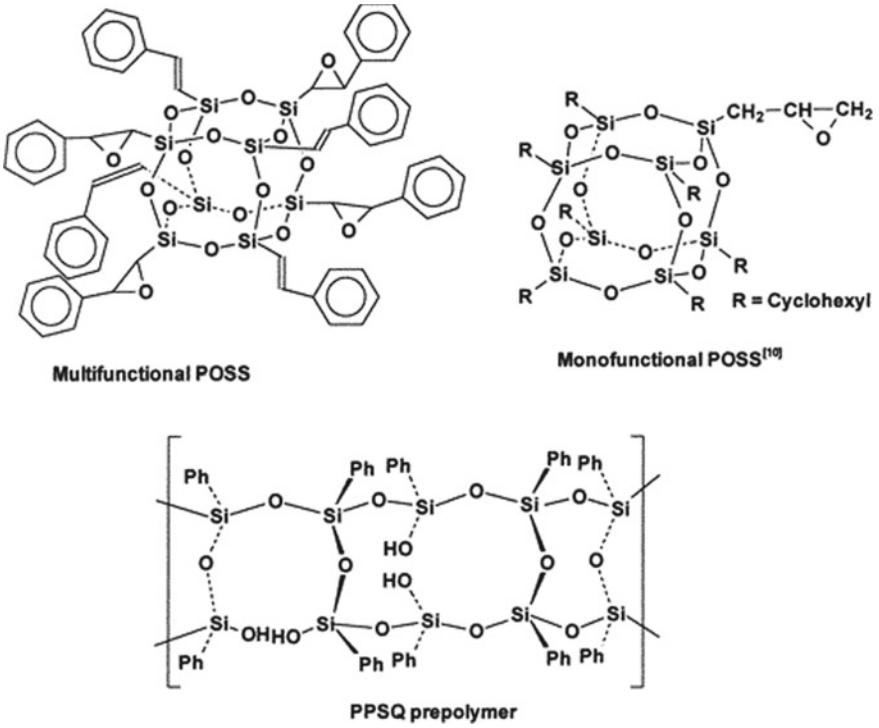

Fig. 2 Structures of the two POSS monomers and PPSQ pre-polymer. Reprinted from [29], © 2001 with permission from ACS Publications

mechanical thermal analysis (DMTA) [29]. They obtained a good dispersion of POSS units in epoxy matrix, even at a nanoparticles weight per cent of 25%.

This molecular dispersion is a result of:

- the mixture of two different corner substituents which enhances the POSS derivative's solubility;
- the ability of epoxy groups to chemically bond to the epoxy resin's matrix as it cures;
- the low tendency for POSS molecules to aggregate when they are originally well dispersed [30].

Therefore confirming how important it is to determine the right balance quantity/dispersion of POSSs in the matrix. Li and co-workers found a good miscibility, among PPSQ and the aliphatic epoxy resin, only at low PPSQ content ($\leq$10 wt%), whilst they observed phase separation starting from 15% of PPSQ. They observed an increase in the cross-linking density due to the high-temperature curing (150 °C) that enhanced cross-linking reactions among residual epoxy functions of the POSS macromer and amine groups, thereby increasing the T_g and the storage moduli (E') values of the formulation with 75% of epoxy and 25% of POSS. In conclusion, the

incorporation of the nanoparticles into the epoxy network broadens the glass transition region but had almost no influence on the T_g values that slightly increased for epoxy/PPSQ blends at $\leq$10 wt% of POSS. On increasing the POSS content in the epoxy matrix, the T_g value decreased in respect to that of neat epoxy probably due to hindrance of epoxy resin cross-linking caused by hard PPSQ-rich particles resulting from phase separation. Nevertheless, the inclusion of PPSQ into epoxy had no effect on the width of the glass transition region of these blends. E' values of epoxy/POSS composites and epoxy/PPSQ blends at $T > T_g$ were higher than those of neat epoxy. Therefore, thermal dimensional stability of epoxy was increased either by the incorporation of POSS or by the inclusion of PPSQ.

Schwab et al. demonstrated the possibility to convert POSS α-olefins into POSS α-epoxides by the means of the reaction of POSS α-olefins with m-chloroperbenzoic acid (MCPBA) [31]. They studied the reactivity of these epoxides in self-polymerization and in reaction with amines and thermally characterized the POSS epoxides. In particular, examined by differential scanning calorimetry (DSC), $[(c\text{-}C_6H_{11})_7Si_8O_{12}CH_2CHCH_2O]$, $[(c\text{-}C_5H_9)_7Si_8O_{12}(CH_2)_6CHCH_2O]$ and $[(c\text{-}C_6H_{11})_7Si_8O_{12}(CH_2)_6CHCH_2O]$ did prove to be reactive in that each of the compounds was observed to undergo an exothermic self-polymerization at a temperature (~250 °C) below the initial decomposition ones (370 °C). Furthermore, in reaction with curative aromatic amines (Shell Epolite 2330), the compounds showed irreversible exothermic transitions near 140 °C. Thermogravimetric analysis (TGA) showed, for these epoxy-POSS system, decomposition temperature ranging from 370 to 400 °C with char yield 10–30%.

Driven by the fact that the reduction of viscosity through the use of POSS-modified epoxies offers significant opportunities for low-cost processing techniques such as vacuum-assisted resin transfer moulding (RTM), the thermomechanical properties of octafunctional cubic silsesquioxane modified epoxy resins associated with dicycloaliphatic hardener were studied by He et al. using TGA, DSC and DMA [32]. Systems of octa(dimethylsiloxy butyl) (OB) epoxide at different ratios of OB/hardener were degraded, showing higher decomposition temperature than the standard Ciba epoxy resin which was ascribed, also in this case, to the POSSs dispersion and the formation of tether structure cage–epoxy matrix. The increase in thermal stability was also confirmed by a higher char yields, in fact they claimed that it is likely that the octafunctional silsesquioxane core preserves the cage structure thus contributing to improve oxidation resistance. He and co-workers observed that the T_g values at low POSS content were similar to that of the standard Ciba epoxy resin and attributed this behaviour to the reduction of overall segmental motion. Whilst at higher OB loading (20 mol% OB), they observed T_g disappearance which suggested them that the segmental motion was prohibited by the presence of the rigid silsesquioxane cage and very high cross-linking density. The papers placed under observation have so far highlighted that the presence of the POSS cages in the epoxy matrix, in the same conditions, significantly slows down the ageing process in the glassy state. However, compounds at high POSS content [29] exhibited a lower T_g which has been ascribed to the possible incomplete curing reaction of epoxy due to the inclusion of the POSS cages.

Williams et al. [33] observed a primary liquid–liquid phase separation occurred at the time of adding the diepoxide to the POSS–diamine precursor due to their incompatibility.

Choi and Laine investigated the modifications of epoxy resin by the inclusion of a series of polyfunctional silsesquioxanes with various R groups (aminophenyl and dimethylsiloxypropylglycidyl ether) [34–37]. The thermal stability of the epoxy hybrids was addressed in terms of the types of the used organic groups, tether structures between epoxy matrices and POSS cages and the defects in silsesquioxane cages. Again, in this series of studies, the authors correlated the favourable combination of properties between POSS and polymers with the dispersion of the nanoparticles. In particular, they demonstrated the possibility to increase the level of POSS dispersion in the matrix by controlling type and reactivity of R groups in silica cages, thus improving the thermal performance of the epoxy-based composites.

Zheng and collaborators continued to evaluate the effect of the type and reactivity of organic groups in POSS cages on phase behaviour and properties of the resulting epoxy hybrids [38]. With the aim to improve the miscibility of POSSs within the diglycidyl ether of bisphenol A (DGEBA), they explored the modification of the phenyl groups attached to the silicon cage by nitration and the resultant effects on the nanoparticles dispersion. It was observed that the replacement of phenyl groups with nitro-phenyl ones enhanced the miscibility, thus leading to a different morphology of the resulting epoxy/POSS hybrids. The T_g values of the obtained composites decreased with increasing POSS content as a result of the increase in total free volume, due to the inclusion of a part of bulky POSS cages at the nanoscale level. They proposed that two competitive factors determine the glass transition temperatures of resulting composites: the hindering effect of POSS cages on polymer chain motions will enhance glass transition temperature, whilst the inclusion of the bulky POSS group could give rise to the increase in free volume of the system, which will result in the decreased T_g. This effect could be comparable to plasticization effect of low-molecular-weight compounds on polymer matrix [27]. Zheng also evaluated the resistance to the thermal degradation; increased initial decomposition temperature (T_i) values and a two-step degradation mechanism were found, suggesting that the presence of POSSs did not significantly alter the degradation mechanism of the epoxy matrix. According to the literature evidence [39, 40], they proposed that mass loss from segmental decomposition via gaseous fragments could be suppressed by well-dispersed POSS cubes at the molecular level. Therefore, the improved thermal stability of epoxy/octaaminophenyl POSS (OapPOSS) vs epoxy/octanitrophenyl POSS (OnpPOSS) could be a result of the combined effects of the formation of aromatic tether structure between epoxy matrix and POSS cages and the dispersion, at nanoscale, of POSS cages in epoxy matrix. Following the peripheral groups setting pathway, they compared the thermal behaviour of OapPOSS-containing nanocomposites with the above-cited OnpPOSS–epoxy system, by founding an increased thermal stability for this latter, thus reaffirming the importance of the nanoscaled dispersion of POSS in epoxy matrices as important factor to contribute the enhanced thermal stability. In OnpPOSS-containing composites, there were no chemical bonds between the matrix and the POSS cages and the heterogeneous morphology was

formed via phase separation induced by polymerization. However, in OapPOSS-containing system, the POSS cages participated in the formation of the cross-linked network, i.e. the POSS cages were tethered onto polymer matrix.

The close link between POSSs dispersion and the degree of functionalization of their organic groups has been confirmed by the studies of Matejka et al. by studying epoxy networks, based on DGEBA and poly-(oxypropylene)diamine (Jeffamine D2000) reinforced with pendant aromatic- and aliphatic-substituted POSS [15]. Improvements of nanoparticles on increasing POSS functionality were observed: in the systems with low-functional POSS cross-links or the POSS units in the backbone, the nanoparticles' dispersion was poor and small amounts of POSS aggregates remained in the network. The aggregation resulted in a possible lower epoxy conversion, lower cross-linking density and deviations from the mean-field statistical theory of network formation [41]. They found that only a very high POSS content results in some immobilization of network chains and therefore the T_g of a majority of systems was not affected (only in a few cases a broadening of the transition was observed). POSS with flexible substituents behaved like a diluent and decreased the network T_g. The only system they possess a strong interactions between POSS and organic chains was the POSS-DGEBA,olig-D2000 network (Fig. 3).

Matejka and co-workers observed a strong increase in T_g by 50 °C due to both POSS–chain interactions and the presence of long stiff oligomer sequences involving several POSS units. Thermal stability of these networks increases with POSS content depending on an extent of protection of organic chains by inorganic structures and also in this case the system showed highest thermal stability was the POSS-DGEBA,olig-D2000 one.

A POSS–epoxy system based on Octakis (dimethylsilyloxypropylglycidylether) silsesquioxane (OG) and meta-phenylenediamine (mPDA) was synthesized and characterized by Chang et al. [42]. The activation energy, based on both Kissinger [43] and Flynn–Wall–Ozawa [44, 45] methods, in curing OG/mPDA system was higher than that of the classic DGEBA/mPDA system as well as the T_g. This increase was explained with the POSS cages capability in hindering the motion of the network junctions. High values of the temperature at the maximum rate of mass loss (T_m) and high char yield were measured for the cured OG/mPDA system, despite a large fraction of unreacted amine groups give raise to low T_i due to their tendency to decompose or volatilize on heating at relatively low temperature.

After their first study on the use of POSS in epoxy matrices, Zheng and his collaborators synthesized an octaammonium chloride salt of octaaminopropyl polyhedral oligomeric silsesquioxane (OapPOSS) to be used as intercalating agent for sodium montmorillonite (MMT) modifying [46]. POSS-intercalated MMT system is shown in Fig. 4. The presence of POSS nanoparticles leads to an expansion of the MMT galleries from 1.3 to 1.7 nm and exploited to prepare epoxy–MMT nanocomposites. No modification in T_g value was observed in respect to the neat epoxy when the POSS–MMT content was less than 10 wt%, whilst a slightly decrease of T_g value was recorded by increasing the POSS–MMT content up to 15 wt%, which was attributed to the incomplete curing reaction resulting from the POSS–MMT loading. Furthermore, an improvement in the thermal stability was evaluated by perform-

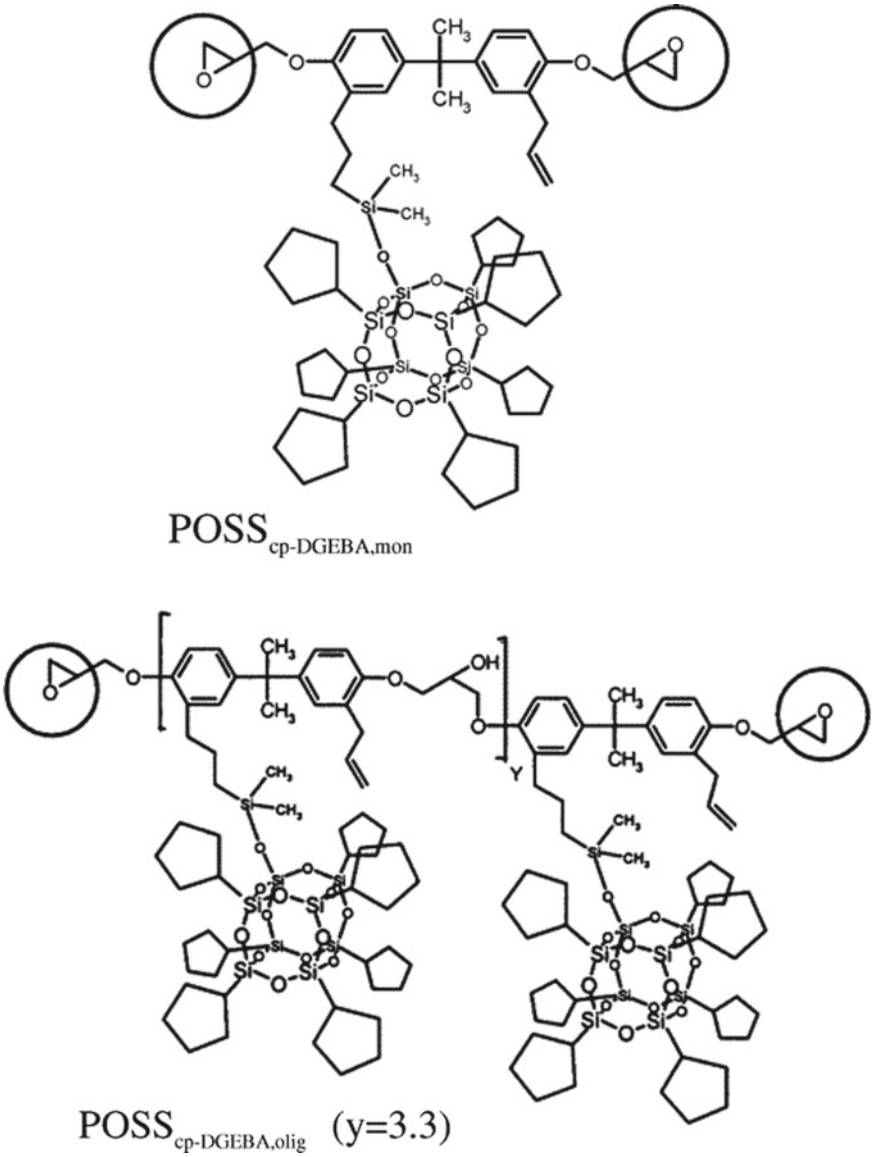

Fig. 3 Structures of the POSS-DGEBA,mon and POSS-DGEBA,olig. Reprinted from [15], © 2004 with permission from ACS Publications

ing thermogravimetric analysis, which showing an increase of the char residue as a function of the POSS–MMT concentration.

The structure and properties of organic–inorganic hybrid nanocomposites prepared from a resole phenolic resin and a POSS-mixture-containing trisilanolphenyl

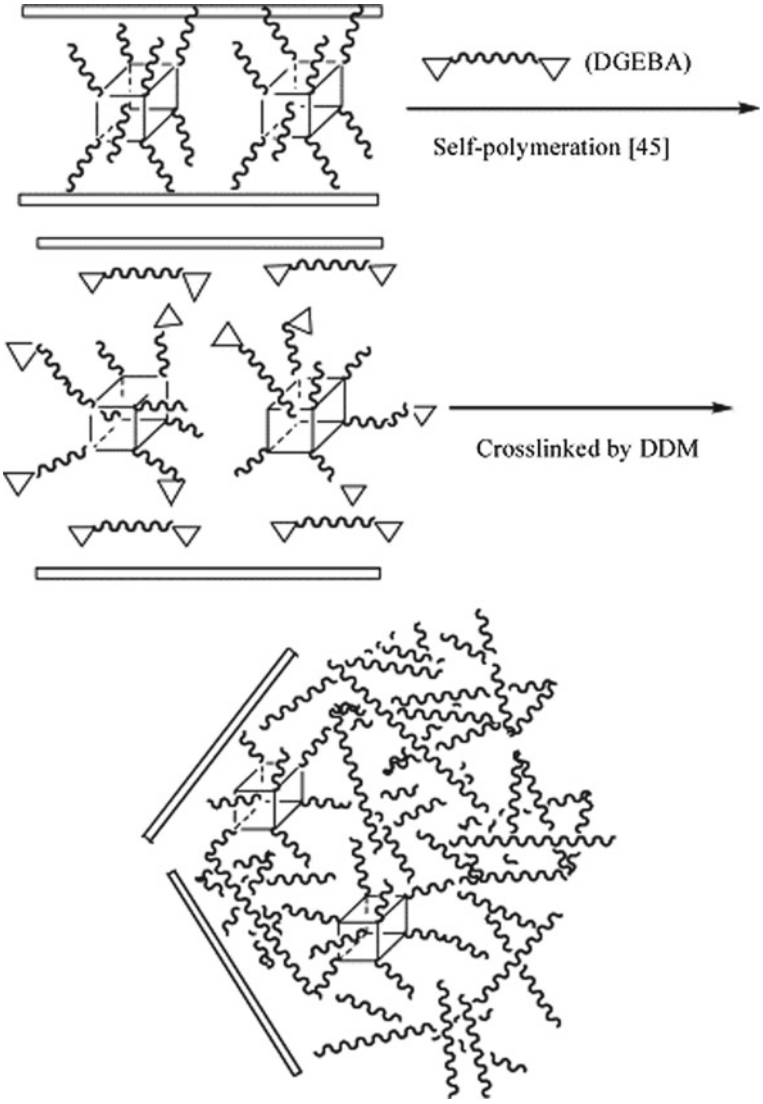

Fig. 4 Formation of epoxy–MMT nanocomposites mediated by ammonium of OapPOSS. Reprinted from [46], © 2005 with permission from Elsevier

POSS were investigated by Pittman et al. [16]. Nanocomposites with POSS, ranging from 1.0 to 10 wt%, heterogeneously dispersed in both cured matrix and dispersed phase domains were thermal characterized by the means of DSC and TGA. The hydrogen bonding between the phenolic resin and POSS Si–OH groups increased their mutual compatibility, but did not prevent POSS aggregation and phase separa-

tion during curing, thus resulting in a slightly increase in the temperature at 5% mass loss ($T_{5\%}$), whilst T_g remained practically constant [16].

Jones and collaborators prepared an epoxy/POSS system based on commercial products (SC-15 epoxy from Applied Poleramic Inc.; Epoxy Cyclohexyl POSS from Hybrid Plastics.). A low-viscosity, two-phased, toughened epoxy resin system consisting of part A (resin mixture of diglycidylether of bisphenol A, aliphatic diglycidlether epoxy toughener) and part B (hardener mixture of cycloaliphatic amine and polyoxylalkylamine) was prepared, showing that the addition of 5 wt% of POSS yielded a considerable increase of 16 °C in T_g but a modest enhancement of 10 °C in T_m. They found that the thermal performance of epoxy is increased with the POSS content, attributing this behaviour to the rigidity of the nanoparticles that would increase the rigidity of the whole epoxy system [47].

Higher T_g than neat epoxy resin was found also by Hu et al. that studied a series of epoxy resin/POSS prepared based on octavinyl polyhedral oligomeric silsesquioxane (OVPOSS) and phosphorus-containing epoxy resin (PCEP synthesized via the reaction between bisphenol A epoxy resin, DGEBA, and 9,10-dihydro-9-oxa-10-phosphaphenanthrene-10-oxide, DOPO) [48]. Their thermogravimetric study evidenced a one-stage degradation process for both OVPOSS–PCEP and PECP and an increase in the temperature at 50% mass loss ($T_{50\%}$) for the hybrid material prepared. Hu and co-workers hypothesized the formation, in inert environment, of a ceramic-like layer that can prevent the inner part of the hybrid from further degradation, and, in air atmosphere, the oxidation of OVPOSS to a silicon dioxide layer that can improve the thermo-oxidation resistance of the EP matrix. Furthermore, they attributed the increase of char yield with the OVPOSS content to the synergistic effect of phosphorus and silicon, where phosphorus-enriched char formation and silicon protected the char from thermal degradation.

Epoxy resin nanocomposites, based on DGEBA and tetraglycidyl diamino diphenyl methane (TGDDM), were prepared by Alagar and his collaborator via in situ copolymerization with 4,40-diaminodiphenylsulphone (DDS) in the presence of octaaminophenyl silsesquioxane (OAPS) up to 20 wt% [49]. Their DSC and DMA results showed an increase in T_g, compared with control epoxy systems, only for the composites at 3 wt% due to the increase of free volume in the hybrid systems by the effect of bulky POSS cage. Differently, TGA experiments indicated an improved resistance to the thermal degradation, explained with both the higher epoxy functionality present in TGDDM and the level of nanoscale POSS dispersion, resulting in the formation of aromatic tether structure among epoxy and nanoparticles cores (Fig. 5).

The kinetics of the degradation of epoxy nanocomposites containing different fractions of *n*-phenylaminopropyl-POSS were studied by Pistor et al. [50] using the Avrami model [51–53]. They observed that the incorporation of POSS monomer reduced the Avrami constant (k') and consequently increased the half-life ($t_{1/2}$) of the degradation reaction. The observed reduction of the k' means that the degradation rate tends to decrease due to the presence of POSS that may be hindering the degradation of the epoxy resin, thereby increasing its resistance to the thermal degradation. In addition, an increase of the POSS content resulted in an increase in the Avrami

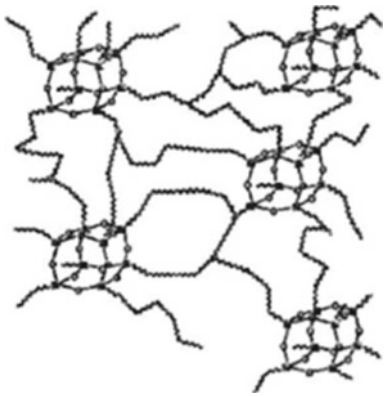

Fig. 5 Schematic representation of POSS-reinforced epoxy nanocomposites. Reprinted from [49], © 2006 with permission from Elsevier

exponent (n). At $2 < n < 3$, the degradation process propagates in two and three dimensions, respectively, thus suggesting that the incorporation of POSS facilitated heat diffusion in three dimensions. Pistor and co-workers observed a decrease in thermal conductivity, due to the increased space among the polymeric chains for the inclusion of POSS. They associated these lower values of thermal conductivity with the Avrami exponent, and thus, the three-dimensional diffusion suggested that there was greater free volume between the chains, which facilitated the dispersion of heat and increased the degradation activation energy (E_a). Consequently, they justified the different thermal performance of the various POSS monomers, used to reinforce epoxy system, with the hybrid characteristic and the ability to change the degradation mechanism by changing the volume of the cage [54]. Finally, they attributed the increase in T_g to the reinforcement effect of POSS-containing amine groups [55]. In their opinion, the change of T_g is not associated with the increased free volume, but with the type of reactive groups present in the POSSs. In the case of a decrease in T_g, a POSS with epoxy reactive groups was used [56], whereas an increase in T_g is related to the influence of the amine-reactive groups present in the nanocages.

More recently, Raimondo et al. studied the degradation mechanism of a multifunctional fire-retardant graphene/polyhedral oligomeric silsesquioxane epoxy resin [57]. In both oxidative and inert environment, a two-step thermal degradation process was observed suggesting that the inclusion of glycidyl polyhedral oligomeric silsesquioxane (GPOSS) and carboxylated partially exfoliated graphite (CpEG) nanoparticles in the matrix did not significantly modify the degradation mechanism of the prepared formulation. TGA experiments in air highlighted that, compared with the unfilled T20BD epoxy resin, the multifunctional epoxy resin T20BD + 5%GPOSS + 1.8%CpEG showed a slight increase in the thermal stability related to the first stage of the degradation process and a substantial increase in the second stage which is even more significant in nitrogen. The higher thermal stability detected for the multifunctional T20BD + 5%GPOSS + 1.8%CpEG, with respect to all the analysed formulations, was attributed by the authors to a synergistic action of GPOSS

and CpEG, even considering that the high thermal conductivity of graphene sheets might facilitate heat dissipation within nanocomposites and consequently improve the thermal stability of the entire composite material [58]. They concluded that the different trend of the degradation in both oxidative and inert atmosphere was a clear evidence that the beginning of the first stage is due to degradation processes which do not involve oxygen (dehydration, random scission, etc.), whereas the second step is strongly dependent on the oxygen availability. The different behaviour observed in inert environment was ascribed to decomposition and release of various fragments over a wider temperature range with respect to the second stage in air. Finally, they observed that the neat T20BD system exhibited a continual crispy char relevant of quite a good thermostability of the neat system. Nevertheless, no intumescence was observed for the system without GPOSS particles, differently than that containing them, for which intumescent char was obtained highlighting that the incorporation of POSS significantly enhances the thermostability.

3 Polypropylene–POSSs Composites

Polypropylene (PP) is probably the most important material among polyolefins because it can couple interesting properties, such as low density and high melting temperature, with low cost of manufacturing and highly versatility thus allowing different structural designs and improving thermomechanical properties. Another aspect not to be underestimated is the possibility of blending PP with other polymers or with reinforcing agents for obtaining materials having superior characteristics [59].

As for almost all the studies concerning the POSS molecules also those on the addition to PP see involved the operative unit at the Edwards Air Force Base Research Laboratory by Phillips, Blanski and their collaborators. They focused their studies on the crystallization, at quiescent and shear states, in isotactic polypropylene (iPP)-containing nanostructured POSSs by the means of DSC [60]. The addition of POSS up to 30 wt% significantly increased the crystallization rate during shear, compared with the rate observed for the neat polymer. Although it is well known that POSS crystals had a limited role in shear-induced crystallization, dispersed POSS molecules behaved as weak cross-linkers in polymer melts and increased the relaxation time of iPP chains after shear. Therefore, a faster crystallization rate was obtained, due to the improvement of the overall orientation of the polymer chains with the addition of nanoparticles, which was faster with higher POSS concentrations. The addition of POSS decreased the average long-period value of crystallized iPP after shear, which indicates that iPP nucleation probably started considerably near molecularly dispersed POSS molecules.

Novel organic/inorganic hybrid copolymers, up to 73 wt% PP–POSS, have been prepared by Coughlin and co-workers, using single-site catalysis, via direct copolymerization of a POSS macromonomer having a polymerizable norbornene linkage and propylene [1]. The obtained copolymers had a slightly decreased melting temper-

ature compared to homo-polypropylene prepared with the same metallocene catalyst, despite the thermal decomposition proceeded, apparently, in a different way. $T_{5\%}$ in air did not increase until high POSS concentration even though the PP–POSS copolymers have a much slower decomposition rate compared with homo-polypropylene, whilst the onset of decomposition temperature in nitrogen increased moderately. They proposed for the PP–POSS decomposition, a mechanism of random chain scission, in which the tertiary carbons were indicated like the more susceptible to degradation site, and attributing to the presence of POSS nanoparticles the slowdown of the degradation process [1].

A fundamental contribution to the study of the thermal properties of PP functionalized POSS nanocomposites was given by the group of Professor Camino in Turin. Camino and his collaborators studied the thermal and thermo-oxidative degradation of PP reinforced, by melt blending, with dimeric $[(i\text{-}C_4H_9)_7Si_7O_{12}Al]_2$ and oligomeric $[\{(i\text{-}C_4H_9)_7Si_7O_{12}\}_2Zn_3]n$ POSSs (Al-POSS and Zn-POSS, respectively) (Figs. 6 and 7) [61]. Their initial purpose was to exploit the ability of metal POSS, under oxidative conditions, to produce a ceramic thermally stable phase. TGA curves in nitrogen atmosphere did not show significant changes in thermal properties with respect to neat PP, whilst thermo-oxidative tests performed in air showed a strong effect of metal POSS compounds on degradation pathways.

In particular when they increased the POSSs content up to 10 wt%, they observed an overall retarded degradation, testified by the shifting of TGA curves with respect to neat PP and a residue at the end of the analysis which was consistent with the amount of POSS inorganic fraction filled in the composites. In the case of both Al-POSS and Zn-POSS, the TGA plots clearly showed two degradation steps, thus indicating two overlapping degradation processes. They supposed that the first one corresponded to the degradation of neat PP on the sample surface since during the first-stage PP macromolecules are degraded into volatile oligomers by the fragmentation process. The second weight loss step was explained with the degradation of the residue formed during the first step. They proposed an interesting three steps mechanism by assuming that the oxidation of the sample surface determines the accumulation of POSS, with formation of a thermally stable phase, similar to the one observed on neat POSS heating. This ceramic superficial layer probably acts as a physical barrier, limiting the gas transport at the interface, thus influencing the kinetics of the degradation reactions. Camino and co-workers continued their studies evaluating the influence of POSS functionalization on PP-based composites, in particular by focusing their research on the effects of the different alkyl substituents (Fig. 8) on the thermal and morphological characteristics of the prepared composites.

They found marked differences in the morphology of the composites by increasing alkyl chain length from octamethyl-POSS (OM-POSS) to octaisobutyl-POSS (oib-POSS): specifically, a higher extent of dispersion for this latter filler. Further increase in the substituent chain length to octaisooctyl-POSS (OIO-POSS) did not bring improvement on POSS dispersion. As regard the thermo-oxidative degradation, they recorded an increase in T_m at high POSS loadings, which was more evident at higher dispersion extents (oib-POSS-based composites). They attributed this behaviour to oxygen scavenging by the inorganic phases cumulating on the surface

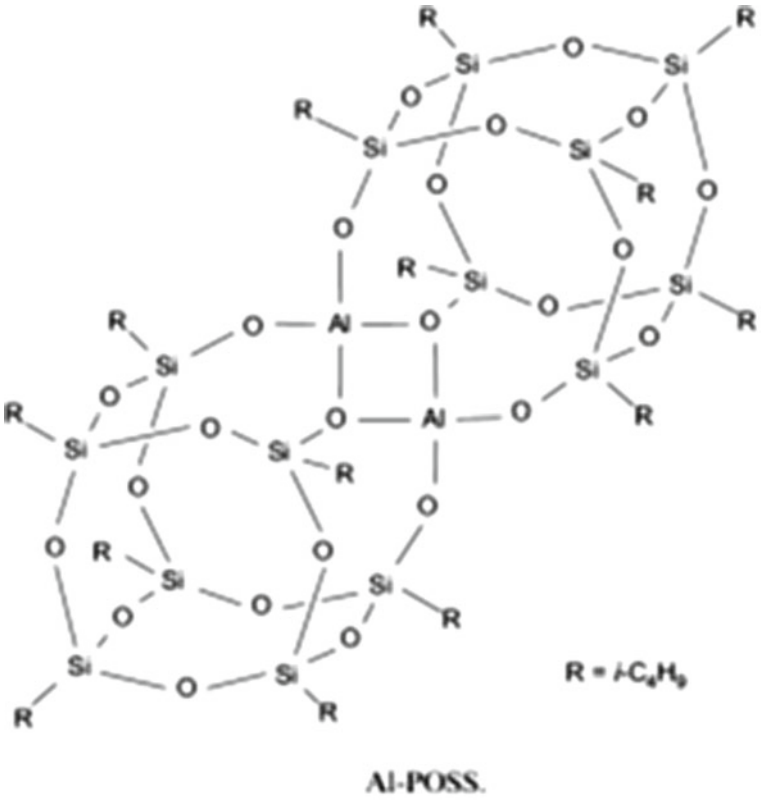

Fig. 6 Molecular structures of Al-POSS. Reprinted from [61], © 2006 with permission from Elsevier

of the material by polymer ablation and concluding that the composite characteristics are not simply driven by the length of the organic substituents, as one could predict on the basis of an expected increase in compatibility between the two phases [62]. The results of the group of Turin indicated that the length of alkyl substituents on POSS cages plays a fundamental role in determining the dispersion degree and the interactions with the PP matrix during the cooling process from the melt. Camino and co-workers supported their finding with microscopic analyses, which showed that OM-POSS gave mainly rise to crystalline aggregates on micron-size scale, whereas OIO-POSS and, partially, oib-POSS were well dispersed in the matrix encouraging interactions of the long alkyl groups with the polymer chains, as compared to POSS–POSS auto-aggregation. At all investigated compositions, the authors found a different behaviour of OM-POSS and OIO-POSS, with this latter that retarded the crystallization kinetics due to its high dispersion as liquid phase component whilst the first one resulted to be a nucleating agent for PP. Finally, they pointed out their attention to the inorganic reinforcement amount by highlighting that oib-POSS

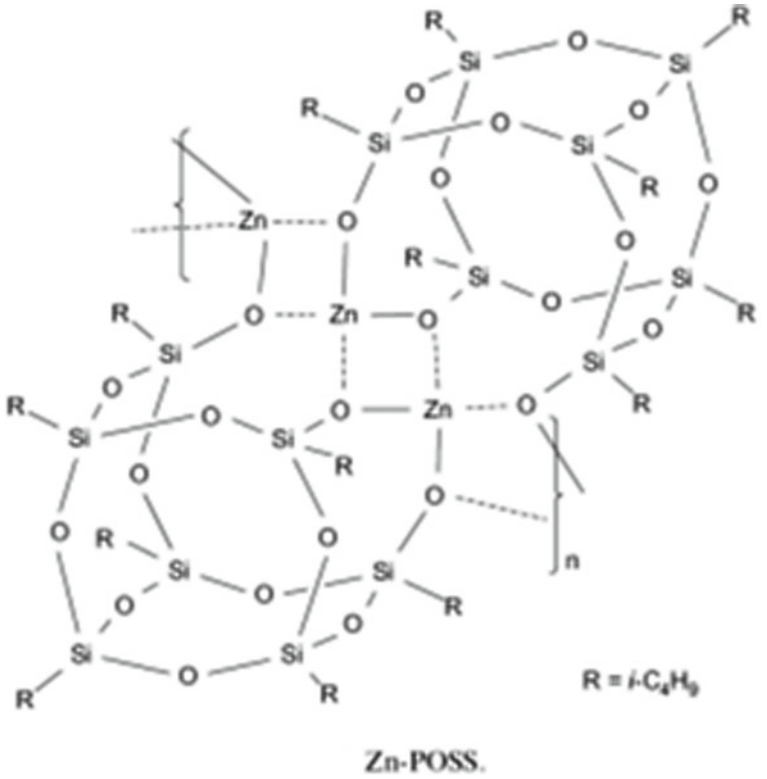

Fig. 7 Molecular structures of Zn-POSS. Reprinted from [61], © 2006 with permission from Elsevier

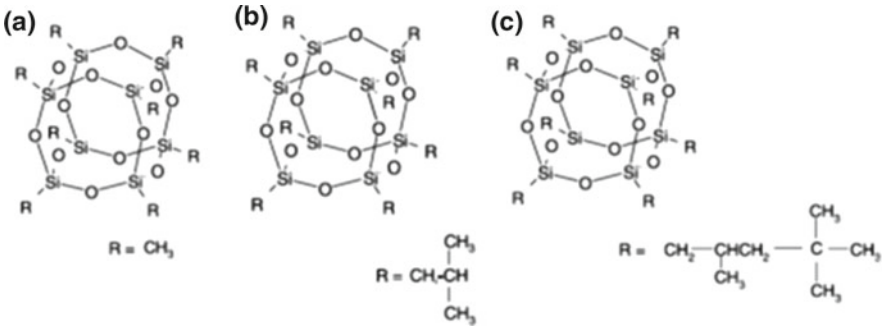

Fig. 8 **a** ome-, **b** oib-, **c** oic-POSS cage structures. Reprinted from [62], © 2005 with permission from Elsevier

showed a different behaviour depending on its content in PP. They observed that at low content (3 wt%), the nanodispersion of oib likely hinders the PP crystal growth, thus resulting in a retarded crystallization; at higher content (10 wt%), this effect is

counterbalanced by the presence of oib crystal aggregates which behave as nucleants for PP [63].

Morgan et al. investigated the bulk and surface properties of POSS–PP composites prepared via high shear melt mixing. They observed POSS aggregates ranging in size from 10 to 100 nm within the matrix, that giving rise to dramatic modification of surface properties. In particular, with the incorporation of 10% oib-POSS, they recorded a 60% reduction in relative COF (from 0.17 to 0.07), a doubling of hardness (109–225 MPa) and a reduction in modulus (1.9–3.9 GPa). Bulk property evaluations by DMA, on the other hand, showed only minimal changes when POSSs were incorporated, thus demonstrated preferential segregation of the POSS aggregates to the surface in comparison to the bulk region [64].

Also Fina et al. observed micron-sized POSS aggregates (Fig. 9) and reinforced the hypothesis of the protective layer formation thanks to the action of the inorganic part of the POSSs, by reporting the study on a maleic anhydride-grafted polypropylene (PPgMA)/POSS. They obtained this system with a one-step reactive blending process by POSS grafting. The thermal performance was evaluated and compared with a non-reactive PPgMA/POSS nanocomposite as a reference, showing advantages in terms of higher thermal stability in the case of the grafting process with respect to simple melt blending [65]. POSS has accumulated on the sample surface during the earlier stage of PPgMA/am-POSS, thus gave rise to higher thermal stability in oxidative environment. Indeed, volatilization of grafted POSS was hindered as compared to unbound oib-POSS, allowing POSS oxidation with the production of a ceramic phase [3], which acts as a protective barrier, limiting the polymer volatilization rate. They put in foreground the role of am-POSS on thermo-oxidative degradation of PP by monitoring the mass loss in air in isothermal conditions at 250 °C, which was approximately the pure matrix T_i. They observed a fast degradation (50% mass loss after 20 min and a stable 6% residue after 300 min) for pristine PP and a similar behaviour for PPgMA/oib-POSS (50% mass loss after 23 min and a stable 9% residue after 300 min), attributing the slightly modification for this latter to the partial formation of a ceramic phase through POSS oxidation in isothermal condition. Indeed, at 250 °C oib-POSS suffered evaporation in competition with oxidation, leading to an insoluble glassy phase [66]. Increasing the degradation time to 45 min, a decrease in mass loss rate was observed for PPgMA/am-POSS (50% mass loss and a 15% residue after 300 min). In this case, POSS was retained in the condensed phase thanks to grafting, resulting in accumulation of a ceramic physical barrier by POSS thermo-oxidation. This accounted for the slower weight loss kinetics and the higher residue compared to PPgMA/oib-POSS. On continuing their studies, Fina and his collaborators investigated polysilsesquioxane (PSS) with different organic groups (methyl, vinyl or phenyl) (Fig. 10) with the aim to correlate dispersion in PP matrix and thermal properties with the silsesquioxane organic fraction type. They prepared polysilsesquioxane-based polymer blends, obtaining a submicronic PSS domain dispersion with vi- and ph-PSS, whereas residual aggregates were found with me-PSS [67].

They generally observed improved performances for the PP/silsesquioxane in terms of higher thermal stability, due to the formation of the above-cited ceramic

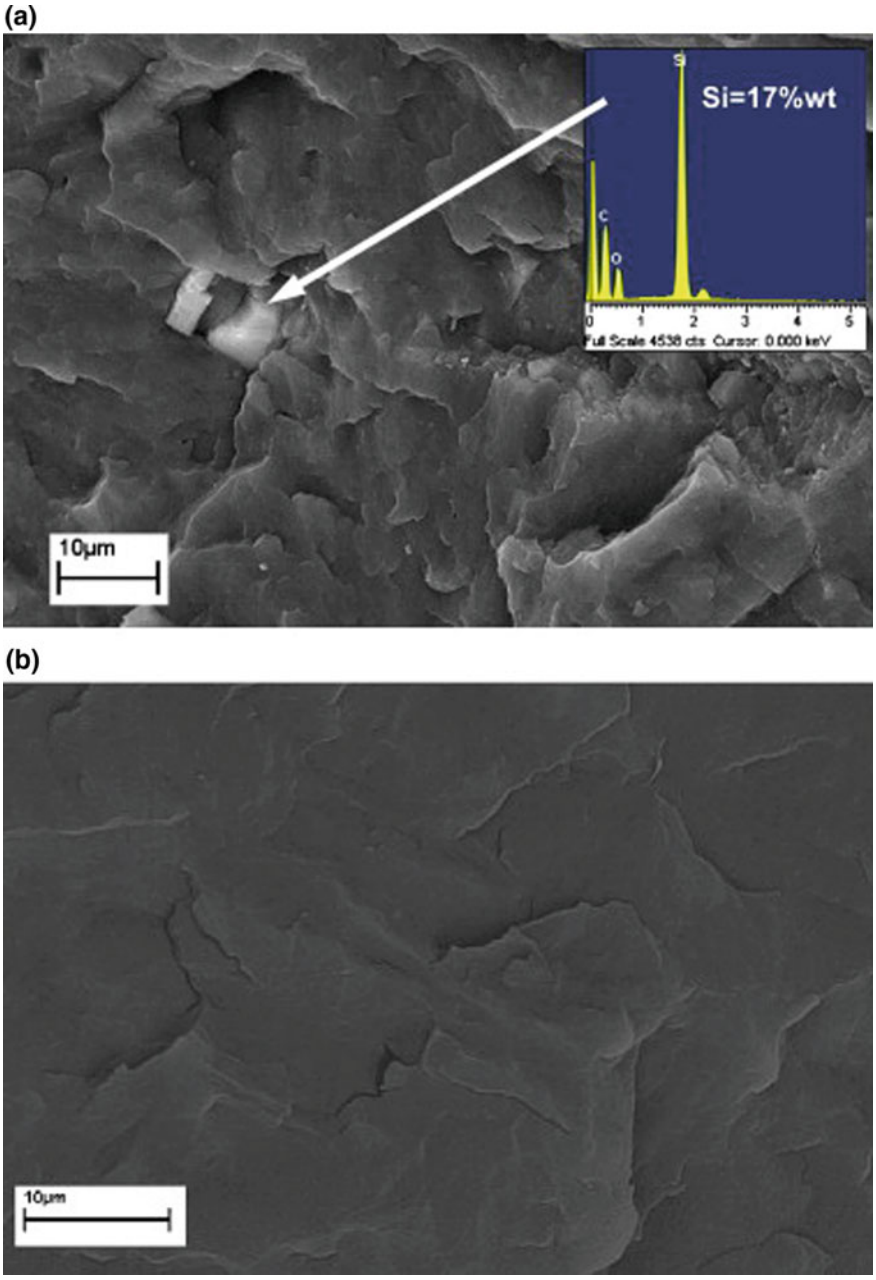

Fig. 9 SEM micrographs of PPgMA/oib-POSS with EDS elemental analysis inset (**a**) and SEM micrograph of PPgMA/am-POSS (**b**). Reprinted from [65], © 2009 with permission from Elsevier

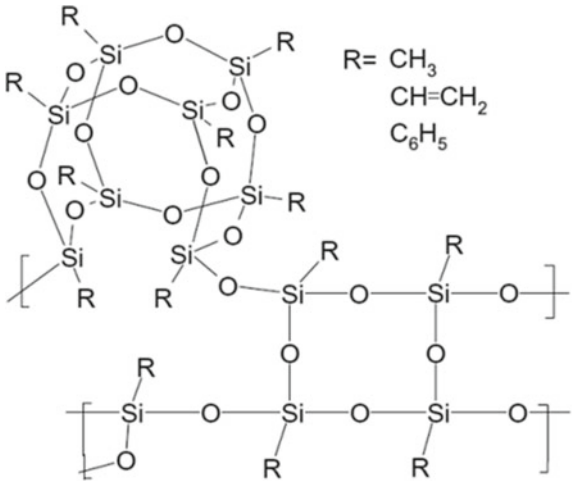

Fig. 10 Polysilsesquioxane approximate structure. Reprinted from [67], © 2010 with permission from Elsevier

superficial layer that acted as a protection towards degradation of the underlying material. PP/me-PSS showed a rapid increase of the weight loss rate above 280 °C, which they attributed to the rupture of the protective layer, with consequent limited delay of T_m (~10 °C). By contrast, PP/vi-PSS showed a lower weight loss rate, reaching a plateau in the range between 320 and 350 °C, thus suggesting that the protective layer from vi-PSS is more thermally stable than the one from me-PSS. They supported this hypothesis by recording an increase in T_m of about 35 °C with respect to neat PP. Finally, PP/ph-PSS showed a higher thermo-oxidative stability, evidenced by the lowest weight loss rate for temperatures below 330 °C and the highest T_m (379 °C).

Successively, the influence of POSS chemical structure and grafting degree on the morphological characteristics and thermal properties of isotactic PP maleic anhydride functionalized PP (PP-g-MA) was investigated by Bartczak et al. [68]. They found that grafting of POSS cages on PP chains leads to the POSS dispersion on the molecular level, unlike when POSS was mixed with plain iPP, which resulted in phase-separated blend with crystallites of POSS dispersed in iPP matrix. They observed a faster degradation of PP in an oxidative atmosphere (air) than in inert conditions due to peroxidation, thus resulting in a decrease of PP-*g*-MA degradation temperature of about 90 °C comparing to degradation in N_2 atmosphere. Samples of PP grafted with POSS demonstrate highly improved thermo-oxidative stability comparing to PP-*g*-MA, giving raise a shift of T_m from 379 to 415 °C for composites. They explained the greatly improved thermo-oxidative stability of PP-*g*-POSS by the accumulation of POSS on the sample surface during the earlier stage of PP-*g*-POSS degradation, thus limiting the polymer volatilization rate.

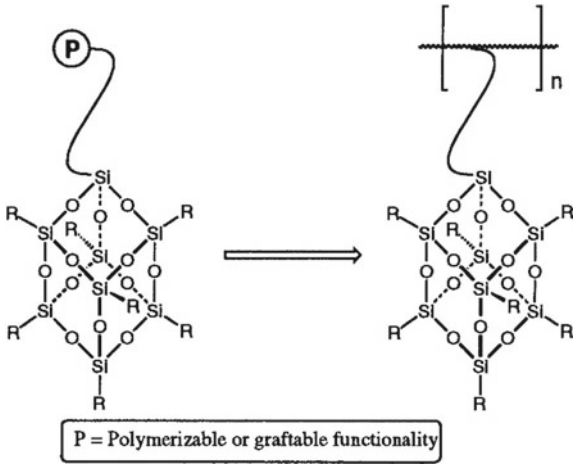

Fig. 11 POSS macromer converted to a hybrid polymer with a pendent architecture. Reprinted from [76], © 1996 with permission from ACS Publications

4 Polystyrene–POSSs Composites

Polystyrene (PS) is one of the more produced thermoplastic polymers due to its versatile application in different fields. Because of its low-cost, good processability, transparency and good electrical property, PS products are present almost everywhere [7]. PS can be found in applications where abrasion, chemical resistance, as well as thermal stability are required [69] and therefore lend it to act as a matrix for polymer composites. When considering the development of composites based on thermoplastic polymers, and more specifically PS, it is particularly difficult to ensure good interfacial adhesion between the matrix and the reinforcing agents. This shortage of compatibility between many reinforcing agents and PS is due to its inert nature and the lack of reactive groups (as compared with thermosetting systems or other engineering thermoplastics), which limits the level of interaction [70]. In the last two decades, hybrid materials, with superior structural and functional properties, have been developed by incorporating nanofillers into polymer matrices. Carbon nanotubes, layered silicates, and others [71–73] were firstly used to prepare organic–inorganic hybrid systems, but, in recent years, polyhedral oligomeric silsesquioxanes have attracted the attention for the use as molecular fillers in the production of PS-based nanocomposites.

Haddad et al. synthesized, by free radical bulk polymerization of cyclohexyl-, cyclopentyl- and isobutyl-substituted POSS-styrenes (Fig. 11), obtaining a series polymers in a high yield and purity [74], that showed a variation in modulus above the T_g. They observed a much more prominent variation for the cycloalkyl POSS copolymer than the isobutyl POSS one, thus speculating on a cage's groups' effect on bulk polymer properties leading to differences in polymer microstructure. They concluded that the packing of the POSS cages in the glassy matrix is strongly affected by the type of group on the POSS moiety.

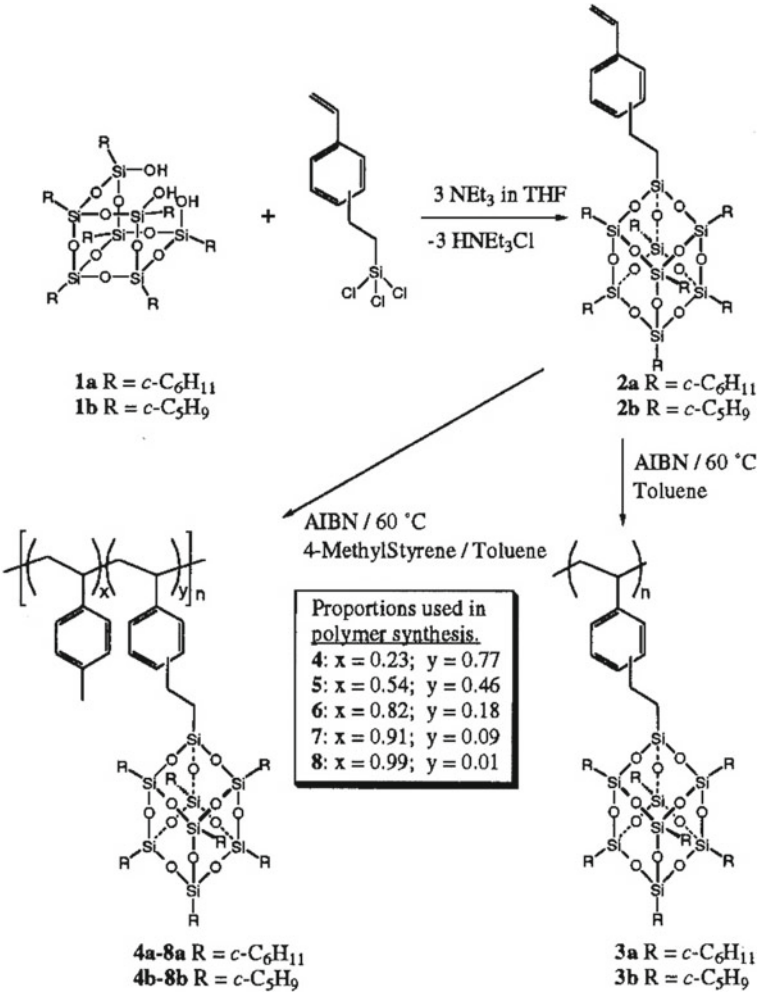

Fig. 12 POSS styryl macromer synthesis and polymerization. Reprinted from [76], © 1996 with permission from ACS Publications

Random copolymers of syndiotactic polystyrene (sPS) and POSS have been synthesized by Coughlin and co-workers [75] through copolymerizations of styrene and (POSS)–styryl macromonomer. Their thermal investigation revealed, not surprisingly, that the copolymers at low POSS content (0–3.2 mol%) had a minor increase in T_g (from 98 to 102 °C), according to Haddad and Lichtenhan [76] that reported a dramatic increase in T_g only at POSS content above 7.8 mol% in atactic poly(4-methyl styrene)–POSS copolymers (Fig. 12).

Coughlin and his collaborators also observed a decrease in melting and crystallinity with increasing the POSS content. Furthermore, they noted that PS–POSS

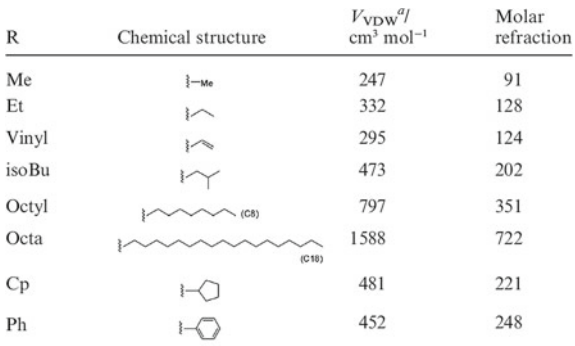

Fig. 13 Chemical structures of octa-substituted POSS fillers. Reprinted from [80], © 2012 with permission from Royal Society of Chemistry

copolymer at 3.2 mol% POSS did not show a melting peak on the second DSC scan, attributing this finding to the disruption of the crystallization process of sPS due to random incorporation of POSS. They completed the investigation with TGA, demonstrating that the inclusion of the inorganic nanoparticles makes the organic polymer matrix more thermally stable. In particular, they recorded $T_{5\%}$ values slightly higher than those obtained from Haddad and Lichtenhan, speculating that this improvement in the resistance to the thermal degradation could arise from the semicrystalline nature of the polymer matrix influencing the aggregation of the inorganic POSS component of the copolymers. Finally, considering the higher values of the residue found at the end of TGA scans, they attributed, in agreement with the literature [77] and with what has already been seen for PP, the thermal oxidative stability to the formation of a silica layer on the surface of the polymer (in the molten state), which acted as a barrier preventing further degradation of the underlying polymer. On continuing their research in this specific field, Coughlin and collaborators wanted to prove that control over the placement of the POSS within an organic polymer is possible using living/controlled polymerization methodologies. The tethering of POSS to an anionically synthesized polymer will extend the range of materials as well as the morphologies that can be achieved. By studying the physical behaviour of the synthesized PS–POSS composites, they observed that the presence of POSS tethered at the end of the polystyrene chain did not alter the T_g, suggesting that the POSS moieties and PS chains are isolated from each others, for the higher-molecular-weight samples [78].

An important contribution to the study of the structure–property relationships between the POSS fillers and the thermomechanical properties of the PS composites was given by the work group of Professor Tanaka at the Kioto University [79], by using eight kinds of octa-substituted aliphatic and aromatic POSS, at different concentrations, as a filler (Fig. 13).

They found homogeneous dispersion and high compatibility for the POSS in the polymer matrices that were valuable for the hybridization with organic and inorganic segments on a nanoscale. The result was a shift to higher values of T_g and decom-

position temperature with increase the POSS content up to 5%. Two tendencies for thermal reinforcement by loading POSS nanoparticles were observed. First, longer alkyl chains in the POSS fillers had a positive effect to enhance thermal stability of the polymer composites (an enhancement ranging from 25 to 30 °C was recorded in the temperature at 20% mass loss, $T_{20\%}$, of composites containing octyl- and octadecyl-POSS), second, the existence of unsaturated bonds in the POSSs. Compared with the $T_{20\%}$ values of the composites containing 5 wt% vinyl- and ethyl-POSS, which have same number of carbon atoms, the former showed significant enhancement to thermal stability of polymer matrices. They speculated that it was likely that longer alkyl chains and unsaturated groups were favourable for enhancing stability due to the strong hydrophobic interaction between POSS and polymers.

Monticelli et al. synthesized, by one-step reactive blending, a copolymer of styrene-maleic anhydride copolymers (PSMA) and a POSS characterized by an amino group as reactive side, obtaining a cyclic imide linkage binding POSS to the polymer backbone due to the occurrence of imidization reaction between the MA group of PSMA and the amino group of POSS molecule. With this typology of synthesis, they obtained a good POSS dispersion, at nanometric level, in the polymer matrix. It is worth to note that when they used a mixing temperature lower than POSS melting one, a surface reaction at the POSS crystal/polymer boundary occurred, leading to the formation of a very peculiar two-phase structure evolving with time at different POSS concentrations. Monticelli and co-workers studied the physical properties of these biphasic systems by the means of DSC and DMTA and found two T_g, depending on the presence of unbound POSS acting as a plasticizer [81].

Wang et al. chemically bonded a mono-functional POSS to a PS chain, modified by the introduction of an active agent [82], observing an increase in T_g of 16 °C that attributed to the rigid nature and diameter (~25–30 Å) of POSS moiety which lead to dominate the movement of the local chain of the polymer [83]. They then confirmed that the incorporation of POSS enhanced the thermal stability of PS by measuring for POSS–PS composites an initial decomposition temperature of about 65 °C and a T_m of 53 °C higher than those of pure PS.

In this context, namely that of the dispersion at nanoscale level of POSSs aiming the enhancement in physical and mechanical properties as compared to virgin PS, fit the studies on POSS of my research group at the University of Catania. Taking advantage of the above-reported literature on the specific topic, we started by the assumption that the different behaviour of each specific POSS in various polymer matrices is attributable to the size of cage, nature of organic periphery, concentration and solubility in the polymer. Thus, the ability of POSS to be dispersed at molecular level is the key to realize physical properties' enhancement like the increase of thermal stability. On considering that symmetric POSSs, with the same height corner organic groups, have been extensively studied in literature and since it is known that aliphatic bonded groups improve solubility and compatibility with polymer matrices but worsen thermal properties [79], whilst aromatic groups act in the opposite way [3], we used, to reinforce PS, some asymmetric substituted POSSs, where a phenyl group was introduced at one of the height cage's slot. POSSs were prepared

by corner-capping reaction of trisilanol with trichlorosilane and/or triethoxysilane [84, 85]. Nanocomposites were obtained by in situ polymerization of styrene in the presence of different quantities of POSS, namely 3, 5 and 10 wt% [86]. Synthesis of mono-substituted silsesquioxanes by a method of corner-capping reactions has been developed by Feher and starts from his pioneering discovery of the synthesis of an incompletely condensed silsesquioxane that contains three reactive hydroxyl groups [87]. The three silanol groups of the incompletely condensed silsesquioxane are very reactive, readily reacting with virtually any organotrichlorosilane ($R'SiCl_3$) to yield the fully condensed cage. A variety of mono-functional silsesquioxanes (as the sole reaction products) can then be easily synthesized by simply varying the R′ group of the organotrichlorosilane. Furthermore, subsequent modifications of this R′ group have since led to the synthesis of various mono-functional monomers that could be polymerized to make organic-inorganic hybrid materials. The first step of our research was to investigate whether and how much the POSS content improves the thermal properties of nanocomposites in respect to neat PS, and on the basis of the obtained thermal parameters, the best filler content was 5 wt% of POSS. Then in the comparison between octaisobutyl-POSS (oib-POSS) and phenyl heptaisobutyl-POSS (ph,hip-POSS), the greatest increases in thermal parameters were recorded for this latter molecular filler as testified from the considerable increase in initial decomposition temperatures (+45 °C about in both oxidative and inert atmosphere) and in degradation activation energy (+40 kJ/mol about) [88, 89]. The better thermal performance showed by nanocomposites filled with the ph,hib-POSS in respect to the octaisobutyl one was attributed to the different structure of the POSSs used as reinforcement. The lower glass transition temperature found for the oib-POSS–PS nanocomposite strengthened this hypothesis. Even though apparently similar, the POSSs we used for nanocomposite design were significantly different: at this stage of the research, we thought that the use of a symmetric POSS, in which stronger POSS–POSS interactions occur, gave rise to auto-aggregation phenomena and thus lower dispersion of filler into polymeric matrix. We got the final confirmation from SEM analysis that showed us this nanometric aggregate (Fig. 14).

On continuing our study in this field, we synthesized nanocomposites based on PS with, this time, seven phenyl and one alkyl groups (Fig. 15). We observed a great increase in both $T_{5\%}$ (+116 °C with respect PS) and E_a of degradation (+105 kJ/mol with respect PS) values. Increase was confirmed, also for the T_g (+28 °C with respect the oib-POSS–PS nanocomposite).

Because of the experience acquired in the reinforcement of polymeric matrices tells us that the compatibility between the matrix and filler in these systems is of great importance, we do not want to limit the introduction of a simple T_8 cage. Always through a corner-capping reaction (Fig. 16), we then synthesized dumb-bell-shaped POSSs with an aromatic thioether bridge [90].

We have already determined that, compared to an unbridged system, dumb-bell-shaped POSS had a better thermal stability and a better viscosity [91]. By checking their compatibility with the polymer matrix, high-magnification Scanning Electron Microscopy revealed that the beads found in the composites with a POSS content of 5 and 10 wt% had a porous structure with squared POSS nanocrystallites that increase

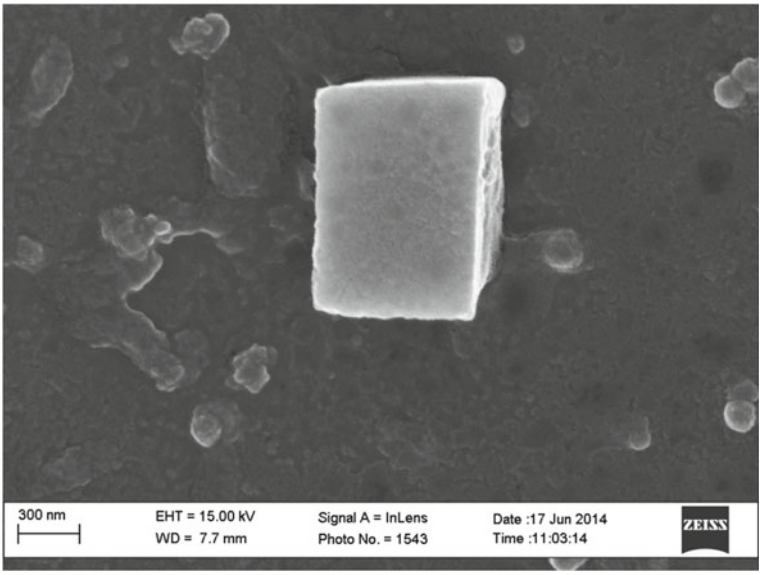

Fig. 14 SEM image of octaisobutyl-POSS–PS nanocomposites.

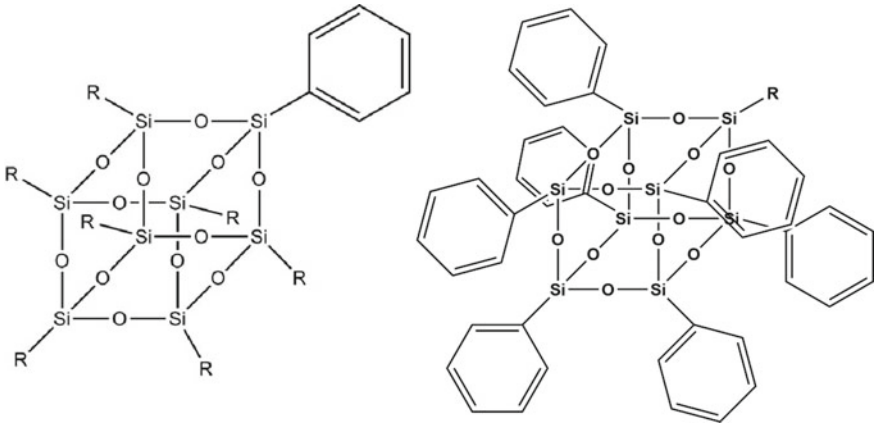

Fig. 15 Molecular structures of phenyl, heptaisobutyl-POSS and isobutyl, heptaphenyl-POSS.

in dimension with the increase of POSS content [92]. The above-observed behaviour could be due to the symmetric structure of the bridged filler that facilitates POSS auto-aggregation phenomena, clearly observed by scanning electron microscopy (Fig. 17).

Consequently, with the aim to enhance the compatibility and miscibility of filler thus leading to the improvement of nanocomposites thermal properties, the idea was to synthesize a series of dumbbell shaped POSSs with aliphatic bridge so that the presence in the filler of jointed chains allows to silicon cages a sufficiently free

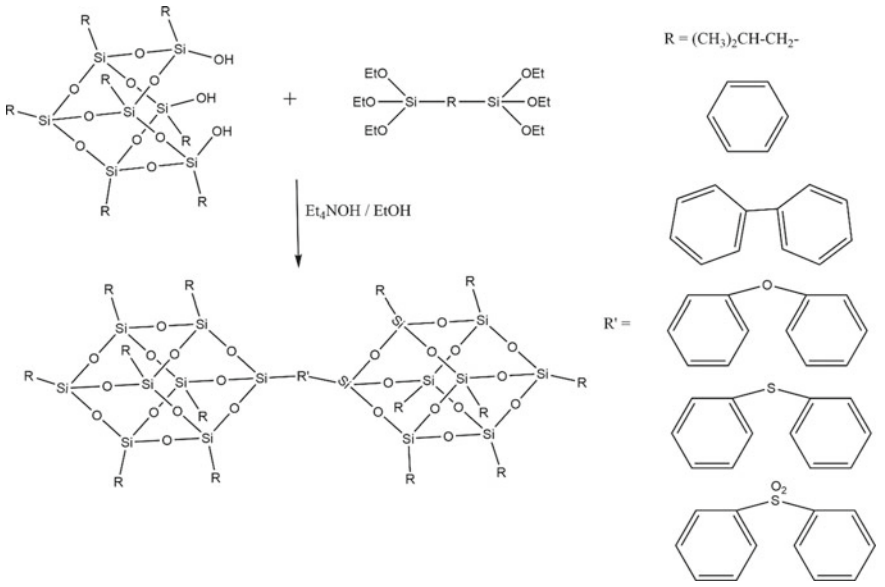

Fig. 16 Corner-capping reaction of hepta isobutyltricycloheptasiloxane trisilanol with triethoxysilyl derivatives for the synthesis of dumb-bell-shaped POSSs.

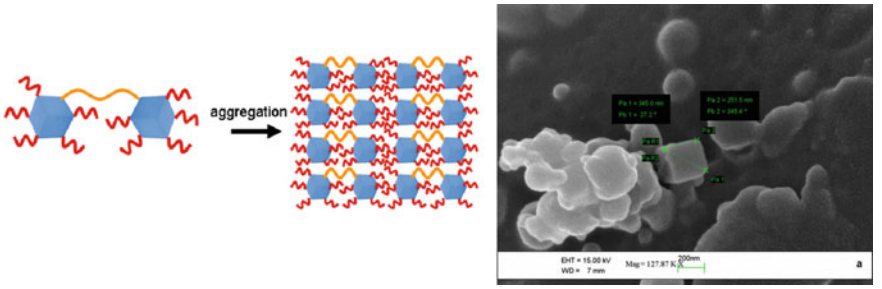

Fig. 17 Aggregation phenomena observed with the incorporation of dumb-bell-shaped POSSs in PS.

movement which should increases as a function of carbon atoms in the bridge (and so chain length) [93, 94]. Indeed, we obtained an increase in the resistance to the thermal degradation, measured with the initial decomposition temperature, with respect to the PS reinforcing with the POSS bearing the aromatic bridge, which increased as a function of the alkyl bridge length [95]. Therefore, in the designing of these materials we must ask whether the priority should be the dispersion in the matrix, and then the possibility to opt for the asymmetric unbridged POSSs, or a higher compatibility with the polymer and then the possibility to opt for the symmetric, but with a bridge that can be functionalized, dumb-bell-shaped POSSs. An alternative way could be

to consider an aliphatic bridge, which allows the freedom of movement of silicon cages, possibility that is not permitted to the spatially blocked aromatic bridge.

5 Polylactide–POSSs Composites

Polylactide (PLA) is a bio-based, biocompatible and biodegradable thermoplastic polyester produced by condensation polymerization of lactic acid (LA; 2-hydroxy propionic acid), which is extracted from fully renewable resources such as corn, sugar beet or rice. PLA has been widely studied and used in medical applications because of its bioresorbable and biocompatible properties in the human body. Furthermore, economic studies showed that PLA can be considered an economically feasible material for use as a packaging polymer, and medical studies have shown that the level of molecules that migrates from packaging containers to food is much lower than the amount of the same molecules used in common food ingredients [96]. However, PLA exhibits some disadvantages, such as low thermo-oxidative stability and slow crystallization rate, which up today greatly limited its application. Several methods, including blending with other polymers and copolymerization, have commonly been used to control PLA properties [97, 98]. The addition of nanoparticles such as nanoclay and carbon nanotubes into PLA has proven to be an attractive way to improve its performance [99, 100]. As for nanoparticles, more and more attention has been paid to POSS.

Poly(L-lactide)s (PLLA) tethered with 0.02–1.00 mol% octaglycidylether polyhedral oligomeric silsesquioxane (OPOSS) were prepared by Huang et al. through solution ring-opening polymerization of L-lactide in the presence of $Sn(Oct)_2$ catalyst [101]. They then prepared a series of PLLA/PLLA-OPOSS 1–30 wt% nanocomposites, by solution blending, that showing similar degradation profiles, indicating that the presence of OPOSS does not significantly altered the degradation mechanism of PLLA matrix. $T_{5\%}$ values of the PLLA/PLLA-OPOSS were higher than those of neat PLLA and increased up to 20 wt% of PLLA-OPOSS content. Huang and co-workers ascribed this improvement in the thermo-oxidative stability to a good dispersion of the POSS cubes in nanocomposites, resulting in a silica layer during the decomposition, which prevents PLLA from further degradation. By the means of DSC measurements, they also observed a shift of the cold-crystallization temperatures of PLLA/PLLA-OPOSS nanocomposites to higher values, compared to that of the neat PLLA. In parallel, the area of the crystallization peak became higher than that of the neat PLLA, thus suggesting an increase in the crystallization rate because of the heterogeneous nucleation effect of the OPOSS molecules dispersed uniformly in the PLLA matrix. On the other side, the glass transition temperature of the PLLA/PLLA-OPOSS nanocomposites remained consistent with that of neat PLLA, regardless their content.

Biodegradable poly(L-lactide) (PLLA)/octamethyl-POSS (ome-POSS) nanocomposites were prepared, by Qiu and Yu via simple melt compounding at various ome-POSS loadings [102]. They obtained a homogeneous dispersion in the matrix and

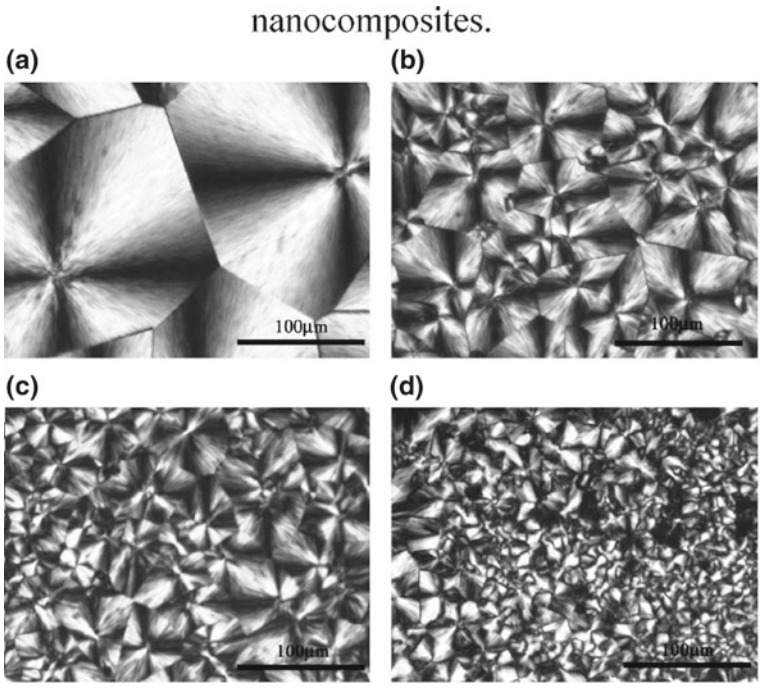

Fig. 18 Polarized optical microscopy (POM) images of neat PLLA and its nanocomposites crystallized at 125 °C; **a** neat PLLA for 90 min, **b** POSS-2 for 35 min, **c** POSS-5 for 18 min and **d** POSS-8 for 12 min. Reprinted from [102], © 2011 with permission from ACS Publications

a similar degradation profile for both neat PLLA and its nanocomposites, suggesting that the presence of ome-POSS did not alter the degradation mechanism of the matrix. They found a $T_{5\%}$ value of about 347 °C for neat PLLA, and a growth from 294, 305 and 321 °C for the PLLA/ome-POSS nanocomposites, with increasing the ome-POSS loading from 2 to 8 wt%, respectively, indicating that the incorporation of ome-POSS reduced the thermal stability of the PLLA matrix. The effect of ome-POSS on the non-isothermal cold and melt crystallization behaviours and isothermal melt crystallization kinetics was further investigated by them. Qiu and Yu found that non-isothermal melt crystallization of PLLA was induced by the presence of ome-POSS in the nanocomposites at a relatively high cooling rate of 15 °C/min, whilst neat PLLA hardly crystallized at the same cooling rate (Fig. 18). Moreover, the overall crystallization rates were faster in the nanocomposites than in neat PLLA and increased with increasing the ome-POSS loading; however, the crystallization mechanism of PLLA remains unchanged despite the presence of ome-POSS. They hypothesized that ome-POSS may act as an effective nucleating agent during the crystallization process of PLLA.

Hu et al., during the attempts to develop a bio-derived polylactide composite with improved flame retardancy and anti-dripping properties, utilized intumescent flame

retardant (IFR) together with trisilanolisobutyl polyhedral oligomeric silsesquioxane (TPOSS) nanoparticles and observed a delay in the thermo-oxidation process of the PLA [103]. They recorded a synergistic effect among microencapsulated ammonium polyphosphate (MCAPP), melamine (MA) and TPOSS that imparted excellent flame retardancy to PLA. The incorporation of TPOSS into PLA obviously decreased the peak heat release rate (PHRR) and total heat released (THR) values of the composites in the microscale combustion calorimeter MCC tests, and effectively delayed the thermo-oxidation process of the PLA. The decomposition of TPOSS gave rise to many active radicals, which interacted with H and OH radicals in the gaseous phase of the fire and retarded polymer degradation and combustion. The additives' actions were explained in the following way: MCAPP catalysed the formation of a protective char whilst TPOSS prevented the char from further thermal degradation, thus shielding the underlying polymeric substrate from further burning.

The effect of screw speed on the thermal and morphological properties of melt compounded plasticized PLA–POSS composites was investigated by Kodal et al. They found that incorporation of POSS particles to the PLA decreased the melt viscosity of the composites due to the slip-agent behaviour of POSS molecules, by improving the yield strength and modulus values. Moreover, they observed a homogeneous POSS particles' dispersion in the matrix at all loadings, regardless of screw speed. It was revealed from DSC that POSS particles acted as a nucleating agent for PLA independently from mixing conditions, thus resulting in an increase of crystallinity as a function of POSS and a slightly decrease of both T_g and cold-crystallization temperature [104].

Monticelli and her collaborators introduced functionalized POSS (one by hydroxyl groups −OH and another with an amino bearing molecule $-NH_2$) into some electrospinning solutions for the preparation of electrospun stereocomplex polylactide (sc-PLA)-based fibres [105]. The thermal decomposition of all the analysed fibres was found to occur in one step, and the presence of POSS in the fibres significantly affected the T_i values, by enhancing those of the fibres containing POSS–OH and POSS–NH_2 at 340 and 338 °C in respect to the 319 °C of sc-PLA fibres. This behaviour, already found for other polymer matrices described elsewhere in this chapter, was ascribed to the formation of a silica layer on the surface of the polymer hence serving as a barrier and limiting the degradation of the polymer. Indeed, as at the T_i, the evaporation of both POSS–OH and POSS–NH_2 is not completed, and the silsesquioxanes can play a protection action towards the polymer. The results found by Monticelli and co-workers point out that not only the formation of stereocomplex can affect PLA degradation, but also the presence of POSS, which in the case of electrospun nanofibres is homogeneously dispersed in the polymer matrix (Fig. 19), can contribute to the increase of the PLA thermal stability. Professor Monticelli group continued their studies by setting a novel strategy for the preparation of bio-hybrid systems based on PLA and POSS, adopting a preliminary functionalization of the matrix and a subsequent reaction of amino or hydroxyl functionalities POSS, potentially capable of reacting with maleic anhydride groups created onto PLA by a free radical process [106].

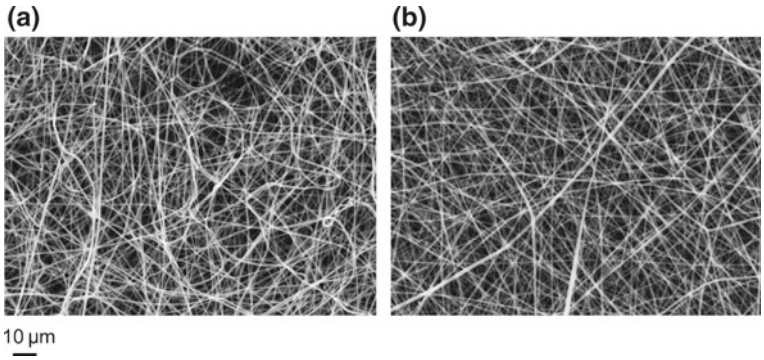

Fig. 19 SEM micrographs of PLLA/PDLA fibres prepared by applying the optimal electrospinning conditions and containing: **a** POSS–NH_2 and **b** POSS–OH. Reprinted from [105], © 2014 with permission from ACS Publications

The main advantage of their preparation method is that it was not accompanied by a change of the polymer molecular mass. By means of DSC, they observed that the incorporation of POSS had little effects on the T_g value of PLA-g-MA, which is around 62.5 °C. Although cold crystallization (T_{cc}) and melting peak (T_m) were found not to change in the hybrid systems, they recorded an increase in the degree of crystallinity related to the amount of POSS grafted onto the polymer, being the degree of crystallinity much higher in the sample based on POSS–NH_2. Finally, they highlighted that in the case of the nanocomposites prepared by melt blending, the addition of POSS was found to enhance the crystallinity of PLA just up to 17% [107], whilst in the synthesized hybrid based on POSS–NH_2 the increment was almost 200%.

Pramoda et al. reported the effects of using graphene oxide (GO) nanosheets and POSS nanocages as filler for in situ ring-opening polymerized PLA [108]. Thermal investigations showed that the nanocomposites reinforced with GO and POSS as nanofillers, either as physical mixture of GO-functionalized and POSS-functionalized or as GO-graft-POSS, were far more superior as compared with the nanocomposites having individually dispersed nanofillers in the PLA matrix. In particular, the nanocomposites produced by incorporating GO-functionalized or POSS-functionalized showed only a slight improvement (i.e. ~10 °C) in thermal properties, whereas the $T_{5\%}$ increased to about 19 °C for PLA/physical mixture of GO and POSS and of about 31 °C for PLA/GO-graft-POSS. The two fillers, when used in combination, worked synergistically to improve the thermal stability of the PLA. The best results, however, were achieved with the GO-graft-POSS for which they hypothesized a more effective improving in thermal property deriving by POSS, with its three-dimensional structure and eight arms, than by the two-dimensional GO. Furthermore, they observed an increase in T_g at 59.5 °C for the PLA/GO-POSS physical mixture and 58 °C for PLA/GO-graft-POSS.

Recently, Ozkoc et al. reported the effects on the thermal properties after the inclusion, at different loading level, of reactive and non-reactive POSSs in PLA matrix [109]. The incorporation of POSS particles into the matrix reduced slightly the T_g value of pure PLA, about 58 °C, independently of POSS used. The decline in T_g showed that both non-reactive and reactive POSSs acted as a plasticizer and affected the free volume of polymer–POSS system by interacting with each other [110, 111]. Ozkoc and collaborators attributed this effect to the dispersion of POSS particles at the nanoscale level in the matrix, which was already observed. In addition, they evaluated the thermal stability of PLA and PLA–POSS composites showing that $T_{5\%}$ of pure PLA (341.4 °C) increased with the addition of POSS particles due to the physical barrier by POSS molecules, which limited the heat flux to the matrix.

6 Polyimides–POSSs Composites

Over the past 20 years, the development of the industrial chemistry leads to improved technologies in producing polymers which are becoming more widely used to improve the quality of human life: from aerospace to high-tech household appliances, textiles, insulation materials in industry and construction, medical and biological field and much more over. An important polymeric materials family, responded to certain technical requirements, are polyimides (PI). Since their first synthesis by Bogert in 1908 [112] and high-molecular-weight aromatic polyimides synthesis in 1955 [113], interest in this class of polymers has been growing steadily because of their thermo-oxidative stability, unique electrical properties, high radiation and solvent resistance, and high mechanical strength [114]. Their characteristics are due to the functional group CO–NR_2 called imide that gives the name to this family of polymers. Specifically, the presence of $n - \pi$ conjugation between non-pair electron of nitrogen atom and π electrons of the carbonyl group makes them resistant to chemical agents and moisture, whilst the type of hydrocarbon residues (arenes, aliphatic) and the presence of other functional groups (Cl, F, NO_2, OCH_3, etc.) determine their physical properties and thus their application [115]. Thanks to its outstanding properties such as high strength and good thermal stability and to the development of the additive manufacturing, PI today has been widely used also as technology material for structural applications [116, 117]. However, the particularity of the applications that see it constantly subjected to solicitations can lead to a premature degradation. Another extensively used of polyimide is as spacecraft material in low Earth orbit (LEO), where hazards such as atomic oxygen (AO) or electrostatic discharge (ESD) act for the material degradation. Thus, the need to develop new high-efficiency techniques to increase the lifetime and enhance its thermal stability. The various methods applied to enhance its resistance to the degradation are generally classified into two categories, namely the application of protective coatings on its surface and the introduction of functional compounds into polyimide by physical blend or chemical bond [118–121].

Mu and collaborators synthesized a series of structural phosphorus-containing POSS–PI nanocomposites at various percentage of phosphorus [122], obtaining nanocomposites displayed outstanding thermal properties. With a phosphorus content of 1.61 wt%, they observed an enhancement of the resistance to the degradation and shift towards higher value of T_g (295 °C). Moreover, the nanocomposites presented much higher atomic oxygen (AO) durability compared with pure PI because of the incorporation of special functional groups of phosphorus oxide and POSS.

With the same phosphorus content (1.61 wt%), the atomic oxygen (AO) erosion yields already decreased to 51.9% of pure POSS–PI nanocomposites. Mu and co-workers continued their studies by synthesizing a series of structural phosphorus-containing POSS–PI hybrid materials, which incorporated phenyl phosphine oxide (PPO) structure into the main chains of POSS–PI. Using the DSC technique, they observed a raising of T_g for the POSS–PI hybrid materials by the incorporation of PPO structure into polymer matrix [123]. With the introduction of PPO structure in PI chains, the C electron cloud density and intermolecular forces increased because of the P=O bond, which provided the electronic properties that resulted in the difficulty of segmental motion and increased T_g. The thermal stability of the prepared composites was evaluated, by Mu and co-workers, using TGA and resulting in an evident increase in $T_{5\%}$ (and thus resistance to thermal degradation) due to the P=O with high bond energy. The phosphorus-containing POSS–PI hybrid materials displayed higher residuals of degradation than reference POSS–PI, that increased as a function of PPO content, which was ascribed to the ceramic formation from POSS moiety during thermal decomposition and to phosphorus oxide.

Atar et al. prepared PI-based nanocomposite films by incorporating POSS and carbon nanotube (CNT) additives (Fig. 20). They investigated the influence of the POSS content on the thermo-optical properties of the CNT–POSS–PI films in comparison to those of control PI and CNT–PI films [124].

CNT–POSS–PI films, with POSS content ranging from 5 to 15 wt%, exhibited sheet resistivities that remained essentially unchanged after exposure to AO with a fluence of ~2.3×10^{20} O atoms cm^{-2}. Atar and co-workers evaluated the possible applications of the prepared composites under simulated space environmental conditions, including thermal cycling, ionizing radiation and AO. The performance of the CNT–POSS–PI films was investigated under extreme thermal cycling, a common hazard of the space environment. The composite films (5 mm × 5 mm) were subjected to 29 thermal cycles from −100 to 140 °C using a temperature-controlled stage in a nitrogen atmosphere. The sheet resistivities of the CNT–POSS–PI films (5 and 15 wt% POSS content) were measured at the conductive bottom surfaces (containing CNTs) using the four-point van der Pauw method [125] at the minimum and maximum temperatures after every second cycle. These properties make the prepared CNT–POSS–PI films with 15 wt% POSS content excellent candidates for applications where AO durability and electrical conductivity are required for flexible and thermally stable materials. Hence, they are suggested here for LEO applications such as the outer layers of spacecraft thermal blankets.

He et al. prepared a series of functional POSS–PI nanocomposites by using a two-step approach (Fig. 21)—first, the octa(aminophenyl)silsesquioxane (OAPS)/NMP

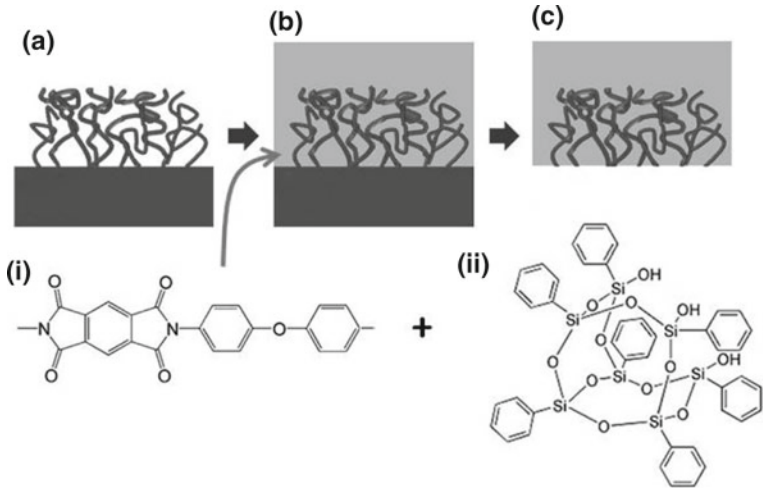

Fig. 20 Schematic illustration of CNT–POSS–PI film fabrication process. **a** A ~9-μm-thick CNT sheet is first grown by CVD on a pre-patterned Si substrate. **b** A POSS–PAA blend, composed of (i) PMDA–ODA monomer and (ii) trisilanolphenyl POSS, is then infiltrated into the CNT sheet. **c** The free-standing CNT–POSS–PI film is mechanically peeled from the substrate after curing. Reprinted from [124], © 2015 with permission from ACS Publications

solution was mixed with polyamic acid (PAA) solution prepared by reacting 4,4′-diaminodiphenylmethane and 3,3′,4,4′-benzophenonetetracarboxylic dianhydride in NMP, and second, the polycondensation solution was treated by thermal imidization [126].

The resulting PI–POSS nanocomposites exhibited excellent thermomechanical properties, such as high T_g and low coefficient of thermal expansion (CTE). The glass transition temperature increased from 301.4 °C for pure PI to 421.0 °C for PI–POSS nanocomposite at an amine group ratio 0.4, due to the significant increase of the cross-linking density in the nanocomposites. The well-defined 'hard particles' (POSS) and the strong covalent bonds between the PI and the 'hard particles' lead to a significant improvement in the thermal stability testified by an increase in $T_{5\%}$ from 513 °C for PI to 551 °C for the nanocomposites.

Another series of functional POSS–PI nanocomposites were prepared, by Sarojadevi et al., using the same two-step approach of He and co-workers. The well-defined 'hard particles' (POSS) and the strong covalent bonds in the amide linkage, between the carbon atom of the carboxyl side group in PAA and the nitrogen atom of the amino group in POSS, led to a significant improvement in the thermal properties. T_g increased from 160.4 to 210.0 °C, and $T_{5\%}$ increased from 321.5 to 496.9 °C by passing from pure PI to PI–POSS nanocomposite. This behaviour was probably due to the homogeneous dispersion of POSS cages in the PI observed by Sarojadevi and co-workers, together with the increase in storage modulus of PI on incorporating POSS within the matrix [127].

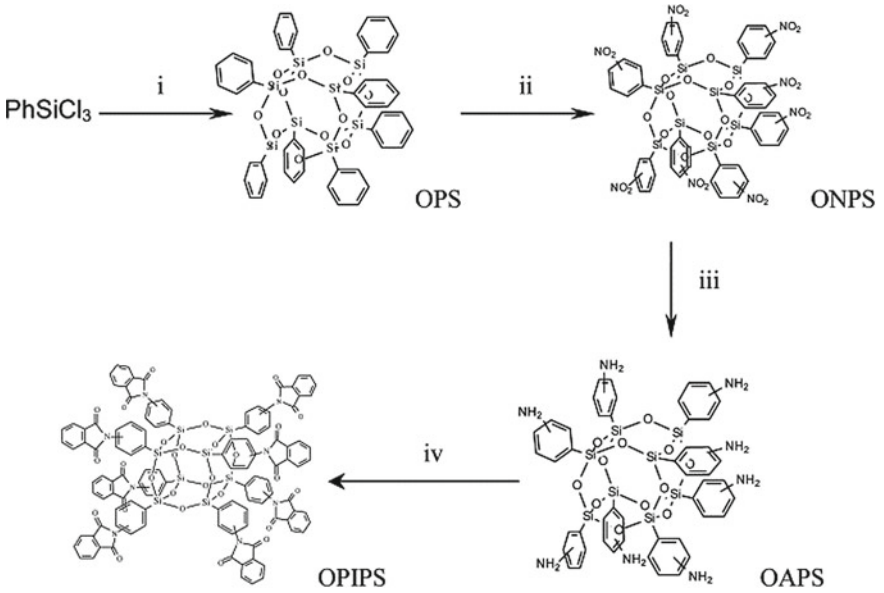

Fig. 21 (i) H_2O, benzene, benzyltrimethylammonium hydroxide, stir at RT/N2; (ii) fuming nitric acid, stir at RT; (iii) Pd/C, THF, NEt3, HCO2H, reflux, 60 °C; (iv) phthalic anhydride, NMP, 270 °C. Reprinted from [126], © 2003 with permission from Elsevier

Pan and his collaborators prepared organic–inorganic hybrid proton exchange membranes (PEMs) using sulphonated polyimides containing benzimidazole (SPIBIs) and glycidyl ether of polyhedral oligomeric silsesquioxanes (GPOSS) [128]. By the means of TGA, they observed two different stages of degradation, for both the membranes and the cross-linked one, with the first step attributed to the decomposition of sulphonic acid groups and the second one to the degradation of the polyimide backbone. All the SPIBIs and cross-linked membranes showed improved resistance to the thermal degradation (higher than 320 °C), indicating their prospective application in high-temperature fuel cells.

Organic–inorganic PI with double-decker silsesquioxane (DDSQ) in the main chains was synthesized by Zheng et al. obtaining composites in which they observed a good dispersion into the continuous polyimide matrix of microphase-separated and self-organized POSS cages, whose spherical microdomains were measured in 5–20 nm in diameter [129]. The TGA results showed that the thermal stability of PI was significantly enhanced with the inclusion of DDSQ in the main chains. They hypothesized that DDSQ cages in place of 4,4′-diaminodiphenyl ether (ODA) in the main chains of PI could significantly retard the chain scission, which resulted in the enhanced decomposition temperature. Successively, the well-dispersed DDSQ microdomains acted to suppress the release of gaseous products from segmental decomposition. On continuing their studies, Zheng and co-workers synthesized a well-defined tetra-amino POSS, 5,11,14,17-Tetraanilinooctaphenyl double-decker

silsesquioxane, always for using in the preparation of polyimide nanocomposites [130]. The thermal stability of the organic–inorganic polyimides was investigated by the means of TGA and upon introducing the tetrafunctional POSS, the temperatures of initial degradation were significantly enhanced, with respect that of plain PI by 30–40 °C, depending on the content of 5,11,14,17-tetraanilino DDSQ. The improved thermal stability was ascribed to two different structural features of the organic–inorganic polyimides: the formation of chemical linkages among PI chains and the POSS cages; the formation of POSS microdomains, with a diameter of 40–80 nm, due to POSS–POSS auto-aggregation phenomena. The chemical linkages between polyimide chains and POSS cages would retard the chain scission, and thus, the T_i value was enhanced. These further studies allowed them to validate their original hypothesis, so the occurring of POSS microdomains leads to the suppression of degradation volatile products, thus giving rise to an increase in the residue yields of degradation.

With the aim to have useful information for designing appropriate molecular architecture, to be used in the fabrication of high performance plastic substrates for display devices, Jung et al. prepared polyimide—organosilicate composite materials by using a new type of polysilsesquioxane (PSSQ) (Fig. 22).

Compared to conventional POSS, this new silane compound has both enhanced thermal stability and improved compatibility with poly(amic acid) [131]. They showed that films made from solutions of the composites exhibited higher optical transparency and superior dimensional stability during thermal treatment than films of pure polyimide or of conventional POSS–PI composites. Bridging of POSS and chemical bonding among POSS and PI chains significantly enhanced the thermal properties. TGA analysis showed an increase in temperature at 1% mass loss of +35 °C by passing from neat PI to composites at 2% of reinforcement.

7 Polyurethane–POSSs Composites

Polyurethane (PU) is one of the most versatile plastic materials and can be considered as the representative of a class of segmented polymers with alternating hard (diisocyanate and chain extender) and soft segments (polyol). Depending on the reactants and process methods, polyurethane polymer can be an elastomer, viscoelastic gel, foam or plastic, offering very good elasticity, high mechanical strength, hardness and abrasion resistance [132, 133]. Polyurethanes are employed in a wide variety of applications, such as adhesives, coatings, construction materials, automotive seating, furniture, packing materials and medical devices [134–139]. There has been much activity in recent years directed towards the covalent incorporation of POSSs into segmented polyurethane elastomers aiming to modify their structure and improve the physical properties of resultant elastomer–POSS composites.

Liu and Zheng used an octaaminophenyl (Oap) POSS as cross-linking agent for PU hybrid networks and observed that its introduction, in small amount (<2 wt%), gave rise to a significant increase in dynamic storage modulus and T_g in respect

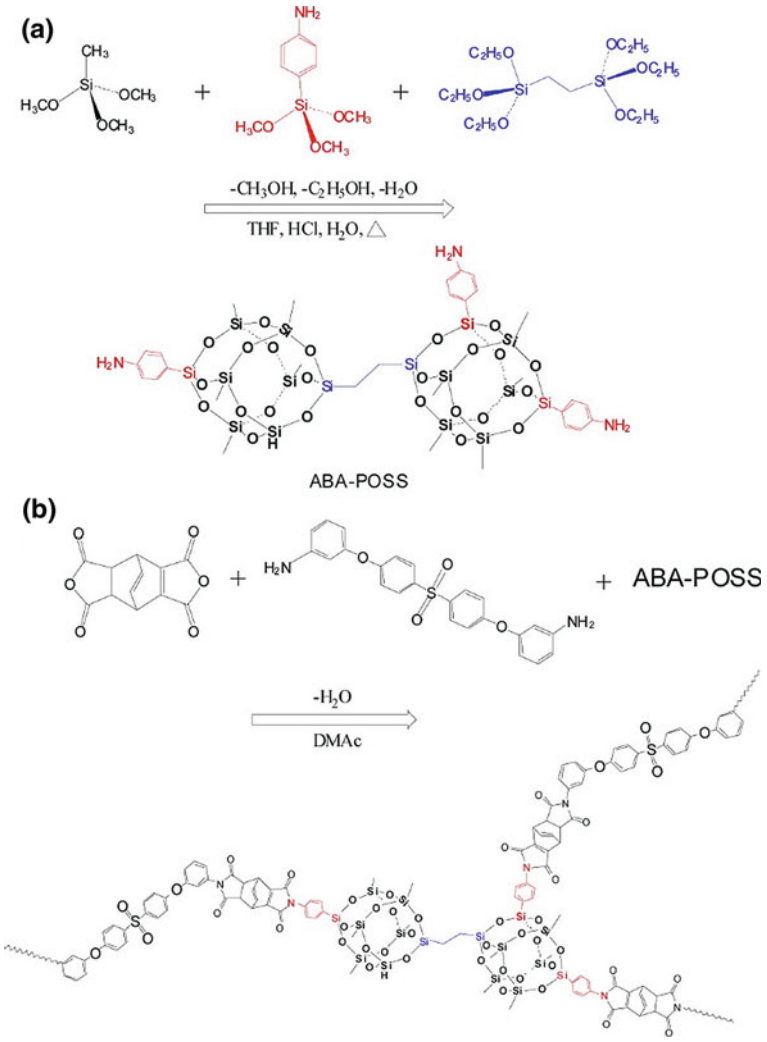

Fig. 22 **a** Possible chemical structure of ABA-POSS and its synthesis through hydrolysis and polycondensation of silane compounds; **b** fabrication of polyimide–organosilicate composite through condensation and imidization. Reprinted from [131], © 2014 with permission from ACS Publications

to the control PU. Furthermore, the improvement in thermal stability was testified by a retarded weight loss rate and an enhanced char yield, by the incorporation of OapPOSS into the PU networks, which was higher with increasing the concentration of nanoparticles [140]. Thus, this improvement was obviously ascribed to the presence of POSS cages, which participated in the formation of a homogeneous hybrid network. They proposed, according to the literature [141], that the

inorganic component provides additional heat capacity, thereby stabilizing the bulk materials against thermal decomposition, except at surfaces where initial decomposition would begin. Liu and Zheng continued their studies on the modification of PU using octa(propylglycidyl ether) polyhedral oligomeric silsesquioxane (OpePOSS) in which additional nanocross-linking reactions occurred, among the amide moiety of PU and the epoxide groups of the OpePOSS, excluding the cross-link among PU pre-polymers and aromatic amines. Also in this case, they observed a T_g enhancement that they attributed not only to the POSS nanoreinforcement in the polymer matrices, which was able to restrict the motions of the macromolecular chains, but also to additional cross-linking among the PU networks and OpePOSS. In fact, it should be noted that, although the nanocomposite containing 20 wt% POSS possessed a T_g of −14 °C, the organic–inorganic network still retained its elastomeric character [142].

Otaigbe et al. obtained a homogeneous dispersion of POSS in polyurethane ureas by a sequencing of reaction steps (Fig. 23), making it possible to prepare nanostructured PU–POSS films with prescribed morphology and superior physical properties [143, 144].

Despite in oxidative environment they observed a slight improvement in the thermal, it has been found a significant increase in the melt viscosity and zero shear viscosity. This behaviour was attributed to the inclusion of diamino-POSS into the PU hard segments, as confirmed by the increase in the storage modulus as a function of increasing POSS concentration only at the high-temperature range of the hard segments, whilst no change has been observed in the low-temperature range of the soft segments.

Similar degradation behaviour was also reported in the work of Zhang and collaborators [145], where diol-functionalized POSS incorporated into a PU network did not alter the onset of thermal degradation, but increased the final char yield.

An important contribution to the effects of POSS addition on the PU thermal stability was given by Prof. Pielichowski, who started his studies in collaboration with the USA Lawrence Livermore National Laboratory and proceeded at the Department of Chemistry and Technology of Polymers of the Cracow University of Technology. Pielichowski and his co-workers started their experiments synthesizing and characterizing, by the means of TGA and thermal volatilization analysis (TVA), a series of PU elastomer systems incorporating varying levels of 1,2-propanediol-heptaisobutyl-POSS (PHIPOSS) as chain extender unit, replacing butane diol. Their results indicated that covalent incorporation of POSS into the PU elastomer network increased the non-oxidative thermal stability of the systems [146]. In particular, with increasing POSS loading from 2 up to 10%, the rate of mass loss increased at temperatures above 300 °C and the total mass loss after 600 °C, thus suggesting a modification in thermal degradation behaviour of POSS–PU hybrid systems. The increase in onset-degradation temperature indicated that the POSS–PU hybrids are more thermally stable with respect to the primary depolymerization, whilst the increased rate of mass loss and lower char yields may be indicative of an acceleration of secondary-stage degradation processes in the hybrid systems. On considering the importance of determining kinetics parameters to better evaluate the thermal stability of a mate-

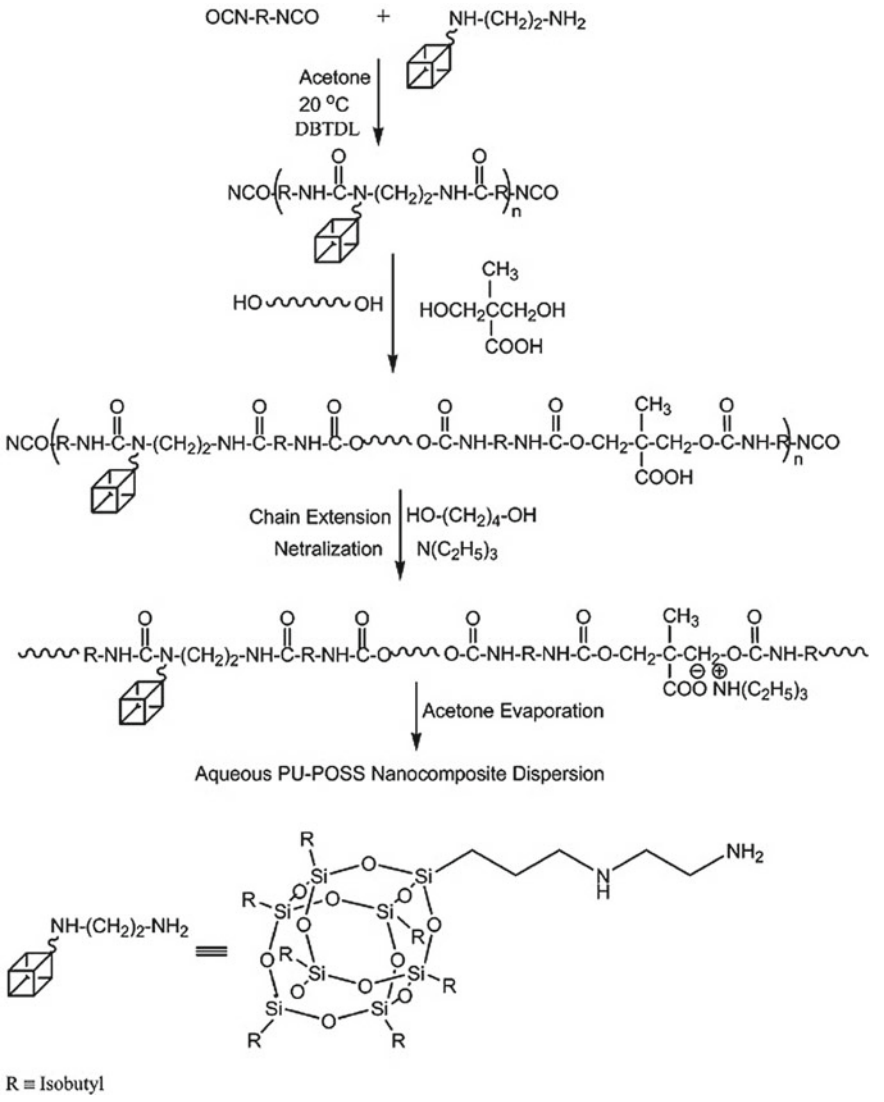

Fig. 23 Elementary steps for the synthesis of the PU–POSS hybrid dispersions and an idealized structure of the diamino-POSS. Reprinted from [143], © 2006 with permission from ACS Publications

rial and to speculate on its degradation mechanisms [147, 148], Pielichowski and collaborators correctly decided to carry out a kinetics study to obtain the apparent activation energy (E_a) of degradation and the pre-exponential factor (A) through the Ozawa–Flynn–Wall (OFW) [149, 150] and Friedman methods [151]. They found that the incorporation of POSS into PU elastomer increased the E_a values in the

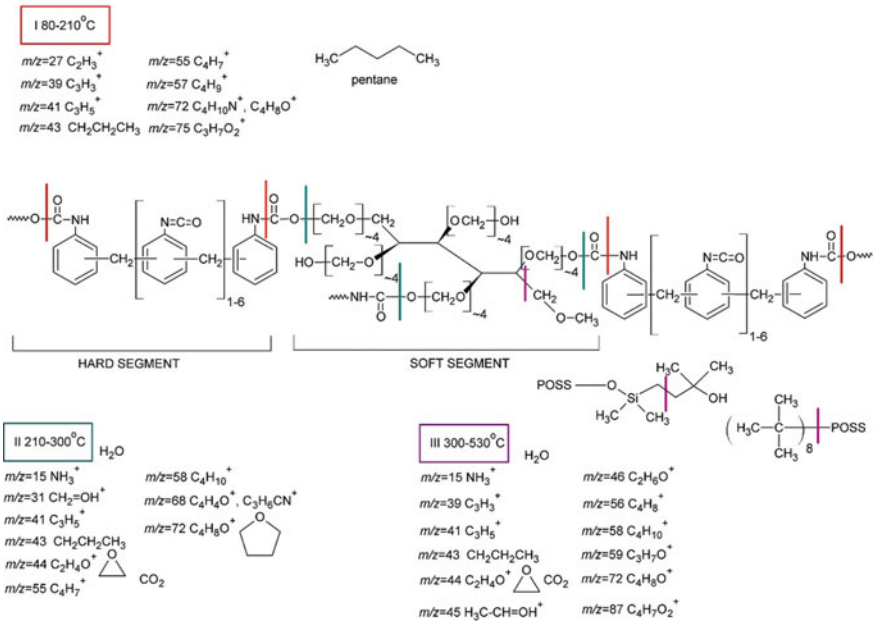

Fig. 24 Thermal degradation of polyurethane materials under inert atmosphere. Reprinted from [153], © 2016 with permission from Elsevier

first stage of the thermal degradation by ~10 kJ/mol and decreased the E_a by about 70 kJ/mol for the second step. The presence of PHIPOSS thus increased the thermal stability of the polymeric material but accelerated the decomposition of the PU at temperatures above 240 °C. The best compliance of experimental data with the considered models was obtained for the two-stage degradation mechanism. The results of isoconversional studies which utilized the Friedman and OFW methods were indicative of autocatalytic behaviour for the first degradation stage in all cases (Cn model) and of the *n*-dimensional nucleation for the second degradation stage (An model) in the case of the unmodified PU elastomer. For the nanohybrid polyurethanes, the second step was altered from an *n*-dimensional nucleation to a reaction of *n*-th order. Thus, with the same *n*-th order followed, neat PU thermal degradation was assumed to occur with autocatalysis/*n*-dimensional nucleation model and for the nanohybrid elastomers with autocatalysis/reaction [152]. Pielichowski group definitively proved that POSS influences the mechanism of PU decomposition by carrying out thermal and spectroscopy characterization of rigid polyurethane foams chemically modified with two functionalized POSS–PHIPOSS as pendant group to the main PU chain and OCTA-POSS (Fig. 24) which acted as a chemical cross-linking agent due to the presence of eight OH-terminated side chains [153].

Their studies showed that the thermal decomposition of PU foams reinforced with POSS started at about 150 °C via urethane linkages scission. They speculated about the formation of low-molecular-weight compounds and intermediates

with ether/ester and alcohol groups at lower temperature. Whilst at higher temperature (>350 °C), they observed the evolution of hydrocarbons, aldehydes, alcohols, ethers, glycols, amines, cyclic species and low-molecular-weight compounds—carbon monoxide, carbon dioxide, water and ammonia. Thus, POSS influenced the degradation mechanism and affected the formation of char, which was demonstrated to act as an insulating barrier limiting heat and mass transfer.

Jiang et al. synthesized a series of hybrid polyurethanes based on sustainable epoxy soybean oil by using double-decker octaphenylsilsesquioxanetetraol (DDT_8OH) to replace 1,4-butanediol (BDO) as chain extender. Through thermogravimetric and calorimetric analyses, they observed an increase in the thermal stability and glass transition temperature, which was attributed to the increased rigidity of molecular chains. Furthermore, although they observed a good homogeneous dispersion of POSS in the polymer matrix up to 12.59 wt% DDT_8OH concentration, serious aggregation phenomena occurred at higher loading [154]. Jiang and his collaborators confirmed that the incorporation of double-decker silsesquioxane into sustainable polyurethane molecular chains can make possible the preparation of hybrids with quite higher physical properties and will open up new pathways for the development of environmentally friendly polymer.

8 Conclusions

Thanks to their rigid heart made of silicon and oxygen, POSS molecules are intrinsically thermally stable. This feature, together with the thousands of possible functionalization due to their organic periphery, has made them one of the most used, in polymeric materials reinforcement, nanomolecule classes in the last 25 years. Moreover, if up to 10–15 years ago POSSs could be considered niche products for their high cost, today the scale-up of POSSs' manufacture has brought down prices dramatically, thus widening the usage categories to the most common ones. In this chapter, I tried to highlight how their ability to modify, generally increasing, the thermal behaviour of the polymeric matrices that host them depends, regardless of the nature of the latter, on the quantity and therefore on their dispersion in the matrix and on the nature, and sometimes length, of the functional groups. Finally, their versatility guarantees that much still can be done and there are still many unexplored paths regarding the preparation of composites reinforced with POSS.

References

1. Zheng L, Farris RJ, Coughlin EB (2001) Novel polyolefin nanocomposites: synthesis and characterizations of metallocene-catalyzed polyolefin polyhedral oligomeric silsesquioxane copolymers. Macromolecules 34:8034–8039

2. Shockey EG, Bolf AG, Jones PF, Schwab JJ, Chaffee KP, Haddad TS, Lichtenhan JD (1999) Functionalized polyhedral oligosilsesquioxane (POSS) macromers: new graftable POSS hydride, POSS α-olefin, POSS epoxy, and POSS chlorosilane macromers and POSS–siloxane triblocks. Appl Organometal Chem 13(4):311–327
3. Fina A, Tabuani D, Carniato F, Frache A, Boccaleri E, Camino G (2006) Polyhedral oligomeric silsesquioxanes (POSS) thermal degradation. Thermochim Acta 440:36–42
4. Bolln C, Tsuchida A, Frey H, Mulhaupt R (1997) Thermal properties of the homologous series of 8-fold alkyl-substituted octasilsesquioxanes. Chem Mater 9:1475–1479
5. Lee A (2002) Proceedings of POSS nanotechnology conference, Huntington Beach, CA, Sept 25–27, 2002
6. Lu S, Hamerton I (2002) Recent developments in the chemistry of halogen-free flame retardant polymers. Prog Polym Sci 27:1661–1712
7. Blanco I, Bottino FA, Cicala G, Latteri A, Recca A (2014) Synthesis and characterization of differently substituted phenyl hepta isobutyl-polyhedral oligomeric silsesquioxane/polystyrene nanocomposites. Polym Compos 35(1):151–157
8. Yei DR, Kuo SW, Su YC, Chang FC (2004) Enhanced thermal properties of PS nanocomposites formed from inorganic POSS-treated montmorillonite. Polymer 45:2633–2640
9. Blanco I, Abate L, Bottino FA, Bottino P (2014) Synthesis, characterization and thermal stability of new dumbbell-shaped isobutyl-substituted POSSs linked by aromatic bridges. J Therm Anal Calorim 117(1):243–250
10. Blanco I, Bottino FA, Abate L (2016) Influence of *n*-alkyl substituents on the thermal behaviour of polyhedral oligomeric silsesquioxanes (POSSs) with different cage's periphery. Thermochim Acta 623:50–57
11. Ni Y, Zheng S, Nie K (2004) Morphology and thermal properties of inorganic–organic hybrids involving epoxy resin and polyhedral oligomeric silsesquioxanes. Polymer 45:5557–5568
12. Zhao L, Li J, Li Z, Zhang Y, Liao S, Yu R, Hui D (2018) Morphology and thermomechanical properties of natural rubber vulcanizates containing octavinyl polyhedral oligomeric silsesquioxane. Composite Part B 139:40–46
13. Blanco I, Bottino FA (2012) Effect of the substituents on the thermal stability of hepta cyclopentyl, phenyl substitued-Polyhedral oligomeric silsesquioxane (hcp-POSS)/polystyrene (PS) nanocomposites. AIP Conf Proc 1459(1):247–249
14. Ghani K, Keshavarz MH, Jafari M, Khademian F (2018) A novel method for predicting decomposition onset temperature of cubic polyhedral oligomeric silsesquioxane derivatives. J Therm Anal Calorim. https://doi.org/10.1007/s10973-017-6881-4
15. Strachota A, Kroutilova I, Kovarova J, Matejka L (2004) Epoxy networks reinforced with polyhedral oligomeric silsesquioxanes (POSS). Thermomechanical properties. Macromolecules 37:9457–9464
16. Zhang Y, Lee S, Yoonessi M, Liang K, Pittman CU (2006) Phenolic resin–trisilanolphenyl polyhedral oligomeric silsesquioxane (POSS) hybrid nanocomposites: structure and properties. Polymer 47:2984–2999
17. Moore BM, Ramirez SM, Yandek GR et al (2011) Asymmetric aryl polyhedral oligomeric silsesquioxanes (ArPOSS) with enhanced solubility. J Organomet Chem 696:2676–2680
18. Blanco I, Bottino FA, Bottino P (2012) Influence of symmetry/asymmetry of the nanoparticles structure on the thermal stability of polyhedral oligomeric silsesquioxane/polystyrene nanocomposites. Polym Compos 33:1903–1910
19. Menczel JD, Prime RB (2009) Thermal analysis of polymers. Fundamentals and applications. Wiley, Hoboken, New Jersey
20. Kandola BK, Biswas B, Price D, Horrocks AR (2010) Studies on the effect of different levels of toughener and flame retardants on thermal stability of epoxy resin. Polym Degrad Stab 95:144–152
21. Blanco I, Oliveri L, Cicala G, Recca A (2012) Effects of novel reactive toughening agent on thermal stability of epoxy resin. J Therm Anal Calorim 108(2):685–693
22. May CA (1988) Epoxy resins, chemistry and technology. Marcel Dekker, New York
23. Ellis B (1993) Chemistry and technology of epoxy resins. Chapman & Hall, London

24. Liu YL, Wu CS, Chiu YS, Ho WH (2003) Preparation, thermal properties, and flame retardance of epoxy–silica hybrid resins. J Polym Sci Part A: Polym Chem 41(15):2354–2367
25. Sprenger S (2013) Epoxy resins modified with elastomers and surface-modified silica nanoparticles. Polymer 54(18):4790–4797
26. Laine RM, Choi J, Lee I (2001) Organic-inorganic nanocomposites with completely defined interfacial interactions. Adv Mater 13(11):800–803
27. Choi J, Harcup J, Yee AF, Zhu Q, Laine RM (2001) Organic/inorganic hybrid composites from cubic silsesquioxanes. J Am Chem Soc 123(46):11420–11430
28. Lee A, Lichtenhan JD (1998) Viscoelastic responses of polyhedral oligosilsesquioxane reinforced epoxy systems. Macromolecules 31(15):4970–4974
29. Li GZ, Wang L, Toghiani H, Daulton TL, Koyama K, Pittman CU Jr (2001) Viscoelastic and mechanical properties of epoxy/multifunctional polyhedral oligomeric silsesquioxane nanocomposites and epoxy/ ladderlike polyphenylsilsesquioxane blends. Macromolecules 34(25):8686–8693
30. Bharadwaj RK, Berry RJ, Farmer BL (2000) Molecular dynamics simulation study of norbornene-POSS polymers. Polym Prepr Am Chem Soc Div Polym Chem 41(1):530–531
31. Shockey EG, Bolf AG, Jones PF, Schwab JJ, Chaffee KP, Haddad TS, Lichtenhan JD (1999) Functionalized polyhedral oligosilsesquioxane (POSS) macromers: new graftable POSS hydride, POSS α-olefin, POSS epoxy, and POSS chlorosilane macromers and POSS-siloxane triblocks. Appl Organometal Chem 13:311–327
32. Mya KY, He C, Huang J, Xiao Y, Dai J, Siow Y (2004) Preparation and thermomechanical properties of epoxy resins modified by octafunctional cubic silsesquioxane epoxides. J Polym Sci Part A: Polym Chem 42(14):3490–3503
33. Abad MJ, Barral L, Fasce DF, Williams RJJ (2003) Epoxy networks containing large mass fractions of a monofunctional polyhedral oligomeric silsesquioxane (POSS). Macromolecules 36(9):3128–3135
34. Choi J, Yee AF, Laine RM (2003) Organic/inorganic hybrid composites from cubic silsesquioxanes. epoxy resins of octa(dimethylsiloxyethylcyclohexylepoxide) silsesquioxane. Macromolecules 36(15):5666–5682
35. Choi J, Tamaki R, Kim SG, Laine RM (2003) Organic/inorganic imide nanocomposites from aminophenylsilsesquioxanes. Chem Mater 15(17):3365–3375
36. Choi J, Kim SG, Laine RM (2004) Organic/inorganic hybrid epoxy nanocomposites from aminophenylsilsesquioxanes. Macromolecules 37(1):99–109
37. Choi J, Yee AF, Laine RM (2004) Toughening of cubic silsesquioxane epoxy nanocomposites using core–shell rubber particles: a three-component hybrid system. Macromolecules 37(9):3267–3276
38. Ni Y, Zheng S, Nie K (2004) Morphology and thermal properties of inorganic–organic hybrids involving epoxy resin and polyhedral oligomeric silsesquioxanes. Polymer 45:5557–5568
39. Le Baron PC, Wang Z, Pinnavaia TJ (1999) Polymer-layered silicate nanocomposites: an overview. Appl Clay Sci 15(1–2):11–29
40. Ray SS, Okamoto M (2003) Polymer/layered silicate nanocomposites: a review from preparation to processing. Prog Polym Sci 28:1539–1641
41. Barabasi AL, Albert R, Jeong H (1999) Mean-field theory for scale-free random networks. Phys A 272:173–187
42. Chen WY, Wang YZ, Kuo SW, Huang CF, Tung PH, Chang FC (2004) Thermal and dielectric properties and curing kinetics of nanomaterials formed from POSS-epoxy and metaphenylenediamine. Polymer 45:6897–6908
43. Kissinger HE (1957) Reaction kinetics in differential thermal analysis. Anal Chem 29:1702–1706
44. Flynn JH, Wall LA (1996) General treatment of the thermogravimetry of polymers. J Res Nat Bur Stand Part: A Phys Chem 70A:487–513
45. Ozawa T (1965) A new method of analyzing thermogravimetric data. Bull Chem Soc Jpn 38(11):1881–1886

46. Liu H, Zhang W, Zheng S (2005) Montmorillonite intercalated by ammonium of octaaminopropyl polyhedral oligomeric silsesquioxane and its nanocomposites with epoxy resin. Polymer 46:157–165
47. Jones IK, Zhou YX, Jeelani S, Mabry JM (2008) Effect of polyhedral-oligomeric-silsesquioxanes on thermal and mechanical behavior of SC-15 epoxy. eXPRESS Polym Lett 2(7):494–501
48. Wang X, Hu Y, Song L, Xing W, Lu H (2010) Thermal degradation behaviors of epoxy resin/POSS hybrids and phosphorus-silicon synergism of flame retardancy. J Polym Sci Part B: Polym Phys 48:693–705
49. Nagendiran S, Alagar M, Hamerton I (2010) Octasilsesquioxane-reinforced DGEBA and TGDDM epoxy nanocomposites: characterization of thermal, dielectric and morphological properties. Acta Mater 58:3345–3356
50. Pistor V, Soares BG, Mauler RS (2013) Influence of the polyhedral oligomeric silsesquioxane *n*-phenylaminopropyl—POSS in the thermal stability and the glass transition temperature of epoxy resin. Polímeros 23(3):331–338
51. Avrami M (1939) Kinetics of phase change. I general theory. J Chem Phys 7(12):1103–1112
52. Avrami M (1940) Kinetics of phase change. II transformation-time relations for random distribution of nuclei. J Chem Phys 8(2):212–224
53. Avrami M (1941) Granulation, phase change, and microstructure kinetics of phase change III. J Chem Phys 9(2):177–184
54. Pistor V, Ornaghi FG, Ornaghi HL, Zattera AJ (2012) Degradation kinetic of epoxy nanocomposites containing different percentage of epoxycyclohexyl–POSS. Polym Compos 33(7):1224–1232
55. Pistor V, Barbosa LG, Soares BG, Mauler RS (2012) Relaxation phenomena in the glass transition of epoxy/*N*-phenylaminopropyl–POSS nanocomposites. Polymer 53(25):5798–5805
56. Pistor V, Ornaghi FG, Ornaghi HL, Zattera AJ (2012) Dynamic mechanical characterization of epoxy/epoxycyclohexyl–POSS nanocomposites. Mater Sci Eng A 532:339–345
57. Raimondo M, Guadagno L, Speranza V, Bonnaud L, Dubois P, Lafdi K (2018) Multifunctional graphene/POSS epoxy resin tailored for aircraft lightning strike protection. Compos B Eng 140:44–56
58. Romano V, Naddeo C, Vertuccio L, Lafdi K, Guadagno L (2017) Experimental evaluation and modeling of thermal conductivity of tetrafunctional epoxy resin containing different carbon nanostructures. Polym Eng Sci 57(7):779–786
59. Maddah HA (2016) Polypropylene as a promising plastic: a review. Am J Polym Sci 6(1):1–11
60. Fu BX, Yang L, Somani RH, Zong SX, Hsiao BS, Phillips S, Blanski R, Ruth P (2001) Crystallization studies of isotactic polypropylene containing nanostructured polyhedral oligomeric silsesquioxane molecules under quiescent and shear conditions. J Polym Sci Part B: Polym Phys 39:2727–2739
61. Fina A, Abbenhuis HCL, Tabuani D, Frache A, Camino G (2006) Polypropylene metal functionalised POSS nanocomposites: a study by thermogravimetric analysis. Polym Degrad Stabil 91:1064–1070
62. Fina A, Tabuani D, Frache A, Camino G (2005) Polypropylene–polyhedral oligomeric silsesquioxanes (POSS) nanocomposites. Polymer 46:7855–7866
63. Pracella M, Chionna D, Fina A, Tabuani D, Frache A, Camino G (2006) Polypropylene-POSS nanocomposites: morphology and crystallization behaviour. Macromol Symp 234:59–67
64. Misra R, Fu BX, Morgan SE (2007) Surface energetics, dispersion, and nanotribomechanical behavior of POSS/PP hybrid nanocomposites. J Polym Sci Part B Polym Phys 45:2441–2455
65. Fina A, Tabuani D, Peijs T, Camino G (2009) POSS grafting on PPgMA by one-step reactive blending. Polymer 50:218–226
66. Fina A, Tabuani D, Frache A, Boccaleri E, Camino G (2005) Isobutyl POSS thermal degradation. In: Le Bras M, Wilkie C, Bourbigot S (eds) Fire retardancy of polymers: new applications of mineral fillers. Royal Society of Chemistry, Cambridge, UK, pp 202–220
67. Fina A, Tabuani D, Camino G (2010) Polypropylene–polysilsesquioxane blends. Eur Polymer J 46:14–23

68. Grala M, Bartczak Z, Pracella M (2013) Morphology and mechanical properties of polypropylene-POSS hybrid nanocomposites obtained by reactive blending. Polym Compos 34(6):929–941
69. Yang M, Yao XX, Wang G, Ding H (2008) A simple method to synthesize sea urchin-like polyaniline hollow spheres. Colloid Surf 324(1–3):113–116
70. Li J, Sun FF (2009) The interfacial feature of thermoplastic polystyrene composite filled with nitric acid oxidized carbon fiber. Surf Interface Anal 41(3):255–258
71. Giannelis EP (1996) Polymer layered silicate nanocomposites. Adv Mater 8(1):29–35
72. Hussain F, Hojjati M, Okamoto M, Gorga RE (2006) Polymer-matrix nanocomposites, processing, manufacturing, and application: an overview. J Compos Mater 40(17):1511–1575
73. Cavallaro G, Lazzara G, Milioto S (2011) Dispersions of nanoclays of different shapes into aqueous and solid biopolymeric matrices. Extended physicochemical study. Langmuir 27(3):1158–1167
74. Haddad TS, Viers BD, Phillips SH (2001) Polyhedral oligomeric silsesquioxane (POSS)-styrene macromers. J Inorg Organomet Polym 11(3):155–164
75. Zheng L, Kasi RM, Farris RJ, Coughlin EB (2012) Synthesis and thermal properties of hybrid copolymers of syndiotactic polystyrene and polyhedral oligomeric silsesquioxane. J Polym Sci Part A Polym Chem 40:885–891
76. Haddad TS, Lichtenhan JD (1996) Hybrid organic–inorganic thermoplastics: styryl-based polyhedral oligomeric silsesquioxane polymers. Macromolecules 29(22):7302–7304
77. Gonzalez RI, Phillips SH, Hoflund GB (2000) In situ oxygen atom erosion study of a polyhedral oligomeric silsequioxanes-siloxane copolymer. J Spacecraft Rockets 37:463–467
78. Cardoen G, Coughlin EB (2004) Hemi-telechelic polystyrene-POSS copolymers as model systems for the study of well-defined inorganic/organic hybrid materials. Macromolecules 37:5123–5126
79. Tanaka K, Adachi S, Chujo Y (2009) Structure-property relationship of octa-substituted POSS in thermal and mechanical reinforcements of conventional polymers. J Polym Sci Part A: Polym Chem 47:5690–5697
80. Tanaka K, Chujo Y (2012) Advanced functional materials based on polyhedral oligomeric silsesquioxane (POSS). J Mater Chem 22:1733–1746
81. Monticelli O, Fina A, Ullah A, Waghmare P (2009) Preparation, characterization, and properties of novel PSMA-POSS systems by reactive blending. Macromolecules 42:6614–6623
82. Guo X, Wang W, Liu L (2010) A novel strategy to synthesize POSS/PS composite and study on its thermal properties. Polym Bull 64:15–25
83. Xu HY, Kuo SW, Lee JS, Chang FC (2002) Glass transition temperatures of poly(hydroxystyrene-covinylpyrrolidone-co-isobutylstyryl polyhedral oligosilsesquioxanes). Polymer 43(19):5117–5124
84. Blanco I, Abate L, Bottino FA, Bottino P, Chiacchio MA (2012) Thermal degradation of differently substituted cyclopentyl polyhedral oligomeric silsesquioxane (CP-POSS) nanoparticles. J Therm Anal Calorim 107(3):1083–1091
85. Blanco I, Abate L, Bottino FA, Bottino P (2012) Hepta isobutyl polyhedral oligomeric silsesquioxanes (hib-POSS) A thermal degradation study. J Therm Anal Calorim 108(2):807–815
86. Blanco I, Abate L, Bottino FA, Bottino P (2012) Thermal degradation of hepta cyclopentyl, mono phenyl-polyhedral oligomeric silsesquioxane (hcp-POSS)/polystyrene (PS) nanocomposites. Polym Degrad Stabil 97:849–855
87. Feher FJ, Budzichowski TA, Blanski RL, Weller KJ, Ziller JW (1991) Facile syntheses of new incompletely condensed polyhedral oligosilsesquioxanes. Organometallics 10(7):2526–2528
88. Blanco I, Abate L, Antonelli ML, Bottino FA, Bottino P (2012) Phenyl hepta cyclopentyl–polyhedral oligomeric silsesquioxane (ph,hcp-POSS)/polystyrene (PS) nanocomposites: the influence of substituents in the phenyl group on the thermal stability. eXPRESS Polymer Letters 6(12):997–1006
89. Blanco I, Bottino FA (2013) Thermal study on phenyl, hepta isobutyl-polyhedral oligomeric silsesquioxane/polystyrene nanocomposites. Polym Compos 34(2):225–232

90. Blanco I, Abate L, Bottino FA, Bottino P (2014) Synthesis, characterization and thermal stability of new dumbbell-shaped isobutyl-substituted POSSs linked by aromatic bridges. J Therm Anal Cal 117(1):243–250
91. Blanco I, Bottino FA, Cicala G, Latteri A, Recca A (2013) A kinetic study of the thermal and thermal oxidative degradations of new bridged POSS/PS nanocomposites. Polym Degrad Stabil 98:2564–2570
92. Blanco I, Bottino FA, Cicala G, Cozzo G, Latteri A, Recca A (2015) Synthesis and thermal characterization of new dumbbell shaped POSS/PS nanocomposites: influence of the symmetrical structure of the nanoparticles on the dispersion/aggregation in the polymer matrix. Polym Compos 36(8):1394–1400
93. Blanco I, Abate L, Bottino FA (2014) Synthesis and thermal properties of new dumbbell-shaped isobutyl-substituted POSSs linked by aliphatic bridges. J Therm Anal Calorim 116:5–13
94. Blanco I, Abate L, Bottino FA (2015) Synthesis and thermal characterization of new dumbbell-shaped cyclopentyl-substituted POSSs linked by aliphatic and aromatic bridges. J Therm Anal Calorim 121:1039–1048
95. Blanco I, Abate L, Bottino FA, Bottino P (2014) Thermal behaviour of a series of novel aliphatic bridged polyhedral oligomeric silsesquioxanes (POSSs)/polystyrene (PS) nanocomposites: the influence of the bridge length on the resistance to thermal degradation. Polym Degrad Stabil 102:132–137
96. Blanco I, Siracusa V (2013) Kinetic study of the thermal and thermo-oxidative degradations of polylactide-modified films for food packaging. J Therm Anal Calorim 112(3):1171–1177
97. Wang L, Ma W, Gross RA, McCarthy SP (1998) Reactive compatibilization of biodegradable blends of poly (lactic acid) and poly(ε-caprolactone). Polym Degrad Stabil 59:161–168
98. Sarazin P, Favis BD (2003) Morphology control in co-continuous poly(L-lactide)/polystyrene blends: a route towards highly structured and interconnected porosity in poly(L-lactide) materials. Biomacromol 4:1669–1679
99. Ray SS, Yamada K, Okamoto M, Ogami A, Ueda K (2003) New polylactide/layered silicate nanocomposites. 3. High-performance biodegradable materials. Chem Mater 15:1456–1465
100. Chen G-X, Kim H-S, Park BH, Yoon J-S (2005) Controlled functionalization of multi-walled carbon nanotubes with various molecular-weight poly(L-lactic acid). J Phys Chem B 109:22237–22243
101. Zou J, Chen X, Jiang XB, Zhang J, Guo YB, Huang FR (2011) Poly(L-lactide) nanocomposites containing octaglycidylether polyhedral oligomeric silsesquioxane: Preparation, structure and properties. eXPRESS Polym Lett 5(8):662–673
102. Yu J, Qiu Z (2011) Preparation and properties of biodegradable poly(L-lactide)/octamethyl-polyhedral oligomeric silsesquioxanes nanocomposites with enhanced crystallization rate via simple melt compounding. ACS Appl Mater Interfaces 3:890–897
103. Xuan S, Hu Y, Song L, Wang X, Yang H, Lu H (2012) Synergistic effect of polyhedral oligomeric silsesquioxane on the flame retardancy and thermal degradation of intumescent flame retardant polylactide. J Combust Sci Technol 184:456–468
104. Kodal M, Sirin H, Ozkoc G (2014) Effects of screw speed on the properties of plasticized PLA/POSS composites. AIP Conf Proc 1593:420–423
105. Monticelli O, Putti M, Gardella L, Cavallo D, Basso A, Prato M, Nitti S (2014) New stereocomplex PLA-based fibers: effect of POSS on polymer functionalization and properties. Macromolecules 47:4718–4727
106. Gardella L, Colonna S, Fina A, Monticelli O (2014) On novel bio-hybrid system based on PLA and POSS. Colloid Polym Sci 292:3271–3278
107. Wang R, Wang S, Zhang Y (2009) Morphology, rheological behavior, and thermal stability of PLA/PBSA/POSS composites. J Appl Polym Sci 113:3095–3102
108. Pramoda KP, Koh CB, Hazrat H, He CB (2014) Performance enhancement of polylactide by nanoblending with POSS and graphene oxide. Polym Compos 35:118–126
109. Sirin H, Kodal M, Ozkoc G (2014) The influence of POSS type on the properties of PLA. Polym Compos 37(5):1497–1506

110. Wu J, Haddad TS, Mather PT (2009) Vertex group effects in entangled polystyrene–polyhedral oligosilsesquioxane (POSS) copolymers. Macromolecules 42(4):1142–1152
111. Ayandele E, Sarkar B, Alexandridis P (2012) Polyhedral oligomeric silsesquioxane (POSS)-containing polymer nanocomposites. Nanomaterials 2(4):445–475
112. Ohya H, Kudryavtsev VV, Semenova SI (eds) (1996) Polyimide membranes—applications, fabrications, and properties. Kodansha Ltd., Tokyo
113. Buhler KU (1978) Spezialplaste. Academie-Verlag, Berlin [in German, Chap. 7.1.11.1]
114. Liaw D-J, Wang K-L, Huang Y-C, Lee K-R, Lai J-Y, Ha C-S (2012) Advanced polyimide materials: syntheses, physical properties and applications. Prog Polym Sci 37(7):907–974
115. Georgiev A, Dimov D, Spassova E, Assa J, Dineff P, Danev G (2012) Chemical and physical properties of polyimides: biomedical and engineering applications. In: Abadie MJM (eds) High performance polymers—polyimides based—from chemistry to applications. Intech
116. Cicala G, Ognibene G, Portuesi S, Blanco I, Rapisarda M, Pergolizzi E, Recca G (2018) Comparison of Ultem 9085 used in fused deposition modelling (FDM) with polytherimide blends. Materials 11(2):285–299
117. Sena SK, Banerjee S (2012) A novel structural polyimide material with phosphorus and POSS synergistic for atomic oxygen resistance. RSC Adv 2:6274–6289
118. Verker R, Grossman E, Gouzman I, Noam E (2007) Residual stress effect on degradation of polyimide under simulated hypervelocity space debris and atomic oxygen. Polymer 48(1):19–24
119. Shimamura H, Nakamura T (2009) Mechanical properties degradation of polyimide films irradiated by atomic oxygen. Polym Degrad Stabil 94(9):1389–1396
120. Gilman J, Schlitzer DS, Lichtenhan JD (1996) Low earth orbit resistant siloxane copolymers. J Appl Polym Sci 60(4):591–596
121. Reddy MR, Srinivasamurthy N, Agrawal BL (1993) Atomic oxygen protective coatings for Kapton film: a review. Surf Coat Tech 58(1):1–17
122. Song G, Li X, Jiang Q, Mu J, Jiang Z (2015) A novel structural polyimide material with phosphorus and POSS synergistic for atomic oxygen resistance. RSC Adv 5:11980–11988
123. Li X, Hao J, Jiang Q, Mu J, Jiang Z (2015) Phosphorus-containing polyhedral oligomeric silsesquioxane/polyimides hybrid materials with low dielectric constant and low coefficients of thermal expansion. J Appl Polym Sci 132(39):42611–42617
124. Atar N, Grossman E, Gouzman I, Bolker A, Murray VJ, Marshall BC, Qian M, Minton TK, Hanein Y (2015) Atomic-oxygen-durable and electrically-conductive CNT-POSS polyimide flexible films for space applications. ACS Appl Mater Interfaces 7:12047–12056
125. van der Pauw LJ (1958) A method of measuring specific resistivity and Hall effect of discs of arbitrary shape. Philips Res Rep 13:1–9
126. Huang J-C, He C-B, Xiao Y, Mya KY, Dai J, Siow YP (2003) Polyimide/POSS nanocomposites: interfacial interaction, thermal properties and mechanical properties. Polymer 44:4491–4499
127. Govindaraj B, Sundararajan P, Sarojadevi M (2012) Synthesis and characterization of polyimide/ polyhedral oligomeric silsesquioxane nanocomposites containing quinolyl moiety. Polym Int 61:1344–1352
128. Pan H, Zhang Y, Pu H, Chang Z (2014) Organic-inorganic hybrid proton exchange membrane based on polyhedral oligomeric silsesquioxanes and sulfonated polyimides containing benzimidazole. J Power Sources 63:195–202
129. Liu N, Wei K, Wang L, Zheng S (2016) Organic-inorganic polyimides with double decker silsesquioxane in the main chains. Polym Chem 7:1158–1167
130. Qiu J, Xu S, Liu N, Wei K, Li L, Zheng S (2018) Organic–inorganic polyimide nanocomposites containing a tetrafunctional polyhedral oligomeric silsesquioxane amine: synthesis, morphology and thermomechanical properties. Polym Int 67:301–312
131. Jung Y, Byun S, Park S, Lee H (2014) Polyimide-organosilicate hybrids with improved thermal and optical properties. ACS Appl Mater Interfaces 6:6054–6061
132. Tu Y-C, Suppes GJ, Hsieh F-H (2009) Thermal and mechanical behavior of flexible polyurethane-molded plastic films and water-blown foams with epoxidized soybean oil. J Appl Polym Sci 111:1311–1317

133. Byczyński Ł, Dutkiewicz M, Januszewski R (2017) Thermal behaviour and flame retardancy of polyurethane high-solid coatings modified with hexakis(2,3-epoxypropyl)cyclotriphosphazene. Prog Org Coat 108:51–58
134. Klempner D, Frisch KC (1991) Handbook of polymeric foams and foam technology. Oxford University Press, New York
135. Wirpsza Z (1993) Polyurethanes: chemistry, technology, and applications. Ellis Horwood, New York
136. Randall D, Lee S (2002) The polyurethanes book. Wiley, New York
137. Król P (2007) Synthesis methods chemical structures and phase structures of linear polyurethanes. Properties and applications of linear polyurethanes in polyurethane elastomers, copolymers and ionomers. Prog Mater Sci 52:915–1015
138. Kang SK, Cho IS, Kim SB (2008) Preparation and characterization of antimicrobial polyurethane foam modified by urushiol and cardanol. Elastomer 43:124
139. Zammarano M, Kramer RH, Harris R, Ohlemiller TJ, Shields JR, Rahatekar SS, Lacerda S, Gilman JW (2008) Flammability reduction of flexible polyurethane foams via carbon nanofiber network formation. Polym Adv Tech 19:588–595
140. Liu H, Zheng S (2005) Polyurethane networks nanoreinforced by polyhedral oligomeric silsesquioxane. Macromol Rapid Commun 26:196–200
141. Zuo M, Chi TT (1999) Preparation and characterization of poly(urethane-imide) films prepared from reactive polyimide and polyurethane prepolymer. Polymer 40:5153–5160
142. Liu Y, Ni Y, Zheng S (2006) Polyurethane networks modified with octa(propylglycidyl ether) polyhedral oligomeric silsesquioxane. Macromol Chem Phys 207:1842–1851
143. Nanda AK, Wicks DA, Madbouly SA, Otaigbe JU (2006) Nanostructured polyurethane/POSS hybrid aqueous dispersions prepared by homogeneous solution polymerization. Macromolecules 39:7037–7043
144. Madbouly SA, Otaigbe JU, Nanda AK, Wicks DA (2007) Rheological behavior of POSS/polyurethane-urea nanocomposite films prepared by homogeneous solution polymerization in aqueous dispersions. Macromolecules 40:4982–4991
145. Zhang S, Zou Q, Wu L (2006) Preparation and characterization of polyurethane hybrids from reactive polyhedral oligomeric silsesquioxanes. Macromol Mater Eng 291:895–901
146. Lewicki JP, Pielichowski K, De La Croix T, Janowski B, Todd D, Liggat JJ (2010) Thermal degradation studies of polyurethane/POSS nanohybrid elastomers. Polym Degrad Stabil 95:1099–1105
147. Rodante F, Vecchio S, Tomassetti M (2002) Kinetic analysis of thermal decomposition for penicillin sodium salts—model-fitting and model-free methods. J Pharm Biomed Anal 29:1031–1043
148. Blanco I, Abate L, Antonelli ML, Bottino FA (2013) The regression of isothermal thermogravimetric data to evaluate degradation E_a values of polymers: a comparison with literature methods and an evaluation of lifetime predictions reliability. Part II. Polym Degrad Stabil 98:2291–2296
149. Ozawa T (1965) A new method of analyzing thermogravimetric data. Bull Chem Soc Jpn 38:1881–1886
150. Flynn JH, Wall LA (1966) A quick, direct method for the determination of activation energy from thermogravimetric data. Polym Lett 4:323–328
151. Friedman HL (1964) Kinetics of thermal degradation of char-forming plastics from thermogravimetry. Application to a phenolic plastic. J Polym Sci Part C 6:183–195
152. Janowski B, Pielichowski K (2016) A kinetic analysis of the thermo-oxidative degradation of PU/POSS nanohybrid elastomers. Silicon 8:65–74
153. Pagacz J, Hebda E, Michałowski S, Ozimek J, Sternik D, Pielichowski K (2016) Polyurethane foams chemically reinforced with POSS—Thermal degradation studies. Thermochim Acta 642:95–104
154. Huang J, Jiang P, Li X, Huang Y (2016) Synthesis and characterization of sustainable polyurethane based on epoxy soybean oil and modified by double-decker silsesquioxane. J Mater Sci 51:2443–2452